Critical Propulsion Components
Volume 1: Summary, Introduction, and Propulsion Systems Studies

Pratt & Whitney
West Palm Beach, Florida

General Electric Aircraft Engines
Cincinnati, Ohio

The NASA STI Program Office . . . in Profile

Since its founding, NASA has been dedicated to the advancement of aeronautics and space science. The NASA Scientific and Technical Information (STI) Program Office plays a key part in helping NASA maintain this important role.

The NASA STI Program Office is operated by Langley Research Center, the Lead Center for NASA's scientific and technical information. The NASA STI Program Office provides access to the NASA STI Database, the largest collection of aeronautical and space science STI in the world. The Program Office is also NASA's institutional mechanism for disseminating the results of its research and development activities. These results are published by NASA in the NASA STI Report Series, which includes the following report types:

- TECHNICAL PUBLICATION. Reports of completed research or a major significant phase of research that present the results of NASA programs and include extensive data or theoretical analysis. Includes compilations of significant scientific and technical data and information deemed to be of continuing reference value. NASA's counterpart of peer-reviewed formal professional papers but has less stringent limitations on manuscript length and extent of graphic presentations.

- TECHNICAL MEMORANDUM. Scientific and technical findings that are preliminary or of specialized interest, e.g., quick release reports, working papers, and bibliographies that contain minimal annotation. Does not contain extensive analysis.

- CONTRACTOR REPORT. Scientific and technical findings by NASA-sponsored contractors and grantees.

- CONFERENCE PUBLICATION. Collected papers from scientific and technical conferences, symposia, seminars, or other meetings sponsored or cosponsored by NASA.

- SPECIAL PUBLICATION. Scientific, technical, or historical information from NASA programs, projects, and missions, often concerned with subjects having substantial public interest.

- TECHNICAL TRANSLATION. English-language translations of foreign scientific and technical material pertinent to NASA's mission.

Specialized services that complement the STI Program Office's diverse offerings include creating custom thesauri, building customized databases, organizing and publishing research results . . . even providing videos.

For more information about the NASA STI Program Office, see the following:

- Access the NASA STI Program Home Page at *http://www.sti.nasa.gov*

- E-mail your question via the Internet to help@sti.nasa.gov

- Fax your question to the NASA Access Help Desk at 301–621–0134

- Telephone the NASA Access Help Desk at 301–621–0390

- Write to:
  NASA Access Help Desk
  NASA Center for AeroSpace Information
  7121 Standard Drive
  Hanover, MD 21076

Critical Propulsion Components

Volume 1: Summary, Introduction, and Propulsion Systems Studies

Pratt & Whitney
West Palm Beach, Florida

General Electric Aircraft Engines
Cincinnati, Ohio

National Aeronautics and
Space Administration

Glenn Research Center

May 2005

Document History

This research was originally published internally in September 2000.

Abstract

Several studies have concluded that a supersonic aircraft, if environmentally acceptable and economically viable, could successfully compete in the 21st century marketplace. However, before industry can commit to what is estimated as a 15-to-20 billion dollar investment, several barrier issues must be resolved. In an effort to address these barrier issues, NASA and Industry teamed to form the High-Speed Research (HSR) program. As part of this HSR program, the Critical Propulsion Components (CPC) element was created and assigned the task of developing those propulsion component technologies necessary to: (1) reduce cruise emissions by a factor of 10 and (2) meet the ever-increasing airport noise restrictions with an economically viable propulsion system. The CPC-identified critical components were ultra-low-emission combustors, low-noise/high-performance exhaust nozzles, low-noise fans, and stable/high-performance inlets. Propulsion cycle studies (coordinated with NASA–Langley sponsored airplane studies) were conducted throughout this CPC program to help evaluate candidate components and select the best concepts for the more complex and larger scale research efforts. The propulsion cycle and components ultimately selected were a mixed-flow turbofan (MFTF) engine employing a lean, premixed, prevaporized (LPP) combustor coupled to a two-dimensional mixed compression inlet and a two-dimensional mixer/ejector nozzle.

The CPC program began in 1994 and was planned for completion in 2002. Unfortunately, in 1999 NASA chose to prematurely end the HSR program. Although terminated early, the HSR program demonstrated that an economically viable and environmentally acceptable supersonic aircraft (and propulsion system) was achievable. The purpose of this document is to document the CPC findings in support of those visionaries in the future who have the courage to once again pursue a supersonic passenger airplane.

Due to the large amount of material presented in this report, it was prepared in four volumes:

Table of Contents

Table of Contents (Continued)

Table of Contents (Concluded)

List of Illustrations

List of Illustrations (Continued)

List of Illustrations (Continued)

List of Illustrations (Continued)

List of Illustrations (Continued)

List of Illustrations (Continued)

List of Illustrations (Continued)

List of Illustrations (Continued)

List of Illustrations (Continued)

List of Illustrations (Concluded)

List of Tables

List of Tables (Continued)

List of Tables (Continued)

List of Tables (Concluded)

Lexicon

16TT	NASA–Langley 16-ft transonic wind tunnel
2D	Configuration similar to two back-to-back letter D's, also two dimensional
2DB	Two-dimensional bifurcated (inlet concept)
2DCD	Two-dimensional convergent/divergent (exhaust nozzle)
2DFC	Two-dimensional fixed chute
2E	Two excitations per rotor revolution (vibration mode)
A_8	Exhaust nozzle throat area
A8CD	Exhaust nozzle effective jet area
A_9	Exhaust nozzle exit area
A16, A_{16}	Variable-area fan/core mixer duct-side area
A56	Mixer-exit area, core stream
AACE	Aeroacoustics collaborative effort
AAPL	Aeroacoustic Propulsion Laboratory
ACE	Axisymmetric coannular ejector (exhaust nozzle)
ADP	Aerodynamic design point
AE8, A_{E8}	Effective exhaust nozzle throat area
AEDC	Arnold Engineering Development Center
AFRL–MMD	Air Force Research Laboratory, Materials and Manufacturing Directorate
AIP	Aerodynamic interface plane (between inlet and engine)
AJ2	Exhaust nozzle suppressed throat area
ALMMC	Aluminum metal-matrix composite
AMEN	Axisymmetric mixer/ejector nozzle
AMT	Airframe Management Team
AN^2	Blade root stress parameter
ANSYS	GEAE design-analysis tool (software)

AR	Aspect ratio, also area ratio
ARP	Aerospace Recommended Practice
ASAR	Flowpath area aft of ejector mixer
ASME	American Society of Mechanical Engineers
AST	Advanced subsonic technology
A_t/A_{mix}	Ratio of acoustic treatment area to mixing area
ATC	Axi-tilt chute
ATCB	Axisymmetric translating centerbody (engine inlet)
AV	Arc valve
AVP	Active-volume parameter
BAC	Boeing Aircraft Company
BCAE	Boeing Commercial Aircraft Group
BDSM	"Best" downstream mixer (exhaust nozzle)
BLISK	Blade on disk (rotor type)
BOAS	Blade outer air seals
BPF	Blade-passing frequency
BPR	Bypass ratio
BS&D	Bearings, seals, and drives
BTSSI	Bifurcated two-stage supersonic inlet
C&A	Controls and accessories
CAFD	Circumferentially averaged flow determination (computer program)
CAM	Cold acoustic model, cold aerodynamic model
CASL	Chute aerodynamics with stereolithography
CB	Customer bleed
CBM	Computation-based method
CDA	Controlled-diffusion airfoil
CDP	Compressor-discharge plane
CER	Chute expansion ratio
CFD	Computational fluid dynamics
CFG, C_{FG}, C_{fg}	Coefficient of gross thrust
CFN, C_{FN}, C_{fn}	Coefficient of net thrust

CG	Center of gravity	DS	Directionally solidified
CG1	Turbomachinery center of gravity	DSM	Downstream mixer (exhaust nozzle)
CG2	Exhaust nozzle center of gravity	DTR	Diffuser test rig
CG3	Overall engine center of gravity	DVM	Discrete-vortex method
CM	Coordination memo	EB	Electron beam
CMC	Ceramic-matrix composite	EDM	Electrical-discharge machining (or machined)
CMMR	Critical major milestone review	EFH	Engine flight hour(s)
CMT	CPC management team	EI	Emissions index: g of pollutant per kg of fuel burned; also, environmental impact
CO	Carbon monoxide		
COTR	Contracting Officer's Technical Representative	EICO	CO emissions index: g CO/kg fuel
CPC	Critical Propulsion Components	EIHC	HC emissions index: g of unburned hydrocarbons per kg of fuel burned
CPR	Compressor pressure ratio		
CR	Contractor report	EINOx	NOx emissions index: g of NOx/kg fuel
CRAFT	Combustion Research and Flow Technology Inc.		
		EPM	Enabling Propulsion Materials
CTOL	Conventional takeoff and landing	EPNdB	Effective perceived noise decibels
dB	Decibels	EPNL	Effective perceived noise level
DEN	Double-edge notch	ER	Extraction ratio: P_{16}/P_{56}
$\Delta H/T$	Specific work	ESF	Engine scale factor
DOC	Direct operating cost	ESP	Electronically scanned pressure
DOC+I	Direct operating cost + interest	ETA (η)	Efficiency
DoD	Department of Defense	f/a	Fuel/air ratio
DOE	Design of experiments	F/C	Fan/core
DOSS	Design optimization synthesis system (Boeing)	FA&M	Florida Agricultural and Mechanical University
DP	Pressure drop or differential	FADEC	Full-authority digital electronic control
DPC	Circumferential pressure distortion	FAR	Fuel/air ratio, also Federal Aviation Regulation
DPC/Pmx	Circumferential-distortion parameter (total pressure)		
		FC	Fixed chute (mixer/ejector nozzle)
DPE	Perfluoroalkyldiphenylether	FCG	Fatigue crack growth
DPR	Radial pressure distortion	FCM	Fixed-chute mixer
DPR/Pmx	Radial-distortion parameter (total pressure)	FCN	Fixed-chute nozzle
		FEGV	Fan exit guide vane
DR&O	Design requirements and objectives (Boeing document)	FEM	Finite-element model
		FENTD	Full-scale engine nozzle technology demonstration/demonstrator (more frequently called FSD)
DRD	Documentation requirements document		

FH	Flight hour(s)	HEAT	High-lift engine aeroacoustic technology
FIAT	Fan inlet/acoustics team (ITD team)	HIN	HEAT isolated nacelle
FLABI	"FLADE" bypass injector valve	HISCAT	Highly integrated supersonic cruise airplane technology
FLADE	Fan-on-blade HSCT engine concept	HMMRA	Highly mixed multistage radial/axial
FN, F_N, F_n	Net thrust	HP	High pressure, also horsepower
FNAA	Fan average	HPC	High-pressure compressor
FNDAB	Net thrust with afterbody drag removed	HPT	High-pressure turbine
FNP	Fixed chute, no plug; unsuppressed primary (idle) thrust; uninstalled net thrust	HPX	Horsepower extraction
		HPXH	Customer (aircraft) power extraction
FNS	Full Navier–Stokes	HPX(2)	Customer (aircraft) power extraction plus engine parasitic requirements
$F_{n\ sup}$	Net thrust with nozzle in noise-suppression mode	HS	High speed; also, Hamilton Sundstrand
FOD	Foreign-object damage	HSCT	High Speed Civil Transport
FPR	Fan pressure ratio	HSR	High Speed Research
FSD	Full-scale demonstrator	HSS	HEAT semispan
FSN	Fluid-shield nozzle	IBR	Integrally bladed rotor
FSPSTD	Full-scale propulsion system technology demonstrator	ICAO	International Civil Aviation Organization
FTR	Formal test report	ICD	Interface control document
γ	Gamma titanium aluminide (TiAl)	ID	Inner diameter
GC/MS	Gas chromatography/mass spectrometry	IFV	Inverter flow valve
		IGV	Inlet guide vane(s)
GE AE	GE Aircraft Engines	IHPTET	Integrated High Performance Turbine Engine Technology
GFY	Government fiscal year		
GI	Ground idle	ILT	Interlaminar tension
GOCAP	Goals, objectives, challenges, approaches, and programs	IMFH	Integrated mixer/flameholder
		IML	Increased mixer length (exhaust nozzle)
GOTCHA	Goals, objectives, technical challenges, and approaches	IMT	Industry method test-bed
GRA	Geared rotary actuator	IR&D	Independent Research and Development
GRC	Glenn Research Center		
HAM	Hot acoustic model	IRR	Internal rate of return
HART	Hot acoustic rig test	ITD	Integrated technology development
HARW	High aspect ratio wing	JBTS	Jet burner test stand (UTRC facility)
HC	Hydrocarbons (unburned, in exhaust gas)	JER	Jet exit rig
HCF	High-cycle fatigue	JN8, Jn8B2	Jet-noise prediction models (P&W)

JNL	Jet Noise Laboratory (NASA–Langley	M14	Mach number at bypass duct inlet
KCAS	Knots, calibrated air speed	M15	Mach number at bypass duct average area
KEAS	Knots, equivalent air speed	$M155, M_{15.5}$	Maximum Mach number in fan duct (bypass duct over rear frame)
KIVA II	A multidimensional CFD code	$M16, M_{16}$	Mach number at fan duct mixing plane (fan/core mixer duct side)
KONA	NASA database Unix server		
KTAS	Knots, true air speed	M2	Mach number at engine inlet
L/D	Lift/drag ratio, also length/diameter ratio	M21ID	Mach number at fan discharge ID
		M21OD	Mach number at fan discharge OD
LAPIN	Large-amplitude perturbation inlet (model)	M25	Mach number at compressor inlet
		M3	Mach number at compressor discharge
LaRC	Langley Research Center		
LBO	Lean blowout	M36	Mach number at combustor inlet
LCF	Low-cycle fatigue	M4	Mach number at HPT vane inlet
LDI	Lean direct (fuel) injection	M49	Mach number at LPT rotor 1 inlet
LDV	Laser doppler velocimeter	M5	Mach number at LPT exit
LE, Le	Leading edge	M54	Mach number at rear frame/diffuser average area
LeRC	Lewis Research Center		
LET	Large Engine Technology	M55	Mach number at mixer entrance, core stream
LF	Linked flap		
LHV	Latent heat value	M56	Mach number at mixer exit, core stream
LOL, LoL	Lobe on lobe		
LP	Low pressure	M68	Mach number at miniaugmentor exit
LPC	Low-pressure compressor (main engine fan)	MAR	Mixing area ratio (duct)
		MCP	Modular component predictor
LPP	Lean premixed/prevaporized	MCTCB	Mixed compression translating centerbody (inlet)
LPT	Low-pressure turbine		
LSAF	Low-speed aeroacoustic facility (Boeing)	MDA	McDonnell Douglas Aircraft
		MDC	McDonnell Douglas Corporation
LSAWT	Low-speed aeroacoustic wind tunnel	MDO	Multidiscipline optimization
LSM	Large-scale model	M–E, M/E	Mixer/ejector (exhaust nozzle)
LSMS	LSM similitude	MFTF	Mixed-flow turbofan
LSWT	Low-speed wind tunnel	MIDIS	Mixer/ejector inlet distortion study
LTO	Landing/takeoff	MIT	Massachusetts Institute of Technology
LV	Laser velocimeter		
M	Mach number	MITCFA	MIT compound flow analysis (computer program)
M_∞	Ambient Mach number		
M_0	Free-stream Mach number	MMC	Metal-matrix composite
		Mn	Mach number

MPC	Multiple-component predictor	OPR	Overall pressure ratio
MRA	Multistage radial/axial	P_{16}	Pressure exiting bypass duct
M&S	Materials and structure	P16Q56	Extraction ratio
MTF	Mid-tandem fan	P_{56}	Pressure exiting core engine
MTOGW	Maximum takeoff gross weight	PAI	Propulsion/airframe integration
MTOW	Maximum takeoff weight	PAIT	Propulsion/airframe integration technology
N1	Low-pressure rotor speed	PC	Power code
N1C2	Low-pressure rotor speed corrected to station 2	PCC	Precision Castparts Co.
N2C2.5	High-pressure rotor speed corrected to station 25 (compressor inlet)	PDF	Probability density function
		PDPA	Phase Doppler particle analyzer
N4	HP spool speed	PDR	Preliminary design (or data) review
N5	LP spool speed	PFPAE	Perfluoropolyakylether
NASA	National Aeronautics and Space Administration	PH3	Tri-perfluoropolyalkylether-phenyl-phosphine
NASA LaRC	NASA Langley Research Center	PIC	Pressure-infiltration casting
NASA LeRC	NASA Lewis Research Center (now NASA Glenn)	PLIF	Planar laser-induced fluoresence
		PLR	Programmable lapse rate
NASTRAN	Computer modeling software	PMT	Propulsion Management Team
NATR	Nozzle acoustic test rig	PMC	Polymer-matrix composite
Nc, N_c	Corrected engine (shaft) speed	PNLT	Tone-controlled perceived noise level
NCP	National cycle program	P&O	Performance and operability
NFM	Nearly fully mixed	PSET	Propulsion System Evaluation Team
NOx	Oxides of nitrogen	PSI	Propulsion system integration, also Pressure Systems Inc.
Noy	Acoustic annoyance parameter		
NPD	Noise power distance	PST	Propulsion selection team
NPSS	Numerical propulsion-system simulation	PT, P_T	Total pressure
		PT8	Exhaust gas total pressure at nozzle throat
NPR	Nozzle pressure ratio	PT14	Total pressure at bypass duct inlet
NRA	NASA Research Announcement	PT15	Total pressure at bypass duct average area
OAC	Optimized aeroelastic concept		
OD	Outer diameter	PT155	Total pressure at bypass duct over turbines and rear frame (mixer entrance)
OEW	Operating empty weight (no fuel, oil, etc.)		
OEW–PR	OEW minus propulsion-system weight	PT16	Total pressure at mixer exit, bypass stream side
OGV	Outlet guide vane(s)	PT21	Total pressure at fan discharge
OML	Outer mold line	PT21A	Average total pressure at fan discharge

PT21ID	Total pressure at fan discharge inner diameter		S2	Second-stage stator
PT21ID	Total pressure at fan discharge outer diameter		S3	Third-stage stator
			SAE	Society of Automotive Engineers
PT25	Total pressure at compressor inlet		SAR	Suppressor area ratio
PT3	Total pressure at compressor discharge		SAVE	Systematic approach to value engineering
PT36, P_{T36}	Total pressure at compressor inlet		SCC	Sizing-code calibration
PT4	Total pressure at HPT vane inlet		SCID	Supersonic cruise integrated design
PT5	Total pressure at LPT exit		SCN	Sliding-chute nozzle
PT55	Total pressure at mixer entrance, core stream side		SD	Stepped dome
			SDOF	Single degree of freedom
PT56	Total pressure at mixer exit, core stream side		SERN	Single-expansion-ramp nozzle
PT68	Total pressure at miniaugmentor exit		SFC	Specific fuel consumption: lbm of fuel per hour per lbf
PT7	Total pressure at convergent nozzle inlet		SFCDAB	SFC based on FNDAB
			SI_{cp}	Stability index
PT8	Total Pressure at nozzle throat		SLA	Stereolithographic apparatus
PTC	Preliminary technology configuration		SLS	Sea-level static
			SLTO	Sea level takeoff
Q	Dynamic pressure		SMFAN	Stall margin, fan
R1	First-stage rotor		SOAPP	State-of-the-art performance program (P&W)
R2	Second-stage rotor			
R3	Third-stage rotor		SPFDB	Superplastic formed, diffusion bonded
RAN	Reynolds-averaged Navier–Stokes		SPL	Sound power level
RC	Round convergent (exhaust nozzle)		SRP	Separate reverser port
RM	Relative "mixedness"		SSC	Supersonic cruise
ROM	Rough order of magnitude		SST	Supersonic transport
RPM	Revolutions per minute		STMT	System technology management team
RQL	Rich (burn), quick (quench), lean (burn)		STOL	Short takeoff and landing
			SW	Sidewall
RR	Rolls Royce		SWET	Substrate welding at elevated temperature
RSQ	Reduced-scale quench			
RTI	Reversing through inlet		SW	Toal wing planform area
RTO	Refused takeoff		SwRI	Southwest Research Institute
Rx4	HPT pitch reaction		SWT	Supersonic wind tunnel
S/MTD	STOL and maneuvering technology demonstratior		T/b	Thickness-to-chord ratio
S1	First-stage stator		T/O	Takeoff

T_3	High-pressure compressor exit temperature	TT4.1	High-pressure turbine rotor inlet total temperature
T_4	Combustor exit temperature	T_{T7}	Augmentor-exit total temperature
T_{41}, $T_{4.1}$	High-pressure turbine rotor inlet temperature	TT8	Exhaust gas total temperature at nozzle throat
TAC	Total accumulated cycles	TTC	Technology transition (or tracking) chart
TBC	Thermal-barrier coating	TTR	Total-temperature ratio
TBE	Turbine bypass engine	UHB	Ultrahigh bypass
TC	Technology configuration	UHC	Unburned hydrocarbons
TCA	Technology concept aircraft	UPS	Universal propulsion simulator
TCB	Translating centerbody (inlet)	UTRC	United Technology Research Center
TCE	Technology concept engine	VABI	Variable-area bypass injector
TCLA	Turbine cooling air	VAM	Variable-area mixer
TCS	Turbulence control structure, also technology concept solution	VAMP	Variable-area mixing plane
TE	Trailing edge	VCE	Variable-cycle engine
TF	Turbofan	VCF	Variable-capacity fan
TF–IFV	Turbofan-inverter flow valve	VDC	Variable-diameter centerbody
TI	Technical integration (team)	VDVP	Variable-displacement vane pump
TIC	Transient inlet/compressor (model)	VEN	Variable exhaust nozzle
TJ	Turbojet	VFX	Variable-capacity fan, experimental
TJ–IFV	Turbojet-inverter flow valve	VG	Variable geometry
TLID	Thrust-lapse parameter	VJIP	Primary ideal jet velocity
TMT	Technology management team	VPI	Virginia Polytechnic Institute
TOBI	Tangential on-board bleed injection	W2AR	Engine corrected airflow
TOC	Top of climb	W5GR	LPT exit gas flow function
TOGW	Takeoff gross weight	W_a	Airflow
TP3	GEAE performance-analysis software	WAE, W_{AE}	Engine airflow
TPS	Thermal-protection system, also turbulence-prevention structure	WB3	Customer bleed
		WBS	Work breakdown structure
TRF	Turbine rear frame	W_c	Corrected airflow, also coolant flow
TRL	Technology readiness level	WG	Air (gas) flow
TSI	Triton Systems Inc.	WG36	Airflow at combustor inlet
TT, T_T	Total temperature	W_p	Primary flow, lbm/s
TT3	Compressor discharge total temperature	W_s	Secondary flow, lbm/s
		XNH	Rotor speed (high-pressure spool)
TT4	Total temperature at HPT vane inlet	XNL	Rotor speed (low-pressure spool)

1.0 Summary

This program has proven that a Mach 2.4 commercial aircraft is a viable concept — if not now, certainly in the near future.

The *Critical Propulsion Components* (CPC) portion of the *High Speed Research* (HSR) program evaluated critical components or subassemblies for the *High Speed Civil Transport* (HSCT) propulsion system. This evaluation considered components both individually and as integrated into an operational system. Cycle studies and limited engine design work were necessary to maintain a system perspective for the component design studies.

Reliability, durability, cost, weight, and performance were key considerations in the evaluation of all components. For particular components, pollutant emissions (combustor) or contribution to acoustic signature (inlet, fan, and exhaust system) were primary considerations.

Phase I of this program determined that the most likely propulsion system for the HSCT would be a mixed-flow turbofan (MFTF) engine with mixed-compression inlet, ultra-low-emissions combustor, and mixer/ejector (ME) noise-suppressor nozzle. Phase II of the CPC program concentrated on optimizing the MFTF configuration by evaluating and downselecting component concepts.

Systems Studies – In conjunction with the focused studies of components, system studies matched combinations of components to each other and to various wing planforms. In 1996, the *Technology Concept Airplane* (TCA) was defined with an MFTF engine having a fan pressure ratio of 3.5 and a ME nozzle with a suppressor area ratio (SAR) of 2.9. The TCA met noise and emission target levels of FAR 36 Stage III –1 EPNdB and EI < 5 NOx at cruise and had a 736,000-lbm maximum takeoff weight. In 1997, a new wing planform was developed, and the *Preliminary Technology Configuration* (PTC) was defined. The PTC had an increased wing aspect ratio that met the more stringent noise requirements of FAR 36 Stage III: –1, –5, and –1 EPNdB (sideline, cutback, and approach, respectively) at an acceptable weight. Initially the PTC retained the 3.5 FPR engine, but reevaluation led to a change to a 3.7 FPR and a 2.7 SAR nozzle. These engine parameters were retained when the *Technology Configuration* (TC) concept was initially defined in late 1997, but FPR was later increased to 3.8. Originally the TC was scheduled for service in the year 2007. At the end of the CPC program, the final TC service date was set at 2015. Concurrently, noise requirements were tightened to FAR 36 Stage III –4 to –6, –8 to –10, and –5 to –6 EPNdB. Three configurations for a "final" TC are defined that meet these more stringent noise constraints.

Combustor – The combustor selection was governed primarily by NOx emissions, both in the stratosphere and in the vicinity of airports, and the impact of these emissions on the ozone layer. Three fundamental combustor concepts were considered during this program: *lean direct injection* (LDI), *lean premixed prevaporized* (LPP), and *rich–quench–lean* (RQL). In the final assessment, the LPP design was selected as best for use in the HSR propulsion system.

Exhaust Nozzle – Nozzle evaluations included consideration of effects on noise, thrust, and weight. All nozzle concepts evaluated were 2D fixed-chute nozzle (FCN) types with mixer/ejector (ME) noise suppression. As a general rule, nozzle size and weight increase as noise constraints are made more stringent. The HSCT noise constraints were reduced twice, and each reduction mandated development of new methodologies to control noise and maintain thrust at a reasonable weight. The ultimate nozzle design was optimized in mixer length and flowpath and included internal and external mixing-enhancement devices (tabs and chevrons).

Inlet – Several mixed-compression inlet concepts were evaluated (see next paragraph). The two-dimensional bifurcated (2DB) concept surpassed the CPC inlet goals. With additional effort, axisymmetric inlets may provide superior aerodynamic performance; however, the HSR program required a downselect decision rather than an optimized inlet, and the 2DB inlet was selected.

Fan/Inlet Acoustics Team (FIAT) – Inlet and fan combinations were evaluated with respect to the amount of noise they generated, effect on engine thrust, and effect on propulsion system weight. Concepts considered included the *variable capacity fan* (VCF), low-noise versions of a *conventional fan,* and an *oversized fan*. These fans were evaluated in conjunction with several mixed-compression inlet concepts: *2D bifurcated* (2DB), *axisymmetric translating centerbody* (TCB), and a *variable-diameter centerbody* (VDC) inlet. One external compression concept, dubbed *waverider*, was evaluated at the end of the program. The evaluations included:

1. Quantifying fan/inlet noise contributions at approach and cutback.

2. Establishing the amount of fan/inlet noise reduction needed to meet HSCT airplane noise goals.

3. Quantifying the noise impact of acoustic liners, inlet flow acceleration (soft choke), inlet auxiliary doors, and fan source reduction concepts.

4. Establishing the fan/inlet acoustic design criteria needed to support engine cycle and inlet downselects.

In the final evaluation, the low-noise fan appeared superior when used with either the 2DB or the waverider inlets.

2.0   Introduction

NASA has projected that a second-generation supersonic commercial airliner could become a major element of the world's air-transportation system. The potential market for a *High-Speed Civil Transport* (HSCT) is predicted to be from 500 to 1500 aircraft over the 2005 – 2030 time period. This potential fleet cannot be marketed and operated unless an HSCT can be developed that is both economically viable and able to meet environmental regulations for noise and pollutant emissions.

Propulsion technology challenges that must be met before developing such an aircraft have been addressed by the *High-Speed Research* (HSR) program, a partnership among NASA, GE Aircraft Engines, Pratt and Whitney, and Boeing.

The vision of the HSR program was to develop high-risk, high-payoff technologies to enable lower risk product-launch decisions by the industry members of the partnership. The HSR program first addressed the environmental challenges (Phase I) of NOx and noise reduction. When it was judged that viable solutions were indeed found, Phase II of the program focussed on development of those technologies with the highest payoff and economic viability.

This final report details the efforts of the *Critical Propulsion Components* (CPC) portion of the HSR program. Broadly, the objective of the CPC program was to develop propulsion technologies and basic critical-component designs for a Mach 2.4 commercial aircraft propulsion system. This was a joint research and development effort by GE Aircraft Engines and Pratt and Whitney, operating as a contractor team and working in concert with NASA. Boeing Commercial Aircraft Group was a subcontractor to GEAE for the inlet portion of the CPC program. Boeing also conducted extensive studies under the airframe portion of the HSR program, from which the CPC effort benefited greatly. Work covered in this report occurred between 1994 and 1999.

Although terminated before the originally designated end date, the CPC program accomplished much. Initially we had only general ideas about the type of propulsion system and the vehicle it would serve. At this writing, we have far surpassed the noise, emission, and weight goals that were set at the beginning of the program, for a year 2005 product, and have nearly achieved the target goals anticipated for the year 2015.

This report describes the sequence of designs, both at component and system level, that were studied and evaluated and the methodologies that led design progressions and downselections. Less successful as well as successful efforts are described in some detail so that future researchers might be spared duplication of prior effort.

The specific technology areas addressed by the CPC program and reported herein are:

Section 3 – Propulsion System Studies: Although the primary CPC program focus was on critical components, system-level studies were necessary to select/define an engine cycle and establish reasonable design envelopes for the component concepts.

Section 4 – Combustor: Design studies and testing focused primarily on low NOx emissions. Testing included evaluation of advanced combustor-liner materials from the HSR *Enabling Propulsion Materials* (EPM) program as well as conventional materials.

Section 5 – Exhaust Nozzle: Design studies and model testing evaluated the acoustic and aerodynamic performance of promising concepts and evaluated advanced materials from the EPM program as well as conventional materials.

Section 6 – Inlet: Design studies and model testing addressed high-performance, integrated-inlet/ engine and controls technology.

Section 7 – Fan/Inlet Acoustic Team: Design studies and subscale model testing addressed fan and inlet noise contribution and suppression.

═══

Due to the large amount of material presented in this report, it is prepared in four volumes:

Volume 1

- Section 1 – Summary
- Section 2 – Introduction
- Section 3 – Propulsion System Studies

Volume 2

- Section 4 – Combustor

Volume 3

- Section 5 – Exhaust Nozzle

Volume 4

- Section 6 – Inlet
- Section 7 – Fan/Inlet Acoustic Team

3.0 Propulsion System Studies

3.1 Overview

3.1.1 Program Flow-Down

The requirement flowdown of the research and development effort established by the High Speed Civil Transport (HSCT) Critical Propulsion Component (CPC) program is depicted graphically in the GOTCHA chart in Figure 1. The acronym GOTCHA refers to the headings of the various levels of the chart (Goals, Objectives, Technical Challenges, and Approaches).
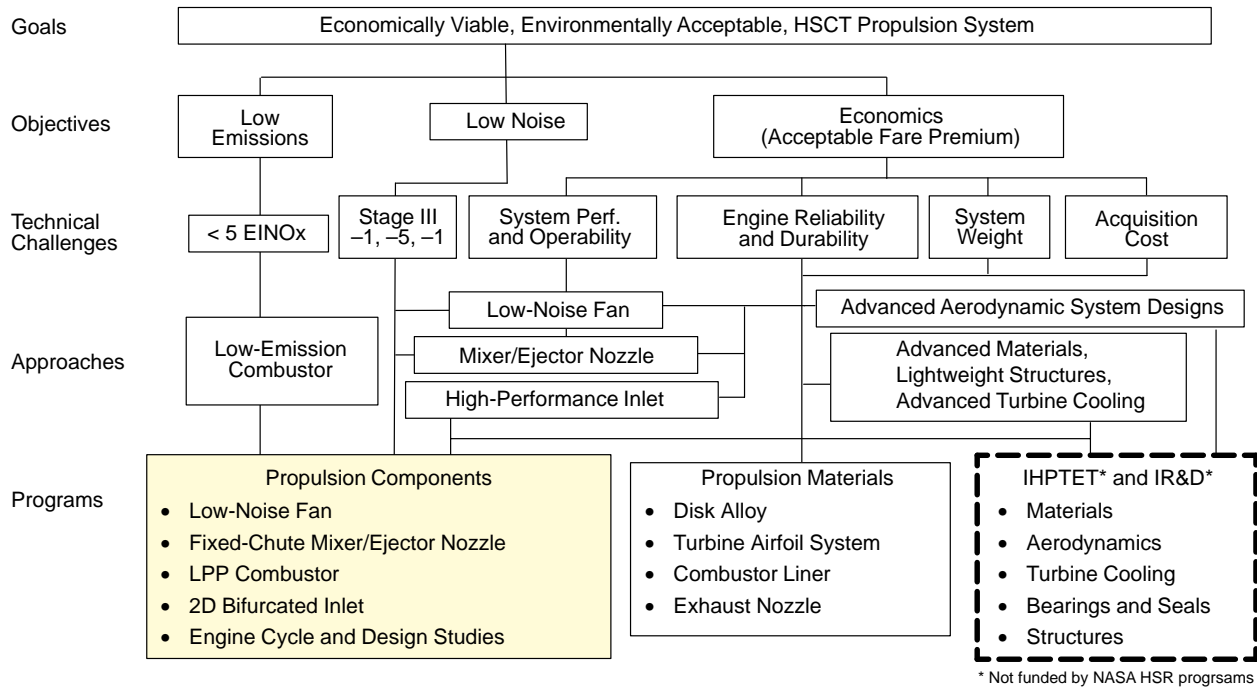
Figure 1. CPC Program GOTCHA chart

The goal of the CPC program has been to develop an environmentally acceptable, economically viable, propulsion system for the HSCT. The goal of environmental acceptability depends primarily on achieving two objectives: low pollutant-emission levels and low noise levels. The goal of economic viability is focused on the objective of economically sound operation with passenger tickets competitive with prices charged by the subsonic fleet.

The low-emissions objective presents the technical challenge of producing an engine that operates with an oxides of nitrogen (NOx) emission index (EI) of less than five grams per kilogram of fuel at supersonic cruise conditions. The low-noise objective presents the technical challenge of producing an engine capable of operating at acoustic levels of –1, –5, and –1 effective perceived-noise decibels (EPNdB) relative to FAR 36, Stage III, at the sideline, takeoff, and approach measuring points respectively.

The economic objective presented technical challenges in the areas of system performance and operability, reliability and durability, system weight, and acquisition cost. The system performance and operability challenge demanded a number of technical approaches that resulted in development

of a low-noise fan, a noise-suppression mixer/ejector nozzle, and a high-performance inlet. The engine reliability and durability challenge combined with the system weight and acquisition cost challenges resulted in development of new, tougher, stronger materials and advanced component designs including lightweight structures and advanced turbine cooling schemes.

The bottom level of the GOTCHA chart shows the programs used to develop each of the items discussed above. The box on the lower right (IHPTET and IR&D) lists technologies that were developed outside of the High Speed Research (HSR) program but used in development of the final HSCT system. The Enabling Propulsion Materials (EPM) program (shown in the center box) developed the advanced material systems needed to meet the HSR program goals. The shaded box (the lower left corner) shows the activities addressed by the CPC program. The last item in this shaded box represents the work described in this *Propulsion System Studies* section of the final CPC report.

3.1.2 Propulsion Concepts Considered

Phase I of this project, which ended in 1995, consisted of evaluation of various engine technology concepts by the HSR team to select an optimum concept to be used in the HSCT. The following concepts were evaluated:

- Mixed-Flow Turbofan (MFTF)
- Turbine Bypass Engine (TBE)
- Variable-Cycle Engine (VCE)
- Fan on Blade (FLADE)
- Turbojet–Inverter Flow Valve (TJ–IFV)

Each concept was analyzed and evaluated for direct operating costs (DOC), aeromechanical risks, and acoustic risks.

3.1.2.1 Propulsion Concept Types

The propulsion concepts considered for the HSCT CPC involved two basic types: high specific thrust and low specific thrust. A high-specific-thrust engine passes a relatively small volume of air at high pressure. A low-specific-thrust engine passes a relatively large volume of air at lower pressure. The first three concepts listed above are considered high-specific-thrust engines, and the last two are low-specific-thrust engines.

During Phase I, the MFTF was selected as the first choice among all the engines analyzed and evaluated. Since the MFTF is a high-specific-thrust engine, a low-specific-thrust alternative was the second choice. That way, Phase II studies could consider two significantly different approaches to meeting system requirements. The high- and low-specific-thrust engines were evaluated separately, but the two concepts were also compared against each other to determine which would best fulfill mission objectives.

For the low-specific-thrust alternative, the team selected the variable-cycle FLADE engine because it showed the lowest TOGW of the low-specific-thrust engine types considered. The team recommended that the TBE, VCE, and TJ–IFV engine concepts be dropped from consideration as each was less effective in achieving the HSCT goals.

3.1.2.2 Primary Concept Selection

The MFTF was clearly the best choice among the engine concepts evaluated. The MFTF is a relatively simple design (Figure 2) that has been used extensively by the USAF and USN for a number of years. The F100, F101, F110, F404, and F414 are all MFTF type engines, and extensive maintenance histories exist for each. These histories clearly demonstrate that the MFTF has high reliability in a wide variety of environments. Consequently, the MFTF is rated as the lowest risk engine for the HSCT, since we can predict future reliability based on this experience. In addition, the projected takeoff and landing noise levels and NOx emission levels were both well within prescribed limits. The acquisition cost and the maintainability cost of the MFTF were projected to be within economic boundaries, and projected direct DOC was the lowest of any engine analyzed.
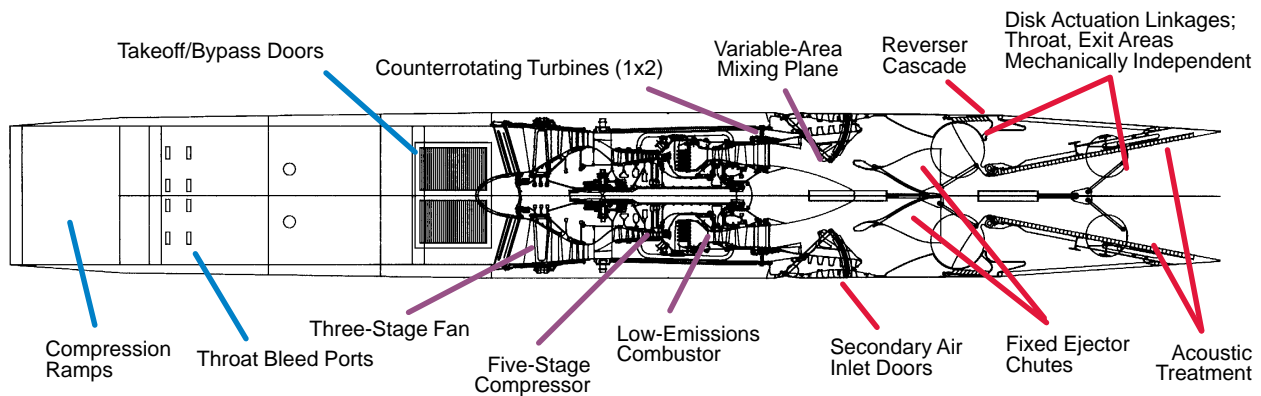
Figure 2.   Typical Mixed-Flow TurboFan (MFTF) Engine

3.1.2.3 First Alternative Concept Selection and Elimination

Reasons for selecting the FLADE engine (see Figure 3) as first alternative may be less obvious than the reasons for selecting the MFTF. The FLADE engine is a departure from conventional types, and the design appeared to offer a substantial potential noise reduction. The FLADE is a variable-cycle type MFTF capable of operating as either a high- or a low-specific-thrust engine. The first stage of the FLADE fan has an extended tip that pumps low-pressure air through an outer bypass duct when
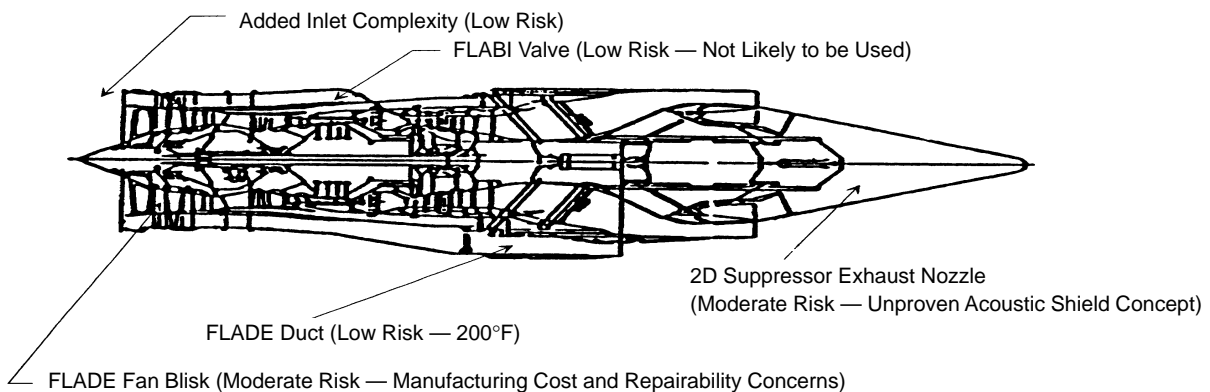
Figure 3.   Typical Fan on Blade Engine (FLADE)

the FLADE bypass injector (FLABI) valve is open. It can produce thrust by passing a larger volume of exhaust gas at a lower average exit velocity than the conventional MFTF. This lower exhaust exit velocity should offer a lower jet exhaust noise level. After careful analysis, it was discovered that the exhaust jet velocity was still too high to meet the stringent noise requirements with a simple nozzle. Some type of noise-suppressor nozzle would be necessary to achieve the desired noise level.

For the HSCT application, a fluid-shield nozzle was developed for the FLADE design. This nozzle vents the outer lower pressure air stream in such a way that it wraps around the lower portion of the main exhaust flow. In theory, this low-pressure air forms a fluid acoustic shield to reduce transmission of the exhaust noise. It was anticipated that the combination of these two features would substantially reduce measured noise levels.

On the negative side, it was noted that the FLADE fan module was slightly more complex than that of the MFTF engine, but it was thought that the FLADE fluid shield exhaust nozzle would be slightly less complex. It was hoped that this would somewhat mitigate the weight. The FLADE met all other criteria.

The projected DOC of the FLADE appeared reasonable, although not as low as that of the MFTF. NOx emissions were expected to be within limits. Acquisition and maintainability costs were both projected to be higher than those of the MFTF, but they were acceptable.

Nevertheless, later analysis and evaluation eliminated the FLADE from further consideration. The primary reason was higher than expected noise levels. Testing in Cell 41 of the GEAE test facility showed that while the fluid acoustic shield worked well at high takeoff power settings the acoustic advantage almost disappeared at takeoff cutback speed. In fact, noise levels at takeoff cutback missed the noise suppression acoustical goal by 4 dB — which was unacceptable.

In addition, the FLADE engine fan blisk (integrally bladed disk) offered a moderate risk. Not only would the complexity have increased engine acquisition cost, the design would have made repair procedures more difficult and costly. Lesser problems were posed by the inlet, the FLADE duct, and the FLABI valve, all of which added complexity without noticeable advantage. These were low-risk items, however, and would not by themselves have eliminated the FLADE if the fluid acoustic shield had worked as anticipated. In final evaluation, further development of the FLADE concept was discontinued.

3.1.2.4 Other Alternative Concepts

The *mid-tandem fan* (see Figure 4), the *variable-capacity fan* (VCF), *variable fan X* (VFX), and the *low pressure ratio turbofan* were all alternative propulsion concepts that were considered after the Phase I engine selections were made. These four engine concepts were each evaluated and finally rejected. The mid-tandem fan and the low-pressure-ratio turbofan are low-specific-thrust concepts that require a large volume of air flow at fairly low pressure. The VCF and VFX are variable-specific-thrust engines; that is, they provide low specific thrust at takeoff and higher specific thrust in supersonic cruise mode.

The mid-tandem fan configuration (Figure 4) has a front end that is a relatively small-diameter spool since there is no fan at the air inlet. A large-diameter, high-volume fan is mounted aft of this spool, where it feeds a large volume of fairly low-pressure air through a set of inlet guide vanes directly into the bypass duct. The engine exhaust passes through a simple exhaust nozzle; the design does not require the complex mixer/ejector-type nozzle. It is necessary, however, for the exhaust nozzle
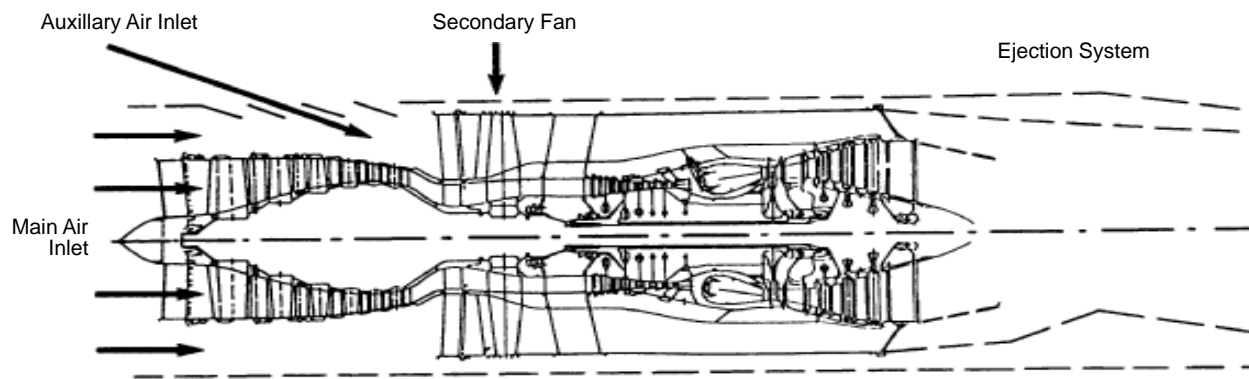
Figure 4.   Typical Mid-Tandem Fan Engine

to be quite large to deal with the large volume of air that passes through the engine. The prime reason the mid-tandem fan was rejected was excessive weight. The small-diameter, multistage spool at the front and the centrally positioned fan require heavy support structures. In addition, the large exhaust nozzle is heavy. Attempts to reduce the mid-tandem fan engine size achieve to acceptable weight were unsuccessful.

The VCF and the VFX are basically the same type of engine except the VFX is larger. Both require large, high-volume fans followed by movable vanes to vary the amount of air flow at different phases of the flight. At takeoff, the movable vanes are in the fully opened position to allow a large volume of air to pass at fairly low pressure. It was felt that the lower pressure would result in a substantial reduction in jet noise at takeoff. When the aircraft reaches cruising altitude and goes into cruise mode, the movable vanes close, causing the engine to pass a lesser volume of air but at higher pressure. Both engines require simple exhaust nozzles with no mixer/ejector hardware, but the nozzles must be quite large to handle the volume of air passing through the engine at takeoff. The problem with both engines is twofold: The complexity of the multistage, movable-vane actuation system and controls poses a slight risk, and the large fan module and exhaust nozzle boost overall propulsion system weight to an unacceptable level.

The low-fan-pressure-ratio turbofan is similar to the MFTF that was selected. However, the selected MFTF is a high-specific-thrust engine, requiring low-volume air flow, and the low-fan-pressure-ratio turbofan is a low-specific-thrust engine, requiring high-volume air flow. The high-volume air flow mandates both a large-diameter fan and a large exhaust nozzle. It was determined that the size and weight of the fan and nozzle combination required to produce the necessary thrust would be beyond the size and weight limits of the HSCT.

3.1.3 Initial Cycle Temperature Selections

The engine temperature requirements of the HSCT mission must be achievable within the capabilities of available materials and the design. Figure 5 shows typical operating temperatures for a current subsonic turbofan and compares them to the temperatures projected for the HSCT reference engine (3770.54). Note that maximum temperatures projected within the HSCT reference engine at supersonic cruise are similar to the maximum temperatures experienced by existing subsonic engines. This implies that materials and designs currently used for subsonic aircraft may be usable in supersonic jets.

Typical Temperatures (°F)					
	Cruise T_{T2}	Max T_{T3}	Cruise T_{T3}	Max T_{T4}	Cruise T_{T4}
Typical Current Engine	−15 to 23	1200	870	3000	2140
HSCT Engine	380	1200	1200	3000	2960
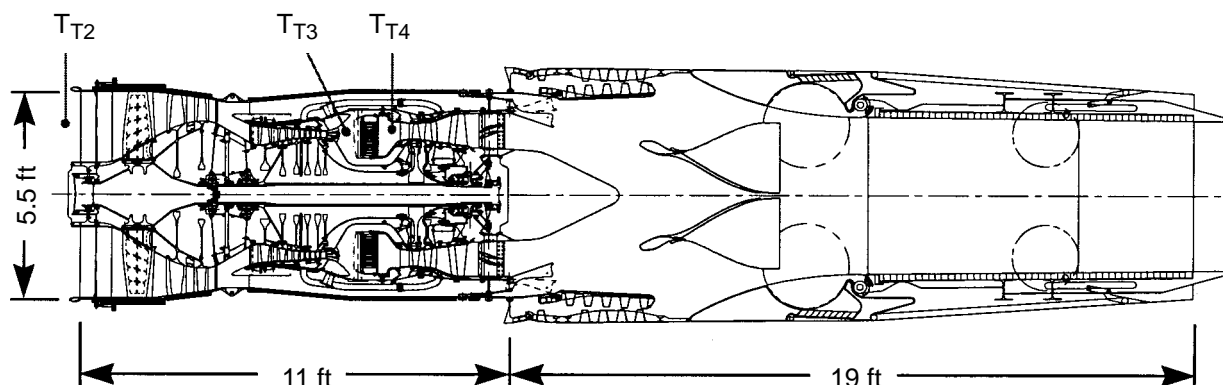
Figure 5. Typical Engine Cycle Temperatures

While it is true that metal stress and fatigue are induced by high engine temperatures and shaft speeds, the extent of the stress and fatigue is the result of the length of time that the metal is exposed to high temperatures. The HSCT requires engines that can perform for long periods at maximum temperatures and speeds. Figure 6 illustrates the differences in mission operating conditions between a typical subsonic transport and the HSCT. The HSCT engine experiences maximum conditions for over half of the time of each supersonic flight, a much longer period than the subsonic engine. Consequently, the HSCT engine must be made of materials capable of handling high temperatures and high stress conditions for a much longer duration than is required for current subsonic engines.

Figure 7 shows some of the key features, cycle parameters, and internal operating temperatures of the 3770.54 MFTF (reference) engine. Operating temperatures vary from a low of 380°F at the engine front face to a peak temperature of 3000°F within the lean premixed/prevaporized combustor. Exhaust gas temperature leaving the combustor is reduced to 1710°F as it enters the exhaust nozzle and is quickly cooled to 1290°F by the bypass air before it exits the nozzle.

3.1.4 System Requirements

System requirements used in the design of the HSCT engine are in accordance with the standards set by the HSCT Preliminary Technical Requirements and Objectives documents (see Subsection 3.3.3). Quantifiable objectives stated were established based on fleet experience with similar designs.

Time at Temperature Sets Allowable Stress

Rotor Speed/Temperature Sets Actual Stress

Δ Rotor Speed/Temperature Impact Fatigue

Operating Condition	Subsonic Transport	Military Fighter	Supersonic Transport
Cumulative High-Temperature/High-Stress Operation (Hours)	<300	<400	9,000
High-Temperature/High-Stress Operation Per Flight (Hours)	0.03	0.15	2.0 – 4.0
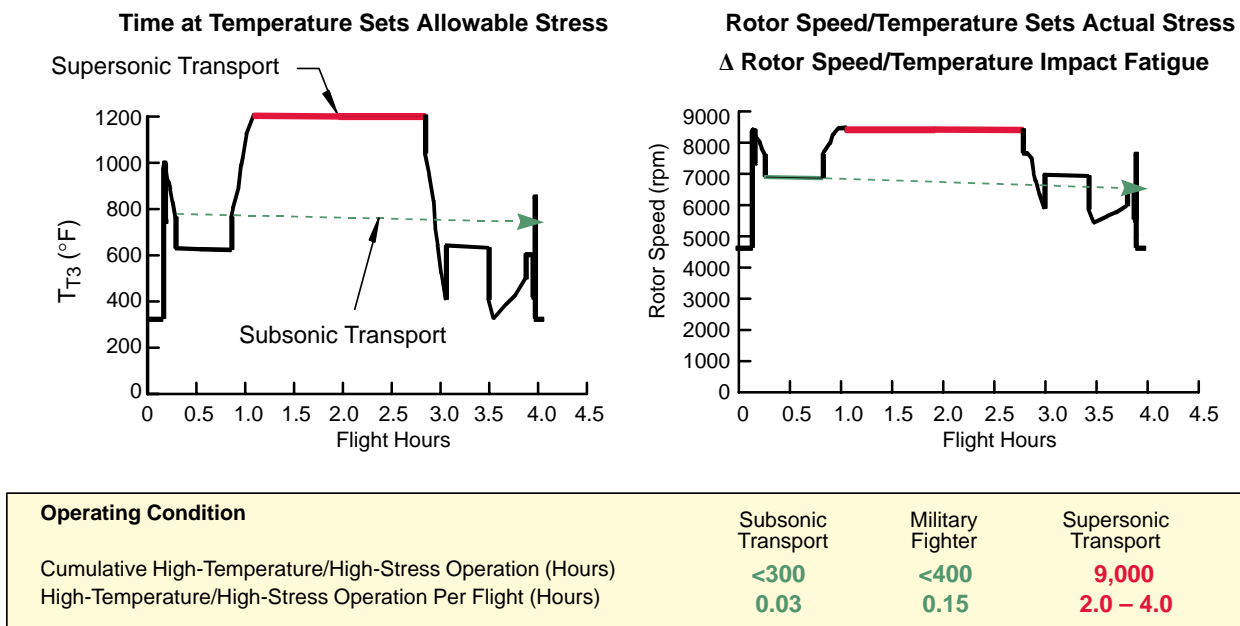
Figure 6.   Hot Life: HSCT vs Subsonic Engine

<u>37</u> <u>70</u> . <u>54</u> <u>MFTF</u>

Mixed-Flow Turbofan

Three-Stage Fan

Pressure Ratio:	3.70
Nominal Corrected Airflow:	800 lbm/s
Mach 2.4 Corrected Airflow:	560 lbm/s (70%)
Takeoff Airflow:	823 lbm/s
Bypass Ratio:	0.54

Six-Stage High-Pressure Compressor

Nominal Corrected Airflow:	172 lbm/s
Pressure Ratio:	5.26

One-Stage High-Pressure Turbine

High-Work, High-Reaction Design

Two-Stage Low-Pressure Turbine

Counterrotating "Vaneless" Design

Cycle Temperatures at Supersonic Cruise

380°F   630°F   1200°F   3000°F   1710°F   1290°F

Ultralow NOx Combustor

Lean Premixed/Prevaporized; EINOx < 5

Figure 7.   Reference 3770.54MFTF Engine Features and Temperatures

The major system requirements considered during this design phase were as follows:

1. Weight
2. Emissions
3. Combustor efficiency
4. Noise
5. Exhaust nozzle performance
6. Durability
7. Engine dynamics
8. Maintainability
9. Thermal management
10. Nacelle integration
11. Fuel consumption

The first six of these requirements are easily quantifiable, so design status can be measured with very specific metrics. Requirements 7 through 10 are not as easily quantifiable but were still used in the assessment of the HSCT design. If the program had continued through to product launch, additional requirements would have been considered, but those requirements would not have affected engine design at this stage of the development cycle.

The initial overall weight requirement for the critical propulsion components was set at 16,675 lbm, which included 8,845 lbf for the engine and 7,830 lbf for the exhaust nozzle. This was based on an initial estimate that maximum takeoff weight (MTOW) for the aircraft should be 750,000 lbm or less. (It was assumed that this MTOW would result in an economically viable aircraft.) Later evaluation determined that the actual weight of the critical propulsion components would probably be higher than this estimate. In addition, more stringent system requirements emerged (see Subsection 3.4.1) and made it necessary to increase the estimated overall weight. Efforts to improve the CPC weight status are discussed in Subsections 3.4.3 and 3.4.4.

To meet emission requirements, a number of technologies were considered. The low-emissions *lean prevaporized premixed* (LPP) combustor concept was selected as the most effective technical approach. Although final regulatory requirements concerning emissions (particularly high-altitude NOx) are not yet certain, from the beginning of the HSR project we have worked toward an emissions index goal of five (EI = 5 g of NOx per kg of fuel) at supersonic cruise speed. To pick this EI level, educated assumptions were made about the size of the HSCT fleet, the quantity of NOx the fleet might produce over time, and the analytically predicted effect of such emissions on atmospheric ozone content.

To ensure that emission suppression technology did not degrade combustor efficiency, the combustor team established combustor efficiency goals. These goals were basically the performance levels of the best combustors currently in use. It was necessary to update the status design levels frequently for combustor performance because flame temperatures and temperature rise across the combustor must be limited when attempting to achieve required EI levels. The combustor team also created maximum EI levels for the NOx and carbon monoxide (CO) that could be produced in the vicinity of airports during takeoffs and landings.

Noise-suppression research also developed a new technology, the mixer/ejector exhaust nozzle. The mixer ejector nozzle achieves noise reduction and high performance through efficient secondary air induction; rapid, complete mixing to lower the exhaust jet velocity; and effective absorption of internally generated mixing noise by means of acoustic liners.

Nozzle performance standards were established, including exhaust nozzle thrust coefficients during takeoff and supersonic cruise operation, in an attempt to ensure that noise-suppression efforts did not degrade nozzle performance. The primary nozzle acoustic-design variable is the suppressor area ratio (SAR, total nozzle mixer area ÷ primary throat area). Increasing SAR increases the nozzle cross-sectional area, weight, and internal noise (requiring more liner area). A large SAR increases

the nozzle secondary area and therefore increases air entrainment and reduces mixed velocity and external jet noise.

The noise requirement changed several times in the course of the HSR program. Initially, the limits were only to meet the FAR36 Stage III requirement. This was upgraded to a limit of –1, –3, –1 EPNdB (relative to FAR 36, Stage III sideline, takeoff, and approach respectively). The noise requirement is now at –1, –5, –1 EPNdB. This noise requirement has had more impact on the engine cycle, engine weight, and aircraft weight than any other system requirement. Changes to the noise requirement reflect the latest estimates from the HSR community of what will be environmentally acceptable in a product HSCT.

Several softer system requirements also affected the engine design studies conducted under the CPC program. The term "softer" indicates that the metrics applied to these requirements either remained undefined or were used only to assess the engine design as it evolved. Included in this category are durability, engine dynamics, maintainability, thermal management, and nacelle integration.

Durability requirements are described in Section 24 of the Preliminary Technical Requirements document (discussed in Subsection 3.3.3 herein). The flight cycle requirement for critical rotating components was used in the preliminary design of the engine, with the rotor structural parts (such as blisks or disks) sized to the required number of flight cycles. The number of flight cycles should be interpreted as the number of representative (or typical) missions (defined in Figure 8) that the part must survive with no failure. Other durability requirements would be verified during the certification process.

Engine dynamics are discussed in Section 23 of the Preliminary Technical Requirements document. This work assessed the engine with respect to the sensitivities that rotor closures would have during various expected commercial aircraft flight maneuvers. This work also helped determine the engine mount locations with acceptable clearance closures. Closure targets were established based on current best practice operating clearances consistent with similar engine designs.

Although no maintainability metrics were established, the engine was evaluated for maintainability. This was done for both the baseline configuration (referred to as the "reference engine") and the final configuration (discussed in Subsection 3.4.3).

Thermal management was another system requirement used in the preliminary conceptual design of the engine. The engine fuel, lubrication, and hydraulic systems were analyzed for adequate thermal performance for several scenarios, and a reasonable system seems possible. Final analysis would be made during the product airplane and engine detail design phase. The adequacy of proper nacelle integration was also addressed by using projected airplane nacelle mold lines and laying out engine hardware to verify proper fit. In this case also, precise system requirements would only be available during the detail design phase.

3.1.5 System Status Vs Requirements (Final Technology Assessment)

Table 1 shows the top level system requirements for the HSCT propulsion system and gives both the final status and best possible status anticipated with future development (beyond HSR). The "Final Status" column indicates the current state of the art. The "Goal" column indicates the target (desired) status.
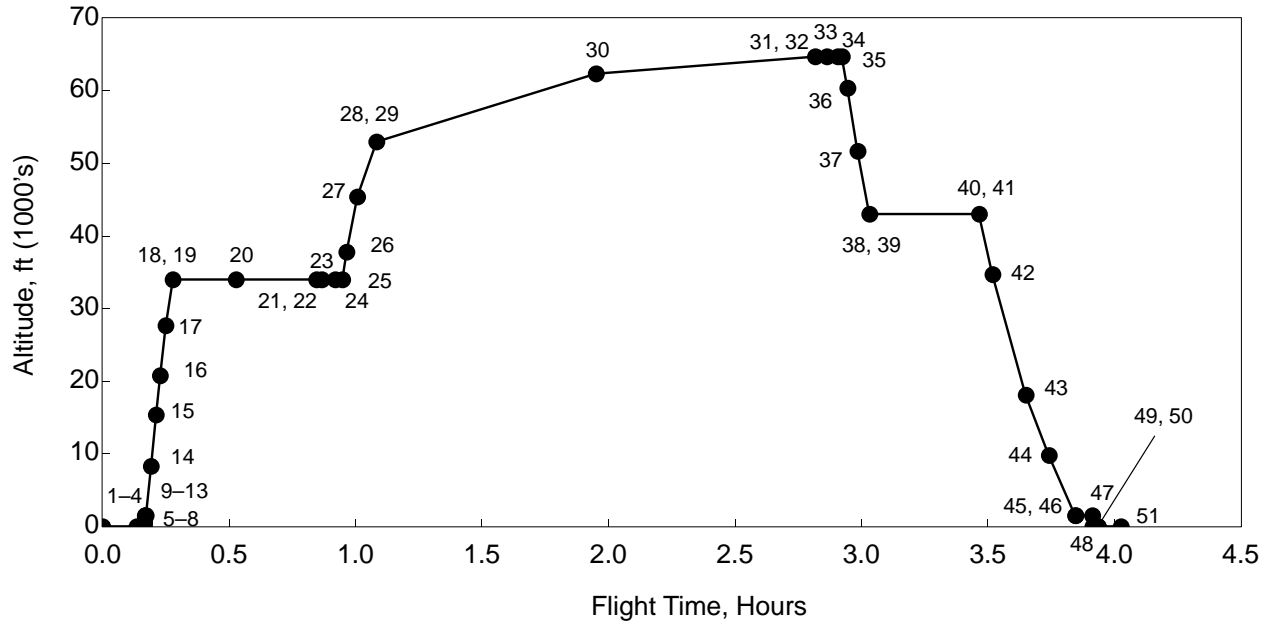
	Mission Segment	Hours	Altitude, ft	Mach	Range, nmi	PC	Ambient Temperature
1.	Begin Taxi	0.000	0	0.00	0.00	5.0	Standard Day +18°F
2.	End Taxi	0.150	0	0.00	0.00	5.0	Standard Day +18°F
3.	Release Brake, Begin Takeoff	0.150	0	0.00	0.00	100.0	Standard Day +18°F
4.	Liftoff from Runway	0.163	0	0.36	1.59	100.0	Standard Day +18°F
5.	Clear 35-ft Obstacle	0.164	35	0.36	1.61	100.0	Standard Day +18°F
6.	Initial Noise Cutback	0.164	35	0.36	1.61	89.6	Standard Day +18°F
7.	Gear Up	0.165	302	0.36	1.82	89.6	Standard Day +18°F
8.	689-ft Sideline Noise Station	0.166	689	0.36	2.14	89.6	Standard Day +18°F
9.	Continue Noise Cutback	0.168	1492	0.36	2.93	89.6	Standard Day +18°F
10.	Cutback for Takeoff Noise Station	0.168	1492	0.36	2.93	49.1	Standard Day +18°F
11.	Flyover Takeoff Noise Station	0.170	1500	0.36	3.51	49.1	Standard Day +18°F
12.	Continue Throttle Cutback	0.172	1500	0.37	4.10	49.0	Standard Day +18°F
13.	Begin Climb to Subsonic Cruise	0.172	1500	0.37	4.10	100.0	Standard Day +18°F
14.	Continue Subsonic Climb	0.192	8300	0.62	10.5	100.0	Standard Day
15.	Continue Subsonic Climb	0.212	15380	0.76	19.2	100.0	Standard Day
16.	Continue Subsonic Climb	0.228	20760	0.85	27.6	100.0	Standard Day
17.	Continue Subsonic Climb	0.250	27670	0.90	39.3	100.0	Standard Day
18.	Subsonic Top of Climb	0.278	34000	0.90	53.6	100.0	Standard Day
19.	Begin Subsonic Cruise	0.278	34000	0.90	53.6	61.5	Standard Day
20.	Continue Subsonic Cruise	0.528	34000	0.90	184.0	60.6	Standard Day
21.	End Subsonic Cruise	0.846	34000	0.90	350.0	59.5	Standard Day
22.	Begin Climb to Supersonic Cruise	0.846	34000	0.90	350.0	100.0	Standard Day
23.	Continue Supersonic Climb	0.867	34000	1.02	361.6	100.0	Standard Day
24.	Continue Supersonic Climb	0.920	34000	1.28	396.4	100.0	Standard Day
25.	Continue Supersonic Climb	0.948	34000	1.52	418.8	100.0	Standard Day
26.	Continue Supersonic Climb	0.965	37790	1.67	434.6	100.0	Standard Day
27.	Continue Supersonic Climb	1.007	45370	2.00	479.3	100.0	Standard Day
28.	Supersonic Top of Climb	1.083	52950	2.40	575.4	100.0	Standard Day
29.	Begin Supersonic Cruise	2.083	52950	2.40	575.4	97.0	Standard Day
30.	Continue Supersonic Cruise	2.950	62329	2.40	1768.4	97.0	Standard Day
31.	End Supersonic Cruise	2.816	64675	2.40	2962.3	97.0	Standard Day
32.	Begin Decel to Subsonic Cruise	2.816	64675	2.40	2962.3	50.0	Standard Day
33.	Continue Decel	2.862	64675	2.02	3020.2	50.0	Standard Day
34.	Continue Decel	2.905	64675	1.63	3064.8	50.0	Standard Day
35.	Continue Decel	2.922	64675	1.45	3079.4	42.3	Standard Day
36.	Continue Decel	2.944	60340	1.31	3096.8	38.6	Standard Day
37.	Continue Decel	2.984	51670	1.06	3124.1	29.8	Standard Day
38.	Continue Decel	3.031	43000	0.86	3150.0	17.9	Standard Day
39.	Begin Subsonic Cruise	3.031	43000	0.90	3150.0	69.0	Standard Day
40.	End Subsonic Cruise	3.464	43000	0.90	3373.4	67.0	Standard Day
41.	Begin Subsonic Descent	3.464	43000	0.90	3373.4	16.5	Standard Day
42.	Continue Subsonic Descent	3.517	34700	0.74	3398.2	6.1	Standard Day
43.	Continue Subsonic Descent	3.649	18100	0.51	3446.0	5.0	Standard Day
44.	Continue Subsonic Descent	3.740	9800	0.43	3472.8	5.0	Standard Day
45.	Continue Subsonic Descent	3.844	1500	0.37	3500.0	5.0	Standard Day +18°F
46.	Begin Approach	3.845	1500	0.24	3501.0	23.3	Standard Day +18°F
47.	Continue Approach	3.911	1500	0.24	3513.2	23.3	Standard Day +18°F
48.	Touchdown	3.912	0	0.24	3513.3	5.0	Standard Day +18°F
49.	Reverse Thrust On	3.933	0	0.10	–	60.0	Standard Day +18°F
50.	Reverse Thrust Off, Begin Taxi	3.934	0	0.0	–	80.0	Standard Day +18°F
51.	End Taxi, Shutdown	4.024	0	0.0	–	5.0	Standard Day +18°F

Figure 8.   Flight Time vs Altitude for the Economic (or Typical) Mission

Table 1.   Final Status of Propulsion System Technology Development

Category	Final Status	Goal
Engine Weight (lbm)	10590	8845
Exhaust Nozzle Weight (lbm)	7833	7830
Supercruise EINOx (g NOx/kg fuel)	3.8	<5.0
Airport NOx (lbm NOx/hr 1000 lbf/cycle)	8.0	<5.0*
Airport CO (lbm CO/hr 1000 lbf/cycle)	8.0	<7.8*
Combustor Efficiency (%) at Cruise	99.98	99.9
Sideline Noise Relative to FAR36 Stage 3 (dB)	−1	−1
Community Noise Relative to FAR36 Stage 3 (dB)	−5	−5
Approach Noise Relative to FAR36 Stage 3 (dB)	−5	−1
Exhaust Nozzle Sideline C_{fg}	0.945	0.960
Exhaust Nozzle Cruise C_{fg}	0.981 −0 .983	0.9385
		* Self-imposed program goal

3.1.6 Sensitivity Studies

Throughout the research portion of the HSCT program, aircraft/propulsion-system sensitivity studies were needed to assist in the development of various design applications. The inlet, combustor, and nozzle research teams all made specific requests for these studies to aid in technologically evaluating components and in developing trade studies.

In these sensitivity studies, "supersonic sensitivity" refers to sensitivities that apply to all supersonic segments of a mission (climb, descent, and cruise). "Subsonic sensitivity" means the same for all subsonic segments of a mission. If only a portion of a flight (such as "cruise") is specified, the sensitivity applies only to that segment, regardless of whether subsonic or supersonic.

All these sensitivities were derived using a reference airplane definition (the *Technology Concept Aircraft,* TCA) and baseline missions. The TCA was the first airplane design considered under Phase II of the HSCT program. The original TCA had an aspect ratio of 2.0 with an outboard panel sweep of 52° and suffered significantly in noise sizing because of poor low-speed lift/drag ratio (L/D). Airframe system studies indicated that using a 2.8 aspect ratio wing with 28° outboard sweep (2.8/28) reduced MTOW by 60,000 lbm when sized to −1 EPNdB sideline and −5 EPNdB community. It was also much less sensitive to changes in noise constraints, weight, and drag. The robust 2.8/28 wing was subsequently chosen for the TCA; it was felt that this planform was most appropriate for use to select the future propulsion components for the TCA.

3.1.6.1 Inlet And Combustor Sensitivity Studies

TCA Studies

The inlet and combustor teams requested aircraft/propulsion system sensitivity studies to aid them in ranking inlets and combustors for their downselection processes. The types of sensitivities requested were inlet pressure recovery, engine weight and performance, inlet bleed, supersonic and subsonic specific fuel consumption (SFC), and supersonic and transonic drag and thrust.

Most of the inlet sensitivity values desired by the team can be derived from three basic sensitivities: inlet weight, pressure recovery, and supersonic thrust. The supersonic thrust and inlet recovery sensitivities in this analysis adjust engine performance from Mach 2.0 to 2.4. The transonic drag sensitivity considered a drag change spread out from Mach 1.0 to 1.6 and an isolated change concentrated at Mach 1.1. (These results are shown later.)

From earlier studies, it was known that a 1% inlet recovery increment caused changes of about 1.4% in net thrust (F_N) and 0.35% in SFC. This meant that for every 1% that inlet recovery increases, absolute airflow increases 1%, thrust increases 1.4%, and fuel flow increases 1.05%. These would be the impacts of a change in inlet recovery on a fixed engine. The impact of eliminating the thrust change by adjusting the extraction ratio (ER) was also investigated. This method, however, changed the bypass ratio and thus could affect engine weight.

On the 3770.60 MFTF engine with a translating centerbody (TCB) inlet, there was about a 3.22% loss in thrust for a 4.13% bleed (656 lbf of bleed drag at Mach 2.4 at 55,000 ft and 560 lbm/s corrected flow). Therefore, a 1% bleed was found to be worth 0.78% thrust, and the 1% supersonic thrust sensitivity can be used. The supersonic thrust sensitivity can also be used to account for supersonic drag change. Basically the effect of a 1% increase in drag is the same as a 1% decrease in thrust without changing fuel flow. Since at supersonic cruise, typically, there are about 100 counts of airplane drag, a 1% thrust change is equivalent to a 1-count drag change.

Table 2 represents GEAE system-study results for the three basic sensitivities. The 1% change in supersonic thrust shown did not change fuel flow. Therefore, there is also a 1% change in SFC associated with the thrust change.

Table 2. Sensitivity Study Results

Parameter	Base	1% Inlet Recovery +	1% Inlet Recovery −	250-lbm Inlet +	250-lbm Inlet −	1% Supersonic F_N −	1% Supersonic F_N +
MTOW (lbm)	725587	721405	730514	729423	722119	734796	716921
Sw (ft^2)	8696	8656	8742	8720	8675	8782	8614
Engine Scale Factor	0.879	0.874	0.885	0.884	0.874	0.890	0.868
F_N (lbf) SLS Hot Day	50721	50432	51067	51009	50432	51356	50086
Airflow (at 100% Corrected Fan Speed, lbm/s)	703.2	699.2	708.0	707.2	699.2	712.0	694.4
OEW w/o Propulsion (lbm)	265087	263911	266478	266952	263336	267687	262642
OEW – Total (lbm)	315302	313787	317104	317516	313239	318667	312142
Block Fuel (lb)	309893	307417	312752	311294	308632	315273	304781
Block Time (min)	326.96	326.96	326.97	326.90	327.01	326.94	326.98
Sizing Constraints:	Noise	Noise	Noise	Noise	Noise	Noise	Noise
	Δ Fuel	Δ Fuel	Δ Fuel	Δ Fuel	Δ Fuel	Δ Fuel	Δ Fuel
3000-nmi Economic Mission:							
Block Fuel (lb)	167298	165729	168987	168138	166516	170232	164341
Block Time (min)	199.19	199.18	199.19	199.18	199.19	199.19	199.18

System Δ's from Table 2 were normalized, and values for impact of inlet recovery, bleed, weight, and supersonic drag were calculated. These values, shown in Table 3, were used to develop the direct operating cost + interest (DOC+I) sensitivities for the inlet downselect.

Table 3.   Inlet Sensitivities for the Base 2.8/28 Aircraft

Sensitivity Parameter	MTOW (lbm)	Engine Air Flow (lbm/s)	Change in Engine Size	OEW Propulsion (lbm)	OEW Total (lbm)	Block Fuel 3000 nmi (lbm)
1% Inlet Recovery	−4555	−4.4	−0.63%	−1284	−1658	−1629
100 lbm Inlet Weight	+1461	+1.6	+0.23%	+ 723	+ 855	+ 324
1 ct Supersonic Drag	+8937	+8.8	+1.26%	+2522	+3262	+2946
1% Inlet Bleed	+6971	+6.9	+0.98%	+1968	+2545	+2298

The inlet team also requested a study of sensitivity to transonic drag. Transonic drag might change for a number of situations: diverter effects, spill drag, lift-induced cowl drag, or lip drag. Some of these drags may cause change over a wide range of Mach numbers and some may cause just a spike at Mach 1.1. Therefore, both types of sensitivities were investigated.

The first sensitivity value for transonic drag was derived by modifying the drag from Mach 1.0 to 1.6 by a constant percentage. Variations in transonic drag were considered from a 10% increase to a 10% decrease. Typically, for the 2.8/28 wing, there are about 140 counts of drag with a L/D ratio of about 10.4 at Mach 1.1 and about 113 counts of drag with an L/D of about 10.0 at Mach 1.5. Therefore, 10% drag was found to represent 14 counts of Mach 1.1 drag. Drag counts represented at Mach 1.6 are less than this value.

The second sensitivity value derived for transonic drag assumes that the Δ is concentrated at Mach 1.1 and disappears linearly by Mach 1.3. Figure 9 shows how the two drag sensitivities are applied.

Table 4 shows the results of the first transonic drag sensitivities study on the 2.8/28 planform. Sensitivity remains fairly linear over a range of ±2% and shows about 1300 lbm of MTOW per 1%
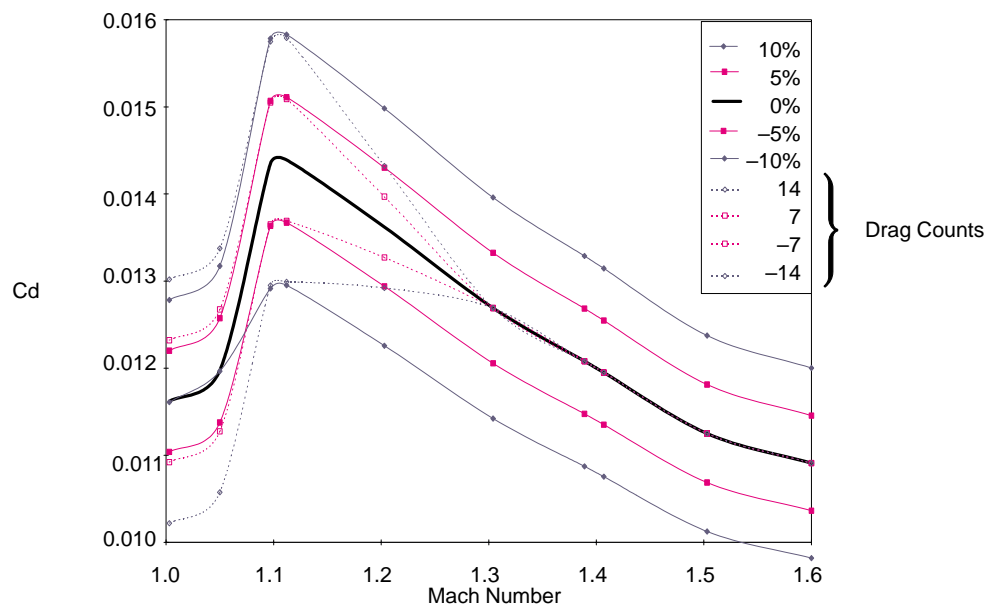
Figure 9.   Transonic Drag Variations: Mach 1.0 to 1.6 for the 2.8/28 Wing

of transonic drag. Sensitivity at +10%, however, is double the sensitivity at –10%. This is not unusual, many sensitivities are linear over only a small range and differ depending on the direction of the penalty or benefit. Table 4 may also be used to develop DOC+I sensitivities for the percent of transonic drag applied over the range of Mach 1.0 to 1.6.

Table 4. First Case, Transonic Sensitivities for Base 2.8/28 Aircraft

Transonic Sensitivity % of Drag, M 1 – 1.6	Δ MTOW (lbm)	Δ Engine Air Flow (lbm/s)	Change in Engine Size	ΔOEW Propulsion (lbm)	ΔOEW Total (lbm)	ΔBlock Fuel 3000 nmi (lbm)
10.0%	19759	19.2	2.74%	5579	7226	5025
5.0%	7824	7.2	1.03%	2209	2860	2057
2.0%	2748	2.4	0.34%	776	1004	809
0.7%	886	0.8	0.11%	249	322	241
–0.7%	–938	–0.8	–0.11%	–265	–344	–246
–2.0%	–2391	–2.4	–0.34%	–675	–874	–648
–5.0%	–5031	–4.8	–0.69%	–1417	–1827	–1429
–10.0%	–9444	–9.6	–1.37%	–2666	–3448	–2576

Table 5 shows the results of the second transonic drag sensitivities study on the 2.8/28 wing planform. In these data, the change in drag value is concentrated at Mach 1.1. This sensitivity is also fairly linear over the range of ±7 counts of Mach 1.1 drag. As before, the sensitivity at +14 counts (of Mach 1.1 drag) is double the sensitivity of –14 counts. These data are used to develop DOC+I sensitivities for transonic drag change concentrated at Mach 1.1.

Table 5. Second Case, Transonic Sensitivities for Base 2.8/28 Aircraft

Transonic Sensitivity Counts of Drag, M 1 – 1.6	Δ MTOW (lbm)	Δ Engine Air Flow (lbm/s)	Change in Engine Size	ΔOEW Propulsion (lbm)	ΔOEW Total (lbm)	ΔBlock Fuel 3000 nmi (lbm)
14 ct	7254	7.2	1.03%	2048	2650	2065
7 ct	2810	2.4	0.34%	794	1027	894
3 ct	1106	0.8	0.11%	311	402	324
1 ct	339	0.0	0.00%	96	124	100
–1 ct	–412	–0.8	–0.11%	–117	–151	–111
–3 ct	–1036	–0.8	–0.11%	–292	–378	–298
–7 ct	–2115	–2.4	–0.34%	–597	–772	–629
–14 ct	–3675	–4.0	–0.57%	–1038	–1342	–1118

General sensitivities were developed for supersonic thrust with no change in SFC (thrust and fuel flow changed together), SFC change alone (fuel flow changed, no change in thrust), and supersonic drag. The supersonic sensitivities developed covered the range of Mach 2.0 to 2.4. As shown in Table 6, SFC variation is fairly linear over a wide range, but drag is less linear. Supersonic thrust is the least linear of the group shown. At higher levels, supersonic thrust and drag would probably require a change in engine bypass ratio to reduce the impact.

Table 6. Overall Sensitivities for Base 2.8/28 Aircraft

Sensitivity Parameter		ΔMTOGW	ΔESF	ΔW_air	ΔBlock F	ΔOEW–PR	ΔOEW
Supersonic Net Thrust / Supersonic Fuel Flow	−10% / −10%	21,727	0.02600	20.8	7,465	6,135	7,947
	−5% / −5%	8,786	0.01100	8.8	3,143	2,482	3,213
	−2% / −2%	3,308	0.00400	3.2	1,104	937	1,217
	+2% / +2%	−2,686	−0.00300	−2.4	−983	−756	−975
	+5% /+5%	−5,835	−0.00700	−5.6	−2,201	−1,644	−2,122
	+10% / +10%	−9,755	−0.01200	−9.6	−3,729	−2,754	−3,561
Supersonic Fuel Flow	+5%	39,664	0.04800	38.4	12,415	11,202	14,522
	+2%	15,240	0.01800	14.4	4,974	4,304	5,573
	+1%	7,620	0.00900	7.2	2,531	2,154	2,791
	−1%	−7,479	−0.00900	−7.2	−2,410	−2,110	−2,728
	−2%	−14,370	−0.01700	−13.6	−4,757	−4,031	−5,177
	−5%	−36,101	−0.04400	−35.2	−11,109	−10,201	−13,189
Supersonic Drag	+5%	47,166	0.05800	46.4	14,320	13,324	17,282
	+2%	18,020	0.02200	17.6	5,805	5,089	6,591
	+1%	9,081	0.01100	8.8	2,883	2,566	3,326
	−1%	−8,765	−0.01100	−8.8	−2,880	−2,473	−3,195
	−2%	−17,316	−0.02100	−16.8	−5,628	−4,887	−6,316
	−5%	−41,968	−0.05100	−40.8	−12,880	−11,852	−15,312
Subsonic Fuel Flow	+10%	17,944	0.02200	17.6	4,494	5,067	6,562
	+5%	8,987	0.01100	8.8	2,281	2,540	3,291
	+2%	3,606	0.00400	3.2	981	1,021	1,325
	−2%	−3,423	−0.00400	−3.2	−887	−964	−1,244
	−5%	−8,670	−0.01100	−8.8	−2,199	−2,446	−3,160
	−10%	−17,146	−0.02100	−16.8	−4,453	−4,844	−6,267
Takeoff Thrust	−10%	43,582	0.12700	101.6	10,321	15,370	24,108
	−5%	14,965	0.04700	37.6	3,552	5,426	8,644
	−2%	4,856	0.01600	12.8	1,119	1,799	2,902
	+2%	−4,228	−0.01500	−12.0	−932	−1,587	−2,578
	+5%	−9,190	−0.03400	−27.2	−2,068	−3,522	−5,790
	+10%	−15,674	−0.06100	−48.8	−2,917	−6,163	−10,275
Dead Weight	+20000 lbm	92,536	0.12700	101.6	19,823	44,283	53,052
	+5000 lbm	21,262	0.02800	22.4	4,647	10,485	12,412
	+1000 lbm	4,280	0.00600	4.8	944	2,107	2,497
	−1000 lbm	−4,149	−0.00600	−4.8	−926	−2,065	−2,437
	−5000 lbm	−20,398	−0.02700	−21.6	−3,966	−10,232	−12,067
	−20000 lbm	−77,611	−0.10300	−82.4	−15,738	−39,611	−46,527
Engine Weight	+500 lbm	9,634	0.01300	10.4	2,150	4,716	5,606
	−500 lbm	−8,995	−0.01200	−9.6	−2,011	−4,456	−5,265
Nozzle Weight	+500 lbm	10,383	0.01400	11.2	2,328	5,146	6,087
	−500 lbm	−10,090	−0.01400	−11.2	−2,176	−4,990	−5,898

Subsonic SFC changes were investigated by determining the changes in fuel flow (including reserve hold) during subsonic cruise. Takeoff thrust was varied over the range of ±10%, and noise was assumed to increase with thrust. Takeoff thrust sensitivity was found to be extremely nonlinear and, when very large, would probably mandate adjustment in the engine cycle. In additional studies, variations in engine and nozzle weight were investigated, as were changes in operational empty weight (OEW) — simulated by applying various dead weight Δ's (constant, not scaled when sized).

Table 7 shows the system-level impacts of 1% changes in the overall propulsion parameters. Delta system-level characteristics are needed for the DOC calculations that assist engine companies in deciding what component technologies produce the best result. To determine DOC+I, values are needed for the block fuel burn of the economic mission, for engine size, and for OEW.

Table 7.   Summary Overall Sensitivities for Base 2.8/28 Aircraft

Sensitivity Parameter	Δ's						
	MTOGW	ESF	W_{air}	Block F	OEW–PR	OEW	%MTOGW
1 Countt Supersonic Drag	8,940	0.01100	8.8	2,940	2,520	3,260	1.2320
1% Supersonic Thrust	−1,499	−0.00175	−1.4	−522	−423	−548	−0.2065
1% SFC Supersonic	7,550	0.00900	7.2	2,470	2,132	2,759	1.0404
1% SFC Subsonic	1,757	0.00200	1.6	467	496	642	0.2422
1% Transonic Thrust	−1,280	−0.00150	−1.2	−360	−360	−470	−0.1764
1% Takeoff Thrust	−2,271	−0.00775	−6.2	−513	−846	−1,370	−0.3130
100 lbm Engine	1,863	0.00250	2.0	416	917	1,087	0.2567
100 lbm Nozzle	2,047	0.00280	2.2	450	1,014	1,199	0.2821
1000 lbm OEW	4,200	0.00600	4.8	935	2,085	2,470	0.5788
1% Engine or 81 lbm	1,503	0.00202	1.6	336	740	877	0.2072
1% Nozzle or 66 lbm	1,345	0.00184	1.5	296	666	787	0.1854
1% OEW or 2651 lbm	11,134	0.01591	12.7	2,479	5,527	6,548	1.5344

Preliminary Technology Configuration Studies

The combustor team also requested sensitivity studies concerning engine weight and performance, supersonic and subsonic SFC, and thrust/drag. Data concerning variations to the combustor inlet and exit temperatures (T_3 and T_4) were also requested. These sensitivities were derived using a *preliminary technology configuration* (PTC) wing planform for the baseline aircraft.

As before, sensitivities were generated for supersonic thrust with no change in SFC and for SFC change alone. Typically, supersonic thrust and drag sensitivities are linear over only small ranges, and at higher levels of change they may mandate a change in the engine bypass ratio (BPR). For the study, the takeoff coefficient of gross thrust (C_{fg}) was varied ±3%. Noise levels remained constant as thrust changed. Takeoff thrust sensitivity is known to be extremely nonlinear and at high sensitivity would probably require an adjustment in the engine cycle. Changes in OEW were investigated by applying a dead weight Δ of 1000 lbm (constant, not scaled when sized) to the base configuration. These studies included investigations into variations in engine and nozzle weight and length.

Table 8 shows values for the more linear parts of sensitivities projected for a 1% change in the parameter of interest.

Table 8. PTC Economic Mission-Change Parameters

Sensitivity Parameter	Δ's						
	MTOGW	ESF	W_{air}	Block F	OEW–PR	OEW	%MTOGW
1% Supersonic Drag	10,000	1.27%	8.8	3,965	2,200	3,160	0.80
1% Supersonic Thrust	−1,500	−0.19%	−1.6	−800	−320	−460	−0.15
1% SFC Supersonic	9,000	1.14%	10.5	3,500	2,000	3,000	0.72
1% SFC Supersonic Cruise	6,100	0.77%	7.2	2,400	1,370	1,960	−0.65
1% SFC Subsonic	4,000	0.51%	4.8	1,350	900	1,250	0.30
1% SFC Subsonic Cruise	1,650	0.21%	2.0	550	370	530	−0.12
1% SFC Overall	13,400	1.70%	16.0	4,900	3,000	4,400	1.02
1% Takeoff C_{fg}	−9,000	−1.14%	−22.0	−2,600	−3,100	−5,000	−0.74
Noise Held Constant							
100 lbm Engine	2,000	0.25%	2.4	530	900	1,100	0.15
100 lbm Nozzle	2,100	0.27%	2.5	560	980	1,200	0.16
No Weight Change							
1-in Engine Length	470	0.02%	0.5	140	245	302	0.04
1-in Nozzle Length	148	0.01%	0.3	39	71	87	0.01
1000 lbm OEW	4,500	0.57%	5.6	694	1,026	1,496	0.21
−50°F T_3	15,620	1.98%	18.4	5,422	4,219	5,815	1.19
−100°F T_{41}	5,850	0.74%	7.2	1,619	2,432	3,031	0.44

For cost analyses, engine sell price is assumed to be $19 million each. A cost-to-price factor of 1.3 is assumed when looking at the impact of variations in engine cost. Thus, a 1% engine cost equals about $146,000 or about 0.11% of DOC+I. Also, in this analysis, engine maintenance cost is assumed to be $392 per engine flight hour (EFH), and a 1% change in engine maintenance cost is worth 0.08% of DOC+I.

The reduced T_3 and T_{41} engines have both been extensively documented. The engines were matched to the same airflow size and approximately the same thrust, thrust lapse, and takeoff jet velocity. Changes in engine weight and length have been accounted for. Nozzle weight is corrected to compensate for physical changes in exhaust nozzle throat area (A_8). Thrust and SFC changes are accounted for throughout the mission flight path based on Δ values taken from the engine design cycle data.

Overall, the reduced-T_3 engine has about a 1% increase in SFC, a 50-lbm increase in propulsion weight, and a 3-in increase in engine length. The reduced-T_{41} engine has the same increase in length, a 150-lbm increase in propulsion weight, and a minimal impact on SFC.

Table 9 summarizes the results of component performance effects on SFC and resultant impact on MTOW and DOC+I. Typically variations in BPR and fan pressure ratio (FPR) were small, and any weight change was unaccounted for. In using these sensitivities, engine weight changes due to changes in components must be accounted for separately using the sensitivities in Table 8.

One pair of columns show Δ values for a 1% change in a parameter, and another pair of columns show Δ values for a 1-point increase. In the case of ΔP's (changes in pressure), the 1-point increase behaves inversely to the specific engine parameter. The cycle input for a ΔP might be PQDxx = 0.98 (pressure ratio — downstream/upstream = 0.98). This would be a 2-point pressure drop. Any increase in the pressure drop reduces the PQDxx.

Table 9. Component Performance Effects on SFC

Parameter	Cycle Label	Base Value	%SFC/%Parameter		1% Increase		1-Pt Increase	
			55K/2.4M PC=50	43K/0.9M PC=40	ΔMTOW	ΔDOC+I	ΔMTOW	ΔDOC+I
SL Des Fan Frame P/P	PQD21	0.9900	−0.163	−0.229	−2388	−0.19	−2412	−0.19
SL Des Fan Duct P/P	PQD14	0.9596	−0.158	−0.232	−2353	−0.18	−2452	−0.19
SL Des Combustor P/P	PQD32	0.9440	−0.234	−0.254	−3120	−0.24	−3305	−0.26
TOC Des Turbine Exhaust P/P	PQD5	0.9890	−0.220	−1.701	−8787	−0.67	−8885	−0.68
TOC Des Turbine Exhaust P/P	PQD55	0.9891	−0.220	−0.478	−3894	−0.30	−3937	−0.31
TOC Des Nozzle Tailpipe P/P	PQD58	0.9650	−0.319	−1.076	−7171	−0.55	−7431	−0.57
SL Des Fan Efficiency	EDD2	0.8828	−0.182	−0.517	−3706	−0.29	−4197	−0.32
SL Des Compressor Efficiency	EDD25	0.8875	−0.249	−0.309	−3477	−0.27	−3918	−0.31
TOC Des HP Turbine Efficiency	EDD41	0.9136	−0.219	−0.291	−3131	−0.24	−3427	−0.27
TOC Des LP Turbine Efficiency	EDD49	0.9250	−0.183	−0.379	−3167	−0.25	−3423	−0.27
TOC Des Comb Efficiency	EDD36	0.9990	−0.998	−0.928	−12693	−1.00	−12706	−1.00
SL Des HPT Cooling Flow	G31W42	0.0951	0.016	0.023	235	0.02	2474	0.19
SL Des LPT Cooling Flow	G28W5	0.0651	0.008	0.017	134	0.01	2064	0.16

An engine component performance sensitivity study was conducted on the 3770.60 MFTF baseline engine to assess the impact of variations in component efficiencies, ΔP's, and cooling flows. For this study, the 3770.60 MFTF engine values were handled in the same way that the reduced-T_3 and T_{41} engine values were handled: thrust, thrust lapse, and takeoff jet velocity were held constant — allowing the SFC, BPR, and FPR to vary. The results of the component variation effect on the SFC are summarized in Table 10, together with resultant impact on MTOW and DOC+I. In general, any variations in the BPR and FPR were quite small, so these and also any weight changes were not considered in the evaluations. In using these sensitivities, engine changes that are due to changes in component performance must be considered separately, using the sensitivities listed in Table 9.

Note: If a change impacts more than one specific area, it may be necessary to refer to previous tables to derive the actual sensitivity value.

3.1.6.2 Engine Duty Cycle

A study was performed by the propulsion companies to determine the average operational duty cycle to be used to support design studies for the PTC 3770.XX aircraft. Missions with ranges of 5000, 3500, and 2700 nmi, with and without 15% subsonic cruise portions, had already been identified by the Technology Integration (TI) team. Because the 3500-nmi range selected for this study was to be a typical mission, it was decided that there would be subsonic cruise both at the beginning and at the end. Operational envelopes for the design and typical usage missions are shown in Figure 10.

Table 10. Combustor Sensitivity Summary

Item	ΔMTOW	%ΔDOC+I
1% Supersonic Cruise Combustion Efficiency	−6,100	−0.65%
1% Subsonic Cruise Combustion Efficiency	−1,700	−0.12%
1% Combustion Efficiency Everywhere	−13,400	−1.02%
1% Subsonic Cruise High-Pressure Turbine Efficiency	−600	−0.04%
1% Subsonic Cruise Low-Pressure Turbine Efficiency	−600	−0.04%
6% Subsonic Cruise HPT Efficiency	−4,000	−0.30%
6% Subsonic Cruise LPT Efficiency	−4,000	−0.30%
1-Pt Combustor Pressure Drop	3,300	0.26%
Combustor Overhaul at 3000 hr (Baseline is 4500 hr)		1.35%
100 lbm Engine	2,000	0.15%
1 in Engine Length, No Weight Change	470	0.04%
−50°F T_3 Engine	15,620	1.19%
−100°F T_{41} Engine	5,850	0.44%
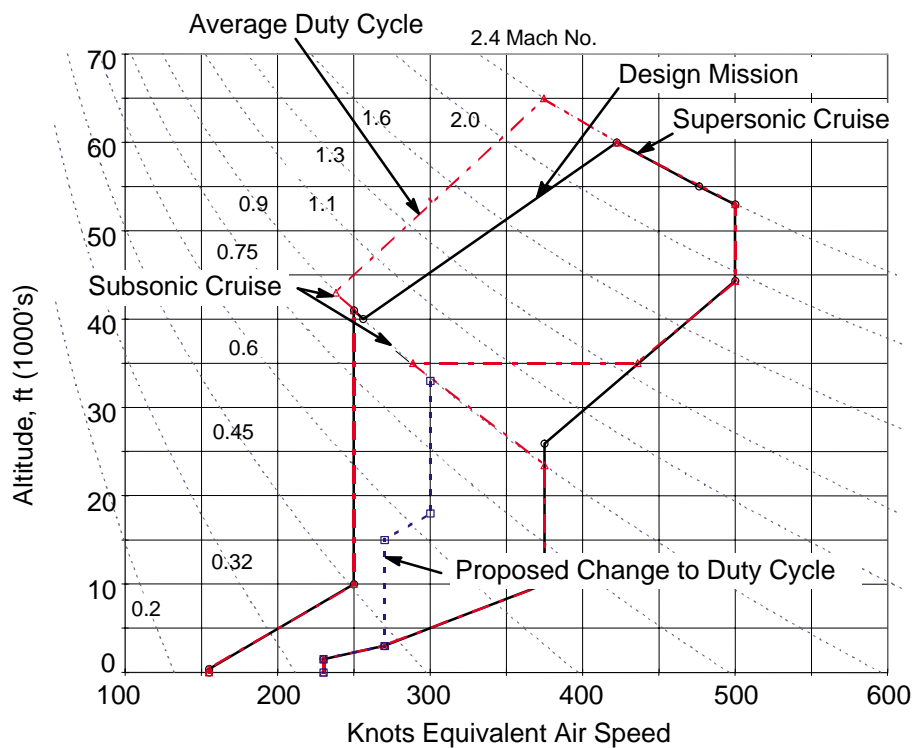
Figure 10. Operational Envelopes for Proposed Missions

Additional definition of the "climb out" phase of the mission was derived from a climb noise procedure trade study. It was decided that the aircraft would climb out initially at 270 KEAS (knots, equivalent air speed) to about 15,000 ft and then proceed at 300 KEAS to 18,000 ft. At that point the nozzle would transition from suppressed to unsuppressed mode. This type of "climb out" path was necessary to minimize the overall community noise footprint. Current supersonic air transports typically perform a similar initial "climb out" to a holding altitude and are then given permission to proceed to supersonic cruise.

Figure 11 shows the operational envelope for the average duty cycle, with descriptions of specific engine/aircraft operations that may be important to the engine design. Figure 12 depicts the altitude/ Mach profile of the mission.

3.1.6.3 Nozzle Sensitivity Studies

The HSCT *Aero Acoustics Collaborative Effort* (AACE) team requested system sensitivities studies of MTOW changes in relation to nozzle noise and performance. These data were used in conducting nozzle technology trade studies. It is difficult to capture all these relationships in a simple sensitivity statement of ΔMTOW per ΔdB or ΔMTOW per ΔC_{fg} because these sensitivities tend to be nonlinear and interdependent. The magnitude of the Δ for one depends on the absolute magnitude of the others. Consequently, improvements are outweighed by attendant penalties.

In the sizing code calibration (SCC) study, when sizing the TCA with a 2.0 aspect ratio wing (TCA_2.0), sensitivities were as shown in Table 11. The planform study was expanded to include sensitivities of other wing planforms with wing aspect ratios of 2.4, 2.8, and 3.2; see Table 12. Note that sensitivities in this table were recorded at only one sideline condition and also that changing the aircraft configuration changes the sensitivity values.

Table 11.   Noise Sensitivities for a 2.0 Aspect Ratio Wing TCA

Fixed Condition	Variation	ΔMTOW				
		Average	BCAG	MDC	NASA	GEAE
Sideline –1 dB	Community –1 to –3	28500	29700	29800	25500	29000
Sideline –1 dB	Community –3 to –5	55000	57300	52900	55600	53200
Sideline –2 dB	Community –1 to –3	33000	34600	31900	29900	35500
Sideline –2 dB	Community –3 to –5	60000	63500	60200	58000	59200
Community –1 dB	Sideline –1 to –2	6200	6400	6500	7000	5200
Community –3 dB	Sideline –1 to –2	10700	11300	8600	11300	11700
Community –5 dB	Sideline –1 to –2	16200	17500	15900	13700	17700

Table 12.   Noise Sensitivities Involving Other Wing Planforms

Condition	Range	ΔMTOW			
		2.0–52	2.4–28	2.8–28	3.2–28
Sideline –1 dB	Community –3 to –5	55000	33000	20000	12000
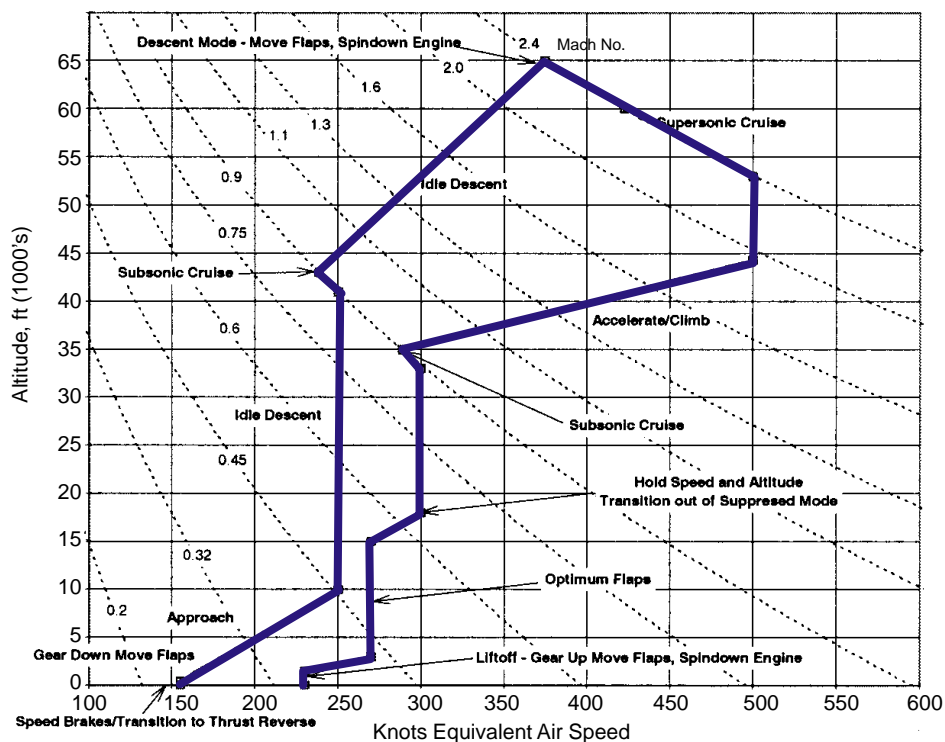
Figure 11.   Operational Envelope for Average Duty Cycle
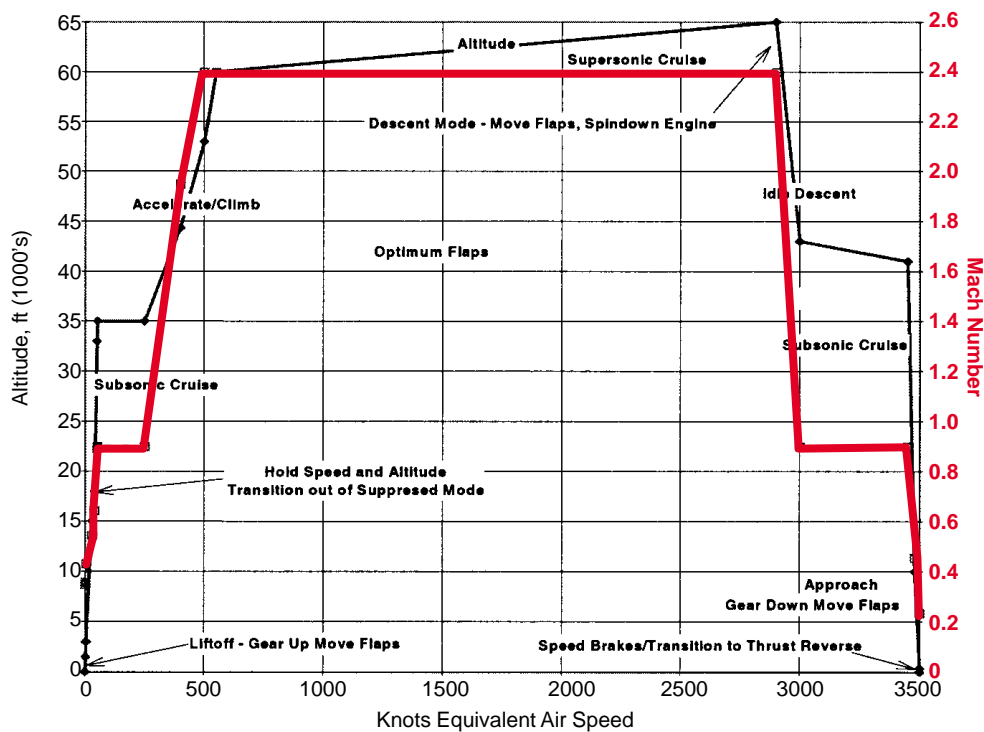
Figure 12.   Flight Profile for Proposed Average Duty Cycle

The sensitivity to community (takeoff) cutback suppression changes significantly with the wing planform. It is important to know both the baseline airplane and the absolute magnitudes of the other important independent variables when using sensitivities. These noise sensitivities assume that the actual nozzle geometry and the nacelle does not change, which means there is no change in nacelle aerodynamics, pylon weight, or landing gear length.

The TCA configuration with a 2.8 aspect ratio wing (TCA_2.8) was used as the baseline for measuring sensitivities in the studies discussed here. Figure 13 represents the jet noise predictions that have been used in all studies since the nozzle preliminary design review (PDR) and hence are the baseline levels from which the noise sensitivities are calculated.
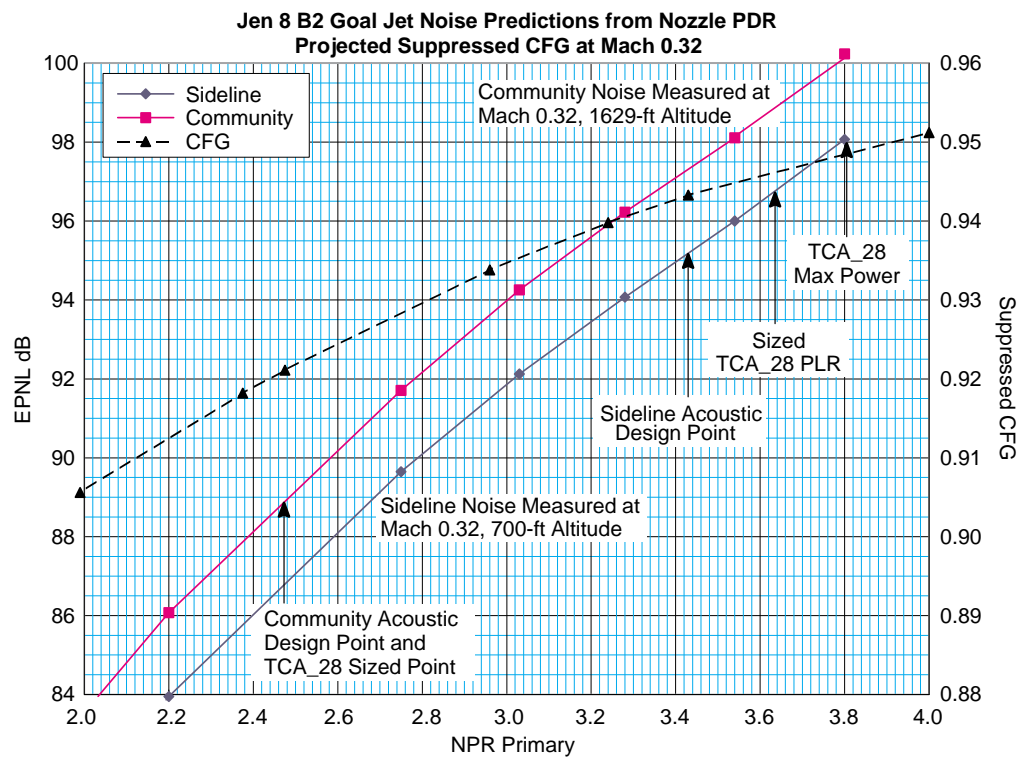
Figure 13.   Goal Jet Noise Predictions (Isolated Single Engine)

Note that the TCA_28 community sizing point and the acoustic design reference point (established by earlier work) are the same. However, the sideline sizing point and the sideline acoustic design point are different. When doing sensitivities, one needs to pay careful attention to where the Δ is occurring and what other items are also changing.

Sensitivities will most likely take the form of variations around the acoustic design points. For example, MTOW for the TCA_28 is a function of sideline and community effective perceived noise level (EPNL) at a fixed suppressed C_{fg} at the acoustic sideline design point. Variations can be developed for different C_{fg}'s.

A preliminary set of sensitivities was developed using the TCA_2.8 with a 28° swept outboard panel. Jn8B2 (P&W software) was used to calculate the noise at sideline and community (takeoff) cutback. Sensitivities were calculated by sizing the plane for sideline noise from a 0 dB to –2 dB margin, using a PLR and constraining the cutback noise to the range of –3 to –7 dB less than Stage III. The baseline

requirements for the TCA_2.8 at this time were –1 dB sideline and –5 dB cutback. Once the multiple component predictor (MCP) results were released, the jet noise component of EPNL that yielded the desired system noise results could be quantified. Sensitivities were considered as variations around those points.

Figure 14 shows MTOW results for most of the sizing runs used to obtain the desired sensitivities. The TCA_2.8 was run with the engines at the same weight as in the 1994 system study. This weight level had been used in system studies for the past several years. The results are indicated on Figure 14 by solid lines designated "Light Engine." Since later mechanical design studies indicated that the 1994 engine weights should increase, a series of sizing runs were made with an engine 1500-lbm heavier to see how much the sensitivity values might change. These results are shown on Figure 14 as "Heavy Engine," plotted with dot/dot/dash lines. Variation of the MTOW with a sized community noise level is shown on the left of the chart. Variation with sideline noise is shown on the right.

MTOW values are obtained from these data by relating model test jet noise results to a specific sizing point on the chart. As an example, if it is assumed that the goal sideline noise margin of –1 dB better than the FAR 36 Stage III levels is met with the P–5 metric, which is a model noise reference level of 96 dB at a nozzle pressure ratio (NPR) of 3.43, then sizing to a 0 dB margin would represent model test data at 95 dB and the –2 level would represent 97 dB. The same goes for community (takeoff) cutback. If is assumed that the P–6 metric of 93.5 dB at a 2.48 NPR at 1300 ft would yield
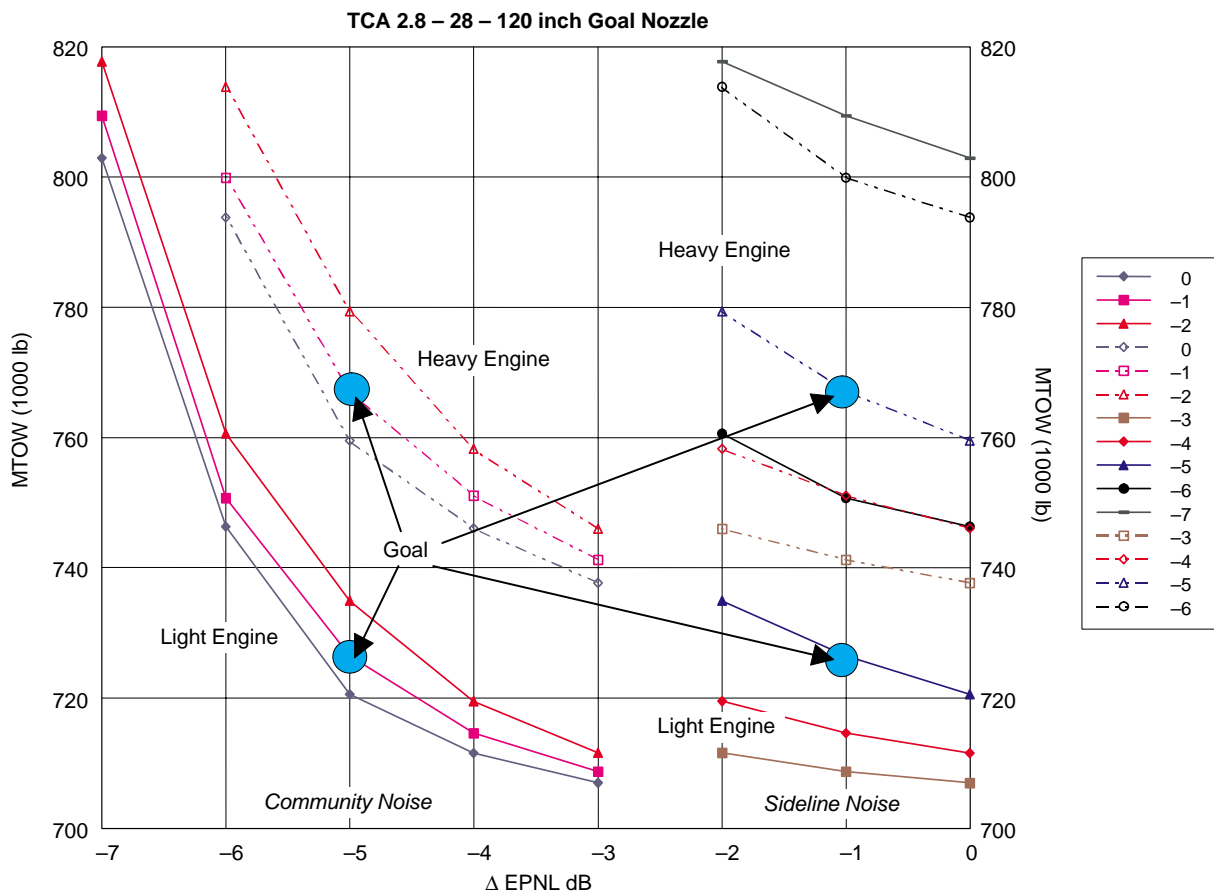
Figure 14.   MTOW for Sizing Runs

performance for the –5 dB community point, then 94.5 dB represents the –6 dB sizing point and 92.5 dB represents the –4 dB point. The exact reference point was calculated when the 1997 MCP noise prediction results were released.

During these studies, sideline variation was handled with the PLR. There is a limit to how much PLR can be used. If PLR use is limited, or if it cannot be used, then variations with sideline noise are handled either by running the engine derated at takeoff or by changing the nozzle configuration. Derating results in severe penalties and is therefore undesirable. It is better to change the nozzle geometry but only if it does not change the nacelle so much that it forces resizing to a new configuration, thus changing the sensitivities.

On Figure 14, note that the slopes of the lines vary with the noise level and therefore are not constant. Note also that the magnitude of sensitivity varies between light-engine cases and heavy-engine cases. If a simple estimate of linear sensitivity is desired, this can be accomplished by choosing a slope somewhere near the goal. Figure 15 shows the same line slopes plotted to indicate the increase in pounds of MTOW per dB for each dB of EPNL. Using this approach, the sensitivity to community noise level is approximately 20,000 lbm MTOW per dB for the goal noise level. For sideline, a sensitivity of 9000 lbm MTOW per dB is probable.

Figure 16 shows the impact of the nozzle-suppressed C_{fg} on the MTOW. For this figure the TCA_2.8 is sized to –1 dB at sideline and –5 dB at cutback. Thrust performance varies around the goal projected performance levels. C_{fg} variations are examined at maximum power, affecting takeoff velocity and altitude and sideline noise. The C_{fg} variation at partial power is examined separately because it affects only the actual throttle setting for community (takeoff) cutback. Typically when the C_{fg} changes, the change does not occur evenly at all throttle settings; higher power settings change less than the lower settings. These data are nonlinear but not nearly as much so as the noise. For this sensitivity a slope of around ±2% ΔMTOW per point of C_{fg} is calculated. It is suggested that for high power a sensitivity of 6000 lbm MTOW per 1% of change in suppressed C_{fg} should be used. For half power, a sensitivity of 3000 lb per 1% of change is appropriate.

These noise sensitivities are based on the assumption that the actual nozzle geometry and nacelle have not changed. If they have changed, there may be a change in nacelle aerodynamics, pylon weight, or landing gear length, so these should be reevaluated.

Nozzle Tab Research

In 1997, a nozzle chute design was tested that used tabs in the primary stream to enhance mixing and reduce noise. Preliminary results showed that the sideline noise was reduced by 1.2 dB, and the takeoff thrust loss was about 1.8%. The community noise level was unchanged.

In further analysis, sensitivity to this sideline noise improvement and takeoff thrust loss was evaluated on a TCA_2.8 sized to –1 dB sideline and –5 dB community noise levels. The 1.8% takeoff thrust reduction equaled a 1.5% reduction in C_{fg} due to ram drag at Mach 0.32. The 1.2-dB sideline noise reduction meant that with a 3.43 NPR the noise level went down from 95.1 dB to 93.9 dB at the sideline acoustic design point. It was also found that a 1.8% reduction in thrust with no change in noise was worth 10,800-lbm MTOW. A 1.2-dB improvement with no change in thrust was worth 6,900-lbm MTOW. Later analysis determined that there was an additional 3.4% thrust loss at half power at the community noise measuring point. This increased the thrust loss penalty to 14,400-lbm MTOW. Adding these sensitivities together produced a 7,500-lbm MTOW increase, but running the

TCA 2.8 – 28 – 120 inch Goal Nozzle

Figure 15. ΔMTOW Versus ΔEPNL

TCA 2.8–28 – 120 inch Goal Nozzle
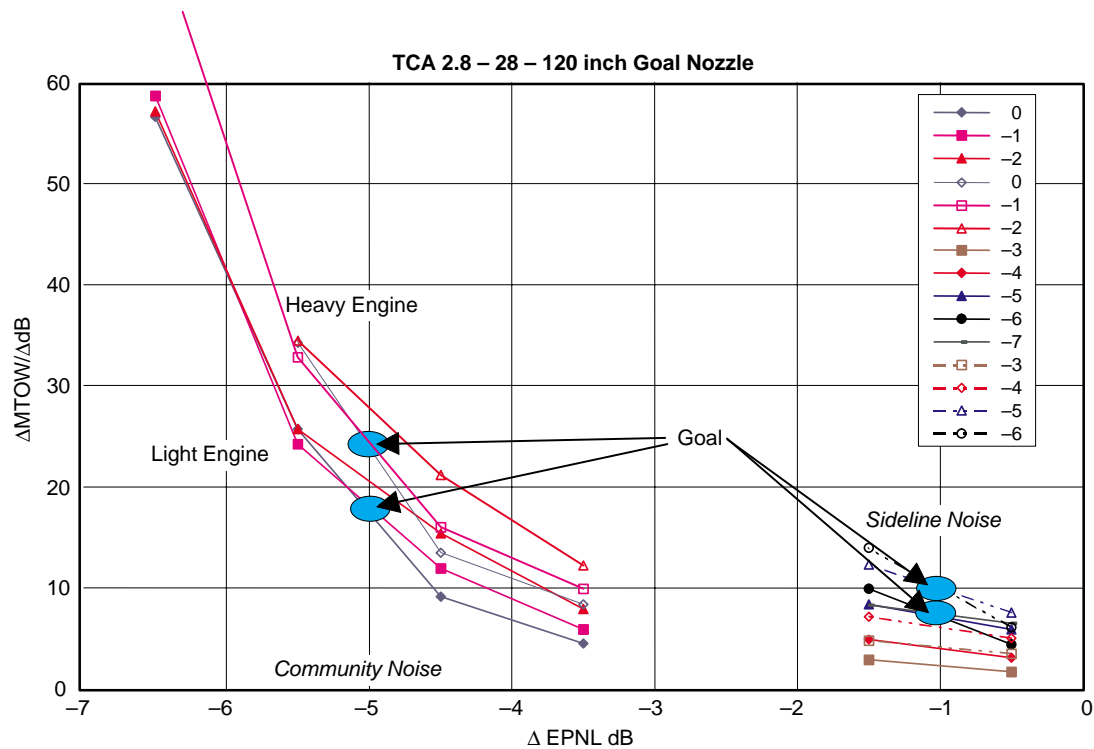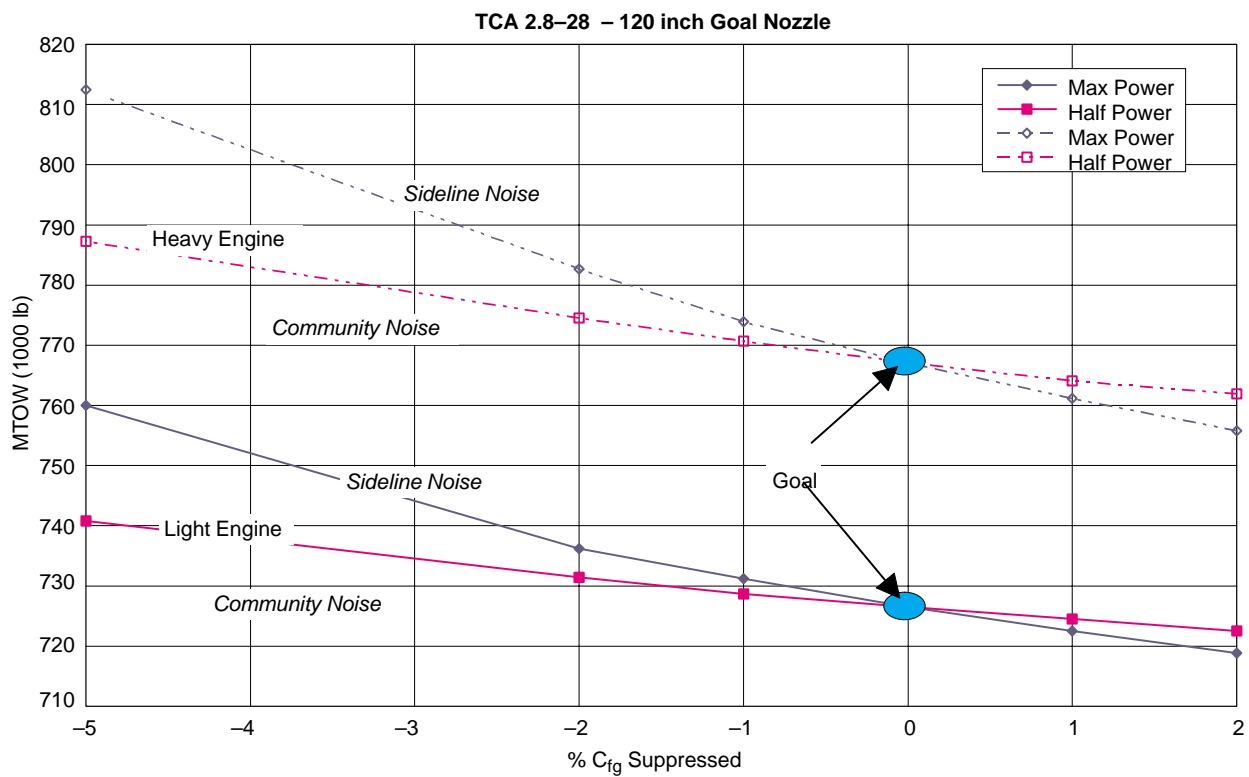
Figure 16. Sensitivity of MTOW to Nozzle Suppressed Coefficient of Gross Thrust

three sensitivities simultaneously and resizing reduced the net increase to 4,800-lbm MTOW, since sensitivities do not always add up linearly.

One of the main benefits of the tabs would be to eliminate the need for PLR. With no tabs the TCA_2.8 needed a 6.5% PLR to meet sideline noise requirements at a 3.64 NPR. If the 1.2-dB improvement from the tabs is factored in, no PLR is required and the noise level is met at 3.8 NPR. This illustrates a problem, however, with simple sensitivities. The 1.2-dB improvement from the tabs was measured at 3.43 NPR, but available acoustic data shows that this is cut in half at 3.8 NPR; see Figure 17.
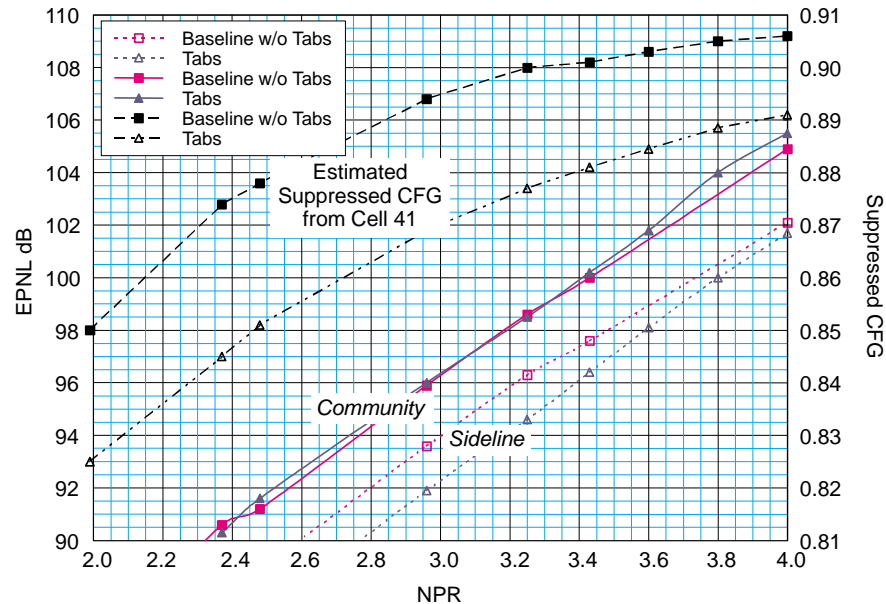
Figure 17.   Impact of Tabs on 8C Ejector, Fully Treated, 160-in Mixing Length

To further illustrate the difficulty in using simple sensitivities, the noise and thrust variations were both modeled in detail and the TCA_28 was resized to –1 dB sideline and –5 dB community noise levels through the use of tabs. The change in EPNL was calculated from the "B Tab" data and used to adjust the noise predictions in the systems studies. The same method was also used for the thrust performance impact on the tabs. The thrust performance yielded an overall MTOW penalty of 10,400 lbm when the preliminary test data was modeled in detail. The PLR used with the tabs was reduced from 6.5% to 4.3% (compared to 0% using the aforementioned sensitivity results).

Table 13 summarizes projection results when using different sensitivity assumptions. The old TCA_2.0 sensitivities (used by AACE) of 1% nozzle performance (worth 6,600-lbm MTOW) and 1 dB sideline (worth 10,000-lbm MTOW) yielded the following result. Using a 1.2 gross to net thrust factor, a 1.8% thrust loss would cost about 10,000-lbm MTOW0 (about the same as the TCA_28 sensitivity above). Using the 1.2-dB sideline-noise benefit from the TCA_2.0, the overall AACE evaluation, the tabs would yield a 2,000-lbm benefit. Using updated AACE sensitivities from the nozzle PDR, the 1.8% thrust loss would cost about 10,900-lbm MTOW, and at 22,700-lbm MTOW per dB for sideline noise the tabs would yield a 16,000-lbm benefit. If simple sensitivities with updated TCA_2.8 data were used, the tabs would have yielded a 4,000-lbm penalty. Using the

sensitivity to part-power thrust increases the penalty to 7,500-lbm MTOW. The final detail evalua-tion indicated a 10,400-lbm penalty in MTOW for the tabs on the TCA_2.8 airplane.

Table 13. Summarizing Impact of Tabs Using Different Analysis Techniques

Assumptions for Sensitivities	Δ MTOW per dB Sideline	Δ MTOW per% Net Thrust	MTOW Results
Old TCA_2.0 AACE Sensitivities	10000 lb	5500 lb	−2000 lb
New TCA_2.0 AACE Sensitivities	22700 lb	6100 lb	−16000 lb
Simple TCA_2.8 Sensitivities	5800 lb	6000 lb	+4000 lb
Detailed TCA_2.8 Sensitivities	5800 lb	6000 lb	+7500 lb
Running Exact Data for Tabs			+10400 lb

This study shows the difficulty of using simple sensitivities. The processes and trends being modeled must be understood completely, including where and how to apply them. Model data must be corrected when going from model to full-scale goal projected values. When one technology item is compared to another, reasonably detailed sensitivities will probably provide reasonable gross trends if it is not necessary to distinguish MTOW closer than several thousand pounds.

Ejector Inlet Notch Study

The nozzle aero team requested a study to determine what impact the ejector inlet notch height has on aircraft performance. The ejector inlet entrance slope had been modeled around various size ellipses. A notch results when the inlet is closed. Nozzle drag was found to be a function of the ratio of the height of the minor axis of the ellipse over the inlet throat height ($2b/H_{th}$). These data were used in a GEAE installation code to modify installed data for 100%, 200%, and 400% ellipses to reflect the inherent drag increase (see Figure 18).

The TCA was the planform used for inlet research. The GEAE TCA model is very similar to the Boeing TCA model: 750,000-lbm MTOW, 8400-ft^2 wing, and scale 1.0 FCN3570.80 engine that
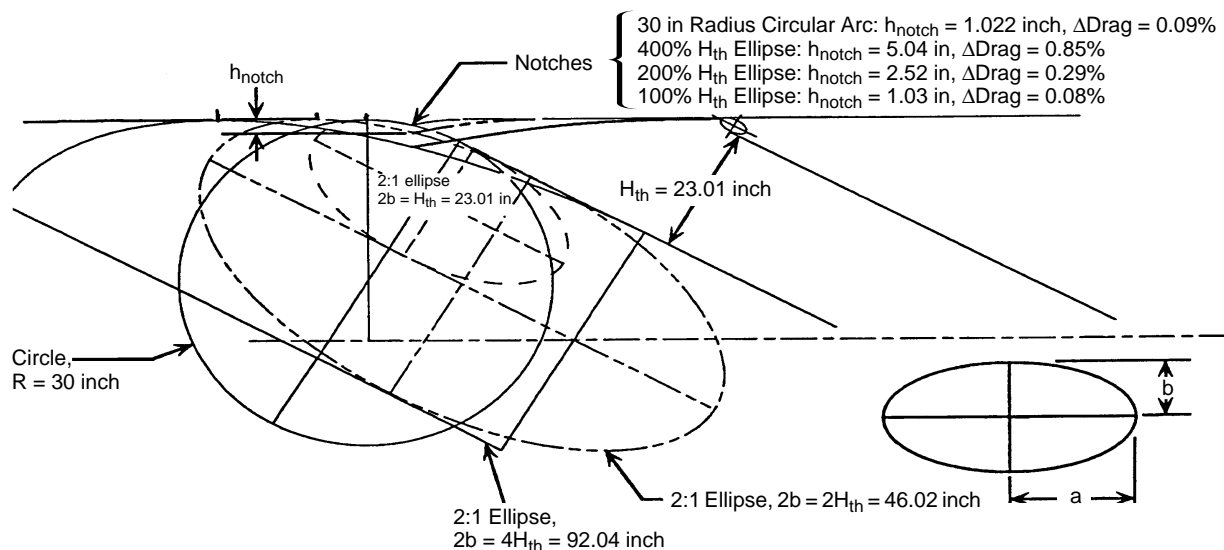
Figure 18. FCN Inlet Shoulder Contouring

meets –1 dB sideline and –3 dB community noise requirements. The noise constraint was relaxed to allow the TCA to be sized by the 60-minute climb time to 742,000-lbm MTOW. Notch drag affects thrust the most at transonic and supersonic speeds. The TCA was sized for climb time to ensure the most realistic impact. The TCA was sized with the installed data for 100%, 200%, and 400% ellipses, as shown in Figures 19 and 20.
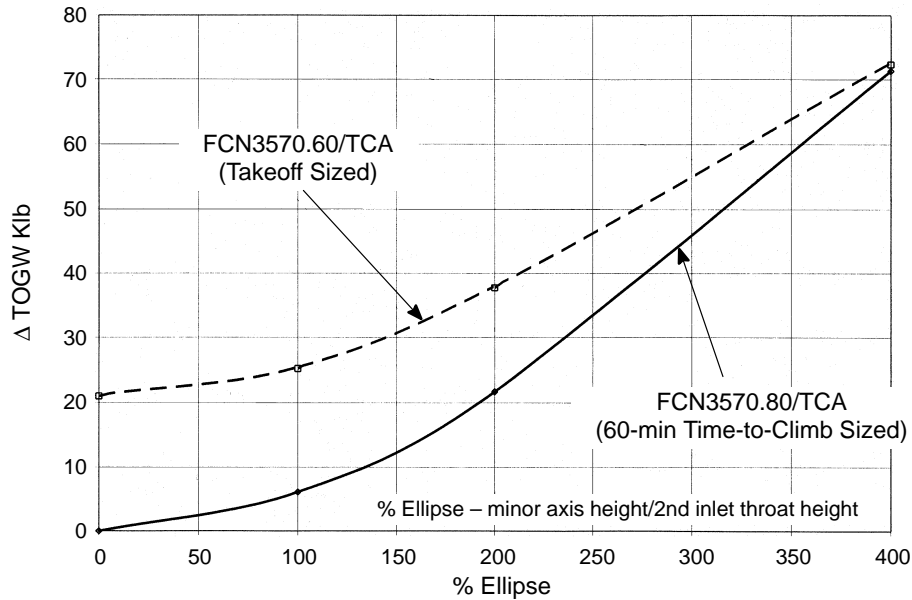
Figure 19.   Delta in TOGW versus Percent of Ellipse
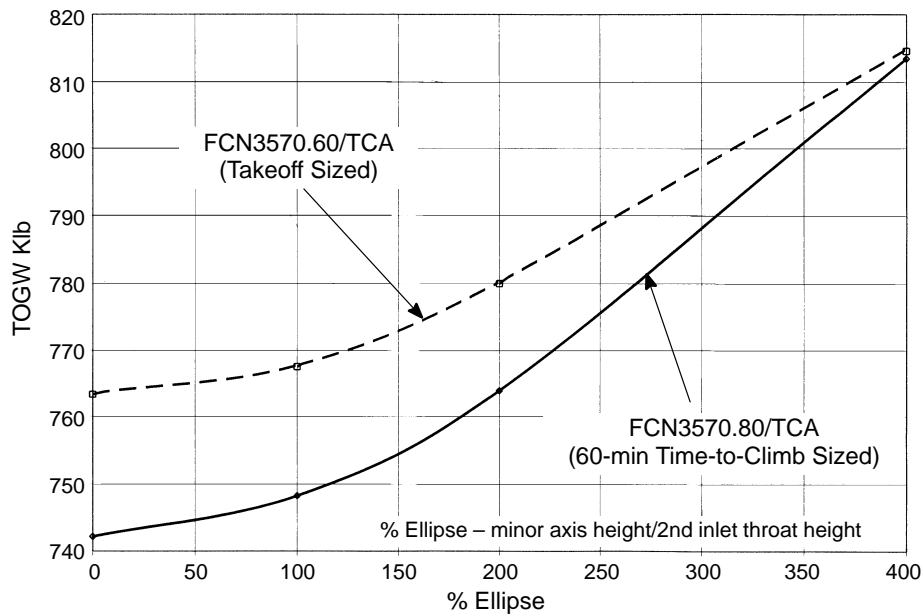
Figure 20.   MTOGW versus Percent of Ellipse

The FCN3570.60 engine was also investigated to determine effects on an engine with much greater supersonic thrust. This engine would be sized by takeoff thrust or noise. A higher SAR nozzle was added so that the FCN3570.60 noise levels would be comparable to the FCN3570.80. This nozzle was heavier, and the aircraft sized out at 763,000-lbm MTOW. Figure 20 shows that the TOGW penalty was less for the FCN2570.60, but this was offset by the fact that the engine started with a 21,000-lbm lb penalty because of greater propulsion weight.

It should be noted that the takeoff thrust penalty from sharp-cornered inlets was not at this time reflected in the engine data packs since the C_{fg} was a fixed value. Impact on the takeoff C_{fg} should be reassessed.

When the 2.0 aspect ratio TCA evolved to a 2.8 aspect ratio PTC, the engine designation changed from 3570.80 to 3770.60, and the fixed-chute nozzle (FCN) SAR increased from 2.5 to 2.9, with a corresponding increase in propulsion weight. At this point, the nozzle aero team requested an update on the impact of ejector inlet notch height on aircraft performance.

To improve the ejector inlet performance, the inlet entrance slope was modeled around ellipses of various sizes. A notch results when the inlet is closed (Figure 18). A study of the impact of the notches determined the relationships of notch drag as a function of the ratio of the height of the minor axis of the ellipse over the inlet throat height ($2b/H_{th}$). These data, shown in Figure 21, were used in the GEAE installation code to modify data installed with the two-dimensional bifurcated inlet for 100% to 400% ellipses, reflecting the drag increases.

The updated PTC model was sized with a 9200-ft^2 wing and 2.9 SAR 3770.60 engine to meet –1 dB sideline and –5 dB community noise. Even though the PTC aircraft was sized by noise, it does not have a significant time-to-climb margin and is therefore sensitive to supersonic climb thrust much the same as the original TCA with the 3570.80 engine. The PTC was sized with GEAE installed data for 100% to 400% ellipses. Figure 22 depicts the ΔMTOW results together with the earlier TCA results.

A missing component in the study was the impact of ellipse size on the ejector inlet performance and thus on takeoff thrust. It is expected that as ellipse size increases, inlet performance improves. Aerodynamic-performance estimates in suppressed mode assume a 200% inlet because this is what was tested and what was planned for the later LSM tests. At present, FCN geometry reflects a 100% ellipse at the secondary inlet throat, with no notch drag impact estimated for the aircraft nacelle.

Figure 22 shows a 6,000-lbm MTOW penalty for the 100% ellipse and an additional 15,000 lbm for the 200% ellipse. It is estimated that there would be a large difference in takeoff performance between a sharp-cornered inlet and a 100% ellipse. It is unknown whether changing from the 100% to the 200% ellipse would yield sufficient improvement in performance to offset the estimated drag penalty. The impact on takeoff performance of nacelle drag and the contouring of the nozzle secondary inlet needs to be assessed and the study redone. Indications are that the MTOW curve will flatten out and reach a minimum between 0% and 200%.

3.1.6.4 Oversized-Fan Study

In August 1998, evaluation of the variable-capacity fan (VCF) engine cycle indicated that the concept offered little advantage. However, the study did indicate there might be some benefit in oversizing the MFTF fan and operating at a higher extraction ratio without the variable fan features. To investigate this premise, several oversized fan cycles were generated. The two cycles that appeared most promising were chosen for detailed FLOWPATH (program) analyses.
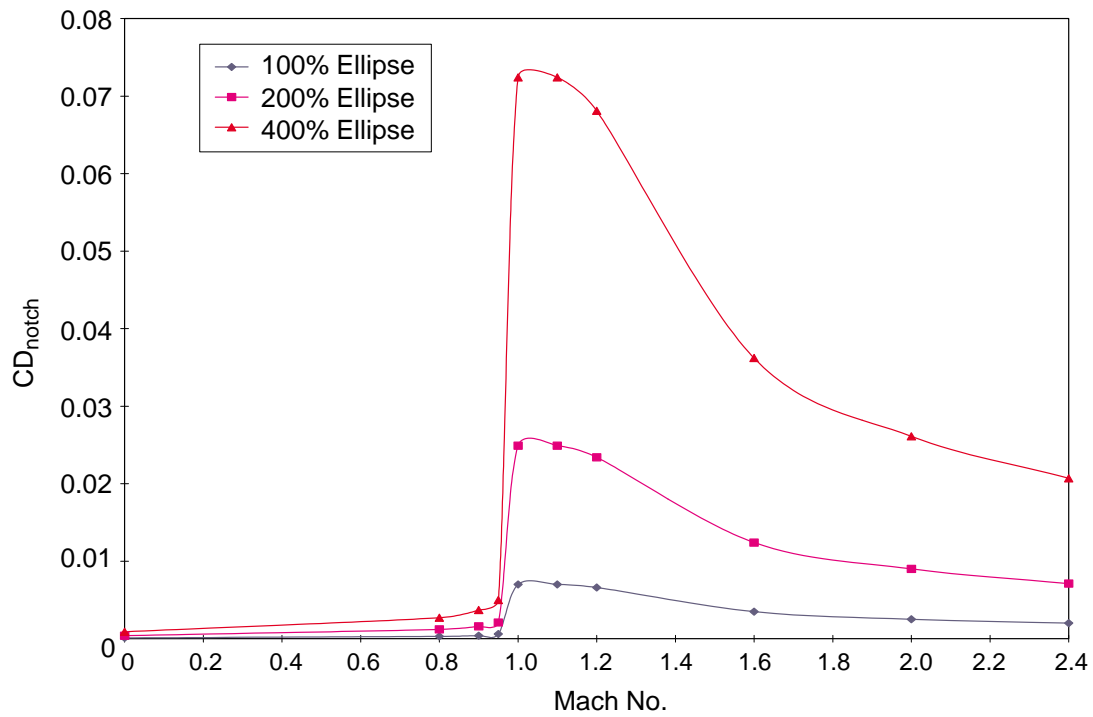
Figure 21. Notch Drag Estimates Used in Installation Studies
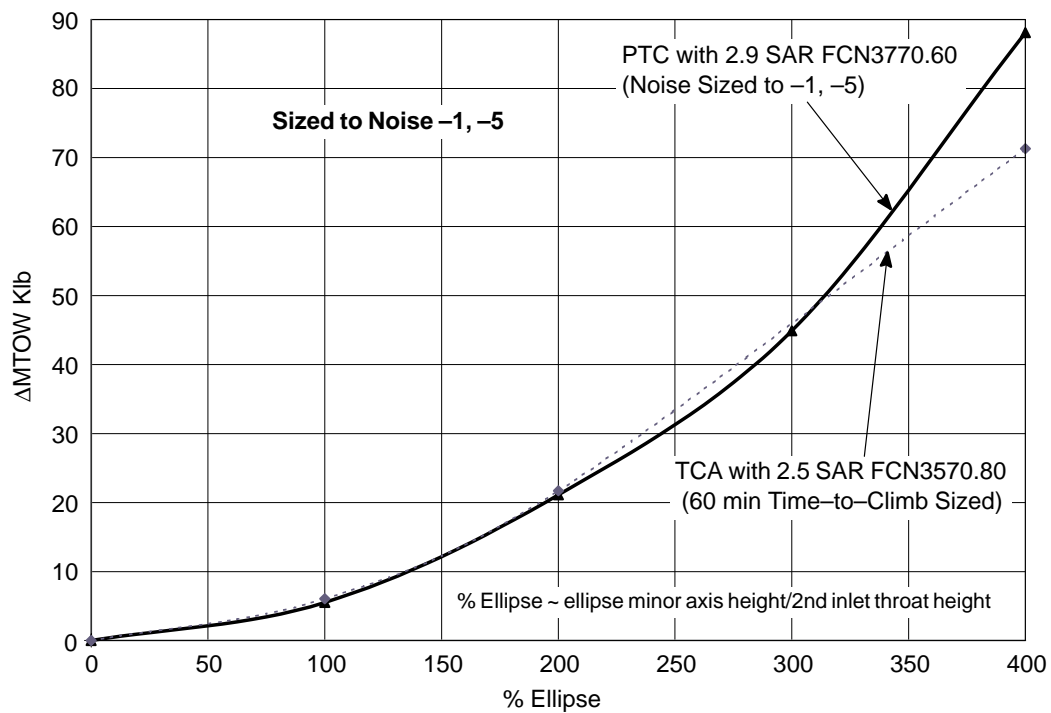
Figure 22. MTOW Impact of Notch Drag Due to Inlet Shoulder Contour

Engine cycle one used a 4.07 FPR in a 0.62 bypass engine with an airflow lapse of 62% relative to top of supersonic climb (TOC). This engine cycle was an attempt to design an oversize fan similar to NASA's VCF but using the 1998 ground rules and assumptions established for the 3770.54 engine, which was the centerline engine from the "Briquette" (see 3.2.3.1, page 84). This engine cycle was designed to handle 920 lbm/s airflow both at the aerodynamic design point and at maximum-power takeoff using an extraction ratio (P16Q56) of 1.15 instead of the normal 1.05. This cycle was also designed to match the original TOC thrust for the 3770.54 while nearly matching jet velocity at takeoff at maximum T_4, thus yielding 11.4% more takeoff thrust at 920 lbm/s.

The supersonic cruise SFC of the VCF was only 0.4% worse than that of the 3770.54, but the engine thrust lapse (TOC to takeoff thrust) decreased to 0.343 as compared to 0.385. The stall margin at cruise also dropped from 23% to 10%. Since this engine is larger than the 3770.54, it was scaled down to the same flow size (800 lbm/s), and the weight was established by the FLOWPATH program. As can be seen in Table 14, at 800 lbm/s the Cycle 1 engine propulsion weight is 4% less than the 3770.54 but it also produces 3% less takeoff thrust and 14% less TOC thrust.

Studies have indicated that a 0.38 lapse is about the minimum required to provide reasonable supersonic thrust margins. If the engine is required to cruise on hot days, the thrust lapse requirement might increase to 0.42 or higher. For this engine to work, the cruise stall margin would have to be increased nearly to the level of the 3770.54. This increase could be accomplished either by putting a variable-area bleed injector (VABI) in the engine or by adjusting the aerodynamic design to produce a higher stall margin. Unfortunately, both of these methods would exact more penalties. The 0.34 thrust lapse of cycle one together with the 10% stall margin at cruise would be unacceptable. From the standpoint of the total aircraft propulsion system, any weight reduction in the Cycle 1 engine would be negated by the loss of thrust at takeoff and TOC.

The Cycle 3 engine was an attempt to follow the same design philosophy as the Cycle 1 but to return the thrust lapse to 0.38. This cycle was designed at 894 lbm/s, but — because of the larger core — the T_4 margin allowed the flow at takeoff to be increased to 920 lbm/s by pushing the throttle. At TOC, however, the Cycle 3 SFC was significantly worse than the Cycle 1 SFC, and the suppressed throat area (AJ2) at takeoff (which drives the nozzle size) had grown considerably.

Cycle 2 (see Table 14) is a 3.91 FPR, 0.46 bypass engine with an airflow lapse of 63%, designed with a thrust lapse of 0.382. This better matches the 3770.54 engine. Just as with Cycle 3, Cycle 2 design flow was 894 lbm/s at a 1.05 extraction ratio, but it had the ability to throttle-push to 920 lbm/s at takeoff. The jet velocity at takeoff matched that of the 3770.54, and the takeoff suppressed throat area was slightly less than that of the Cycle 3 engine. Supersonic cruise SFC was better than that of the Cycle 3 engine but still 1% higher than that of the 3770.54 engine.

Since the Cycle 2 engine is also larger than the 3770.54, it was scaled down to the same flow size (800 lbm/s), and the weight was then set by the FLOWPATH program. As can be seen in Table 14, at 800 lbm/s the propulsion weight of the Cycle 2 engine is about equal to that of the 3770.54 engine, but it produces 1% more thrust both at takeoff and at TOC. From a total aircraft-propulsion-system standpoint, this 1% additional thrust will be more than negated by the 1% SFC penalty. To add to this, the 10% fan stall margin at cruise would still be unacceptable.

Table 14. Summary of the Oversized Fan

Parameter		Base 3770.54	Cycle 1 4161.62	Cycle 1 Scale 4161.62	Cycle 2	Cycle 2 Scale	Cycle 3
Design Point Sea-Level, Static, Standard Day	P16Q56	1.05	1.15	1.15	1.05	1.05	1.13
	BPR	0.5364	0.618	0.618	0.455	0.455	0.462
	OPR	19.68	21.785	21.785	20.53	20.53	20.24
	FPR	3.7	4.07	4.07	3.91	4.1	
	T_{T4} (°R)	3086	3216.2	3216.2	3107.3	3107.3	3126.5
	$T_{T4.1}$ (°R)	2840	2958.3	2958.3	2860.9	2860.9	2877.3
	W2AR (lbm/s)	800	920	800	894.25	800	894.25
	SM Fan	24.8	24.8	24.8	24.8	24.8	24.8
Projected Propulsion Weight at 800 lbm/s	Engine	8845		8581		8833	
	Nozzle at 2.9	7830		7360		7870	
	Total	16675		15941		16703	
Sea Level, Mach 0.3, Standard Day +18°F	FNMIX (lbf)	54300	60493	52603	61518	55034	61474
	W2AR (lbm/s)	823	919.2	799	920	823	920
689-ft, Mach 0.32, Standard Day +18°F	T_{T4} (°R)	3460	3458.9	3458.9	3424.9	3424.9	3449.6
	SM Fan	19.99	19.93	19.93	24.2	24.2	24
	P16Q56	1.029	1.098	1.098	1.05	1.05	1.13
	A8CD (in^2)	1258.7	1361	1183	1414	1265	1434
	AJ2 (in^2)	1292	1397	1215	1451	1298	1472
	T_{T8} (°R)	1745	1690.7	1690.7	1747.9	1747.9	1756.8
	P_{T8} (psi)	52.18	53.04	53.04	52.02	52.02	51.43
	VJIP (ft/s)	2557	2529	2529	2558	2558	2556
	W2AR (lbm/s)	823	920	800	920	823	920
	FPR	3.97	4.24	4.24	4.05	4.05	4.26
	Efficiency	0.8566	0.8594	0.8594	0.825	0.825	0.8127
55,000-ft, Mach 2.4, Standard Day	T_{T3} (°R)	1660	1659.8	1659.8	1658	1658	1660
	T_{T4} (°R)	3460	3460	3460	3460	3460	3460
	$T_{T4.1}$ (°R)	3210	3210.4	3210.4	3211.4	3211.4	3211.2
	P16Q56	1.165	1.224	1.224	1.085	1.085	1.176
	W2AR (lbm/s)	560	560	487	560	501	560
	F_{NP} (lbf)	20886	20751	18044	23499	21022	23388
	SFC_{STW}	1.2237	1.2284	1.2284	1.2367	1.2367	1.2427
	$F_{N lapse}$ (lbf)	0.385	0.343	0.343	0.382	0.382	0.38
	T_{T8} (°R)	1748	1745.8	1745.8	1861.8	1861.8	1861.7
	P_{T8} (psi)	31.48	31.12	31.12	33.93	33.93	33.26
	$T_{T4.1}$ Throttle Ratio	1.130	1.085	1.085	1.123	1.123	1.116
	A_{16} (in^2)	475	436.5	379.6	455	407.0	361.8
	SM Fan	22.9	9.7	9.7	9.9	9.9	8.8

In conclusion, there does not appear to be any system advantage to oversizing the fan. The oversized fan cycles described above tend to be no different than scaling up the engine with a different airflow lapse. The oversize-fan engines provide no thrust margins for the propulsion system. This does not mean that an actual product would not have to oversize the fan or the core to produce margins that can be held in reserve for hot-day requirements, growth, or uncertainty. Margins are a different issue and will never show a MTOW advantage unless they are part of the system requirements.

3.2 Cycle and Flowpath

3.2.1 Technology Concept Aircraft (TCA)

In 1994, at the beginning of the CPC contract, there were two airframe configurations, the Boeing Commercial Aircraft Group (BCAG) *Reference H* and the McDonnell Douglas Corporation (MDC) *M2.4–7A Arrow Wing*. These two configurations had different requirements, making selection of a single engine baseline difficult. Since the two companies were partners in the HSR program, they agreed to work towards a common HSR baseline for the NASA program. Together they worked out common design approaches, bookkeeping systems, mission sizing rules and methodologies, and finally aircraft configuration. The first of these common industry baselines was designated *Interim Baseline Reference H* (BCAG configuration 1080–1410). This was followed by the *Industry Method Test-bed* (IMT or BCAG configuration 1080–1404). The IMT was used by GEAE, NASA, MDC, and BCAG to resolve differences between analytical methods and ensure that all HSR participants could arrive at very similar system solutions when using the same information.

Work on these configurations, plus a number of additional planforms, lead eventually to an official HSR common baseline at the end of 1995. This was designated the *Technology Concept Aircraft* (TCA). The TCA design assumptions were based on aerodynamic testing, computational fluid dynamics (CFD), mechanical design, and sizing trade studies. Further, more detailed, studies modified and improved the TCA design, resulting in an updated final configuration in late 1996. All propulsion system studies from 1994 to 1996 were aimed at defining the optimum engine configuration for this aircraft.

3.2.1.1 Engine Study Matrices

1994 Engine Study Matrix

As noted earlier, HSR Phase 1 had downselected to an MFTF engine with a mixer/ejector (M/E) nozzle as the propulsion concept for HSR Phase 2, but there were still a number of unknowns to be dealt with. The inlet concept, which would directly affect the air flow and pressure going into the engine, had yet to be determined. Of primary concern when setting thrust at top of climb (TOC) is the inlet flow lapse (maximum corrected airflow at TOC over nominal engine corrected airflow at the sea-level static design point). The inlet pressure recovery also has an impact on TOC thrust.

Another area of uncertainty was the relatively immature M/E nozzle concept. The design philosophy for this concept was still evolving in terms of setting the nozzle length and the suppressor area ratio for optimum performance and acoustic suppression. The mechanical configuration for best implementing and integrating the suppression system while optimizing performance, weight, and life was also still in development. Much of the research for the M/E nozzle concept was concurrent with system studies; hence, assumptions were continuously changing. Each time the expected suppression capability changed, either the nozzle size or the takeoff jet velocity had to change. A number

of alternative nozzle concepts were still being considered, ranging from a simple performance nozzle with no suppression capability to more sophisticated axisymmetric nozzles with limited suppression capability — axisymmetric coannular ejector, fluid shield etc.

In addition to these propulsion uncertainties, the airframe configuration, high- and low-speed characteristics, and exact methodology for flying and sizing the aircraft were also evolving. The airframe design team was concerned with these unknowns and also about the size, weight, and complexity of the M/E system.

For these reasons, it was determined that a wide range of MFTF designs had to be generated to cover the wide variety of potential thrust and jet velocity requirements. It was also decided that a matrix of engines would provide the capability of better optimizing the propulsion system characteristics for whatever concept was being studied. The 1994 HSR engine matrix that evolved to meet all these needs is shown in Figure 23. This matrix covers a range of SLSS fan pressure ratios (2.9 to 4.3) and inlet corrected flow lapses from takeoff to TOC (0.65 to 0.75).

Basically, the FPR is setting the ideal primary jet velocity at takeoff, and the flow lapse is determining the TOC to takeoff thrust-lapse. Principal cycle design assumptions were the desire to maintain a 25% stall margin to provide adequate operability margins and a 1.05 extraction ratio (ER) at maximum power. The ER is simply P_{16}/P_{56}, the ratio of the pressure coming out of the bypass duct to the pressure coming out of the core before it is mixed (sometimes referred to as the mixing-plane pressure ratio). At the TOC design point, maximum turbine rotor inlet temperature (T_{41}) was set at
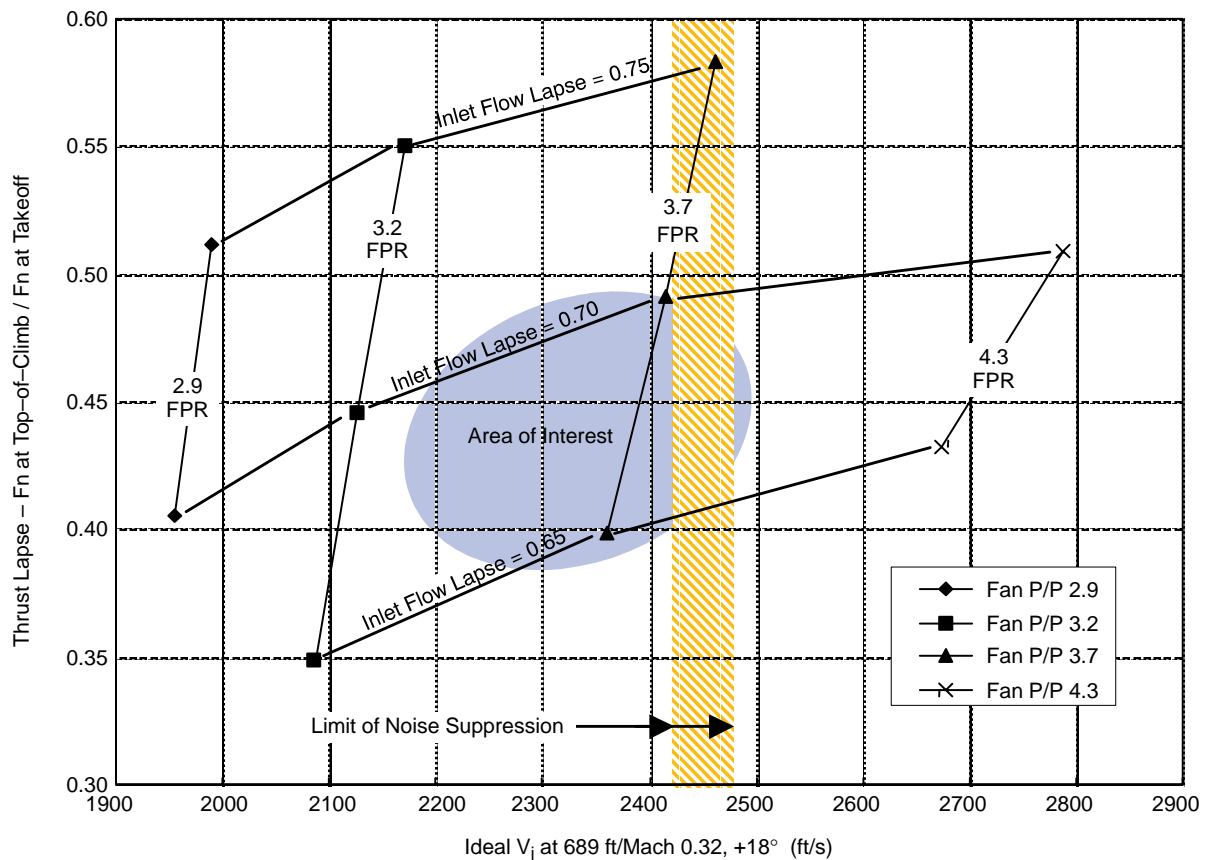
Figure 23.   Engine Matrix, 1994

2800°F, and the maximum compressor exit temperature (T_3) was set at 1200°F to satisfy mechanical design and life concerns.

Any engine in this matrix can be designated by the FPR, the flow lapse, and the suppression. For example, 3770.100 means an engine with a 3.7 FPR at 70% flow lapse with a nozzle designed to meet FAR Stage III sideline noise levels with the engine operating at 100% takeoff power. Nozzle suppression and engine characteristics can then be traded to determine the best propulsion system to meet airframe requirements for a particular configuration.

Nozzles with downstream mixers (DSM) were designed for these engines at three levels of noise suppression (ejector flow entrainment): Separate nozzles were designed to meet FAR Stage III sideline noise levels with the engine operating at 80% takeoff power, 100% takeoff power, and 110% jet velocity (at 689-ft altitude, Mach 0.32, standard day +18°F ambient temperature). These nozzles were later updated and designated "Best" DSM or BDSM. A number of axisymmetric and 2D nonsuppressing performance nozzles were also designed for these engines to allow quantification of the acoustic suppression penalty in meeting the HSCT noise requirements. These nozzles also made it possible to explore the possibility of finding a simpler, nonsuppressor-nozzle solution to meet noise requirements.

Early studies with these engines indicated that it was best to keep the FPR up near the noise suppression limit for the nozzle. Hence, the best system solutions were typically near 3.7 FPR. The BCAG *Reference H* aircraft tended to favor the 3770.100 engine (3.7 FPR at 70% flow lapse with a 100% nozzle). On the other hand, the MDC *Arrow Wing* aircraft favored the 3765.100 engine, and eventually propulsion studies at both BCAG and MDC also favored the thrust-lapse of the 3765.100 engine with the latest BDSM nozzle. The 3765.100 also remained the favored baseline engine on the interim baseline aircraft configuration.

Studies using the simple "performance nozzle" (without noise-suppression features) showed that, in order to achieve the desired noise levels, the engine had to have a very low FPR but the engine airflow had to be very large. This meant that a large fan was required, which resulted in a very heavy, uneconomical aircraft. None of the simple performance nozzle configurations analyzed could meet the HSCT noise requirements at any size when used with the 2.9 FPR. Therefore, a much lower FPR than 2.9 was required if the simple nozzle was used, and this would have made the vehicle much heavier. Studies with the simple performance nozzles showed that the penalty for the amount of acoustic suppression needed was approximately 7% of the MTOW. The studies also proved that the optimal range for the FPR was the same with simple performance nozzles as with acoustically suppressed M/E nozzles.

1996 Engine Study Matrix

The 1994 matrix focused on systems that used MFTF engines with M/E nozzles (Figure 24). It was decided to investigate these engines more carefully. Studies up to this point had proved that takeoff requirements were the prime factor in determining the low-pressure spool design parameters (FPR and airflow size). The TOC thrust requirement sets the engine bypass ratio. In the 1994 engines, the TOC thrust requirement had been set by adjusting the air flow lapse. At the time, the thrust-lapse of the 3765.100 system appeared to be attractive in most system studies, but there was concern about the 65% flow lapse requirement. It was determined that none of the inlet concepts being studied could handle a 65% flow lapse. Considering this, it was decided that a 70% flow lapse engine would be more desirable since it would match (or accomodate) any of the inlet concepts being considered.
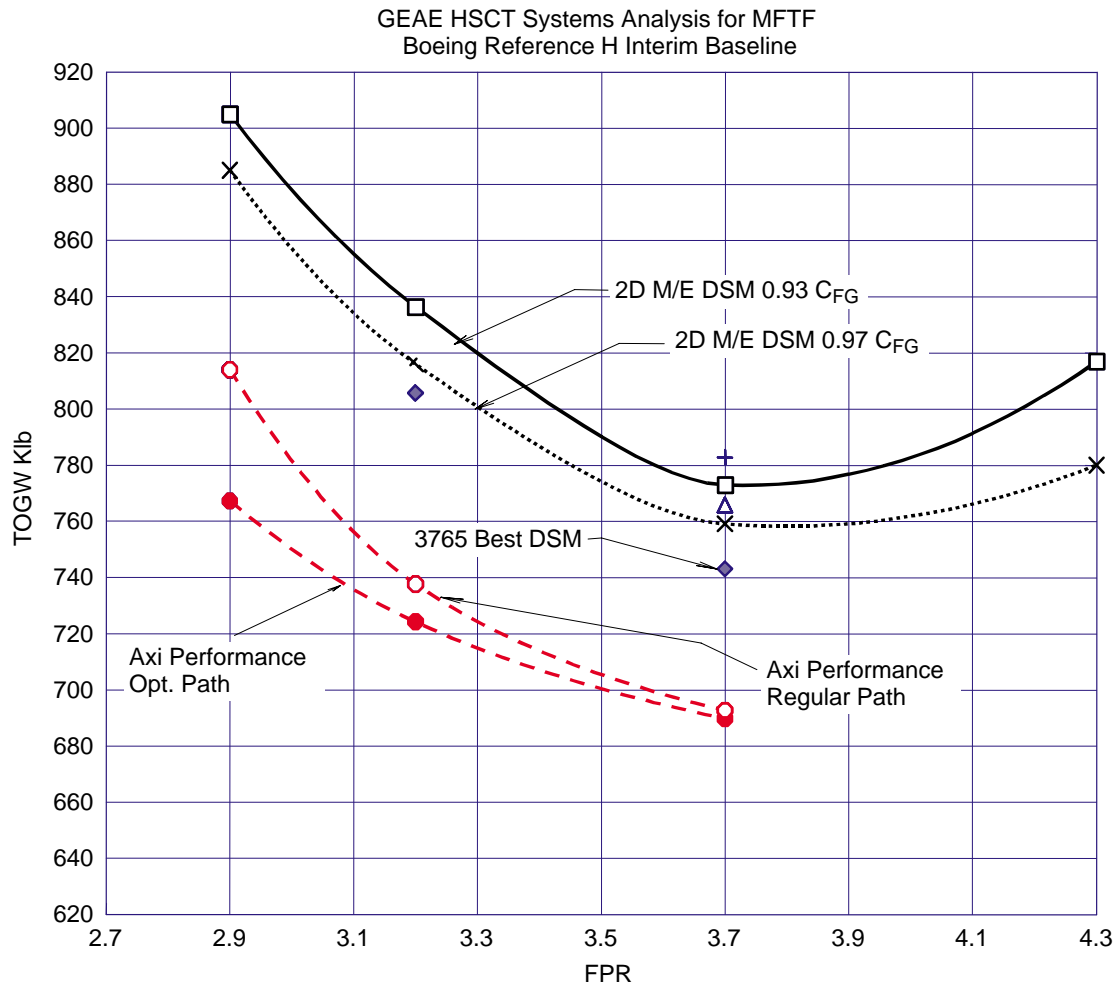
Figure 24. System Study Results for the 1994 Matrix

A study was launched to find out if there were other ways to set the thrust-lapse or BPR other than by adjusting the airflow lapse. The maximum T_3 and T_{41} temperatures depended on mechanical design considerations, and these could not be changed, but it was found that the stall margin and the ER could be increased above the minimum 25% and 1.05 limits.

Figure 25 shows the results of a study that used a constant 70% airflow lapse with varying stall margin and TOC ER. In the figure, when the airflow lapse is constant, any thrust-lapse value can be achieved at a higher BPR simply by varying the ER. it should be noted that the higher BPR provides a smaller core, which typically improves both the weight and the SFC of the engine. This technique was used in the design of the next engine matrix.

As a result of these early studies, a new matrix was produced in late 1995 and 1996 (Figure 26). This new matrix covered a smaller range of FPR (3.5 and 3.7) and inlet flow lapses (0.65 and 0.70). The matrix added TOC extraction ratio variations to facilitate thrust matching independent of flow lapse. Engine designations within this matrix take the form: *FPR, flow lapse . BPR*. For example, *3570.80* refers to a 3.5 FPR, 0.70 flow lapse engine with 0.80 BPR.
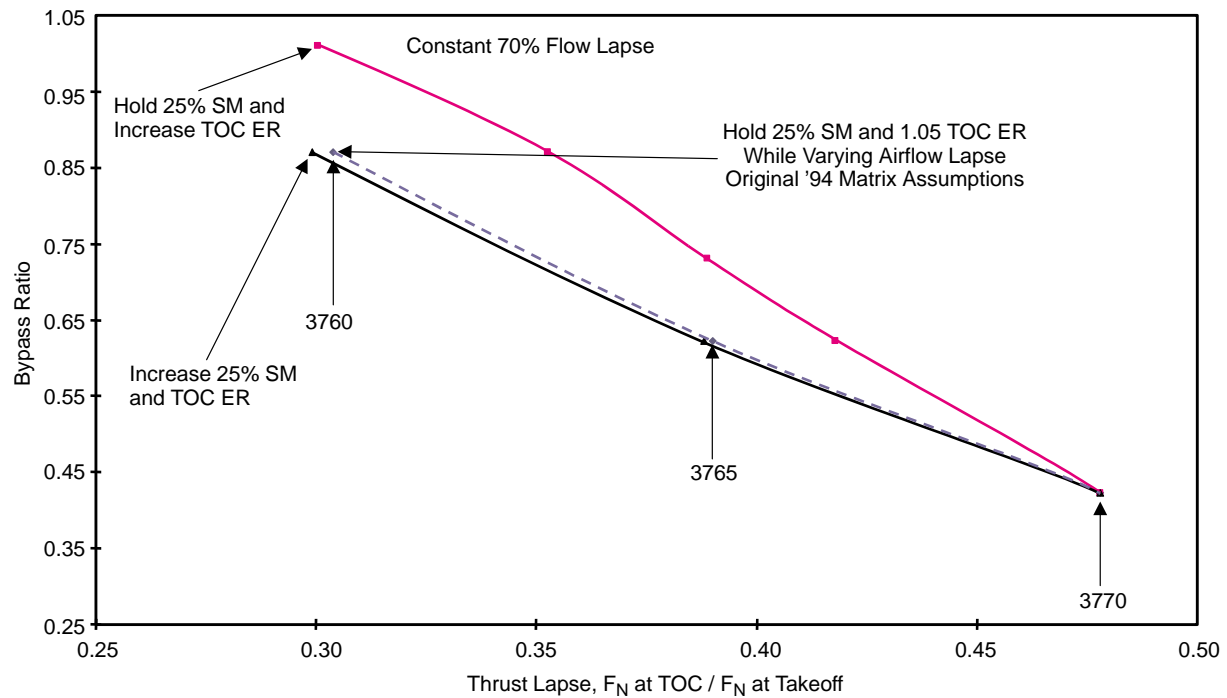
Figure 25.   Bypass Ratio vs Thrust-Lapse
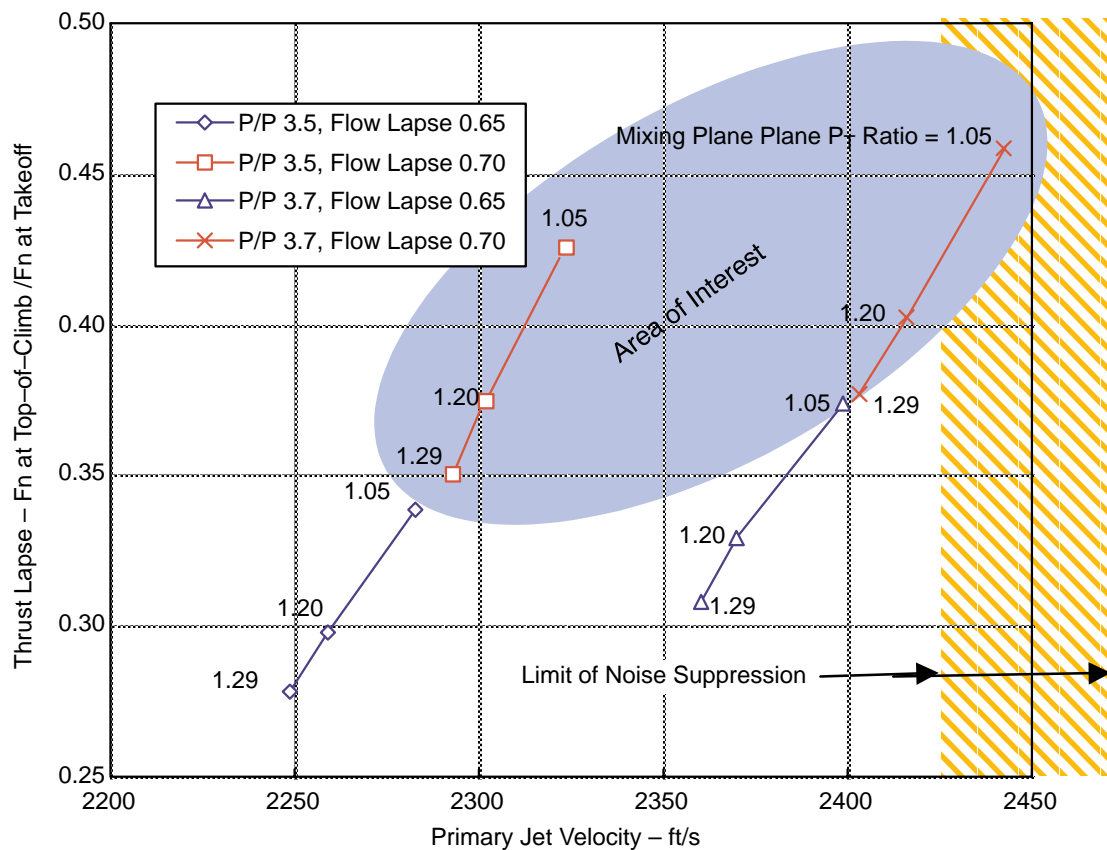
Figure 26.   Engine Matrix, 1996

Noise Level Change

In 1995, more emphasis was placed on reducing community noise at takeoff cutback. At that time, the noise goals for the program had been to achieve FAR 36 Stage III levels with a 1-dB margin for sideline, community, and approach. The Environmental Impact (EI) team convinced the program managers that this goal would not be sufficient, so the community goal at takeoff cutback was dropped from –1 dB to –3 dB. It was later felt by many that eventually a –5 dB margin would be required for community noise levels. This change in noise goals plus concern about the size of the M/E nozzle required for the 3.7 FPR engines prompted exploration of the possibility of changing the baseline engine to a 3.5 FPR. Figure 27 shows sizing comparisons between the interim baseline engine and the IMT engine. As shown in the figure, when the engines are performance sized the 3.7 FPR engine is superior, but when the engines are sized acoustically (to Stage III –1 dB sideline and –3 dB community) the two engines appear almost equal. Because of the lower acoustic suppression risk presented by the lower jet velocity cycle, the 3570 engine with the most aggressive or "Best" DSM nozzle (BD3570) was chosen to be the HSR baseline engine for the first TCA.

As research progressed on the IMT for the first TCA, projected drag estimates worsened. It became apparent that the original 3570.80 engine would not achieve a reasonable MTOW. More thrust was needed along the entire flight path, and the change in thrust could not cause changes in the propulsion system size and weight. Figure 28 shows an installed thrust comparison of the five engines that were considered for use on the TCA.

The original 3570.80 engine was selected because it yielded a lower TOGW than the 3765.65 engine when sized to a –5 dB community noise level, although when performance-sized the 3570.80 yielded a heavier TOGW. On the last IMT, the 3570.80 did not fare as well, because takeoff and transonic thrust requirements had increased.

Nozzle Selection

Based on the 1995 nozzle downselect, a fixed-chute nozzle was designed for use with the TCA engine — which changed the designation to FC3570.80. This new FC3570.80 engine was designed to use a significant throttle push (fan overspeed) at takeoff and through transonic speeds until it reached the maximum airflow the inlet could handle. This new FC3570.80 engine increased the FPR at takeoff to about 3.7 at 839-lbm/s airflow and 109% corrected speed. These changes resulted in 11% more takeoff thrust. The engine also had 15% more thrust at Mach 1.1 and only a minimal penalty on thrust and SFC (0.3%) at cruise speed when compared to the original BD3570.80 (see Figure 28).

To deal with the higher takeoff jet velocity, the engine control system implemented a programmable lapse rate to slow down the fan to 100% of the corrected speed and thereby reduce jet velocity at the sideline noise-measuring point. The nozzle aerodynamics group also improved the supercruise coefficient of gross thrust of the FCN nozzle by almost 0.5%. These changes provided a significant improvement in MTOW when compared to the original BD3570.80 engine. This engine was one of the first produced from the new matrix. The fan overspeeding technique developed for this engine was later adopted for use with all the engines in the matrix, although after review it was decided to limit fan overspeeding to 105% of normal speed or about 3% more air flow than nominal because of specific flow limitations. The thrust characteristics of this new engine are shown in comparison to nonoversped engines in Figure 28.
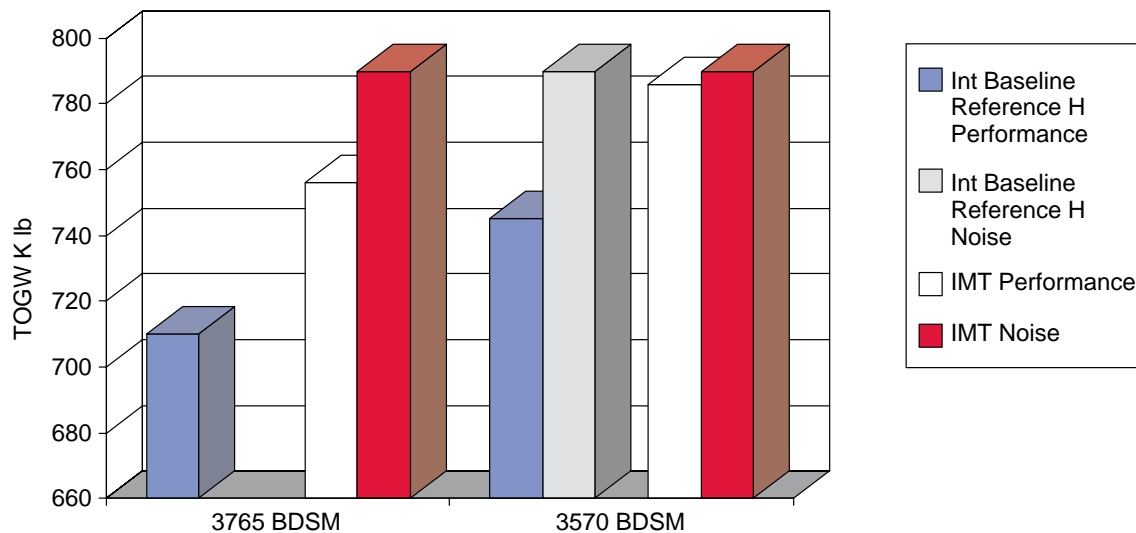
Figure 27.   Impact of New 3570 Baseline on System Studies
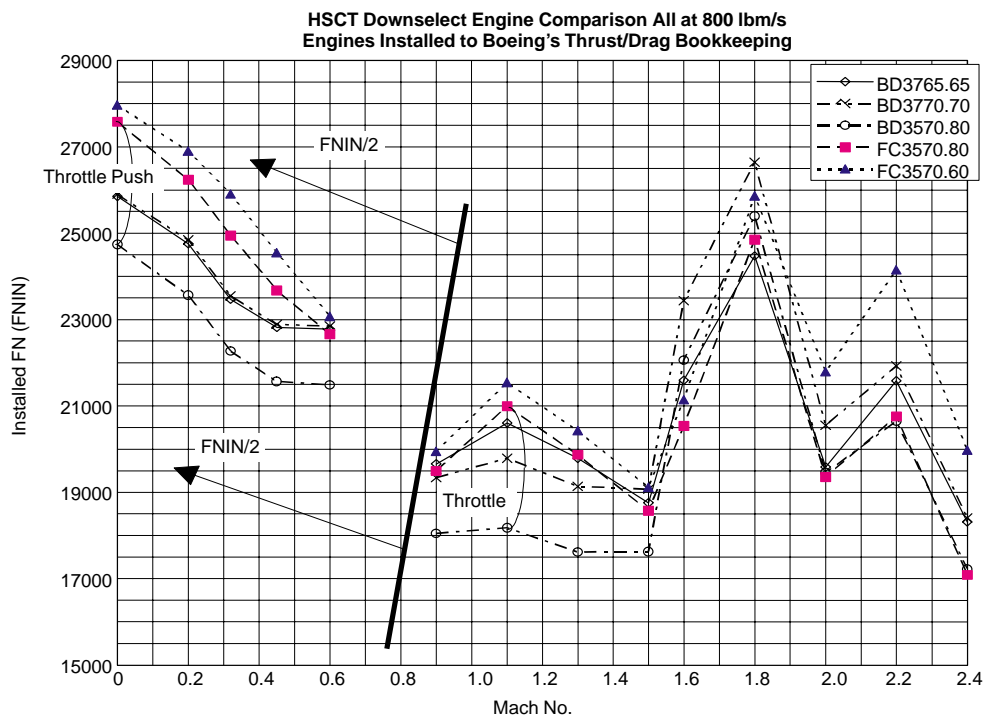
Figure 28.   Impact of Fan Overspeed on Cycle Performance

Interim TCA

The first or "interim" TCA was defined in late 1995 to meet the HSR Level 1 milestone. This interim TCA (Figure 29) weighed 783,000 lbm MTOW using the FC3570.80 engine described above. When Boeing and MDC agreed on drag and weight for the TCA, technology projections became more aggressive. The goal for high-speed drag reduction was increased another 3 to 4%, and a policy was established to minimize structural weight increases during the structural design review process. In April 1996, this new approach brought the TOGW of the TCA (with FC3570.80) down to about 740,000 lbm. This interim TCA was sized to meet FAR 36 Stage III –1 dB at sideline, –3 dB at cutback noise requirements and all other mutually agreed on sizing criteria shown in Figure 30).
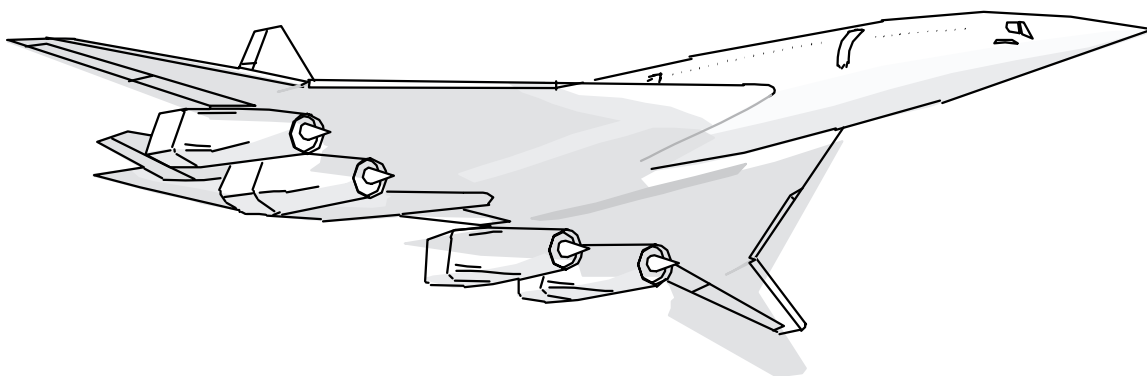
Figure 29.   Late 1995 Interim Technology Concept Airplane

Data Packs

After definition of the first TCA, work progressed on the actual definition of the matrix of engines identified in Figure 26. Because of the three-dimensional variations, this engine matrix was dubbed the "Brick" (see Figure 31). Inlet airflow ratio varies along the X axis while FPR varies along the Y axis. The three levels of ER at TOC are shown along the Z axis. BPR values for each engine are shown in parenthesis. As can be seen in the figure, ER at TOC sets the BPR at a constant airflow lapse. Figure 32 shows how this impacts the thrust lapse. For this study, the fixed-chute nozzles were designed at three levels of acoustic suppression (SAR = 2.5, 2.7, and 2.9) but were not designed for a specific throttle position as in the earlier configuration. The three levels of nozzle suppression (ejector flow entrainment) at each cycle were developed to allow proper matching of acoustic suppression to the specific engine. The throttle position for the PLR and community (cutback) would develop naturally depending on the noise requirements and engine/nozzle/aircraft combinations. These propulsion systems could be sized up or down together with the aircraft wing to define the best overall combination to minimize MTOW for the sizing requirements shown in Figure 30.

Thirty-six data packs were produced from the 1996 brick matrix, each corresponding to one of the engine values noted in the matrix. Figure 32 shows the results of the brick evaluation done by both Boeing and GEAE to determine the best propulsion system for the 1996 TCA. All these aircraft were sized to Stage III –1 dB sideline and –3 dB community. The results showed that most of the 65% flow lapse engines had high nacelle drag and suffered from a lack of TOC thrust. Only the ones designed at a TOC ER of 1.05 could be sized to a reasonable MTOW. The 3765.61 was the closest engine to the old 3765 baseline and proved to be the best of the 65% flow lapse engines. In general, the 70% flow lapse engines performed better than the 65% flow lapse engines. The 2.7 SAR nozzles

Figure 30.   HSR Sizing Criteria
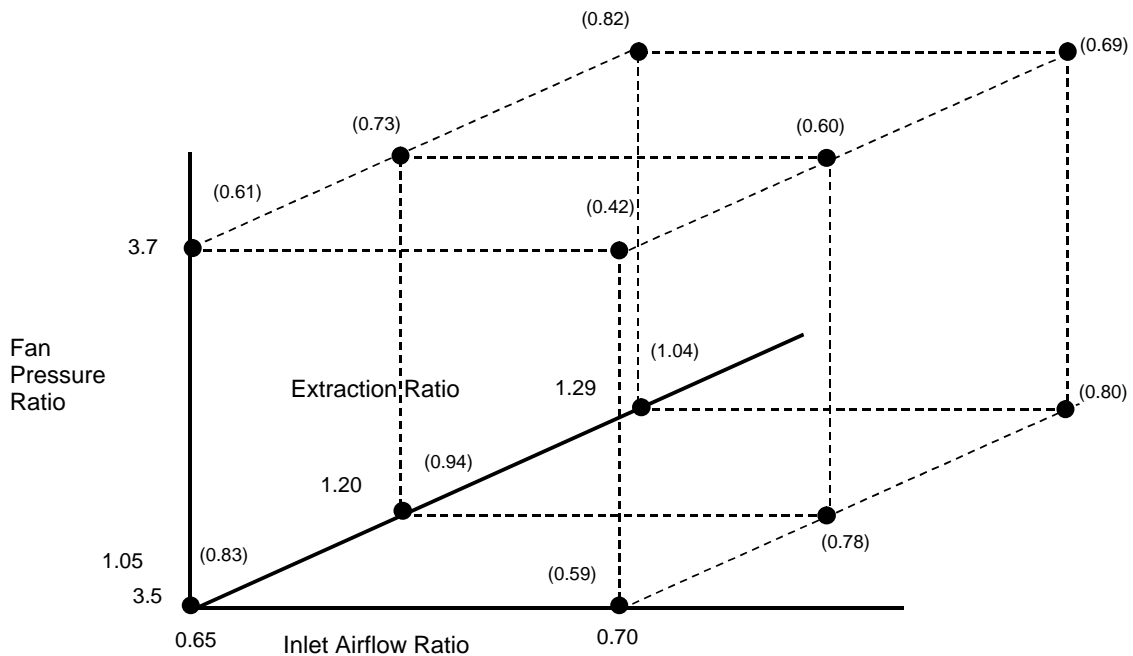
Figure 31.   The 1996 Brick
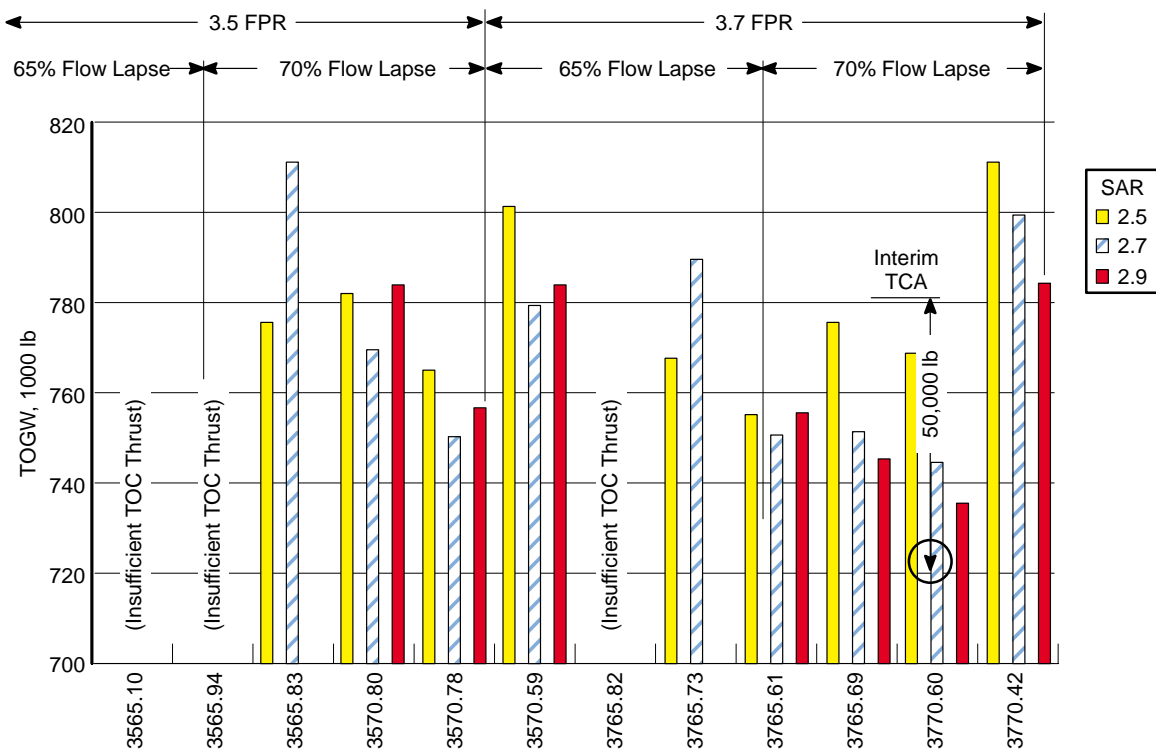
Figure 32.   Evaluation of 1996 Brick on TCA

were found to work better on the 3.5 FPR engines with little or no PLR required. The 2.9 SAR nozzles proved better on the 3.7 FPR engines, but typically these required about a 10% PLR to meet the sideline requirement. The 3770.60 engine with a 2.9 SAR FCN produced the lowest MTOW (under 740,000 lbm).

During evaluation of the data packs, it was determined that the 70% flow lapse 3.7 FPR series engines were less likely to be limited in the amount of climb thrust they produced. Also, a 70% airflow lapse is achievable with all inlet types. Figure 33 shows sized trends for the TCA 70% flow lapse at 3.7 FPR propulsion systems. This figure shows that 2.9 SAR FCN offered the best weight-to-noise-suppression trade for the 3.7 FPR engine, and the 3770.60 yields the lightest airplane. This engine was chosen for the 1996 update that produced the interim TCA.

3.2.1.2 Updated TCA Definition

In 1996, the airplane sizing thumbprint was determined for the updated TCA (see Figure 34). The pertinent characteristics of the sized configuration are shown in the box to the right. This updated TCA had a 2.0 aspect ratio wing planform with 52° outboard-swept wing panels. The propulsion system was the 3770.60 engine with a 2.9 SAR fixed-chute nozzle. This updated aircraft was sized to meet FAR 36, Stage III noise margins of –1 dB sideline and –3dB community.

Updated TCA Engine Description

The baseline engine for the final TCA was the GEAE/P&W FCN3770.60: a Mach 2.4, dual-spool, mixed-flow turbofan with a 2.9 SAR fixed-chute mixer/ejector nozzle. Engine maximum takeoff is
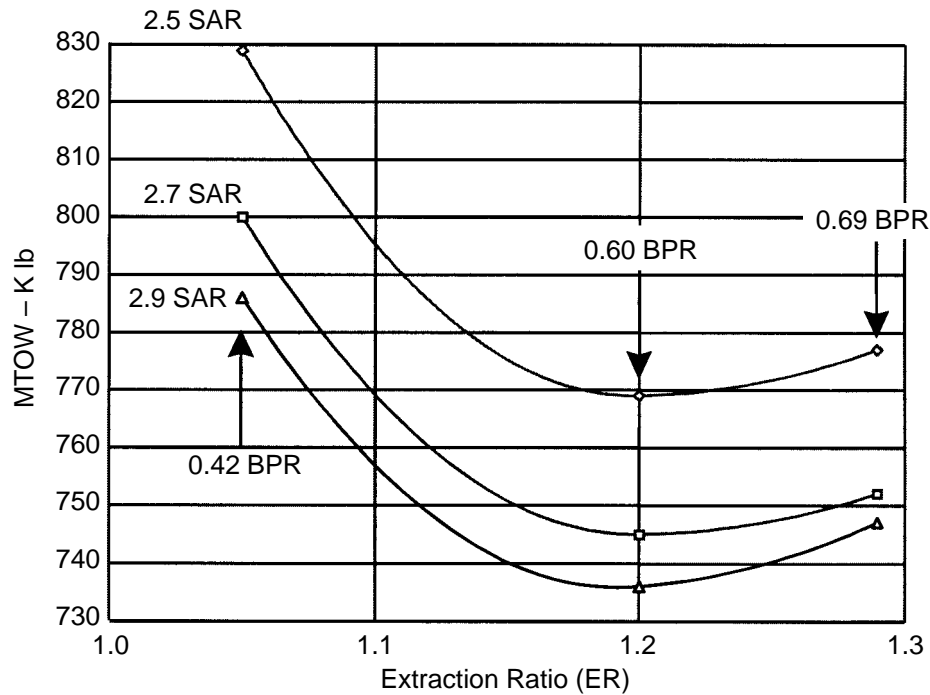
Figure 33.   MTOW Matrix for 3.7 FPR at 70% Flow Lapse

MTOW	736,000 lb
Wing Area	8,350 ft^2
Range	5,000 nm
Payload	63,000 lb
Engine Thrust	54,000 lb/eng
Engine Airflow	754 lbm/s
OEW	315,000 lb
Block Fuel	318,000 lb
Reserve	42,800 lb
Block Time	5 hr 15 min
Climb Time	35 min
T/O FL, act.	10,000 ft
(1st and 2nd segment grad based on 10,800 ft FL)	
V$_{approach}$	154 KEAS
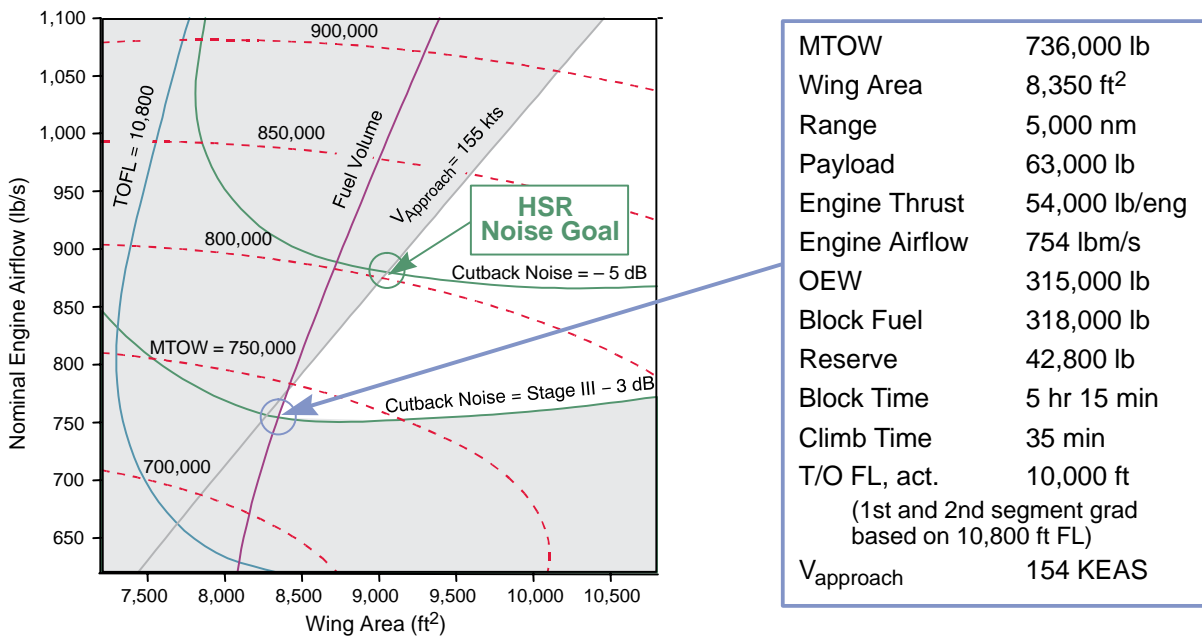
Figure 34.   Thumbprint of TCA Engine

rated below Mach 0.45 to match inlet capability. Maximum takeoff rated power increases airflow from 800 to 823 lbm/s at sea-level static Other salient engine design characteristics are as follows:

- Three-stage fan
- Five-stage high-pressure compressor
- Single-stage high-pressure turbine
- Two-stage low-pressure turbine

Engine Performance Characteristics

Cycle characteristics for design reference conditions (SLS +18°F, ejector deployed), are:

- Reference corrected inlet airflow   800 lbm/s
  (at 100% corrected fan speed)

- Fan pressure ratio   3.7

- Overall pressure ratio   21.8

- Bare engine weight   8070 lbm

- Max turbine rotor inlet total temperature (T_{41})   2800°F

- Max compressor discharge total temperature (T_3)   1200°F

- Customer bleed from HPC   1 lbm/s

- Power extraction   200 hp

- Installed net thrust   57703 lbf

Baseline Nozzle Concept

The baseline nozzle concept used with the final TCA engine was the 2D FCN with mixer/ejector suppressor (Figure 35). The mixer design has two banks of chutes totalling 20 secondary chutes and 18 primary chutes, plus 4 half primary chutes sized for a suppressor area ratio of 2.90. The nozzle has an isolated maximum cross-sectional area of 6911 in^2. The aspect ratio of the nozzle operating at a mixer area ratio of 0.95 is 1.5.

The advantages of the FCN design are:

1. No plug- or splitter-associated cooling problems.

2. Fixed chutes reduce design complexity and required sealing.

3. Ejector inlet and reverser ducts are separate and can be optimized for each function.

4. Acoustic liners are always in low-pressure area.

5. Single-piece divergent flap simplifies nozzle actuation.

6. Convergent flap also serves as reverser blocker.

7. Concept has demonstrated good potential through system studies and model-scale testing. Concept should meet and exceed HSCT acoustic and performance goals.

The materials used to fabricate this nozzle are consistent with 2001 technology. The nozzle design uses engine bay purge flow to cool various elements and ensure that they meet durability requirements. Nozzle weight is based on engine manufacturer's estimates. The nozzle external flap lines

Takeoff

Subsonic Cruise

Supersonic Cruise

Reverse
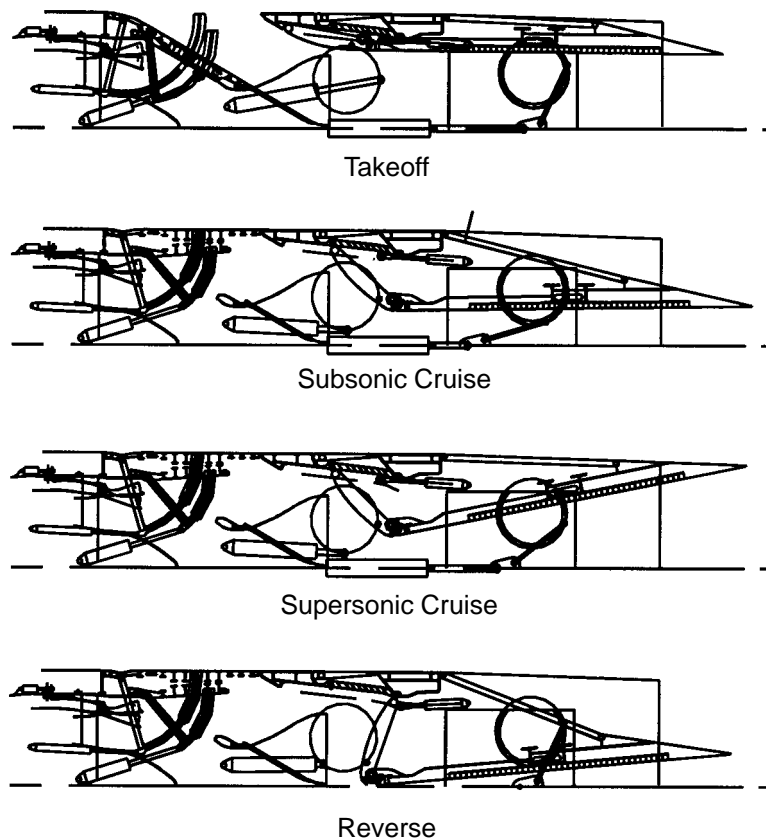
Figure 35.   Fixed-Chute Nozzle Configuration

are designed to meet the 4° local boattail requirement; however, the sidewall closeout angle exceeds this requirement.

The FCN was designed for use with the 3770.60 MFTF. The nozzle thrust coefficient for sideline (M 0.32, 689 ft) at maximum power is 0.946. The nozzle thrust coefficient for cruise (M 2.4, 60,000 ft) at maximum continuous power is 0.983. The 2.9 suppressor area ratio aspirates 70%, relative to engine mass flow, at full power. This aspirated flow mixes with the engine flow in the 120-in long mixing duct and reduces jet velocity at the ejector exit to acceptable levels. Internal shocks and mixing of the engine and aspirated flows produces internally generated noise that is held at acceptable levels by acoustic lining in the ejector. The effective acoustic lining is 4.0 times the ejector flow area (A_{mix}) and begins 10 mixing lobe widths downstream of the mixer exit. The minimum mixing duct length is set by aerodynamic performance considerations. If the resulting treatment area proved to be insufficient, length was added. In the 3770.60 case, the minimum (aerodynamic performance) length and the length required for acoustic treatment were essentially the same.

Inlet Configuration

The inlet for the TCA was a mixed-compression, axisymmetric, translating-centerbody design. The inlet and cowl are constructed of titanium. A vertical cross section view of the inlet is shown in Figure 36. The main components of the inlet are as follows.
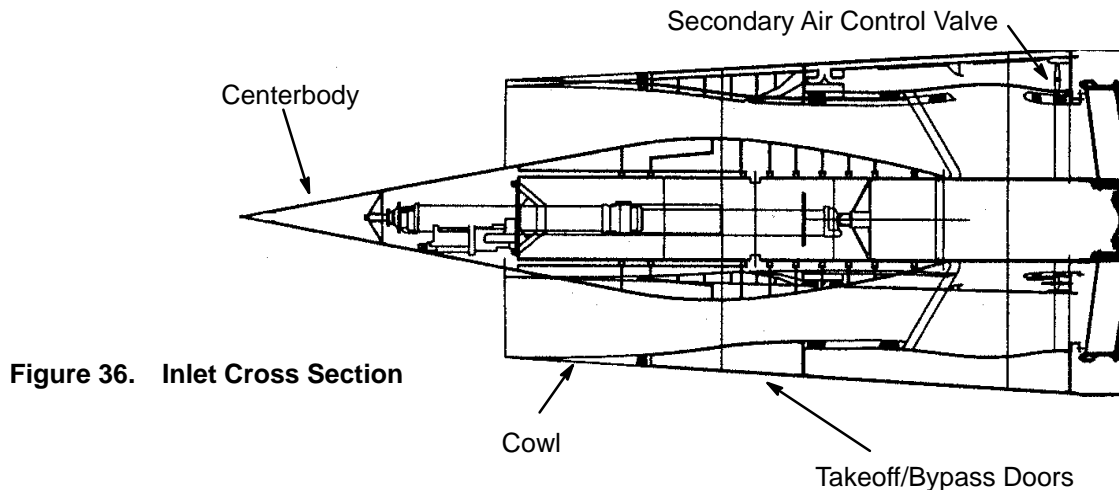
Figure 36.   Inlet Cross Section

Cowl: The cowl has a sharp leading edge. The supersonic diffuser and throat regions of the internal cowl are perforated with bleed holes, and a bleed slot is located at the throat. The cowl contains four bleed compartments with individual overboard exits. The cowl also houses six fluidic vortex valves. The internal surfaces of the aft cowl are lined with acoustic absorbing material.

Takeoff/Bypass Doors: Near the engine face the cowl contains six blow-in type auxiliary inlet doors, located circumferentially, to be used during takeoff. These doors are self actuating but may require return springs. In tandem with each takeoff door is an outward-opening bypass door to be used during supersonic flight. The bypass doors require continuous control and actuation.

Centerbody: The centerbody slides forward from the cruise position by a distance of 1.35 cowl lip radii for low-speed operation. The centerbody support tube is attached to the cowl structure by radial struts. The centerbody requires continuous control and actuation during operation above the starting Mach number of 1.6. The centerbody surface is perforated with bleed holes. Eight bleed plenums are separated by bulkheads. Bleed air is vented overboard via the support tube and support struts.

Secondary Air System: A secondary air control valve assembly has been incorporated into the baseline inlet design to control the flow of inlet air into the engine compartment bypassing the compressor. The capacity of the system has not been determined since engine/nacelle and nozzle cooling requirements have not been defined.

Inlet Performance

- Design Mach number   2.35
- Starting Mach number   1.6
- Cruise total pressure recovery   93%
- Cruise bleed mass-flow ratio   0.041
- Cruise/transonic corrected flow supply ratio   0.70

Excess inlet flow is spilled below Mach 1.2 and is bypassed above Mach 1.2. With the engine at takeoff power setting, auxiliary inlets are required below Mach 0.25.

Additions to the 1996 Brick

In 1997 the system studies matrix was extended in an attempt to locate the optimum FPR for the HSCT. The original 1996 Brick showed only the 3.5 and 3.7 FPR, but additional engines were added to the Brick at a 3.8 and 3.9 FPR in an attempt to find the best engine with the lowest MTOW. This addition to the chart is shown in Figure 37. The engines shown had 2.9 and 3.1 SAR fixed-chute nozzles designed for them.

These engines were sized on the updated TCA to FAR 36, Stage III –1 dB sideline and –3 dB community standards just as the rest of the Brick. Results are shown in Figure 38. The trends for the 1997 Brick matrix at a 70% flow lapse show that at this point the best choice engine would use a 3.8 FPR at a 1.29 ER with a 2.9 SAR fixed-chute nozzle.

Even though the 3.8 FPR engine came out better in this study, there was reluctance to change the HSR baseline from the 3770.60. The PLR for the 3870 engine had increased to 14% compared to a 7% rate in the 3770.60. The acoustics group had wanted to keep this PLR below 10%. A number of design changes were evaluated that could have impact. Engine weights were reevaluated to set a new propulsion baseline, and new nozzle design criteria were developed. Basic cycle assumptions were also reevaluated. System noise, particularly at sideline, was felt to be too optimistic, and a major update was expected for 1998. For that reason, the1997 HSR baseline remained the 3770.60.

3.2.1.3 Cycle Development – TCA

It was decided at the GEAE/P&W team meeting in November of 1993 to achieve common performance cycle modeling between the companies. To do this, a set of ground rules was established such that, when either GEAE or P&W defined a cycle, the model-producing cycle output of the other company would be consistent with it. This was necessary to avoid duplicate efforts between the two companies.

Once the cycle output was established, it was decided that P&W would provide cycle performance studies of the MFTF (the primary concept chosen from the 1993 downselect process) and GEAE would provide cycle performance studies of the fan-on-blade (Flade) engine (the backup concept from the 1993 downselect process). Each company could then be confident that the other's output would be consistent with theirs, if they were to execute their model. Figure 39 illustrates the paths used in cycle matching.

Working together, GEAE and P&W developed preliminary MFTF cycle requirements. A matrix that included the optimum Mach 2.4 MFTF cycle selected for the TCA was developed from these requirements and provided to NASA, Boeing, and McDonnell Douglas. Multiple fan pressure ratios, inlet corrected airflow rates (W2AR), and lapse rates (TOC W2AR/design W2AR) were considered to ensure coverage of both Boeing's and McDonnell Douglas' requirements for the TCA.

Parameter Selections

The rates for the fan inlet corrected airflow were selected based on the results of the 1993 systems analyses of similar cycles. The cycles were selected to cover the range of thrust lapse (net thrust at top of climb Mach 2.4 / net thrust at sea level takeoff Mach 0.3) from 0.35 to 0.57.

Boeing's mixed compression, translating centerbody No. 2 inlet and P&W's downstream mixer nozzle were selected for the July 1994 MFTF data packs. GEAE's fixed-chute nozzle with plug was selected for use in the additional November 1994 MFTF data packs.
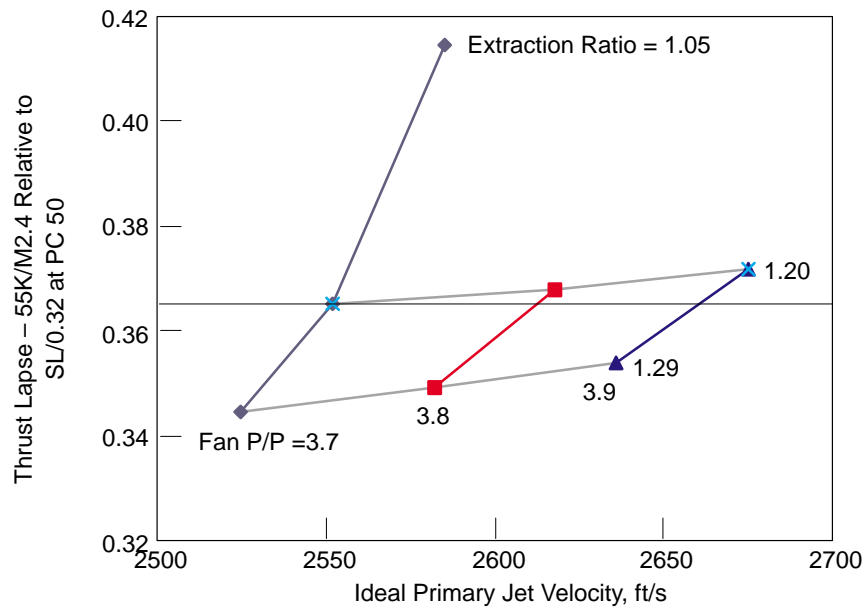
Figure 37.   The 1997 Brick Extension
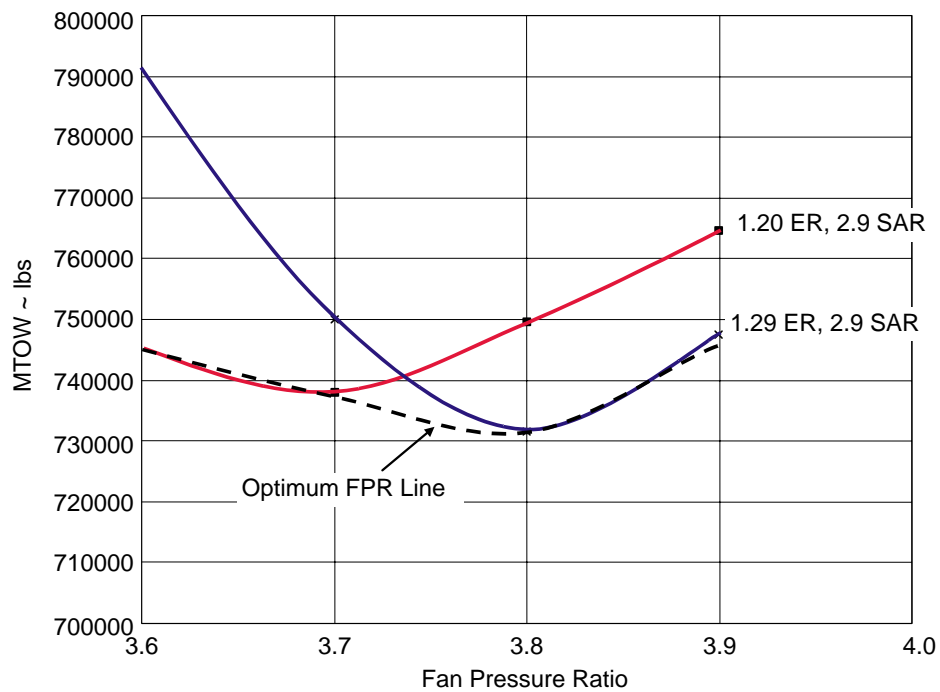
Figure 38.   Brick-Extension Sizing Evaluation on the TCA
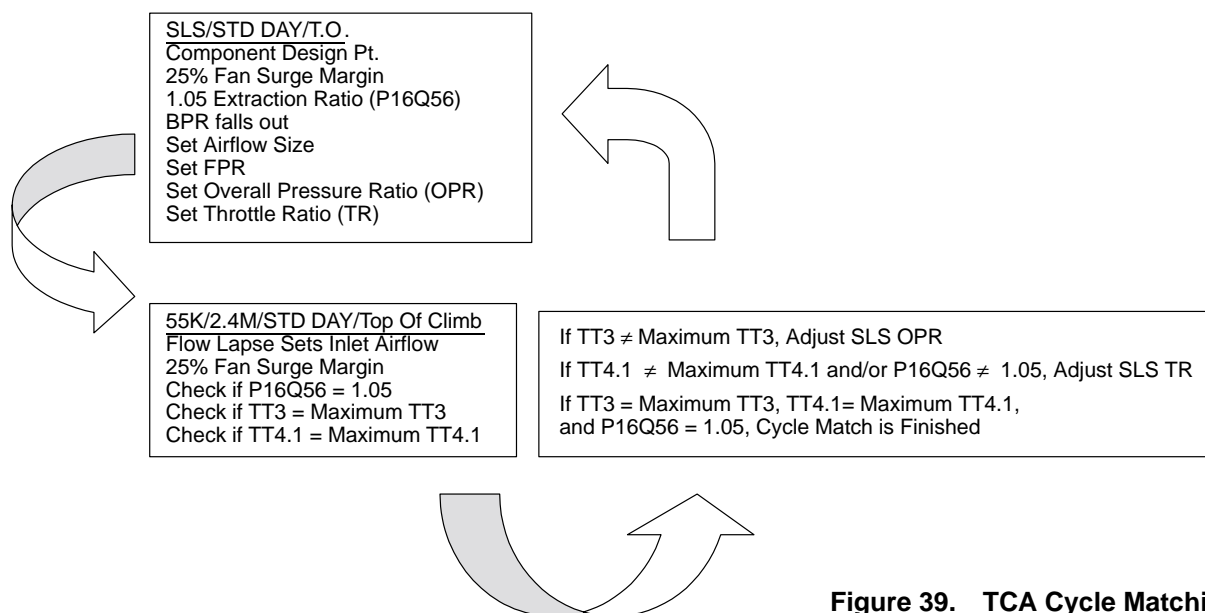
Figure 39. TCA Cycle Matching

A fan surge margin of 25% was selected to ensure adequate surge margin over the life of the engine. Holding extraction ratio of 1.05 from takeoff (design point) to top of climb ensures the availability of the pressure needed when nozzle cooling is required. This ratio also resulted in an increase in TOC net thrust that more than made up for relative increases in engine weight and TOC SFC. The impact of this ratio on maximum TOGW was unknown at the time of the extraction-ratio selection.

Off-Design Operation

Maximum-Augmented-Power Operation, Power Code (PC) = 100: The maximum augmentor exit temperature (T_{T7}) was defined as the same value as that of the maximum dry T_{T7}. This was set so that the nozzle would not change (materials, dimensions, etc.) if an augmentor was added to the design.

The flight Mach number range of augmentation was 0.9 to 1.8. A T_{T2} bias was applied to the inlet corrected airflow to limt airflow and protect the fan and core from overspeeding.

The effective throat area (A_{E8}) was varied to hold the inlet corrected airflow stable. (Inlet corrected airflow schedule was defined by establishing a takeoff design value and flow lapse and then applying the T_{T2} bias.)

Fuel flow was varied to hold extraction ratio (P16Q56) at 1.05, unless limited by maximum turbine rotor inlet temperature ($T_{T4.1}$) of 2800°F or maximum compressor exit temperature (T_{T3}) of 1200°F.

The variable-area fan/core mixer, duct side area (A_{16}) was varied to hold the fan surge margin at 25%. This holds the fan operating point.

Maximum-Power Operation, PC = 50: A T_{T2} bias was applied to the inlet corrected airflow to limit airflow and protect the fan and core from overspeeding.

A_{E8} was varied to hold the inlet corrected airflow. (Inlet corrected airflow schedule was defined by setting the takeoff design value and the flow lapse and then applying the T_{T2} bias.)

Fuel flow was varied to hold P16Q56 = 1.05, unless limited by maximum turbine rotor inlet temperature ($T_{T4.1}$) of 2800°F or maximum compressor exit temperature (T_{T3}) of 1200°F.

A_{16} was varied to hold the fan surge margin at 25%. This holds the fan operating point.

Part-Power Operation, PC = 47–26: A_{E8} was varied to hold maximum power W2AR until limited by maximum variable-area fan/core mixer duct side Mach number (M_{16}) of 0.8.

Fuel flow was varied to obtain a percentage of the maximum power uninstalled primary net thrust.

A_{16} was varied to hold the fan surge margin at 25% until limited by the maximum bypass duct over turbine rear frame Mach number ($M_{15.5}$) of 0.8. The fan surge margin was reduced when $M_{15.5}$ reached 0.8.

Idle-Power Operation, PC = 21: At $M \leq 1.5$, fuel flow was varied to obtain 5% of the maximum power primary net thrust.

At $M > 1.5$, in order to minimize inlet spillage drag, idle was defined as the primary net thrust required to hold W2AR at or above 80% of maximum power W2AR. The primary net thrust required to do this was 50% of the maximum power primary net thrust. Therefore, fuel flow was varied to obtain 50% of the maximum power primary net thrust. This was done to avoid inlet unstart and adverse (stress-inducing) thermal gradients on the compressor disks.

A_{E8} was varied to hold maximum power W2AR until limited by maximum M_{16} of 0.8.

At $M < 1.5$, A_{16} was varied to hold the fan surge margin at 15% until limited by the maximum $M_{15.5}$ of 0.8 or the maximum A_{E8} of ($1.8 \times A_{E8}$ at design). When $M_{15.5}$ reached 0.8, fan surge margin was reduced.

At $M \geq 1.5$, A_{16} was varied to hold the fan surge margin at 25%.

Engine Performance Data Packs

Table 15 is a summary of the 1994 HSCT engine performance data packs. These included:

1. Design (sea level static/standard day/takeoff power) FPR

2. Inlet corrected airflow lapse rate: (TOC W2AR/design W2AR) $\times$ 100

3. Design BPR (fan duct inlet mass flow/core inlet mass flow)

4. Design overall pressure ratio (OPR)

5. $T_{T4.1}$ throttle ratio (TOC $T_{T4.1}$/design $T_{T4.1}$)

6. Uninstalled net thrust lapse

7. Top of climb extraction ratio (TOC P_{T16}/P_{T56})

8. Design inlet corrected airflow (lbm/s)

9. Data pack date completed for an engine with a DSM nozzle sized to meet FAR Stage III sideline noise levels and with the engine operating at:

   - 80% takeoff power
   - 100% takeoff power
   - 110% jet velocity at 689 ft/M0.32/standard + 18°F day

Table 15. Summary of 1994 HSCT Engine Performance Data Pack *Exhaust nozzles sized to meet FAR Stage III noise.*

			Design Parameter					DSM Nozzle			FCN with Plug		
FPR	Flow Lapse Rate, %	BPR	OPR	T_{T41} Throttle Ratio	Thrust Lapse	TOC ER	W2AR, lbm/s	80% Power	100% Power	110% Jet Velocity	80% Power	100% Power	110% Jet Velocity
2.9	70	1.16	20.31	1.17	0.41	1.05	1070	07/12/94	07/12/94	07/12/94			
	75	0.88	17.56	1.23	0.51	1.05	970	07/15/94	07/15/94	07/15/94			
3.2	65	1.08	22.89	1.12	0.35	1.05	1070	07/06/94	07/06/94	07/06/94			
	70	0.81	19.64	1.19	0.44	1.05	970	07/08/94	07/08/94	07/08/94	11/18/94	11/18/94	11/21/94
	75	0.58	17.19	1.25	0.54	1.05	870	07/13/94	07/13/94	07/13/94			
3.7	65	0.62	21.78	1.14	0.40	1.05	900	07/07/94	07/07/94	07/07/94			
	70	0.42	19.05	1.20	0.49	1.05	800	07/06/94	07/06/94	07/06/94	11/18/94	11/18/94	11/21/94
	75	0.26	16.91	1.24	0.57	1.05	700	07/18/94	07/18/94	07/18/94			
4.3	65	0.28	21.09	1.15	0.43	1.05	700	07/21/94	07/21/94	07/22/94			
	70	0.10	18.54	1.19	0.51	1.05	600	07/22/94	07/22/94	07/22/94	11/18/94	11/18/94	11/21/94

10. Data pack date completed for an engine with a FCN with plug, sized to meet FAR Stage III sideline noise levels with the engine operating at:

- 80% takeoff power
- 100% takeoff power
- 110% jet velocity at 689 ft/Mach 0.32/standard + 18°F day

Performance Model Methods

The P&W performance model was modified such that one model could output multiple MFTF cycles. This helped reduce the turnaround time to produce a performance data pack and enabled P&W/GEAE to go from producing 2 MFTF data packs in 1993 to 39 in 1994. Some of the modifications performed this way included:

- Multiple inlet airflow maps to cover the range of airflow sizes and airflow lapses.
- Multiple fan maps to cover a wide range of design fan pressure ratios.
- Multiple compressor maps to cover a wide range of design compressor pressure ratios.
- Multiple nozzles to include the different types and sizes.
- Cycle selectors once initial cycles were defined.

Flowpath Development (Technology Concept Aircraft)

The engine matrix developed for the technology concept aircraft (TCA) was supported by a wide range of engines and nozzles based on the cycle matrix defined in the previous section. The goals and the high-level process definition of this activity are shown in Figure 40. The focus of this flowpath activity was to satisfy HSCT design limits while maintaining consistency among the various engines. The deliverables for this work were data packs containing the engine and nozzle configuration geometry and weights.

Engine consistency is best achieved by rigorously defining the database of the engine components. This includes defining the aerodynamic and mechanical design technologies used for each of the major components of the engine. Figure 41 shows this process to be an important part of the design activity. The baseline components were selected from the Pre-1994 study engine A31.

The A31 engine used a generic combustor configuration that was an average representation between the rich burn/quick quench/lean burn (RQL) and lean/premixed/prevaporized (LPP) combustor alternatives. Previous engine design activity that supported the A31 engine was also incorporated into the component definitions. The nozzle designs used a set of acoustic design rules to ensure that noise suppression would be consistent with the current acoustics database.

The steps involved in the second-level engine design process are shown in Figure 42. The boxes shaded in blue required either external data or hands-on activity. The yellow boxes represent computer models that automatically perform the task listed. At the heart of this activity is the GEAE FLOWPATH software design tool. This tool, developed in an earlier activity, is used to design engine components rapidly from a specific set of base data. The tool greatly facilitates satisfying specific requirements such as compressor rim speed, turbine loading, or fan stall margin when designing an

Objectives

- To Support 1994 Aircraft Matrix
- Define Engines and Nozzles Satisfying HSCT Design Limits
- Maintain Engine Design Consistency

Process

- Define the Engines Focused on Weight Impact:
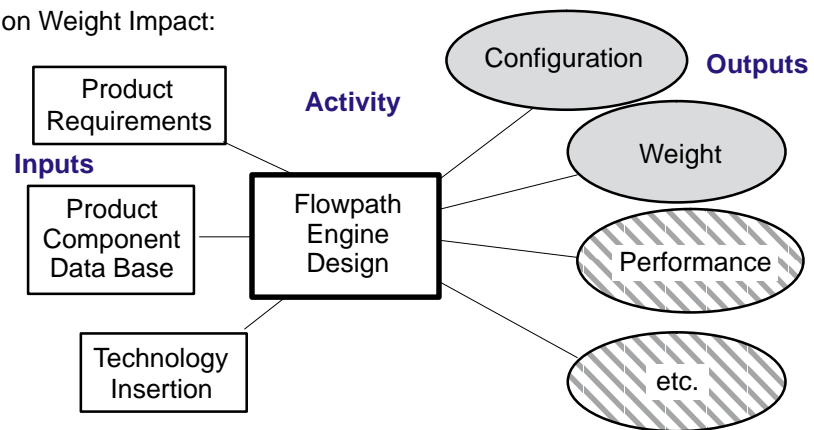
Figure 40.   TCA Flowpath Design Process
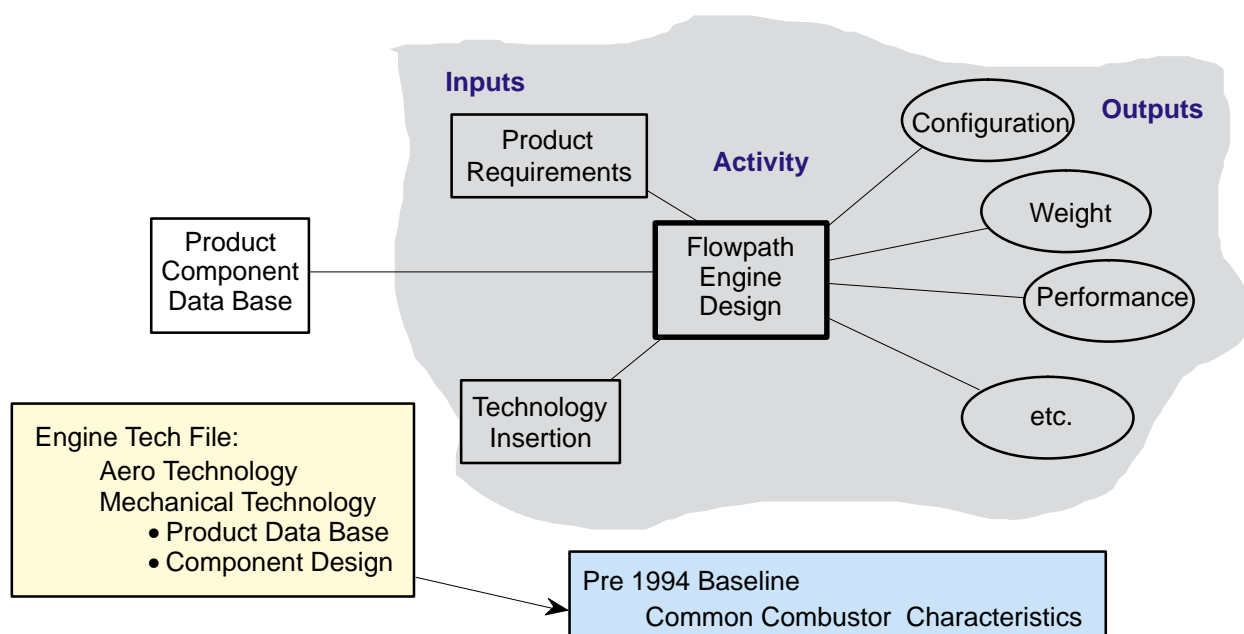
Figure 41.   Development of TCA Component Data Base
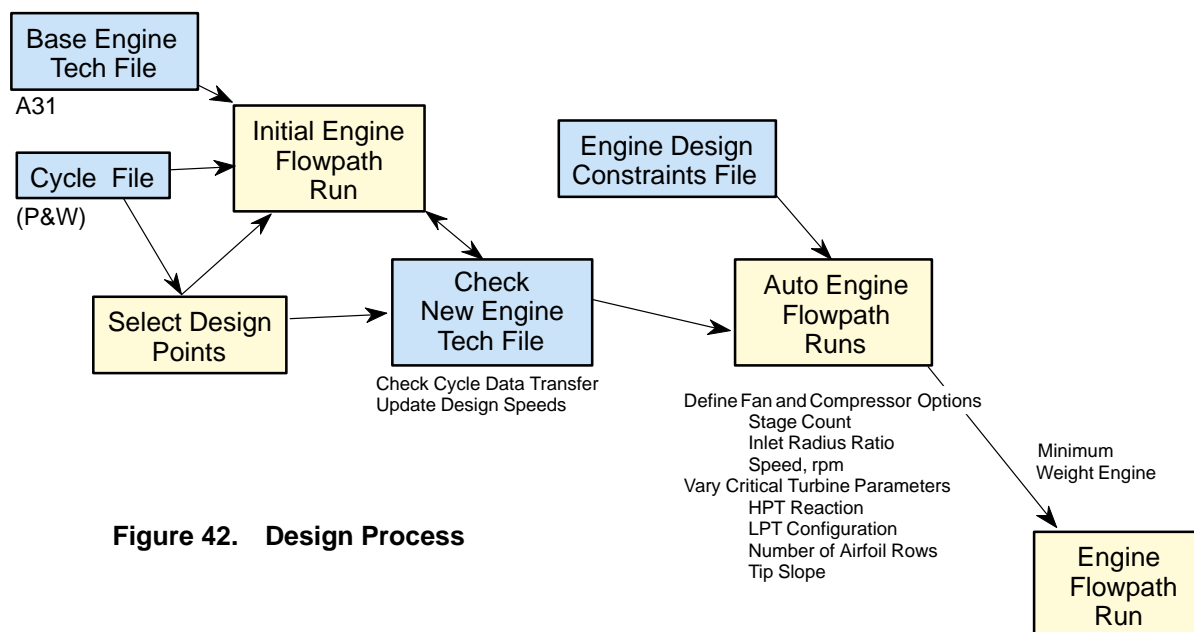
Figure 42. Design Process

engine. Generally, designs developed by FLOWPATH cover a wide range of cycle variations and thus are able to provide data packs that define an appropriate aircraft system very effectively.

The engines developed by this process are designed for multiple cycle points. Cycle point selection is based on the severity of impact on the configuration components. Data for a selected cycle point are transferred to the base engine file and then used to develop an engine that can satisfy the thermodynamic requirements specified. The FLOWPATH tool can determine what values are needed for the initial run of any given cycle. Run values selected are then thoroughly examined to ensure that the transfer has been successful and that the engine can be defined as initially conceived. This process is repeated until all issues are satisfied.

The data in the engine technology file (assumptions of component performance levels, materials, etc.) are coupled with the design constraint file for that specific engine to develop inputs for the *Auto* engine design function. That function provides a balanced engine relative to the design constraints mandated by the selected component architecture. During this effort, the number of turbomachinery component stages is varied to determine what impact each change will have on the engine configuration and weight. This procedure is used to automatically develop 10 complete engines that will each satisfy the design constraints. Selection of a single option is based on engine weight.

For each of the baseline turbomachinery sets, four nozzle designs were specified. All designs met the same supersonic cruise requirements, but different power settings were used to satisfy takeoff acoustic requirements. Power variations included 40, 45, and 50 power codes and a high power setting defined by 110% of PC50 ideal jet velocity. The first three power codes were developed with the assumption that engine takeoff would be at 80%, 90%, or 100% power. The fourth and subsequent power codes were an attempt to define the impact of ultrahigh takeoff power on the nozzle.

Figure 43 shows a typical deliverable engine configuration. The nozzle at the acoustics takeoff point is shown in solid lines. Dashed lines represent the nozzle in a Mach 2.4 cruise configuration.

Core turbomachinery is shown in Figure 44. The engine shown consists of a three-stage fan; five-stage compressor; single-stage, high-pressure turbine; and two-stage, low-pressure turbine.
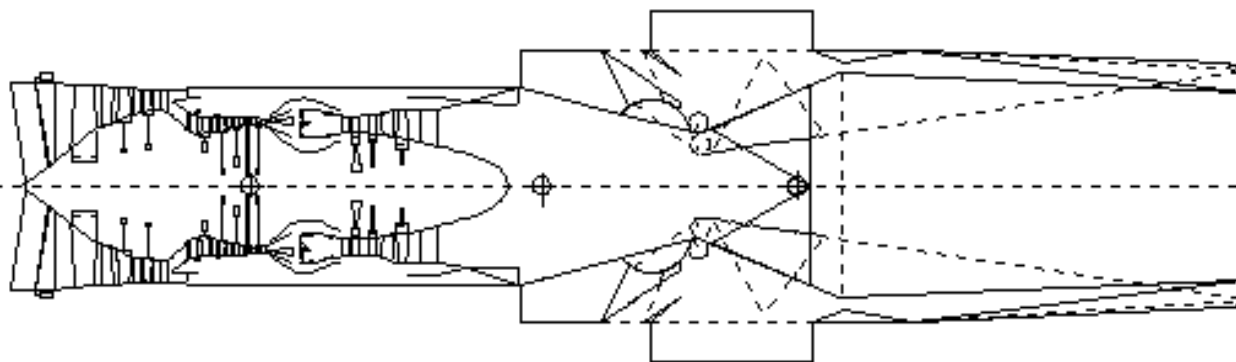
Figure 43. Typical Deliverable Configuration
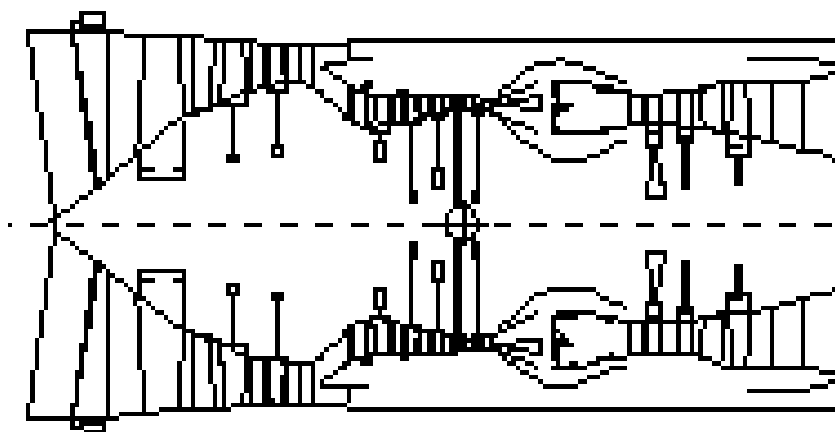
Figure 44. Core Turbomachinery (Typical)

The engine spools are counterrotating, which allows the nozzle between the two turbines to be omitted and still provides acceptable design performance. This configuration leads to a reduction in engine weight and reduced turbine cooling flow usage. Throughout this work, a fan-stage count of three and a single-stage, high-pressure turbine appeared to be optimum component selections, although there were a few exceptions.

The main differences in stage count from engine to engine appeared to be in the compressor and the low-pressure turbine. The cycles selected for the technology concept aircraft were defined with critical mission thrust levels held constant. This caused the flow size of the various cycles to vary from 600 lbm/s to nearly 1200 lbm/s. This, in turn, meant the three-stage fan varied in diameter 40% over this range.

Table 16 lists values for the configuration variations of the 10 cycles examined in this study. The compressor stage count was the only parameter to vary in this part of the study. The low-bypass engines were developed with a five-stage compressor. The high-bypass ratio designs required a seven-stage machine. Moderate-bypass ratio engines between 0.6 and 0.9 were specified with a six-stage compressor.

Table 16. Technology Concept Engine Matrix

FPR	Parameter	Flow Lapse		
		65	70	75
2.9	Engine Bypass Ratio		1.204	0.896
	Designation HSCT–		2970	2975
	Tip Speed, ft/s		1268	1268
	HPC Stage Count		7	6
	LPT Stage Count		2	2
3.2	Engine Bypass Ratio	1.128	0.823	0.579
	Designation HSCT–	3265	3270	3275
	Tip Speed, ft/s	1303	1303	1303
	HPC Stage Count	7	6	5
	LPT Stage Count	2	2	2
3.7	Engine Bypass Ratio	0.622	0.410	0.254
	Designation HSCT–	3765	3770	3775
	Tip Speed, ft/s	1370	1370	1370
	HPC Stage Count	3	5	5
	LPT Stage Count	2	2	2
4.3	Engine Bypass Ratio	0.274	0.096	
	Designation HSCT–	4365	4370	
	Tip Speed, ft/s	1370	1370	
	HPC Stage Count	5	5	
	LPT Stage Count	2	2	

Significant design activity for this effort was concentrated on the nozzle. As in the case of the turbomachinery, previous technology was captured over a wide range of flow sizes. The main problem was that the rules for designing the nozzle to achieve the desired acoustics level and satisfy the aerodynamic requirements changed during the study. In addition, the order of the configuration fundamentals was changed significantly during this design activity to reduce the work effort. The takeoff configuration was affected first. Later, a change to the acoustics requirements made it necessary to change the entire set of four nozzles designed for each engine. Finally, the supersonic requirements and the structural requirements were modified at the same time.

Over 250 nozzles were designed to satisfy the deliverable requirements of this activity. The FLOW-PATH model was coupled to a knowledge-based system to develop the lightest nozzle that could meet takeoff acoustics requirements while simultaneously achieving adequate supersonic cruise performance and thrust reverse performance. Figure 45 shows the 3770.42 DSM nozzle solution that was ultimately developed.

Each of the resulting engine and nozzle configurations and weights were delivered to the aircraft companies for evaluation. Engine configuration was defined by two mechanisms. First, the geometry files for the turbomachinery and each of the nozzles were delivered separately. Second, each critical dimension of the engine configuration was defined for each nozzle variation. Figure 46 is
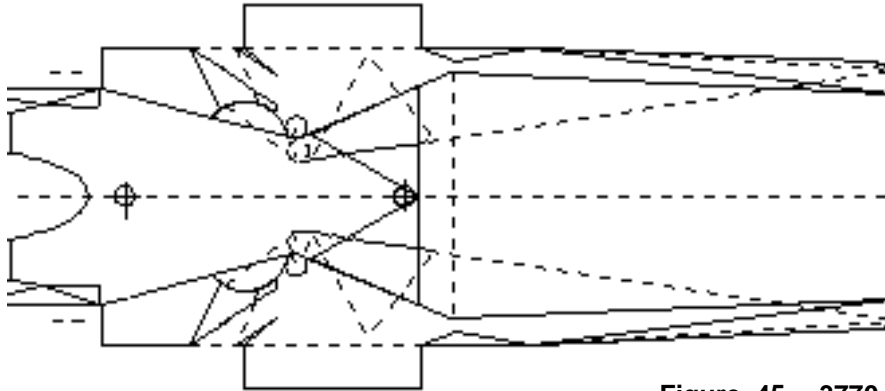
Figure 45.   3770.42 DSM Nozzle
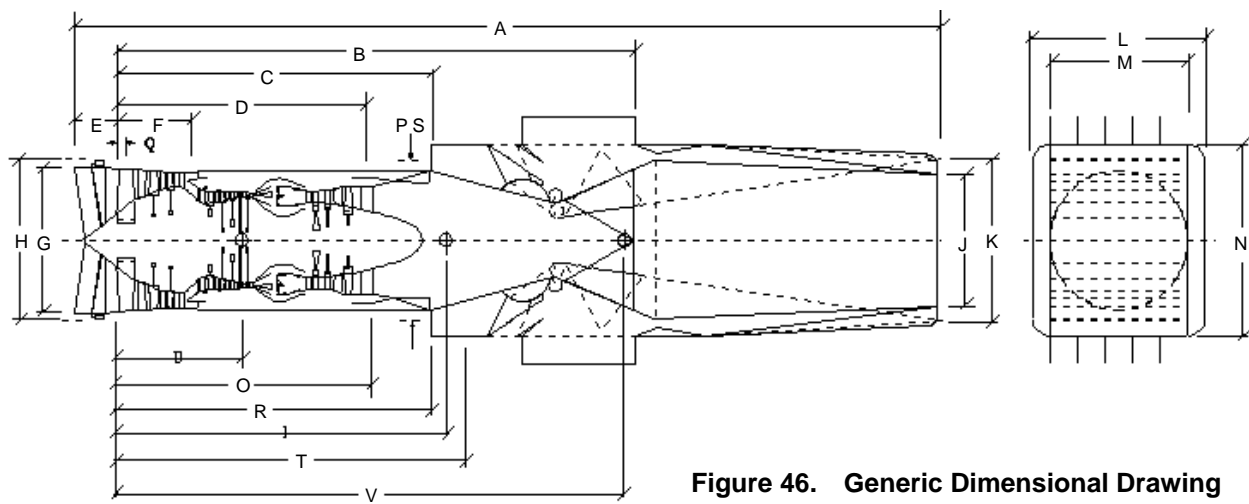
Figure 46.   Generic Dimensional Drawing

Table 17.   Engine and Nozzle Parameters

Engine	Core Weight	PC40				PC45				PC50				110% V$_j$ PC50			
		Nozzle Weight	Total Weight	Length		Nozzle Weight	Total Weight	Length		Nozzle Weight	Total Weight	Length		Nozzle Weight	Total Weight	Length	
2970	11932	5189	17121	362.2		5067	16999	353.2		5753	17685	372.4		7226	19158	400.5	
2975	10763	4374	15137	335.3		4590	15353	335.6		5375	16138	357.0		6600	17363	381.2	
3265	11454	5585	17039	364.8		6252	17706	375.7		6840	18294	385.2		7226	18680	389.2	
3270	10411	4699	15110	340.6		5559	15970	362.4		6040	16451	370.3		6598	17009	381.8	
3275	9533	4198	13731	318.9		4936	14469	339.3		5364	14897	346.4		6378	15911	373.7	
3765	9387	5911	15298	363.8		6396	15783	370.4		6576	15963	376.6		11495	20882	450.9	
3770	8462	5013	13475	340.6		5292	13754	343.6		5990	14452	365.6		10384	18846	436.4	
3775	7923	4153	12076	320.0		4372	12295	323.3		5209	13132	353.0		8987	16910	420.4	
4365	7234	5290	12524	338.3		5297	12531	340.9		9289	16523	411.1		19793	27027	516.6	
4370	6726	4065	10791	312.5		5001	11727	341.6		8036	14762	398.1		17114	23840	498.8	

an example of the type of dimensional drawing used. Table 17 lists the engine and nozzle weights and the total engine length of each of the 40 engine/nozzle combinations defined in the 1994 study.

3.2.2 Preliminary Technology Configuration (PTC) Aircraft

3.2.2.1 Wing Planform Studies Leading to PTC Planform Selection

In 1996, it was decided that the acoustic goals for the HSR program needed to be changed to achieve a FAR 36, Stage III –5 dB reading at the community measuring point. In Figure 34 it was shown that the TCA thumbprint sized for this acoustic goal grew from 736,000-lbm to nearly 800,000-lbm MTOW. Program management considered this weight increase unacceptable. Since there did not seem to be any additional suppression techniques that could improve the noise level of the propulsion system, it was decided to launch a number of wing-planform studies to see if a change in the aircraft could achieve the values desired. The basic goal of the studies was to find a planform with better low-speed lift-to-drag characteristics without sacrificing abilities at the high-speed end. Conventional aerodynamics indicated that this could most likely be achieved by increasing the wing aspect ratio. Therefore, two alternate wing planforms were developed as shown in Figure 47.

As can be seen in the figure, aspect ratio changes were achieved merely by varying the outer wing panel. Since this panel is very thin, the impact on supersonic drag was minimal, but there was significant improvement in low speed L/D as the panel swung outward. When sized to –5 dB, the 2.8–36 is lightest at slightly under 730,000-lbm MTOW. The 3770.60 2.9 SAR FCN was still projected to be the best propulsion system for all three wings.

Another benefit to the higher aspect ratio wing is shown in Figure 48 The penalty to go from –3 dB to –5 dB on the 2.8–36 planform is half that of the same change for the 2.0–52 TCA. This meant that the 2.8–36 planform projected a lower MTOW when sized to –5-dB community noise than the 2.0–52 wing planform did at –3 dB. Since the higher aspect ratio wing is more robust to changes in noise requirements, on the final HSCT configuration it would show less impact on payload or range if noise regulations changed.

Since the highest aspect ratio wing proved best in the first study, a follow-on study was launched to examine even higher aspect ratios and more outboard wing sweeps. Structural weight estimates for these designs were a big concern with the wing structural weight group, and it was hoped that a lighter configuration could be found. The matrix is illustrated in Figure 49.

As part of the sizing code calibration (SCC) study, all configurations in the study were sized by all team members. The SCC team was made up of people from Boeing, MDC, NASA–Langley, and GEAE. Typical results are shown in Figure 50. The 2.8 aspect ratio wing was best, with the 28° swept outboard panel showing a slight advantage, although the 36° panel was close. The results from the wedge study were used to guide the planform selection of the next baseline update at the end of 1997.

3.2.2.2 Preliminary Technology Configuration (PTC) Definition

The purpose of the PTC was to determine which direction configuration development should go to reach the Technology Configuration (TC) milestone at the end of 1998. By mid-1996, it was obvious that the configuration integration requirements for the HSCT had deviated too much to continue using the TCA configuration for technology development. Changes from the original TCA configuration had been many. The inlet had changed from axisymmetric to 2D bifurcated. The wing

- Increasing aspect ratio reduces TOGW penalty sizing to –5 dB noise
- 2.8 AR wing reduced TOGW 74,000 lb relative to 2.0 baseline
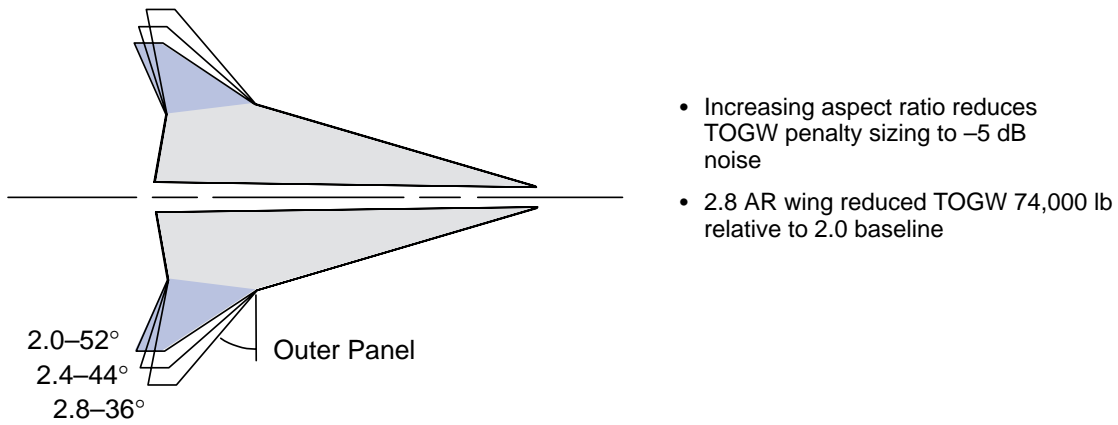
Noise Sized (–1, –5, –1) Airplanes with 3770.60 MFTF with 2.9 SAR Nozzle

AR – Sweep	2.0 – 52°	2.4 – 44°	2.8 – 36°
MTOW, lbm	803,000	766,800	729,100
Wing Area, ft^2	955	8760	8710
Airflow, lbm/s	800	815	730

Figure 47.   Increased Wing Aspect Ratio Achieves Noise Goal
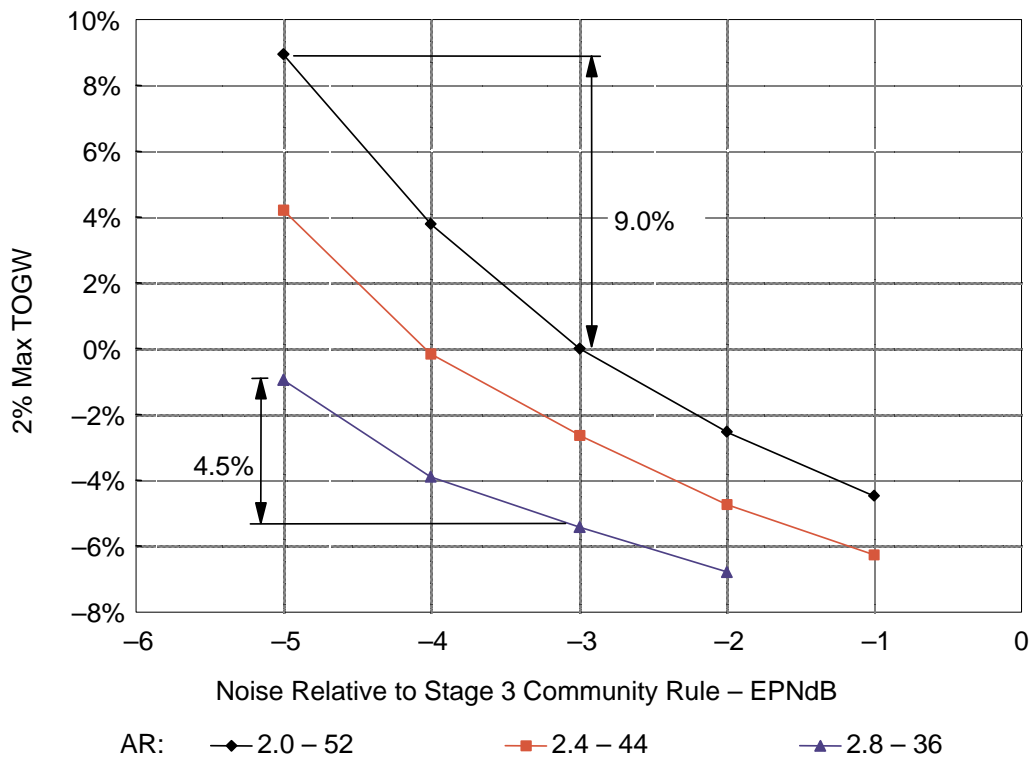
Figure 48.   Increased Aspect Ratio Improves Noise Robustness
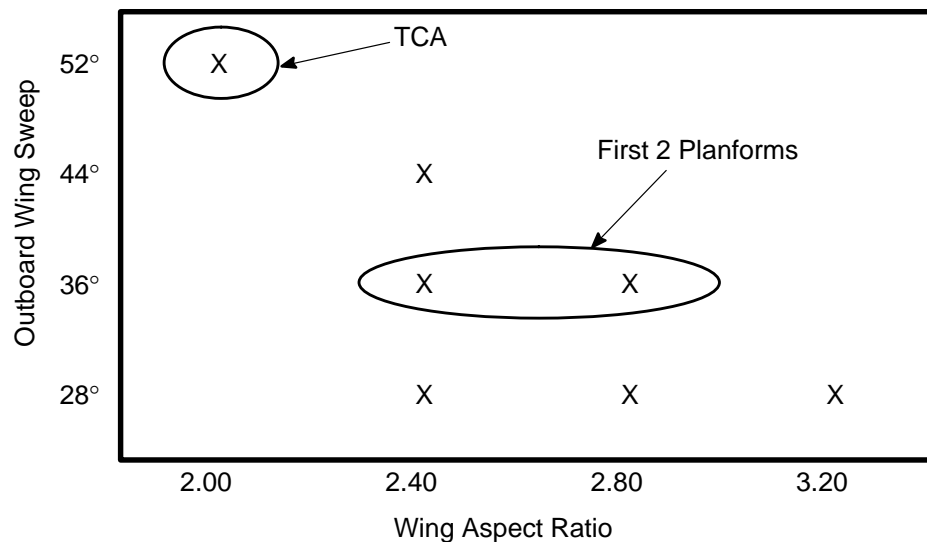
Figure 49.   Wedge Wing Planforms
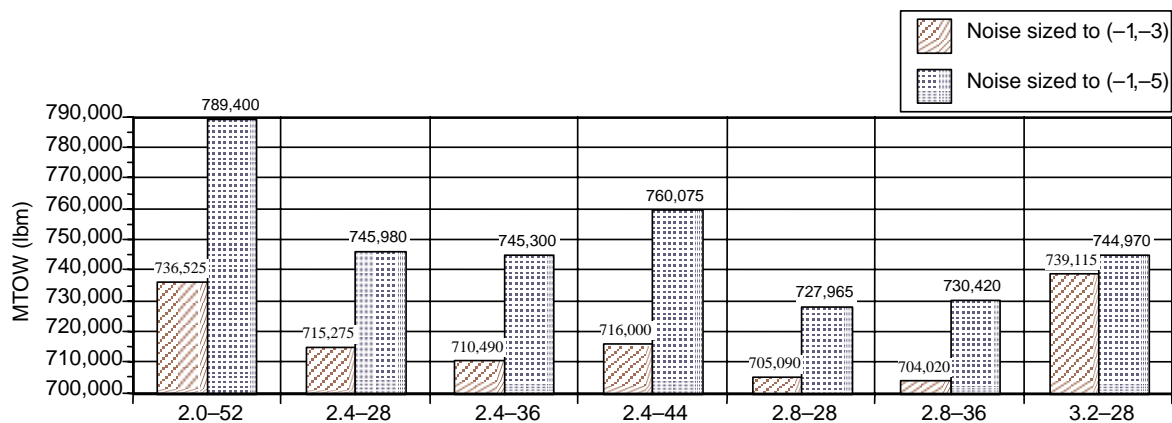
Figure 50.   Wedge Sizing Results Still Favor 2.8 Aspect Ratio

planform went to a higher aspect ratio to meet the more aggressive noise goals (Stage III –3 to Stage III –5). The structural mode control now required three wing surfaces on the aircraft (Figure 51). Even the engine cycle selected had changed. However, the PTC left the entire inboard wing and body of the TCA unchanged to preserve the finute-element models.

3.2.2.3 Sizing the PTC

The sizing conditions were set by the minimum wing area and the desired takeoff/cutback noise (Stage III –5 dB). The wing area was constrained to 9200 ft^2 to maintain the existing inboard section of the wing. This also allowed the existing engine installation and parts of the finite-element models to remain unchanged. The thumbprint chart for the new PTC is shown in Figure 52.

The PTC aircraft incorporated changes in the propulsion system, wing, and methodology. The propulsion system had a two-dimensional bifurcated (2DB) inlet. The engine and nozzle weights, dimensions, and performance values changed to reflect the new design and more realistic range.

Figure 51. PTC Three View

220 sq.ft.

158' 6"11

25 sq.ft.

WL 200 (REF)

11.1 n

326 ft.

ΔCB=−8.0   860000

850000

840000

830000

ΔCB=−7.0
820000

VA
PPDF
=1V=550000   ΔCB=−6.0   810000

TOFL = 108000   800000

ΔCB=−5.0   790000

780000

CT=60
770000   ΔCB=−4.0

760000

750000   ΔCB=−3.0

MTOW=740000   ΔCB=−2.0   ΔCB=−1.0

Engine Airflow, lbm/s

850
800
750
700
650

8500   9000   9500   10000   10500

Wing Area, ft²

MTOW..........lb 788500

Sw. ....sq.ft 9200

Wa.........lb/sec 728

Range..........nm 5000.0

Payload........lb 63001

SLST/eng.........lb 54194

OEW...........lb 347600

Block Fuel.....lb 338227

Reserve Fuel...lb 42360

Fuel Vol Req lb 399613

Fuel Vol Avail.lb 423860

Block Time .....hr 5.35

Climb Time ....min 51.89

TOFL.........ft 10106

NOTE: 1st and 2nd Seg Grad

based on 10800 ft FL

1st Seg Grad..... 0.0528

2nd Seg Grad 0.0692

Vappr ....keas 149.4

CLappr 0.680000

SL Margin...(dB) −1.00

CB Margin ....(dB) −5.00

ASAP Version A16 20–Nov–97

Figure 52.   PTC Thumbprint

3.2.2.4 PTC Propulsion System

Changes to the propulsion system from the TCA configuration are as follows:

- The inlet changed to a 2D bifurcated type from the axisymmetric translating-centerbody inlet used in the TCA. The 2D inlet improved operability and transonic flow margin and is more tolerant of Mach and angle-of-attack variations relative to the axisymmetric inlet. The 2D inlet, however, was 520 lbm heavier than the axisymmetric inlet. Figure 53 compares the profile of the 2D bifurcated inlet with the axisymmetric translating-centerbody inlet.

- Inlet doors are closed at the cutback point for additional noise attenuation.

- The engine cycle remained the 3770.60 FCN but with changes. The engine front flange diameter was slightly smaller, although the airflow was the same. The engine rear flange and overall length was slightly greater. In addition, the weight increased by 772 lbm per engine. Figure 54 compares the engine of the PTC with the 1996 TCA model. The performance of the installed, updated engine cycle was reduced at transonic conditions and improved at cruise conditions. Figure 55 shows SFC differences between the two engines.

- The nozzle concept is the same fixed-chute, no-plug type, but the mixing length is changed to 135.4 versus 120 inches on the 1996 TCA aircraft. In addition, the weight increased 1260 lbm on each updated nozzle. Figure 56 compares the updated and the old nozzle configurations.

- More realistic propulsion system designs and technology projections added substantial weight to the system. The inlet increased 520 lbm. The engine increased 772 lbm, and the nozzle increased 1260 lbm for a total of 2552 lbm per system.

PTC Engine Description

The baseline PTC engine was the GEAE/P&W FCN3770.60 SAR 2.9, a Mach 2.4, dual-spool, MFTF engine with a 2.9 SAR fixed-chute nozzle with a mixer/ejector suppressor. Engine maximum takeoff power is rated below Mach 0.45 to match inlet capability. Maximum takeoff rate increases airflow from 800 to 823 lbm/s at sea-level static up to Mach 1.1. Other salient engine design characteristics are:

- Three-stage fan
- Six-stage HPC
- Single-stage HPT
- Two-stage LPT

Engine Performance Characteristics

Cycle performance characteristics for the design reference condition (SLS +18°F, suppressor deployed), are:

- Reference corrected inlet airflow   800 lbm/s
  (100% corrected fan speed)

- Fan pressure ratio   3.7

Dimensions in inches.

	1996 TCA	1997 PTC
Cruise Recovery	93%	93%
Cruise Bleed (%Wc)	4.1%	3.0%
Weight	3360 lb	3880 lb

2D Bifurcated Inlet
(1997 PTC)

Translating Centerbody Inlet
(1996 TCA)
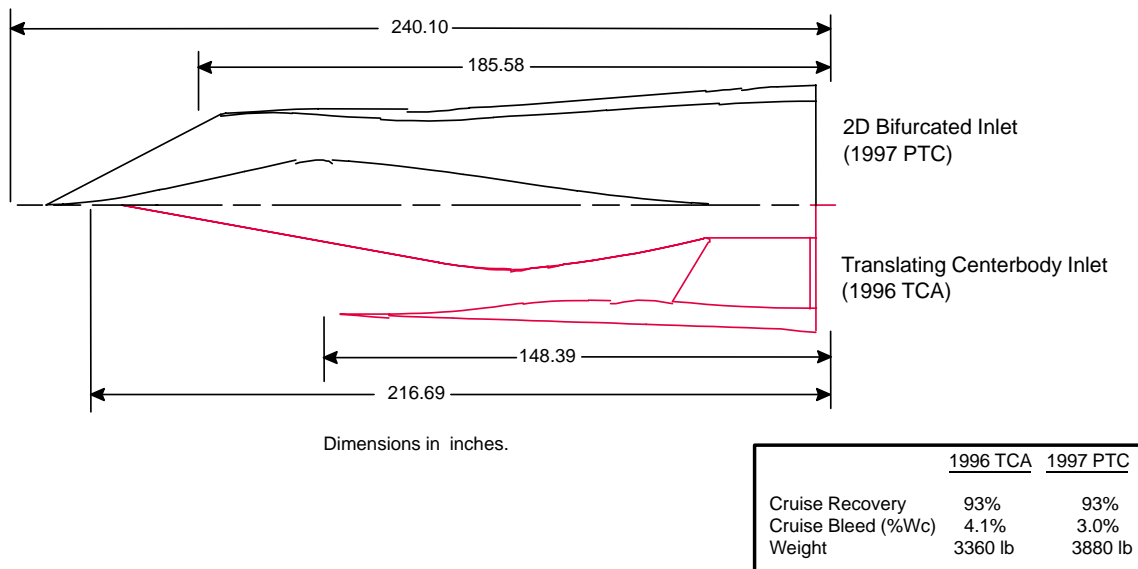
Figure 53.   Inlet Geometry Comparison: 1996 TCA Vs 1997 PTC

Engine	1996 TCA	1997 PTC
Fan Stages	3	3
Comp Stages	5	6
HPT Stages	1	1
LPT Stages	2	2
Weight	8073 lb	8845 lb
Thrust/Weight	7.14	6.74

**MFTF 3770.60 Flowpath
(1997 PTC)**

**MFTF 3770.60 Flowpath
(1996
TCA)**

Dimensions in inches.
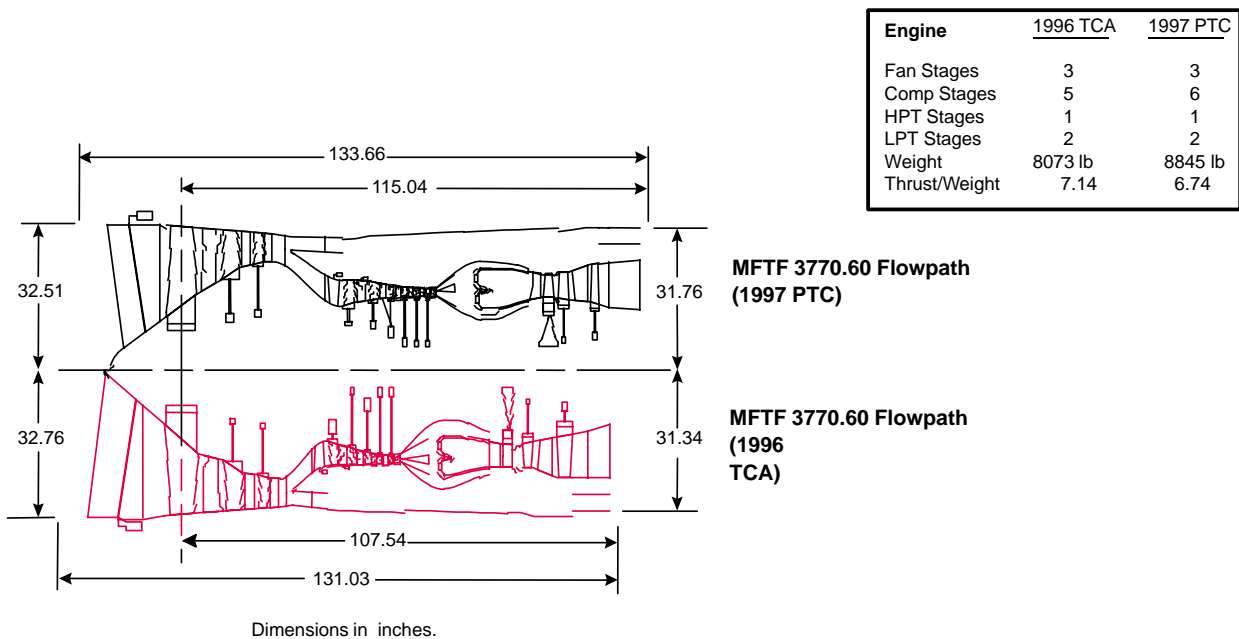
Figure 54.   Engine Geometry Comparison: 1996 TCA Vs 1997 PTC
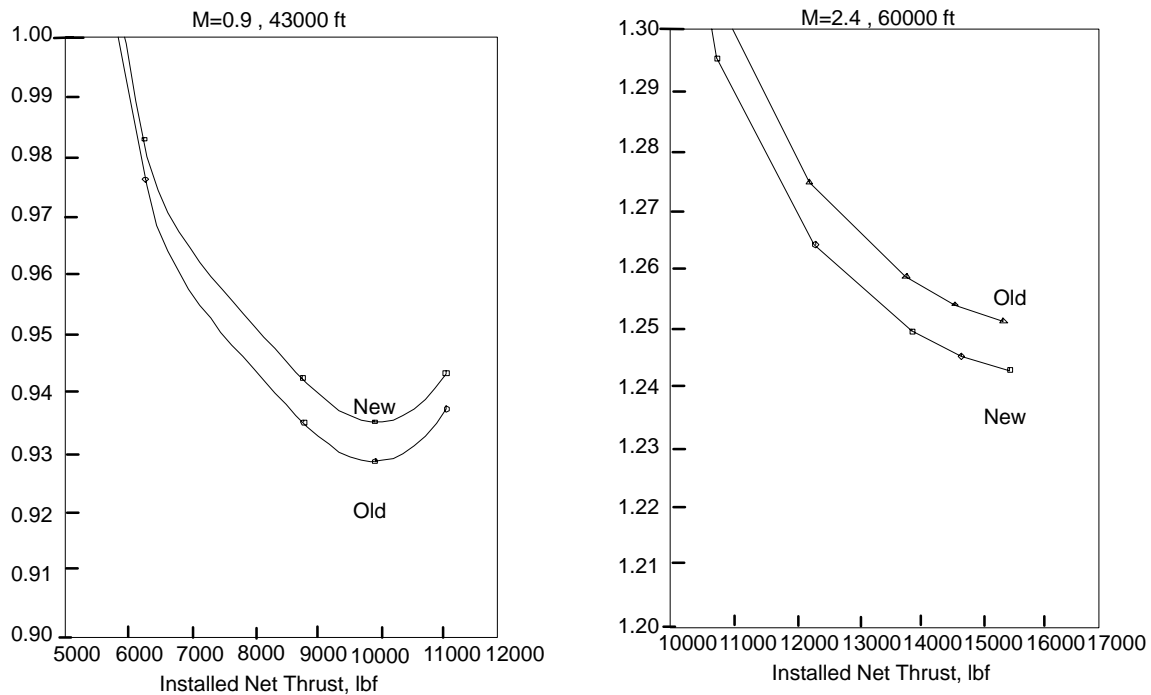
Figure 55. Engine Performance Comparison (3770.60)
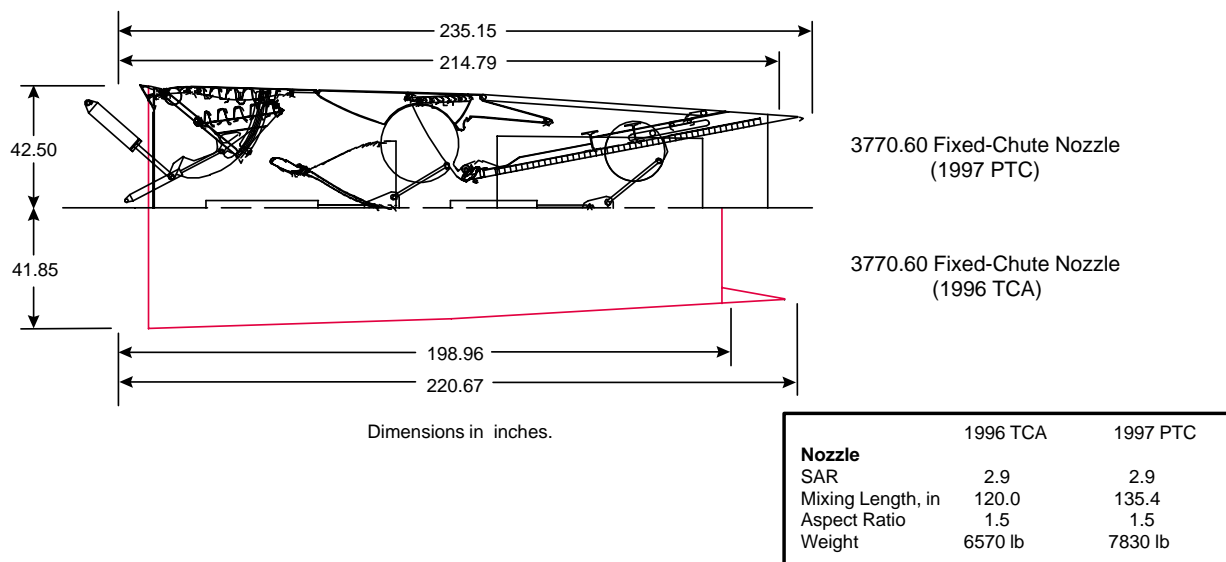
Figure 56. Nozzle Geometry Comparison: 1996 TCA Vs 1997 PTC

- Overall pressure ratio   20.3
- Bare engine weight   8845 lbm
- Maximum T_{41} 2800°F
- Maximum compressor discharge total temperature   1200°F
- Customer bleed from HPC   1 lbm/s
- Power extraction   200 hp
- Installed net thrust   59,544 lbf

Nozzle Design

The baseline nozzle concept used in the PTC is the 2D FCN mixer/ejector suppressor designed by the CPC nozzle team of P&W and GEAE. Figure 35 (page 49) shows the FCN. The nozzle is designed with 20 secondary chutes and 18 full, plus 4 half primary chutes sized for SAR = 2.90. The nozzle has an isolated maximum cross-sectional area of 6911 in^2. The aspect ratio of the nozzle operating at MAR = 0.95 is 1.5. FCN design features are:

1. No plug- or splitter-associated cooling problems.

2. Fixed chutes reduce design complexity and required sealing.

3. Ejector inlet and reverser ducts are separate and can be optimized for each function.

4. Acoustic liners are always in low-pressure area.

5. Single-piece divergent flap simplifies nozzle actuation.

6. Convergent flap also serves as reverser blocker.

7. Concept has demonstrated good potential through system studies and model-scale testing. Concept should meet and exceed HSCT acoustic and performance goals.

Materials used to fabricate the nozzle are consistent with 2001 technology and include nickel-based super alloys. To meet durability requirements, this nozzle design uses engine bay purge flow to cool various elements. Physical properties are not yet available on these materials, but the nozzle weight is based on an engine manufacturer's 2006 projected goal weight of 7830 lbm per nozzle. The nozzle external flap lines are designed to meet the 4° local boattail requirement, but the sidewall close-out angle currently exceeds this requirement.

The FCN is designed to be used with the 3770.60 MFTF engine. The nozzle thrust coefficient for sideline (Mach = 0.32, Altitude = 689 ft, NPR= 3.8) is 0.964. The nozzle thrust coefficient for cruise (Mach 2.4, Altitude = 60,000 ft) at maximum power is 0.983. The 2.9 suppressor area ratio aspirates 70%, relative to engine mass flow, at full power. This aspirated flow mixes with the engine flow in the 135.5-in-long mixing duct and reduces jet velocity at the ejector exit to acceptable levels. Internal shocks and mixing of the engine and aspirated flows produces internally generated noise that is reduced to acceptable levels by acoustic lining in the ejector. Effective acoustic lining is 4.0 times the ejector flow area and is located 10 mixing lobe widths downstream of the mixer exit, towards the ejector exit. Note that the mixing duct length specified above (135.5 inches) is the physical dimension of the mixing duct and correlates to the 140-in duct length used in analytical studies. The mixing duct length of 140 inches corresponds to the 1/7-scale model test database.

Inlet Design and Characteristics

The inlet baseline design is a mixed compression, 2D bifurcated design with variable-position ramps. The inlet and cowl are constructed of titanium. A vertical cross section view of the inlet is shown in Figure 57.
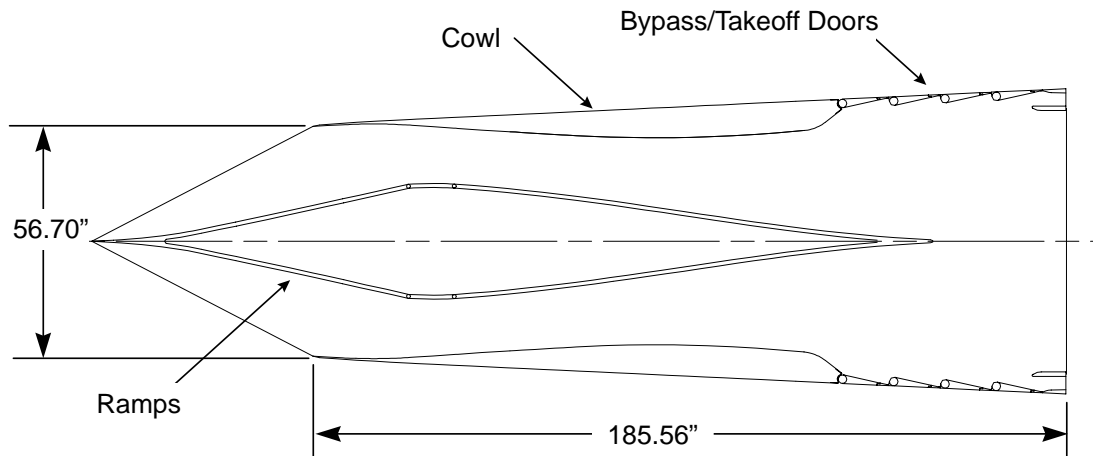
Figure 57.   PTC Inlet Cross Section

The main components of the inlet are the following:

Cowl: The cowl has a sharp leading edge. It contains 18 bleed compartments with individual overboard exits. The cowl houses the six fluidic vortex valves. The cowl also houses the supersonic diffuser, and throat regions of the internal cowl are perforated with bleed holes. The internal surfaces of the aft cowl are lined with acoustic-absorbing material.

Takeoff/Bypass Doors: Near the engine face, the cowl contains four louvered auxiliary inlet doors, two per side of the inlet, to be used during takeoff. These doors are self-actuating but may require actuation to force them closed at the cutback condition. In tandem with each takeoff door is an outward-opening bypass door to be used during supersonic flight. The bypass doors require continuous control and actuation.

Ramps: Contoured ramps are oriented vertically, spanning the entire inlet and bifurcating into two equivalent passages. The ramps require continuous control and actuation during operation above Mach 1.6. For low-speed operation, the ramps are actuated to open the throat. In the supersonic diffuser and throat regions, the ramp surfaces feed bleed air through perforations into four bleed plenums separated by bulkheads. The bleed air is vented overboard via exits in the cowl. The aft portions of the ramps are lined with acoustic-absorbtion material.

Secondary Air System: A secondary air control valve is incorporated into the baseline inlet design to control the flow of inlet air into the engine compartment and bypass the compressor.

Inlet Performance Characteristics

- Design Mach number   2.35
- Starting Mach number   1.6

- Cruise total pressure recovery   93%
- Cruise bleed mass-flow ratio (W_{bld}/W_{cap})   0.03
- Acoustic treatment area (ft^2)   274

Excess inlet flow is spilled below Mach 1.6 and bypassed above Mach 1.6. With the engine at takeoff power setting, auxiliary inlets are required below Mach 0.4.

3.2.2.5 Cycle Development – PTC

A number of MFTF propulsion systems were studied during 1994 and 1995, comprising various combinations of inlet, engine cycle, and nozzle configurations. Inlet variations included the variable-diameter centerbody (VDC) inlet, the 2D bifurcated (2DB) inlet, and the translating centerbody (TCB) inlet. Engine cycles evaluated incorporated fan pressure ratios that ranged from 2.9 to 4.3, bypass ratios from 0.26 to 1.16, and flow lapse rates from 65 to 75%. Nozzles considered for use with these engines included a number of mixer/ejector configurations. The nozzle types judged to have the most potential were the downstream mixer nozzle with sliding chutes, the downstream mixer nozzle with rotating chutes, and the fixed-chute no-plug nozzle.

The prime criteria in the downselect process was TOGW. For this purpose, TOGW values were developed from mission studies by the propulsion system evaluation team (PSET) and technology integration (TI) team. The inlet and nozzle teams, however, both needed more criteria to complete their downselect processes.

The inlet team used inputs from the controls and fan/inlet acoustics teams and ranking factors with values that had been determined by the inlet team. Their analysis of the best inlet candidates resulted in the selection of the VDC and the TCB inlets for further study. The 2D bifurcated inlet was rejected because it was found to result in a substantially heavier vehicle than would be developed from either the VDC or TCB configurations.

The nozzle team evaluated studies that had been performed by the acoustics team and the aero team. The nozzle team also considered the results of a review of several designs by experts from GEAE and P&W. Analysis of the best candidate nozzles showed that the fixed-chute, no-plug nozzle resulted in a slightly heavier vehicle than either of the two downstream mixer nozzles (sliding chutes and rotating chutes), but the FCN was a close competitor and definitely still in the running.

Analysis of engine cycles resulted in selection of the 3570.80 cycle (3.5 FPR, 70% airflow lapse rate, 0.80 BPR). The 3570.80 was projected to provide the lowest vehicle TOGW of all engines analyzed, and it produced a favorable cutback noise level in the range of –3 to –5 dB relative to Stage III.

These downselected configurations were analyzed and evaluated further during 1996 and 1997 to ensure that the HSCT propulsion system would include the best possible combination of inlet, engine cycle (Figure 58 illustrates the paths used in PTC cycle matching), and nozzle.

Summary of 1996 – 1997 Studies

Significant facts about the 1996 – 1997 studies are as follows:

- The VDC inlet was used with most of the data packs. However, in 1996 a few studies were performed that used the mixed-compression TCB (MCTCB) inlet. Since inlet recovery values varied between the two inlet types, the data pack simulations had to be changed accordingly.
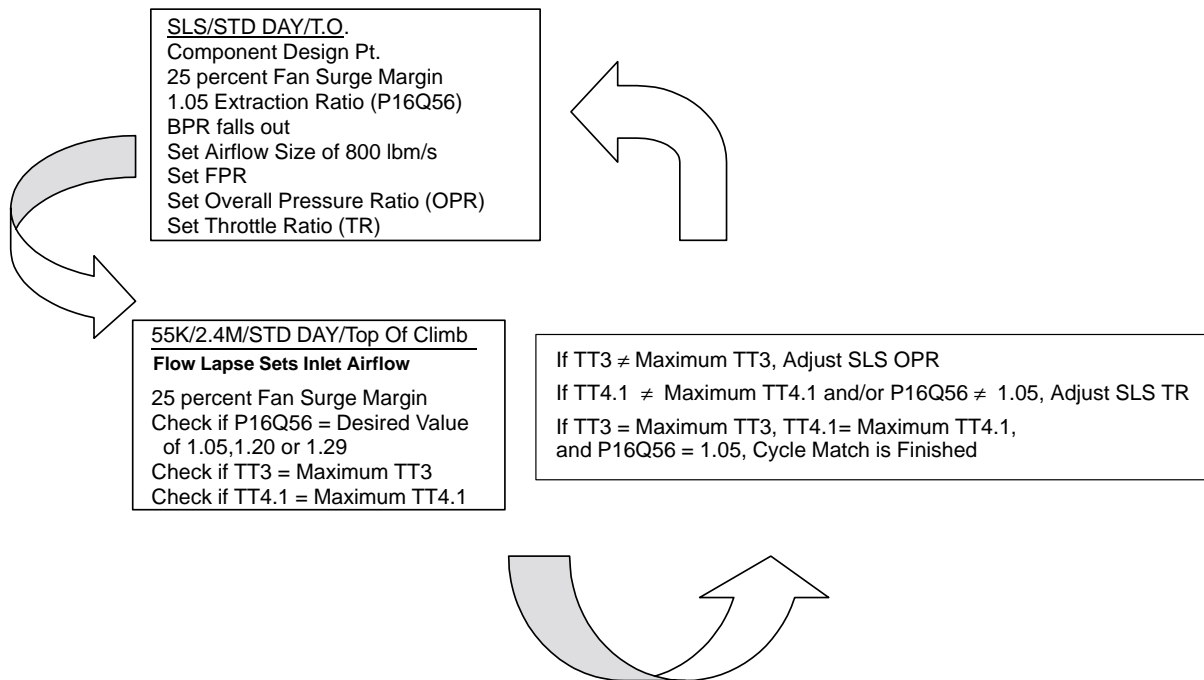
Figure 58. PTC Cycle Development

- The VDC inlet was later replaced with the 2D bifurcated (2dB) inlet. The airflow characteristics of the 2DB inlet fell within the range of the VDC inlet; therefore, the characteristics of the data packs were similar for the two inlets.

- The nozzle selected for use was the FCN, and most studies used that nozzle. A few studies were run in 1996 that used the axisymmetrical-tilt chute nozzle. The throat area of the FCN remains at a constant value all during suppressed operation, but the A_8 of the axisymmetrical-tilt chute nozzle is variable.

- The amount of entrained air incorporated into the system was also analyzed in 1996 – 1997. One factor used for determining the amount of entrained air is the size of the nozzle. The term used for this factor has been "suppressor area ratio." During 1996 – 1997, SAR's from 2.5 to 3.1 were analyzed and evaluated.

- In early 1996, the range of FPR used was from 3.5 to 3.7. This range was increased as the study continued to analyze a variety of aircraft/engine configurations. In July 1996, an FPR of 3.2 was added to the list. An FPR of 3.8 was added in August 1996, and in April 1997 an FPR of 3.9 was added.

- The inlet corrected airflow lapse rate originally selected for these studies ranged from 65 to 70%, but in mid-1996 Boeing reported that the 65% lapse rate had no benefit over the 70% lapse rate, even though the 65% lapse rate resulted in a slightly lighter aircraft system. For this reason, Boeing recommended using just the 70% lapse rate. Accordingly, data packs from July 1996 forward use only the 70% lapse rate.

Design Point and Cycle Definitions

The inlet corrected airflow (W2AR) used at design (SLS, standard day, takeoff) was set at 800 lbm/s. A previous study had determined that 800 lbm/s was closest to the airflow size required for the TCA airframe/engine configuration. This value was used for all data packs throughout 1996 and 1997.

For the first half of 1996, the maximum W2AR was held at 800 lbm/s during takeoff and at suppressed flight operations at any Mach number below 0.45. As the study progressed, the need for extra takeoff thrust was noted. Later data packs included overflow points where the maximum takeoff suppressed W2AR was increased by 2.9%, by increasing the low rotor speed while moving up the fan operating line, to a value of 823 lbm/s. One benefit of overflowing the engine at takeoff was the scaled-down engine/airframe configuration. Overflowing the engine at takeoff created an increase in thrust that overcame size limits. After rotation, the PLR procedure was used to control sideline noise.

At a flight Mach number of 0.45 and above, the maximum power W2AR was 823 lbm/s. This airflow was maintanied during climb flight conditions until limited by maximum low rotor speed (XNL) or maximum low-pressure turbine exit gas flow function (W5GR). This climb procedure was used while executing the design table flight matrix. After running the design table (used for engine flowpath design), the W2AR schedule for use in the data packs was developed. The limits were turned off and W2AR was run to the schedule defined above, for the data pack, at maximum power.

When W2AR was run to 823 lbm/s during suppressed operation, the extraction ratio was allowed to drop from 1.05 to 1.00. The top of climb extraction ratio was expanded to include values of 1.05, 1.20, and 1.29. The design point extraction ratio continued to be fixed at 1.05, but the top of climb extraction ratio was expanded for a given FPR in order to cover a range of thrust lapses.

- A fan surge margin of 25% was selected for the simulations to provide adequate surge margin over the life of the engine.

- Unsuppressed idle definition was changed from the 1994–95 study as a result of the analyses of turbine disk life. During descent, the step change from 50% thrust (Mach 1.5) to 5% thrust (Mach 1.49), resulted in a rapid temperature change. This temperature change adversely affected the turbine life; a series of smaller step changes was used instead:

  - For $M < 1.1$. idle = 5% maximum primary nozzle net thrust (FNP)
  - For $M < 1.2$. idle = 14% maximum FNP
  - For $M < 1.3$. idle = 23% maximum FNP
  - For $M < 1.4$. idle = 32% maximum FNP
  - For $M < 1.5$. idle = 41% maximum FNP

For $M \geq 1.5$, idle was defined as: the thrust required to hold W2AR at or above 80% of the maximum power W2AR. The thrust required to do this was 50% of the maximum-power thrust.

Off-Design Operations, Unsuppressed

Maximum-Augmented-Power Operation, PC = 100: The maximum augmentor exit temperature (T_{T7}) was defined as the same value as that of the maximum dry T_{T7}. This was set so that the nozzle would not change (materials, dimensions, etc.) if an augmentor was added to the design.

The flight Mach number range of augmentation was 0.9 to 1.5.

The inlet corrected airflow schedule was defined by taking the maximum climb to TOC W2AR values from the flowpath design table.

A_{E8} was varied to maintain the inlet corrected airflow schedule unless a maximum XNL of $1.09 \times$ XNL_{design} was obtained. If this occurred, the W2AR would be reduced and the A_{E8} varied to satisfy the XNL requirement.

Fuel flow was varied to hold extraction ratio (P16Q56) = 1.05, unless limited by maximum turbine rotor inlet temperature ($T_{T4.1}$) of 2800°F or maximum compressor exit temperature (T_{T3}) of 1200°F.

The variable-area fan/core mixer, duct side area (A_{16}) was varied to hold the fan surge margin at 25%. This holds the fan operating point.

Maximum-Power Operation, PC = 50: The inlet corrected airflow schedule was defined by taking the maximum climb to TOC W2AR values from the flowpath design table.

A_{E8} was varied to maintain the inlet corrected airflow schedule unless a maximum XNL of $1.09 \times$ XNL_{design} was obtained. If so, the W2AR would be reduced and the A_{E8} varied to satisfy the XNL requirements.

Fuel flow was varied to maintain P16Q56 = 1.05, unless limited by maximum turbine rotor inlet temperature ($T_{T4.1}$) of 2800°F or maximum compressor exit temperature (T_{T3}) of 1200°F.

A_{16} was varied to hold the fan surge margin at 25%. This holds the fan operating point.

Part-Power Operation, PC = 47–26: A_{E8} was varied to hold maximum power W2AR until limited by maximum variable-area fan/core mixer duct side Mach number (M_{16}) of 0.8 or maximum A_{E8} of $1.45 \times A_{E8\ design}$.

Fuel flow was varied to obtain a percentage of the maximum power uninstalled primary net thrust.

A_{16} was varied to hold the fan surge margin at 25% until limited by the maximum $M_{15.5}$ of 0.8 or maximum A_{16} of $1.45 \times A_{16\ design}$.

Idle-Power Operation, PC = 21: At $M \leq 1.0$, fuel flow was varied to obtain 5% of the maximum power primary net thrust. Between $M = 1.0$ and 1.5, idle was a series of step changes as follows:

- For M < 1.1. idle = 5% maximum FNP
- For M < 1.2. idle = 14% maximum FNP
- For M < 1.3. idle = 23% maximum FNP
- For M < 1.4. idle = 32% maximum FNP
- For M < 1.5. idle = 41% maximum FNP

At $M \geq 1.5$, idle was defined as the FNP required to hold W2AR at or above 80% of maximum power W2AR. The FNP required to do this was 50% of the maximum power FNP. Therefore, fuel flow was varied to obtain 50% of the maximum power FNP.

A_{E8} was varied to hold maximum power W2AR until limited by maximum M_{16} of 0.8 or maximum A_{E8} of $1.45 \times A_{E8\ design}$.

A_{16} was varied to hold the fan surge margin at 25% until limited by the maximum $M_{15.5}$ of 0.8 or maximum A_{16} of $1.45 \times A_{16\ design}$.

Off-Design Operations, Suppressed

Maximum-Power Operation, PC = 50: Fuel flow was varied to reach maximum scheduled W2AR at 823 lbm/s unless limited by maximum $T_{T4.1}$ of 2800°F or maximum T_{T3} of 1200°F. A_{E8} was fixed. A_{16} was varied to hold the fan surge margin at 25%.

Part-Power Operation, PC = 47–26: Fuel flow was varied to obtain a percentage of the maximum power uninstalled FNP. A_{E8} was fixed. A_{16} was varied to hold the fan surge margin at 25% until limited by the maximum $M_{15.5}$ of 0.8 or maximum A16 of $1.45 \times A_{E8 \, design}$.

Idle-Power Operation, PC = 21: Fuel flow was varied to obtain a percentage of the maximum power uninstalled FNP. A_{E8} was fixed. A_{16} was varied to hold the fan surge margin at 25% until limited by the maximum $M_{15.5}$ of 0.8 or maximum A16 of $1.45 \times A_{E8 \, design}$.

Engine Performance Data Packs

The airframe manufacturers cycle of choice from the 1996–1997 study was the 3770.60 because it provided the lowest TOGW. The 3770.54 cycle was selected by the engine manufacturers to be used for their in-house design efforts. The 3770.54 cycle was defined by running the 3770.60 cycle with updated (increased) turbine cooling levels. Table 18 is a summary of the 1996–1997 HSCT engine performance data packs. The increased turbine cooling levels were defined after the matrix of cycles in Table 18 was defined. The table shows:

1. Design (sea level static/standard day/takeoff power) FPR

2. Inlet corrected airflow lapse rate: (TOC W2AR/design W2AR) $\times$ 100

3. Design BPR (fan duct inlet mass flow/core inlet mass flow)

4. Design overall pressure ratio (OPR)

5. $T_{T4.1}$ throttle ratio (TOC $T_{T4.1}$/design $T_{T4.1}$)

6. Uninstalled net thrust lapse

7. Top of climb extraction ratio (TOC P_{T16}/P_{T56})

8. Data pack date completed for an engine with a variable-diameter-centerbody inlet and a fixed-chute nozzle, with plug. The FCN was sized at four suppressor area ratios and a variety of mixing lengths. SAR was defined as the mixing plane area (including chute base area), A_{mix}/A_8 (physical throat area) The four SAR values were 2.5, 2.7, 2.9, and 3.1. Since A_8 was fixed during suppressed operation, SAR defined the size of the nozzle mixing area and amount of airflow entrainment. Entrainment increased as SAR increased.

9. Data pack date completed for an engine with a VDC inlet and a axitilt chute nozzle. The axitilt chute nozzle was sized at SAR's of 2.9 and 3.1.

10. Data pack date completed for an engine with a MCTCB inlet and FCN, with plug. The fixed-chute nozzle was sized at SAR's of 2.5 and 2.55.

3.2.2.6 Flowpath Development – PTC

The engine design goals developed for the PTC airplane were similar to those used for the TCA. Therefore, the engine matrix developed for the PTC was based on design data determined for the

Table 18. Summary of 1996/97 HSCT Engine Performance Data Pack

| | Design Parameter | | | | | | Variable-Diameter-Centerbody (VDC) Inlet | | | | | | | | MCTCB Inlet | | |
| | | | | | | | FCN | | | | | | Axitilt Chute Nozzle | | FCN | | |
FPR	Flow Lapse Rate, %	BPR	OPR	T_{T41} Throttle Ratio	Thrust Lapse	TOC ER	2.5 SAR	2.7 SAR	2.9 SAR	2.9 SAR IML	3.1 SAR	3.1 SAR IML	2.9 SAR	3.1 SAR	2.5 SAR	2.55 SAR**	2.9 SAR
3.2	70	0.92*	20.97	1.135	0.37	1.20	07/02/96	07/03/96	07/05/96								
3.5	70	0.59	19.80	1.183	0.43	1.05	04/22/96	04/22/96	04/23/96								
		0.78	21.02	1.131	0.38	1.20	04/17/96	05/02/96	05/02/96						05/15/96		
		0.80*	21.65	1.106	0.35	1.29	04/15/96	04/15/96	04/16/96								
	65	0.83	23.06	1.124	0.34	1.05	04/24/99	04/24/96	04/24/96								
		0.94*	24.56	1.075	0.30	1.20	05/01/96	05/01/96	05/01/96								
		1.04*	25.28	1.054	0.28	1.29	05/01/96	05/01/96	05/01/96								
3.7	70	0.42	19.11	1.197	0.47	1.05	04/22/96	04/22/96	04/22/96								
		0.54	20.32	1.141	0.41	1.20				03/21/97						10/08/96	
		0.60	20.28	1.143	0.41	1.20	05/02/96	04/18/96	01/13/97	11/27/96		12/05/96			05/29/96		
		0.69	20.86	1.115	0.38	1.29	05/02/96	05/02/96	05/02/96			02/15/97	07/19/96	07/19/96	05/16/96		
	65	0.61	21.88	1.143	0.38	1.05	04/30/96	04/30/96	04/30/96								
		0.73*	23.30	1.092	0.33	1.20	04/30/96	04/30/96	04/30/96								
		0.82*	23.93	1.069	0.31	1.29	04/30/96	04/30/96	04/30/96								
3.8	70	0.54	20.23	1.141	0.41	1.20		09/03/96	08/19/96			02/18/97					
		0.62	2084	1.117	0.39	1.29		08/28/96	08/20/96			02/19/97					
3.9	70	0.48	20.11	1.141	0.42	1.20			04/23/97			04/04/97					
		0.56	20.72	1.116	0.39	1.29			04/22/97			04/18/97					

* Three-stage LPT (all other engine cycles have a two-stage LPT).

** In-house study engine (W2AR = 839 lbm/s); W2AR overflowed at takeoff by 29% from M = 0 to M = 0.32, sea level to 5000 ft.

IML = increased mixer length (nozzle)

Objectives

- To Support 1994 Aircraft Matrix
- Define Engines Satisfying HSCT Design Limits
- Maintain Engine Design Consistency

Process

- Define the Engines Focused on Sensitivity Impact:
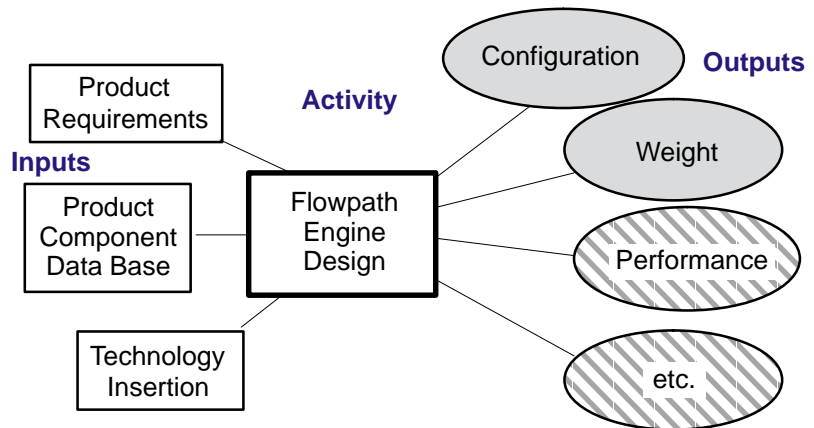
Figure 59.   PTC Engine Design Process

HSCT 3770.42 engine used in the TCA. The main difference in the process was that while the TCA engine selection focussed primarily on weight, engine selection for the PTC concentrated on system sensitivities. Figure 59 shows the goals and high-level process definition used for the PTC. As before, the focus of this flowpath activity was to satisfy HSCT design limits and still maintain consistency among the various engines.

Engine consistency required rigorously defining the database of engine components. Initially, the design focussed primarily on weight reduction, and engine components were selected accordingly (see Figure 60). Once these choices were made, however, component evaluations focussed on other features. The combustor downselect process was still in the future at this time, but test data at the subscale level had indicated the LPP combustor would be the best and possibly the only choice that would meet HSCT system emission goals. Therefore, the flowpath model was changed to include the characteristics of the LPP combustor.

During this PTC activity, the focus changed from a design mission to a more typical mission. This new mission profile was designated "mission 2 usage." The profile covered an average usage flight activity from initial start up to final shutdown of the engine. The main difference that resulted from this change was in the content and arrangement of subsonic and supersonic segments. The new profile included subsonic legs both before and after the supersonic cruise segment. This new mission profile became part of the product requirements shown in Figure 61.

From a flowpath perspective, the PTC offered one new design constraint: engine size. It was anticipated that the PTC engine would have flow between 800 and 900 lbm/s. An engine this size would have required a core turbine disk and blisks (for the last few compressor stages) that would have exceeded current manufacturing facility size limitations. While it would be possible to make the components, the investment in new manufacturing equipment was thought to be more than system economics could handle.
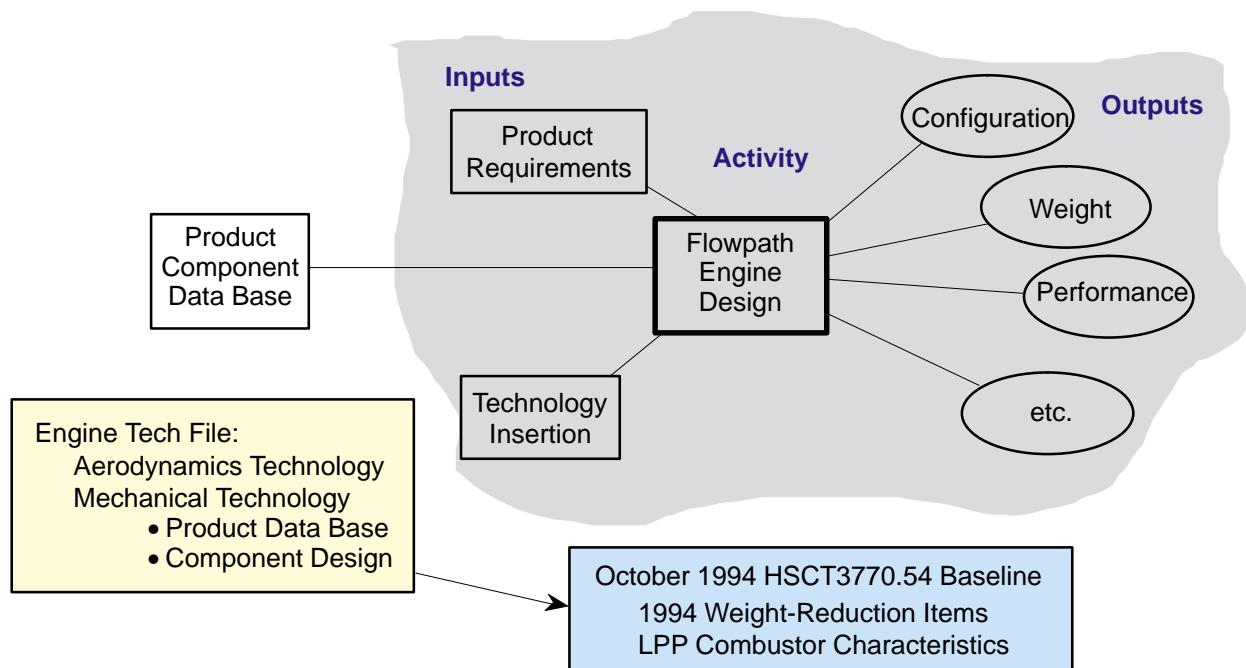
Figure 60.   Development of PTC Component Database

Key Cycle List

Point	Flight Operation	Altitude (ft)	Flight Mach No.	Power Code % FN	DTAMB (F)
1	Aero Design Point SLS	0	0	50	0
2	Begin Taxi	0	0	5.0%	18
3	Taxi	0	0	5.0%	18
4	Release Brake, Begin Takeoff	0	0	100.0%	18
5	Lift Off	0	0.36	100.0%	18
6	Initial Noise Cutback	35	0.36	89.6%	18
7	689 ft Sideline Noise Station	689	0.36	50	18
8	Noise Cutback	689	0.36	47	18
9	Noise Cutback	689	0.36	44	18
10	Continue Noise Cutback	1492	0.36	89.6%	18
11	Cutback from Takeoff Noise Station	1492	0.36	49.1%	18
12	Begin Climb to Sub Cruise	1500	0.37	100.0%	18
13	Climb to Sub Cruise – overflow	10K	0.65	50	0
14	Climb to Sub Cruise – overflow	10K	0.8	50	0

Design and Usage Cycles
Performance and Weight Goals
Cost Objectives

Transfer Function

Δ TOGW = + A Δ Weight + B Δ SFC + C Δ …
Δ SFC = a + b $\Delta \varepsilon$ fan + c $\Delta \varepsilon$ HPC + e $\Delta \varepsilon$ HPT + f Δ …

Define and Weight for Usage Mission

Design Constraints

AN^2, $U_{t\,max}$, $U_{r\,max}$, T_{bulk}, …

Figure 61.   Product Requirements

The engine matrix developed for the PTC incorporated the latest component designs together with the most advantageous materials defined by the Enabling Propulsion Materials program. As HSCT program requirements evolved, engine design became more complicated (Figure 62). The AUTO engine design activity remained focussed on the TOGW metric through the sensitivities that had been defined for the TCA concept. This approach provided balanced engines that included all the component design constraints including the manufacturing size-limitation constraint.
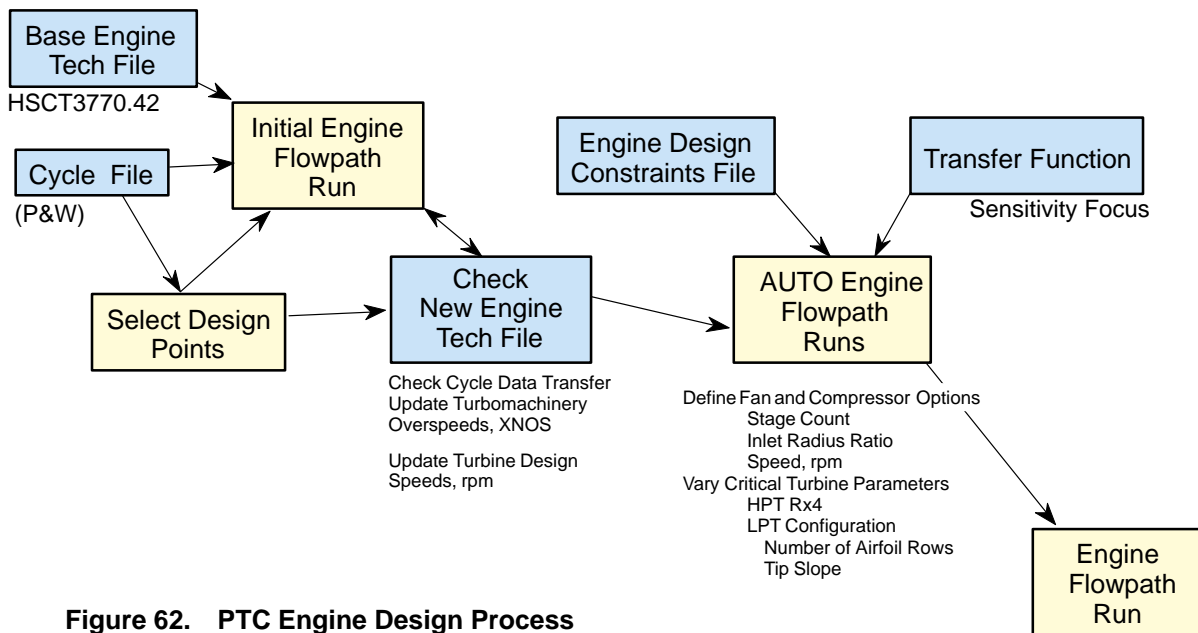
Figure 62.   PTC Engine Design Process

Many design variations were investigated, each of which satisfied a set of design constraints. This process defined 15 to 25 candidate engines, all of which satisfied the design constraints mentioned. Engine selection from this list of candidates was based on comparison of minimum specific fuel consumption values. Each SFC parameter was defined through the use of an equation that included engine weight and the component efficiencies of the fan, compressor, and turbines used.

The sensitivities used in the selection process described above are defined in Table 19, which shows the relationship between efficiency and weight variation. The weight increments shown were defined by the FLOWPATH program. Efficiency differences were established by linking configuration data using GEAE performance-prediction tools. The cooling flow was determined by a process of defining the configuration details of stages, surface area, and the number of airfoils estimated.

This data matrix led to the larger variations in engine parameters shown in Table 20, where the engine bypass ratio is varied from 0.417 to 1.122. The turbomachinery components listed define compressors with from five to seven stages and low-pressure turbines with from two to three stages. All of these systems have counterrotating spools, which allows a vector diagram solution that includes the removal of the stator vane row between the two turbines. This vaneless arrangement was selected because of the engine weight and cooling flow improvements that resulted from removing the hot airfoil row.

Table 19. Efficiency Effects on SFC and Engine Weight

Mission Sensitivities	
+1000 lbm Weight	+1.256% SFC
+2 Points Fan Efficiency	−0.41% SFC + 58.9 lbm
+2 Points High-Pressure Compressor Efficiency	−0.50% SFC + 54.6 lbm
+2 Points High-Pressure Turbine Efficiency	−0.56% SFC + 56.5 lbm
+1% HPT Cooling Flow	+0.20% SFC + 20.2 lbm
+2 Points Low-Pressure Turbine Efficiency	−0.45% SFC + 49.1 lbm
+1% LPT Cooling Flow	+0.24% SFC + 24.7 lbm

Table 20. Preliminary Technology Configuration Engine Matrix

FPR	Flow Lapse	Parameter	Data			
3.5	65	Engine Bypass Ratio	0.825	1.0243	1.122	
		Designation FCN–	356B.83	3565B1.02	3565B1.12	
		Tip Speed, ft/s	1344	1344	1344	
		HPC Stage Count	6	6	7	
		LPT Stage Count	2	3	3	
	70	Engine Bypass Ratio	0.588	0.775	0.798	0.871
		Designation FCN–	3570B.59	3570B.78	3570B.80.3	3570B.87
		Tip Speed, ft/s	1344	1344	1344	1344
		HPC Stage Count	6	6	6	6
		LPT Stage Count	2	3	3	3
3.7	65	Engine Bypass Ratio	0.61	0.80	0.895	
		Designation FCN–	3765B.61	3765B.80	3765B.90	
		Tip Speed, ft/s	1370	1370	1370	
		HPC Stage Count	6	6	6	
		LPT Stage Count	2	3	3	
	70	Engine Bypass Ratio	0.417	0.600	0.690	
		Designation FCN–	3770B.42	3770B.60	3770B.69	
		Tip Speed, ft/s	1370	1370	1370	
		HPC Stage Count	5	5	6	
		LPT Stage Count	2	3	2	
3.5	70	Engine Bypass Ratio	0.54	0.62		
		Designation FCN–	3870B.54	3870B.62		
		Tip Speed, ft/s	1383	1383		
		HPC Stage Count	5	5		
		LPT Stage Count	2	2		

As was the case with the TCA engines, the PTC engines studied had from two to four fan stages. The three-stage version defined the best engine for this range and fan pressure ratio.

Figures 63 and 64 illustrate the configuration differences. Figure 63 shows the impact of varying the engine bypass ratio on turbomachinery. Note that the lower BPR engine is shorter because of the smaller core flow size. Figure 64 shows the configuration differences that result from compressor and LPT stage count variations.

3570.54

3770.42
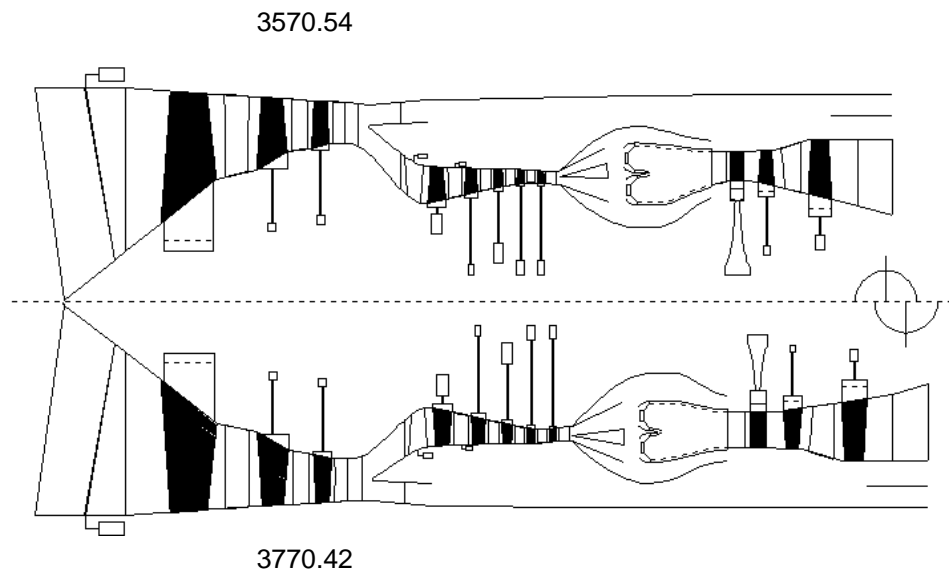
Figure 63.   Effect of Bypass Ratio Variation

3570.102

3770.42
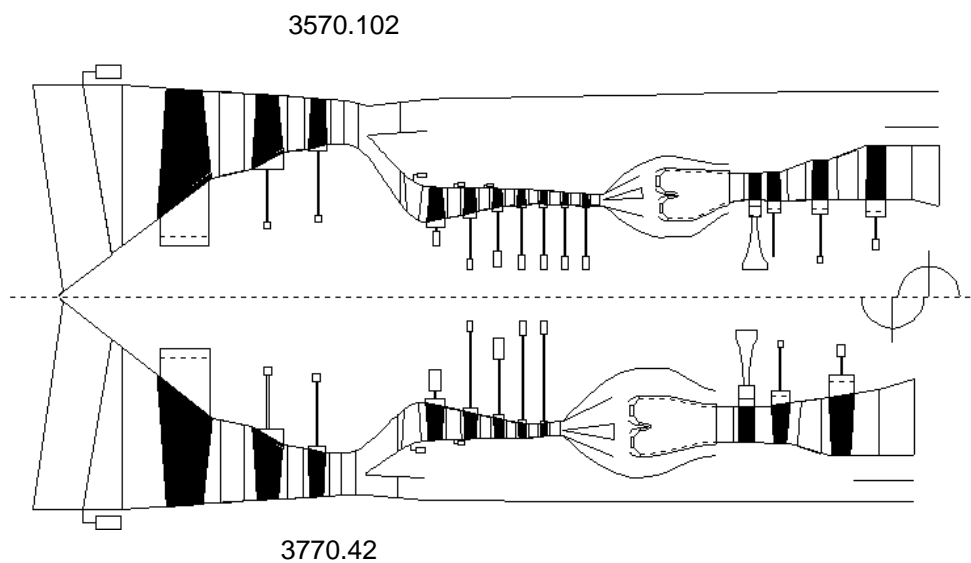
Figure 64.   Effect of Compressor and LPT Stage Count Variation

An example of a study engine is shown in Figure 65. The figure presents a cross section of the engine and specific component data including the geometry and aerodynamic description of the component in the accompanying table. All of this information was generated for all of the engines designed for this series.

The deliverable items listed for the flowpath design activity portion of the program are the engine weight and length. Table 21 lists these data for the 15 sets of engines that ultimately ended up in the PTC system matrix.

HSCT3770.69

	Fan	Compressor		HPT	LPT
No. Stages	3	6	No. Stages	1	2
Pressure Ratio	3.7	5.7	Expnsion Ratio	2.5	2.3
Corrected Flow	800	159	Flow Parameter	78.0	189.3
Rotor Speed, rpm	4848	8401	Rotor Speed, rpm	8341	4815
Corrected Tip Speed, ft/s	1370	1136	*Mean Velocity Ratio	0.48	0.71
Inlet Specific Flow, lbm/ft^2	40.5	38.0	Max AN^2 x 10^9, in^2/min	44.5	28.9
Inlet Hub/Tip	0.37	0.69	Max Exit Rim Speed, ft/s	1393	803
Exit Mach No.	0.50	0.31	Total Cooling and Leakage	14.0%	7.0%
Exit Hub/Tip Ratio	0.79	0.89	Flow (%W25a)		
Max Exit Rim Speed, ft/s	1088	1283	No. Airfoils	114	180
No. Variable Stages	1	2	Length	6	17
No. Airfoils	353	834			
Length, in	29	26			

Figure 65.   Typical Study Engine and Components

Table 21. Deliverable Parameters for PTC System Matrix Engines

Cycle	Engine BPR	Weight (lbm)																	TRF Length (in)
		Front Frame	Fan Rotor	Fan Stator	Main Frame	Compressor Rotor	Compressor Stator	Comb	HPT Rotor	HPT Stator	LPT Rotor	LPT Stator	Rear Frame	Outer Duct	Diffuser	Exhaust Nozzle	C&A	Total	
3565	0.825	151	1026	746	502	689	417	670	668	217	851	268	562	164	1100	2696	595	8039	108.30
	1.0243	151	1021	747	481	587	365	560	453	173	898	404	510	178	1100	2696	577	7705	115.90
	1.122	151	1021	746	476	598	461	520	448	181	914	424	512	193	1100	2696	571	7822	121.20
3570	0.588	151	1029	746	549	793	551	793	600	228	913	330	552	201	1100	2696	621	8595	122.50
	1.775	151	1028	747	541	687	562	715	628	217	894	324	559	181	1100	2696	600	8253	114.90
	0.798	151	1023	746	523	665	461	640	451	183	962	443	509	203	1100	2696	598	8070	126.00
	0.871	151	1023	746	568	634	439	626	428	179	938	438	493	198	1100	2696	591	8070	124.70
3765	0.61	150	1058	728	519	682	379	717	550	212	819	269	493	162	1100	2696	610	8279	117.00
	0.8	150	1050	728	509	625	420	626	454	188	937	439	474	186	1100	2696	590	7989	121.75
	0.895	150	1057	728	581	781	470	900	552	241	872	274	528	179	1100	2696	635	8180	120.30
3770	0.417	150	1057	728	581	781	470	900	552	241	872	274	528	179	1100	2696	635	8482	116.40
	0.6	150	1057	728	574	682	390	793	505	226	870	292	515	166	1100	2696	612	9073	111.80
	0.69	150	1055	728	553	673	476	731	620	214	811	258	530	179	1100	2696	601	8093	116.90
3870	0.54	151	1053	714	582	672	411	840	674	235	901	282	539	169	1100	2696	618	9368	111.90
	0.62	151	1049	714	584	631	376	792	657	232	904	278	537	157	1100	2696	607	8187	107.25

During this phase of activity, nozzle design responsibility was transferred to the nozzle team. The design data for the nozzle were established, and the weight and dimensional data were described as shown in Table 22. These 22 primary dimensions along with electronic files of the geometry were transferred to the airframe designers for evaluation in conjunction with the entire aircraft system.

Table 22. Typical Design Data (HSCT3770 1994 Rotating Chute DSM) *Axial dimensions are from fan front face.*

Component	Dimension, in
Overall Length (Supercruise)	336.7
Fan Face to Nozzle Throat (Takeoff)	201.2
Maximum Nozzle Height Location	120.0
Turbine Rear Frame Location (Thrust Mount)	119.5
Bulletnose and Front Frame (Forward Flange, Mount)	19.2
Main Frame Location (Power Takeoff Shaft)	34.0
Fan Diamter	64.8
Fan Case Diameter (Forward Flange Outer Diameter)	70.8
Center of Gravity Location (Engine)	120.8
Exit Height at Takeoff	51.0
Exit Height at Cruise	72.0
Maximum Nozzle Width	78.3
Internal Nozzle Width	62.3
Maximum Nozzle Height	75.2
Turbine Rear Frame Aft Flange Location	123.4
Turbine Rear Frame Aft Flange Outer Diameter	66.0
Fan First-Stage Disk Center of Gravity Location	4.3
Nozzle Forward Flange Location	122.0
Nozzle Forward Flange Outer Diameter	75.0
Nozzle Support Location	122.4
Turbomachinery Center of Gravity Location	64.9
Nozzle Center of Gravity Location	209.0
	Weight, lbm
Core Engine	8449
Exhaust System	5358
Total	13807

3.2.3 Technology Configuration (TC) Aircraft

3.2.3.1 Engine Study Matrices

A number of studies led to final definition of the Level 1 milestone TC at the end of 1998. Of prime concern to the CPC team were the propulsion studies to select the configuration for the *Technology Concept Engine* (TCE) that was to go on the TC aircraft In 1998. Due to the impending Phase IIA

downselect for the HSR demonstrator engine, there were major revisions to improve the accuracy of the predicted propulsion system weights. A new matrix of engines developed from these studies covered a tighter range than was covered in the original 1997 "Brick." This new matrix, which was dubbed the "Briquette," is shown in Figure 66.
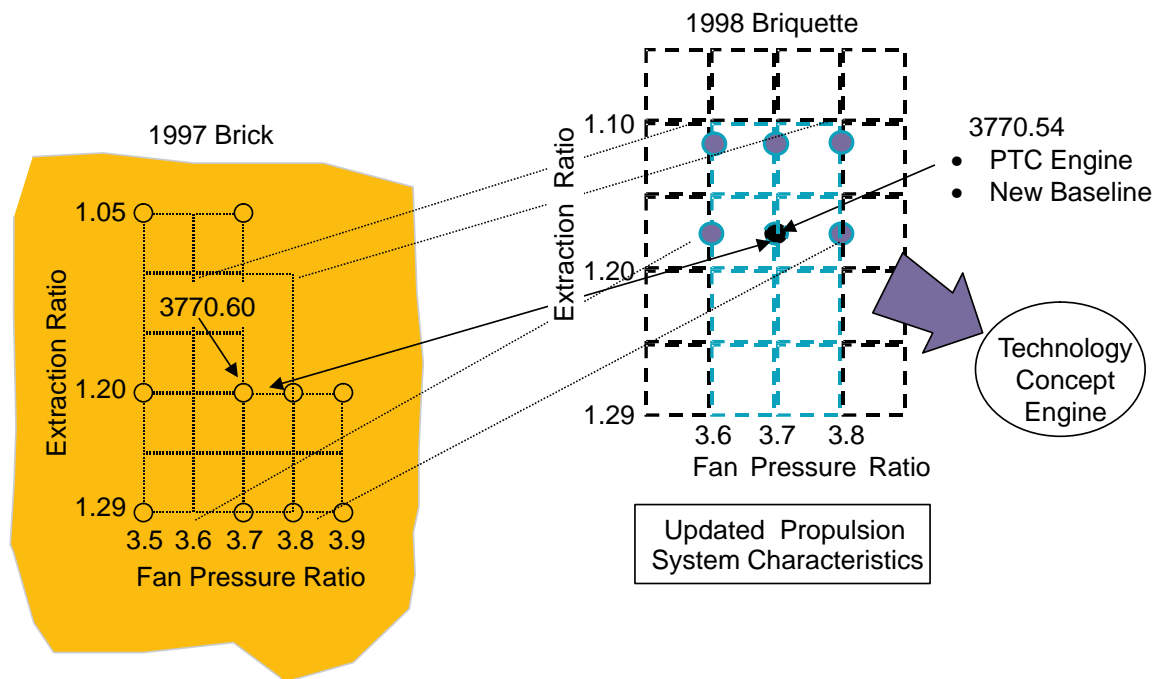
Figure 66.   Engine Study 1998 Matrix Refines Previous Studies

GEAE and P&W cycle audits resulted in updated values for component performance and pressure losses to be used for this new matrix. Table 23 shows the actual changes that appeared at the Mach 2.4 design point when progressing from the (3770.60) PTC engine to the new Briquette (3770.54) centerpoint engine. These updates ensured much greater confidence in the propulsion system performance projected for the product engine but had a negative impact on installed performance. Supersonic cruise SFC increased by 1.5%, and subsonic cruise SFC increased by over 4%.

The cycle design philosophy for this new engine matrix also changed. The original Brick matrix was designed to a specific FPR and ER at TOC. It was noted that some of these engines were operating at less than the full 103% fan airflow possible; they were limited by the maximum turbine inlet temperature because of cooling-flow changes. These were not satisfactory with the restricted airflow. Therefore, it was decided that at a minimum the new engines would be designed to achieve full 103% airflow at maximum T_4. This criterion set the maximum BPR and therefore the minimum thrust-lapse for each FPR.

Table 23.   Briquette Performance Update   *Analysis: 55,000 ft, Mach 2.4, standard day, design point.*

Parameter		Engine	
		3770.60	3770.54–6/98
Pressure Ratio	Fan	2.31	2.34
	HPC	4.47	4.30
	HPT	2.47	2.54
	LPT	2.14	2.10
Extractions	Power, hp	200	338.1
	Bleed, lbm/s	1.0	1.25
Pressure Losses, %	Fan Exit Guide Vanes	1.1	0.0
	FEGV Core	0.0	0.5
	FEGV Duct	0.0	1.0
	Duct	7.0	6.4
	Diffuser/Combustor	6.1	7.2
	Turbine Rear Frame	1.1	0.7
	FCM Core	0.0	1.9
	FCM Duct	0.0	2.5
	Nozzle	3.5	3.5
Efficiency, %	Inlet	92.5	93.0
	Fan	90.8	89.4
	HPC	90.1	89.6
	Combustor	99.9	99.9
	HPT	91.4	90.8
	LPT	92.3	90.4
	FCM	80.0	80.0
Cooling and Leakage Air, % HPC Flow	Turbine	23.0	28.9

The Briquette engines were designed at two levels of thrust-lapse as shown in Figure 67. The engine thrust-lapse parameter is referred to in these system studies as TLID. The minimum thrust-lapse engines (identified as TLID = 0) were limited either by maximum T_4 or by a minimum thrust-lapse limit of 0.375. Other engines (TLID = 10) were designed at a higher thrust-lapse of about 0.42 to enable exploration of the impact of hot day operation, engine deterioration, and minimum engine margins. The higher thrust-lapse engines have approximately an 80°F T_4 margin at takeoff. The initial 1998 Briquette matrix which only covered 3.6 to 3.8 FPR is shown in a box in Figure 67. The remaining engines, which were used to enable exploration of other propulsion and airframe alternatives, were added in 1999 after TC definition.

The 1998 propulsion trade study, the Briquette, evaluated a total of 12 GEAE/P&W engine cycles with two SAR variations (2.7 and 2.9) for use with the PTC. A complete propulsion data pack was generated for each of these engine cycles. The propulsion data packs consisted of cycle performance data, thrust, and SFC power hooks at multiple altitudes and Mach numbers. (A power hook is a complete range of part-power data for a set altitude and Mach number.) The data packs also included specific propulsion geometry and blade count information that was used to predict acoustic levels for each engine. The propulsion weight and center of gravity were also issued together with specific outer mold lines for configuring the nacelle.
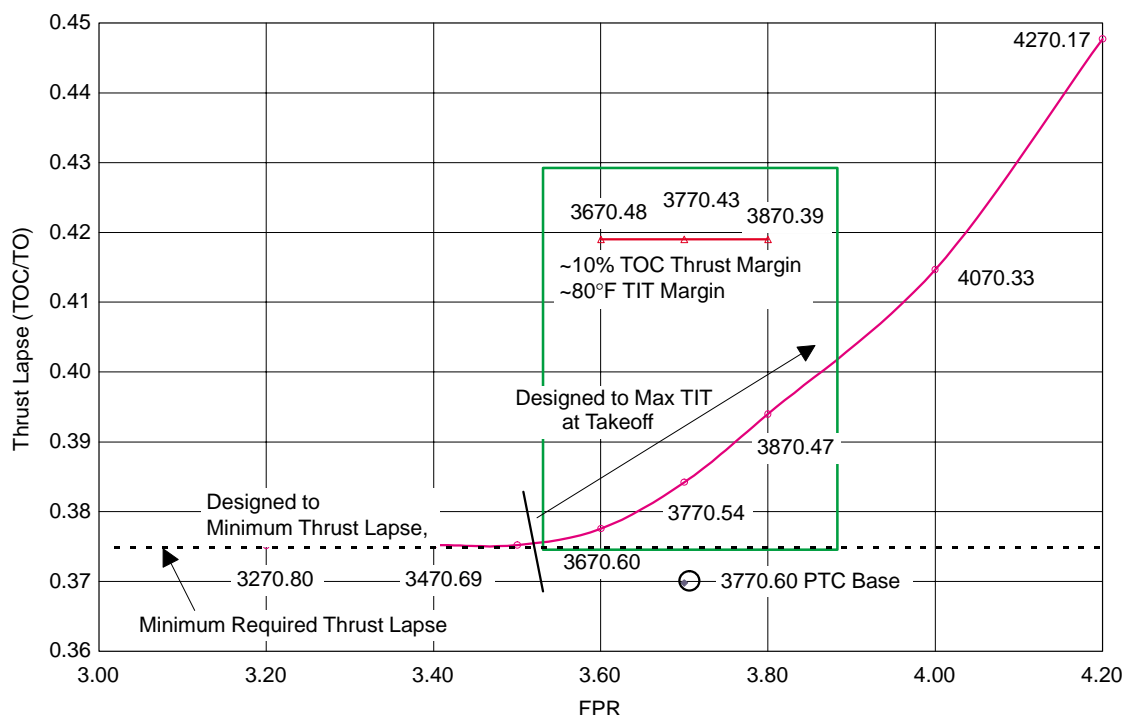
Figure 67.   Design Philosophy for the Briquette Matrix of Engines

The following is a list of the engine datapacks delivered in 1998 for Briquette trade studies that led to selection of the engine for the TC.

TLID_1	**TLID_10**
3670.60	3670.48
3770.54	3770.43
3870.47	3870.39

3.2.3.2 System Trade Studies

The data from these engines were represented parametrically in the optimized aeroelastic concept (OAC) study conducted by Boeing using their *Design Optimization Synthesis System* (DOSS). The goal of the OAC was to develop an airplane configuration by simultaneously optimizing the wing planform, the wing thickness distribution, the engine cycle, and the takeoff flight profile parameters. The results of the OAC were primary inputs for developing the 1998 Technology Concept aircraft.

The design space covered by the OAC design study is shown in Figure 68. Planform data for the OAC study were developed in a configuration trades study conducted during 1998 called the "Prism." The Prism was similar to the earlier "Wedge" study but with added wing design parameters and hence more configurations. The propulsion data for the Prism came from the Briquette and was represented by response surfaces as is shown in Figure 69.

In all, the configuration trades produced a total of 300 possible design concepts comprising 25 aspect ratio, outboard sweep, and leading-edge-break combinations; three engine fan pressure ratios; two thrust-lapse rates; and two suppresser area ratios. The Briquette was initially evaluated separately on a fixed Prism planform, the 1504, which was similar to the PTC. The results of this are shown in Figure 70.
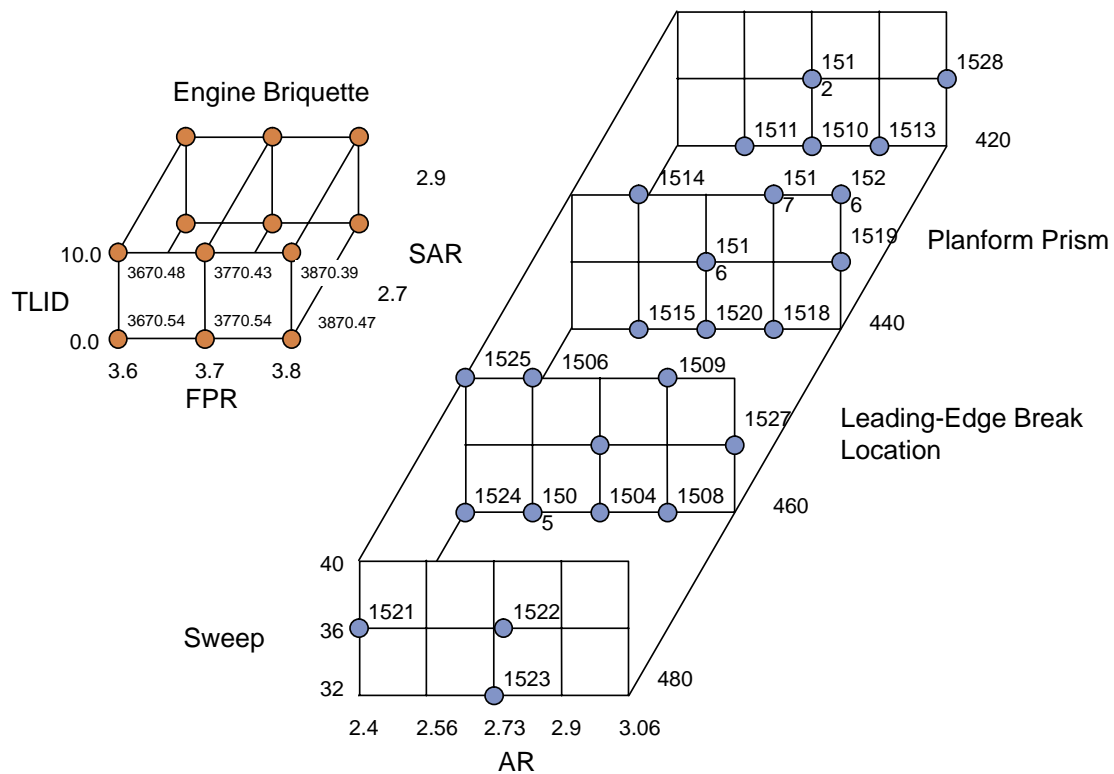
Figure 68. OAC Design Space
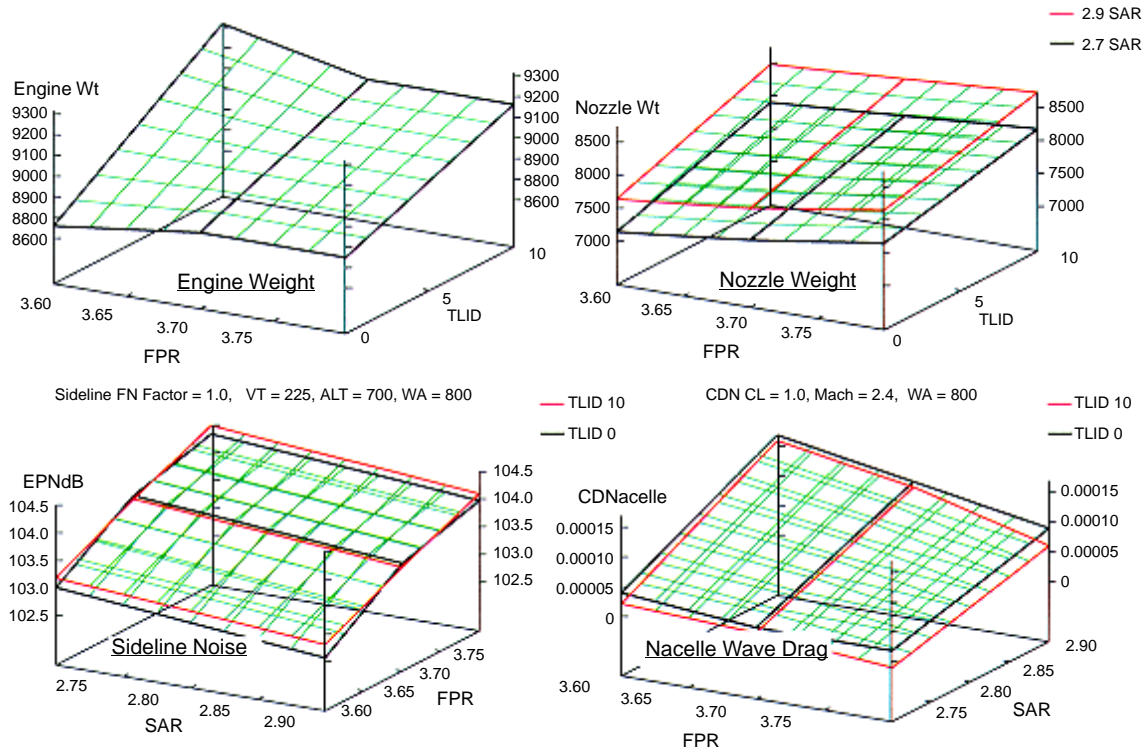
Figure 69. Propulsion Response Surfaces Used in OAC Study
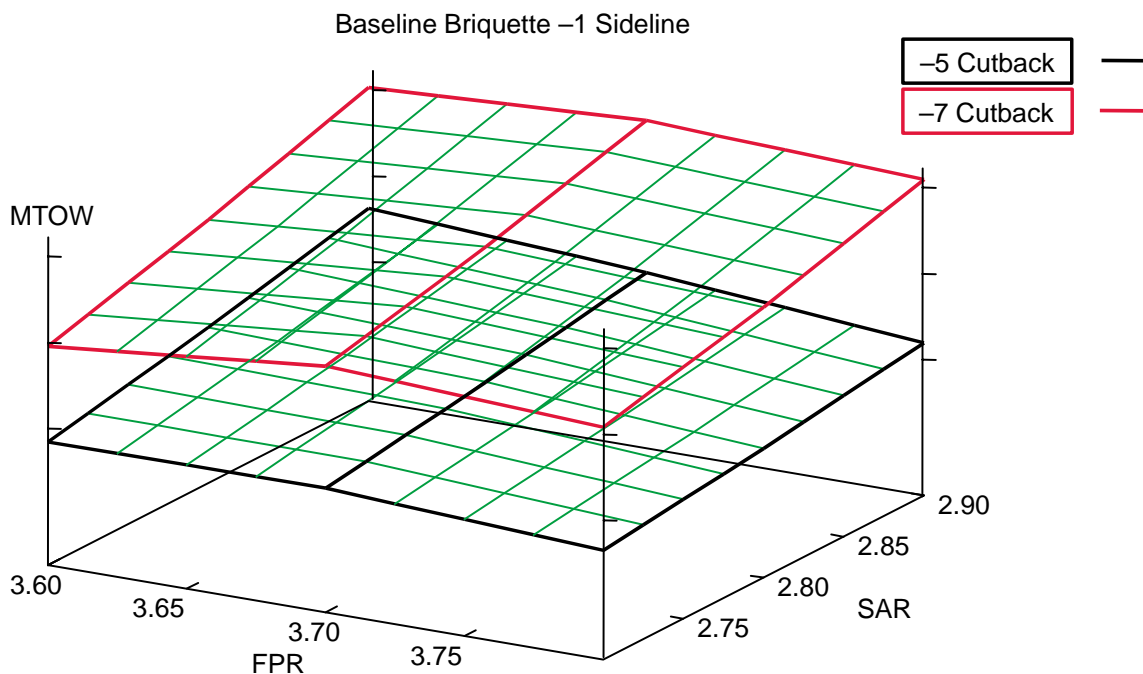
Figure 70.   DOSS Sizing Results for Briquette
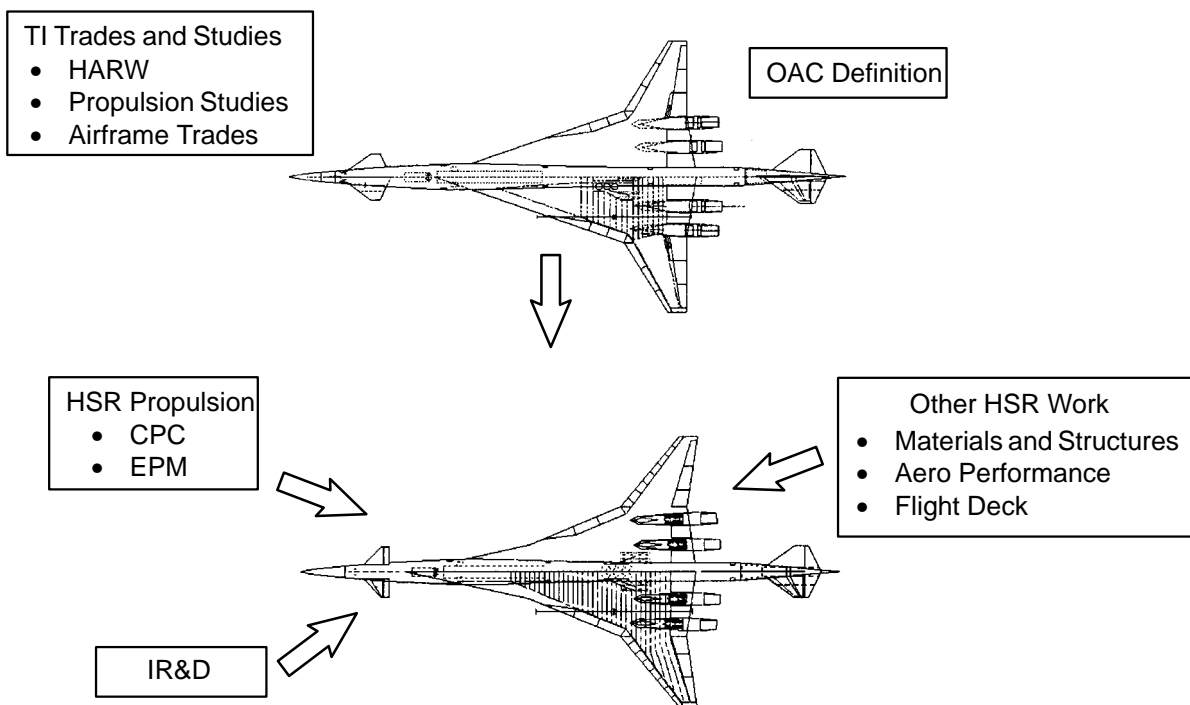
Figure 71.   Studies that Defined the TC

None of the high thrust-lapse engines (TLID = 10) are shown because all of these engines were projected to be too heavy. There were no Phase II CPC requirements for margins. Therefore, engines with margins were too heavy. There was no advantage inherent in the heavier weight and poorer SFC if additional climb thrust is not required. In all cases, the 2.7 SAR nozzles proved to be best at meeting the Phase II noise requirements (FAR 36, Stage III –1 dB sideline and –5 dB community). The best engine listed in the Briquette appeared to be the 3870.47 with a 2.7 SAR FCN nozzle. Engine optimization in this Briquette study saved about 50,000-lbm MTOW over the original Briquette baseline engine (the 3770.54 with a 2.9 SAR nozzle).

Eventually a full configuration optimization of the engine was performed. All planform, engine, wing thickness, and sizing variables were allowed to vary. The optimum engine cycle remained the same as in the Briquette study, and this was chosen for use in the TC aircraft. The optimum planform determined in the OAC was used together with information from the high-aspect-ratio wing (HARW) study to set the wing characteristics of the TC aircraft. Figure 71 shows all the various studies that contributed to the definition of the TC aircraft.

3.2.3.3 Technology Configuration Design

The 1998 baseline TC aircraft evolved from the PTC, which in turn evolved from the TCA. Each configuration was selected because, given the current state of the art, it was deemed a suitable planform for developing the enabling technologies for a commercially viable HSCT. The TC was to be the first baseline that was a direct result of a fully automated multidiscipline optimization (MDO) process in which an optimizer is used to pick the airframe/engine match. Unfortunately, program time constraints limited the design process to one cycle. Therefore, a number of design issues were not fully addressed during the TC development.

The TC was sized to an MTOW of 753,500 lbm and an operating empty weight (OEW) of 324,500 lbm. This TC OEW was a decrease of 1.5% from the OEW of the 1997 HSR baseline (PTC). The major driver in lowering the OEW was the wider main wing box chord: 245 inches compared to the 210-inch chord used in the PTC. This wider chord design was developed as a result of the 1997 high-aspect-ratio-wing integration study. The TC carries a 3,000-lbm weight allowance for wing flutter, the same as the PTC. Figure 72 shows a three view and the thumbprint of the TC aircraft.

TC Engine Description

The baseline engine used in the TC aircraft is the GEAE/P&W FCN3870.47 SAR 2.7, a Mach 2.4, dual-spool, MFTF with a 2.7 SAR, fixed-chute nozzle, mixer/ejector suppressor. Engine is maximum takeoff rated below Mach 0.45 to match inlet capability. This increases the airflow from 800 to 823 lbm/s at SLS to Mach 1.1 TC-sized airflow was 690 lbm/s at SLS). Other salient engine design characteristics are as follows:

- Three-stage fan
- Six-stage HPC
- Single-stage HPT
- Two-stage LPT

TC Engine Performance Characteristics

Cycle performance characteristics for the design reference condition are:
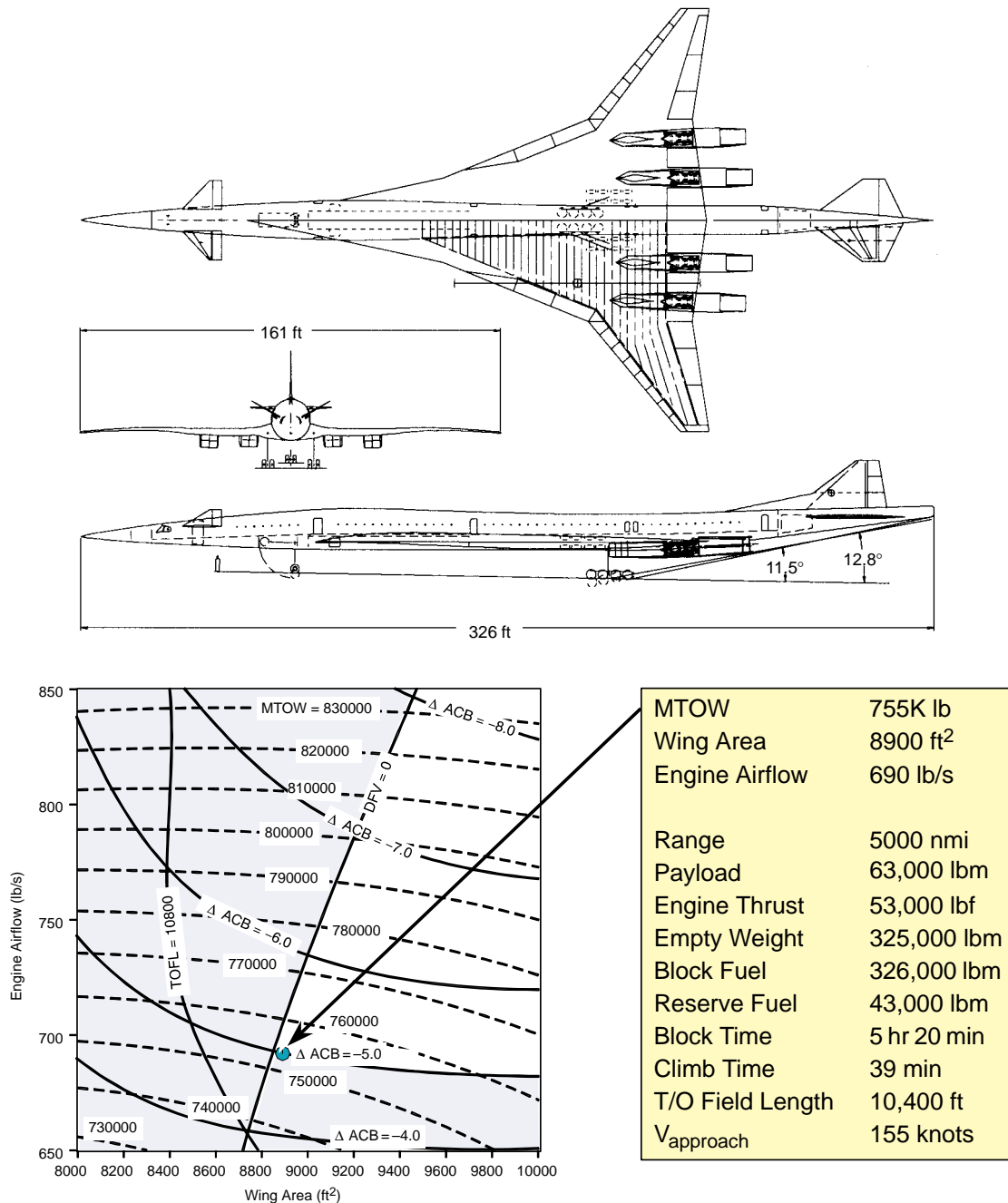
Figure 72. TC Aircraft Three View and Thumbprint

- Reference corrected inlet airflow   = 800 lbm/s
  (100% corrected fan speed)

- Fan pressure ratio   = 3.8

- Overall pressure ratio   = 20.55

- Bare engine weight   = 8848 lbm

- Max T_{41} = 2751°F
  (preserves 3000°F max combustor exit temprature)

- Maximum compressor discharge total temperature   = 1200°F

- Customer bleed from HPC   = 1.25 lbm/s

- Maximum power extraction   = 500 hp

- Installed net thrust at SLS, +18°F   = 61,388 lbf
  (suppressor deployed)

TC Nozzle Design

The baseline nozzle concept is the 2D FCN mixer/ejector suppressor designed by the CPC nozzle team of P&W and GEAE, Figure 35 (page 49). The nozzle is designed with a multilobed mixer sized for SAR = 2.70. The nozzle has an isolated maximum cross-sectional area of 7053 in^2. The aspect ratio for the nozzle operating at a mixer area ratio of 0.95 is 1.5. FCN design features are:

1. Fixed multilobed mixer reduces design complexity and required sealing.

2. Ejector inlet and reverser ducts are separate and can be optimized for each function.

3. A single-door ejector inlet concept is incorporated to reduce weight and complexity.

4. Acoustic liners are always in low-pressure areas.

5. The convergent flap also serves as reverser blocker.

6. The concept has demonstrated, through system studies and model-scale testing, good potential to meet and exceed HSCT acoustic and performance goals.

Materials used in the nozzle are consistent with 2001 technology, including nickel-based superalloys. To meet durability requirements, this nozzle design uses engine bay purge flow to cool various elements. Physical properties are not yet available on these materials, but the nozzle weight is based on an engine manufacturer's projected goal weight of 7657 lbm per nozzle. The nozzle external flap lines are designed to meet the 4° local boattail requirement; however, the sidewall close-out angle currently exceeds this requirement.

The FCN is designed to be used with the 3870.47 MFTF engine. The nozzle thrust coefficient for sideline (Mach = 0.32, Altitude = 689 ft, NPR = 3.16) is 0.964. The nozzle thrust coefficient for cruise (Mach = 2.4, Altitude = 60,000 ft) at maximum power is 0.983. The 2.7 suppressor area ratio aspirates 70%, relative to engine mass flow, at full power. This aspirated flow mixes with the engine flow in the 142-in-long mixing duct and reduces jet velocity at the ejector exit to acceptable levels.

Internal shocks and mixing of the engine and aspirated flows produces internally generated noise. This noise is reduced to acceptable levels by acoustic lining in the ejector. The effective acoustic lining length over duct diameter ratio is 1.38 and is located five mixing lobe widths downstream of the mixer exit.

Note that the mixing duct length specified above (142 inches) is the physical dimension of the mixing duct and correlates to a 140-inch duct length used in analytical studies. The mixing duct length of 140 inches corresponds to the 1/7-scale model test database.

TC Inlet Design

There was no change in the design of the 2DB inlet from that used in the PTC aircraft.

3.2.3.4 Cycle Development – TC

During 1996 and 1997 the mechanical design of the 3770.54 cycle advanced to the point where it was necessary for the cycle performance simulation to be updated in order to improve the engine component models. In addition, GEAE and P&W had agreed on a common design by the end of 1997, so components designed by one company would be accepted by the other. Preparation for the anticipated (but later dropped) full-scale demonstrator engine program began at that same time. Thus, the performance model was updated in anticipation of generating another matrix of mixed-flow turbofan cycles.

Customer bleed was taken from either of two locations in the HPC and modeled as a function of bleed temperature. Customer power extraction varied as a function of nozzle mode (suppressed or unsuppressed). Engine parasitic power extraction was modeled as a function of fuel flow. Figure 73 depicts the station designations used for the HSCT program. Figure 74 shows the cycle-matching procedure.

Component inlet and exit Mach numbers were added to the simulation to better represent the aerodynamic conditions throughout the cycle.

Inlet Selection

The inlet chosen for the 1998/99 studies was Boeing's 2D bifurcated design. This inlet was designed for a 70% corrected engine inlet airflow lapse ratio (W2AR at 55,000 ft, Mach 2.4, standard day, PC = 50) / design W2AR at sea level static, standard day, takeoff design). When it was designed, the W2AR was set to 800 lbm/s, which was consistent with the 1996/97 cycles. This airflow was allowed to increase to 823 lbm/s during takeoff and climb.

Nozzle Selection

The fixed-chute nozzle was retained for the 1998/1999 studies, but the simulation was changed to incorporate a constant value for A_8 during suppressed operation. A range of suppressor area ratios from 2.5 to 2.9 was analyzed.

Fan Selection

The fan incorporated radial pressure and temperature differentials (warpage or stratification), so two fan maps were created. The first represented fan average performance, and the second represented
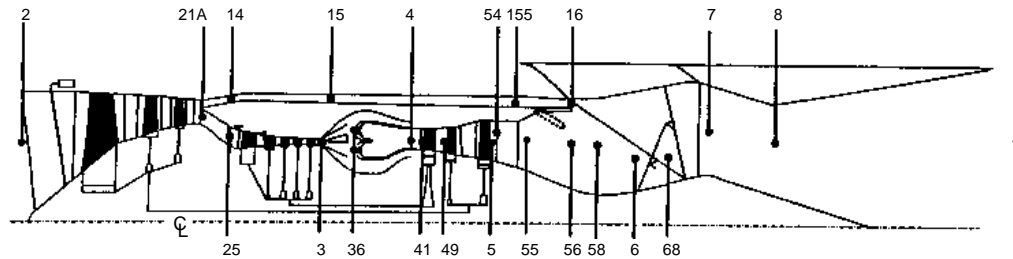
Legend

14	Bypass Duct Inlet	49	LPT Rotor 1 Inlet
15	Bypass Duct Average Area	5	LPT Exit
155	Bypass Duct at Mixer Entrance	54	Rear Frame/Diffuser Average Area
16	Mixer – Bypass Stream Side	55	Mixer Entrance – Core Stream
2	Engine Inlet	56	Mixer Exit – Core Stream
21A	Average Fan Discharge	58	Totally Mixed
25	Compressor Inlet	6	Miniaugmentor Inlet
3	Compressor Discharge	68	Miniaugmentor Exit
36	Combustor Inlet	7	Convergent Nozzle Inlet
4	HPT Vane Inlet	8	Nozzle Throat
41	HPT Rotor Inlet	9	Nozzle Exit (Based on Complete Expansion)

Note: 1. This schematic is not intended to imply details of an actual engine cross section
2. The miniaugmentor is no longer part of the HSCT schematic. Miniaugmentor stations are shown for designation purposes only.

Figure 73.   HSCT Station Designation Schematic

SLS/Standard Day/Takeoff
Component Design Point
25% Fan Surge Margin
1.05 Extraction Ratio (P16Q56)
BPR Falls Out
Set Airflow Size of 800 lbm/s
Set FPR
Set Overall Pressure Ratio (OPR)
Set Throttle Ratio (TR)

55K/2.4M/Standard Day/Top of Climb (TOC)
Flow Lapse Sets Inlet Airflow
Fan Surge Margin Falls Out (A_{16} Fixed)
Either Check if Thrust Lapse = Desired Value or
T_{T4} = Max at (689 ft/0.32 Mn/Std + 18°F Day/PC = 50)
Check if TOC T_{T3} = Maximum T_{T3}
Check if TOC T_{T4} = Maximum T_{T4}

If TOC $T_{T3} \neq$ Maximum T_{T3}, Adjust SLS OPR
If TOC $T_{T4} \neq$ Maximum T_{T4}, and/or
Thrust Lapse $\neq$ Desired Value (or T_{T4} 0 Maximum at
(689 ft/0.32 Mn/Std + 18°F Day/PC = 50)),
Adjust SLS TR.
If TOC T_{T3} = Maximum T_{T3}, TOC T_{T4} = Maximum T_{T4}
and Thrust Lapse = Desired Value (or T_{T4} = Max at
(689 ft/0.32 Mn/Std + 18°F Day/PC = 50)),
Cycle Match is Finished

Note: Thrust Lapse = Uninstalled primary net thrust (FNP) at (55K ft/2.4 Mn/Std Day/PC = 50) / Uninstalled mixed out net thrust (FNMIX) at (SL/0.30 Mn/Std + 18°F Day/PC = 50)

Figure 74.   Matching Diagram for 1998–1999 Cycle

the fan inner-diameter performance. The fan outer-diameter performance was calculated from these two maps. The fan pressure ratio range used was 3.2 to 4.2 with a bypass ratio range of 0.17 to 0.80. The fan average efficiency, ID efficiency, and ID pressure ratio at design were adjusted as a function of BPR and average FPR.

Compressor Modeling

The high pressure compressor was modeled by using two maps, chosen to better represent the compressor stator schedules and engine rotor speed variations during subsonic and supersonic flight. These maps were biased to the engine inlet total temperature. The first map was a nominal (low T_{T2} stator schedule) map used to simulate subsonic flight conditions. The second was a high T_{T2} stator schedule map used to simulate supersonic flight conditions. For transonic flight conditions, a linear interpolation was applied between the two maps.

Combustor Simulation

A new correlation was added to the simulation to represent combustor pressure loss. The combustor pressure loss was split between a diffuser loss (which varied as a function of dynamic pressure, Q) and a fixed burner loss (defined at design).

Turbine Development

The HPT map was based on design results for 199619/97. A table was also added to to calculate the angle of the HPT exit air. The exit air angle was a function of the HPT expansion ratio and the HPT inlet corrected speed. This exit air angle was also considered to be the LPT inlet air angle.

The LPT had a vaneless first-stage design that used interpolation of six maps representing inlet air angles of 21°, 28°, 35°, 41.78°, 47°, and 52°. Both the LPT exit air angle and the LPT exit Mach number were functions of the LPT expansion ratio and the LPT inlet corrected speed. The LPT exit air angle was used together with the LPT exit Mach number to calculate the exit guide vane loss.

The number of turbine cooling bleeds was expanded from 3 to 36 to provide a better representation of the turbine cooling process. The bleed percentage varied slightly from cycle to cycle for the 1998/99 matrix of cycles. The bleed percentage increased from the 1996/97 level of 23% of the airflow entering the compressor (WAE) to 28.1%, plus 1.3% of the fan duct airflow.

Due to this increase in turbine cooling, there was a significant change in the way the cycle operates. Since the amount of cooling for the HPT vane increased from 9.5% to 13.4% W_{AE}, the maximum HPT temperature used for limiting fuel flow at maximum-power operation, switched from the HPT rotor inlet temperature ($T_{T4.1}$) to the combustor exit temperature (T_{T4}). This was necessary because the increase in cooling caused the temperature exiting the HPT vane to decrease so much that it was no longer the limiting parameter.

The turbine design cooling flows and efficiencies were adjusted because of the variations in enthalpy (Δh) values from cycle to cycle in both the HPT and the LPT. These adjustments varied as a function of $\Delta h/T_{T4.1}$ for the HPT and $\Delta h/T_{T4.5}$ for the LPT.

Fan/Core Mixer Selection

After extensive comparison of the fixed fan/core mixer versus the variable fan/core mixer, it was concluded that the complexity and weight of the variable mixer negated any performance benefits.

Therefore, the 1998/99 cycles all were performed using a fixed fan/core mixer. Core side diffusion losses were combined with the friction loss. This resulted in a core side pressure loss at design of 2%. The duct-side friction loss at design was 1.5%. Off-design these losses varied as a function of local Q. For all flight conditions, the mixing effectiveness was set at 80%.

Top of Climb Thrust and SFC Trends

Figure 75 displays the 1998/1999 cycle thrust and SFC trends. Primary nozzle net thrust (FNP) at top of climb (TOC) is plotted on the X axis; the corresponding SFC is plotted on the Y axis. Seveal curves are shown, each corresponding to a constant parameter.
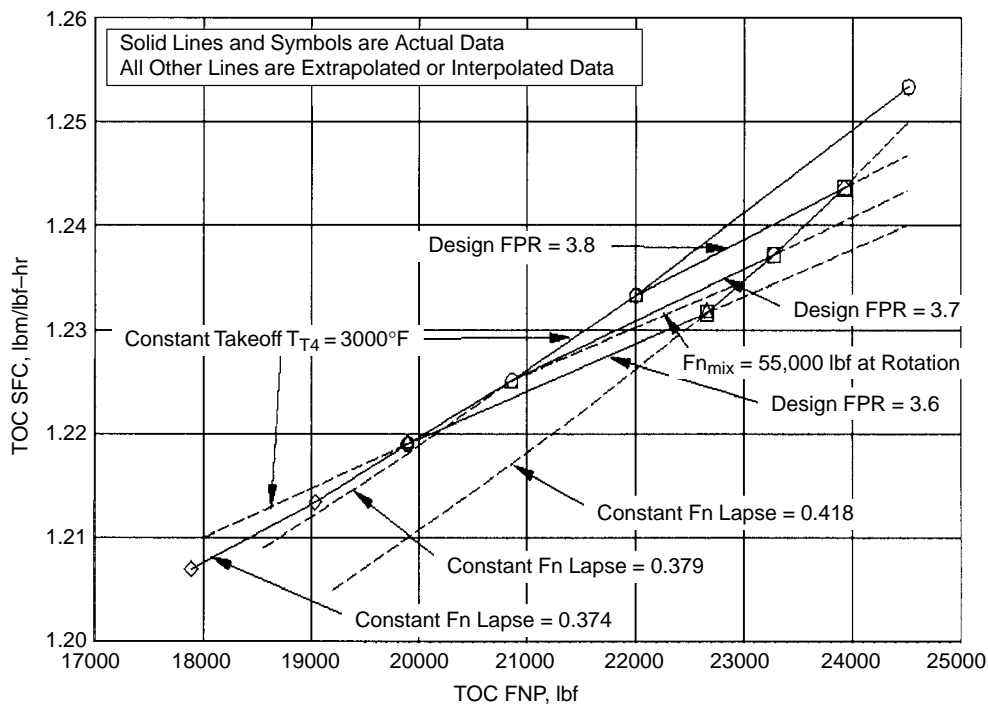
Figure 75. Cycle Trends: 1998 – 1999

- T_{T4} of 3000°F (maximum limit) at the takeoff sideline noise flight condition (689 ft, Mach 0.32, Std +18°F day, PC = 50). All cycles falling on this curve will have a takeoff TT4 of 3000°F; this curve defines the upper TT4 boundary. Any cycle falling below this curve would not be a candidate for HSCT.

- F_{Nmix} of 55,000 lbf at the takeoff rotation flight condition (sea level, Mach 0.30, Std +18°F day, PC=50). All cycles falling on this curve will have a takeoff thrust of 55,000 lbf. Since 55,000 lbf at takeoff meets the requirements of an engine sized at a fan inlet corrected airflow of 823 lbm/s, any cycle falling above or below this curve would need to be scaled.

  - Design FPR = 3.6
  - Design FPR = 3.7
  - Design FPR = 3.8
  - Thrust lapse = 0.374
  - Thrust lapse = 0.379
  - Thrust lapse = 0.418

Figure 75 enables the designer to estimate an HSCT cycle. When using a TOC FNP, the thrust lapse and design FPR are selected to provide a desired TOC SFC.

Off-Design Operations, Unsuppressed

Maximum-Power Operation, PC = 50: The inlet corrected airflow schedule was defined by Boeing, and a maximum limit of 823 lbm/s was applied to that schedule.

A_{E8} was varied to hold the inlet corrected airflow schedule unless the maximum XNL of $1.09 \times XNL_{design}$ or the maximum LPT exit flow parameter (W5GR, which was defined at 10,000 ft, Mach 0.8, Standard day, PC = 50) was obtained. If so, the W2AR would be reduced and the A_{E8} varied to satisfy the new requirements.

Fuel flow was varied in order to hold a P16Q56 of 1.05, unless limited by the maximum combustor exit total temperature (T_{T4}) of 3000°F and/or the maximum compressor exit temperature (T_{T3}) of 1200°F.

A_{16} was fixed at the value defined for the aerodynamic design point.

Part-Power Operation, PC $\leq$ 50 and > 21: A_{E8} was varied to hold maximum power W2AR until limited by maximum W5GR, maximum M_{16} of 0.8, maximum $M_{15.5}$ of 0.8, or a maximum A_{E8} of $1.6 \times A_{E8\ design}$.

Fuel flow was reduced to obtain a percentage of the maximum power uninstalled primary net thrust (FNP) until limited by the minimum combustor inlet total pressure (P_{T36}) of 30 psia.

A_{16} was fixed at the value defined for the aero design point.

Idle-Power Operation, PC = 21: A_{E8} was varied to hold maximum power W2AR until limited by maximum W5GR, maximum M_{16}, maximum $M_{15.5}$, or maximum A_{E8}.

At a static conditions, fuel flow was varied to obtain the minimum FNP possible. This ranged from 5% to 6% of the maximum power FNP, depending on the cycle.

At Mach numbers > 0 and $\leq$ 1.0, fuel flow was varied to obtain 5% of the maximum power FNP.

At Mach numbers $\geq$ 1.5, idle was defined as the FNP required to hold W2AR at or above 80% of maximum power W2AR. The FNP required to do this was 50% of the maximum power FNP. Therefore, fuel flow was varied to obtain 50% of the maximum power FNP.

Between M = 1.0 and 1.5, idle was a linear interpolation between 5% and 50% maximum power FNP. If P_{T36} reached the minimum value of 30 psia, idle was reset so that P_{T36} was held at 30 psia.

A_{16} was fixed at the value defined for the aero design point.

Off-Design Operations, Suppressed

Maximum-Power Operation, PC = 50: Fuel flow was varied to hold W2AR unless limited by maximum T_{T4} or maximum T_{T3}.

A_{E8} was fixed at a value such that the surge margin of the fan was 20% and P16Q56 was 1.03 at the sideline noise flight condition of 689 ft, Mach 0.32, Std +18°F day, PC = 50.

A_{16} was fixed at the value defined for the aero design point.

Part-Power Operation, PC < 50 and > 21: Fuel flow was varied to obtain a percentage of the maximum power uninstalled FNP unless limited by the minimum P_{T36} of 30 psia.

A_{E8} was fixed at the value set for the maximum power operation.

A_{16} was fixed at the value defined for the Aero Design Point.

Idle-Power Operation, PC = 21: At static to Mach 0.2, fuel flow was varied to obtain the minimum FNP possible. This ranged from 5% to 9.9% of the maximum power FNP, depending on the cycle.

At Mach numbers > 0.2 and ≤ 0.9, fuel flow was varied to obtain 5% of the maximum power FNP unless limited by the minimum P_{T36} of 30 psia.

A_{E8} was fixed at the value set for the maximum power operation.

A_{16} was fixed at the value defined for the aero design point.

Engine Performance Data Packs

Table 24 is a summary of the 1998/1999 HSCT engine performance data packs. The table shows:

1. Design (sea level static/standard day/takeoff power) FPR

2. Inlet corrected airflow lapse rate: (TOC W2AR/design W2AR) × 100

3. Design BPR (fan duct inlet mass flow/core inlet mass flow)

4. Design overall pressure ratio (OPR)

5. $T_{T4.1}$ throttle ratio (TOC $T_{T4.1}$/design $T_{T4.1}$)

6. Inlet corrected airflow (W2AR) at takeoff

7. T_{T4} at sideline noise condition (689 ft, M 0.32, Std +18°F day, PC=50)

8. Uninstalled net thrust lapse

9. Top of climb extraction ratio (TOC P_{T16}/P_{T56})

10. Data pack completion date

The nozzle was sized at three different suppressor area ratios: 2.5, 2.7, and 2.9. Since A_8 was constant during suppressed operation, SAR defined the size of the nozzle mixing area and the amount of airflow entrainment. The entrainment increased as the SAR increased.

> *Note: Parameters listed or mentioned in the following tables and discussions are generally represented by "cycle deck" nomenclature (all capitals, no subscripts) according to the station designations illustrated in Figure 73. Some of these parameters may not be described in the tables or foregoing text, but definitions are listed in the* Lexicon *at the front of this report (page lxv).*

Tables 25 and 26 summarize engine performance data at key flight conditions for the 1998/99 HSCT Briquette cycles. Table 25 presents data for six cycles, run to a constant T_{T4} = 3000°F at sideline noise condition, 689 ft, Mach 0.32, std +18°F day, PC=50. The SAR for the entire table was 2.7. Table 26 presents data for six cycles, run to a constant thrust lapse = 0.374 plus three cycles run to a constant thrust lapse = 0.418. The SAR for the entire table was 2.7.

Table 24.   HSCT Engine Performance Data Pack Summary, 1998 and 1999   *Design inlet corrected airflow is 800 lbm/s.*

FPR	Flow Lapse Rate, %	BPR	OPR	T_{T41} Throttle Ratio	Takeoff W2AR, lbm/s	T_{T41} at Sideline Noise Condition, °F	Thrust Lapse	TOC ER	2D Bifurcated Inlet Fixed-Chute Nozzle		
									2.5 SAR	2.7 SAR	2.9 SAR
3.2	70	0.80	19.56	1.146	823	2942	0.37	1.12	03/22/99	03/19/99	
3.4	70	0.69	19.69	1.139	823	2965	0.37	1.14	03/24/99	03/23/99	
3.6	70	0.48	18.52	1.166	823	2898	0.42	1.11		07/15/98	07/14/98
		0.60	19.88	1.130	823	3000	0.37	1.16		07/07/98	07/06/98
3.7	70	0.43	18.52	1.160	823	2917	0.42	1.12		07/14/98	07/13/98
		0.54	19.68	1.130	823	3000	0.38	1.17		07/02/98	07/02/98
3.8	70	0.39	18.49	1.154	823	2939	0.42	1.13		07/11/98	07/10/98
		0.47	19.37	1.131	823	3000	0.39	1.17		07/11/98	07/11/98
4.0	70	0.33	18.67	1.130	823	3000	0.41	1.17		09/29/98	09/30/98
4.2	70	0.17	17.39	1.133	823	3000	0.45	1.15		09/29/98	10/01/98

Table 25. Data Summary A for 1998/1999 Briquette Cycles

Operating Point	Parameter	Cycle				
		B3670.60	B3770.54	B3870.47	B4070.33	B4270.17
Design Point: Sea Level Static, Standard Day, PC = 50	P16Q56	1.05	1.05	1.05	1.05	1.05
	BPR	0.604	0.536	0.465	0.331	0.172
	OPR	19.880	19.677	19.368	18.669	17.394
	FPR	3.60	3.70	3.80	4.00	4.20
	TT4 (°F)	2627.9	2625.8	2624.7	2629.5	2624.2
	TT4.1 (°F)	2381.2	2380.0	2378.8	2382.5	2376.6
	W2AR (lbm/s)	800.0	800.0	800.0	800.0	800.0
	SMFAN	24.8	24.8	24.8	24.8	24.8
Sea Level, Mach 0.3, Std +18°F Day, PC50	FNMIX (lbf)	53435	54988	56499	59630	63790
	W2AR (lbm/s)	822.3	822.2	822.4	822.1	822.0
689 ft, Mach 0.32, Std +18°F Day, PC50	TT4 (°F)	3000.1	3000.4	3000.4	3000.6	3000.6
	SMFAN	20.02	19.99	20.34	21.18	22.45
	P16Q56	1.0303	1.0286	1.0285	1.0289	1.0292
	A8CD* (in^2)	1275.0	1258.7	1250.0	1237.0	1235.0
	AJ2 (in^2)	1308.5	1291.7	1282.8	1269.4	1267.3
	TT8 (°F)	1235.9	1285.5	1338.0	1451.6	1618.0
	PT8 (psia)	50.71	52.18	53.43	55.86	58.62
	VJIP (ft/s)	2495	2557	2618	2743	2910
	W2AR (lbm/s)	822.9	822.7	822.9	823.0	822.86
	FPR	3.86	3.97	4.06	4.25	4.42
	ETA (FNAA)	0.8292	0.8271	0.8225	0.8124	0.7973
55,000 ft, Mach 2.4, Standard Day, PC50	TT3 (°F)	1200.0	1200.2	1200.4	1200.1	1199.9
	TT4 (°F)	3000.1	2998.7	2999.2	2999.5	3000.2
	TT4.1 (°F)	2750.5	2750.2	2751.0	2751.8	2753.2
	P16Q56	1.1618	1.1650	1.1669	1.1704	1.1533
	W2AR	560.0	560.0	560.0	560.0	559.9
	FNP	19891	20860	22009	24515	28386
	SFC	1.2190	1.2251	1.2333	1.2533	1.2881
	FN Lapse*	0.372	0.379	0.390	0.411	0.445
	TT8 (°F)	1245.2	1288.3	1340.1	1455.2	1638.1
	PT8 (psia)	30.77	31.48	32.28	33.92	36.27
	TT4.1 Throttle Ratio**	1.1300	1.1304	1.1311	1.1299	1.1328
	A16 (in^2)	523.0	475.1	423.5	319.1	181.0
	SMFAN	24.33	22.93	21.31	17.79	12.43
* From 55,000-ft, Mach 2.4 to sea level, Mach 0.3						
** From 55,000-ft, Mach 2.4 to sea level design point						

Table 26. Data Summary B For 1998/1999 Briquette Cycles

Operating Point	Parameter	B3270.80	B3470.69	B3670.60	B3670.48	B3770.43	B3870.39
Design Point:	P16Q56	1.050	1.050	1.05	1.050	1.050	1.050
Sea Level Static,	BPR	0.796	0.685	0.604	0.477	0.431	0.387
Standard Day,	OPR	19.556	19.693	19.880	18.520	18.522	18.491
PC50	FPR	3.20	3.40	3.60	3.60	3.70	3.80
	TT4 (°F)	2583.8	2602.5	2627.9	2529.9	2545.6	2563.1
	TT4.1 (°F)	2333.1	2354.3	2381.2	2293.7	2307.7	2323.3
	W2AR (lbm/s)	800.0	800.0	800.0	800.0	800.0	800.0
	SMFAN	24.8	24.8	24.8	24.8	24.8	24.8
Sea Level, Mach 0.3,	FNMIX (lbf)	47868	50876	53435	54362	55828	57297
Std +18°F Day, PC50	W2AR (lbm/s)	823.0	823.0	822.3	823.0	823.0	823.0
689 ft, Mach 0.32,	TT4 (°F)	2942.4	2965.3	3000.1	2898.7	2917.5	2939.1
Std +18°F Day,	SMFAN	20.00	20.01	20.02	20.29	20.39	20.56
PC50	P16Q56	1.0336	1.0320	1.0303	1.0286	1.0276	1.0271
	A8CD (in^2)	1365.3	1319.0	1275.0	1295.0	1277.5	1263.0
	AJ2 (in^2)	1401.7	1353.9	1308.5	1329.2	1311.1	1296.2
	TT8 (°F)	1084.0	1161.7	1235.9	1274.9	1320.7	1368.9
	PT8 (psia)	44.98	47.83	50.71	50.568	52.005	53.388
	VJIP (ft/s)	2277	2389	2495	2524	2583	2642
	W2AR (lbm/s)	823.0	823.0	822.9	823.0	823.0	823.0
	FPR	3.42	3.64	3.86	3.85	3.95	4.06
	ETA (FNAA)	0.8288	0.8288	0.8292	0.8290	0.8264	0.8222
55,000 ft, Mach 2.4,	TT3 (°F)	1200.0	1200.3	1200.0	1200.0	1200.0	1199.8
Standard Day, PC50	TT4 (°F)	3000.0	3000.8	3000.1	3000.0	2999.7	3000.3
	TT4.1 (°F)	2740.9	2746.6	2750.5	2751.8	2751.6	2752.3
	P16Q56	1.1217	1.1385	1.1618	1.1129	1.1217	1.1319
	W2AR	560.0	560.0	560.0	560.0	560.0	560.0
	FNP	17887	19033	19891	22663	23280	23922
	SFC	1.2070	1.2134	1.2190	1.2316	1.2372	1.2436
	FN Lapse*	0.374	0.374	0.372	0.417	0.417	0.418
	TT8 (°F)	1156.7	1207.0	1245.2	1365.0	1365.0	1424.0
	PT8 (psia)	29.35	30.19	30.77	33.23	33.61	33.94
	TT4.1 Throttle Ratio**	1.146	1.1394	1.1300	1.1664	1.1604	1.1542
	A16 (in^2)	676.5	591.2	523.0	449.6	410.7	372.5
	SMFAN	25.38	24.66	24.33	18.72	18.43	17.99
* From 55,000-ft, Mach 2.4 to sea level, Mach 0.3							
** From 55,000-ft, Mach 2.4 to sea level design point							

At the conclusion of the 1998/1999 study, the 3870.47 was selected as the best cycle based on mission requirements. The nomenclature of 3870.47 is interpreted as follows:

- 38 is the design FPR
- 70 is the inlet corrected airflow lapse (%)
- 0.47 is the design BPR

However, the B3770.54 cycle was selected by the engine manufacturers, prior to the final engine selection, to perform detailed component designs. Tables 27 through 35 present configuration data concerning the B3770.54 engine cycle.

A total of 36 bleeds are defined for turbine cooling. Table 36 is a summary of the B3770.54 turbine cooling bleeds in % of total engine airflow (WAE) or % of fan duct airflow.

Engine Mixer Effectiveness

Engine mixer effectiveness (PCMX) is 0.80 and is fixed for all flight conditions and power settings (affects thrust).

Trade Study

Tables 37 and 38 present the results of a trade study conducted on the 6/98 B3770.54 cycle. Table 37 summarizes the effect of increasing fan, HPC, HPT, and LPT average efficiencies by 0.01 (absolute) on uninstalled net thrust and SFC at the sideline noise, subsonic cruise, and supersonic top of climb flight conditions. This table also summarizes the effects of reducing turbine cooling air (TCLA) by 1% and increasing nozzle C_{FG} by 0.002 (absolute).

Table 38 summarizes the effect of reducing pressure loss by 0.005 (absolute) at nine locations: (1) fan exit guide vane, core side (FEGV,C), (2) fan exit guide vane, duct side (FEGV,D), (3) fan duct (Duct), (4) diffuser, (5) combustor (Burner), (6) turbine exit case (TEC), (7) fan/core mixer, core side (FCM,C), (8) fan/core mixer, duct side (FCM,D), and (9) nozzle tail pipe (Nozzle), on uninstalled net thrust and SFC at the sideline noise, subsonic cruise, and supersonic TOC flight conditions.

Table 27. HSCT MFTF FCN B3770.54 Customer Parameters

Parameter	Description/Comments
η (Inlet)	Boeing's 2D bifurcated Inlet as of 2/13/98. Inlet recovery is a function of flight Mach no.
W2AR	Boeing's 2D bifurcated Inlet as of 2/13/98. Inlet corrected airflow is a function of flight Mach no. The cycle runs to this airflow schedule unless it is limited by the maximum turbine exit flow parameter (W5GR), defined at 10000 ft, M 0.8, std day, PC50 or the max XNL of 9% above the design point N1 value.
HPXH	Customer (airframe) power extraction: 500 hp suppressed, 150 hp unsuppressed.
HPX(2)	Customer (airframe) horsepower extraction: 500 hp suppressed, 150 hp unsuppressed plus engine parasitic horsepower requirements (function of fuel flow).
WB3	Customer bleed requirement: 1.25 lbm/s.

Table 28. HSCT MFTF FCN B3770.54 Cycle Parameters

Parameter	Value	Description/Comments
PT16/PT56	1.05	Sets BPR
SMFAN	25	Defined by fan map characteristics; FPR (3.7), surge PR, and corrected airflow (800 lbm/s)
W2AR	800 lbm/s	Engine inlet corrected airflow
Fuel Flow	10.322 lbm/s	Set by TT4.1
TT4.1	2380°F	Set by throttle ratio to get max. TT4 (3000°F) at 689 ft, Mach 0.32, std+18°F day and max. TT4 at 55000 ft, Mach 2.4, std day
OPR	19.677	Set to obtain max. TT3 (1200°F) at 55000 ft, Mach 2.4, std day
FPR	3.70	Set to match VJIP (2553 ft/s) of the 3770.60 cycle, at 689 ft, Mach 0.32, std+18°F day, PC50
CPR	5.260	Determined from OPR and FPR
N1C2	100	Low-pressure rotor speed corrected to station 2
XNL	100.00 RPM	To calculate actual physical speed use the following equation: $$XNL_{actual} = 5007.51 \times XNL/97.135$$ (Equation is good only for the B3770.54 cycle.)
N2C2.5	100	High-pressure rotor speed corrected to station 2.5
XNH	123.23 RPM	To calculate actual physical speed use the following equation: $$XNH_{actual} = 7899.92 \times XNH)/119.02)$$ (Equation is good only for the B3770.54 cycle.)
A8CD	945 in^2	Effective nozzle throat area; varied to maintain engine inlet corrected airflow

Table 29. HSCT MFTF FCN B3770.54 Cycle Engine Limits, 6/98

Engine Limit	Value
Max. Combustor Exit Total Temperature (TT4)	3000°F
Max. HPT Rotor Inlet Total Temperature (TT4.1)	2800°F
Max. Compressor Discharge Total Temperature (TT3)	1200°F
Max. Nozzle Effective Jet Area (A8CD or AE8)	1.6 × Aero Design Point A8CD
Max. Fan Duct Mach Number (M155)	0.8
Max. Fan Duct Mixing Plane Mach Number (M16)	0.8
Max. Low-Pressure Spool Speed (XNL)	1.09 × Aero Design Point N1
Max. LPT Exit Flow Parameter (W5GR)	Defined at 10,000 ft, Mach 0.8, std day, PC50
Max. LPT Exit Mach Number (M5)	0.55
Fan Duct Mixing Plane Area (A16)	Fixed at The Aero Design Point Value
Min. Combustor Inlet Total Pressure (PT36)	30 psia

Table 30. HSCT MFTF FCN B3770.54 Input Emissions Parameters

Parameter	Value/Unit of Measure	Comment
Volume	4.81991 ft^3	Volume defined at 55,000 ft, Mach 2.4, std day, PC50, top of climb as: TT4 $\times$ WG36 / PT4 / 932.0
NOx – EINOx (output)	g/kg fuel	Function of volume, TT3, WG36, TT4 and PT4
HC – EIHC (output)	g/kg fuel	Function of combustor efficiency
CO – EICO (output)	g/kg fuel	Function of combustor efficiency and fuel/air ratio
H_2O EIH$_2$O (output)	g/kg fuel	Function of EIHC
CO_2 EICO$_2$ (output)	g/kg fuel	Function of EIHC and EICO
SO_2 EISO$_2$ (output)	g/kg fuel	Set equal to 1.0

Table 31. HSCT MFTF FCN B3770.54 Input Pressure Losses

Parameter	Value	Description/Comment
(PT21ID–PT25)/PT21ID	0.007	Varies off design as a function of Q (dynamic pressure)
(PT21OD–PT14)/PT21OD	0.010	Fixed for all flight conditions
(PT3–PT36)/PT3	0.027	Varies off design as a function of Q
(PT36–PT4)/PT36	0.0414	Combined with (PT3–PT36)/PT3), is defined by Combustor team. (Fixed for all flight conditions.)
(PT5–PT55)/PT5	0.0077	Turbine exit guide vane loss is a function of LPT exit air angle and LPT exit Mach number. Varies off design as a function of LPT exit air angle and LPT exit Mach number)
(PT55–PT56)/PT55	0.020	Varies off design as a function of Q
(PT14–PT15)/PT14	0.040	Varies off design as a function of Q
(PT155–PT16)/PT155	0.015	Varies off design as a function of Q
(PT68–PT7)/PT68	0.000	In suppressed mode tailpipe pressure loss is recorded in nozzle C_{FG}. In unsuppressed mode the loss is not recorded in C_{FG}. Therefore, (PT68–PT7)/PT68 = 0.035 at 55,000 ft, M2.4, std day, PC50. (PT68–PT7)/PT68 then varies off design as a function of the local Mach number squared.

Table 32. HSCT MFTF FCN B3770.54 Input Mach Numbers

Parameter	Value	Description/Comment
M2	0.465	Recommended value based upon P&W fan design. Set at IGV strut L/E
M21ID	0.560	Based upon P&W fan design and fan exit warpage effects
M21OD	0.390	Based upon P&W fan design and fan exit warpage effects
M25	0.600	At HPC IGV L/E
M3	0.3237	Set so that at 55,000 ft, Mach 2.4, std day, PC50, M3 = 0.35
M36	0.170	
M4	0.120	
M49	0.650	
M5	0.500	Off design function of LPT exit angle, corrected speed and PR
M54	0.380	
M55	0.380	
M56	0.300	Set not to exceed M55, otherwise design integration problems could occur
M14	0.350	Duct stream Mach number at exit of intermediate case
M15	0.359	Set equal to M14+.009
M155	0.346	Set equal to M16–0.05 (need to run one pass first in order to get M16)
M16		Output from static pressure balance and PT16
M68	0.250	Per the 1996 version of the 3770.60 cycle.

Table 33. MFTF FCN B3770.54 Engine Component Inputs, Fan

Item	Value	Comment
FPR (average)	3.70	Input
η(fan average)	0.8710	Read from fan average map and then adjusted by the fan adjustment tables
FPR(ID)	3.768	Read from fan I.D. map and then adjusted by the fan adjustment tables
η(fan ID)	0.8840	Read from fan I.D. map and then adjusted by the fan adjustment tables

Notes:

1. Fan O.D. PR and η are outputs and a function of the fan average and ID values.

2. FPR(OD) = 3.574, η(fan OD) = 0.8462

3. The fan OD to ID pressure ratio difference (warpage) is represented by a fan average map and a fan ID map and applying adjustments when needed.

4. The fan adjustment tables are used on design to adjust η(fan aver), η(fan ID) and FPR(ID) for changes in cycle BPR and FPR(average).

5. The average fan map was designed at FPR(average)=3.70 and BPR=0.54.

6. The map fan average surge line is defined by taking the fan average map maximum pressure ratio and the associated corrected airflow for each of the N1C2's and combining them into one table. The surge margin is calculated at a constant fan average map corrected airflow value.

7. Not using Reynolds effects.

Table 34. MFTF FCN B3770.54 Engine Component Inputs, Compressor

Item	Value	Comment
Pressure Ratio	5.260	Output, function of OPR and fan average PR
Polytropic Efficiency	0.9100	Input
Adiabatic Efficiency	0.8881	Output

Notes:

1. Two compressor maps used to better model the compressor stator schedules. The first is a nominal (low TT2 stator schedule) map. The second is a high TT2 stator schedule map. The maps work in the following way:

   – The low TT2 map is used for TT2 ≤ 120°F
   – The high TT2 map is used for TT2 ≥ 200°F and
   – For TT2 > 120°F and < 200°F, values are interpolated between the maps as a function of TT2.

2. The map HPC surge line is defined by taking the maximum pressure ratio and the associated corrected gas flow for each of the N2C25's and combining them into one table. There is one table for the low TT2 map and another for the high TT2 map.

3. The surge margin is calculated at a constant map WC value, using the low TT2 table for TT2 ≤ 120°F, the high TT2 table for TT2≥200°F and interpolating between the two tables for TT2>120°F and <200°F.

Table 35. MFTF FCN B3770.54 Engine Component Inputs, Combustor and Turbines

Item	Value	Comment
Combustion Efficiency	0.9990	Input
Fuel LHV	18,580 Btu/lbm	Input
HPT Expansion Ratio	2.530	Input
HPT Efficiency	0.8880	Input
LPT Expansion Ratio	2.214	Input
LPT Efficiency	0.9002	Input

Notes:

1. The HPT is represented by one map plus a table of exit-air angles.

2. The LPT is modeled via interpolation of six maps for inlet air angles of 21°, 28°, 35°, 41.78°, 47°, and 52°. An LPT exit air-angle table is used with the LPT exit Mach number to read the exit guide vane loss.

3. At design, turbine cooling and both the HPT and LPT efficiencies are adjusted as a function of $\Delta H/T_{T4.1}$ (for HPT) and $\Delta H/T_{T4.5}$ (for LPT).

Table 36.   Turbine Cooling Bleeds

Bleed	Source	Value
% Engine Airflow (WAE)	HPT Vane	13.4200
	HPT Blade	7.2300
	LPT First-Stage Blade	3.2330
	LPT Vane	2.1034
	LPT Second-Stage Blade (from HPC)	2.1061
	Total %WAE	28.0925
% Fan Duct Air	LPT Second-Stage Blade (from Fan Duct)	0.7600
	Turbine Exit Case	0.5000
	Total % Fan Duct Air	1.2600

Table 37.   Summary: 11/10/98, B3770.54 (6/98) Thrust and SFC Trade Study

All Δ's are relative to the baseline value. All entries use a SAR of 2.7.

Operating Point	Parameter	Baseline	+0.01 $\Delta\eta$				−1% ΔTotal TCLA	+0.002 Δ C_{FG}
			Fan (avg) ID and OD	HPC	HPT	LPT		
Sideline Noise Takeoff Point: 689 ft, Mach 0.32, Std+18°F Day, PC50	FN_{mix}, lbf	53634						
	SFC_{mix}, lbm/lbf/hr	0.9279						
	ΔFN_{mix}, %	0	−0.8%	−0.2%	−0.1%	−0.7%	−0.1%	0.24%
	ΔSFC_{mix}, %	0	−0.8%	−0.3%	−0.2%	−0.7%	0.0%	−0.24%
Subsonic Cruise Point:36,089 ft, Mach 0.9, Standard Day, PC38	FNP, lbf	9849						
	SFC, lbm/lbf/hr	0.8969						
	ΔFNP, %	0	−0.7%	−0.6%	−0.6%	−0.3%	−0.1%	0.31%
	ΔSFC, %	0	−0.5%	−0.4%	−0.4%	−0.5%	−0.1%	−0.36%
Supersonic Top of Climb Point: 55,000 ft, Mach 2.4, Standard Day, PC50	FNP, lbf	20860						
	SFC, lbm/lbf/hr	1.2251						
	ΔFNP, %	0	1.0%	0.7%	−1.7%	0.1%	−0.6%	0.58%
	ΔSFC, %	0	−0.24%	−0.24%	−0.25%	−0.23%	−0.04%	−0.58%

Table 38.   Summary: 11/10/98, B3770.54 (6/98) Thrust and SFC Trade Study

All Δ's are relative to the baseline value. All entries use a SAR of 2.7.

Operating Point	Parameter	Baseline	−0.005 ΔPR								
			FEGV,C	FEGV,D	Duct	Diffuser	Burner	TEC	FCM,C	FCM,D	Nozzle
Sideline Noise Takeoff Point: 689 ft, Mach 0.32, Std +18°F Day, PC50	FN_{mix}, lbf	53634									
	SFC_{mix}, lbm/lbf/hr	0.9279									
	ΔFN_{mix}, %	0	−0.2%	−0.2%	−0.2%	0.0%	0.0%	−0.3%	−0.2%	−0.1%	0.0%
	ΔSFC_{mix}, %	0	−0.25%	−0.11%	−0.08%	−0.06%	−0.06%	−0.32%	−0.30%	−0.08%	0.00%
Subsonic Cruise Point:36,089 ft, Mach 0.9, Std Day, PC38	FNP, lbf	9849									
	SFC, lbm/lbf/hr	0.8969									
	ΔFNP, %	0	−0.5%	0.3%	0.3%	−0.2%	−0.2%	−0.2%	−0.2%	0.3%	0.2%
	ΔSFC, %	0	−0.11%	−0.07%	−0.08%	−0.13%	−0.11%	−0.25%	−0.26%	−0.08%	−0.32%
Supersonic Top of Climb Point: 55,000 ft, Mach 2.4, Std Day, PC50	FN_{mix}, lbf	20860									
	SFC_{mix}, lbm/lbf/hr	1.2251									
	ΔFNP, %	0	0.5%	−0.1%	−0.2%	0.3%	0.2%	0.0%	0.0%	−0.2%	0.2%
	ΔSFC, %	0	−0.08%	−0.02%	−0.04%	−0.08%	−0.07%	−0.14%	−0.13%	−0.04%	−0.16%

Note: All pressure loss deltas were applied at SLS/std day, PC50, W2AR = 800 lbm/s, except for nozzle pressure loss which was applied at 55,000 ft, Mach 2.4, std day, PC50, W2AR = 560 lbm/s. The losses would then vary by either the local Mach number squared or Q, or remain constant.

3.2.3.5 Flowpath Development – TC

The 1998 engine matrix designated the "Briquette" was the basis for the propulsion system studies performed for the Technology Configuration aircraft. The objective of this engine design effort was to optimize previously explored concepts and so to develop a design suitable for the demonstrator engine program. To ensure that all factors were considered, "design of experiment" techniques were used in the flowpath definitions of the Briquette matrix engines.

The design process for the TC propulsion system was very similar to that used for the PTC (Figure 76). The HSCT3770.54 engine developed in October 1997 and used in all 1997 weight-reduction studies was the baseline for TC system development.
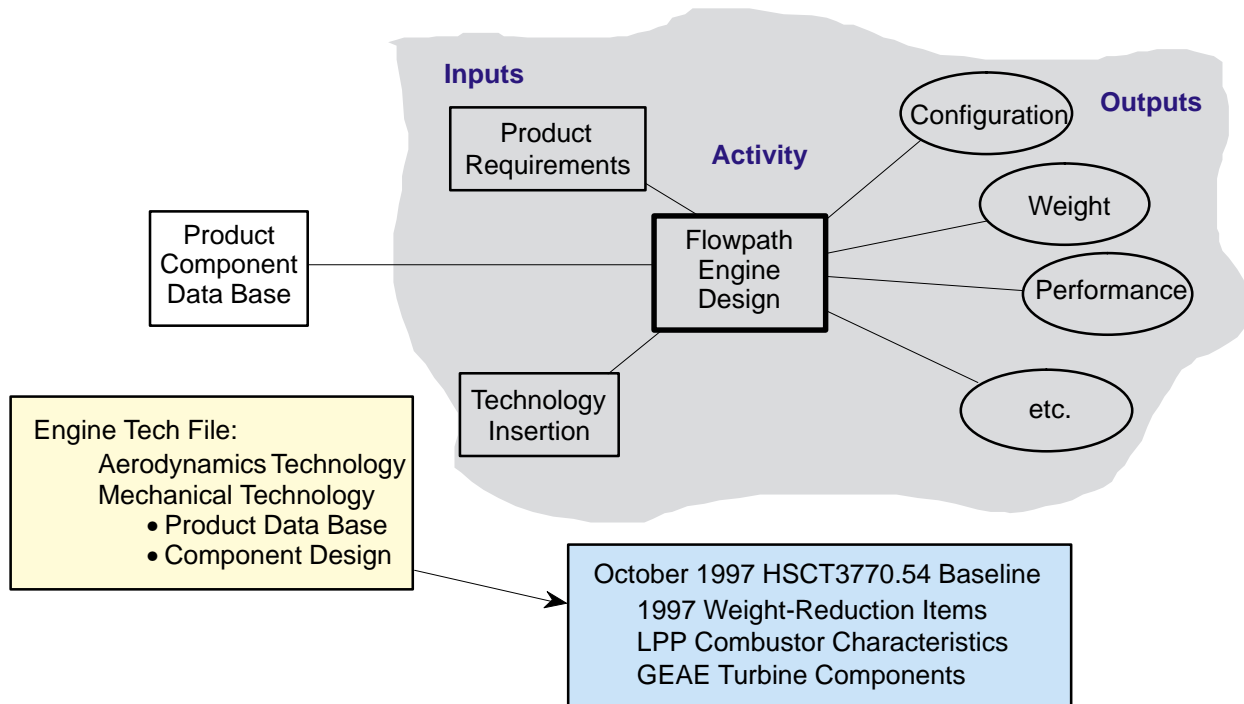
Figure 76.   TC Engine Design Process

Product Requirements

Mission requirements for the TC were basically the same as those used for the PTC. The main difference was that the PTC used specific fuel consumption as the prime criteria for engine selection, but the TC used aircraft gross takeoff weight. To ensure that the engine analysis was both complete and comprehensive, performance was developed for all engines defined in this study. Also, a term was included in the TC transfer function to define the impact of engine length on the bending moment of the airplane wing (see Figure 77).

TC Engine Design Process

The engine-design process for the TC focused on weight-reduction via component-design activities. For the core engine, the component split gave P&W design responsibility for the compression components and GEAE design responsibility for the turbines (Figure 78). Design responsibility for

Key Cycle List

Point	Flight Operation	Altitude (ft)	Flight Mach No.	Power Code % FN	DTAMB (F)
1	Aero Design Point SLS	0	0	50	0
2	Begin Taxi	0	0	5.0%	18
3	Taxi	0	0	5.0%	18
4	Release Brake, Begin Takeoff	0	0	100.0%	18
5	Lift Off	0	0.36	100.0%	18
6	Initial Noise Cutback	35	0.36	89.6%	18
7	689 ft Sideline Noise Station	689	0.36	50	18
8	Noise Cutback	689	0.36	47	18
9	Noise Cutback	689	0.36	44	18
10	Continue Noise Cutback	1492	0.36	89.6%	18
11	Cutback from Takeoff Noise Station	1492	0.36	49.1%	18
12	Begin Climb to Sub Cruise	1500	0.37	100.0%	18
13	Climb to Sub Cruise – overflow	10K	0.65	50	0
14	Climb to Sub Cruise – overflow	10K	0.8	50	0
15	Subsonic top of Climb	34K	0.9	100.0%	0

Design and Usage Missions
Performance and Weight Goals
Cost Objectives
Life Requirements
Maintenance Strategy

Transfer Function

Δ TOGW = A Δ Weight + B Δ SFC + C Δ …
Δ SFC = a + b Δ ε fan + c Δ ε HPC + e Δ ε HPT + f Δ …

Define and Weight for Usage Mission

Design Constraints

AN^2, $U_{t\ max}$, $U_{r\ max}$, T_{bulk}, …

Figure 77. Design Requirements

1998 Component Descriptions:

P&W Compression Configurations
    Aero
    Mechanical Construction
    Material Usage

GEAE Turbine Components
    Aero
    Mechanical Construction
    Material Usage

Unique or Advanced Features:
    Special Configurations
    Acoustics Restrictions
    Aero and Mechanical Configurations

Design Constraints:

Ut corr, Vane to blade ratio, ...
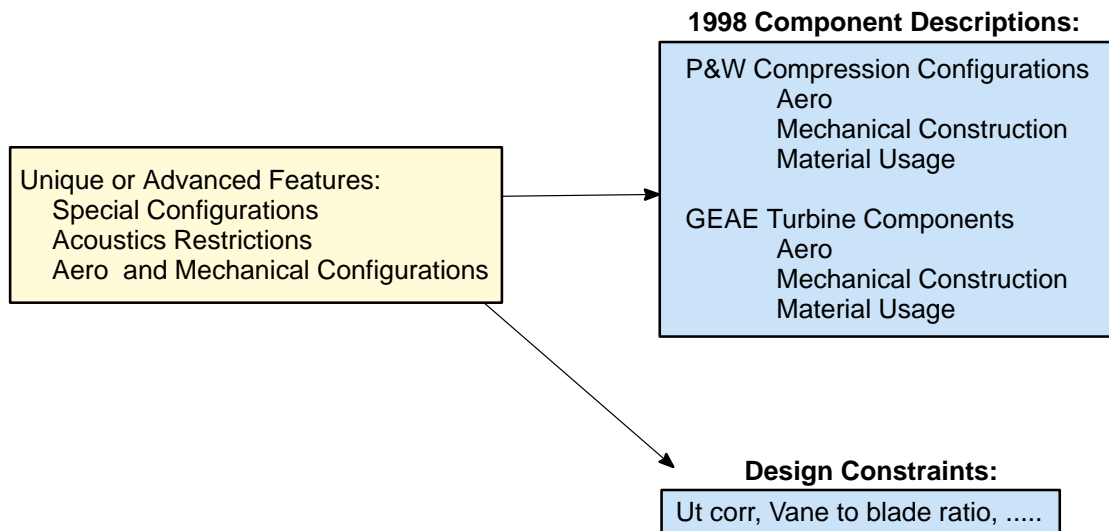
Figure 78. Technology Insertion

the combustor was split between the two companies. The baseline combustor continued to be the LPP, which turned out to be a good decision since the LPP later became the combustor of choice.

The design process was extended to include a DOE activity as shown in Figure 79. The initial configurations for 25 cycles were developed by AUTO engine flowpath design software, which specified the compressor component nominal stage count and inlet radius ratios.
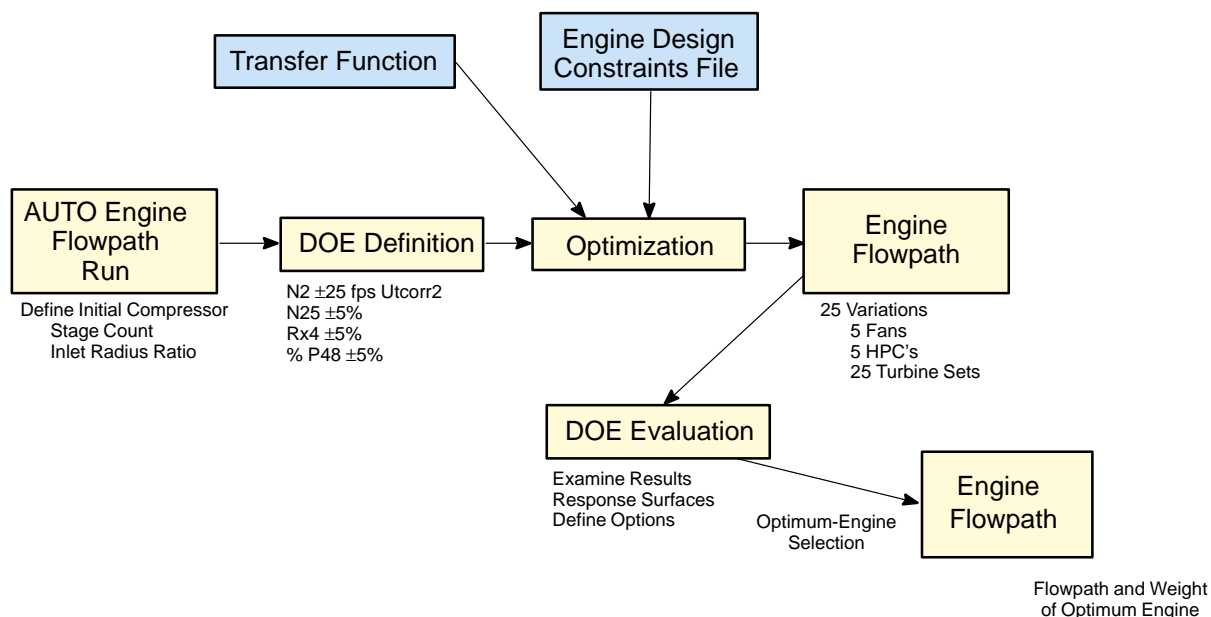
Figure 79.   Design Process Flow

Design of Experiments

The experiment used for DOE evaluation was developed from the HSCT3770.54, the engine that served as the basis for this matrix. Normally, the DOE focussed on four important engine variables. Each of these 25 engine experiments was passed through an optimization activity that defined the most appropriate configuration for experiment values. The resulting engine was selected using TOGW as a "figure of merit" via the transfer function shown in Figure 77.

The result of this evaluation was that 25 engines were defined, each required to satisfy all of the design constraints. These engines involved 5 unique fans, 5 compressors and 25 unique sets of turbines. Using the underlying mathematics of the DOE techniques, an evaluation was performed on the data for these components. This technique was also used to generate response surfaces for the many engine variables. First, the options were selected, then the most appropriate engine configuration was defined. In some cases, additional engines were defined from the 25 in the DOE to establish the best engine configuration.

The typical DOE setup is illustrated in Figure 80. The four engine variables used for this calculation were the two spool speeds, the HPT reaction, and the LPT stage work distribution. This last variable was defined by specifying the percentage of total work for the first stage of the two-stage turbine. This process was also used for single-stage and three-stage LPT's. The fourth variable so derived was modified to fit the needs of the configuration.

DOE Results for the 3770.54 Engine

The DOE setup and some of the resulting data for the 3770.54 engine are shown in Table 39. These results are Δ's from the initial engine. The experiments were configured such that the initial engine was not an element in the DOE.

- 2^4 Central Composite Analytical DOE

- DOE Analysis Integrating Flowpath and TP3

- Variables:
  - LP Spool Rotational Speed, N5 (rpm)   4920 –> 5094
  - HPT Pitch Reaction, Rx4   56% –> 64%
  - LPT Stage 1 Work Fraction, %psi48   35% –> 45%
  - HP Spool Rotational Speed, (rpm)   7296 –> 8064
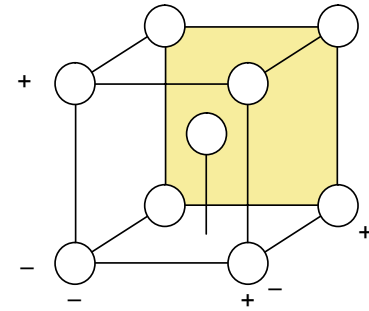
Figure 80.   Typical Central Composite DOE

Table 39.   Results of DOE for 3770.54 Engine   *DOE comprises 25 engine variations; another 10 to 20 subsequent finalize configuration choice. Average 40 configurations per cycle.*

Run	N5	Rx4	%psi48	N4	ΔTOGW, lbm	Δ Engine Weight, lbm	η Fan	η HPC	η HPT, pts	η Fan, pts
1	5094	56	35	7296	2.871	−55.350	0.620	0.180	−0.500	0.010
2	4920	64	35	7296	0.923	−598.560	0.930	0.330	−0.510	−0.030
3	5094	64	35	8064	2.765	−271.480	0.620	0.560	−0.180	−1.460
4	5007	60	40	8448	2.509	−922.430	0.130	0.580	−0.610	−4.360
5	4920	56	35	7295	1.037	−608.370	0.930	0.330	−0.550	−0.230
6	5094	64	45	7295	2.925	−30.890	0.620	0.180	−0.370	−0.180
7	5094	56	45	8064	4.182	−265.110	0.620	0.560	−0.570	−4.240
8	4833	60	40	7680	1.262	−767.850	0.130	0.250	−0.140	−0.950
9	5007	52	40	7680	1.503	−90.110	0.130	0.250	−0.200	−1.120
10	4920	56	45	7296	1.136	−08.930	0.930	0.330	−0.620	−0.460
11	5094	56	45	7296	3.026	−73.970	0.620	0.180	−0.570	−0.410
12	4920	64	45	8064	1.365	−1049.590	0.930	0.740	−0.920	−3.320
13	5094	56	35	8064	2.646	−383.920	0.620	0.560	−0.090	−1.760
14	4920	64	45	7296	1.036	−613.580	0.930	0.330	−0.560	−0.440
15	5007	60	50	7680	1.650	−822.830	0.130	0.250	−0.130	−2.280
16	4920	56	45	8064	1.320	−1044.080	0.930	0.740	−0.830	−3.270
17	5007	68	40	7680	1.341	−701.870	0.130	0.250	−0.520	−0.530
18	5007	60	30	7680	1.221	−646.860	0.130	0.250	0.200	−0.570
19	5181	60	40	7680	1.097	−773.460	0.130	0.250	0.020	−0.910
20	5094	64	45	8064	2.887	−488.370	0.620	0.560	−0.480	−2.710
21	5007	60	40	7680	1.105	−830.500	0.130	0.250	−0.140	−1.000
22	5007	60	40	6912	2.286	−197.960	0.130	−0.290	−0.740	0.530
23	4920	56	35	8064	0.595	−1017.270	0.930	0.740	−0.330	−2.030
24	4920	64	35	8064	0.973	−789.500	0.930	0.740	−0.240	−1.650
25	5094	64	35	7296	2.662	−128.930	0.620	0.180	−0.540	0.130

The data for the 3770.54 engine defined response surfaces representing complex, multiterm expressions of the four DOE variables. Figure 81 illustrates the usefulness of the response-surface approach. In this example, turbine reaction and core speed are the DOE variables displayed for each of the four output surfaces. The TOGW surface is the primary selection criteria. The other three surfaces in this example are subsets of the transfer function for TOGW.

The implication from the chart is that the TOGW solution is at a lower core speed than the minimum engine-weight solution. System performance is best achieved with a balanced engine approach through the transfer function.
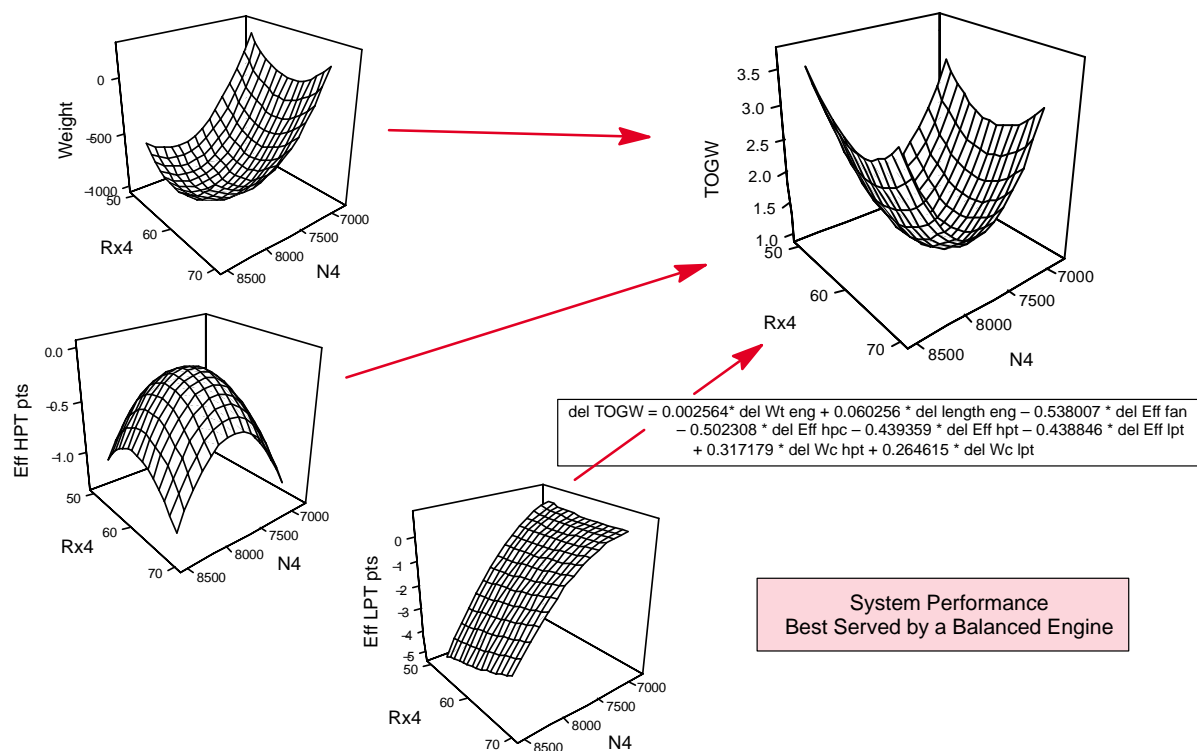
Figure 81.   Response-Surface Results

Response Surfaces

Response surfaces are very complex expressions. The three dimensional visualization shown in Figure 81 does not describe the whole picture, but the charts are very useful in defining the trends that lead to the results from the DOE. Figure 82 shows several three-dimensional illustrations of the weight response of the four DOE variables. The chart makes it easy to determine the best position in regard to weight.

Once these design process improvements were in place, a significant design activity was initiated. The engine cycles were defined at three discrete fan pressure ratios (FPR) and three extraction ratio (ER) settings. Thus, this initial activity defined nine engines.

Engine Performance

At the same time that the flowpath design baseline and processes were improved, the fidelity of the cycle model was increased. The new cycle model indicated lower performance. These changes had a significant impact on the resulting engine geometry and system performance. Figure 83 shows the differences between the middle engine in the April 1998 Brick matrix and the 3770.54 engine selected from the 1997 work. The design inlet flow size is the same in both engines, so the fans are very similar. There are some rotor construction differences and slight changes due to the different pressure ratios. The major change, however, is in the core elements downstream of the fan frame.

The increased losses in cycle as well as operational differences at low altitude made a significant increase in the LPT corrected flow necessary. In order to design for the same flowpath Mach number,
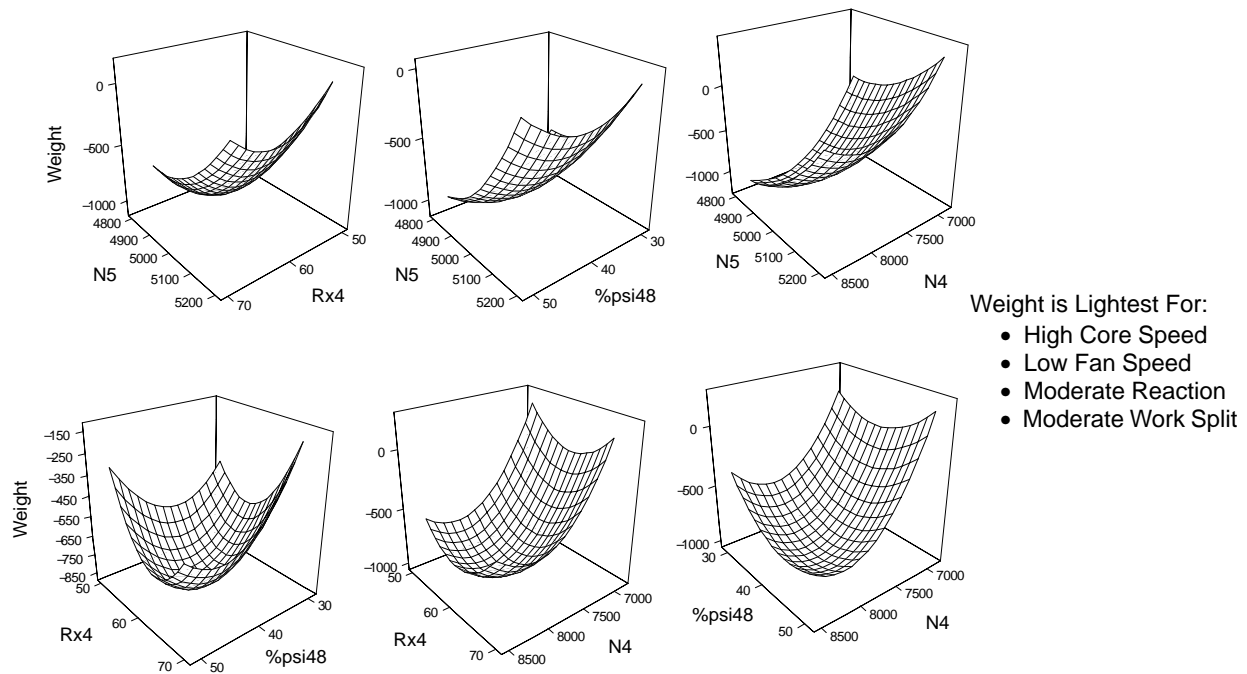
Figure 82. Response Surfaces for Weight

Weight is Lightest For:
- High Core Speed
- Low Fan Speed
- Moderate Reaction
- Moderate Work Split
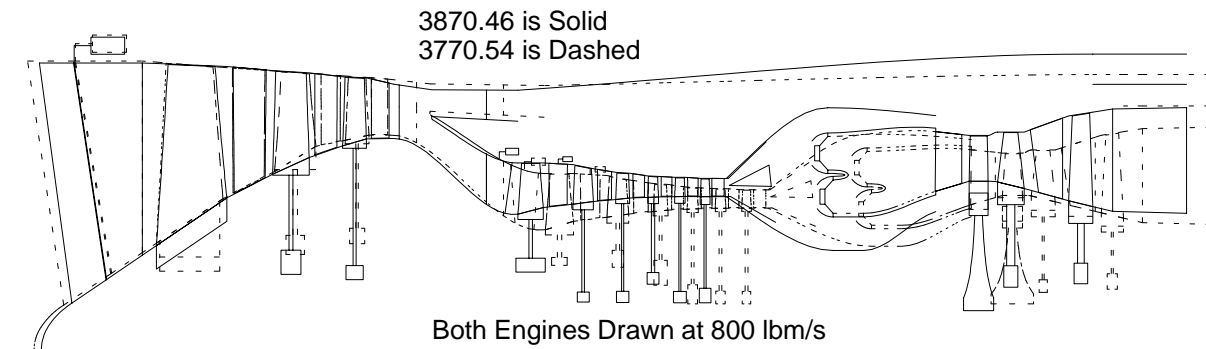
Figure 83. April Brick Engine: HSCT 3870.46 Vs 3770.54(97) Flowpath

a large increase was required in turbine exit area. These changes forced the core to have a larger diameter than was required by the front of the compressor and increased the outer bypass duct diameter. Other impacts included:

- Fans are very similar (common flow size, radius, and exit Mach number)

- Bypass ratio reduced from 0.54 to 0.46 (core flow is 5.5% larger)

- Fan pressure ratio is up 5%

- LPT loading is higher

- LPT design problems ($AN^2 = 50 \times 10^9$ in^2/min, exit radius ratio = 0.5, exit Mach = 0.6)

- Core location set by LPT

These changes led to larger volume parts with increased weight. The blade root stress parameter (AN^2), turbine exit radius ratio, and exit Mach number were the design limits for the LPT. The resulting area increase stretched the ability of the design to satisfy these constraints.

The engine weight increase was quite a bit more than had been estimated in the 1997 interim projection and projected product levels (Table 40). This exacerbated the weight problem for the propulsion system. The nozzle throat area was increased significantly relative to the 1997 engine, and the core engine and nozzle system were both over the goal by a ton apiece. As a result, even with the much improved design process, the engine characteristics were less than acceptable for the TC airplane.

Table 40.   Weight Impact on Engine

Component	Engine Weight (lbm)		
	1997 3770.54		1998 3870.46
	Interim Projection	Projected Product	2.9 SAR Engine
Core	7,218	6,551	8,253
Combustor	1,461	1,315	1,381
Controls and Accessories	798	718	976
Gearboxes	290	261	335
Engine	9,767	8,845	10,945
Exhaust Nozzle	8,700	7,830	9,939
Total	18,467	16,675	20,884

All nine of the engines were designed and released to the aircraft system analysis group. Before any additional work was done in the study, the design team realized that major changes would be needed to achieve the engine weight and performance goals. Figure 84 summarizes the major differences for engines of a common cycle from 1997 to April 1998.
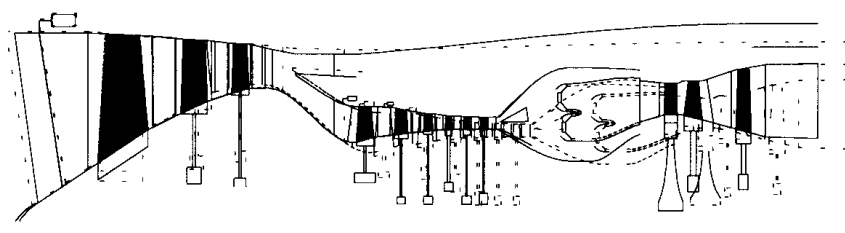
1998 Version is Solid and Shaded: 3770.54(A98)
1997 Version is Dashed: 3770.54(97)

Figure 84.   Engine Differences, 1997 to 1998

Summary

Engine Weight Increase Due to Two Major Items:

1. Flow Holding in Product Usage Mission 2
    –   Dramatic LPT Area Increase, +14%
    –   Increased Diameters, HPC Aft

2. Cycle Losses Drive A_8 and T_8 Up
    About 1000-lbm Increase in Nozzle Weight

Several design improvements were found to be significant in enhancing engine performance and weight characteristics:

- Performance:
    - Modified off-design efficiency Δ's on HPC maps (1%)
    - Increased HPT efficiency at SLS/standard day design (0.2%)
    - Increased LPT efficiency at SLS/standard day design (1%)
    - Fixed 1% constant fan frame pressure loss at all conditions
    - HPC M3 = 0.35 at 55,000-ft/Mach 2.4 – 0.35 design to 0.32 design (SLS standard day)
      – Reduced combustor pressure loss
    - Exit area ratio = 1.03 at 689-ft/Mach 0.32
- Jet Noise: 3770.60 takeoff flow, jet velocity, and thrust
- Part-Power Operation: LPT extraction limited (flow function at 10,000-ft/Mach 0.8)

For the compressor, an error in the cruise exit Mach number led to additional combustor losses. The minimum extraction ratio at the sideline acoustics point was reduced to the 1.03 value.

The takeoff noise setup in the cycle was modified from the previous levels in the April engines. For the Briquette, these parameters were returned to the old characteristics. In the initial set of engine cycles the LPT was overextracted in critical mission regions. This contributed to the increased turbine areas. Turbine work extraction was limited to turbine discharge corrected flow (flow function) consistent with the cycle value at 10,000-ft/Mach 0.8. This was found to have little impact on system performance, but it had a major effect on engine design.

Figure 85 shows the resulting engine designed to the 3770.54 cycle of the June Briquette, compared to the 1997 engine. The exit area of the LPT is still slightly larger but is very close to the older engine. The major weight improvements of the common cycle engine between 1997 and two sets of 1998 cycles are as follows:

- Lighter engine relative to May 1997 Brick:
    - Turbomachinery   880 lbm
    - Exhaust Nozzle   1135 lbm

- Status weight up 349 lbm relative to 1997; holding 16675 becomes more challenge

1998 Version is Solid and Shaded: 3770.54(J98)
1997 Version is Dashed: 3770.54(97)
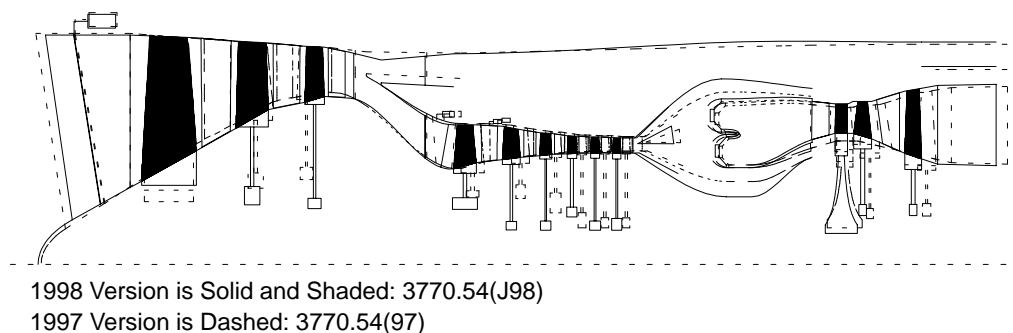
Figure 85.   Flowpath Changes, 1997 to 1998

The new design nearly achieves the 1997 projection, but the engine is still far heavier than a product engine should be.

Tables 41 and 42 summarize the engine weight and dimensions for the April 1998 Brick and the June 1998 Briquette engines. All of the engines have counterrotating spools, and all have a single-stage HPT. The three-stage configuration was found to be best for all of the fans. There are several missing values in the Briquette table. These engines were designed near the end of the year, and the missing data were never defined.

Table 41.   April 1998 Brick

Parameter	Component	Engine Cycle								
		3770.31	3770.54	3770.71	3870.25	3870.46	3870.63	3970.20	3970.39	3970.59
Stage Count	Compressor	6	6	6	6	6	6	6	6	6
	LPT	2	2	2	1*	2	2	1*	2	2
Weight, lbm (Interim Projection)	Core Engine	11,965	11,233	10,591	11,795	10,945	10,980	11,881	11,137	10,702
	Exhaust Nozzle	11,965	9,600	9,110	12,316	9,939	9,320	13,156	10,389	9,606
	Total Engine	23,931	20,833	19,701	24,111	20,884	20,300	25,036	21,526	20,307
Counterrotating spools; no vane between HPT and LPT unless noted with asterisk (*).										

Table 42.   June 1998 Briquette

Parameter	Component	Engine Cycle								
		3270.80	3470.69	3670.48	3670.60	3770.43	3770.54	3870.39	3870.47	4070.33	4270.17
Stage Count	Comp	6	6	6	6	6	6	6	6	6	5
	LPT	2	2	2	2	2	2	2	2	2	1*
Weight, lbm (Interim Projection)	Core	10,310	10,428	10,905	10,242	10,732	10,351	10,734	10,354	11,020	11,440
	Nozzle			8,541	7,716	8,689	7,959	8,849	8,278		
	Total			19,446	17,958	19,421	18,310	19,583	18,632		
Dimensions (Inches)	CG1	67.37	66.77	66.91	65.29	65.60	65.60	68.73	63.68	67.23	70.57
	CG2			87.80	88.30	87.50	88.10	87.60	87.90		
	CG3			134.08	130.72	133.61	131.00	138.98	131.03		
	TRF	119.67	117.13	125.47	122.69	123.70	121.48	130.07	120.96	121.43	129.49
Counterrotating spools; no vane between HPT and LPT unless noted with asterisk (*).											
Dimensions are measured from fan rotor leading edge: CG1 is turbomachinery center of gravity; CG2 is exhaust nozzle center of gravity relative to rear frame aft flange; CG3 is overall engine center of gravity; TRF is turbine rear frame (aft flange).											

3.2.4 Alternate Propulsion Concepts

3.2.4.1 Mid-Tandem Fan

Flowpath Development (MTF)

During the 1994 system studies, interest in alternative engine concepts was sparked by reports of an engine known as the midtandem fan (MTF) developed jointly by Rolls Royce in England and SNECMA in France. To determine the efficacy of this design, GEAE and P&W developed their own study version of the MTF. This GEAE/P&W configuration is shown in Figure 86. (The Rolls Royce version of this engine is not shown.)

The objective of the MTF configuration was to achieve the necessary noise reduction at takeoff by routing a large volume of relatively low-pressure air through a simple nozzle and then switching to
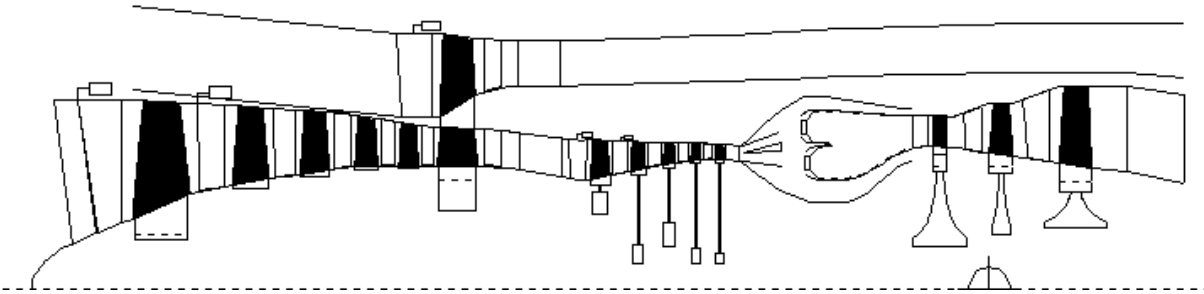
Figure 86.   GEAE/P&W Midtandem Fan Engine

route a smaller volume of higher pressure air through the nozzle for supersonic cruise. In other words, provid low specific thrust at takeoff but change to high specific thrust during supersonic cruise. The intent was to provide the same noise suppression that would have been achieved by a more conventional engine via the more complex mixer/ejector nozzle system. It was hoped that the result would be a lighter, less complex system overall.

The design for the MTF started with two-spool turbomachinery comprising a fan, compressor, combustor, and two turbines, much like the engines described in the prior system studies but without any bypass flow in the high Mach cruise mode. An extension is added to the last compressor rotor along with a second duct to handle takeoff bypass flow which is required to lower the exhaust velocity below the point where it needs noise suppression. The resulting fan-on-blade engine is similar to the rotor configuration used in the GEAE TF39 product engine. The theory is that the midfan and second duct plus a simpler nozzle will be lighter and more reliable than the complex mixer/ejector nozzle system.

Study Activity – For the MTF study, the GEAE/P&W team examined three versions of the engine:

1. A direct simulation of the cycle (Engine 3)
2. A best cycle for the Boeing airplane (G1)
3. A best cycle for the MDA airplane (G2)

The aerodynamic, mechanical, and material technologies and the groundrules for these configurations were the same as used for the MFTF engines. The focus of the studies was to characterize the design issues of the configuration. Since weight has been a strong factor in all HSCT design, the primary focus was to minimize weight.

To produce the desired effects, the tip speed of the tandem fan blade should be held at 1900 ft/s or less. For this reason, the tandem fan is attached to the fan of the main engine, often called the low-pressure compressor (LPC) in these tandem-fan configurations, which impacts all main engine components. Because the engine airflow at takeoff must achieve the desired takeoff thrust at a reasonable jet velocity, the ratio of the tandem fan tip diameter to the mean diameter of the LPC is close to 2 to 1. It was felt that this ratio kept the tandem-fan speed in the acceptable range and eliminated the need for the more complex suppressor nozzle.

The average rotational speed of the low-pressure spool is half of what it would be if the tandem fan were not attached. Since stage loading increases by the square of the speed, this configuration increases the fan and LPT loading requirements by a factor of four.

Figure 87 shows the impact of this speed reduction on the fan module and compares this impact to that of the equivalent 3770 MFTF engine. The LPC required six stages to do the job that the fan of the MFTF did in three. The MTF engine requires a fan system 20% longer than the fan system used in the 3770 MFTF. While the rotor structure diameter is greatly reduced, the weight of the airfoil and case structure needed for the added length dominates the component weight. The fan-on-blade last stage shown in Figure 87 offers several mechanical challenges:
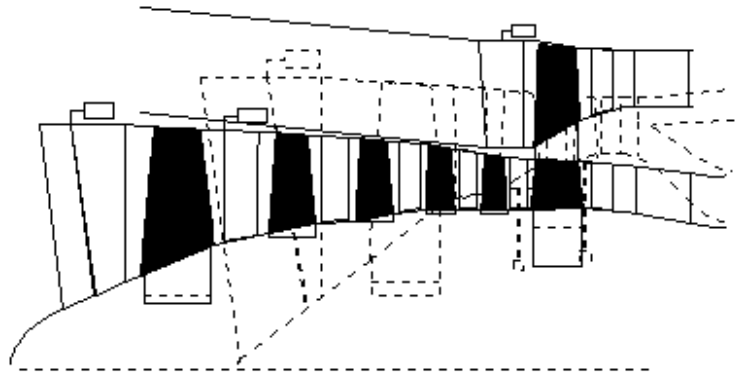
Figure 87.   Comparison of 3770 with MTF Engine

- The radius ratio is quite low (0.28) for a bladed rotor in the middle of the engine. The usual value is 0.37.

- To minimize the tip radius of the tandem-flow fan, which was modeled after the CF6–80E fan design, the fan specific flow (flow per annulus) area was designed at 42.5. This high value compromises fan efficiency.

- Input flow for the fan is delivered through blow-in doors located in proximity to the fan inlet. This location makes high specific flow difficult to achieve.

To reduce airfoil weight and minimize the containment requirements of the high-tip-speed rotor, the outer portion was assumed to be of hollow construction. However, even with optimistic assumptions, the figure shows increased structural volume in the fan frame and the inlet guide vane in front of the outer part of the tandem fan rotor. The IGV system is needed to sustain flow-modulation requirements from takeoff to high Mach cruise flight.

A core comparison between the MTF engine and the MFTF is shown in Figures 88 and 89. For this comparison, both engines have a five-stage compressor. The MTF compressor shown with solid rotors in Core Comparison A has a slightly lower radius. The primary difference between the two engines is in the turbine designs.

One main design issue had to do with the low LP rotor speed discussed previously. The LPT loading that resulted mandated the increase in diameter shown on Figure 89. Adding a third stage to the LPT allowed the diameter to be closer to that of the MFTF. Weight and preformance favored this solution.

Design Issues – The bladed MTF rotor preliminary design:

- Defined tip speed limit
- Set LP spool rotational speed
- Set minimum blade radius ratio

The core stream fan stage count was set by the speed and stall margin The turbine diameters were set by extraction requirements on the LPT. This established:

- Loading
- Size of blades
  (very large due to amount of airflow)
- Exit Mach number
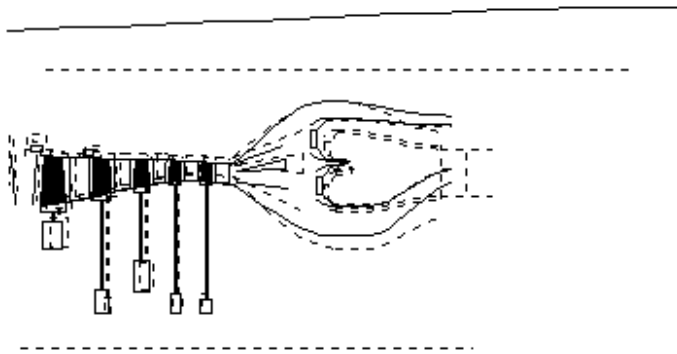
Figure 88.   Core Comparison A
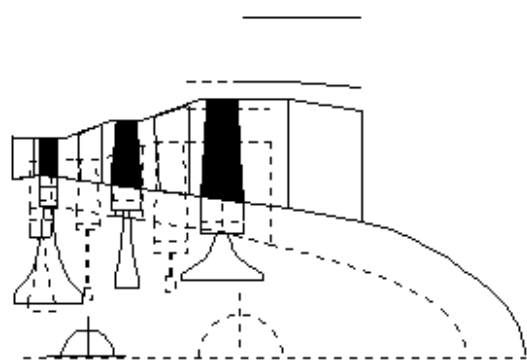
Figure 89.   Core Comparison B

The three-stage LPT helped reduce the turbine diameter with no impact on turbine exit location. This resulted in a lighter engine.

MTF engine parts are very large. The volume of these parts creates a length and diameter problem relative to the MFTF system. Figure 90 is a comparison of MTF with the turbomachinery of the base MFTF engine.

The idea that a simpler exhaust system would lead to improved system weight was examined during these studies. Figure 91 shows that the MTF total engine length is longer that the baseline system. The turbomachinery for configuration G1 is four feet longer than the equivalent mixed-flow turbofan (HSCT3770.4). Using a large, simple nozzle does not overcome this length problem.

Weight analysis of these studies assumed that hollow airfoils would be used on the fan, both tandem and mainstream. The turbines were assumed to require cooled airfoils.

Table 43 presents the weight prediction results of the three MTF engine configurations relative to two of the mixed-flow turbofan configurations. The top part of the table defines the engine cycle parameters that resulted from matching the system thrust requirements. Flow size requirements contributed to the weight conflict between the MTF engines and the system.

Summary – The turbomachinery size and configuration complexity dominated the engine weight results. The FLOWPATH model representation of the MTF that was used is missing the midturbine frame required for this structural arrangement. The large, simple nozzle used is at best 2000 lbm lighter than the mixer/ejector nozzle configuration. The turbomachinery used is between 4000 and 9000 lbm heavier than the mixed-flow turbofans, as shown in Table 43. Thus, the advantage that was hoped for from the MTF was not realized in the cycles examined in this study.

Engine Cycle Development

In 1994 Boeing and McDonnell Douglas had an interest in an alternative propulsion concept referred to as the mid-tandem fan (MTF). The MTF was provided to Boeing and MDA by Rolls Royce (RR)/SNECMA to be used in a Mach 2.0 and a Mach 2.4 configuration. At that time RR estimated the total engine/nozzle weight to be about equal to the weight of their mixed-flow turbofan and much lighter than the current U.S. MFTF. During 1994 and 1995, P&W and GEAE were given the task of evaluating this concept by designing their own MTF.
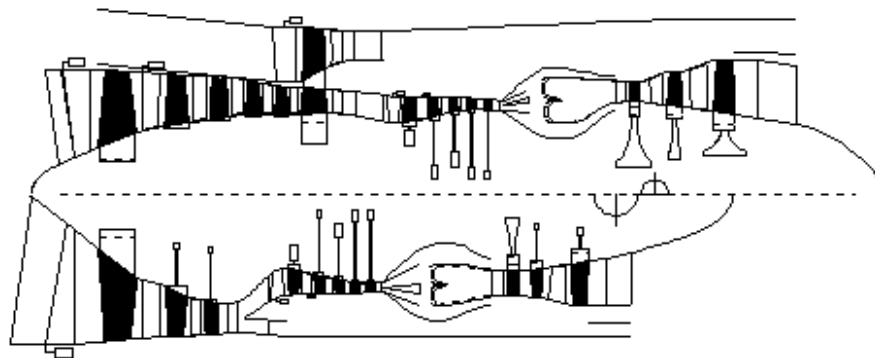
Figure 90.   MTF Over HSCT3770 Turbomachinery
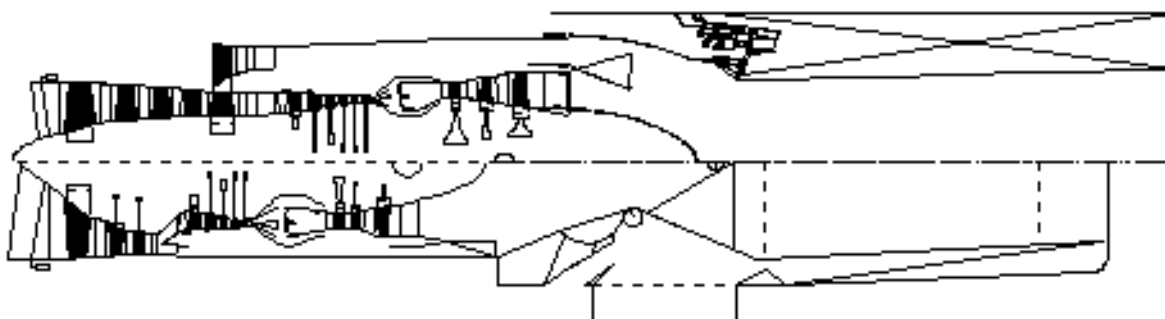
Figure 91.   MTF G1 Over HSCT3770 Turbomachinery

Table 43.   Weight Predictions for MTF and MFTF Engines

Parameter	Cycle				
	MTF3	**MTF G2**	**MTF G1**	**HSCT2970**	**HSCT3770**
Flow Size	1279	1636	1466	1170	800
FPR	4.80	3.20	3.20	2.89	3.70
BPR	1.16	1.78	1.57	1.20	0.41
OPR	19.5	21.6	19.5	20.4	19.0
Component	**Engine Weight (lbm)**				
Fan	5,148	5,782	4,726	3,882	2,728
HPC	1,351	1,682	1,693	1,674	1,247
HPT+Combustor	2,606	3,128	2,924	2,418	1,711
LPT+Frame	4,032	4,731	4,426	2,450	1,690
Turbomachinery	15,236	17,753	16,089	11,932	8,597
Exhaust Nozzle		3,935	3,935	5,753	5,990
Engine + Nozzle		21,688	20,024	17,685	14,587

The MTF is a low-specific-thrust concept that requires a large volume of airflow at fairly low pressure. The front end has a relatively small-diameter spool since there is no fan at the air inlet. A large-diameter, high-volume fan mounted aft of this spool feeds a large volume of low-pressure air through a set of inlet guide vanes directly into the bypass duct. The engine exhaust passes through a simple exhaust nozzle, since the design does not require the more complex mixer/ejector type nozzle. It is necessary, however, for the exhaust nozzle to be quite large to deal with the volume of air that passes through the engine.

Data Provided – Data concerning RR, P&W, and GEAE mid-tandem fans are presented as follows.

Table 44 is a comparison of the P&W Mach 2.0 MTF (CSTF1072) performance compared to available RR performance data at sea-level takeoff, 31,000 ft/Mach 0.95 subsonic cruise, and 53,000 ft/Mach 2.0 supersonic top of climb. P&W's data matched well with the RR MTF data.

Table 44.   Mach 2.0 Mid-Tandem Fan Engine Performance

Mach Number	0		0.95		2.0	
Altitude, ft	0		31,000		55,000	
Engine	**RR**	**P&W**	**RR**	**P&W**	**RR**	**P&W**
Net Thrust, lbf	50,000	50,000		12,300		13,900
SFC, lbm/hr/lbf		0.51		0.784	1.10	1.10
Fan Pressure Ratio	2.1	2.1		1.72		1.51
Bypass Ratio	2.0	2.0		1.50		1.44
Overall Pressure Ratio	25.4	25.4		23.6		19.2
T_{T3}, °R		1424		1316		1742
$T_{T4.1}$, °R		2640		2220		3050
W_C, lbm/s LPC		427		427		350
Fan		854		640		504
Total		1281		1067		854
Total W_C, %		120		100		80

Table 45 compares the P&W Mach 2.4 MTF performance to available RR performance numbers at sea-level takeoff, 31,000 ft/Mach 0.95 subsonic cruise, and 55,000 ft/Mach 2.4 supersonic TOC. P&W's Mach 2.4 MTF, designated either STF1073 or PW2163, performed better than the RR MTF.

Table 46 compares component performance of the Mach 2.4 MTF engines at SLS. The PW2163, GEAE G1 (Mach 2.4 MTF per Boeing requirements), and GEAE G2 (Mach 2.4 MTF per MDA requirements) are compared to the RR Mach 2.4 MTF. The projected turbine cooling bleed for the RR MTF was very optimistic (13.7%) compared to the levels listed for P&W and GEAE (23%).

Table 47 is a comparison of the MTF relative to the MFTF flow size and engine/nozzle weight used in the U.S. and British studies. The cycles for the U.S. comparison were the PW2163 and the HSCT 1994 MFTF 3770.42. Note that the British weights were much lower. The weight difference between the British MTF and MFTF was less than the weight of the corresponding U.S. units. This indicates that the British were not as far along in the detailed design process as the U.S. studies were. The U.S. studies showed that, with realistic accounting, the weight of the MTF would increase greatly.

Table 45.   Mach 2.4 Mid-Tandem Fan Engine Performance

Mach Number	0		0.95		2.4	
Altitude, ft	0		31,000		55,000	
Engine	**RR**	**P&W**	**RR**	**P&W**	**RR**	**P&W**
Net Thrust, lbf	50,000	50,000		12,800		20,050
SFC, lbm/hr/lbf		0.51	0.87	0.86	1.29	1.18
Specific Thrust, lbf/lbm/s		1.0		0.26		0.40
Fan Pressure Ratio	2.07	2.10		1.72		1.57
Bypass Ratio	1.16	1.16		0.87		1.48
Overll Pressure Ratio	22.1	22.1		21.1		10.4
Jet Velocity, ft/s		1310				
T_{T3}, °R		1367		1278		1744
$T_{T4.1}$, °R		2347		2060		3260
W_C, lbm/s LPC Fan Total		592 687 1279		592 687 1279		296 438 734
Total W_C, %		116		100		66

Table 46.   HSCT Component Performance (SLS)

Parameter	Engine			
	RR/SNECMA	**PW2163**	**GEAE G1**	**GEAE G2**
LPC Adiabatic Efficiency, %	87	84.6	88.8	88.8
Mid-Fan Efficiency, %	84	85.0	85.0	85.0
HPC Efficiency, %	87	90.0	89.1	89.1
Turbine Cooling, % HPT Vane HPT Blade LPT	13.7 6.7 4.7 2.3	23.0 10.0 6.0 7.0	23.0 10.0 6.0 7.0	23.0 10.0 6.0 7.0
HPT Efficiency, %	88	90.0	91.3	91.3
LPT Efficiency, %	89.5	90.0	91.0	91.0
Burner $\Delta P/P$	5.0	4.6	5.6	5.6
Bypass Duct $\Delta P/P$	4.0	4.0	2.5	2.5
Horsepower	200	200	200	200
Bleed, lbm/s	1.0	1.0	1.0	1.0

Table 47.   Engine Dimensions and Weights

Parameter	1994 U.S. Study		Circa 1990 British Study	
	MFTF	**MTF**	**MFTF**	**MTF**
Engine Cycle	3770.42	2163		
Cruise Mach Number	2.4	2.4	2.0	2.0
Takeoff Thrust, lbf	53,000	50,000	50,000	50,000
Flow Size, lbm/s	800	1279		1280
Engine and Nozzle Weight, lbm kg	14,120	18,970	11,350 5,150	11,700 5,300

Figure 92 presents a set of curves showing the maximum-power fan inlet corrected airflow versus flight Mach number, along a given flight path, for the P&W PW2163, GEAE G1, and GEAE G2 MTF cycles. The PW2163 airflow is designed to be less so as to match the RR MTF value. The G1 and G2 were sized to meet Boeing's and MDA's requirements, respectively.
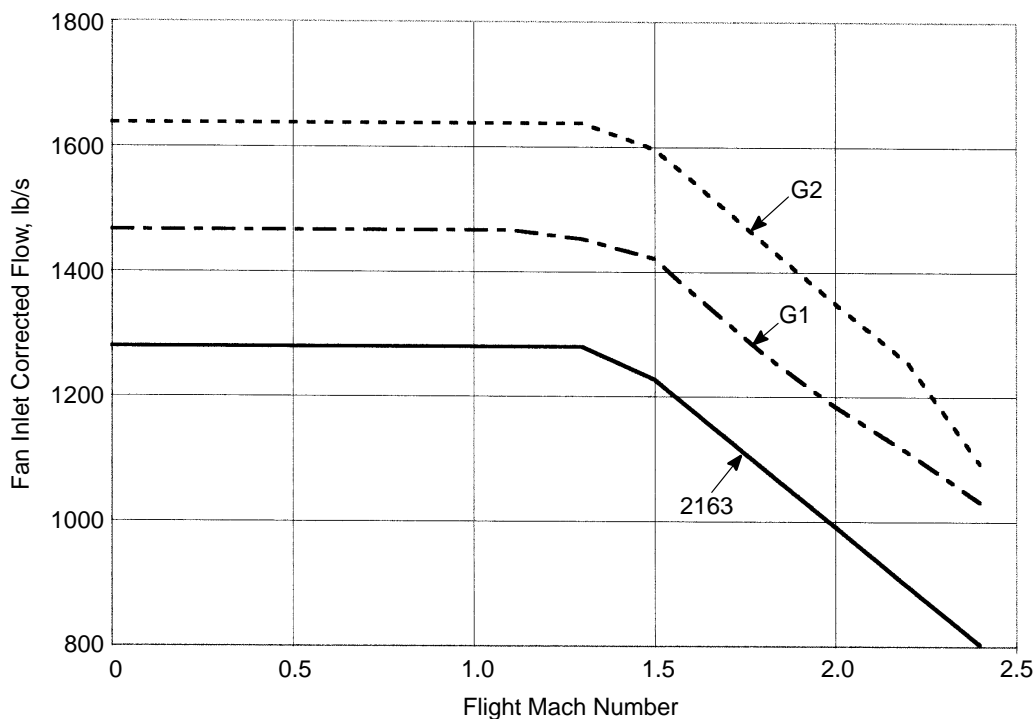
Figure 92.   Mach 2.4 Mid-Tandem Fan Flow Schedule

Table 48 summarizes the GEAE G2, P&W PW2163, and RR STF1072 engine parameters. The STF1072 matched the RR engine configuration for a six-stage front compressor, single-stage mid-fan, five-stage rear compressor, and single-stage HPT. The LPT had a vaneless first stage to make it a 2.5-stage LPT instead of the three-stage LPT used in the RR version. Again, note the difference between the RR weight and the PW2163 and G2 weights.

Table 48. Mid-Tandem Fan Engine Summary

Parameter		Engine		
		RR	PW2163	GEAE G2
Mach Number		2.0	2.4	2.4
Total Flow Size, lbm/s		1280	1279	1637
Mid-Fan Pressure Ratio		2.1	2.1	2.1
Bypass Ratio		2	1.16	1.78
Overall Compression Ratio		25.4	18.6	21.8
Configuration RR		6/1–5–1–3		
P&W			4/1–5–1–2.5	
GEAE			5/1–5–1–2	4/1–6–1–2
Engine Weight, lbm			15,236	17,753
Nozzle Weight, lbm			3,374	3,935
Total Weight, lbm		11,700 (RR)	18,970	21,688
Weight / Flow, lbm/(lbm/s)		9.14	14.83	13.25

Figure 93 presents a flowpath for the STF1072 Mach 2.0 MTF together with component design characteristics. Figure 94 is a similar presentation for the STF1073/PW2163 Mach 2.4 MTF.

Data Summary – In summation, the U.S. MTF weights were derived using a process similar to that used for the HSCT MFTF 3770.42. The result, Table 47, was that the MTF engine weighed 34% more than the MFTF engine, obviously more than the 3% figure used by RR in their calculations. This weight increase negated the performance benefits that the MTF engine might have produced relative to the MFTF engine. In brief, the study efforts were:

- P&W conducted flowpath analysis of Mach 2.0 MTF to evaluate the RR design philosophy.
- P&W conducted performance analysis of the RR Mach 2.0 and 2.4 cycles to assess the off-design operation.
- P&W conducted flowpath analysis and mechanical design of the Mach 2.4 engine.
- GEAE conducted another flowpath analysis to ensure that MTF tests would be conducted on a weight-consistent basis with the HSCT MFTF engines.
- GEAE conducted performance and flowpath analyses of two MTF engines (G1, G2).
- The mid-tandem fan was rejected, primarily because of weight. There were at least two causes for this excess weight: (1) The small-diameter multistage spool front end and centrally positioned fan made a heavy support structure necessary and (2) the volume of airflow through the MTF mandated use of a large, heavy exhaust nozzle.
- Attempts to reduce the weight of the mid-tandem fan engine to within acceptable limits were unsuccessful.

3.2.4.2 VFX/VCF

Engine Cycle Development

In 1995 the variable-capacity fan, experimental (VFX) concept was proposed to NASA–Lewis by a company called Diversitech. The VFX concept involved using variable fan stators, inlet guide

Component Design Characteristics

6–Stage LPC

N1C2	: 5091.0	rpm
WAT2C	: 427.0	lbm/sec
PR	: 4.67	
η_{adi}	: 89.40	
Wc/A	: 41.05	lbm/sec–ft²
Mn_{exit}	: 0.48	
λ_{inlet}	: 0.37	
λ_{exit}	: 0.77	
N1des	: 5091.0	rpm
UTIPC	: 1049.4	ft/sec
UTIPmax	: 1154.4	ft/sec
URIMmax	: 738.0	ft/sec

Mid–Fan I.D.

N1C25H	: 4000.4	rpm
W25HC	: 116.4	lbm/sec
PR	: 1.25	
η_{adi}	: 80.00	
Wc/A	: 35.56	lbm/sec–ft²
N1des	: 5091.0	rpm

Mid–Fan O.D.

N1C25C	: 5081.3	rpm
WAT25C	: 854.0	lbm/sec
PR	: 2.08	
η_{adi}	: 85.40	
Wc/A	: 43.10	lbm/sec–ft²
N1des	: 5081.0	rpm
UTIPC	: 1552.0	ft/sec
UTIPmax	: 1710.6	ft/sec

5–Stage HPC

N2C27H	: 7173.4	rpm
W27HC	: 110.73	lbm/sec
PR	: 5.08	
η_{adi}	: 88.70	
Wc/A	: 37.50	lbm/sec–ft²
Mn_{exit}	: 0.30	
λ_{inlet}	: 0.73	
λ_{exit}	: 0.91	
N2des	: 9300.8	rpm
UTIPC	: 1071.0	ft/sec
UTIPmax	: 1510.0	ft/sec
URIMmax	: 1368.0	ft/sec

1–Stage HPT

FP	: 49.84	
PR	: 2.92	
$\eta_{TCOOL66}$	: 90.00	
ν_{rim}	: 0.45	
ν_{mean}	: 0.51	
Reaction	: 0.57	
Max AN²	: 450	x10⁸ in²–rpm²

2.5–Stage LPT

FP	: 151.66	
PR	: 4.23	
$\eta_{TCOOL66}$	: 90.5	
ν_{rim}	: 0.38	
ν_{mean}	: 0.50	
Reaction	: 0.5	
Max AN²	: 445.0	x10⁸ in²–rpm²
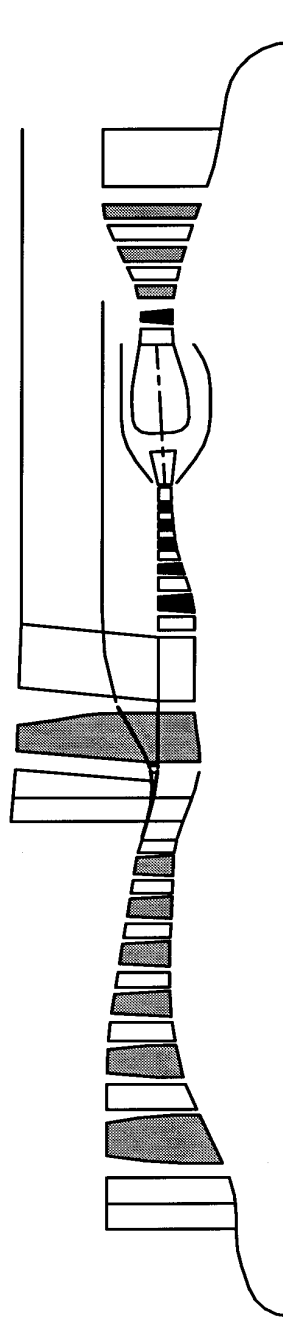
Figure 93.   P&W STF1072 Mach 2.0 Mid-Tandem Fan Engine

Component Design Characteristics

4-Stage LPC

N1C2	:	5036.0	rpm
WAT2C	:	592.0	lbm/sec
PR	:	3.45	
η_{adi}	:	87.0	
Wc/A	:	42.50	lbm/sec-ft²
Mn$_{exit}$	:	0.50	
λ_{inlet}	:	0.40	
λ_{exit}	:	0.70	
N1des	:	5036.0	rpm
UTIPC	:	1220.0	ft/sec
UTIPmax	:	1220.0	ft/sec
URIMmax	:	714.0	ft/sec

Mid-Fan I.D.

N1C25H	:	4131.6	rpm
W25HC	:	209.2	lbm/sec
PR	:	1.22	
η_{adi}	:	77.5	
Wc/A	:	36.10	lbm/sec-ft²
N1des	:	5036.0	rpm

Mid-Fan O.D.

N1C25C	:	5036.0	rpm
WAT25C	:	687.0	lbm/sec
PR	:	2.10	
η_{adi}	:	85.00	
Wc/A	:	42.50	lbm/sec-ft²
N1des	:	5036.0	rpm
UTIPC	:	1570.0	ft/sec
UTIPmax	:	1570.0	ft/sec

5-Stage HPC

N2C27H	:	5439.5	rpm
W27HC	:	177.71	lbm/sec
PR	:	4.42	
η_{adi}	:	90.00	
Wc/A	:	37.50	lbm/sec-ft²
Mn$_{exit}$	:	0.30	
λ_{inlet}	:	0.73	
λ_{exit}	:	0.90	
N2des	:	6858.0	rpm
UTIPC	:	1029.0	ft/sec
UTIPmax	:	1460.0	ft/sec
URIMmax	:	1300.0	ft/sec

1-Stage HPT

FP	:	87.76	
PR	:	2.86	
$\eta_{TCOOL66}$	:	90.00	
ν_{rim}	:	0.45	
ν_{mean}	:	0.52	
Reaction	:	0.57	
Max AN²	:	450	x10⁸ in²-rpm²

2.5-Stage LPT

FP	:	216.25	
PR	:	3.29	
$\eta_{TCOOL66}$	:	90.0	
ν_{rim}	:	0.55	
ν_{mean}	:	0.71	
Reaction	:	0.45	
Max AN²	:	440.0	x10⁸ in²-rpm²
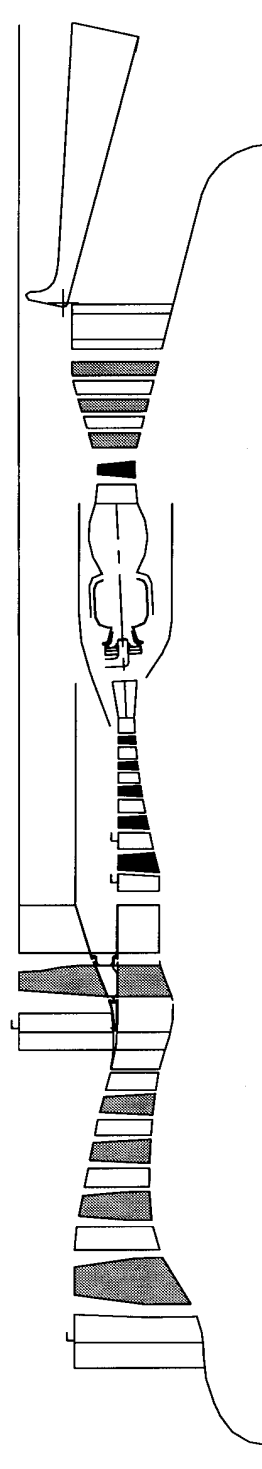
Figure 94.   P&W STF1073 Mach 2.4 Mid-Tandem Fan Engine

vanes, and split outlet guide vanes to create a high-flow, high-specific-thrust MFTF at takeoff and convert it to a low-flow, high-specific-thrust engine during climb and supersonic cruise. The high-flow condition at takeoff was to be achieved by high-flowing the fan to produce about twice the normal airflow. The advantages were expected to be lower takeoff noise (due to reduced jet velocity) and elimination of the need for the large, heavy, mixer/ejector (noise suppression) nozzle.

NASA–Lewis undertook a study of the VFX concept, and initial evaluation was that the VFX cycle advantages came with a severe TOGW penalty. The weight increase was primarily due to the added inlet/turbomachinery and the larger nozzle required by the doubled airflow.

NASA–Lewis then proposed a hybrid cycle that capitalized on the VFX fan and mixer/ejector nozzle contributions to reduce noise and at the same time reduce TOGW. The hybrid cycle studies (which included the use of a mixer/ejector nozzle) did demonstrate reduced noise.

In 1996 NASA–Lewis completed mean-line and two-dimensional aerodynamic evaluations of several hybrid fans which were referred to as variable capacity fans (VCF). The new designs were restricted to the baseline HSR fan aeromechanical design envelope, including the elimination of the OGV and third-stage stator variability. The variable IGV and stators for the VCF were designed to maintain constant corrected speed above 800 lbm/s inlet corrected airflow while increasing the FPR, as shown in Figure 95.

By November 1996, NASA–Lewis came to a conclusion that a lower SAR mixer/ejector nozzle in conjunction with a lower airflow VCF would reduce TOGW with lower acoustic risk and minimal impact on the baseline MFTF design. In 1997, GEAE and P&W were given this "optimum" hybrid cycle for aerothermal and mechanical evaluation. The evaluation concluded that the design was heavier (TOGW) than the comparable 1996 3770.60 MFTF, when evaluated at constant noise and
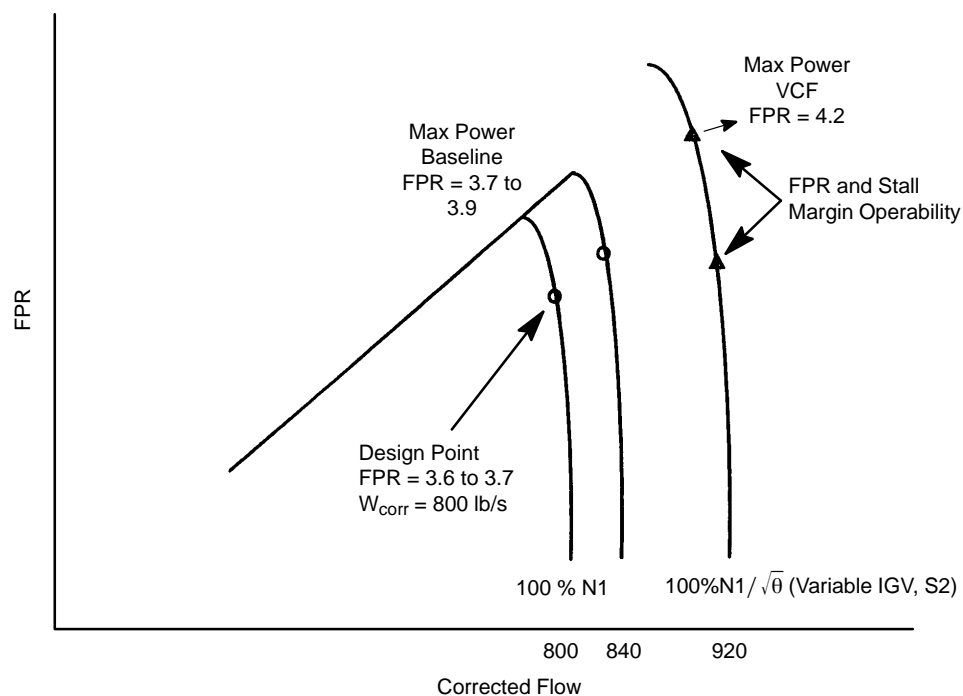
Figure 95.   Variation in Pressure Ratio at High-Flow Condition, Constant Corrected Speed

mission requirements. In 1998 a revised VCF cycle was provided to GEAE and P&W for another aerothermal and mechanical evaluation. Conclusions are summarized as follows:

- GEAE FLOWPATH assessment of VCF engine is "heavy"
  - Turbomachinery weight up 32%, mostly in fan module
  - Nozzle weight up 8% due to A_8 increase
  - Engine is 20.6% heavier; more than thrust gain
- Fan weight increased 2800 lbm for the projected product
  - Large airfoil weight increases
  - Significant cascading impact on disks, case, and containment
- 1997 Mechanical rules and 1996 performance used
  - 1998 Characteristics will further increase LPT flow and energy extraction
  - Anticipate larger turbine weight impact
- The VCF engine does not show a benefit over the MFTF

Subsequently, GEAE and P&W evaluated the VCF engine on the 1504 planform, otherwise known as the *Preliminary Technology Configuration.* The groundrules and assumptions for the 1504 baseline were weights and aerodynamic input from Boeing on the 1504 planform (PTC). Aerodynamics were provided for high-speed high-lift (10° flaps) 1504 wings. The baseline engine for comparison was the 3770.60 MFTF with 2.9 SAR 135-in FCN installed with 2DB inlet, and the HSCT noise prediction (approximate) method from MCP was used. The MFTF-powered aircraft sizes to 798,000 lbm with P&W cycle data installed by Boeing and to 790,000 lbm with NCP cycle data installed by GEAE. Other particulars of the VCF evaluation were as follows:

- Installation
  - Afterbody – 3770.60 2.9 SAR FCN
  - Inlet – Boeing 2DB inlet map
- Engine Assuming 43.5-lbm/s/ft^2 Inlet Specific Airflow
  - 11,646 lbm Turbomachinery Weight
  - 6% Longer than MFTF
- 2.9 SAR Nozzle
  - Scale by A_8 Ratio (8%)
  - 8456 lbm Nozzle Weight
- Adjusted Noise at Same Jet Velocity for 2.9 SAR Nozzle
  - $10 \log_{10} (1.08) = 0.3$ dB
  - Used VJIP vs EPNL Relationship from 3770.60 Acoustic Data
  - Small Fan Noise Penalty for Increased Tip Speed and Fewer Blades
- 1504 is 60-min Climb-Time Sized at 820,000-lbm MTOW
  - 30,000-lbm Penalty Relative to MFTF

Comparisons were based on the engine data tabulated in Table 49, and the resulting engine design is described in the Flowpath Development discussion beginning on page 130.

Table 49.   MFTF and VCF Engine Propulsion Statics

MFTF engine data provided by P&W/GEAE for 3770.60 SAR 2.9; this is the PTC engine that was used in all the ongoing HSCT system studies. VCF engine data provided by NASA from NCP (installed by GEAE) for 4260.60 SAR 2.9.

Parameter	MFTF 3770.60	VCF 4260.60
Fan Pressure Ratio	3.7	4.2
Bypass Ratio	0.60	0.60
Extraction Ratio	1.20	1.20
Inlet Airflow Ratio	0.70	0.60
SAR	2.9	2.9
Mixer Length, in	135	135
Reference Airflow, lbm/s	800	920
Reference Thrust, lbf (SLS, +18°F, Installed, Suppressor Deployed)	59,800	65,800
Turbomachinery Weight, lbm	8,845	11,646
Nozzle Weight, lbm	7,840	8,456
Engine Weight, lbm (Includes Nozzle)	16,675	20,102
T/W (SLS suppressed)	3.59	3.27
Cruise SFC: P&W NASA NCP	1.242 1.237	 1.237

The "Briquette" data were used to estimate the penalty for 10% more TOC thrust:

- 300 lbm for engine, 800 lbm for nozzle
- 10% more Mach 2.4, 55,000 ft thrust at 1% SFC penalty

The 1504 was noise-sized at 820,000-lbm MTOW. As with the 60-min climb time sizing, there was a 30,000-lbm penalty, but the thrust margin is more desireable at TOC.

In summary, three engines were evaluated, with the following salient results.

- MFTF 3770.60 baseline, from planform study
  - Sized to –1 dB sideline, –5 dB community noise
  - Time to climb to Mach 2.4: 50 minutes
- VCF engine 4260.60 – 30,000 lbm heavier than MFTF
  - Sized to 60-min time to climb
  - Top of climb thrust inadequate
- VCF engine 4260.60 – 30,000 lbm heavier than MFTF
  - Sized to –1 dB sideline, –5 dB community noise
  - Time to climb to Mach 2.4: 48 minutes
  - Sufficient top of climb thrust margin

If the evaluation assumed no turbomachinery weight penalty and that 920 lbm/s with 11% more thrust in the same engineis possible, it would still require an 8% larger nozzlewith a 2.9 SAR to comply with noise constraints.

In conclusion, the revised VCF concept showed no benefit. It produces 10% more thrust but at 20% more weight, and it is unrealistic to assume the turbomachinery weight penalty will go away while the thrust increase is retained. Some ideas from this study might be useful in future MFTF studies.

- Oversized Fan with Takeoff at Higher Extraction Ratio
- Better Matching of Inlet Airflow Characteristics

A rig test of this VCF concept is not warranted at this time. Future studies may identify a fan concept using some VCF cycle features worthy of rig testing.

Flowpath Development

Throughout the CPC program, the goal has been to define a configuration that could operate economically at high Mach cruise and meet HSCT noise requirements. The VCF and the VFX concepts attempted to accomplish this in a manner somewhat similar to that used by the fan-on-blade (FLADE) and midtandem fan engines. The VCF and VFX concepts both counted on a low-specific-thrust takeoff to eliminate the need for a heavy noise-suppression nozzle. In other words, at takeoff the engine provides thrust by very high airflow and relatively low pressure. This reduces jet noise below HSCT limits. Once at cruising altitude, engine airflow is decreased in volume but increased in pressure to provide high-specific-thrust operation for supersonic cruise.

The VFX concept was first proposed in 1996. NASA picked up the idea and developed a cycle engine system they thought would blend noise and mission requirements with a much simpler nozzle system The main feature of the VFX engine was potential to significantly increase fan inlet flow through the use of variable stators installed throughout the fan assembly. The objective of this design feature was to pass 17% more air through the engine during takeoff operation. It was hoped the constant-thrust line could be followed down to lower jet velocity because of the increased flexibility in the fan assembly enabled by three rows of variable stators. This proposed solution to the engine noise challenge was examined by the GEAE/P&W team during April 1997. The study strove to maintain consistent constraints in all facets of the engine design.

VFX Fan

MFTF3770.60 Fan

Figure 96. Comparison of VFX and MFTF3770.60 Designs

Figure 96 compares the proposed VFX fan design with the design of the MFTF3770.60 fan, the base engine used for studies at the time of this analysis.

The HCST mission is extremely sensitive to engine weight, so any oversized engine concept faces a system challenge. Engine size and weight have a dominant impact on aircraft size. Large size yields large drag in an aircraft. To offset the drag and accomplish the mission, the size of the propulsion system must be increased. This, in turn, forces system size to increase to enable it to do the mission and threatens the

system economic viability. Engine weight has a similar impact on aircraft size and viability. Engine specific fuel consumption is dominated by the high-Mach nozzle performance.

The GEAE/P&W team replicated the intent of the NASA engine. Because of the nature of the evaluation results, other engine options were defined to understand the key elements of the conclusions. The steps involved in evaluation of the VFX engine were:

- P&W defined the cycle
  - Maintains fixed A_8 during suppressed mode
  - Uses overflow capacity of VFX component

- GEAE captured NASA VCF technology
  - Created FLOWPATH model of fan
  - Used system study mechanical design suite

- Defined engine that best satisfies P&W engine cycle

- Defined similar-technology component-to-system study constraints
  - W/A set to 42.5 (maximum available to matrix engine)
  - Stage 1 radius ratio set to 0.37

- Compared geometry and weights with matrix engine 3770.60
  - 800 lbm/s
  - 937 lbm/s

The most crucial factor in VFX system design is the overflow capacity of the fan system. The particular cycle for this overflow point is summarized as follows:

- Airflow: 939 lbm/s
- FPR: 4.24
- BPR: 0.49
- OPR: 21.9
- Net Thrust: 67,024 lbf

The lower BPR and OPR require larger core geometry than the 3770.60 engine.

The baseline 3770.60 system used in this study produces 50,000-lbf net thrust with a fan pressure ratio of 3.7, an inlet flow of 800 lbm/s, and a bypass ratio of 0.60.

Originally, NASA assumed the VFX engine would operate at a fan pressure ratio of 3.7 or lower in this high-flow case. This required a significant change in fan design and engine logic to be successful. The flow areas at the fan exit are usually established at a fan exit Mach number of 0.5. As the operating line of the engine is lowered, the exit Mach number increases.

Studies showed that the operating line could not be lowered to the 3.7 level when the engine operated at high flow because the fan frame could not accept the high flow. When the fan frame was sized to accept the high flow, the design base exit Mach number was significantly reduced. Levels between Mach 0.3 and 0.35 were predicted. This design would necessitate a four-stage fan and very long chords to achieve the needed stall margin. Neither of these options was studied because of the projected adverse impact to the engine performance and weight. Instead, the design was performed on the fan at 4.24 pressure ratio stipulated above.

It was hoped that it would be possible to use the same core from the fan frame aft to drive the VFX fan. The only way that this could be accomplished was if the baseline fan had excess turbine

capability. The engine with the higher flow fan required an increase in horsepower extraction in the low-pressure turbine. Both the engines are already designed to operate near the temperature limits for the system, so operating at higher temperature was not an option. The power increase desired for the VFX could only be achieved through the use of a larger low-pressure turbine than was used for the base engine.

The baseline engine was designed with the smallest exit diameters thought to be possible. The increased turbine size mandated a larger diameter and area to handle the power increase. Because of internal coupling between engine components, the core diameters were increased from the compressor inlet aft. The result of this design activity is illustrated in Figure 97; the two engines are lined up at the compressor inlet plane. The VFX fan is on the top, and the base 3770 engine is on the bottom. The larger fan shows up in the front, and the larger core shows up in the back of the engine schematic.
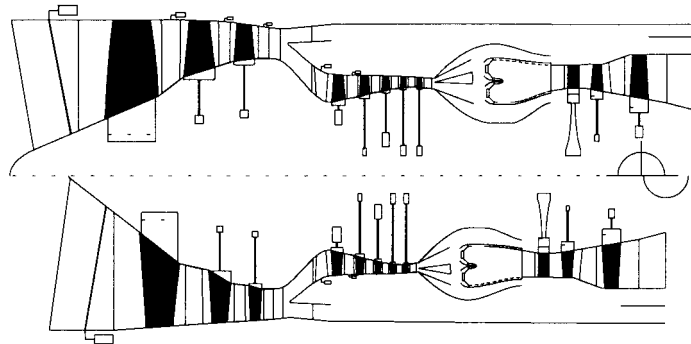
Figure 97.   NASA VFX Fan Engine Comparison

Geometry value changes were:

- Turbomachinery 14 inches longer (fan contributes 8 inches)

- All component diameters larger,

Fan Stage 2:	3.4 inches
HPC Exit:	1.0 inches
HPT:	4.0 inches
LPT:	3.6 inches

One scenario proposed that the inlet of the fan be made smaller by designing the engine for a higher inlet Mach number than was used for the base engine. This specific flow increase would have driven the VFX fan much closer to the (theoretical) ideal limits than was deemed prudent.

Examination revealed that the second fan stage was larger than the base (Figure 97). This attempt to minimize the impact of the high-flow design on the fan influenced only the inlet plane. The resulting engine still was at risk of high-specific-flow problems, and accepting the risk still did not result in a fan of similar size. The results were discouraging relative to the original concept.

Several alternatives to the assumptions were also examined to describe the sensitivity of the problem. The first of these alternatives was to redesign the VFX fan at the baseline specific flow. Fan length was improved slightly by this option, again indicating that the higher risk specific-flow design did not produce any benefit to the system. This first alternative is captured graphically in Figure 98, and the numerical impact is as follows; note that the diameter and length changes are similar to the original design.

- Turbomachinery 10 inches longer (fan contributes 6 inches)

- All component diameters larger,

Fan Stage 2:	5.2 inches
HPC Exit:	1.4 inches
HPT:	4.4 inches
LPT:	4.2 inches
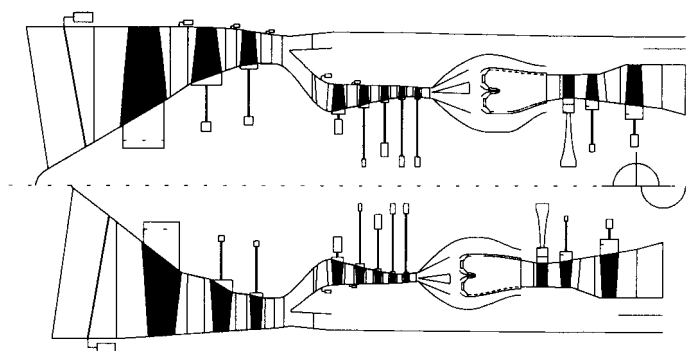
Figure 98.   Comparison to Modified Fan

A second alternative was to oversize the baseline engine to the higher flow of the VFX. The fan pressure ratio and engine thrust are not the same as the VFX, but the flow impact is illustrated. As shown schematically in Figure 99 and summarized below, this option yields the least length impact. Diameters throughout the engine are increased proportionately. These changes are similar to both of the first two options. The increased complexity of the VFX fan does not appear to provide a quantifiable advantage in engine geometry.

- Turbomachinery 9 inches longer (fan contributes half)

- All component diameters larger,

Fan Stage 2:	4.6 inches
HPC Exit:	3.5 inches
HPT:	3.4 inches
LPT:	3.6 inches

Weight Impact

The weights of these engine configurations are what could be expected from the volume and length discussion above. As shown in Table 50, the high-specific-flow initial VFX case yielded the heaviest fan. The core engine is the heaviest in the case of the low-specific-flow, high-volume engine, but the advantage was small. Variations on this model could change the weight impact. Just scaling the engine to match the MFTF TOC thrust would provide significantly better

Figure 99.   Comparison to 3770.60 Engine Scaled to 937 lbm/s

weight figures than were obtained with either of the VFX options examined. The impact of the VFX relative to the mixed-flow turbofan configuration is summarized as follows.

Advantages	**Negatives**

- Thrust to Weight at SLS Takeoff
  - +4.8% to Base
  - +5.9% to Scale of Base

- Thrust to Weight at Top of Climb
  - –4% to Base
  - –3% to Base Scaled

- Increased Engine Length
  - +10 Inches to Base
  - +1 Inch to Scale of Base

- Increased weight and complexity will increase cost

Table 50. Weight Impacts of the VFX Engine Variations

	MFT3770.60 Base Engine	VCF3670.49 W/A = 44.54		VFX3670.49 W/A = 42.54		MFTF3770.60 Scaled Base	
FPR	3.69	3.60		3.60		3.69	
BPR	0.60	0.49		0.49		0.60	
OPR	20.3	18.0		18.0		20.3	
Component	**Engine Weight, lbm**		Δ	**Engine Weight**	Δ	**Engine Weight**	Δ
Fan	1936	2918	982	2860	925	2354	418
Fan, Compressor and Combustor	2439	2770	331	2841	402	2892	453
Turbines	2407	2765	358	2836	429	2850	443
Core Engines	8073	9942	**1869**	10033	**1960**	9547	**1474**

The preceding comparisons did not include the nozzle because the cycles were defined to maintain the nozzle throat areas. Conclusions for this engine concept are as follows:

- This version of the VFX concept is neutral to the product performance.
- Weight, complexity, and cost impacts are negative.

1998 VCF Engine Studies

As the VFX study described above drew to a close, NASA decided to to modify the effort to develop a high-flow fan engine that could solve the takeoff noise problem. This new concept was given the name *variable-capacity fan* (VCF). For the VCF, NASA defined a cycle with a smaller overflow level. There was also a smaller push on increased fan specific flow.

As in the earlier study, a more conventional fan approach was also studied to understand what improvements resulted from the VCF approach and what came just from the flow increase.

The base engine used in the VCF study was the same as the engine used in the earlier VFX study.

The DOE methodology that was used in the 1998 TC systems studies was applied to the VCF study. The system objective parameter for this work is takeoff gross weight. The fan design specified by NASA in a memo by Dr. Adamczyk was captured by the FLOWPATH model. Figure 100 defines the salient features of that fan configuration, including the aerodynamic design point and geometry features.

The DOE parameter variation was as follows:

- Test matrix: 2^3 central composite analytical DOE
- DOE analysis integrating the FLOWPATH and TP3 software tools
- Variables
  - LP spool RPM: Fixed by NASA
  - HPT pitch reaction (R×4):   55% ▶ 65%
  - LPT Stage 1 work fraction: 38% ▶ 45% P_{48}
  - HP spool RPM: 7800 ▶ 8500
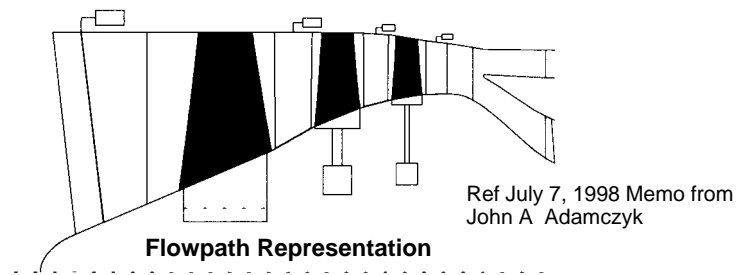
ADP
W_c = 920 lbm/s
P_r = 4.2
Utc i = 1500 ft/s
rr i = 0.342
W/A = 43.8
D_{max} = 66.276 in

Ref July 7, 1998 Memo from
John A Adamczyk

Flowpath Representation

Stage	Aspect Ratio		Airfoil Count	
	R	S	R	S
1	1.36	2.85	22	56
2	1.48	2.78	42	106
3	1.36	2.51	46	136

Figure 100.   NASA 1998 VCF Design

LP spool rotational speed was held at the NASA value and was not considered a variable in the experiment. The DOE design and results relative to the baseline engine for the initial run are shown in Table 51. A second DOE was run over a narrower range of parameters to verify the results.

Table 51.   DOE Design and Results

%P_{48}	Rx_4	N_4	Deltas					
			TOGW	Weight	Fan Eff	HPC Eff	Eff HPT pts.	Eff LPT pts
38	0.55	8500	7.627	2537.090	–0.870	–0.900	–0.420	1.050
45	0.55	7800	8.329	2982.520	–0.870	–1.400	–0.790	2.460
41.5	0.51591	8150	7.926	2645.320	–0.870	–1.100	–0.790	1.470
45	0.65	7800	8.268	3040.170	–0.870	–1.400	–0.480	2.630
38	0.65	7800	8.755	3124.110	–0.870	–1.400	–1.080	2.830
38	0.55	7800	8.349	3003.820	–0.870	–1.400	–0.790	2.520
41.5	0.6	8738.63	7.416	2372.780	–0.870	–0.760	–0.300	0.370
45	0.55	8500	7.553	2506.980	–0.870	–0.900	–0.040	0.700
41.5	0.68409	8150	7.677	2525.820	–0.870	–1.100	–1.420	2.030
45	0.65	8500	7.395	2361.040	–0.870	–0.900	–0.700	0.870
35.6137	0.6	8150	7.767	2641.100	–0.870	–1.100	–0.760	1.810
47.3863	0.6	8150	7.627	2559.850	–0.870	–1.100	–0.590	1.420
38	0.65	8500	7.577	2596.510	–0.870	–0.900	–0.640	1.570
41.5	0.6	7561.37	9.285	3487.390	–0.870	–1.250	–1.040	3.190

• 14 Engine Variations in DOE

• Repeated DOE Over Narrow Range

• Total of 28 Configurations

A comparison of the resulting engine and the baseline 3770.60 engine is shown in Figure 101. The core compressors in the two engines are virtually identical. As shown in the chart, the total VCF engine is nearly 21% heavier than the equivalent baseline engine. For the product engines, this is 3400 pounds heavier, and 2/3 of that weight is in the fan. In this cycle the exhaust throat areas areas are increased, which results in increased weight for the nozzle.

In Figure 102 the size increases of the VCF fan relative to the baseline are shown. Summarized in this chart are the major geometric differences that led to the 2324-lbm weight increase. As in the case of the earlier study, the specific flow increase reduced only the annulus at the fan inlet plane. All other parts of the VCF are much larger.

The power needed to drive the larger VCF forced the change in turbine diameter shown in Figure 103. In this example, the compressor size was held constant while the VCF turbine component weights increased 6%.

As was the case in the first study described in this subsection, the question arose as to what a more conventional fan for the cycle sized at this inlet flow would weigh. Figure 104 shows the VCF fan in comparison to a 4.0 FPR MFTF of similar maximum size.

As shown in Figure 105, the turbomachinery portion of the conventional fan was shown to be 2250 pounds lighter than the VCF. This is very significant to the system, since the oversized turbofan turbomachinery is only 500 pounds heavier than the baseline 3770.60 engine used in the PTC.

Both of the high-flow engine configurations discussed in this subsection were very large and heavy compared to the baseline mixed-flow turbofan. The only justification for using them would be if the noise-suppression mixer/ejector nozzle did not achieve the noise goals.

The VCF study is summarized as follows:

- GEAE FLOWPATH assessment indicates VCF engine is heavy.
  - Turbomachinery weight up 32%, mostly in fan module.
  - Nozzle weight up 8% due to large A_8.
  - Engine is 20.6% heavier; more than thrust gain.
- Fan weight increased 2800 lbm for the projected product engine.
  - Large airfoil-weight increases
  - Significant cascading impact on disks, case, and containment
- The 1997 mechanical groundrules and 1996 performance groundrules were used.
  - The 1998 characteristics would further increase LPT flow and energy extraction.
  - Larger turbine weight impact is anticipated.
- The VCF engine is competitive with the MFTF engine.
- Cycle concepts are competitive and should be explored further.

1998 VCF Version is Solid and Shaded
3770.60 Version is Dashed
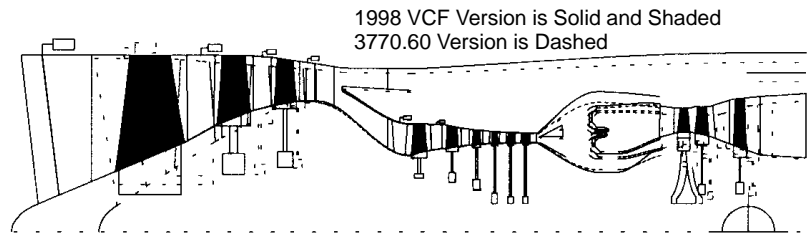
Component	Weight, lbm					
	HSCT3770.60		1998 VCF			
	Interim	Projected Product	Interim	Projected Product	Diff	
Front Frame	222	200	243	220	20	
Fan Rotor	1253	1141	2307	2099	958	
Stator	651	636	1800	1758	1122	
HP Turbine Rotor	641	577	763	687	110	
Stator	245	221	242	218	–3	
LPT Rotor	740	670	797	721	51	
Stator	254	232	262	239	7	
Rear Frame	614	541	678	597	56	
Outer Duct	349	310	360	319	9	
Fan Containment	126	125	353	349	224	
Combustor	1402	1262	1416	1274	12	
Total Core	9460	8845	12338	11646	2801	31.7%
Nozzle	8700	7830	9396	8456	626	8.0%
Total Engine	18160	16675	21734	20102	3427	20.6%

Summary

Engine Weight Increase
Due to Three Major Items:

- Fan → +2324
- Nozzle ~ +626
- Turbines → +224

  Dramatic LPT Area
  Increase, +13%
  Increased Diameters,
  HPT Aft

Figure 101.   VCF Vs Baseline Design

VCF is Solid
3770.60 is Dashed
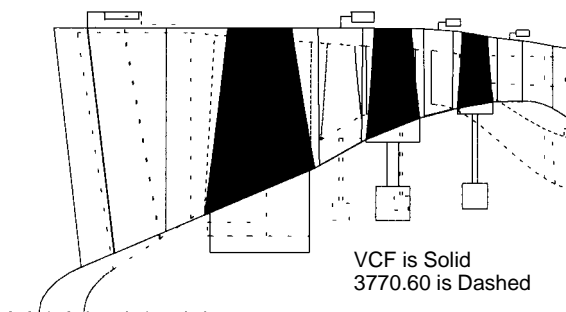
VCF Fan vs. 3770.60 Fan Flowpath

Component	HSCT3770.60		1998 VCF		
	Interim	Projected Product	Interim	Projected Product	Diff
Front Frame	222	200	243	220	20
Fan Rotor	1253	1141	2307	2099	958
Stator	651	636	1800	1758	1122
Fan Containment	126	125	353	349	224

Major Differences

- Airfoil Size:
  - Stage 1 A_{ann} +13%
  - Stage 2 A_{ann} +24%
  - Stage 3 A_{ann} +21%
  - Rotor Ave AR –22%
  - Stator Ave AR –24%

- Airfoil Weights:
  - Rotors 2.2 X Heavier
  - Stators 4.0 X Heavier

- Drives Disk and Case Weights:
  - Disks +77%
  - Case +67%
  - Containment +2.8X

- Stator Variability: +155 lb

- Fan Component Weights:
  - VCF → 4426 lb
  - 3770.60 → 2102

Figure 102.   Fan Comparison, VCF to Baseline

VCF is Solid
3770.60 is Dashed
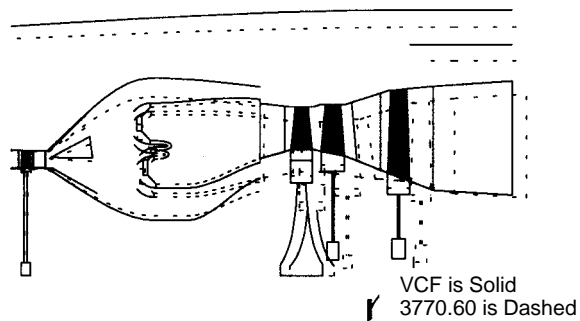
VCF vs. 3770.60 Flowpath

| Component | HSCT3770.60 | | 1998 VCF | | |
	Interim	Projected Product	Interim	Projected Product	Diff
HP Turbine Rotor	641	577	763	687	110
Stator	245	221	242	218	–3
LPT Rotor	740	670	797	721	51
Stator	254	232	262	239	7
Rear Frame	614	541	678	597	56
Outer Duct	349	310	360	319	9
Combustor	1402	1262	1416	1274	12
Total Core	9460	8845	12338	11646	2801

Major Differences

- Energy Extraction, Δh/t
  - HPT   +3%
  - LPT   +15%
- Exit Corrected Flow, w√(T)/P
  - HPT   +1%
  - LPT   +14%
- HPT Diameter Increases:
  - LPT limits → OD Slope, Me and rre
  - Larger HPT Diameters Result
- Turbine Component Weights:
  - VCF →   4056 lb
  - 3770.60 →   3815 (+6%)

Figure 103.   Turbine Comparison

VCF Fan

Conventional 4.0 Fan
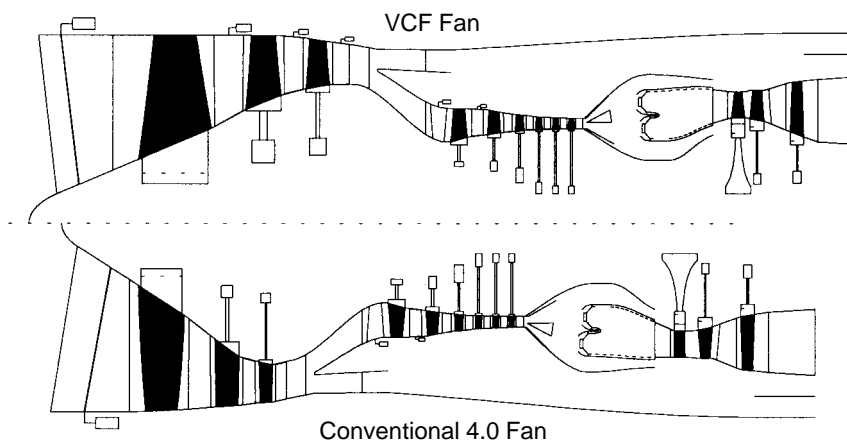
**Figure 104.   Comparison of VCF Engine with 4.0 Conventional Fan
Engine**   *VCF engine is longer.*

1998 VCF Version is Solid and Shaded
Conventional Fan Version is Dashed

Conventional Fan Version 2250 lb Lighter than VCF
Initial Configuration 500 lbm Heavier than PTC
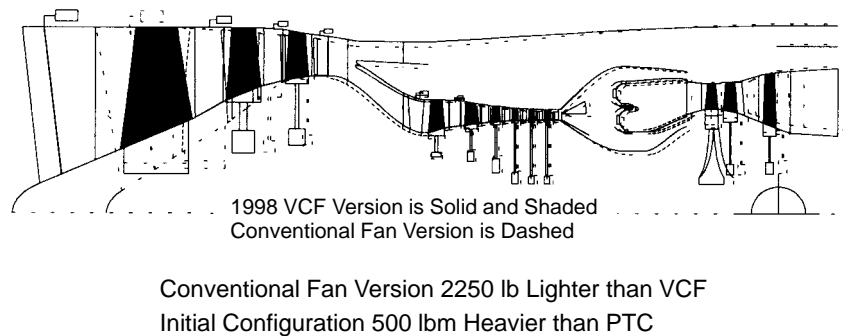
Figure 105. Comparison of Weight Characteristics, VCF Vs Conventional

3.2.5 Product Margins and Requirements

3.2.5.1 Cycle Audit

The changes made in transition from the 1996 3770.60 cycle to the June 1998 3770.54 cycle are
summarized as follows:

- New "stratified fan" performance model from detailed design
- New HPC
- New HPT
- Vaneless LPT stacked maps
- High-fidelity turbine cooling model
- Detailed turbine cooling accounting (3 cooling bleeds increased to 36)
- Fixed fan/core mixer
- Updated customer extractions
- Increased pressure-loss fidelity

In this transformation, the fan incorporated a radial pressure and temperature differential (warpage
or stratification), so two fan maps were created. The first represented the fan average performance
and the second represented the fan inner diameter performance. Fan outer diameter performance was
calculated based on the average and the ID outputs. The fan pressure ratio range was 3.2 to 4.2, and
the bypass ratio range was 0.17 to 0.80. Due to the FPR and BPR ranges, at design the fan average
efficiency, ID efficiency, and ID pressure ratio were adjusted as a function of BPR and average FPR.

The high-pressure compressor was modeled with two maps, chosen to better represent the compres-
sor stator schedules and the engine rotor speed variations during subsonic and supersonic flight.
These maps were biased to engine inlet total temperature (T_{T2}). The first map was nominal (low T_{T2}
stator schedule) and was used for subsonic flight conditions. The second was a high T_{T2} stator
schedule map and was used for supersonic flight conditions. A linear interpolation between the two
maps was used for transonic flight conditions.

A new combustor pressure loss correlation was added to these calculations. This loss was split
between a diffuser loss, which varied as a function of dynamic pressure (Q) and a fixed burner loss

defined at design. Pressure losses throughout the model were updated based on the latest design information available. Design Mach numbers were added to better represent aerodynamic conditions throughout the cycle.

The map for the high pressure turbine was generated based on 1996–97 design results. In addition, a table was added to calculate the HPT exit air angle. The exit air angle was a function of the HPT expansion ratio and the HPT inlet corrected speed. This exit air angle was also considered to be the low pressure turbine inlet air angle.

The LPT had a vaneless first-stage design that used six maps (one for each of the following six inlet air angles: 21°, 28°, 35°, 41.78°, 47°, and 52°). Each map was read as a function of air inlet angle and interpolated where needed. Two tables were used for (1) LPT exit air angle and (2) LPT exit Mach number. Both the LPT exit air angle and the LPT exit Mach number were functions of the LPT expansion ratio and the LPT inlet corrected speed. The LPT exit air angle was used together with the LPT exit Mach number to derive the exit guide vane loss. (This output is a function of exit angle and exit Mach number.)

The number of turbine cooling bleeds was expanded from 3 to 36 to provide better representation of the turbine cooling. A small portion of these bleeds was diverted from the fan duct. The percent of bleed increased from the 1996–97 level, which was 23% of engine airflow entering the HPC (WAE), to 28.1% WAE, plus an additional 1.3% from the fan duct.

3.2.5.2 Operability Audit

The percent of bleed varied slightly from cycle to cycle in the 1998–99 matrix. There was a significant change in the way the cycles operated due to the increase in turbine cooling. Since the amount of cooling for the HPT vane increased from 9.5% to 13.4% WAE, the HPT maximum temperature used for limiting was changed from the HPT rotor inlet temperature ($T_{T4.1}$) to the combustor exit temperature (T_{T4}). This was done because the increase in cooling caused the temperature exiting the HPT vane to drop so much that it no longer was the limiting parameter. The design turbine cooling flow and both the HPT and LPT design efficiencies had to be adjusted due to the cycle-to-cycle variation in HPT and LPT specific work ($\Delta h/T$). These adjustments varied from cycle to cycle as a function of $\Delta h/T_{T4.1}$ for the HPT and $\Delta h/T_{T4.5}$ for the LPT.

The fixed fan/core mixer and the variable fan/core mixer were evaluated and compared extensively. It was decided that the complexity and weight of the variable fan mixer negated any performance benefits; therefore, the fixed fan/core mixer was used for all 1998–99 cycles. Mixer was improved by addition of pressure losses through the mixer. On the core side, the diffusion loss was combined with the friction loss and resulted in a 2% pressure loss at design. Duct-side friction loss at design was 1.5%. Off-design, these losses varied as a function of local Q. Mixing effectiveness was set at 80% for all flight conditions.

Customer bleed was taken from one of two locations in the HPC and modeled as a function of bleed temperature. Customer power extraction varied as a function of nozzle mode (suppressed or unsuppressed). Engine parasitic power extraction was added and applied as a function of fuel flow.

Table 52 is a comparison of the 3770.54–6/98 cycle and the 3770.60 cycle at the top of climb flight condition. Figure 106 shows the results of these changes in cycle components. Supersonic cruise SFC increased by about 1.5%, subsonic cruise SFC increased by about 4.4%, thrust/airflow had little change, and thrust/weight dropped by about 2.5% relative to the PTC.

Table 52.   Cycle Performance Tracking

Component analysis: 55,000 ft, Mach 2.4, standard day, top of climb

Parameter		Engine	
		3770.60	**3770.54–6/98**
Pressure Ratio	Fan	2.31	2.34
	HPC	4.47	4.30
	HPT	2.47	2.54
	LPT	2.14	2.10
Extractions	Power, hp	200	338.1
	Bleed, lbm/s	1.0	1.25
Pressure Losses, %	Fan Exit Guide Vanes	1.1	0.0
	FEGV Core	0.0	0.5
	FEGV Duct	0.0	1.0
	Duct	7.0	6.4
	Diffuser/Combustor	6.1	7.2
	TEC	1.1	0.7
	FCM Core	0.0	1.9
	FCM Duct	0.0	2.5
	Nozzle	3.5	3.5
Efficiency, %	Inlet	92.5	93.0
	Fan	90.8	89.4
	HPC	90.1	89.6
	Combustor	99.9	99.9
	HPT	91.4	90.8
	LPT	92.3	90.4
	FCM	80.0	80.0

Figure 106.   Revised Reference Engine Cycle Performance

3.2.5.3 Power and Bleed Extraction

In 1997 the effect of increasing customer horsepower extraction (HPX) and customer bleed (CB) air requirements was evaluated. A study was undertaken at P&W to evaluate the effect of varying the HPX and CB on the 3770.60 engine cycle. All cycles in the 1996–97 matrix included an HPX of 200 hp and a CB of 1 lbm/s.

The 3770.60 SAR 2.9 engine cycle (short 122-in mixing length, fixed-chute nozzle) was used as a constant design base. This base-condition engine was first run with the HPX at 200 hp and the CB at 1 lbm/s. The HPX then was varied from 200 to 350 and 500 hp, and the customer bleed was varied from 1 to 2 and 3 lbm/s. In all a total of nine combinations were studied, and the engine cycle was examined in four flight configurations:

    A. 55,000 ft, Mach 2.4, standard day, supersonic cruise

    B. 36,089 ft (11 km), Mach 0.9, standarad day, subsonic cruise

    C. 689 ft, Mach 0.32, standard day +18°F, suppressed takeoff (823 lbm/s)

    D. 30,000 ft, Mach 1.1, standard day, transonic climb (823 lbm/s)

Tables 53 through 56 each show results for one of the four configurations listed. Data presented in these tables include:

- HPX (horsepower extraction)
- CB (customer bleed air),
- FNDAB (net thrust with afterbody drag removed),
- SFCDAB (specific fuel consumption based on FNDAB),
- %ΔSFCDAB from base and for the supersonic cruise point only
- %ΔDOC+I (percent of change in direct operating cost + interest

The last parameter is based on a P&W study that showed +1% supersonic SFC to be worth +0.94% in DOC+I. Each table uses a fixed FNDAB so that variations in SFCDAB can be easily compared. The results show that the %ΔSFC for changes in bleed and HPX are both linear and additive.

Table 57 is summary data for three conditions. Case 1 shows that for constant HPX the change in %ΔSFC is linear as it goes from 1 to 2 to 3 lbm/s. This is true also in Case 2, which shows constant CB and varying HPX. In Case 3, an even-increment change in both HPX and CB is also shown to be linear. Adding the %ΔSFC across, Case 1 + Case 2 ≃ Case 3 shows that the %SFC changes are essentially additive.

The information in Table 57 was provided to the airframe companies, in the form of three data packs, so they could evaluate the effect of variations in customer HPX and CB on maximum TOGW.

3.2.5.4 Minimum Engine Definition and Hot Day Operation

A performance evaluation study was conducted in an effort to understand what the performance of a minimum deteriorated engine would be for the HSCT flight mission. This study took into account engine-to-engine, nozzle-to-nozzle, and control variations together with development margin (for LPT only) and deterioration.

Table 53.   Customer Bleed and Horsepower Extraction Study A (5/2/97)

Study conditions are: 55,000 ft, Mach 2.4, Std Day, PC Near 50, Supersonic Cruise

HPX (hp)	CB (lbm/s)	FNDAB (lbf)	SFCDAB (lbm/lbf/hr)	%ΔSFCDAB from Base (%)	%Δ DOC+I
200	1.0	19000	1.2505	0	0
350	1.0	19000	1.2522	+0.1359	+0.13
500	1.0	19000	1.2539	+0.2719	+0.26
200	2.0	19000	1.2588	+0.6637	+0.62
350	2.0	19000	1.2605	+0.7997	+0.75
500	2.0	19000	1.2622	+0.9356	+0.88
200	3.0	19000	1.2671	+13275	+1.25
350	3.0	19000	1.2688	+1.4634	+1.38
500	3.0	19000	1.2704	+1.5914	+1.50

Table 54.   Customer Bleed and Horsepower Extraction Study B (5/2/97)

Study conditions are: 36,089 ft (11 km), Mach 0.9, Std Day, PC38 (60% Power), Subsonic Cruise

HPX (hp)	CB (lbm/s)	FNDAB (lbf)	SFCDAB (lbm/lbf/hr)	%ΔSFCDAB from Base
200	1.0	9000	0.9388	0
350	1.0	9000	0.9435	+0.5006
500	1.0	9000	0.9482	+1.0013
200	2.0	9000	0.9486	+1.0439
350	2.0	9000	0.9530	+1.5126
500	2.0	9000	0.9576	+2.0026
200	3.0	9000	0.9584	+2.0878
350	3.0	9000	0.9628	+2.5565
500	3.0	9000	0.9671	+3.0145

Table 55.   Customer Bleed and Horsepower Extraction Study C (5/2/97)

Study conditions are: 689 ft, Mach 0.32, Std+18°F Day, PC50 (W2AR = 823 lbm/s), Suppressed Takeoff

HPX (hp)	CB (lbm/s)	FNDAB (lbf)	SFCDAB (lbm/lbf/hr)	%ΔSFCDAB from Base
200	1.0	53100	0.8971	0
350	1.0	53100	0.8977	+0.07
500	1.0	53100	0.8984	+0.14
200	2.0	53100	0.8997	+0.29
350	2.0	53100	0.9003	+0.36
500	2.0	53100	0.9009	+0.42
200	3.0	53100	0.9024	+0.58
350	3.0	53100	0.9030	+0.65
500	3.0	53100	0.9036	+0.72

Table 56.   Customer Bleed and Horsepower Extraction Study D (5/2/97)

Study conditions are: 30,000 ft, Mach 1.1, Std Day, PC50 (W2AR=823 lbm/s), Transonic Climb

HPX (hp)	CB (lbm/s)	FNDAB (lbf)	SFCDAB (lbm/lbf/hr)	%ΔSFCDAB from Base
200	1.0	22260	1.1819	0
350	1.0	22260	1.1831	+0.1015
500	1.0	22260	1.1844	+0.2115
200	2.0	22260	1.1881	+0.5246
350	2.0	22260	1.1894	+0.6346
500	2.0	22260	1.1906	+0.7361
200	3.0	22260	1.1943	+1.0492
350	3.0	22260	1.1956	+1.1592
500	3.0	22260	1.1968	+1.2607

Table 57.   Three-Case Comparison

Conditions for this study are: 55,000 ft, Mach 2.4, Std Day, Supersonic Cruise

Case 1			Case 2			Case 3		
HPX (hp)	Bleed (lbm/s)	ΔSFC (%)	HPX (hp)	Bleed (lbm/s)	ΔSFC (%)	HPX (hp)	Bleed (lbm/s)	ΔSFC (%)
200	1	0	200	1	0	200	1	0
200	2	+0.6637	350	1	+0.136	350	2	+0.80
200	3	+1.3275	500	1	+0.272	500	3	+1.59

An effort was made, based on a P&W in-house study, to estimate the component (fan, HPC, HPT, LPT, and nozzle) variation as well as the development margin and deterioration for a minimum engine and nozzle. Table 58 lists the recommended component allocations to model engine-to-engine, nozzle-to-nozzle, and control variations; development margin; and deterioration. The worst case (most deteriorated) engine must meet thrust requirements at the end of engine life. This worst case engine can be modeled by applying all of the recommended allocations at one time.

Note: The 1-point reduction in LPT efficiency, allocated as development margin, was a result of a redesign of the LPT to reduce weight. This weight reduction caused a 1-point degradation in efficiency relative to that quoted in the cycle deck. All other component efficiency targets, for the nominal engine, are assumed to be attainable.

Table 58.   Recommended Component Performance Variations

Variation	Δη (Adiabatic)				Nozzle Cooling Flow and Leakage
	Fan	HPC	HPT	LPT	
Engine to Engine and Control or Nozzle to Nozzle Variation	–0.30	–0.65	–0.30	–0.35	+10%
Development Margin	——	——	——	–1.00	——
Deterioration	–0.33	–0.40	–0.63	–0.57	——
Minimum Deteriorated Engine	–0.63	–1.05	–0.93	–1.92	+10%

Table 59 lists the results of a minimum deteriorated engine run made with the 3870.47. briquette cycle (FPR = 3.8, flow lapse = 0.70, TOC relative to takeoff, BPR = 0.47). These results were from runs on a standard day and a hot day (standard +18°F). In both cases, takeoff suppressed mode was run on a hot day. The unsuppressed mode data were also run on a standard day and a hot day. These data should be compared to the baseline 3870.47 briquette cycle data listed in Table 60.

At 55,000 ft, Mach 2.4, top of climb, on a standard day, the minimum deteriorated engine thrust matches the baseline 3870.47 thrust. The thrust lapse (FNP at 55,000 ft, Mach 2.4 relative to FNMIX at sea level, Mach 0.3) is maintained. There is a 1.2% increase in TSFC at the top of climb.

In order to maintain the baseline thrust characteristics for a minimum deteriorated engine throughout the entire flight matrix, an EPR versus T_{T2} schedule was developed. EPR (defined as P_{T7}/P_{T2}) was found to be the best parameter to use to maintain the baseline thrust. Two schedules were developed: One for unsuppressed flight conditions (Figure 107) and the other for suppressed flight conditions (Figure 108). Each schedule had one unique curve, which defined EPR. It should be noted that these two figures reflect values developed from the 3870.47 baseline data pack flight matrix. The EPR versus T_{T2} schedules for other cycles would be different.

Taking into account a deteriorated engine, the turbines have been designed with a 75°F temperature margin. Therefore, when running the minimum deteriorated engine, the maximum T_{T4} increases from 3460° to 3535°R. If the net thrust required for top of climb at 55,000 ft, Mach 2.4, standard day, nominal engine (22,000 lbf) was to be maintained on a hot day for a minimum deteriorated engine, the aircraft would have to drop to either:

- 51,200 ft, Mach 2.3, where Mach 2.4 standard day T_{T2} (838°R) is maintained and fan corrected inlet airflow (W2AR) is 570 lbm/s. TSFC increases by 2.0% relative to the baseline 55,000 ft, Mach 2.4, standard day value

or

- 51,800 ft, Mach 2.25, where T_{T2} = 820°R, W2AR = 591 lbm/s, T_{T3} and T_{T4} are at their maximum values, 1660° and 3535°R respectively. TSFC increases by 1.2% relative to the baseline 55,000 ft, Mach 2.4, standard day value.

To minimize the effects of a minimum deteriorated engine and hot-day operation, the another cycle was developed, labeled 3670.51 because it has a 3.6 fan pressure ratio, a 70% engine inlet corrected airflow lapse, and a bypass ratio at design of 0.51. Table 61 is a summary of the performance of the 3670.51 at various flight conditions, for the nominal engine and the minimum deteriorated engine. As was the case with the 3870.47, the minimum deteriorated engine uninstalled TSFC at 55,000 ft, Mach 2.4, standard day, PC50 TOC increases by 1.2% relative to the nominal engine value. Table 62 presents a similar summary of the performance of the 3870.47 engine.

When the 3670.51 cycle is compared to the 3870.47, the 3670.51 appears to have advantages and disadvantages. The 3670.51 offers three advantages.

First, the minimum deteriorated engine uninstalled TSFC for the 3670.51 is 1.0% greater (versus 1.2% for the 3870.47) than the 3870.47 nominal engine TSFC at TOC. This is at a constant uninstalled net thrust.

Second, on a hot day, maximum climb power, the 3670.51 is able to operate closer to the standard day W2AR by +4.0 to +4.5% relative to the 3870.47. This lowers the inlet spillage drag for the 3670.51. Figure 109 shows the relationship of hot day, 51,800 ft, Mach 2.25, maximum power

Table 59. B3870.47S27 Minimum Deteriorated Engine, 6/01/99

Parameter	SLS Design	Takeoff Rotation	Sideline Noise	55k/M2.4 Std Day	55k/M2.4 Std +18°	51k/M2.3 Std +18°	52k/M2.25 Std +18°
ALT (ft)	0	0	689	55000	55000	51200	51800
XM	0	0.3	0.32	2.4	2.4	2.3	2.25
DTAMB (°R)	0	18	18	0	18	18	18
PC	50	50	50	50	50	50	50
PAMB (psia)	14.696	14.696	14.3337	1.3227	1.3227	1.5877	1.5426
TAMB (°R)	518.67	536.67	534.2129	389.97	407.97	407.97	407.97
ERAM	0.924	0.964	0.963	0.93	0.93	0.9325	0.9337
PT2A (psia)	13.5791	15.0795	14.8182	18.0121	18.027	18.546	16.6819
TT2A (°R)	518.6698	546.3335	545.1585	837.789	875.7552	838.1154	819.8505
W2AR (lbm/s)	800	816.6419	816.8362	559.9999	527.9858	569.6796	591.1241
TT3 (°R)	1296.406	1421.31	1419.014	1659.776	1660.016	1660	1659.324
TT4 (°R)	3084.361	3500.974	3496.523	3503.183	3353.177	3478.677	3534.915
TT41 (°R)	2838.48	3219.903	3215.711	3249.738	3117.458	3228.138	3277.756
PT7 (psia)	44.6848	54.3367	53.423	32.416	27.7406	32.5403	31.1695
W8 (lbm/s)	748.7988	830.1758	816.8237	546.3857	503.253	572.0082	540.0841
TT8 (°R)	1568.234	1824.2	1821.487	1805.602	1720.367	1778.4	1805.135
PT8 (psia)	44.6848	54.3367	53.423	31.1977	26.5833	31.223	29.9253
FNP (lbf)	51396.78	57807.36	56457.07	21882.2	16982.7	22033.26	22008.4
WFT (lbm/hr)	39055.03	53871.85	52928.1	27323.86	21878.79	27729.58	27461.33
SFCSTW (lbm/lbf/hr)	0.7599	0.9319	0.9375	1.2487	1.2883	1.2585	1.2478
FNMIX (lbf)	54467.72	56617.85	55136.97	0	0	0	0
SFCMIX (lbm/lbf/hr)	0.717	0.9515	0.9599	0	0	0	0
VJMIX (ft/s)	1377.003	1717.584	1725.997	0	0	0	0
VJIP (ft/s)	2271.858	2630.391	2635.141	3648.259	3497.43	3550.339	3572.998
CVPSTW	0.9721	0.9791	0.9792	0.9829	0.9837	0.9836	0.9834
CVMIX	0.9219	0.9679	0.9676	0	0	0	0
CV9TD	1.0301	0.9616	0.9595	0	0	0	0
SMFAN	24.8159	19.642	19.6227	21.7441	22.0374	23.6921	24.3195
P16Q56	1.05	1.0279	1.0279	1.1999	1.3025	1.2401	1.2148
A16 (in²)	423.5059	423.5059	423.5059	423.5059	423.5059	423.5059	423.5059
A8CD (in²)	1266.304	1249.985	1249.939	1424.189	1500.726	1477.965	1467.565
A8GEOSUP (in²)	1299.85	1282.158	1282.11	0	0	0	0
A8GEOUNSUP(in²)	1299.549	1281.313	1281.264	1465.263	1545.213	1521.45	1510.601
FPR	3.8	4.0603	4.0621	2.4159	2.2313	2.431	2.5376
BPR	0.4653	0.4275	0.4274	0.6645	0.7361	0.6909	0.6703
OPR	19.3679	21.2578	21.2699	10.0973	8.7058	10.0714	10.7934
EPR7	3.2907	3.6034	3.6052	1.7997	1.5388	1.7546	1.8685
RPMC(FAN) (rpm)	100	102.2662	102.2916	82.2311	79.5117	82.8715	84.5068
Δη(ad), (FAN,OD)	0	–0.0063	–0.0063	–0.0063	–0.0063	–0.0063	–0.0063
Δη (ad), (FAN,ID)	0	–0.0063	–0.0063	–0.0063	–0.0063	–0.0063	–0.0063
Δη (ad), (HPC)	0	–0.0105	–0.0105	–0.0105	–0.0105	–0.0105	–0.0105
Δη (ad), (HPT)	0	–0.0093	–0.0093	–0.0093	–0.0093	–0.0093	–0.0093
Δη (ad), (LPT)	0	–0.0192	–0.0192	–0.0192	–0.0192	–0.0192	–0.0192
η (ad), (FAN,AVG)	0.8665	0.8308	0.8303	0.8833	0.8831	0.8824	0.882
η (ad), (FAN,OD)	0.8385	0.7926	0.7921	0.8439	0.8449	0.8455	0.8468
η (ad), (FAN,ID)	0.8794	0.8473	0.8468	0.9086	0.9101	0.9071	0.9048
η (ad), (HPC)	0.8887	0.8779	0.8779	0.8885	0.8856	0.8881	0.8884
η (ad), (HPT)	0.8882	0.8777	0.8777	0.8858	0.8875	0.8861	0.8852
η (ad), (LPT)	0.9004	0.878	0.878	0.8784	0.8795	0.8796	0.8796
WCOOLSUP (lbm/s)	0	0	0	0	0	0	0
WLEAKSUP (lbm/s)	2.2839	2.9622	2.9146	0	0	0	0
WCOOLUNSUP(lbm/s)	0	0	0	0	0	0	0
WLEAKUNSUP (lbm/s)	2.2839	2.9622	2.9146	1.7111	1.4956	1.7262	1.6414

Table 60.   B3870.47S27 Baseline Engine, 6/01/99

Parameter	SLS Design	Takeoff Rotation	Sideline Noise	55k/M2.4 Std Day	55k/M2.4 Std +18°	51k/M2.3 Std +18°	52k/M2.25 Std +18°
ALT (ft)	0	0	689	55000	55000	51200	51800
XM	0	0.3	0.32	2.4	2.4	2.3	2.25
DTAMB (°R)	0	18	18	0	18	18	18
PC	50	50	50	50	50	50	50
PAMB (psia)	14.696	14.696	14.3337	1.3227	1.3227	1.5877	1.5426
TAMB (°R)	518.67	536.67	534.2129	389.97	407.97	407.97	407.97
ERAM	0.924	0.964	0.963	0.93	0.93	0.9325	0.9337
PT2A (psia)	13.5791	15.0795	14.8182	18.0121	18.027	18.546	16.6819
TT2A (°R)	518.6698	546.3335	545.1585	837.789	875.7552	838.1154	819.8505
W2AR (lbm/s)	800	822.3417	822.9008	559.999	536.1061	578.7532	598.7941
TT3 (°R)	1296.406	1425.673	1424.594	1660.021	1660.003	1659.998	1656.606
TT4 (°R)	3084.361	3460.184	3459.739	3458.975	3296.246	3415.389	3459.936
TT41 (°R)	2838.48	3184.271	3183.75	3210.741	3067.449	3172.332	3211.164
PT7 (psia)	44.6848	54.2741	53.4326	33.4446	28.0038	32.8299	31.2813
W8 (lbm/s)	748.7988	835.6313	822.5869	546.3348	510.8109	580.8695	546.7953
TT8 (°R)	1568.234	1797.867	1797.562	1799.777	1694.776	1748.575	1768.543
PT8 (psia)	44.6848	54.2741	53.4326	32.275	26.8421	31.5083	30.0386
FNP (lbf)	51411.56	57691.26	56440.73	22008.54	16875.51	21893.7	21673.46
WFT (lbm/hr)	39055.03	52997.41	52202.57	27143.85	21490.53	27201.7	26692.05
SFCSTW (lbm/lbf/hr)	0.7597	0.9186	0.9249	1.2333	1.2735	1.2424	1.2316
FNMIX (lbf)	54483.71	56502.75	55115.61	0	0	0	0
SFCMIX (lbm/lbf/hr)	0.7168	0.938	0.9471	0	0	0	0
VJMIX (ft/s)	1377.376	1708.649	1719.426	0	0	0	0
VJIP (ft/s)	2271.858	2610.085	2617.698	3655.015	3473.919	3522.947	3536.57
CVPSTW	0.9723	0.9795	0.9796	0.9832	0.984	0.9839	0.9837
CVMIX	0.9217	0.9706	0.9702	0	0	0	0
CV9TD	1.0304	0.9619	0.9598	0	0	0	0
SMFAN	24.8159	20.5117	20.3327	21.3065	23.4672	25.2491	25.8502
P16Q56	1.05	1.0287	1.0284	1.167	1.3007	1.239	1.2159
A16 (in²)	423.5059	423.5059	423.5059	423.5059	423.5059	423.5059	423.5059
A8CD (in²)	1266.304	1250.044	1249.812	1374.24	1496.742	1474.101	1464.297
A8GEOSUP (in²)	1300.361	1282.809	1282.57	0	0	0	0
A8GEOUNSUP (in²)	1300.075	1281.984	1281.737	1413.44	1541.653	1518.016	1507.788
FPR	3.8	4.0582	4.0643	2.4248	2.2495	2.4502	2.5483
BPR	0.4653	0.4243	0.4237	0.6284	0.7253	0.6803	0.6616
OPR	19.3679	21.3151	21.3626	10.2505	8.8136	10.1939	10.8601
EPR7	3.2907	3.5992	3.6059	1.8568	1.5534	1.7702	1.8752
RPMC(FAN) (rpm)	100	102.9267	102.996	82.2632	80.0942	83.5175	85.0233
Δη (ad), (FAN,OD)	0	0	0	0	0	0	0
Δη (ad), (FAN,ID)	0	0	0	0	0	0	0
Δη (ad), (HPC)	0	0	0	0	0	0	0
Δη (ad), (HPT)	0	0	0	0	0	0	0
Δη (ad), (LPT)	0	0	0	0	0	0	0
η (ad), (FAN,AVG)	0.8665	0.8238	0.8226	0.8898	0.8888	0.8874	0.8867
η (ad), (FAN,OD)	0.8385	0.7833	0.7818	0.848	0.8505	0.8507	0.852
η (ad), (FAN,ID)	0.8794	0.8413	0.8401	0.915	0.9154	0.9114	0.9088
η (ad), (HPC)	0.8887	0.8784	0.8781	0.8954	0.8919	0.8945	0.8948
η (ad), (HPT)	0.8882	0.8869	0.8869	0.8962	0.8955	0.8958	0.8957
η (ad), (LPT)	0.9004	0.8995	0.8994	0.8988	0.9007	0.901	0.901
WCOOLSUP (lbm/s)	0	0	0	0	0	0	0
WLEAKSUP (lbm/s)	2.0763	2.7104	2.6686	0	0	0	0
WCOOLUNSUP(pp)	0	0	0	0	0	0	0
WLEAKUNSUP(lbm/s)	2.0763	2.7104	2.6686	1.612	1.3838	1.5977	1.5141
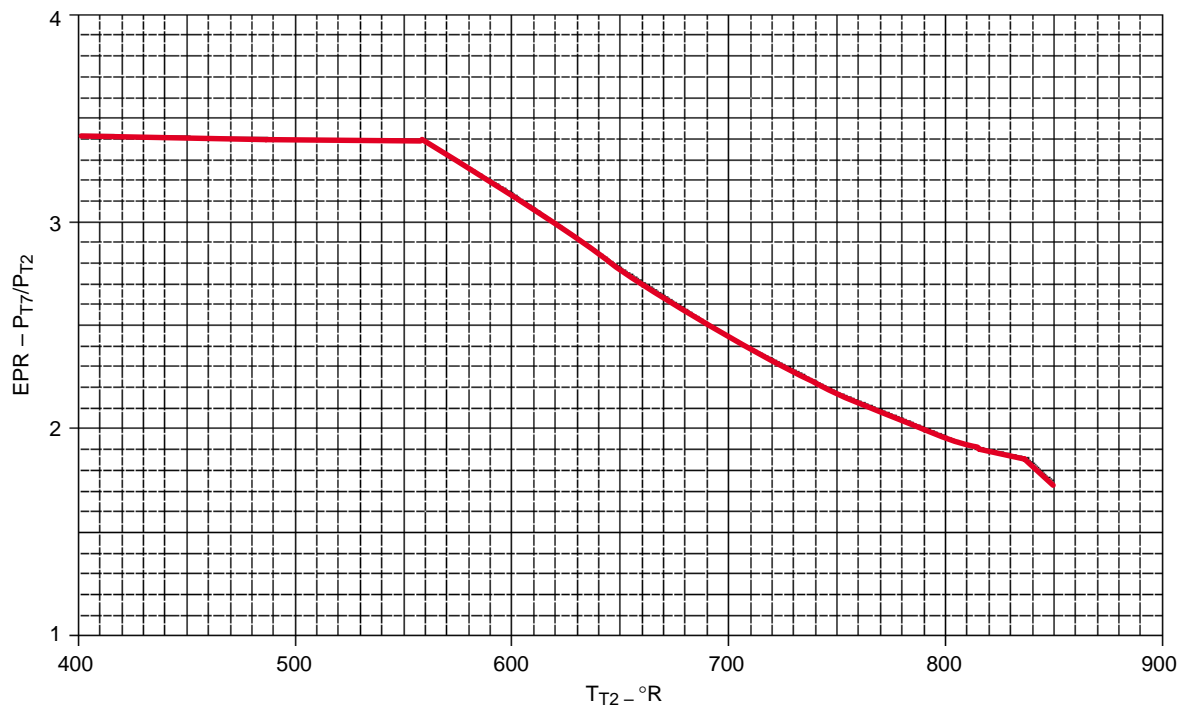
Figure 107.   B3870.47 Unsuppressed EPR Vs T_{T2} Schedule
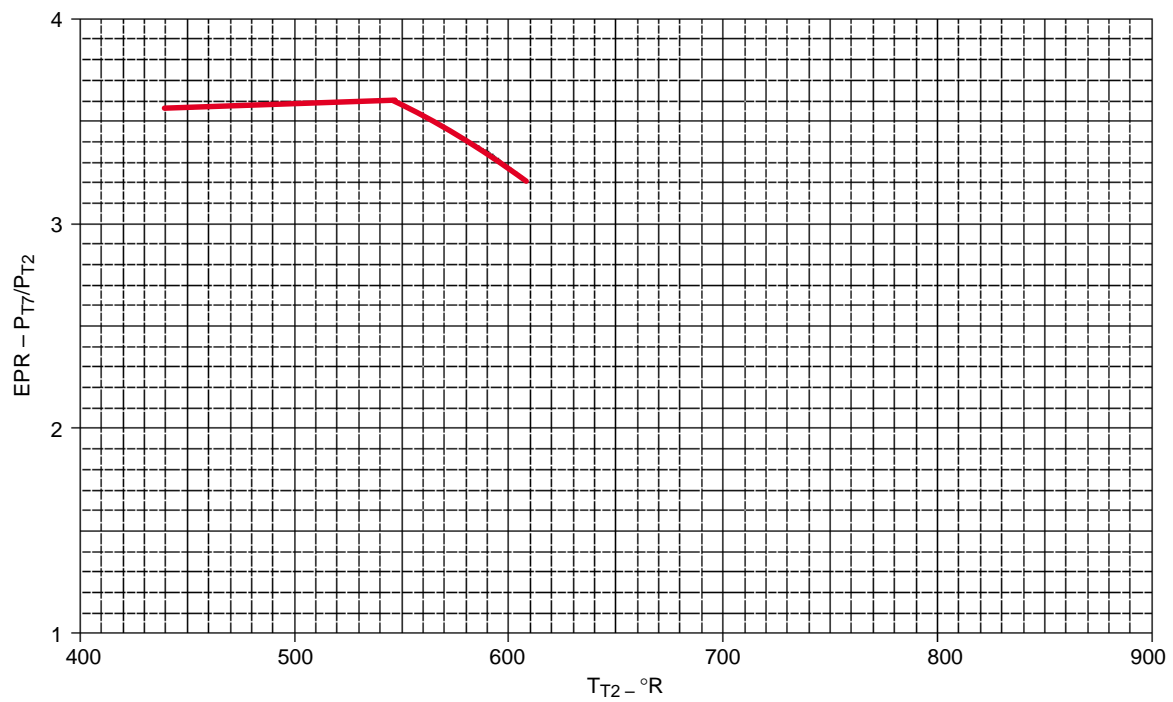
Figure 108.   B3870.47 Suppressed EPR Vs T_{T2} Schedule

Table 61. Comparison of the HSCT MFTF Cycle 3670.51 Minimum Deteriorated to Nominal Engine

Parameter		Cycle	
		Nominal B3670.51	Min. Deteriorated B3670.51
Design Point Sea Level, Static, Standard Day **PC50**	P16Q56	1.05	1.05
	BPR	0.5145	0.5145
	OPR	18.645	18.645
	FPR	3.60	3.60
	TT4 (°R)	3102.5	3102.5
	TT4.1 (°R)	2851.1	2851.1
	W2AR (lbm/s)	800.0	800.0
	SMFAN	24.8	24.8
Sea Level, Mach 0.3 Standard Day +18°F, PC50	FNMIX (lbf)	53518	55096
	W2AR (lbm/s)	823.2	823.0
689 ft, Mach 0.32 Standard Day +18°F, PC50	TT4 (°R)	3368.7	3474.4
	SMFAN	22.01	20.03
	P16Q56	1.0321	1.0292
	A8CD (in^2)	1309.3	1309.3
	VJIP (ft/s)	2493	2555
	W2AR (lbm/s)	823.1	823.0
55,000 ft, Mach 2.4 Standard Day, PC50	TT3 (°R)	1653.5	1659.2
	TT4 (°R)	3459.7	3534.7
	TT4.1 (°R)	3208.4	3275.3
	P16Q56	1.1157	1.1315
	W2AR (lbm/s)	560.0	560.0
	FNP (lbf)	22137	22451
	SFC (lbm/lbf/hr)	1.2302	1.2452
	FN lapse (55k/sl/M0.3)	0.414	0.407
	TT8 (°R)	1802.7	1826.1
	PT8 (psia)	32.74	32.22
	SMFAN	20.77	20.80
55,000 ft, Mach 2.4 Standard Day +18°F, PC50	W2AR (lbm/s)	560.0	551.2
51,800 ft, Mach 2.25 Standard Day +18°F, PC50	TT3 (°R)	1657.3	1660.0
	TT4 (°R)	3458.9	3531.2
	W2AR (lbm/s)	623.4	615.0
	FNP (lbf)	21882	22098
	SFC (lbm/lbf/hr)	1.2284	1.2443

Table 62. Comparison of Minimum Deteriorated to Nominal 6/98 Minibriquette Engine 3870.47

Parameter		Cycle	
		Nominal B3670.47	Min. Deteriorated B3670.47
Design Point Sea Level, Static, Standard Day PC50	P16Q56	1.05	1.05
	BPR	0.465	0.465
	OPR	19.368	19.368
	FPR	3.80	3.80
	TT4 (°R)	3084.4	3084.4
	TT4.1 (°R)	2838.5	2838.5
	W2AR (lbm/s)	800.0	800.0
	SMFAN	24.8	24.8
Sea Level, Mach 0.3 Standard Day +18°F, PC50	FNMIX (lbf)	56499	56618
	W2AR (lbm/s)	822.4	816.6
689 ft, Mach 0.32 Standard Day +18°F, PC50	TT4 (°R)	3460.1	3496.5
	SMFAN	20.34	19.62
	P16Q56	1.0285	1.0279
	A8CD (in2)	1250.0	1249.9
	VJIP (ft/s)	2618	2635
	W2AR (lbm/s)	822.9	816.8
55,000 ft, Mach 2.4 Standard Day, PC50	TT3 (°R)	1660.1	1659.8
	TT4 (°R)	3458.9	3503.2
	TT4.1 (°R)	3210.7	3249.7
	P16Q56	1.1669	1.1999
	W2AR (lbm/s)	560.0	560.0
	FNP (lbf)	22009	21882
	SFC (lbm/lbf/hr)	1.2333	1.2487
	FN lapse (55k/sl/M0.3)	0.390	0.386
	TT8 (°R)	1799.8	1805.6
	PT8 (psia)	32.28	31.20
	SMFAN	21.31	21.74
55,000 ft, Mach 2.4 Standard Day +18°F, PC50	W2AR (lbm/s)	536.1	528.0
51,800 ft, Mach 2.25 Standard Day +18°F, PC50	TT3 (°R)	1656.6	1659.3
	TT4 (°R)	3459.9	3534.9
	W2AR (lbm/s)	598.8	591.1
	FNP (lbf)	21673	22008
	SFC (lbm/lbf/hr)	1.2316	1.2478
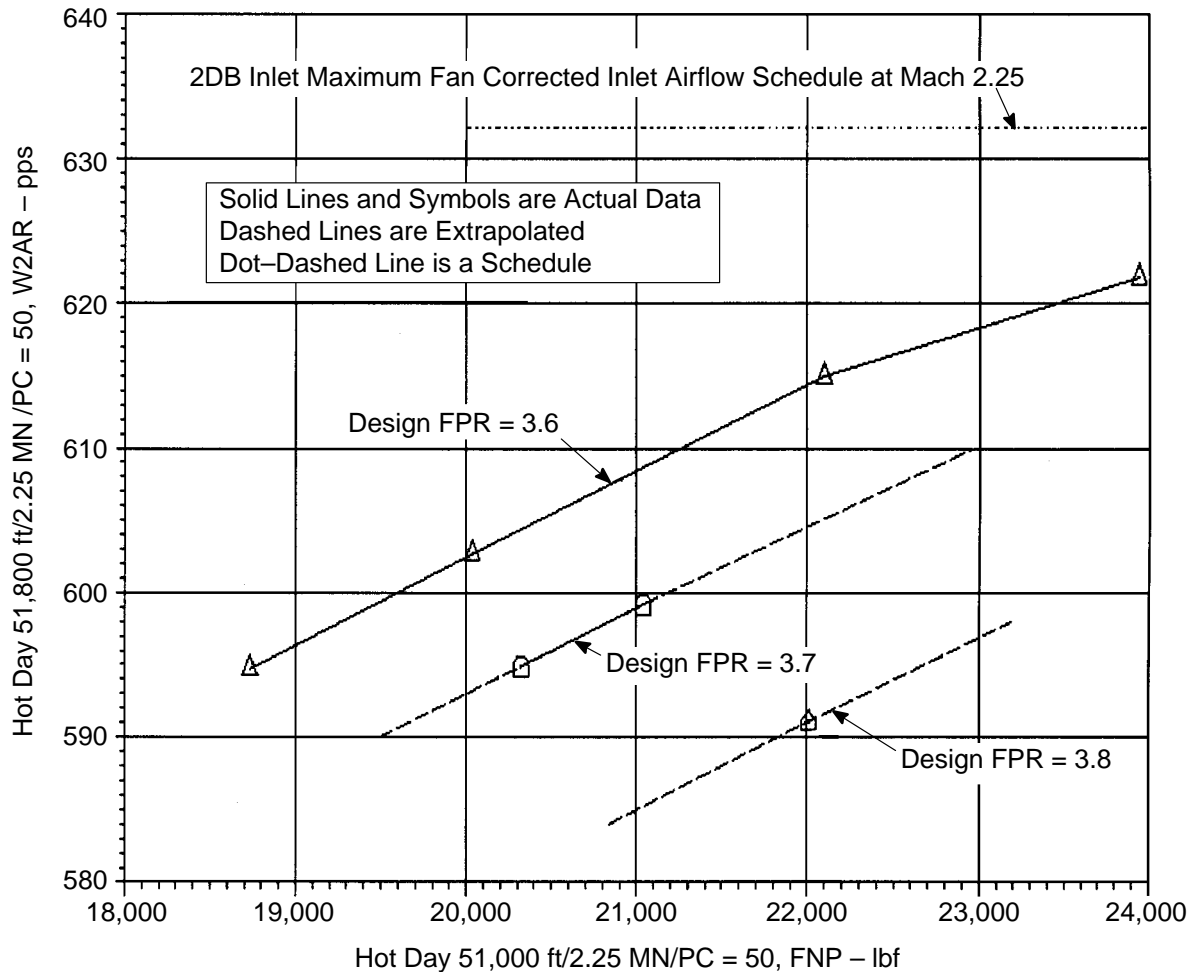
Figure 109.   HSCT Hot Day Minimum Deteriorated Cycle Trends

W2AR at a given uninstalled net thrust, for various design fan pressure ratios. The plot shows a 4% increase in W2AR for a FPR of 3.6 relative to 3.8 FPR. The 3.6 FPR cycle has a larger throat area, enabling it to pass more flow. Thus, a lower FPR cycle is capable of accepting more airflow at a given thrust than a higher FPR cycle. This reduces inlet spillage drag. For example, at Mach 2.25, the 2D bifurcated inlet will accept up to 632 lbm/s W2AR. The 3.6 FPR cycle is capable of a W2AR flow of 615 lbm/s at FNP = 22,000 lbf, while the 3.8 FPR cycle is capable of a flow of 591 lbm/s. The 3.6 FPR cycle has a W2AR airflow penalty of 2.7%, while the 3.8 FPR cycle has a W2AR airflow penalty of 6.5%. A mission analysis must be conducted to determine the impact of this difference.

Finally, the primary ideal jet velocity (VJIP) at the sideline noise flight condition (689 ft, Mach 0.32, standard +18°F day, PC50) is reduced by 4.8% for the nominal engine and 3.0% for the minimum deteriorated engine.

The one disadvantage of the 3670.51 cycle is at takeoff, suppressed mode. The uninstalled mixed out net thrust for the 3670.51 cycle is 5.3% below that of the 3870.47 cycle for the nominal engine and 2.7% below for the minimum deteriorated engine. This is consistent with the reduction in VJIP.

A mission analysis is needed to further evaluate these cycles.

3.2.6 Numerical Propulsion-System Simulation (NPSS) Modeling Assessment

The *Numerical Propulsion–System Simulation* (NPSS) is a thermodynamic computer modeling environment that uses the latest computer science and information technology as system-level modeling tools. Development of this environment is the result of years of participation in the NPSS Development Project by NASA–Glenn and aerospace industry members. Early versions of the NPSS software were used in the development of the HSCT

A steady-state model of the HSCT engine was created by the NPSS program before the release of NPSS version 1.0, and a comparison was made of this model to the official P&W *State-of-the-Art Performance Program* (SOAPP) HSCT system model. The design point values of the NPSS model were a close match to the values used by the SOAPP system, which indicated that the thermodynamic component representations were being implemented properly. The comparisons between NPSS and SOAPP did show some off-design discrepancies, however, primarily at flight idle conditions. These off-design discrepancies were not deemed significant enough to be pursued as part of the HSR program. Instead, the discrepancies will be addressed in the normal NPSS development effort at NASA–Glenn.

During the HSR evaluation, P&W and GEAE users were able to rapidly update and run the model, run multipoint design cases, and exercise the simulation in the interactive run environment. These aspects of the NPSS program were found to be mature, robust, and quite user friendly. Model troubleshooting was expedited by the NPSS diagnostics, which can specify the location and nature of most problems encountered. Development of new NPSS elements is facilitated by the NPSS interpreted input language; the robust, flexible NPSS architecture; and the object-oriented design.

One disadvantage of the NPSS is that it has a slower run time for individual points than does the typical industry simulation system. For example, NPSS executes approximately four times slower for an individual point than the current P&W SOAPP modeling system does. Although this lack of speed would not in itself preclude use of NPSS in an engine design/development environment, users have noted the slower speed, and the NASA–Glenn team will consider it in future releases. The NPSS multipoint design capability has reduced an 8-hour (typically) manual process to an NPSS process that takes less than 25 minutes.

Work is continuing on resolution of issues uncovered during the NPSS evaluation of the HSR program. P&W and GEAE continue to participate in development of NPSS together with NASA–Glenn and other industry development team members. The HSR Program has provided valuable insight into the functionality of NPSS in a realistic preliminary design environment. Because of issues that surfaced during the HSR program, many improvements have been identified and implemented in NPSS. Use of NPSS by the HSR Program has definitely resulted in an improved NPSS that more closely reflects industry needs.

3.3 Mechanical Design

3.3.1 Temperature, Durability, Manufacturing, and Material Challenges

Development of the HSCT propulsion system presented four technical challenges that set the HSCT propulsion system apart from those used in subsonic commercial transports and supersonic military aircraft:

1. Due especially to the HSCT operating environment, the engine must emit ultralow levels of NOx.

2. The engine must be capable of producing high specific thrust to meet the HSCT Mach 2.4 flight requirement, but jet noise must remain below the limits set by FAR 36 Stage 3.

3. To fly the HSCT mission, the engine and nozzle materials must be capable of withstanding maximum temperatures and stresses for up to 30 times longer than experienced by subsonic power plants.

4. Engine core sizes must be so large, to meet the HSCT high-volume/high-thrust requirements, that they may exceed the limits of current material processing, component manufacturing, and repair technologies.

3.3.1.1 Emissions Challenge

The HSCT is designed to fly in the stratosphere, at or above 60,000 feet in altitude, because that is the optimum supersonic cruise altitude for a Mach 2.4 airliner. At this altitiude, however, NOx emissions are extremely damaging to the ozone layer, and are only acceptable evironmentally at or below a specified level. The ozone layer is vital to a stable earth environment, so NOx emissions must be minimal and carefully controlled. The HSR team's main approach to controlling NOx emission has been to develop and expand new combustor technologies for the HSCT engine. The results of these efforts have been a dramatic and substantial decrease in NOx emissions projected for the HSCT propulsion system.

3.3.1.2 Noise Challenge

Environmental acceptability also requires that the HSCT comply with Federal community noise regulations (FAR36, Stage III). Engines capable of efficient supersonic cruise must produce high specific thrust and are therefore characterized by high exhaust jet velocities. Since jet noise is a function of jet velocity, an unsuppressed HSCT propulsion system can easily exceed the Stage 3 noise limits by 15 to 20 EPNdB. The most successful approach to suppressing this noise without substantial loss in thrust has been the development of advanced mixer/ejector exhaust nozzle concepts that also enable the performance vital to meeting the economic goals.

3.3.1.3 Durability Challenge

The HSCT propulsion system must have the durability (life expectancy) to operate at nearly maximum thrust throughout the entire supersonic cruise portion of each flight. This means that the propulsion system components must endure nearly maximum cycle temperatures and nearly maximum stresses (rotor speeds) for more than 50% of each flight (see Figure 110). Conventional aircraft propulsion system components experience maximum conditions for a much shorter period (see Figure 111).

The total accumulated (life) high-stress time projected for HSCT engine components is approximately 30 times the amount of high stress time experienced by components in current commercial aircraft or military aircraft. Because of this extended exposure to extreme operating conditions, it has been necessary to develop advanced engine materials, advanced structural concepts, and advanced disk and turbine airfoil cooling technologies.

3.3.1.4 Physical Limitations Challenge

The supersonic mission has also presented problems in dealing with the physical size of the HSCT engine. While it is true that the HSCT engine employs many of the same principles and in many ways
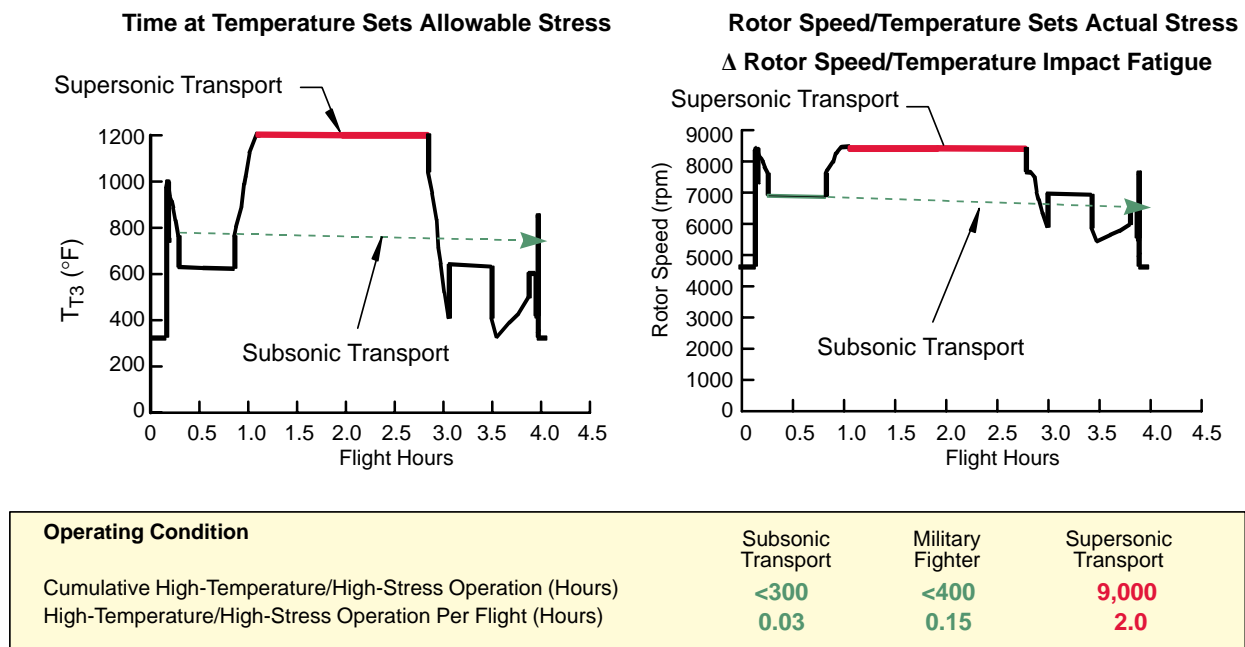
Figure 110.   High-Temperature/High-Stress Requirements

	Typical Temperatures (°F)				
	Cruise T_{T2}	Max T_{T3}	Cruise T_{T3}	Max T_{T4}	Cruise T_{T4}
Typical Current Engine	−15 to 23	1200	870	3000	2140
HSCT Engine	380	1200	1200	3000	2960
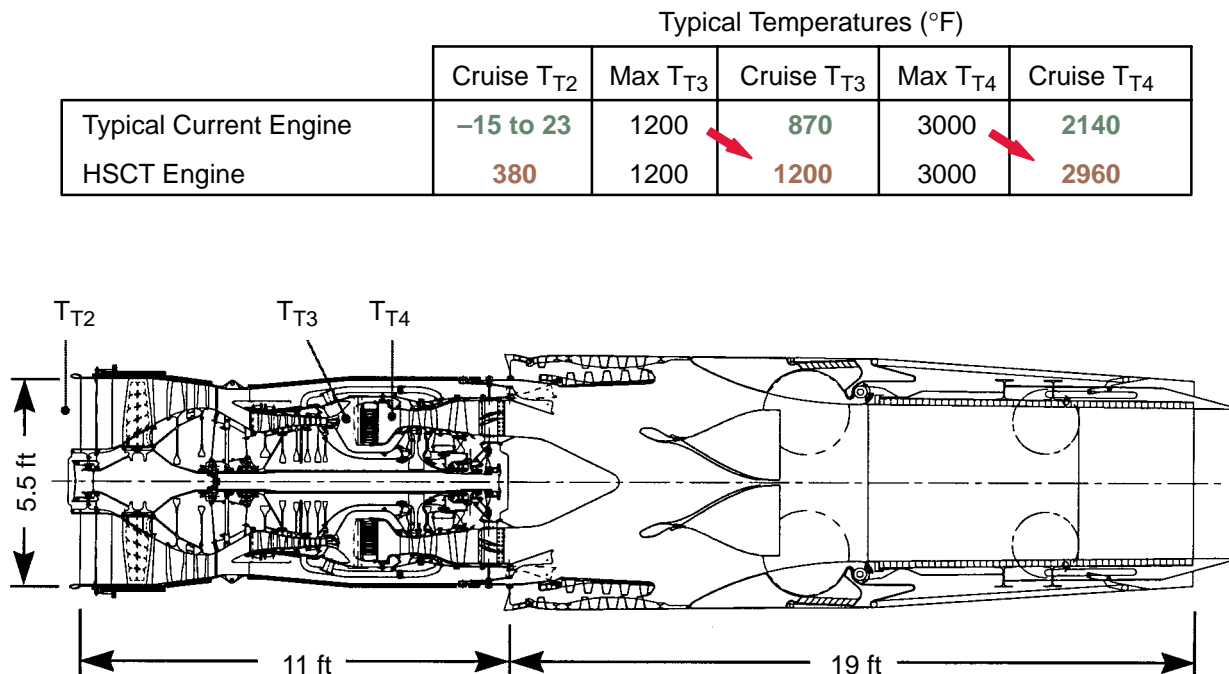
Figure 111.   Engine Temperature Comparison, HSCT to Existing Subsonic Aircraft

is similar to military supersonic aircraft, the HSCT propulsion system poses a size problem. In order to meet the noise and thrust requirements imposed on the HSCT, the power plant design has been based on a much larger airflow relative to a supersonic military jet. Typically, a current fighter engine has an inlet airflow of less than 300 lbm/s, but the HSCT engine may require an airflow greater than 800 lbm/s. This airflow requirement has forced the development of new material processing, manufacturing, handling, and repair technologies (see Figure 112).

3.3.2 MFTF Mechanical Design Studies (3770.54 Reference Cycle)

3.3.2.1 Thrust Balance

During the design activity, the issue of balancing the axial load on the high-pressure rotor came up several times. In the engine world, this force balance is called thrust balance. Any remaining unbalance due to pressure forces translates into a load on the thrust bearing — normally located under the compressor. The magnitude of this load directly impacts the life of the thrust bearings. As shown in Figure 113, bearing life is actually controlled by two load issues.

The first issue is the maximum instantaneous load, which usually occurs at takeoff power. Traditionally this point is used as the key when defining a balanced thrust system. The second issue is the sustained-load level. For long-range missions, this is the dominant factor that governs the life of the bearing system.

A third important issue impacting the life of the bearing system is bearing load crossover. A crossover occurs when force on the bearing changes direction. During engine operation, pressure changes in the cavities around the rotor structure often cause direction reversals. Because of the tight clearances in the bearing structure, sudden large-magnitude changes in force direction can severely reduce the life of the bearing system.

A well-balanced rotor thrust system only encounters crossovers at low power and at very short-duration operating points. To achieve long bearing-system life, average thrust must be kept low, but a near-zero steady-state load is a condition of continuous crossover and severely reduces bearing life.

One of the thrust balance analyses is summarized in Figure 114. This study focused on the September 1997 3770.54 engine. The steady-state rotor thrust for this analysis was defined using loads and pressures developed by GEAE compressor and turbine preliminary design tools. The cavity pressures and geometry needs were defined by a rule-of-thumb approach using knowledge from previously balanced systems. Rotor thrust characteristics were derived from 18 points of Mission 2.

The loads for several of these mission points are shown in Table 63. The initial goal was to keep the maximum load below 10,000 lbf. The difficulty was that some of the points were at or above that goal. Pressurization of the forward cavity in front of the compressor reduced the maximum load somewhat (from 20,150 to 13,426 lbf). In the process of reducing the the force by approximately 6,700 lbf, the supersonic end-of-cruise point at 64,000-ft altitude dropped from 370 to 192 lbf. Essentially, this is a no-load situation and is not desirable.

Achieving proper rotor thrust balance to satisfy all bearing life criteria involves the design of turbomachinery for the shaft, compressor, and turbine. It also involves cavity seal location and cavity pressurization strategy as discussed above.
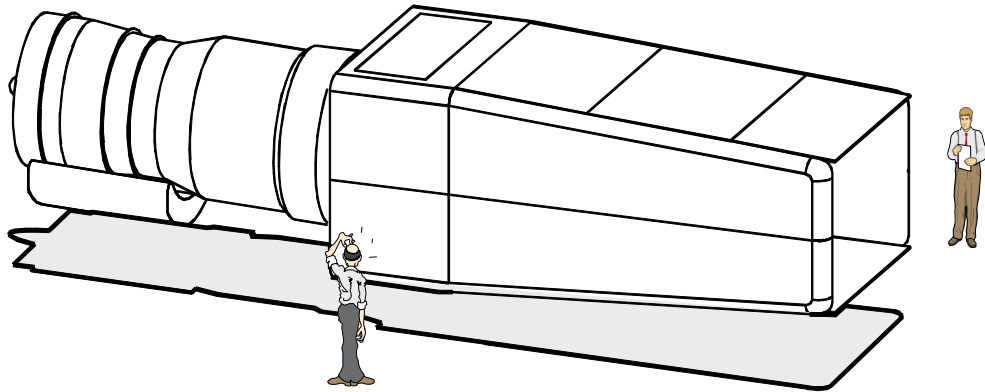
- Forging Limits For Fan and Compressor Disks
- Heat Treatment for Thick-Bore Turbine Disks
- Casting of Large Turbine Airfoils with Complex Internal Features
- Thin-Wall Casting of Large Nozzle Components
- Large-Diameter Ceramic-Matrix Composite Combustor Liners

Figure 112.   HSCT Material Processing, Manufacturing, Handling, and Repair Problems

Load Magnitude: Two Issues
- Maximum instantaneous load (strength)
- Sustained load level (life)
    HSCT life goal is 36,000 hours

Load Magnitude and Crossover

Bearing Load Crossovers
- Avoid crossovers in operating range
- If crossovers cannot be avoided, then:
    1. Tailor to occur during transients on the flight map
    2. Preclude at rotor dynamic critical speeds
- Avoid steady zero load on bearing

Figure 113.   Factors Affecting Bearing Life
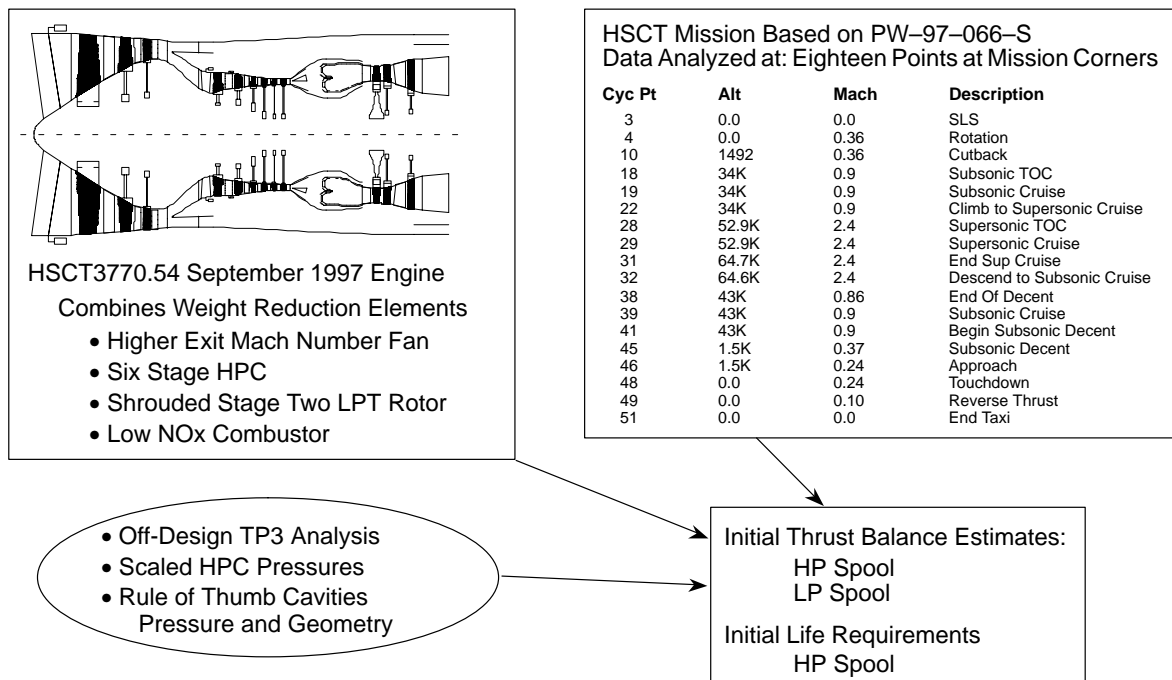
Figure 114. HSCT3770.54 September 1997 Engine Thrust Balance Analysis

Table 63. Thrust Balance Calculations

- MFTF 3770.54 Engine, Mission 2

- Design Load Limit for Thrust Bearing: 10,000 lbf

Compressor Forward Cavity at Hub Pressurized ?				Yes	No
Case	**Flight Condition**			**Bearing Load (lbf)**	
	Altitude, ft	Mach No.	Power Code	All ⇐ Forces	
Baseline Test Case	35,000	0.36	Takeoff + 18°F	14,641	21,102
HSCT Mission 2 Flight Points	Ground	0	Idle	170	370
	35	0.36	Takeoff	13,426	20,150
	34,000	0.9	38.5	791	2,715
	34,000	0.9	50.0	6,474	9,088
	57,300	2.4	50.0	324	3,607
	64,000	2.4	50.0	192	370
	43,000	0.9	40.0	9,742	11,092

The compressor discharge pressure (CDP) seal, usually located under the combustor, controls the leakage flow at the hub of the compressor and thus has the most impact on the balanced rotor thrust condition. Figure 115 shows the impact on bearing load of a 3-in radial relocation in the CDP seal. The load at the high radius seal is 40,000 lbf in the forward direction. Moving the seal to the smaller radius results in a 30,000-lbf load in the aft direction. Thus, the 3-in movement causes a net load change of 70,000 lbf.

The tangential on-board injector (TOBI) seals listed in Figure 115 are the turbine inducer seals on the front side of the turbine rotor. These seals were held constant during this exercise.
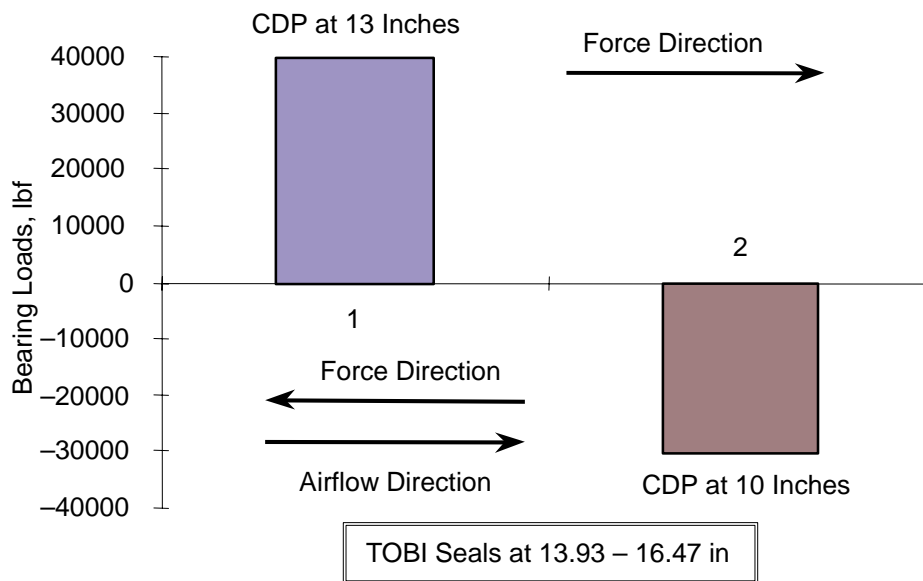
Figure 115. Effect of 3-in CDP Seal Movement

It is obvious that a solution exists where the average mission load will be at a level that satisfies the goals for maximum bearing life. Figure 116 illustrates the bearing load for the entire mission when a CDP seal radial location between 9.3 and 10.8 inches is used. Remember that the low-radius average load described above was for the 10.00-in location. As the figure shows, the load reverses for all of these locations. If the seal is located between 10.45 and 10.8 inches, the reversal occurs during the long-duration supersonic cruise, and this is a very undesirable condition.

Figure 117 depicts the average mission load variation when the seal is increased from a radial location of 11.0 to 12.0 inches. The characteristic has a change of slope near the zero-load condition; again, this is undesirable.

Examination of the predicted bearing life that results from CDP seal movement makes it possible to quantify the location choices to best satisfy all requirements. Figure 118 shows the life predictions for the low-load portion of the study. As shown in the figure, a life goal of 36,000 hours can be met when the seal is located between 11.37 and 11.4 inches.
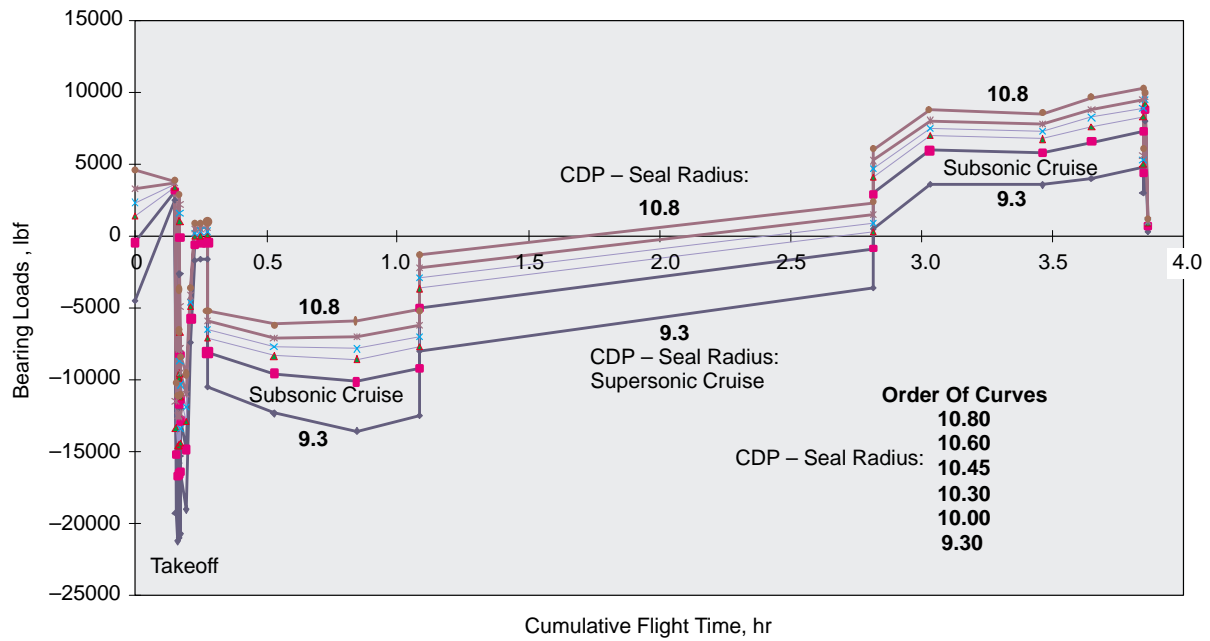
Figure 116.   Bearing Load for Mission with CDP Locations Between 9.3 and 10.8 Inches
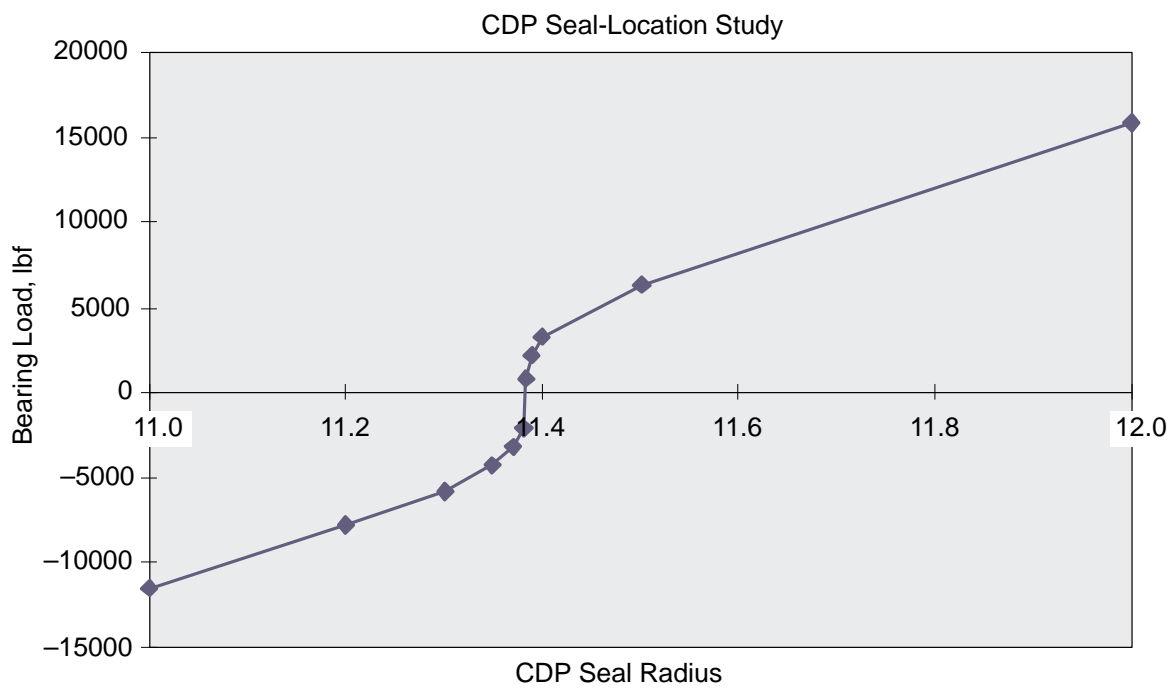
Figure 117.   Average Mission Load Variation When CDP Seal Is Raised From 11.0 to 12.0 Inches
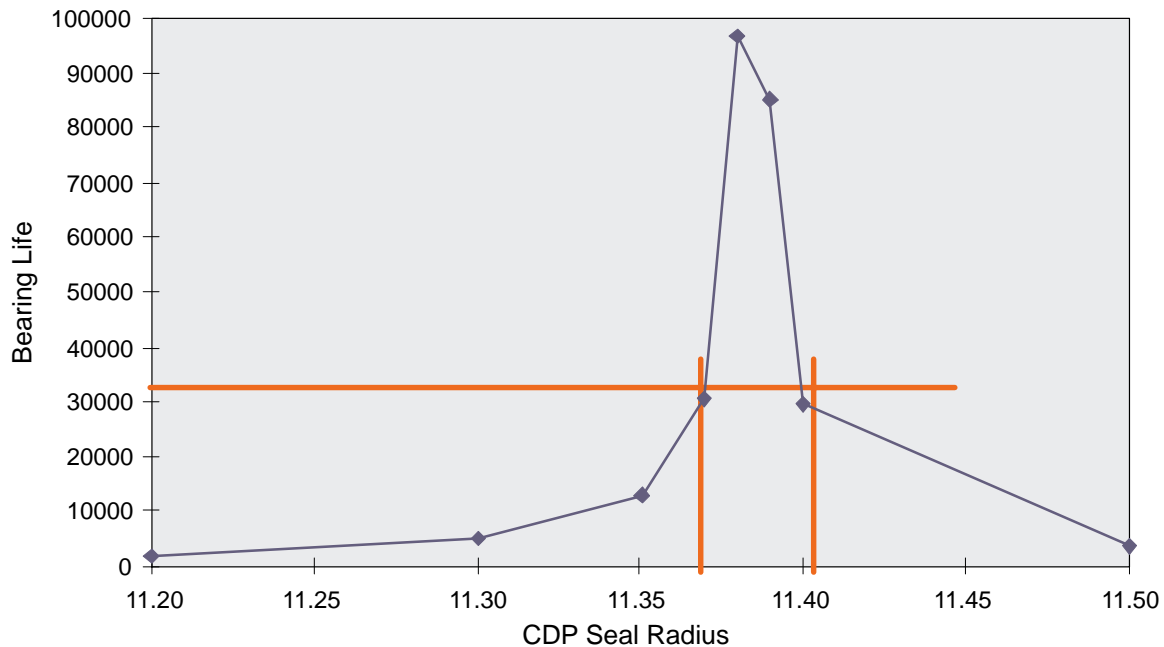
Figure 118.   CDP Seal Location Study Results

An alternate configuration that would eliminate the CDP seal, and thus reduce weight, was also examined. In this alternate configuration the turbine rotor seal, located in front of the HPT disk, performed the sealing function of the CDP seal, and the radial location of the seal was varied to achieve the proper load balance. The resulting predicted load distribution is shown in Figure 119, and it can be seen that the zero average load point occurs between 10.2 and 10.4 inches.

The bearing life predictions for this analysis are shown in Figure 120. The 33,000-hour life prediction occurs between 10.3 and 10.5 inches based on previously examined life-prediction characteristics. In this analysis, a load reversal is predicted above 10.3 inches during the supersonic cruise leg of the mission. If the bearing life goal is reduced to 25,000 hours, a solution can be found between 10.2 and 10.3 inches.

In conclusion, this work has indicated that setting the turbine rotor seal location at 10.25 inches can effectively eliminate the CDP seal. This configuration avoids bearing load crossover throughout the supersonic cruise leg, and the life of the bearing can still be expected to exceed 25,000 hours. It appears that this would be an acceptable rotor thrust balance for the HSCT engine.

3.3.2.2 MFTF3770.54 Fan Aerodynamic and Mechanical Design

P&W conducted in-depth aerodynamic and structural design studies of the MFTF3770.54 fan to validate projected performance, dimensions, and weight. Design studies included: (1) parametric aero/mechanical optimization to identify a configuration that meets all required design objectives, (2) CFD optimization of the stage aerodynamics, (3) preliminary disk sizing, (4) blade and vane vibration, (5) blade flutter, (6) bird strike, and (7) blade out. Key fan design requirements are summarized in Table 64, and a summary of the aerodynamic and mechanical design characteristics is provided in Figure 121.
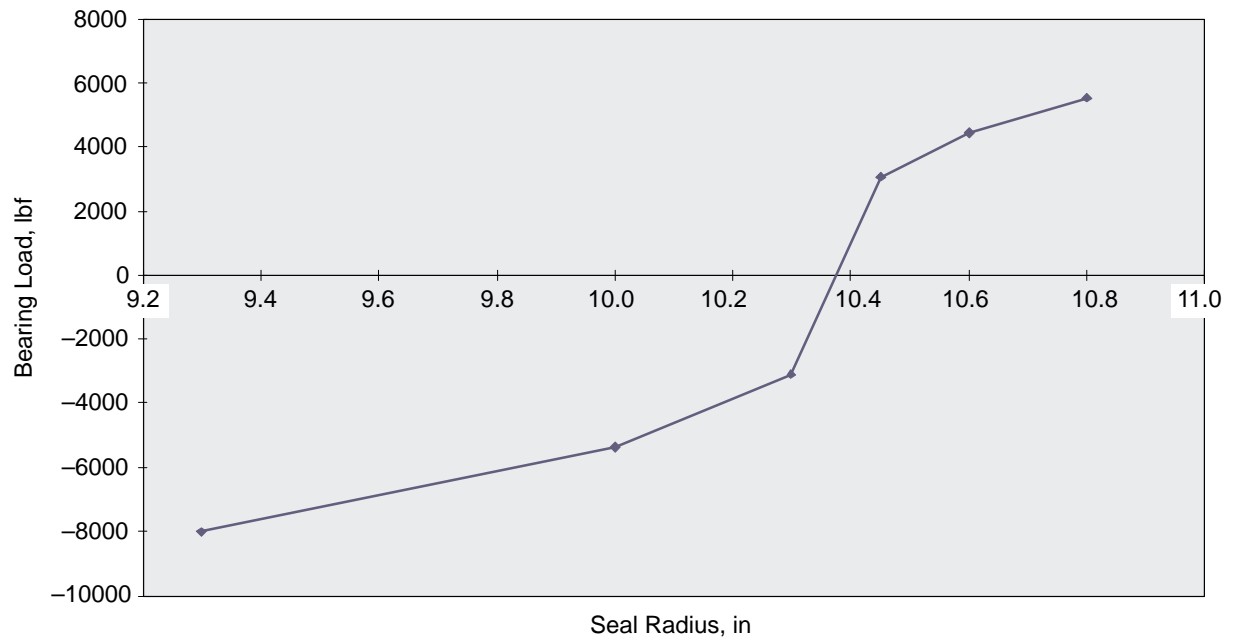
Figure 119. Turbine Rotor Seal Locations to Achieve Zero Load
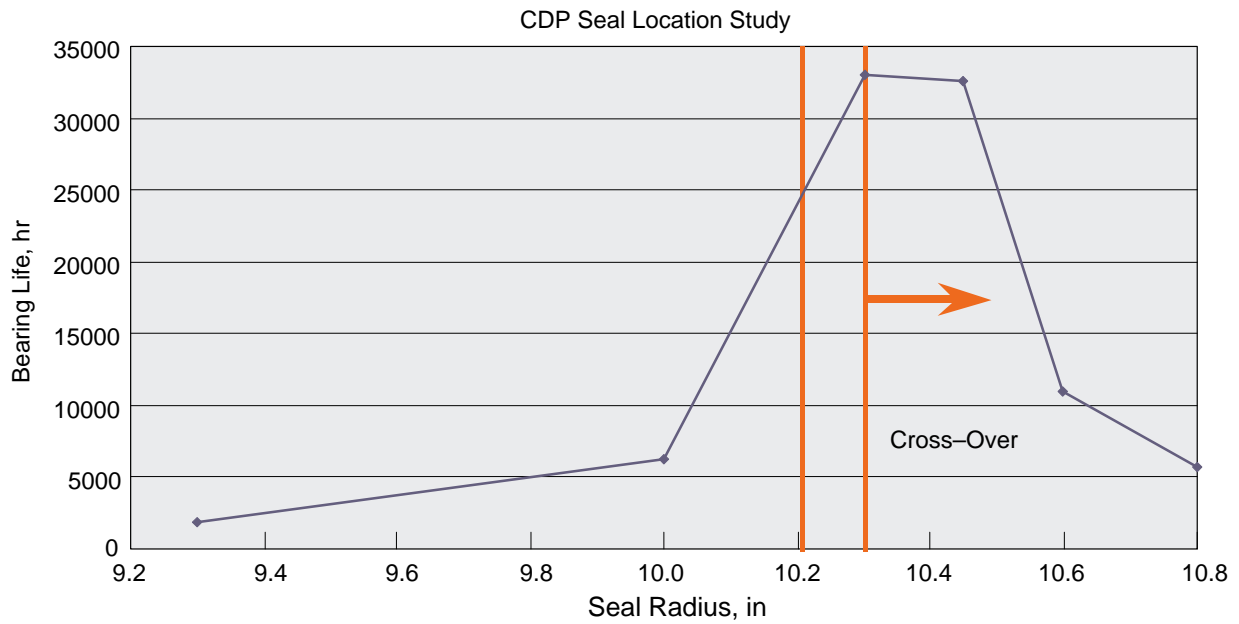
Figure 120. Bearing Life Predictions

Table 64.   Key Design Requirements for the HSCT Fan

- Adequate Airflow Capacity During Sea-Level Takeoff and Transonic Climb

- High Efficiency During Part-Power Supersonic Cruise (70% Flow)

- Acceptable Stall Margin Throughout the Operating Range, With Special Emphasis on Low-Power Operation

- Acceptable Acoustic Characteristics During Takeoff, Cutback, and Approach

- Compatibility With Circumferentially Averaged Radial Pressure Profiles Supplied by the Two-Dimensional Bifurcated Mixed Compression Inlet

- Avoidance of 2E Resonance Induced by the Flow Splitter in the Two-Dimensional Bifurcated (2DB) Mixed-Compression Inlet

- Minimum Fan Module Weight

MODERATE TIP CORRECTED SPEED
Minimizes Rotor Shock Noise

MODERATE STAGE AERODYNAMIC LOADING
Minimizes Rotor/Stator Interaction Noise

3D MULTISTAGE VISCOUS AERO DESIGN
Reduced Endwall and Profile Losses
Improved Efficiency and Stall Margin

TANGENTIALLY SWEPT ROTORS
Increased Rotor Tip Chord/Solidity
Improved Efficiency From Reduced Shock Loss
Improved Stall Margin From Increased Tip Solidity

BOWED STATORS
Improved Endwall Flows
Improved Efficiency and Stall Margin

HYBRID FAN DESIGN
Low-Aspect-Ratio Rotors
High-Aspect-Ratio, High-Solidity Stators
Provides Blade/Vane Count For Acoustics

HIGH-SOLIDITY IGV FLAPS
Improved Low-Speed Stall Margin

INCREASED IGV–R1 TIP GAP
Reduced Interaction Noise

COMPATIBILITY WITH 2D BIFURCATED INLET
Avoidance of 2E Vibration Driven By Inlet Splitter
Aero Compatibility With Circumferentially Averaged
Radial Pressure Profile

HOLLOW ROTOR 1
Reduced Airfoil and Disk Weight

INTEGRALLY BLADED ROTORS
2E Vibration Margin
Significant Weight Reduction
Reduced Parasitic Leakage

Fan Performance Characteristics

Parameter	Fan ADP	Cycle ADP	Max Power
Corrected Speed (rpm)	4918.0	5155.2	5311.3
Corrected Airflow (lbm/s)	747.83	800.0	823.04
Pressure Ratio	3.438	3.700	3.968
Pressure Warpage (P_{Tcore} / P_{Tduct})	1.054	1.054	1.055
Mass-Averaged Adiabatic Efficiency	89.21	87.10	82.65
Core Stream Adiabatic Efficiency	90.20	88.40	84.43
Rotor 1 Corrected Tip Speed (ft/s)	1386.1	1452.9	1497.0
Rotor 1 Specific Airflow (lbm/sec–ft^2)	38.33	41.00	42.15
Exit Mach Number	0.50	0.50	0.50

Figure 121.   MFTF3770.54 Fan Configuration and Projected Performance

Conclusions from the fan design study are summarized below, and the aerodynamic and mechanical design analyses are discussed in following paragraphs.

1. The fan design met or exceeded all performance goals, including: maximum flow capacity, supersonic cruise efficiency, and low-power stall margin.

2. Fan noise is the major element of the acoustic signature during approach. The baseline fan design is predicted to provide acceptable approach acoustics. However, uncertainty in the engine component and airframe noise predictions may result in overall system acoustics exceeding the goal level by 2.5 EPNdB. Design features have been identified to further reduce fan noise. Incorporation of these features would increase fan-module weight by approximately 200 lbm.

3. The projected weight of the baseline fan module is 2871 lbm relative to the target of 2731 lbm. Quoted weight includes the inlet case, fan rotor, fan stator and case, intermediate case, No. 1 bearing compartment, No. 2/3 bearing compartment (including two towershaft assemblies), and inlet guide vane (IGV) lever arms and synchronization rings. IGV actuator weights are not included. Target weight was established by allocating module weights based upon a goal weight of 16,675 lbm for the engine and exhaust nozzle.

4. As noted above, the baseline fan module is 140 lbm over the target goal. Design modifications have been identified that have the potential to reduce fan weight by approximately 156 lbm with no change to the aerodynamic flowpath.

   Low- to moderate-risk design modifications will reduce fan weight by 121 lbm. These include use of high-temperature composites (such as PETI–5) in the inlet case and nosecone, incorporation of a hollow second-stage blade, and use of a fabricated rather than cast intermediate case.

   A higher risk innovative disk design using a monolithic titanium bore for the first stage has shown a 25-lbm weight reduction potential. Combining the innovative disk design with a titanium composite bore will provide an additional 10 lbm weight reduction.

5. All airfoils can be designed to avoid resonance resulting from the 2E driver inherent in the 2D bifurcated mixed compression inlet.

   Avoidance of 2E resonance had a significant impact on the first-stage rotor. Initial fan designs featured a bladed rotor assembly to allow replacement of individual blades in the event of foreign-object damage (FOD). Design studies indicated that a bladed disk design that met all structural and vibratory requirements was possible. However, the airfoils had to be removed from the rear of the disk, necessitating a teardown of the fan and No. 1 bearing assemblies.

   Use of an integrally bladed rotor (IBR) for the first stage (R1) reduced weight by 195 lbm relative to the bladed disk design.

   Avoidance of 2E resonance for the R1 IBR resulted in a 90-lbm weight penalty relative to an IBR design allowing a 2E crossing. However, the latter design was predicted to encounter flutter dangerously close to the supersonic cruise operating condition. Avoidance of flutter resulted in an airfoil design and rotor weight similar to that required to avoid 2E resonance. Thus, elimination of the 2E driver in the inlet is not anticipated to provide a significant fan weight reduction.

6. Rotor 1 was designed to avoid flutter and a 2E crossing when matched on the nominal operating line. R1 is predicted to encounter a subsonic stalled flutter boundary when matched near the stall line at 82% corrected rotor speed (which corresponds to the supersonic cruise rotor speed).

Avoidance of flutter at this match point requires either a blade redesign with an associated weight penalty or incorporation of a positive damping device. Innovative positive damping systems are being developed under industry and Department of Defense funded programs.

7. The fan is predicted to meet all bird-impact requirements. Impact by an 8-lbm bird will produce significant deformation of the first blade but will not produce tears in the blade material.

8. An innovative containment system has shown the potential to provide significant weight reduction relative to conventional designs. The innovate "catenary" design is predicted to fully contain the blade.

Fan Aerodynamic Design

The MFTF3770.54 fan flowpath and aerodynamic design characteristics are summarized in Figure 122, and the aerodynamic design procedure is illustrated in Figure 123. The overall aerodynamic configuration was derived from a meanline parametric analysis that considered the impact of flow-path shape, flowpath elevation, inlet specific airflow, R1 hub/tip ratio, R1 tip speed, stage pressure ratio distribution, stator exit swirl distribution, exit Mach number, airfoil aspect ratio, and airfoil

Location	X_{id}	R_{id}	X_{od}	R_{od}
Nosecone LE	−61.155	0.000	—	—
Nosecone TE	−43.261	8.199	—	—
IGV Strut LE	−43.261	8.199	−49.314	31.772
IGV Strut TE	−39.538	9.704	−45.985	32.415
IGV Flap LE	−39.454	9.738	−45.661	32.477
IGV Flap TE	−35.796	11.215	−37.785	33.126
Rotor 1 LE	−33.932	11.968	−33.318	32.339
Rotor 1 TE	−25.944	17.398	−27.628	31.874
Stator 1 LE	−23.896	18.357	−25.707	31.717
Stator 1 TE	−21.495	19.256	−21.512	31.274
Rotor 2 LE	−20.349	19.648	−19.680	31.158
Rotor 2 TE	−15.868	20.966	−16.425	30.784
Stator 2 LE	−15.010	21.170	−15.590	30.654
Stator 2 TE	−12.632	21.633	−12.468	30.218
Rotor 3 LE	−11.585	21.808	−11.585	30.118
Rotor 3 TE	−8.677	22.234	−8.985	29.708
Stator 3 LE	−7.792	22.298	−7.934	29.473
Stator 3 TE	−5.610	21.972	−5.611	28.652
I/C LE	−5.100	21.787	−5.100	28.505
I/C Splitter LE	−0.409	24.907	—	—
Station –0– Core	0.000	18.511	0.000	24.467
Stator –0– Duct	0.000	25.192	0.000	28.191
I/C TE Core	4.900	15.181	4.900	21.050
I/C TE Duct	4.900	25.192	4.900	28.191

MFTF3770.54 Projected Performance

Performance Parameter	Fan ADP	0/0K Takeoff	0.9/34K Cruise	2.4/53K Cruise
Corrected Rotor Speed (rpm)	4918.0	5311.3	4759.8	4231.1
Corrected Airflow (lbm/s)	747.83	823.04	710.50	560.00
Mass-Average Pressure Ratio	3.438	3.968	3.027	2.323
Core Stream Pressure Ratio	3.768	4.037	3.093	2.386
Mass-Average Adiabatic Efficiency	89.21	82.65	88.73	89.32
Core Stream Adiabatic Efficiency	90.20	84.43	89.94	91.89
Bypass Ratio	0.54	0.49	0.69	0.75
Stall Margin	22.2	19.9	29.6	24.0
Corrected Tip Speed	1386.1	1497.0	1341.5	1192.5
IGV Exit Air Angle (Degrees)	80.0	89.5	76.2	63.4
R1 Specific Flow (lbm/s–ft^2)	38.33	42.15	36.42	28.70
Exit Mach Number	0.560	0.50	0.51	0.51
Physical Rotor Speed (rpm)	4918.0	5402.6	4492.4	5377.4
Physical Tip Speed (ft/s)	1386.1	1522.7	1266.1	1515.6

MFTF3770.54 Stage Design Parameters

Design Parameter	Stage 1	Stage 2	Stage 3
Stage Pressure Ratio	1.589	1.524	1.400
Stator Exit Air Angle (Deg)	85.0	87.0	90.0
Rotor LE Mean Mrel	1.027	1.071	1.023
Stator LE Absolute Mach No.	0.732	0.718	0.692
Number of Blades	26	46	64
Number of Vanes	68	100	120
Rotor Mean Aspect Ratio	1.76	1.78	1.85
Stator Mean Aspect Ratio	3.20	3.22	3.10
Rotor Mean Gap/Chord	0.620	0.596	0.606
Stator Mean Gap/Chord	0.593	0.591	0.602
Rotor Root Thickness/Chord	0.116	0.092	0.080
Rotor Mean Thickness/Chord	0.070	0.048	0.046
Rotor Tip Thickness/Chord	0.020	0.020	0.020
Stator Mean Thickness/Chord	0.053	0.052	0.052

Figure 122.   MFTF3770.54 Fan Flowpath and Aerodynamic Design Characteristics

1D Meanline Analysis

Radius, in

Axial Length, in

2D Streamline Analysis

3D NASTAR Analysis

3D Airfoil Generator
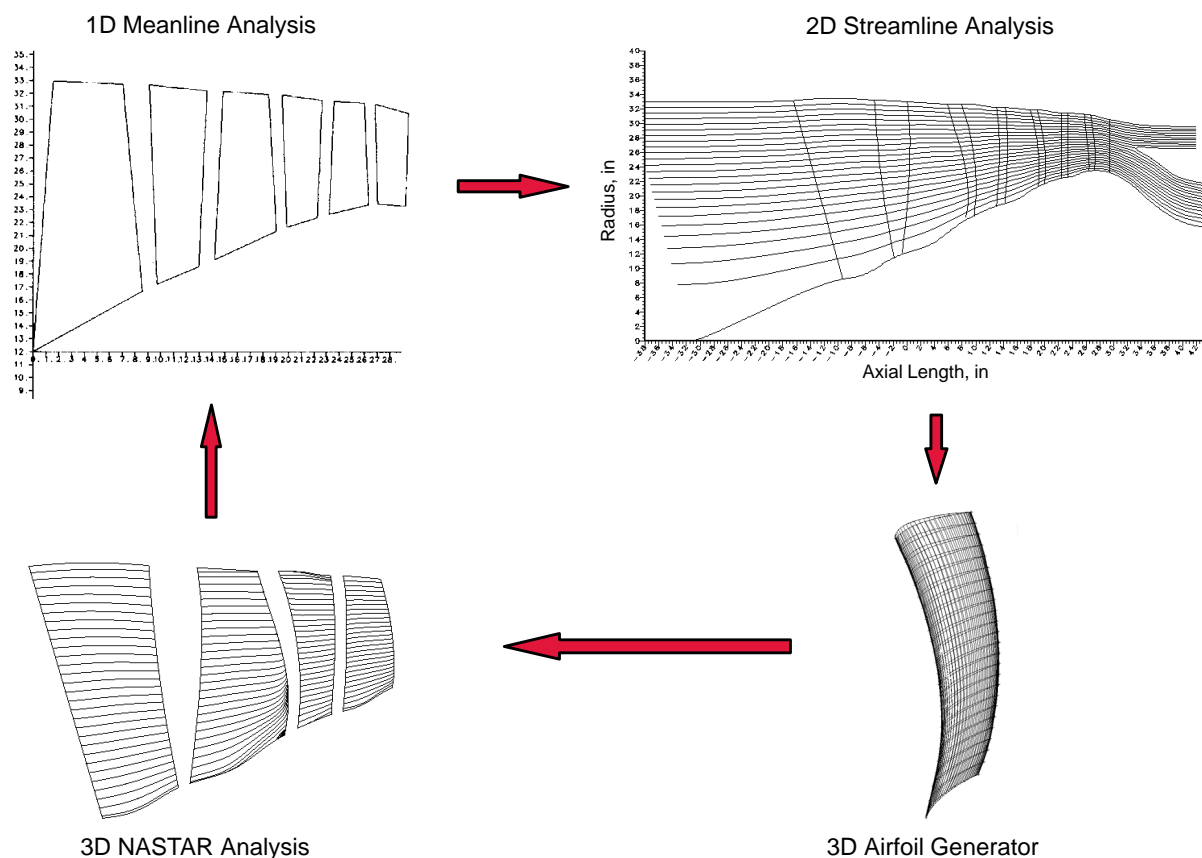
Figure 123. MFTF3770.54 Fan Aerodynamic Design Procedure

solidity. Design parameters were selected to achieve a fan configuration that balanced the requirements summarized in Table 64. Once the overall configuration was defined, a two-dimensional, axisymmetric, streamline analysis was used to optimize the radial distributions of rotor work and stator turning. Two-dimensional cascade theory and 2D viscous blade-to-blade design codes were used to generate initial airfoil profiles consistent with the streamline velocity triangles. Final aerodynamic optimization was performed with a 3D viscous Navier–Stokes computer code capable of analyzing flows through multiple turbomachinery stages. Aerodynamic optimization was conducted in conjunction with structural iterations to ensure that the final design met both aerodynamic and structural design requirements.

Fan aerodynamic design was significantly influenced by six critical operating points within the flight envelope: (1) takeoff, (2) subsonic cruise, (3) transonic acceleration, (4) supersonic cruise, (5) approach to landing, and (6) sea-level idle. Thrust, and therefore flow capacity, is of primary concern for takeoff and transonic acceleration; fuel consumption, and therefore efficiency, is critical during subsonic and supersonic cruise. Fan acoustics is a significant contributor to the overall system noise during approach. The HSCT engine cycle characteristics result in a relatively high operating line match during low-power operating conditions such as idle. As a result, achievement of acceptable stall margin level during sea-level idle also had a significant impact on the fan configuration. Other factors having a significant impact on the fan aerodynamic design included: (1) compatibility with the circumferentially averaged radial pressure profiles delivered to the fan face by the 2DB inlet,

(2) compatibility with the 2E vibration driver inherent in the 2DB inlet, and (3) compatibility of the exit pressure profiles with the bearing compartment buffer air supply.

The *aerodynamic design point* (ADP) refers to the operating condition at which the fan velocity triangles are defined and the corresponding airfoil geometries generated. Parametric studies indicated that optimizing the fan at the high flow/pressure ratio sea-level takeoff condition yielded unacceptable compromises for the supersonic cruise efficiency and sea-level idle stall margin. Attempts to balance takeoff, supersonic cruise, and idle performance by biasing individual blade and vane rows resulted in an excessive number of design iterations. To minimize the number of iterations, the ADP was selected at a part-power operating condition lying between the takeoff and supersonic cruise points. Initially, all airfoil rows were designed for optimum efficiency at the ADP. A subsequent off-design analyses indicated that only minor modifications to the optimum incidence were required to meet takeoff and transonic flow requirements, supersonic cruise efficiency, and sea-level idle stall margin.

Parametric flowpath studies were conducted by GEAE to assess the impact of fan exit Mach number on fan performance and overall engine weight. Fan designs were evaluated with exit Mach numbers ranging from 0.45 to 0.55. An exit Mach number of 0.50 yielded a fan configuration that balanced engine weight, engine length, and fan efficiency; that configuration was selected for the MFTF3770.54 design.

Acoustic considerations had a significant impact on the fan configuration. As shown in Figure 124, noise generated by the fan is a significant contributor to the overall acoustic level at the approach flight condition. Three key features are incorporated into the baseline fan design to achieve the required acoustic goal: (1) moderate tip speed, (2) increased axial spacing at the flowpath outer diameter (OD) between the IGV trailing edge (TE) and R1 leading edge (LE), and (3) rotor/stator counts selected to provide acoustic cutoff. Although the engine is projected to meet approach noise goals (Stage 3 –1 EPNdB), the large uncertainty for engine component and airframe noise predictions may result in a system noise exceeding the goal level by 2.5 EPNdB. Fan noise can be reduced further by increasing the axial spacing between the IGV TE and R1 LE and possibly between the R1 TE and first-stage stator (S1) LE. Incorporation of increased axial spacing between the IGV, R1,
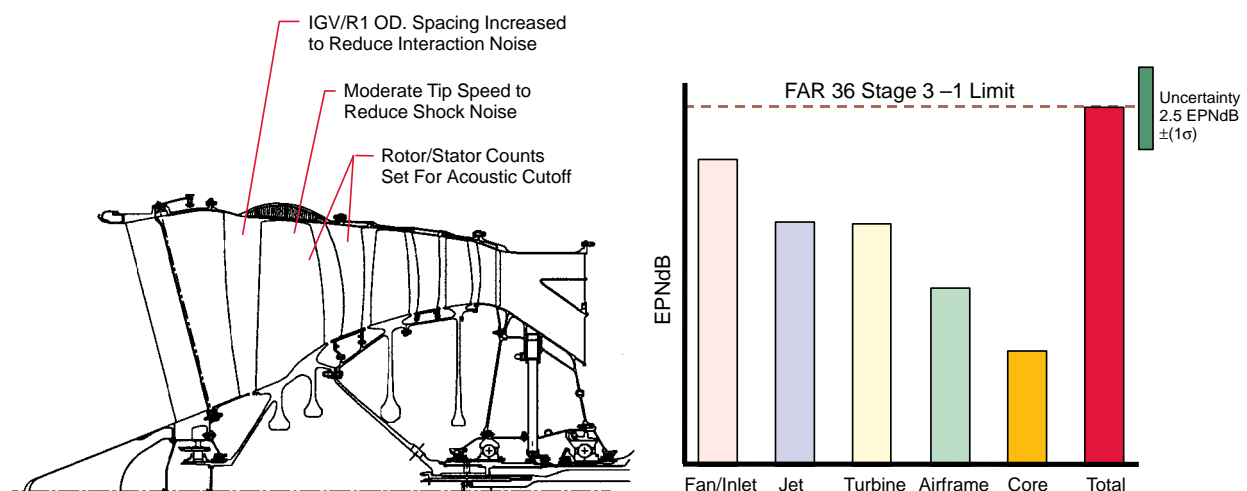
Figure 124.   Fan Design Features Compatible with Approach Acoustic Goals

and S1 is projected to have minor impact on fan aerodynamic performance but add approximately 200 lbm to the fan weight. Acoustic constraints and the impact on the fan configuration are discussed further in following paragraphs.

Shocks generated in rotor passages are significant contributors to the acoustic signature of turbomachinery. The typical method of minimizing shock-induced noise is to limit fan tip corrected speed. Preliminary system studies indicated that the R1 tip corrected speed should be less than 950 ft/s at the part-power approach condition, resulting in a maximum allowable corrected tip speed of 1500 ft/s at sea-level takeoff.

Turbomachinery acoustics is also significantly impacted by aerodynamic interactions between closely spaced rotating and stationary airfoil rows. An obvious method of minimizing the interaction noise is to increase axial gaps. A second method is to "cutoff" acoustic interactions by judicious selection of the airfoil counts between adjacent airfoil rows. Limited acoustic testing of multistage fans for military fighter applications has indicated that interaction noise can be minimized if the ratio of airfoils between adjacent rows equals or exceeds 2.2. The desired ratio was achieved between R1 and S1 and between R2 and S2 by combining low-aspect-ratio, moderate-solidity blade rows with high-aspect-ratio, high-solidity vane rows. Use of low-aspect-ratio rotors provides additional benefits to the fan design, including elimination of the part-span shroud and associated aerodynamic losses, improved distortion tolerance, and improved resistance to erosion and FOD.

A variable-camber IGV has been incorporated into the baseline design to provide the required low-power fan stall margin. Mechanical and aerodynamic constraints did not allow the ratio of the IGV-to-R1 airfoil counts to approach the desired value of 2.2. Limited engine testing indicated the axial spacing between the IGV TE and R1 LE must approach 170 to 190% of the IGV axial chord to eliminate blade-passing tones generated as the rotor interacts with wakes shed from the IGV. In the HSCT fan this would result in an axial gap of approximately 18 inches and a corresponding weight increase of approximately 150 lbm. To accommodate acoustic concerns within acceptable aerodynamic and mechanical constraints, the IGV was leaned axially forward to increase the gap at the flowpath outer diameter, where the strongest interaction effects occur. The resulting OD gap is 40% of the IGV tip chord, much less that the desired value. Acoustic tests of a subscale fan rig have been proposed to determine whether or not the tip gap is acceptable. As previously mentioned, incorporation of unequal circumferential spacing for the IGV may reduce interaction noise with minimum impact on weight and performance. Acoustic liners placed in the outer flowpath between the IGV and R1 may also provide an acoustic benefit. Additional acoustic tests for the subscale fan rig have been proposed to evaluate both features.

Since the desired IGV/R1 axial spacing could not be implemented without an unacceptable weight penalty, it was suggested to design the fan without an IGV. System-level studies indicated that this was not a viable solution. The operating characteristics of the HSCT engine yield an operating line lapse rate having relative high pressure ratios at low corrected flow conditions such as idle. Elimination of the IGV resulted in the low-power operating line exceeding the predicted stall line. Supposing this problem could be fixed with an innovative casing treatment over the rotor tips, an additional serious problem remained. The engine cycle matches the fan corrected airflow and pressure ratio to the required thrust level at any flight condition. Removal of the IGV results in the fan running at a lower corrected speed for a given part-power flow and pressure ratio. This lower speed resulted in excessive aerodynamic loading for the baseline low-pressure turbine (LPT). Either of two design changes could provide a suitable LPT design. The first change involved increasing the diameter of

the LPT flowpath to increase the wheel speed and lower the loading. The second change involved maintaining the baseline flowpath diameters and adding a third LPT stage. Both design changes resulted in a weight penalty exceeding 300 lbm and were therefore deemed unacceptable.

The fan aerodynamics were designed for compatibility with the 2DB mixed-compression inlet. The nominal inlet airflow schedule, provided by Boeing, is shown in Figure 125. As will be discussed later, the first-stage blade root to midspan thickness was increased significantly relative to conventional blading to avoid flutter during supersonic cruise and a 2E vibration crossing throughout the operating range. A high-solidity stator cascade was used for the first stage to provide the desired rotor-to-stator counts for acoustic cutoff. The combination of thick blades and high-solidity S1 cascade made achievement of the desired maximum flow capability and the part-power speed/flow relationship difficult to achieve. Optimization with the 3D viscous computational fluid dynamics (CFD) computing code allowed the final design to achieve both flow goals with sufficient margin to allow for manufacturing tolerances.
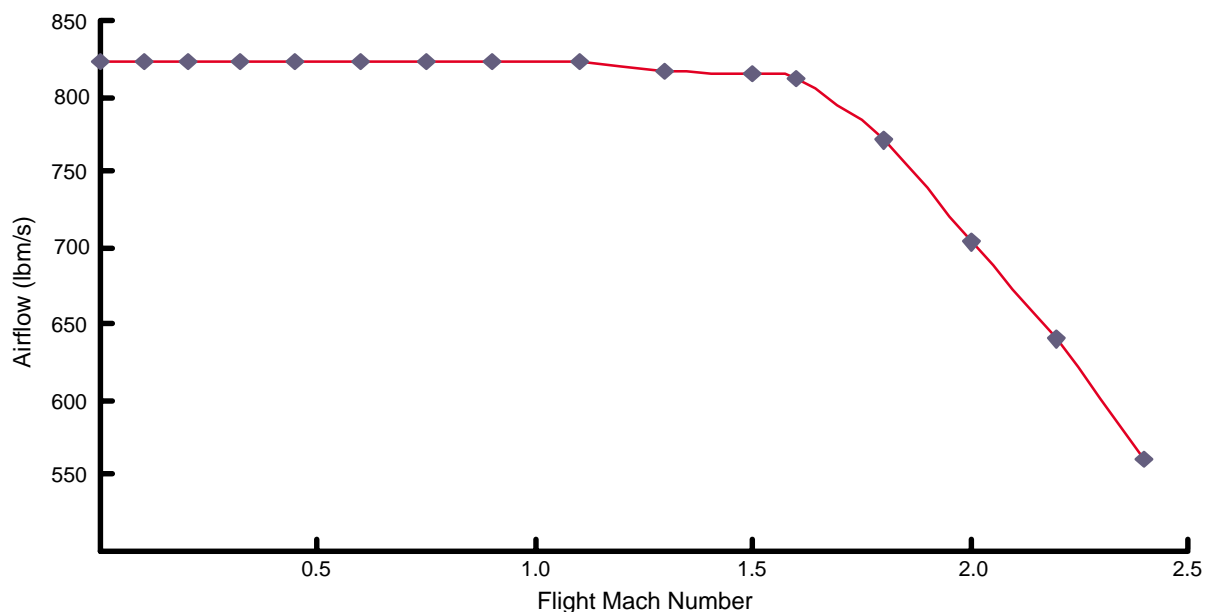
Figure 125.   Nominal Inlet Airflow Schedule for 2DB Mixed-Compression Inlet

The 2DB inlet features a flow splitter extending from the entrance to approximately ½ diameter upstream of the fan face (Figure 126). Incorporation of the splitter allows a significant reduction in inlet length and weight relative to a conventional 2D design. However, proximity of the splitter to the fan face exposes the airfoils to a 2E vibration driver (two excitations per rotor revolution). Fan face pressure profiles were defined during tests of a subscale inlet in the NASA–Glenn 10×10 wind tunnel. Profiles for uniform, zero-incidence flow entering the inlet are shown in Figure 126. Even for this optimum flow situation, the presence of the 2E driver is clearly indicated. Flow distortion is projected to be aggravated in the presence of crosswinds. In such a case, the flow may separate off one side of the splitter. The resulting pressure and flow disturbance will be transmitted by the splitter to the fan face, resulting in a severe 180° distortion pattern.

To avoid potential vibration problems, the fan airfoils were designed with no 2E crossing in the anticipated running range. This had a significant impact on the first-stage blade. Avoidance of a 2E

2DB Mixed Compression Inlet

Fan Face Pressure Profiles During Supersonic Cruise

Inlet Bifurcation

Inlet Bifurcation

Contour Label	Contour Value
A	0.875
B	0.895
C	0.915
D	0.935
E	0.955
F	0.975
G	0.995
H	1.015
I	1.035
J	1.055
K	1.075

* Data From NASA–Glenn 10x10-ft Model Test
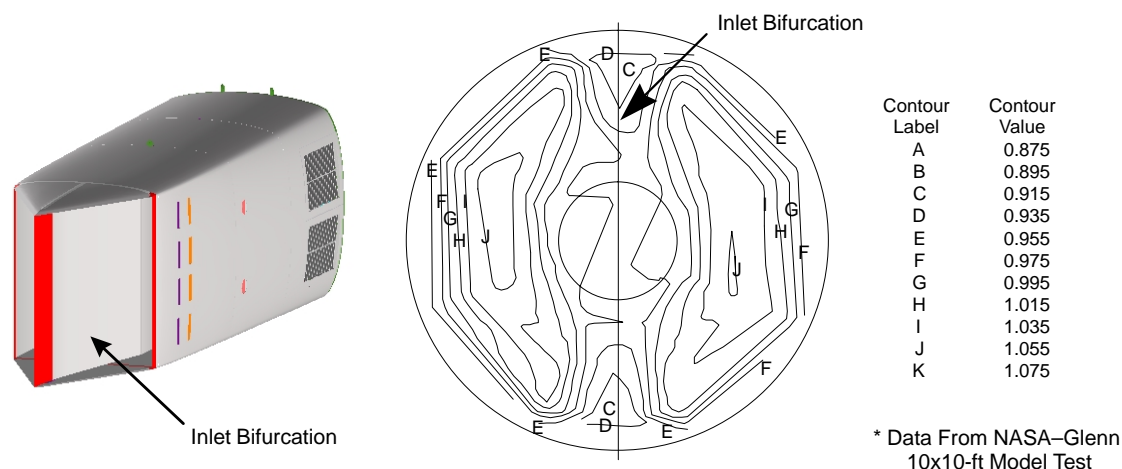
Figure 126.   Fan Face Pressure Profiles and 2DB Inlet   *The MFTF3770.54 fan was designed for aerodynamic and structural compatibility with the 2DB inlet.*

crossing required a stiffened airfoil with a thicker than normal root section. The thickness was extended from the root to slightly below midspan. Although a hollow airfoil configuration was selected to minimize weight, the stiffened airfoil weighed more than an airfoil having a conventional thickness/chord distribution. Increased airfoil weight had a cascading impact on the weight of the attachment, disk, and containment designs. Overall fan weight was increased by approximately 285 lbm. In addition, the airfoils had to be inserted from the rear of the disk rather than the front. Thus, teardown, reassembly, and balance of the No. 1 bearing and fan modules would be required to change a blade. To reduce the weight penalty, the configuration was changed from a bladed disk to an integrally bladed rotor. Fan weight still increased by 90 lbm relative to an equivalent IBR design allowing a 2E crossing. However, continued design studies indicated that the latter design encountered a flutter boundary dangerously close to the supersonic cruise operating condition. Attainment of the required flutter margin required a rotor weight penalty similar to that required to avoid a 2E crossing. Accordingly, the weight penalty initially associated with avoidance of a 2E crossing was ultimately required to avoid flutter.

Controlled-diffusion airfoil (CDA) profiles were used for the stators to minimize profile losses while improving durability. CDA's are optimized specifically for high subsonic and transonic applications to reduce boundary layer separation and, in the transonic regime, allow diffusion from supersonic to subsonic local suction surface velocity without the development of strong shocks (Figure 127). The suction surface of a CDA is precisely contoured to cause left-running expansion waves to be reflected from the sonic lines as strong right-running compression waves. By preventing the expansion and compression waves from coalescing, a weak shock or shock-free flow is obtained. In addition, CDA's typically incorporate thicker leading edges than conventional airfoils, providing superior incidence range and durability.

The design radial distributions of total pressure and total temperature at the fan face and exit are shown in Figure 128. The inlet pressure is consistent with the circumferentially averaged profiles delivered by the 2DB inlet. The exit pressure profile was selected for compatibility with No. 2/3
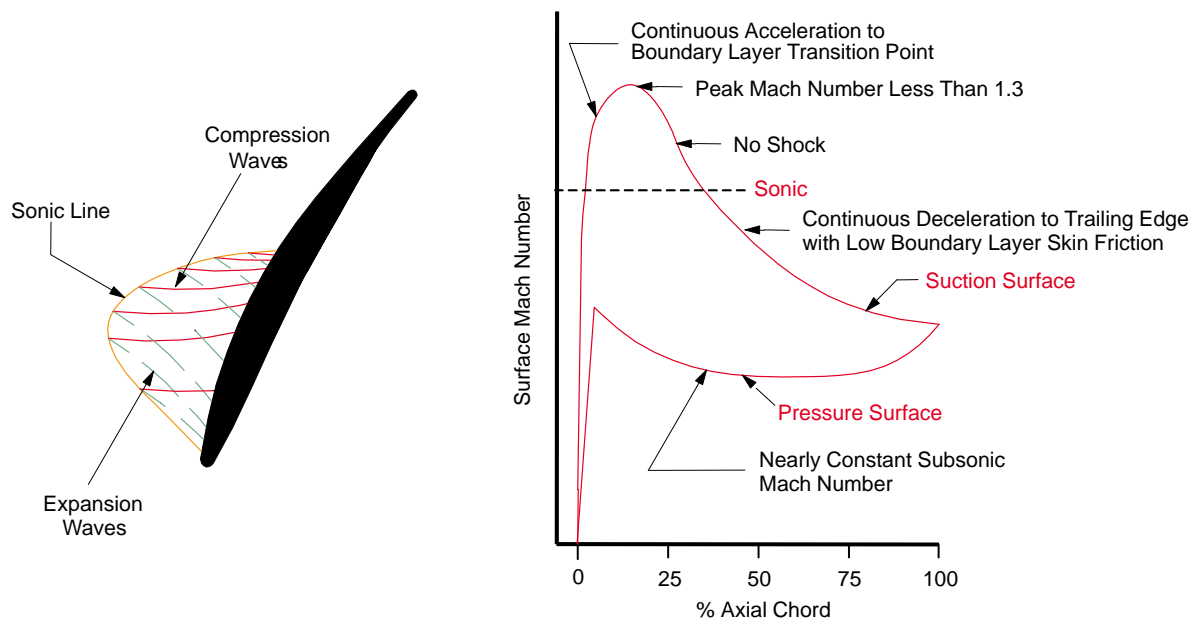
Figure 127. Controlled-Diffusion Airfoil Design Characteristics
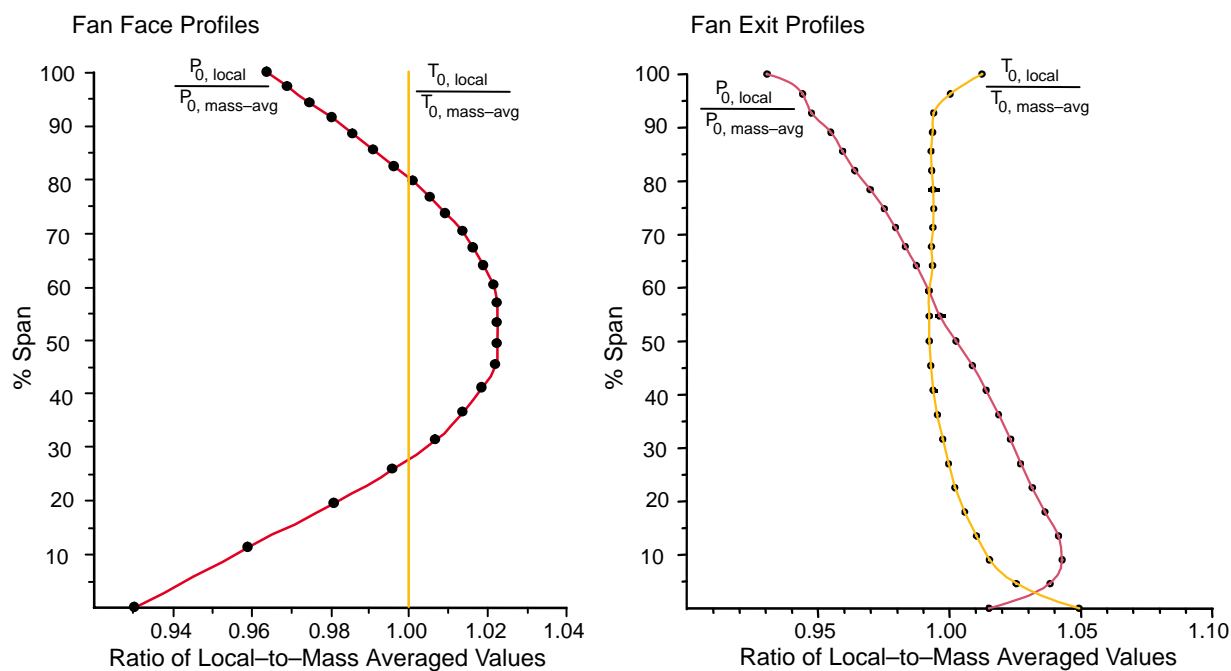
Figure 128. Fan Face and Exit Pressure and Temperature Profiles

bearing compartment buffer air and low shaft cooling requirements. To ensure sufficient flow, it was necessary to provide a slightly higher pressure in the fan core stream. The design point pressure warpage (P_{Tcore}/P_{Tduct}) is 1.054 for a corresponding bypass ratio of 0.54.

The fan aerodynamics were optimized with a 3D viscous multistage CFD design code. Full speed lines, from slightly below the operating line to stall, were generated at the supersonic cruise (maximum operating-line efficiency), fan ADP, and sea-level takeoff (maximum corrected airflow) conditions. The resulting streak lines, airfoil loading distributions, and blade-to-blade flowfields were examined and the flowpath and airfoil geometry iteratively adjusted until the performance requirements were achieved. Aerodynamic iterations were conducted in conjunction with structural iterations to ensure that the final airfoil shapes met all required vibratory margins. An example of the computed streak lines for the IGV and first two fan stages is shown in Figure 129. The computed R1 blade-to-blade Mach number distribution at various spanwise locations is illustrated in Figure 130, and the associated airfoil surface Mach numbers are illustrated in Figure 131.

The mass-averaged fan map resulting from the fan aerodynamic design is shown in Figure 132. Since the fan was designed with pressure warpage, it was also necessary to generate a corresponding core stream performance map (Figure 133).

Fan Structural Design

Figure 134 is a summary of the MFTF3770.54 fan mechanical features and materials. The rotor is an all-titanium design featuring integrally bladed rotors in all stages. IBR technology saves weight, increases reliability, and reduces parasitic leakage by eliminating the dead rim area associated with mechanical attachments and cascading impact on the disk, shaft, and bearing designs. Reliability is increased by eliminating life-limiting stress concentrations associated with disk rim slots. Elimination of parasitic leakage around blade/disk attachment points improves aerodynamic performance
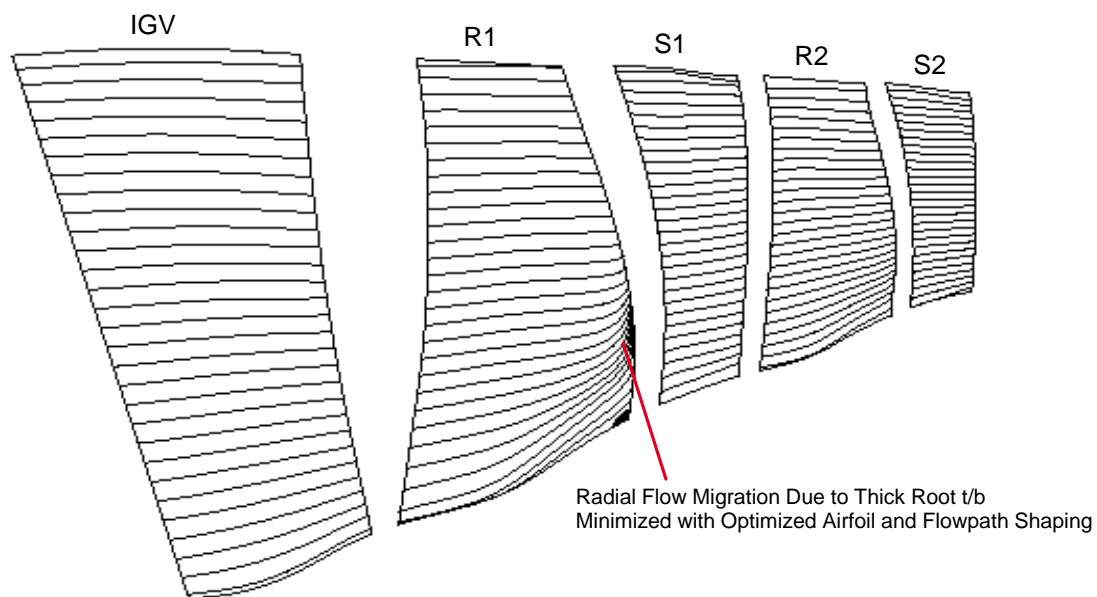
Figure 129.   CFD Computed Suction-Surface Streak Lines at the Fan ADP

Aerodynamic Design Point

90% Span   60% Span   40% Span   10% Span

Maximum Corrected Airflow
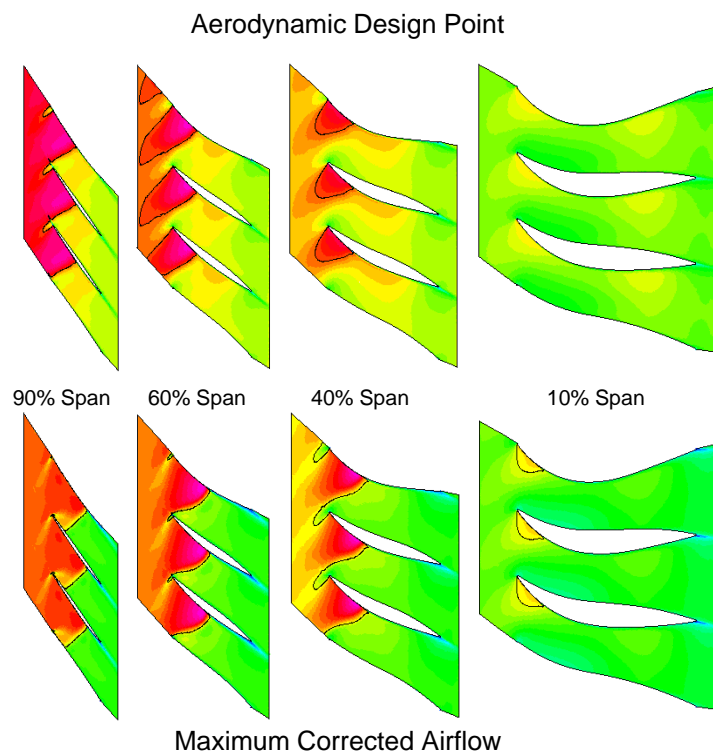
Figure 130.   CFD Computed Rotor 1 Blade-to-Blade Mach Number Distribution at the Fan ADP and Maximum Airflow Operating Conditions
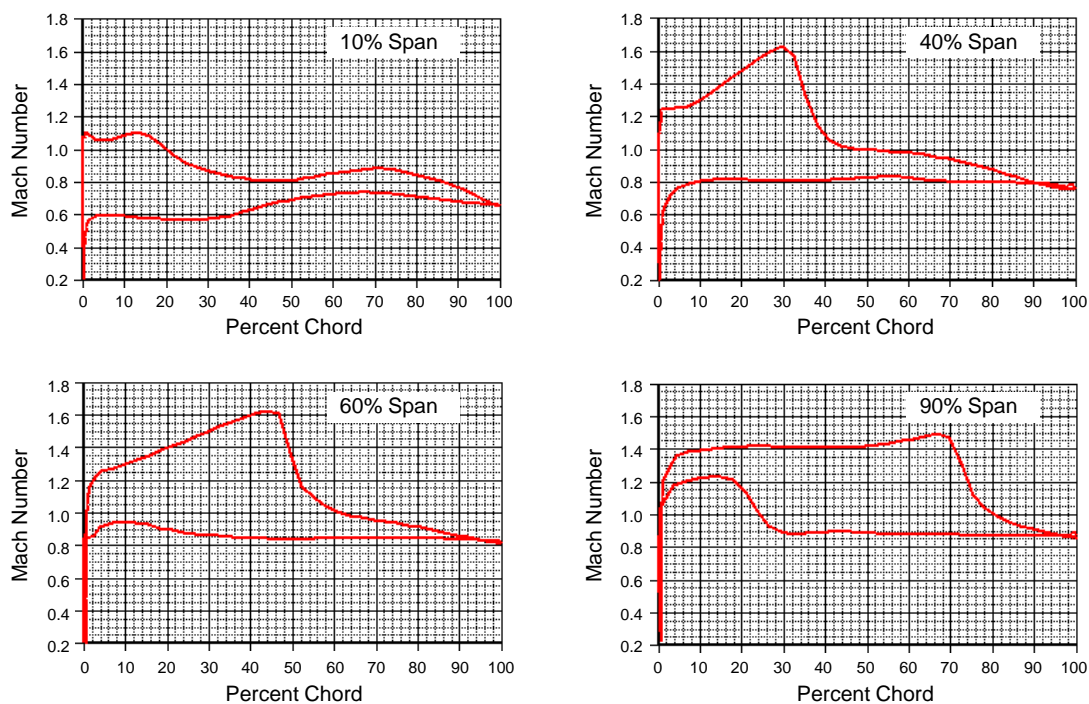
Figure 131.   CFD Computed Rotor 1 Surface Mach Number Distribution at the Maximum Corrected Airflow Operating Condition
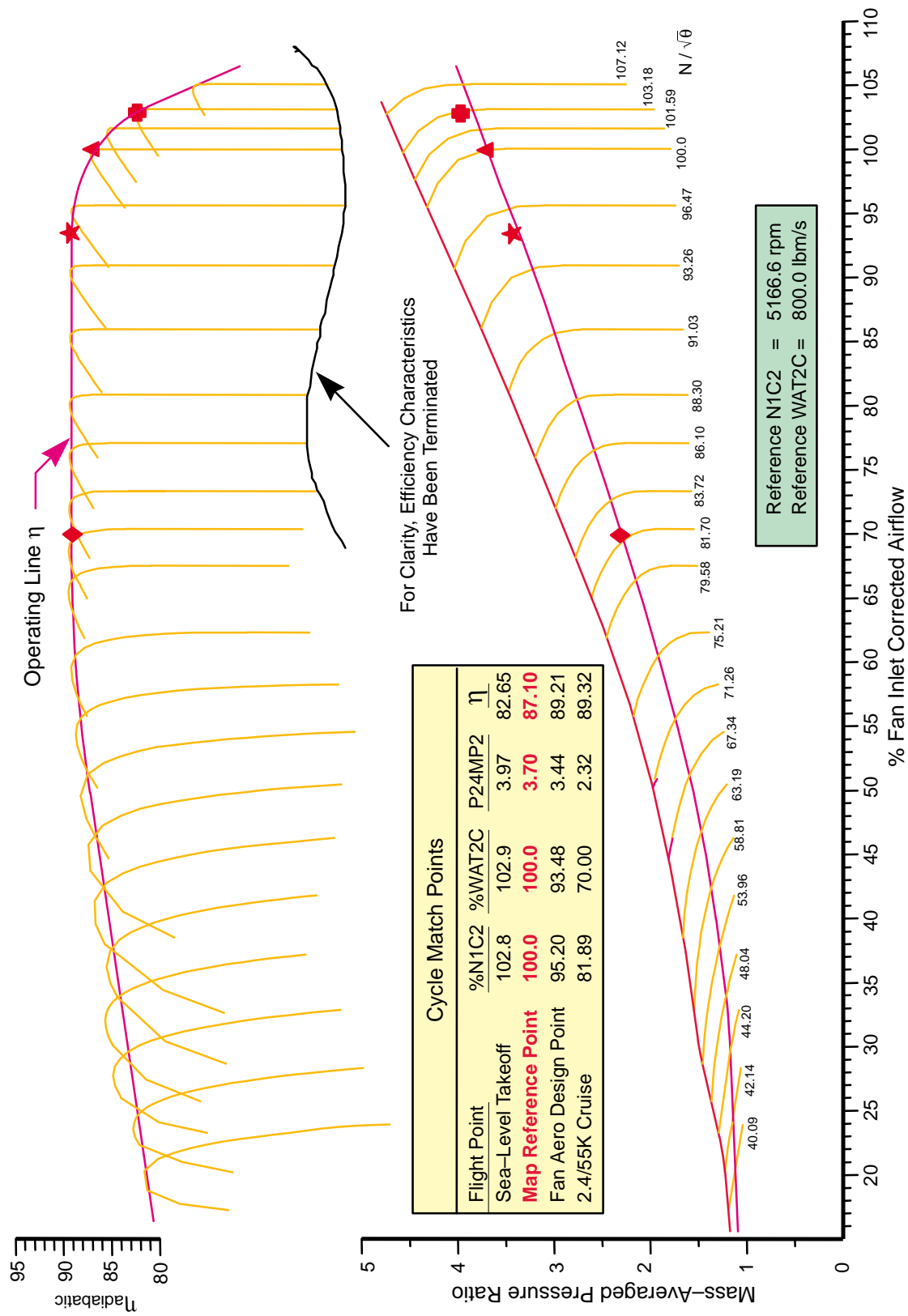
Figure 132. MFTF3770.54 Mass-Averaged Fan Performance Map

Cycle Match Points				
Flight Point	%N1C2	%WAT2C	P24MP2	η
Sea–Level Takeoff	102.8	102.9	3.97	82.65
Map Reference Point	**100.0**	**100.0**	**3.70**	**87.10**
Fan Aero Design Point	95.20	93.48	3.44	89.21
2.4/55K Cruise	81.89	70.00	2.32	89.32

Reference N1C2 = 5166.6 rpm
Reference WAT2C = 800.0 lbm/s

For Clarity, Efficiency Characteristics Have Been Terminated
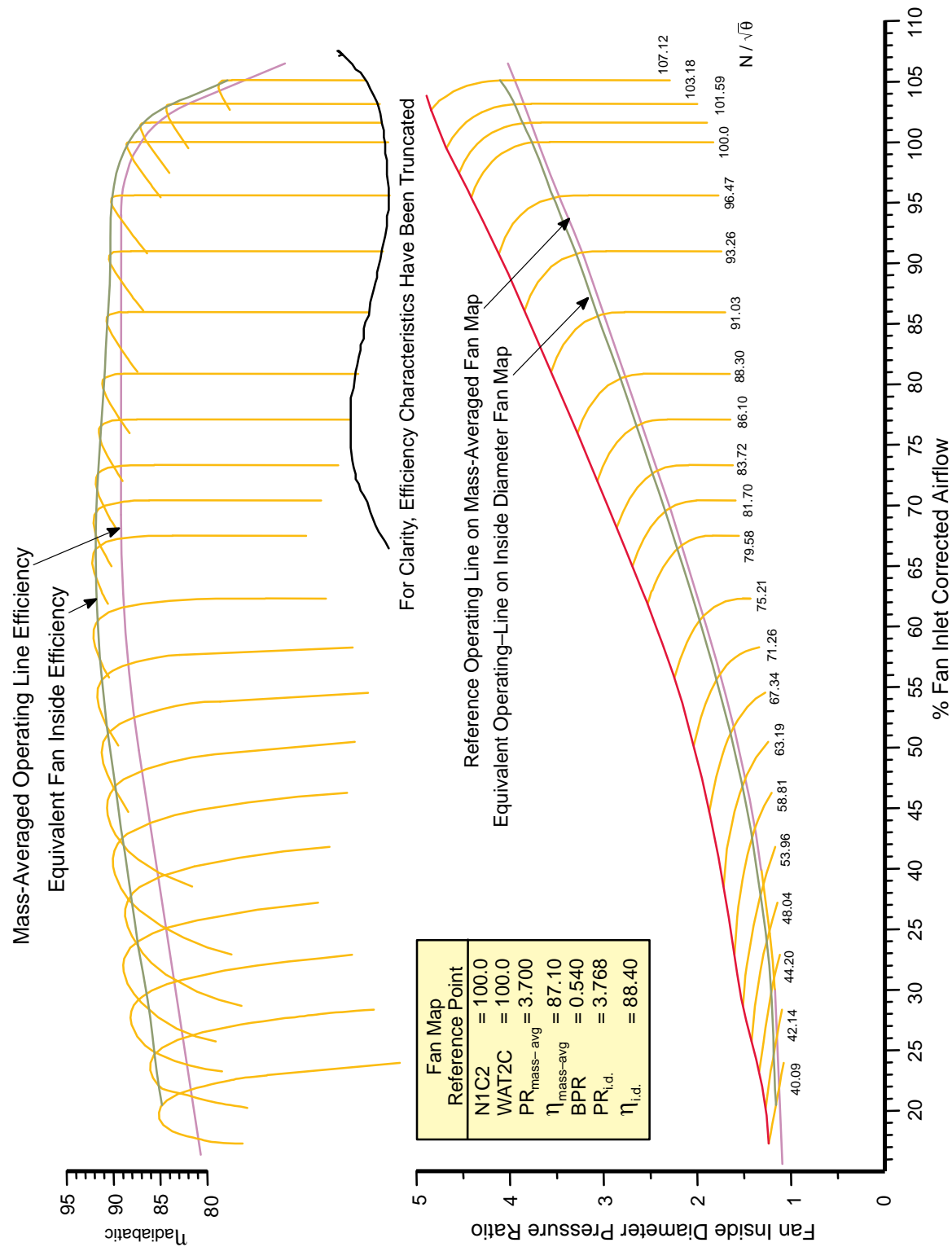
Figure 133. MFT3770.54 Fan Core Stream Performance Map
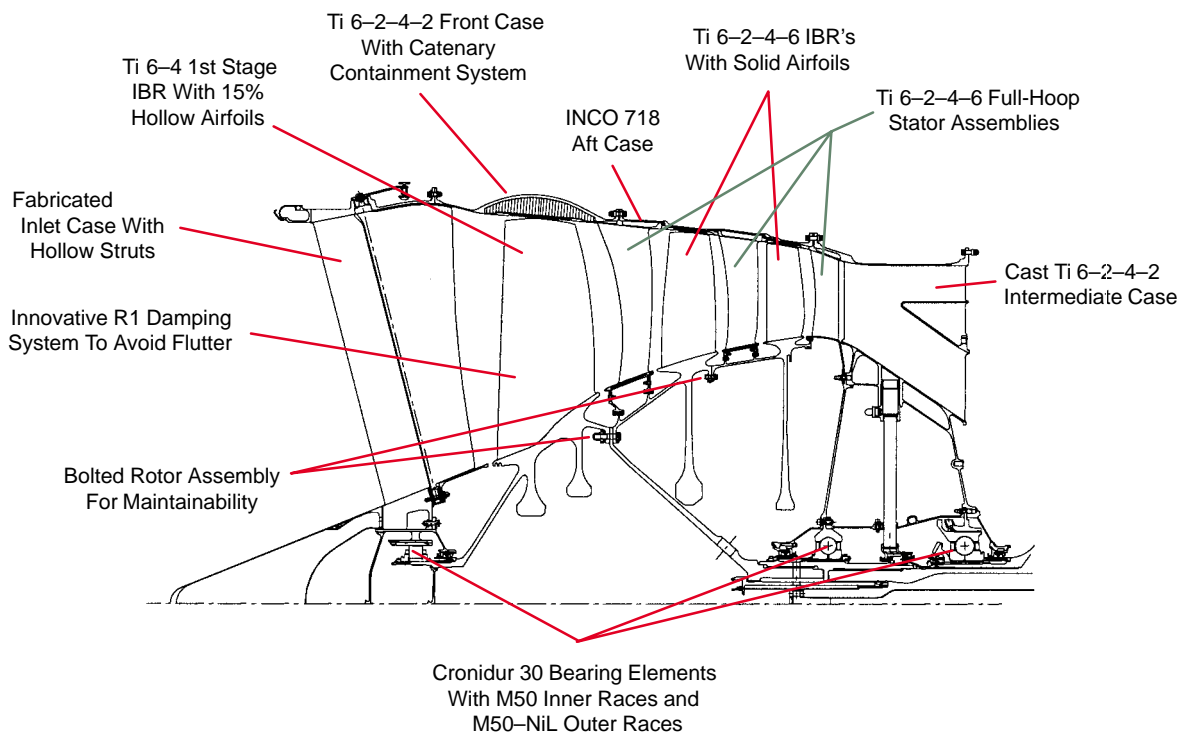
Figure 134.   Summary of Fan Materials and Design Features

and reduces local metal temperatures. Each stage is bolted together to allow removal and replacement of individual IBR's.

The fan outer case consists of forward and aft full-hoop assemblies. The front case is fabricated from titanium and consists of: (1) a curved (catenary shaped) outer hard wall to provide containment in the event of blade loss, (2) a honeycomb grid to catch the released blade and prevent it from falling back into the flowpath, and (3) a thin-wall liner that forms the flowpath outer diameter. A proprietary P&W abradable material is applied to the inner surface of the liner to provide a sacrificial surface for blade rubs. The abradable material incorporates circumferential grooves to improve part-power stability. The "catenary" containment system provided a significant weight reduction relative to conventional hard-wall designs.

The lightest weight containment system for the aft two stages was a conventional hard-wall design fabricated from Inco 718. Full-hoop titanium tip shrouds incorporating a grooved abradable material are located over rotors 2 and 3. All three stator assemblies are fabricated from high-temperature titanium. Individual vanes are mounted in full-hoop ID and OD rings. Stator 1 is held in place by a bolted flange between the front and aft case. Stator 2 is inserted into the case and pinned in place. Stator 3 is bolted to the intermediate case at the inner and outer diameters.

The intermediate case is a single-piece cast titanium structure. Axial and radial loads are transferred from the ID ring to the OD ring through eight struts evenly spaced around the circumference. Two thick struts are located at 135° and 225° from top dead center to allow power takeoff shafts to transfer load from the No. 3 bearing compartment to engine and airframe accessory gearboxes. The remaining six struts are hollow to allow flow of oil or air to the No. 2/3 bearing compartment.

Fan Duty Cycle and Life Requirements: An average flight profile, shown in Figure 135, was used for structural design of the MFTF3770.54 fan. Fan airflow, rotational speed, and inlet and exit pressures and temperatures at each flight point are tabulated in the figure.

Rotating components were designed for 9,000 hours of supersonic cruise operation. Based upon the composite profile, 9,000 hours of supersonic cruise yields a total operating life of 20,890 hours accumulated during 5,190 flights. The cumulative operation at near maximum temperature and stress is 9,422 hours. Depending upon the specific flight profile, the engine will spend from 1.6 to 3 hours of operation per flight at these most severe conditions. The engine thrust request, fan temperature, fan pressure, and fan rotor speed histories for the composite profile are shown graphically in Figure 136.

During each flight the engine experiences one Type I cycle (cold start – maximum power – shutdown), two Type III cycles (idle – max power – idle), and two Type IV cycles (cruise – max power – cruise). This results in 1.55 total accumulated cycles (TAC) per flight, or 8,045 TAC for 5,190 flights. For the fan conceptual design, one TAC was considered equivalent to one Type I cycle. Life goals for the fan rotating components are summarized in Table 65. For conceptual design purposes, the life goal for the fan static structure were set at twice that of the rotating components.

It is important to note that the HSCT propulsion system operates near maximum temperature and stress throughout supersonic cruise. Detailed design studies have indicated that although the HSCT propulsion system spends 43% of its time (9000 hours) at supersonic cruise, approximately 95% of the damage occurs at this flight condition. Accordingly, an accurate estimate of the fan rotor design can be achieved by basing creep life calculations on 9,475 hours ($9,000 \div 0.95$) at supersonic cruise conditions and low-cycle fatigue (LCF) lives based upon 8,045 zero-stress/room temperature to max-stress/cruise temperature cycles. Fatigue life debits resulting from sustained high-stress/high-temperature dwell must be applied as required.

Fan Thermal Analysis: Prior to fan structural design activities, it was necessary to estimate the rotor thermal stresses. Thermal profiles during steady-state and transient operation impact stresses in the part and the allowable stress level. A detailed thermal analysis was not performed during this study. Thermal conditions were estimated using an empirically based system calibrated with thermal data from P&W military engines. The fan secondary flow is shown in Figure 137, and the associated rotor thermal profiles for supersonic cruise are summarized in Figure 138. Disk rim temperatures for rotors 1 and 2 were set equal to the average relative total temperature across the blade. The large radius change for rotor 1 resulted in a correspondingly large difference between the LE and TE rim relative total temperatures. Thus, for this stage both temperatures were calculated and the thermal gradient included in the stress analysis. Web and bore temperatures were based on the aforementioned empirical calculation procedure that accounts for entry temperature of the bore cooling air, windage and mixing effects as the cooling air flows through the bore region, convection between the disk surfaces and bore flow, and heat conduction between the rim and bore.

Rotor Design Summary: The major design features of the MFTF3770.54 fan rotor were described previously. A 3D model of the fan rotor with a 90° section removed is shown in Figure 139.

The first stage of the HSCT fan features an integrally bladed rotor configuration in which the hollow titanium 6–4 blades are linear friction welded to the twin-web titanium 6–4 disk. The front hub is integral to the disk. Initial design efforts for the first-stage rotor focused on a bladed disk assembly with individually removable airfoils. As described in the fan aerodynamic design discussion, the

Parameter Names and Units

Time : Cumulative Flight Time (hours)
Altitude : Flight Altitude (feet)
Distance : Cumulative Distance (nm)
WAT : Inlet Physical Airflow (lb/sec)
PT2 : Inlet Total Pressure (psia)
PT25H : Exit Core Stream Total Pressure (psia)
TT2 : Inlet Total Temperature (°F)
TT25H : Exit Core Stream Total Temp (°F)
N1 : Rotational Speed (rpm)

3513 Nautical Miles
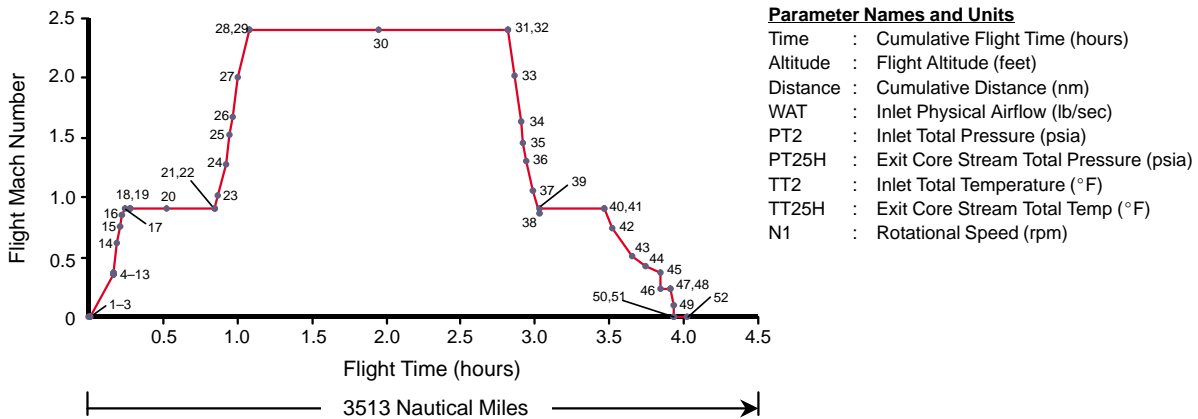
PT.Flight Operation	Time	Altitude	Mn	Distance	WAT	PT2	PT25H	TT2	TT25H	N1
1 Begin Taxi From Gate	0.000	0	0.00	0	206.62	13.579	18.913	77.0	138.9	2432.3
2 End Taxi	0.150	0	0.00	0	206.62	13.579	18.913	77.0	138.9	2432.3
3 Release Brake, Begin Takeoff	0.150	0	0.00	0	747.62	13.579	54.819	77.0	385.9	5402.6
4 Liftoff From Runway	0.163	0	0.36	1.59	838.85	15.488	62.093	90.9	403.2	5452.2
5 Clear 35 ft. Obstacle	0.164	35	0.36	1.61	837.99	15.468	62.019	90.8	403.1	5452.1
6 Initial Noise Cutback	0.164	35	0.36	1.61	810.54	15.468	58.505	90.8	375.4	5280.5
7 Gear Up	0.165	302	0.36	1.82	804.09	15.320	58.013	89.8	374.3	5279.4
8 689 ft Sideline Noise Station	0.166	689	0.36	2.14	794.65	15.100	57.279	88.3	372.7	5277.4
9 Continue Noise Cutback	0.168	1,492	0.36	2.93	776.20	14.671	55.859	85.4	369.6	5274.8
10 Cutback For Takeoff Noise Station	0.168	1,492	0.36	2.93	607.28	14.671	41.562	85.4	291.2	4605.2
11 Flyover Takeoff Noise Station	0.170	1,500	0.36	3.51	607.13	14.667	41.556	85.4	291.2	4605.4
12 Continue Noise Cutback	0.172	1,500	0.37	4.10	623.01	14.742	41.710	86.2	292.0	4606.0
13 Begin Climb to Subsonic Cruise	0.172	1,500	0.37	4.10	804.14	14.742	59.436	86.2	399.3	5444.4
14 Continue Subsonic Climb	0.192	8,300	0.62	10.5	749.95	13.497	52.467	67.1	361.5	5345.9
15 Continue Subsonic Climb	0.212	15,380	0.76	19.2	647.96	11.559	44.946	57.9	347.5	5299.0
16 Continue Subsonic Climb	0.228	20,760	0.85	27.6	572.49	10.128	39.383	49.4	334.6	5255.7
17 Continue Subsonic Climb	0.250	27,670	0.90	39.3	456.85	7.915	30.806	28.6	302.8	5148.0
18 Subsonic Top of Climb	0.278	34,000	0.90	53.6	351.24	5.919	23.096	2.3	262.7	5007.5
19 Begin Subsonic Cruise	0.278	34,000	0.90	53.6	304.79	5.919	18.424	2.3	199.2	4502.2
20 Continue Subsonic Cruise	0.528	34,000	0.90	184.0	303.20	5.919	18.305	2.3	197.8	4492.4
21 End Subsonic Cruise	0.846	34,000	0.90	350.0	301.36	5.919	18.167	2.3	196.2	4480.8
22 Begin Climb to Supersonic Cruise	0.846	34,000	0.90	350.0	351.24	5.919	23.096	2.3	262.7	5007.5
23 Continue Climb/Accel	0.867	34,000	1.02	361.6	394.68	6.783	26.449	20.7	290.9	5105.8
24 Continue Climb/Accel	0.920	34,000	1.28	396.4	521.96	9.404	36.560	68.3	363.7	5353.2
25 Continue Climb/Accel	0.948	34,000	1.52	418.8	663.13	12.692	47.711	121.8	427.7	5544.9
26 Continue Climb/Accel	0.965	37,790	1.67	434.6	670.81	13.420	48.440	148.2	449.9	5559.9
27 Continue Climb/Accel	1.007	45,370	2.00	479.3	629.18	15.430	46.615	242.4	525.7	5493.4
28 Supersonic Top of Climb	1.083	52,950	2.40	575.4	595.97	19.877	47.827	378.1	629.0	5382.0
29 Begin Supersonic Cruise	1.083	52,950	2.40	575.4	595.97	19.877	47.424	378.1	626.5	5377.4
30 Continue Supersonic Cruise	1.950	62,329	2.40	1,768.4	379.71	12.664	30.192	378.1	626.3	5376.9
31 End Supersonic Cruise	2.816	64,675	2.40	2,962.3	339.22	11.314	26.963	378.1	626.2	5376.9
32 Begin Decel to Subsonic Cruise	2.816	64,675	2.40	2,962.3	307.05	11.314	23.665	378.1	585.6	5067.1
33 Continue Decel	2.862	64,675	2.02	3,020.2	201.66	6.292	14.381	248.6	450.9	4887.1
34 Continue Decel	2.905	64,675	1.63	3,064.8	138.60	3.472	9.256	137.9	349.1	4825.1
35 Continue Decel, Start Descent	2.922	64,675	1.45	3,079.4	110.53	2.665	7.162	94.7	292.9	4650.3
36 Continue Decel/Descent	2.944	60,340	1.31	3,096.8	115.55	2.759	7.260	64.5	247.5	4480.7
37 Continue Decel/Descent	2.984	51,670	1.06	3,124.1	126.84	3.046	7.545	18.2	172.9	4162.2
38 Continue Decel/Descent	3.031	43,000	0.86	3,150.0	143.60	3.684	8.181	−11.9	113.1	3817.0
39 Begin Subsonic Cruise	3.031	43,000	0.90	3,150.0	208.56	3.844	12.629	−6.4	198.2	4569.6
40 End Subsonic Cruise	3.464	43,000	0.90	3,373.4	206.32	3.844	12.461	−6.4	195.4	4536.5
41 Begin Subsonic Decel/Descent	3.464	43,000	0.90	3,373.4	145.72	3.844	8.344	−6.4	116.1	3791.0
42 Continue Decel/Descent	3.517	34,700	0.74	3,398.2	163.10	4.870	9.227	−21.4	74.8	3441.6
43 Continue Decel/Descent	3.649	18,100	0.51	3,446.0	274.19	8.424	16.058	18.1	124.1	3619.8
44 Continue Decel/Descent	3.740	9,800	0.43	3,472.8	355.10	11.158	21.262	42.0	153.1	3711.7
45 Continue Decel/Descent	3.844	1,500	0.37	3,500.0	325.62	14.742	22.876	86.2	167.1	3210.4
46 Begin Approach	3.845	1,500	0.24	3,501.0	455.86	14.008	29.962	77.8	218.9	4005.9
47 Continue Approach	3.911	394	0.24	3,513.2	410.02	14.567	27.377	81.5	198.1	3713.7
48 Touchdown	3.912	0	0.24	3,513.3	273.27	14.776	21.054	83.0	148.5	2858.8
49 Initiate Thrust Reverse	3.933	0	0.10	–	631.25	14.148	43.432	78.0	300.5	4726.4
50 Cancel Thrust Reverse	3.934	0	0.00	–	688.70	13.579	48.381	77.0	335.8	5039.1
51 Begin Taxi	3.934	0	0.00	–	206.62	13.579	18.913	77.0	138.9	2432.3
52 End Taxi at Gate	4.024	0	0.00	–	206.62	13.579	18.913	77.0	138.9	2432.3

Figure 135.   Fan Operating Conditions Along the 3500-nmi Composite Flight Profile
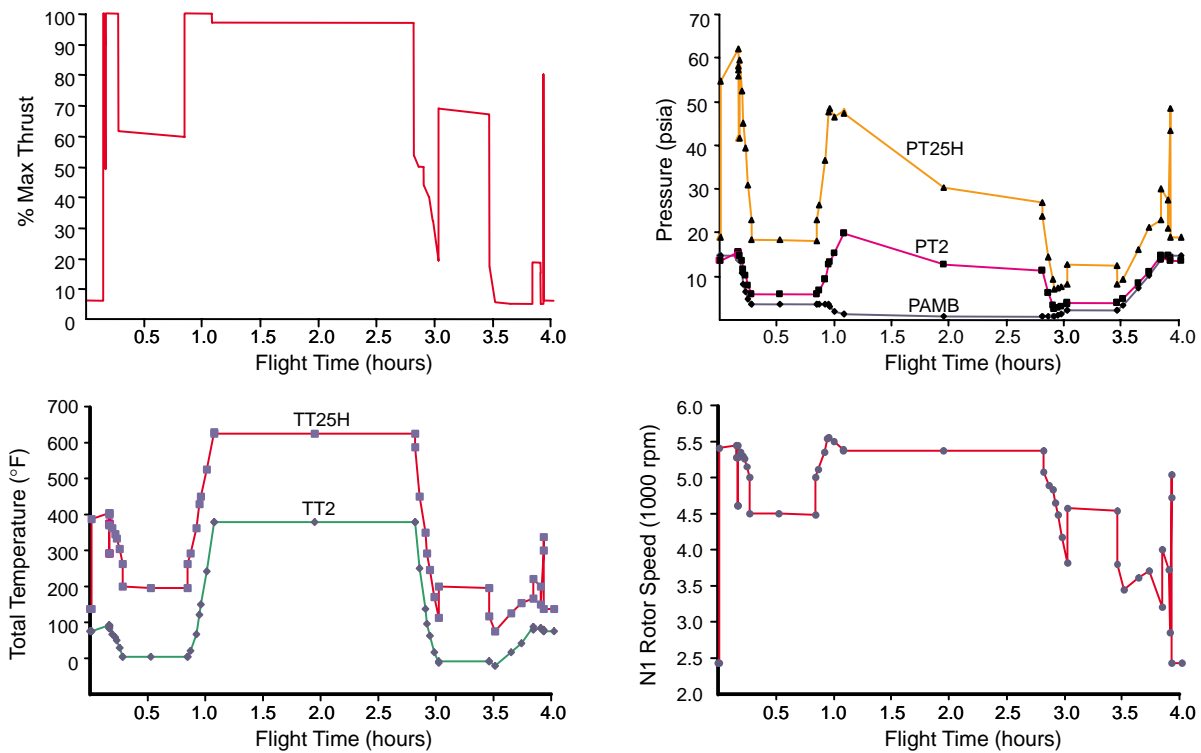
Figure 136. **Engine Thrust Request and Fan Rotational Speed/Pressure/Temperature Histories for the Composite Flight Profile**

Table 65. **MFTF3770.54 Fan Rotating Component Life Goals Based on 3500-nmi Design Flight Profile**

Total Operating Hours	20,890
Total Engine Flight Hours	19,644
Total Supersonic Cruise Hours	9,000
Average Flight Hours	4
Type I Cycles	5,190
Type III Cycles	10,380
Type IV Cycles	10,380
Total Accumulated Cycles[*]	8,045
High-Temperature/Stress Hours	9,422
Sustained High-Temperature/Stress Hours/Flight	2–3

*TAC's = Type 1 Cycles + 0.25 × (Type III Cycles) + 0.025 × (Type IV Cycles)
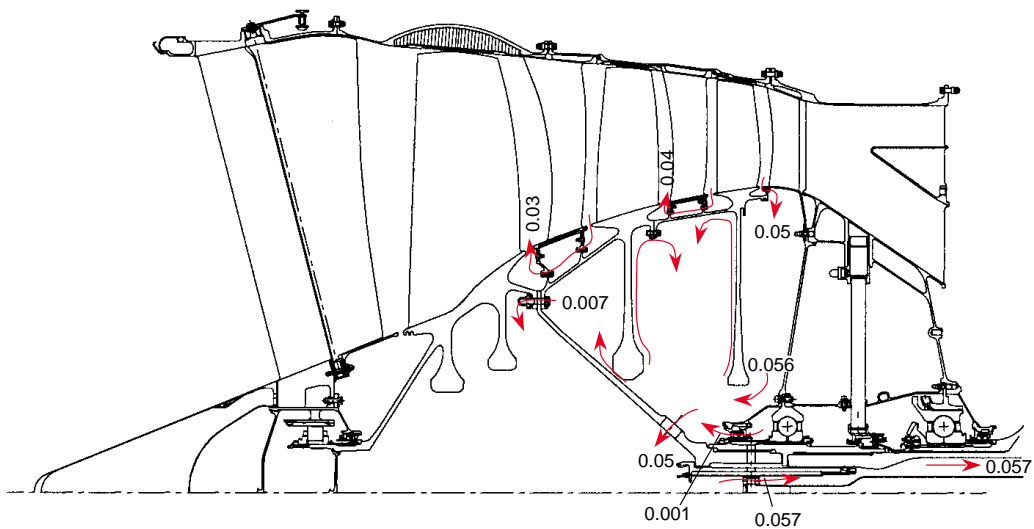
Figure 137.   MFTF3770.54 Fan Secondary Flows
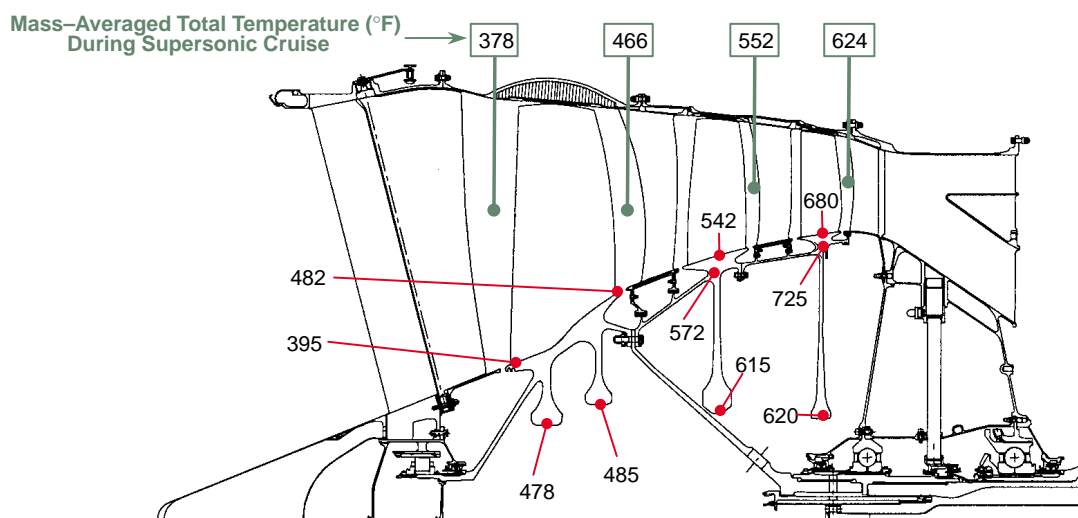
Figure 138.   MFTF3770.54 Rotor Thermal Conditions During Supersonic Cruise
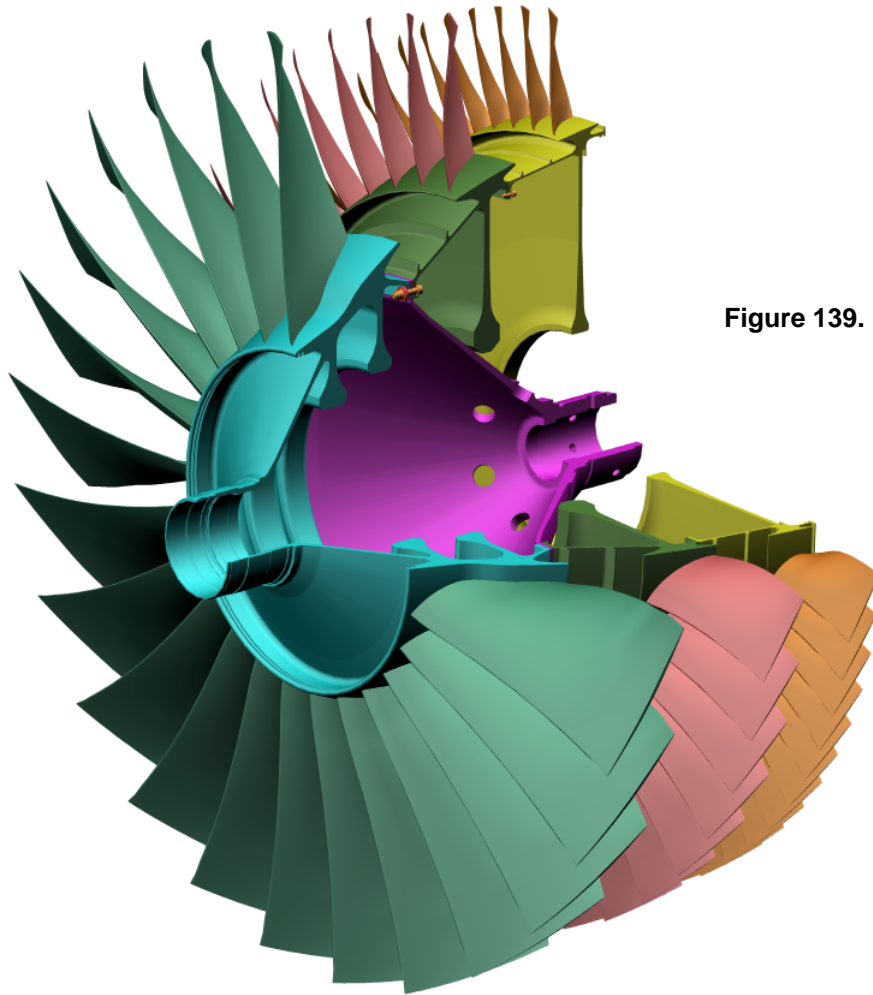
Figure 139. Solid Model 3D of MFTF3770.54 Fan Rotor

2DB inlet incorporates a splitter extending from the entrance to approximately ½ diameter upstream of the fan face. The proximity of the splitter to the fan face exposes the airfoils to a 2E vibration driver (two excitations per rotor revolution). To avoid potential vibratory problems, R1 was designed with no 2E crossing in the projected operating range. Avoidance of a 2E crossing required that the thickness-to-chord (t/b) ratio of the airfoils be increased relative to a design allowing a 2E crossing. Root t/b was set at 11.5%, held constant to approximately 20% span, and then tapered linearly to a tip t/b value of 2%.

The weight increase associated with the thicker airfoils had a cascading impact on the design of the attachment and disk. Conventional axial dovetail attachments were severely overstressed, necessitating the use of a sloped, curved attachment to increase the area of the load bearing surfaces. Elimination of a 2E crossing also required that the attachment neck height be minimized. A solution was obtained only when a complex platform and attachment concept was configured (Figure 140). To minimize attachment neck height, the disk live rim radius was increased as much as possible. A miniplatform was also incorporated into the design — in which the disk dead rim forms the flowpath ID surface at the blade leading edge. At approximately 30% axial chord the flowpath ID begins to transition from the disk dead rim to the miniplatform. The design resulted in a 285-lbm weight increase relative to the goal. Of this, 188 lbm is attributed to the increased airfoil, attachment, and

Very Thick Airfoil Root Section

Tip Section

Root Section

Conventional Design Does Not Meet 2E Criteria

Flowpath Surface Defined by Platform

Dead Rim

Attachment

Disk Live Rim

Unconventional Design Required to Meet 2E Criteria

Flowpath Surface Defined by
• Airfoil Platform
• Disk Dead Rim

Increased Live Rim Radius
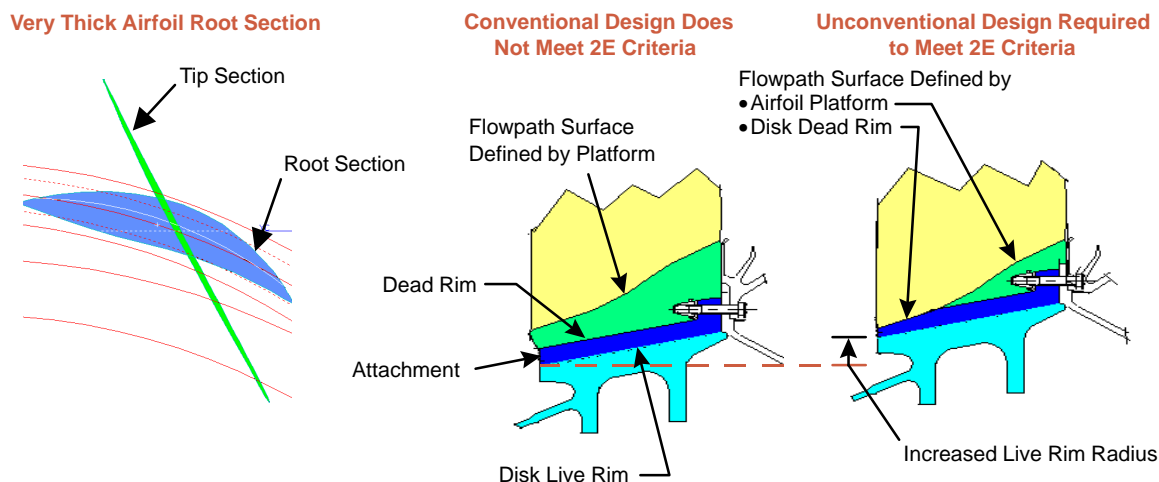
Figure 140.   Platform and Attachment   *Avoidance of 2E vibration crossing with a bladed disk assembly required a thick airfoil root section and complex platform and attachment configuration.*

disk weight. The remaining 97 lbm is attributed to weight increases in the containment, inlet case, and No. 1 bearing to handle blade-out loads.

The primary advantage of a bladed disk assembly relative to an IBR is the ability to remove and replace individual airfoils in the event of FOD. It is highly desirable to remove and insert blades from the front of the fan to avoid teardown of the fan module and No. 1 bearing compartment. Assembly studies indicated the curved dovetail attachment would prevent front loading of the airfoils due to interferences between adjacent blades. Figure 141 shows the tip interference that occurs if airfoils are fully inserted one at a time. Assembly was also attempted by partially inserting one blade, followed by an adjacent blade. This process was continued until all of the airfoils were partially inserted in the disk. The blades were then individually adjusted in an attempt to obtain full insertion. No satisfactory front assembly method was achieved. Failure to achieve front assembly with the baseline airfoil design led to a short study to determine the aerodynamic impact of redesigning the blades. Changes in tip chord and camber were evaluated. All proposed aerodynamic modifications led to unacceptable loss in fan stall margin. As a result, the baseline aerodynamic design was retained. Assembly requires that the airfoils be inserted from the rear of the disk. Replacement of blades requires teardown of the fan module and No. 1 bearing.

The large weight penalty and difficult assembly associated with a bladed disk configuration led to evaluation of a integrally bladed rotor design in which individual airfoils are linear friction welded to the disk. Fan IBR's are being introduced in the latest generation of military fighter engines such as the F119–PW–100 and in business jet engines such as the Williams–Rolls FJ44. Repair capabilities are being developed with industry and Department of Defense funding. As shown in Figure 142, an IBR design that avoided a 2E crossing in the projected operating range was achieved. The IBR design imposed a 90-lbm weight penalty compared to the 285-lbm penalty associated with the bladed disk.

The weight penalties discussed in the above paragraphs were originally attributed solely to avoidance of 2E resonance associated with the 2DB inlet. In fairness, it should be noted that the design also avoided flutter during supersonic cruise. Subsequent design studies of a blade having a 2E crossing identified a flutter boundary dangerously close to the supersonic cruise operating point.

Airfoil and/or Attachment Interference Prohibits Front Loading Into Disk
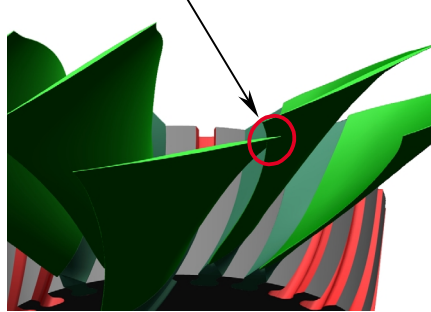
Solution is to Load Airfoils From Rear of Disk

Sloped, Curved Attachment

Blades Inserted From Rear of Disk
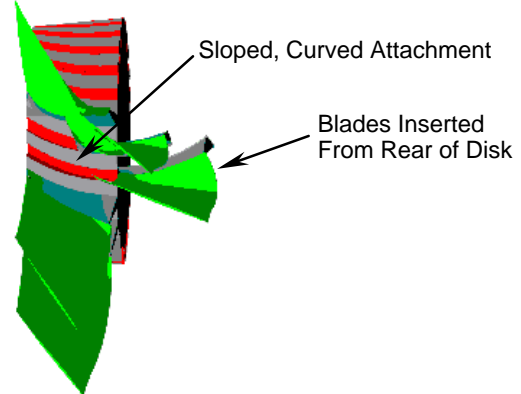
Figure 141.   Tip Interference   *The curved attachment requires the airfoils to be inserted from the rear of the disk.*
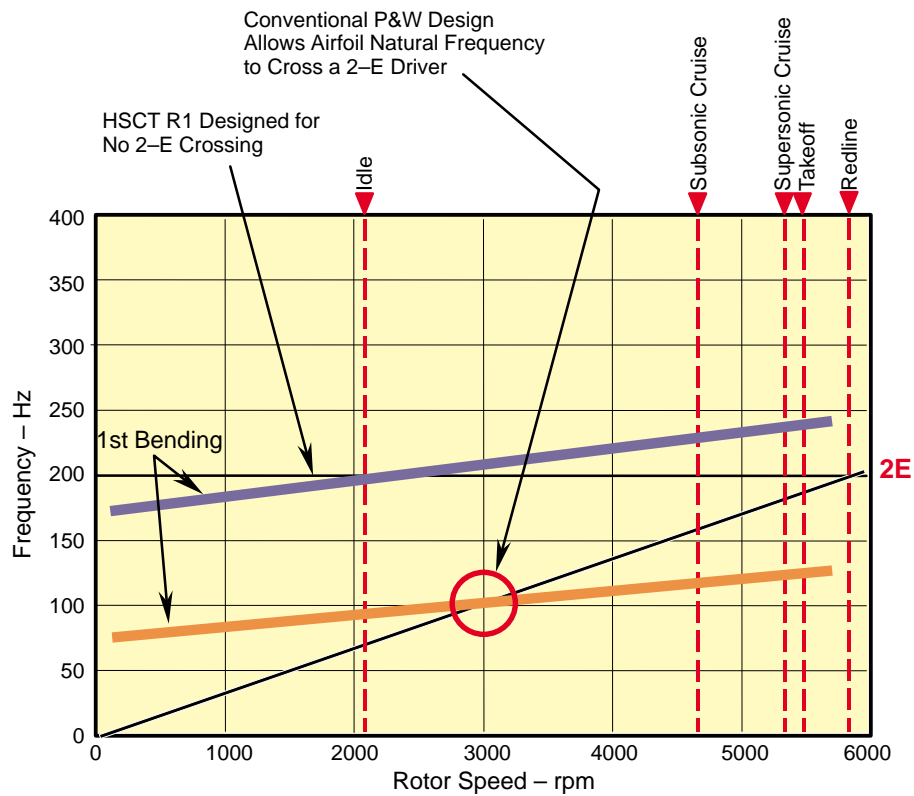
Figure 142.   The Final First-Stage IBR Design Avoids a 2E Crossing

Moving this flutter boundary to a safe location of the fan map resulted in a weight penalty similar to that required for avoidance of a 2E crossing.

The disks for all three rotor stages were sized to meet creep, LCF, and burst requirements. Creep and LCF stress allowables were established consistent with achieving 9,475 hours of supersonic cruise operation in 5,190 flights (8,045 equivalent Type I cycles). A minimum of 25% burst margin was required at maximum nominal rotor speed. Airfoils were designed to avoid a 2E crossing throughout the operating range and to provide acceptable high-cycle fatigue (HCF) life. Steady-state stress analysis was performed using the ANSYS finite-element modeler. The structural model consisted of an axisymmetric segment of the disk that included one airfoil (Figure 143). Disk materials, operating temperatures, and damage mechanisms are summarized in Table 66. The lightest disk is achieved when actual stresses equal the design allowables. High local stresses, which exceeded allowables, may be observed at the intersection of the airfoils with the disk rims. These locally high stresses result from: (1) modeling the airfoil/disk intersection as a sharp corner rather than a contoured fillet and (2) excessive bending of the baseline airfoil. Both of these effects are traditional problems that can be fixed with little or no weight impact. Bending-induced stresses can be significantly reduced by adjusting the airfoil stacking line to balance the blade. Stress concentrations resulting from the sharp corner at the blade/disk intersection can be reduced by using a double-curved fillet. Both fixes are typically incorporated during detailed design.

Rotor 1 Flutter Analysis: Airfoil flutter can occur when aerodynamic forces couple with the airfoil elastic and inertia forces to increase the kinetic energy of the blade, a process referred to as "negative damping." When the aerodynamic energy exceeds the positive mechanical damping energy, airfoil oscillations will grow to dangerous amplitudes and catastrophic failure of the airfoil may occur. As shown in Figure 144, there are four potential flutter zones of interest: (1) supersonic unstalled flutter which typically occurs near the operating line at maximum corrected rotor speed, (2) supersonic stalled flutter which typically occurs near the stall line at maximum corrected rotor speed, (3) choked
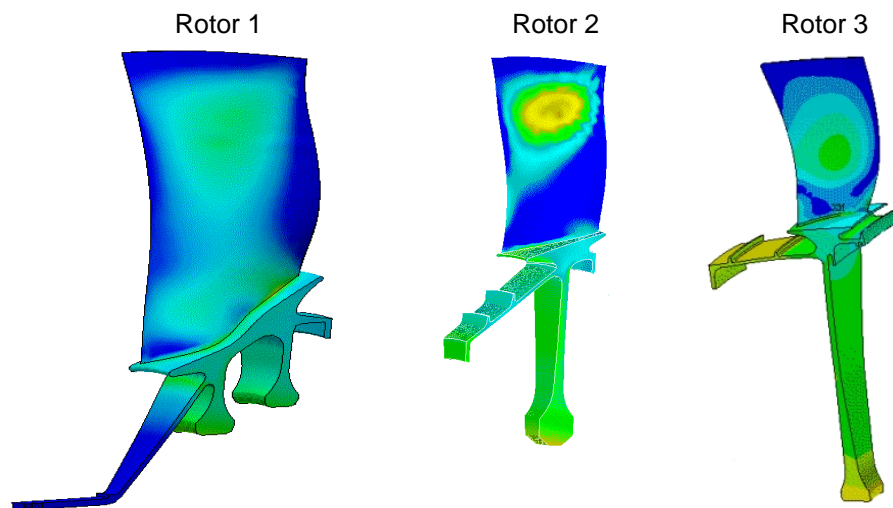
Figure 143.   Structural Finite-Element Model   *Individual fan IBR's were modeled in ANSYS using an axisymmetric disk segment with one airfoil.*

Table 66. Summary of Fan Disk Design Stress Allowables

Fan Disk	Location	Temp (°F)	Material	Limit
1	Rim	482	Ti 6–4	Creep
	Web	483	Ti 6–4	Creep
	Bore	485	Ti 6–4	Creep
2	Rim	542	Ti 6–2–4–6	Creep
	Web	600	Ti 6–2–4–6	LCF
	Bore	615	Ti 6–2–4–6	LCF
3	Rim	680	Ti 6–2–4–6	LCF
	Web	715	Ti 6–2–4–6	Creep
	Bore	620	Ti 6–2–4–6	LCF
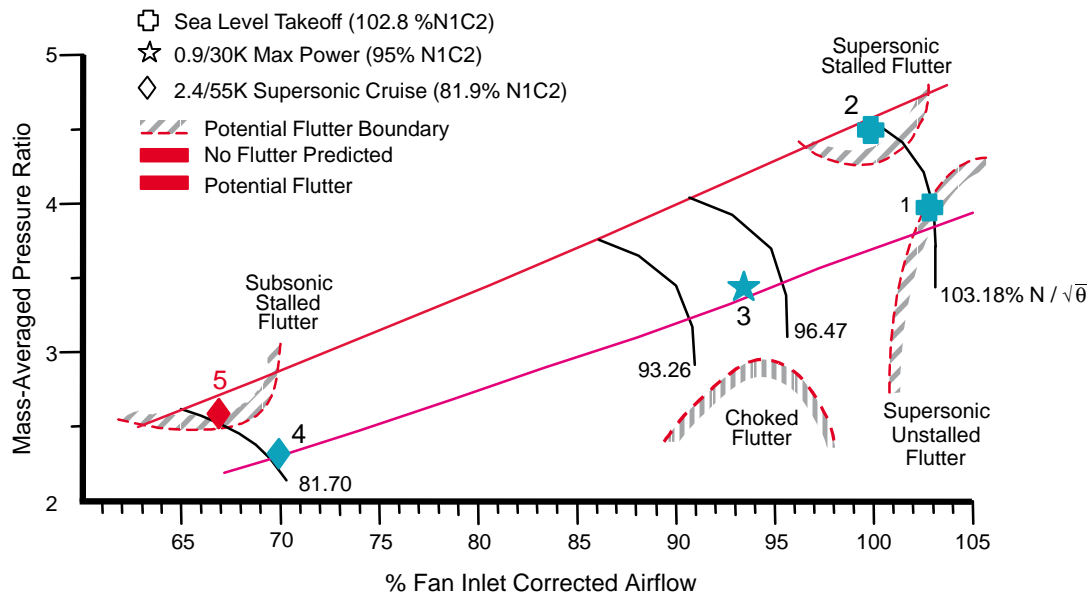
Figure 144.   Rotor 1 Flutter Potential *Evaluated at corrected rotor speeds corresponding to three flight conditions.*

flutter which typically occurs at part power on the choked section of a speed line, and (4) subsonic stalled flutter which typically occurs at part power near the stall line. Subsonic stalled flutter is of particular concern for the HSCT since it can occur at rotor speeds at or near those encountered during supersonic cruise. The elevated supersonic cruise temperature can aggravate the flutter problem due to the impact on material properties.

All three fan stages were evaluated for flutter potential using a simple empirical method derived from extensive component and engine test experience. Rotors 2 and 3 were determined to have adequate flutter margin. However, the need for a more detailed analysis of the first stage was indicated. Flutter analysis was performed at rotor speeds corresponding to three fight points: (1) sea-level takeoff, (2) Mach 0.9/30,000-ft altitude, and (3) Mach 2.4/55,000-ft altitude. The super-

sonic and subsonic flutter regimes both required evaluation of match points near the operating and stall lines (Figure 144). A semiempirical flutter model was used in which airfoil frequency and modal displacements were predicted by an ANSYS finite-element model. Unsteady, unseparated aerodynamic loads acting on the airfoils are calculated from mass-averaged inlet flow conditions determined using a streamline model. In the case of high aerodynamic loading, the impact of flow separation on the unsteady loads is obtained by applying an empirical correction factor. Correction factors were determined from an experimental airfoil database for unstalled and stalled flow conditions.

As previously discussed, flutter can occur when aerodynamic forces couple with the blade inertia and elastic forces to increase the kinetic energy of the airfoil. In the P&W analysis, this coupling can occur when the aerodynamic damping is negative. Match points 1 through 4 were determined to have positive aerodynamic damping, and therefore flutter free operation, for all vibratory modes. However, match point 5 was determined to have negative damping for the third vibratory mode (Figure 145).
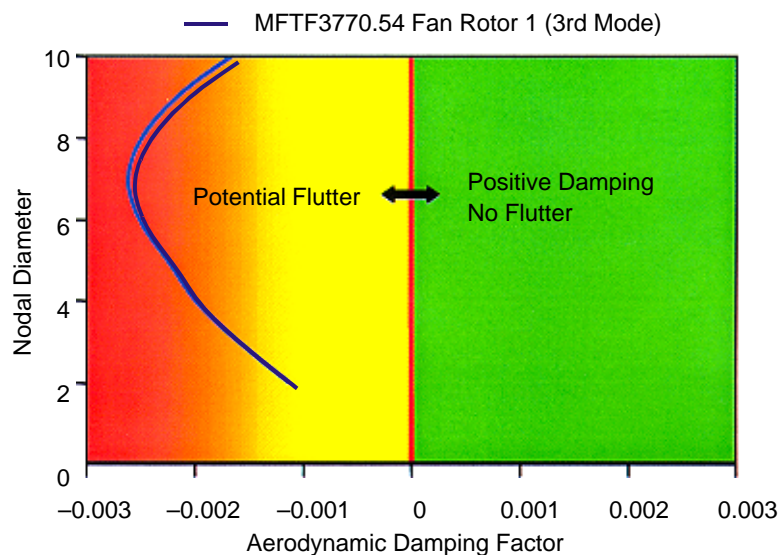
Figure 145.   Rotor 1 Negative Aero Damping in the Third Mode

Point 5 is matched near the stall line at the rotor temperature and corrected speed occurring at the supersonic cruise flight condition. Operation at this match can result from flight through atmospheric temperature and/or pressure perturbations. Thus, it is critical that flutter be avoided. This can be achieved by further thickening the airfoils to increase stiffness or by adding a means to provide positive damping. Increasing airfoil thickness will result in a corresponding increase in airfoil and disk weight and a potential loss in fan flow capacity. Advanced damping concepts that have little to no impact on rotor weight are being evaluated under industry and Department of Defense funding.

Rotor 1 Bird-Strike Analysis: The HSCT fan must be compatible with the bird-ingestion requirements defined in FAR 33.76. Simulated bird strikes were performed using advanced finite-element modeling. General features of the model are summarized in Figure 146. Three fan blades were modeled using shell elements; the disk was modeled with brick elements. The soft-body bird was modeled as a series of fluid elements that interact dynamically with the deforming airfoils. Impact accounts for forces generated by blade rotation and projectile forward velocity. During each time step the impact zones are determined, impact forces calculated, and blade stresses, strains, and

Bird Model

Weight (lbm)	Diameter (in)	Length (in)
2.5	3.88	9.72
4.5	4.72	11.82
8.0	5.72	14.30

Bird Velocity	=	300 ft/s
Fan RPM	=	5300 rpm
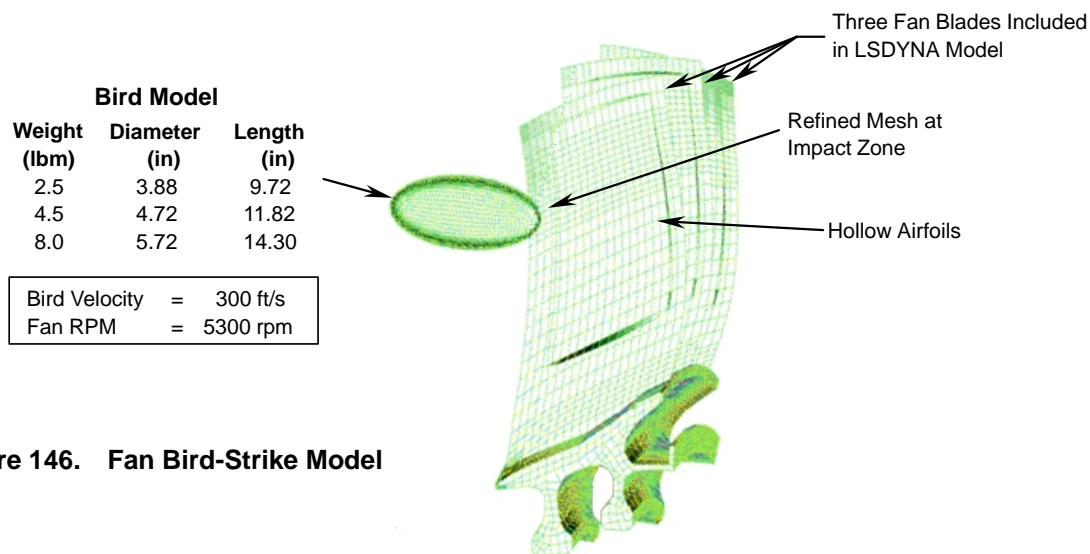
Figure 146.   Fan Bird-Strike Model

deflections generated. Airfoil rotational speed was set at takeoff conditions, and bird axial velocity relative to the engine was set to a typical value of 300 ft/s. Initial impact occurred at approximately 75% of the leading-edge span.

Three bird sizes were analyzed to determine the potential blade damage. The largest size, 8 pounds, exceeds currently defined ingestion requirements. Calculated blade damage for each bird size is shown in Figure 147. Ingestion of an 8-lbm bird is predicted to result in significant distortion of the airfoil leading edge; however, no tears or loss of blade material should occur.
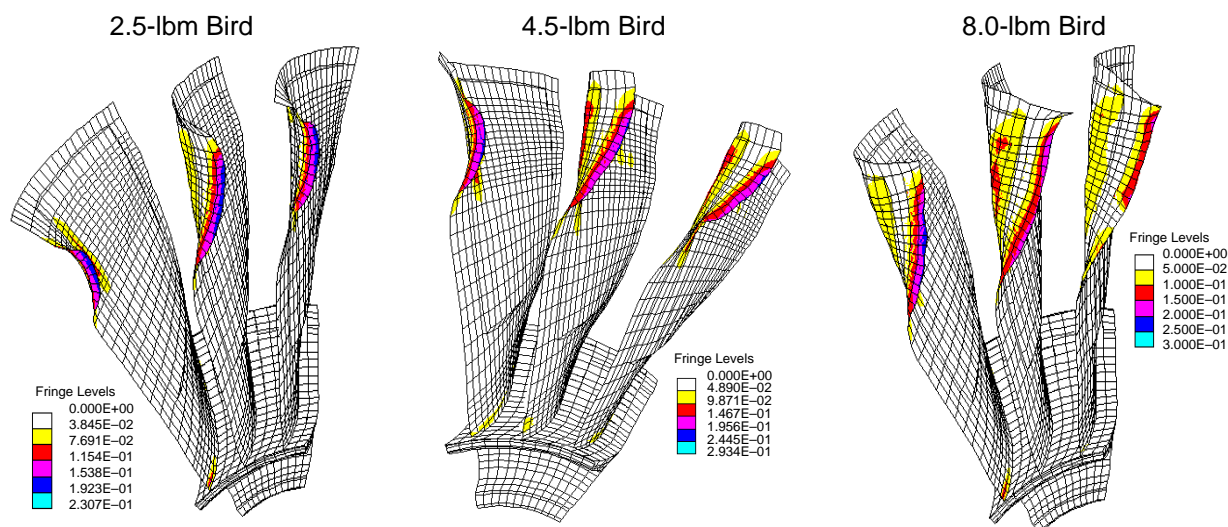
Figure 147.   Predicted Rotor 1 Airfoil Damage From Bird Ingestion *Bird impact resulted in significant airfoil deformation but produced no tears in material.*

Rotor 1 Containment: Three rotor 1 containment concepts were evaluated (Figure 148): (1) a conventional "flat" hard-wall configuration, (2) a flat hard-wall configuration incorporating honeycomb to trap the released blade and prevent it from exiting the flowpath, and (3) a curved hard-wall configuration incorporating a honeycomb blade trap. All three configurations were evaluated with Inco 718 and 6–4 titanium. Wall thicknesses were varied from a minimum of 0.25 inches to a maximum of 0.36 inches. The blade-out event was simulated in LSDYNA using a three-blade rotor sector and a 30-in axial case length. Case length was selected to ensure containment 20° forward of the blade centerline and 1.5× the blade axial chord length rearward. The case length also ensures that the front and aft flange locations are outside of the event zone. As shown in Figure 149, the LSDYNA model was capable of predicting case penetration, collateral damage to the rotor, and exit of blade particles from the case. Results from the LSDYNA analyses are summarized in Table 67.

Conventional Hard Wall

Hard Wall With Honeycomb Blade Catchment

Figure 148. Rotor 1 Containment Configurations

Hard Wall With Catenary Honeycomb Catchment
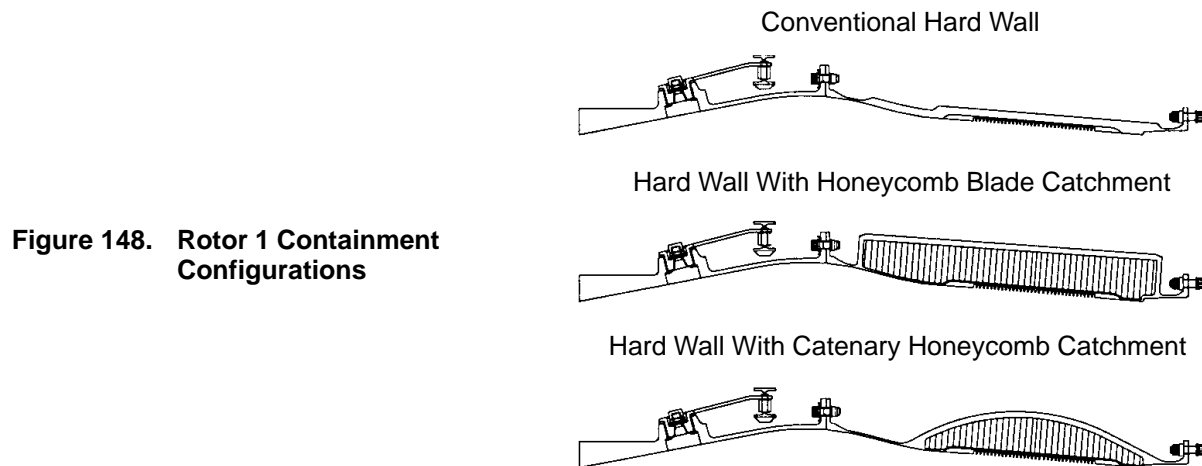
Table 67. Results of LSDYNA R1 Containment Analyses

Case Configuration	Material	Case Thickness (Inches)	Case Penetration	Parts Exited Case	Cascading Blade Failures
Flat Hard Wall	Titanium 6–4	0.35	YES	YES	YES
	INCO 718	0.25	YES	YES	YES
	INCO 718	0.30	YES	YES	YES
	INCO 718	0.35	NO	YES	NO
Flat Hard Wall With Honeycomb Trap	INCO 718	0.35	NO	NO	NO
Catenary Case	INCO 718	0.23	YES	NO	NO
	INCO 718	0.30	NO	NO	NO
	Titanium 6–4	0.25	YES	NO	NO
	Titanium 6–4	0.30	NO	NO	NO

Only two configurations prevented case penetration, collateral damage, and exit of rotor parts from the case. Both incorporated honeycomb to trap the released blade above the rotor. Of these two, the catenary design provided a weight savings exceeding 200 lbm and was therefore selected for incorporation into the baseline design. Snapshots from the blade-out event with the 0.3-inch thick titanium catenary case design are provided in Figure 150.
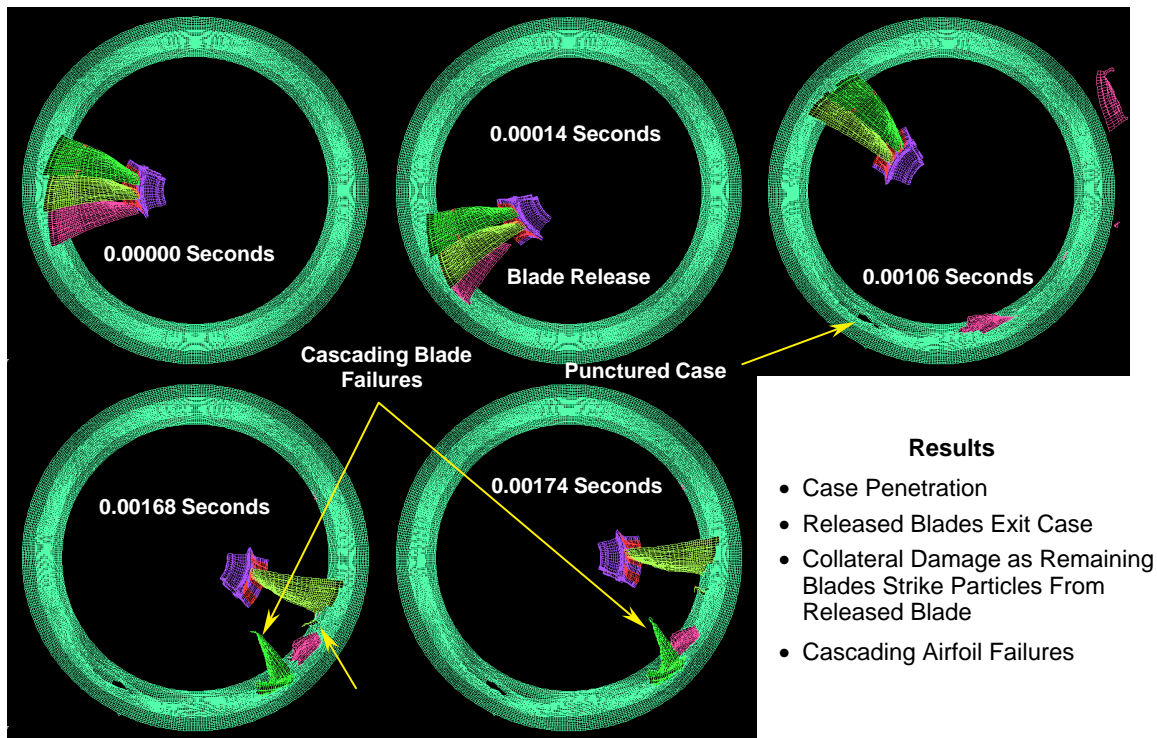
Figure 149. Rotor 1 Blade Out Results: 0.25-in Thick Flat Titanium Case
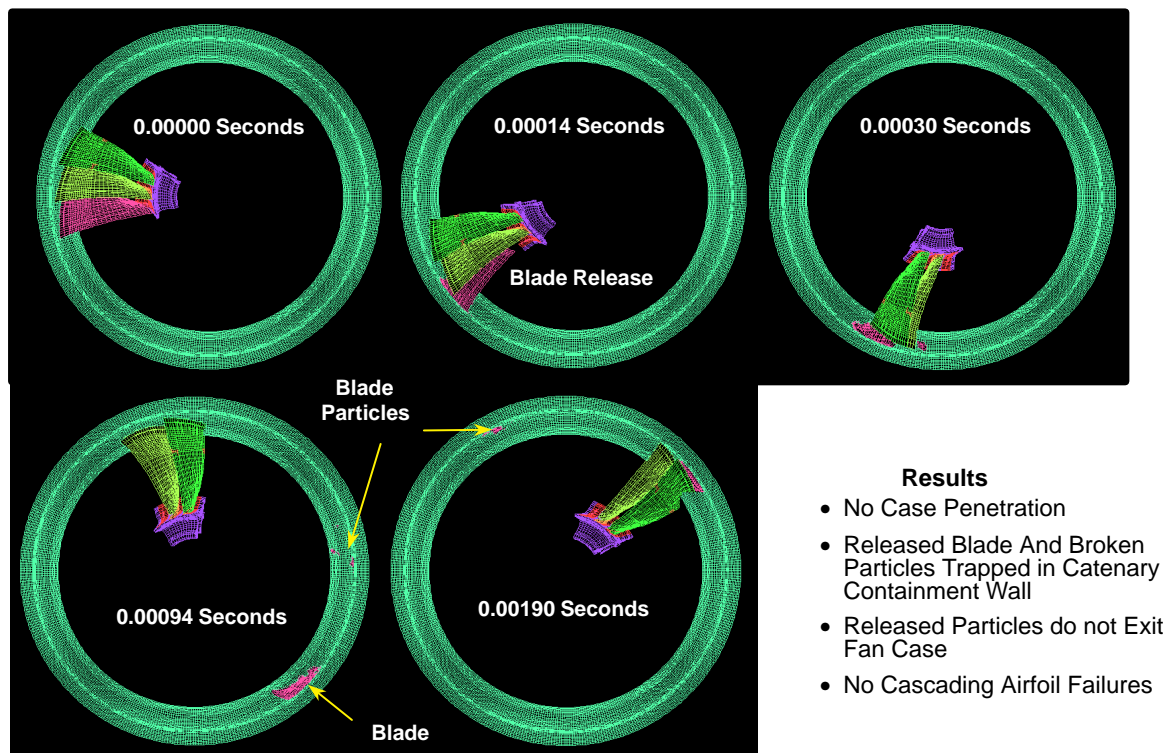
Figure 150. Rotor 1 Blade-Out Results: 0.30-in Thick Titanium Catenary Case

Fan Material and Weight Summary

Detailed part breakdowns with accompanying material and weight list are provided in Figures 151 through 155. The axial location of the center of gravity, x_{cg}, is referenced relative to the towershaft centerline. Polar moments of inertia for rotating parts are defined relative to the engine centerline.

Description	Material	Weight (lbm)	X_{cg} (inches)	I_{xx} (ft–lbf–sec^2)
Inlet Case OD Ring	Ti 6–4	82.5	–44.4	0.0
Inlet–to–Engine Interface	Ti 6–4	30.2	–50.8	0.0
Inlet Case Struts (23)	Ti 6–4	52.9	–45.2	0.0
Inlet Case ID Ring	Ti 6–4	19.0	–41.2	0.0
OD Nosecone	Ti 6–4	8.9	–47.5	0.0
ID Nosecone	INCO 625	4.4	–45.1	0.0
IGV Flaps (23)	Ti 6–4	83.7	–40.4	0.0
IGV Flap ID Shroud	Ti 6–4	8.0	–37.3	0.0
IGV Flap ID Wear Insert	Ti 6–4	7.0	–39.0	0.0
IGV Flap Lever Arms & Sync Ring	Ti 6–4	33.0	–42.9	0.0
Oil Supply Tubes	Ti 6–4	3.2	–45.2	0.0
Miscellaneous Hardware	Ti 6–4	1.4	–45.2	0.0
Nuts and Bolts	Ti 6–4	6.7	–39.2	0.0
Total		**340.9**	**–43.5**	**0.0**

Figure 151.   Fan Frame Weight Summary
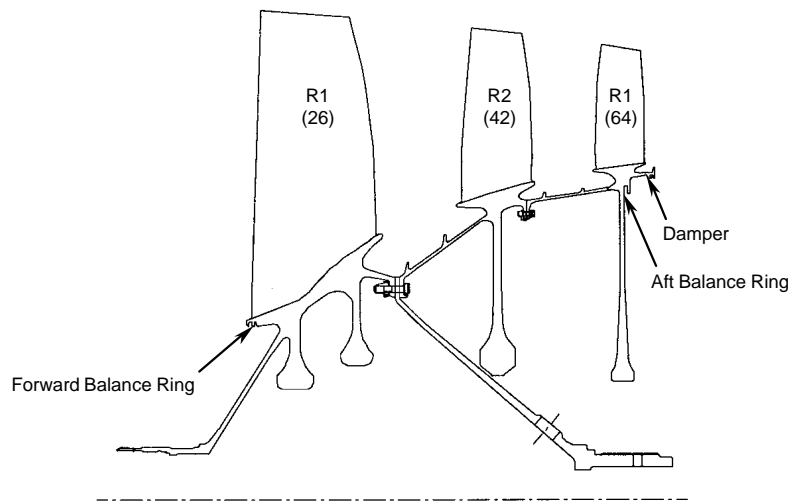
Description	Material	Weight (lbm)	X_{cg} (inches)	I_{xx} (ft–lbf–sec^2)
Rotor 1 Integrally Bladed Rotor				
• Airfoils	Ti 6–4	319.8	−30.2	409.197
• Disk	Ti 6–4	254.3	−29.2	107.277
• Integral Front Hub	Ti 6–4	28.6	−35.0	4.261
• Integral Aft Flange	Ti 6–4	19.2	−25.7	10.640
Rotor 2 Integrally Bladed Rotor				
• Airfoils	Ti 6–2–4–6	99.7	−18.2	156.853
• Disk	Ti 6–2–4–6	216.4	−18.0	153.042
• Integral R2–R1 Spacer	Ti 6–2–4–6	36.5	−21.8	25.676
Rotor 3 Integrally Bladed Rotor				
• Airfoils	Ti 6–2–4–6	60.2	−10.2	102.800
• Disk	Ti 6–2–4–6	130.9	−10.2	102.180
• Integral R3–R2 Spacer	Ti 6–2–4–6	29.4	−13.6	30.634
• Integral Aft Seal Arm	Ti 6–2–4–6	9.3	−8.6	11.073
Aft Hub	Ti 6–4	71.7	−17.6	13.086
Nuts and Bolts (Total)	INCO 718	8.9	−23.3	5.158
Balance Rings (Total)	INCO 718	6.4	−20.7	5.294
Rotor 3 Seal Arm Damper	INCO 718	1.2	−8.1	1.476
Total		**1292.5**	**−22.5**	**1138.647**

Figure 152.   Fan Rotor Weight Summary

Front View

Aft View

174 Bolt Holes

OD Case

Ground Handling Mount

208 Bolt Holes

Splitter

88 Bolt Holes

Thick Struts (2)
Thin Struts (6)

76 Bolt Holes

28 Bolt Holes

ID Case

30 Bolt Holes
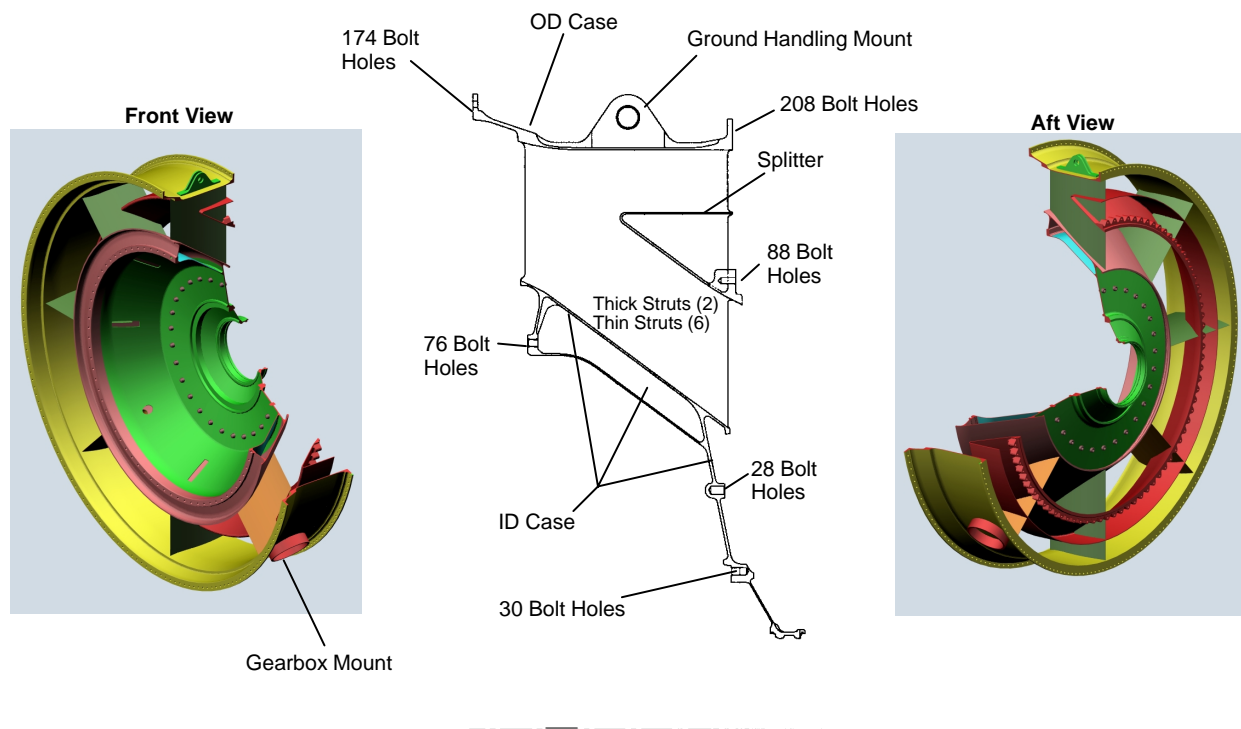
Gearbox Mount

Description	Material	Weight (lbm)	X_{cg} (inches)	I_{xx} (ft–lbf–sec^2)
OD Case				
• Outer Case	Ti 6–2–4–2	89.6	−1.8	0.0
• Oil Line & Borescope Bosses	Ti 6–2–4–2	6.3	0.0	0.0
• Gearbox Mounts	Ti 6–2–4–2	2.5	0.0	0.0
ID Case	Ti 6–2–4–2	81.7	0.7	0.0
Splitter	Ti 6–2–4–2	47.5	3.3	0.0
Struts				
• Thin Struts (4)	Ti 6–2–4–2	22.9	0.5	0.0
• Thick Struts (2)	Ti 6–2–4–2	10.2	0.5	0.0
Total		**260.7**	**0.3**	**0.0**

Figure 153.   Intermediate Case Weight Summary
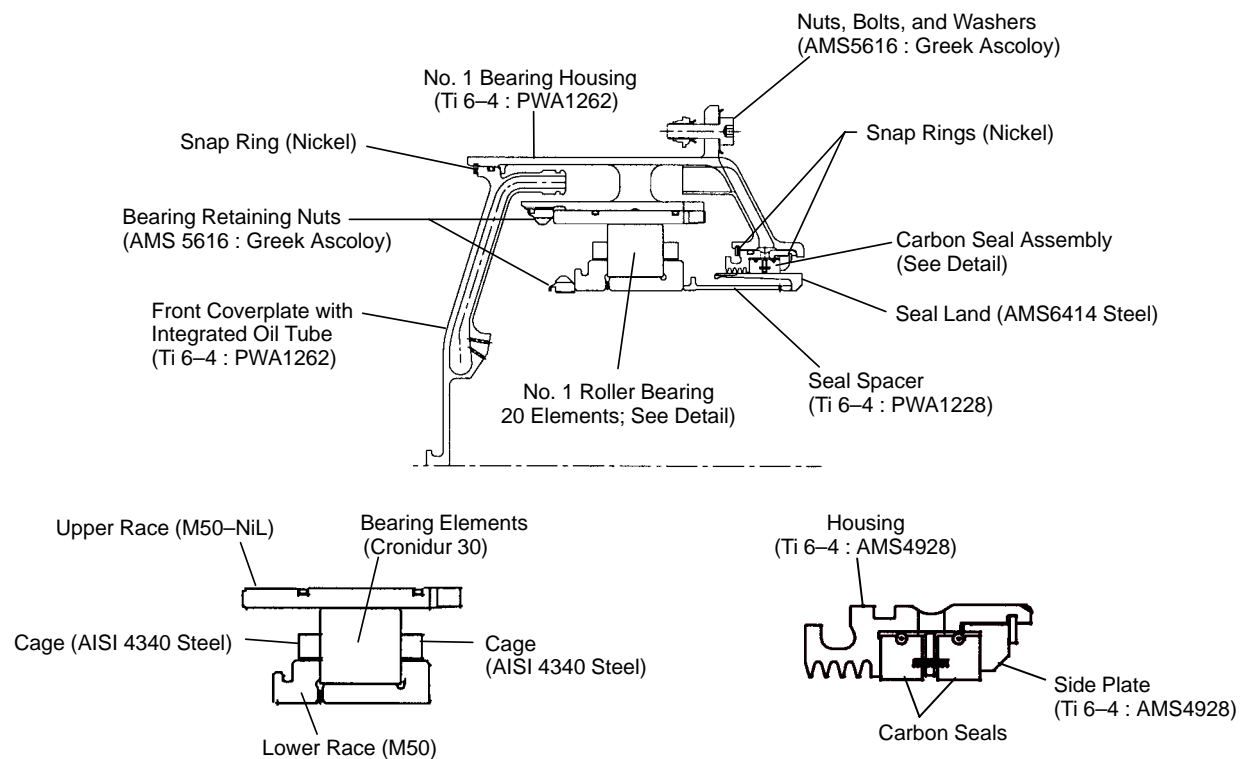
Description	Material	Weight (lbm)	X_{cg} (inches)
Front Coverplate	Ti 6–4	2.8	–43.8
Bearing Housing	Ti 6–4	11.3	–40.7
Roller Bearing Assembly			
• Bearing Elements	Conidur 30	5.4	–40.7
• Bearing ID Race	M50	5.5	–40.9
• Bearing OD Race	M50–Nil	6.8	–40.9
• Forward and Aft Cages	Steel	1.5	–40.7
Carbon Seal Assembly			
• Housing	Ti 6–4	0.94	–38.9
• Side Plate	Ti 6–4	0.21	–37.8
• Carbon Seals (2)	Carbon	0.52	–38.1
• Front Snap Ring	Nickel	0.11	–38.7
• Aft Snap Ring	Nickel	0.05	–37.6
Seal Land	Steel	1.4	–38.1
Seal Spacer	Ti 6–4	0.7	–38.7
Bearing OD Retaining Nut	Nickel	1.0	–42.8
Bearing ID Retaining Nut	Nickel	0.7	–42.3
Front Coverplate Snap Ring	Nickel	0.2	–43.9
Nuts and Bolts (16)	Nickel	0.8	–39.3
Total		**40.0**	**–40.8**

Figure 154.   No. 1 Bearing Compartment Weight

Description	Material	Weight (lbm)	X_{cg} (inches)
No. 2 Bearing Support	Ti 6-2-4-2	37.7	-5.9
No. 2 Bearing Assembly			
• Ball Bearing Elements (16)	Cronidur 30	6.7	-6.7
• Upper Race	M50-Nil	18.3	-6.4
• Lower Race	M50	10.1	-6.5
• Cage	Steel	3.0	-6.4
No. 2 Bearing Retaining Nut	Nickel	1.0	-10.3
No. 2 Seal Land	Steel	1.7	-9.4
No. 2 Seal Spacer	Ti 6-4	0.8	-8.8
No. 2 Carbon Seal Assembly	Ti/Ni/C	2.9	-9.3
Coupling	Ti 6-2-4-6	25.6	-6.0
Actuator	Steel	0.8	-5.0
Mid-Compartment Seal Assembly			
• Forward Seal Housing	Ti 6-4	2.0	-1.0
• Forward Carbon Seal	Carbon	0.2	-1.4
• Forward Seal Snap Ring	Nickel	0.2	-1.2
• Forward Seal Land	Steel	0.9	-1.3
• Forward Seal Lock Nut	Nickel	0.9	-0.5
• Aft Seal Land	Steel	2.6	0.9
• Aft Seal Housing	Ti 6-4	0.7	0.2
• Aft Carbon Seal	Carbon	0.2	0.0
• Aft Snap Ring	Nickel	0.2	-0.2
No. 3 Bearing Assembly			
• Ball Bearing Elements (16)	Cronidur 30	9.0	4.9
• Upper Race	M50-Nil	22.4	4.4
• Lower Race	M50	13.4	5.1
• Cage	Steel	3.2	4.9
No. 3 Bearing Support	Ti 6-4	8.4	4.9
Bevel Gear	Steel	12.8	3.8
Bevel Gear Lock Nuts	Nickel	4.5	3.5
No. 3 Bearing Damping Rods (16)	Ti 6-4	0.8	3.9
No. 3 Seal Spacer	Ti 6-4	0.7	7.4
No. 3 Seal Land	Steel	1.6	7.9
No. 2 Carbon Seal Assembly	Ti/Ni/C	2.5	7.6
No. 2/3 Housing Assembly	Ti 6-2-4-2	14.5	-1.2
Housing Nuts & Bolts	Nickel	3.0	-1.1
Towershaft Assemblies (2)			
• Towershaft Drive Gears (2)	Steel	12.3	0.0
• Towershafts (2)	Steel	3.6	0.0
• Towershaft Bearing Spacers (2)	Ti 6-4	1.2	0.0
• Driver Gear Bearings (2)	M50	4.4	0.0
• Towershaft Bearings (2)	M50	3.4	0.0
• Bearing Retaining Nuts (2)	Nickel	0.4	0.0
• Towershaft Bearing Covers (2)	Ti 6-4	0.1	0.0
Miscellaneous	Ti 6-4	1.0	-1.3
Total		**239.6**	**-1.4**
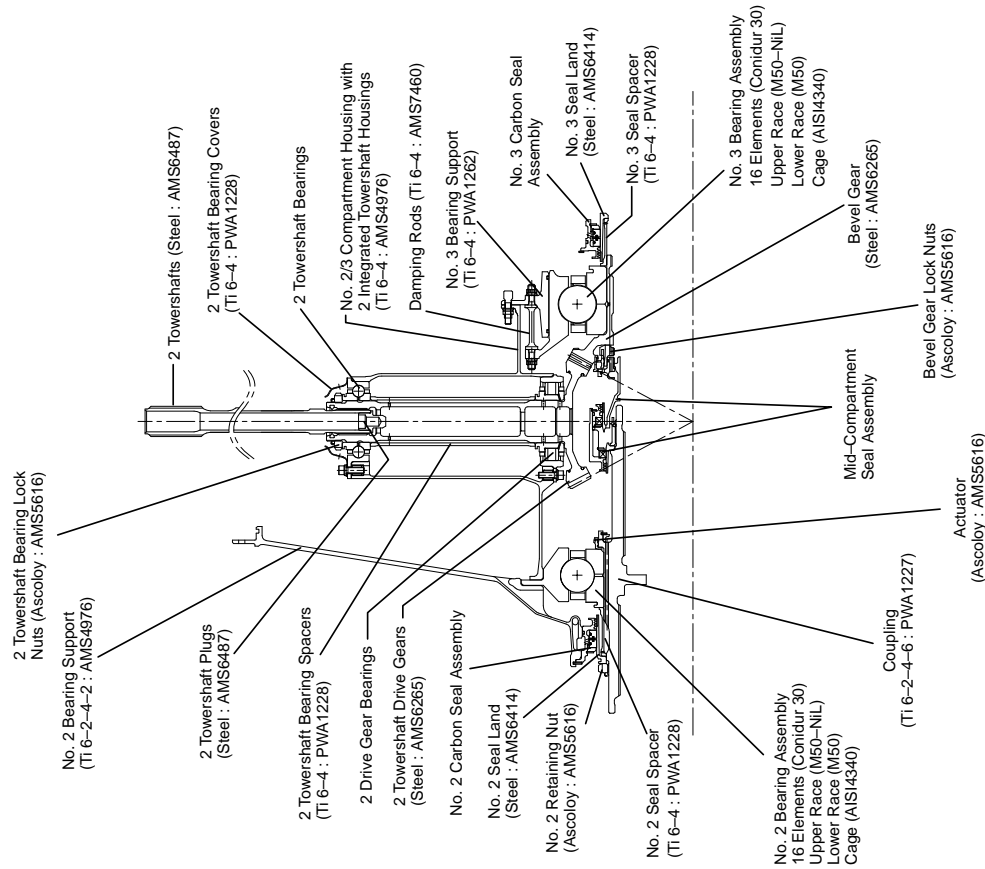
Figure 155. No. 2/3 Bearing Compartment Weight Summary

3.3.2.3 Compressor Aerodynamic and Mechanical Design

In 1997 GEAE initiated mechanical design studies of the compressor rotor structure. The GEAE compressor rotor and stator conceptual/preliminary design specifications were to this point, like most of the turbomachinery components, established by the Preliminary Design organization using the FLOWPATH engine model analysis tool. Detail preliminary design analysis using finite-element methods had not been performed. The core rotor heat transfer transient mission analyses conducted in 1996 and 1997 was used to identify rotor structure temperatures at operating points throughout the mission (Usage Mission 2). The rotor structure was analyzed using ANSYS models and designed to meet HSCT application requirements for burst, creep, and life based on LCF and residual life (crack propagation life). Although on-going engine system level studies had shown that a six-stage compressor might be a better solution based on weight and thrust balance considerations, the detail compressor rotor structure analysis was performed on the five-stage compressor configuration used for the core rotor heat transfer studies. The objective of this study was to improve the fidelity of the compressor rotor design definition, material selection, and weight estimates.

Figure 156 shows the initial five-stage compressor rotor with steady-state temperatures (supersonic cruise operating condition in mission) indicated. The disk and blade materials considered for the compressor rotor structure were as follows:

- IMI834 Titanium: 75°F better creep strength than Ti6–2–4–2 and about the same HCF strength.

- Nickel powder alloys developed under the EPM program for HSCT applications:

  - Subsolvus – LCF strength 10% greater than current production powder alloy. Fracture mechanics 50°F greater than the current production powder alloy.

  - Supersolvus – Fracture mechanics 150°F greater than the current production powder alloy.

A comprehensive preliminary design evaluation of the compressor rotor structure considered the stress/sizing criteria used for the disk (blisk) rim, web, bore, and attachment spacer arms. The stress concentration areas at the bolt holes and flowpath secondary bleed holes were also evaluated. Figure 157 shows results for the preliminary model stage 2 and 3 blisks. This preliminary study identified the critical sizing areas and developed the appropriate criteria for the compressor rotor structure.
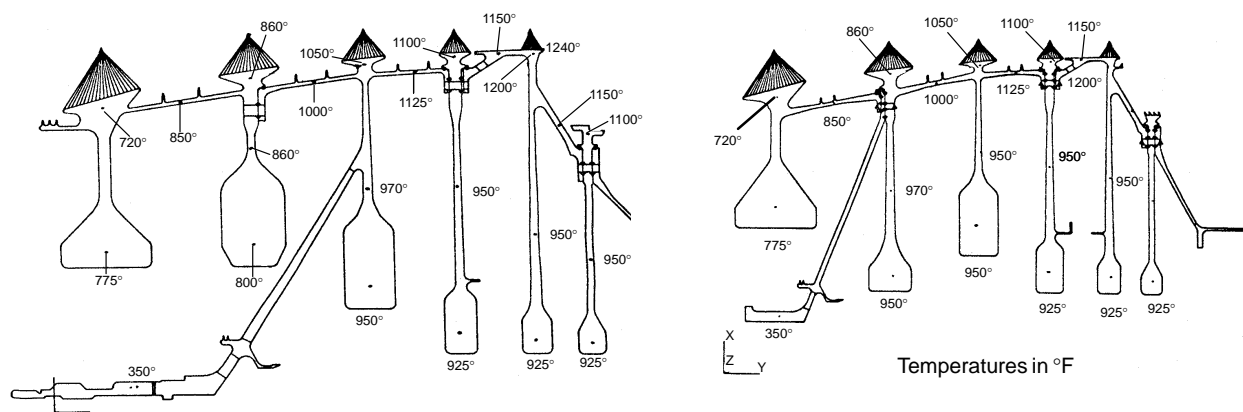
Figure 156.   Intial Model, 5-Stage Compressor Rotor

Stage 2 and 3 Nickel Power
Hoop Stress, Mechanical Only

- LCF >10,000 cycles

- Web Sized by Radial Burst

- Bore Stress Limited to 140 ksi for Residual Life

- $\overline{\sigma}_{Hoop}$ = 100 ksi
- Burst Margin 0.2%

- $\overline{\sigma}_{Hoop}$ = 80 ksi
- 75 ksi is 0.2% Creep Limit
- 30% Burst Margin
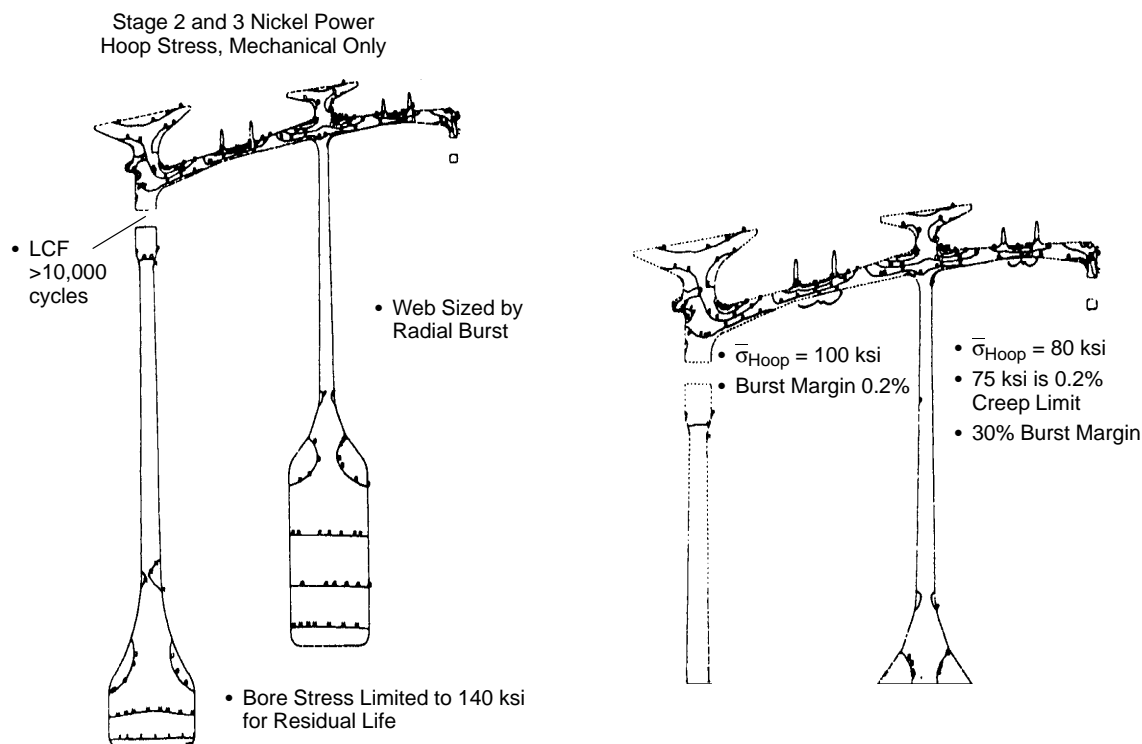
Figure 157. Preliminary Model, Stage 2 and 3 Blisk

The study also determined the selection of IMI834 material for Stage 1 and the selection of an advanced EPM nickel powder alloy for stages 2 through 5. These selections resulted in the forward shaft and attachment changes shown in Figure 156.

During the study, the material selection and component configuration were evaluated extensively to ensure that they would meet requirements. Detailed weight calculations were not performed until the selection of the final system-level compressor rotor configuration.

Weight reduction studies were performed on preliminary design FLOWPATH models to evaluate system-level changes such as compressor exit Mach numbers (0.30, 0.35, 0.40) and compressor configuration types (five stage versus six stage). These studies were used to determine the lightest compressor solution while considering overall system impact on parameters such as engine weight, length, performance, and core-rotor thrust balance (bearing life).

The preliminary design effort for the GEAE compressor was put on hold until after the annual CPC Systems Mechanical Design Review in October 1997. Following this review, plans were made for the 1998 work, which included preliminary design to support a full-scale demonstrator engine program. This program was scheduled to start in the middle of 1999. The demonstrator engine program made it necessary for GEAE and P&W to jointly develop a common engine configuration and assign component responsibilities to each company.

The original work assignment of late 1997 gave fan and compressor design responsibility to P&W and turbine responsibility to GEAE. This was consistent with the mechanical design study efforts performed up to this point in the program. A change in late 1997 assigned the compressor study to GEAE and placed additional emphasis on the need to execute a detailed preliminary design for the

compressor in 1998. Figure 183 (page 216) shows the common engine configuration concept and, the design lead assignments, and the engine specifications required.

The scope of work for the 1998 GEAE compressor aerodynamic and mechanical design studies was defined as follows:

- Develop a compressor mechanical configuration to meet component and system requirements

- Define compressor mean-line aerodynamics including end-wall estimates (to support the LPT secondary flow cooling circuit trade studies)

- Conduct a weight study of the five-stage compressor design versus the six-stage compressor design

The results of the compressor five-stage versus six-stage study are shown in Figure 158 and Table 68. The figures show a 258-lbm weight advantage of the six-stage compressor. Table 69 shows the aerodynamic preliminary design that was established for the compressor, and Figure 159 shows stage pressure and temperature profile estimates that support the secondary flow configuration shown in Figure 160.

The compressor rotor blisks were designed to achieve the life requirements shown in Figure 161. The results of these evaluations are as listed. It was determined that the subsolvus EPM advanced nickel disk alloy selected for the stage 2–6 blisks exhibited superior HCF properties when used for the blisk airfoils. Figure 162 illustrates the advantages of the subsolvus material. Figures 163 through 164 define the resulting compressor mechanical configuration, and the material selections. This compressor design provided the best solution combining the component and system requirements for the HSCT 3770.54 mixed-flow turbofan. The key features were as follows:

- Bolted blisks
  - Projected inertia weld fracture mechanics properties at elevated temperatures limit weld use
- Material forging size limits configuration to one stage per blisk
- Variable vanes
  - IGV, stages 1 and 2
  - Aerodynamic analysis shows three variable stages required, but not by a significant margin
    - Primarily for starting
    - Future testing may reduce variable stages to 2
  - Vane actuator mounted external, typical of mixed-flow turbofan
- Low-α compressor case
  - Split forward case for maintainability
  - 360° aft case for clearance control
- Forced-vortex air tube
  - Prevents vortex whistle
  - Lowers turbine cooling air temperature

5 Stage Design   **6 Stage Design**

R 18.2   **R 15.1**
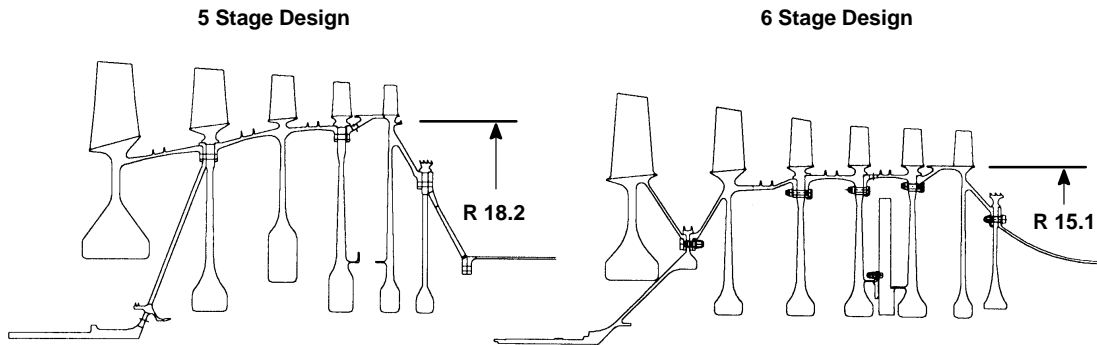
Figure 158.   Compressor Rotor Configurations, 5-Stage Vs 6-Stage

Table 68.   Compressor Weight Study, 5-Stage Vs. 6-Stage   *Six-stage compressor rotor weighs 258 lb less than the five-stage (same rpm for both designs).*

		6 Stage HPC				5 Stage HPC		
		Weight, lbm				Weight, lbm		
Stage	Material	Disk	Blades	Total		Disk	Blades	Total
1	IM1834	119	24	143		190	27	217
2	Subsolvus	172	23	195		181	21	202
3	Subsolvus	117	10	127		309	8	317
4	Subsolvus	138	8	146		203	7	210
5	Subsolvus	138	8	146		187	4	191
6	Subsolvus	116	6	122				
Total		**800**	**79**	**879**		**1070**	**67**	**1137**

Table 69.   Compressor Aerodynamic Description

HPC T/O (Design Point)

- Corrected Flow   171.5 lb/s
- Corrected RPM   6638
- Corrected Tip Speed   1158.5 ft/s
- Pressure Ratio   5.27
- Adiabatic Efficiency   0.890
- Inlet Radius Ratio   0.710
- Exit Radius Ratio   0.865
- Inlet Tip Radius   20.0 in.

- High Confidence Compressor Aero Design
  - Fliight Mach No. & T_3 Limit Results in low HPC Pressure Ratio
  - Corresponding Stage Loading is within Experience Range
  - 25% Stall Margin

Stage	Rotor Aspect Ratio	Stator Aspect Ratio	Rotor Pitch Solidity	Stator Pitch Solidity	Stage Pressure Ratio
1	1.81	2.04	1.40	1.40	1.453
2	1.88	1.90	1.40	1.40	1.433
3	1.91	1.80	1.40	1.40	1.339
4	1.62	1.74	1.40	1.40	1.252
5	1.38	1.68	1.40	1.50	1.230
6	1.32	1.44	1.40	2.30	1.223

Compressor Exit (Plane 3)
Pressure and Temperature Profiles

HSCT Compressor Exit (Plane 3)
Total Pressure Profile

HSCT Compressor Exit (Plane 3)
Total Temperature Profile

Immersion

0.94 0.96 0.98 1 1.02 1.04 1.06
Normalized Total Pressure

0.94 0.96 0.98 1 1.02 1.04 1.06
Normalized Total Temperature

- Profiles support multi-pass diffuser aerodynamics
- End wall losses cause pressure and temperature profile

Rotor 4 Exit
Pressure and Temperature Profiles

HSCT Compressor Rotor 4 Exit
Total Pressure Profile

HSCT Compressor Rotor 4 Exit
Total Temperature Profile

0.94 0.96 0.98 1 1.02 1.04 1.06

0.94 0.96 0.98 1 1.02 1.04 1.06

- Profiles developed to support Stage 4 bleed for turbine cooling air
- Total pressure profile per GE experience
- End wall losses cause pressure and temperature profile

Figure 159.   Exit Pressure and Temperature Profiles

Customer Bleed

Seal
Pressurization

Stage 4 Rotor Bleed –
Turbine Cooling Air

Fan Shaft Cooling Air

Vent Air

Aft Sump Pressurization
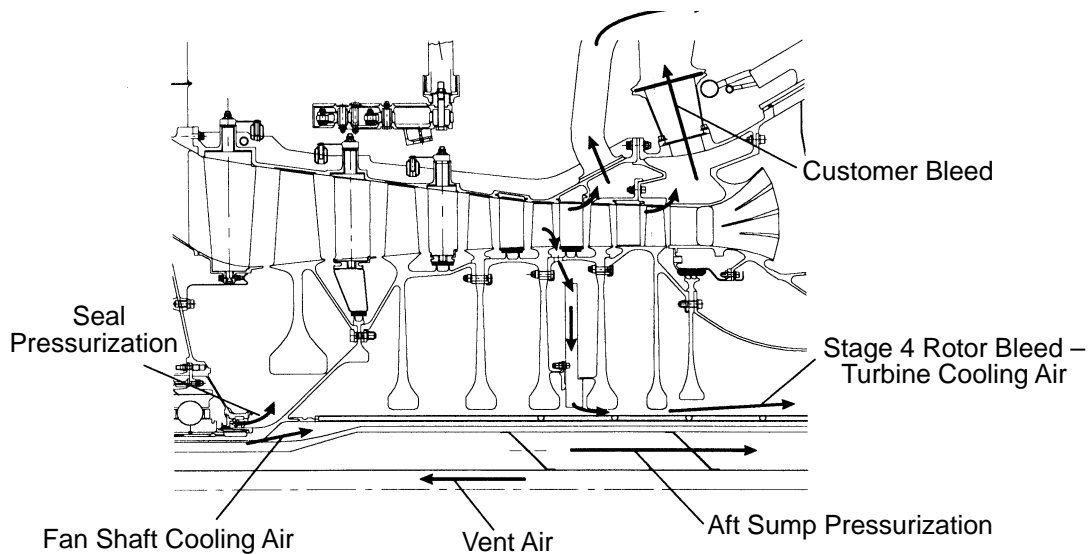
Figure 160.   Compressor Secondary Flow Configuration
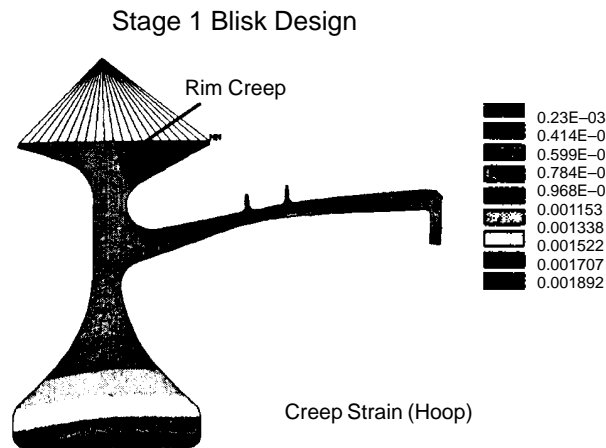
Stage 1 Blisk Design

Rim Creep

▮	0.23E–03
▮	0.414E–03
▮	0.599E–03
▮	0.784E–03
▮	0.968E–03
▮	0.001153
▨	0.001338
▯	0.001522
▮	0.001707
▮	0.001892

Creep Strain (Hoop)

Requirements

- Flight Cycles   5000
- Burst Margin   125%
- Total Operating Hours   20,000

*JAR-E-840 Compressor & Turbine Rotor Integrity Tests

Results

- Material: IM1834
- Stage 1 Bore Sized to Limit Rim Growth
- Flange Sized by LCF
- Burst Margin: 131%
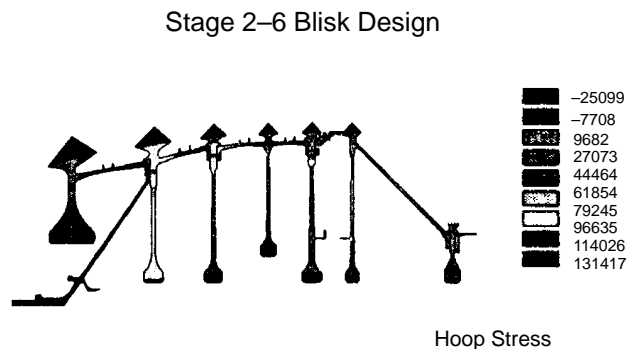
Stage 2–6 Blisk Design

▮	–25099
▮	–7708
▨	9682
▮	27073
▮	44464
▨	61854
▯	79245
▮	96635
▮	114026
▮	131417

Hoop Stress

Requirements

- Flight Cycles   5000
- Burst Margin   125%
- Total Operating Hours   20,000

*JAR-E-840 Compressor and Turbine Rotor Integrity Tests

Results

- Material: EPM Disk Allo (Subsolvus)
- Bores Sized by Fracture Mechanics
- Flanges Sized by LCF

Figure 161.   Compressor Rotor Blisk Designs   *Meet life requirements.*
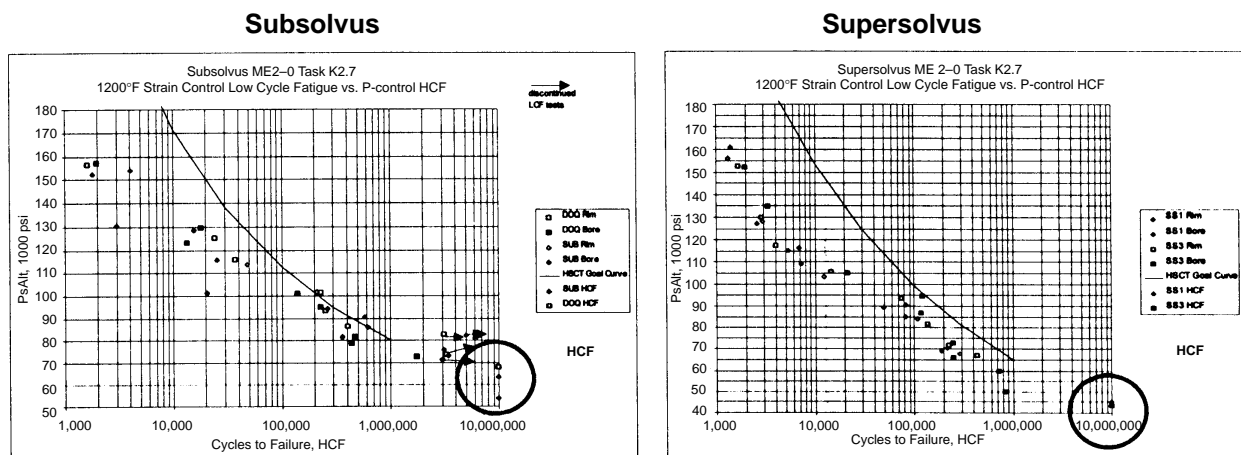
Figure 162.   Compressor Blisk/Blade HCF Material Properties   *Subsolvus material HCF properties are 40% better than supersolvus; that is, blade vibratory endurance capability is better with subsolvus.*
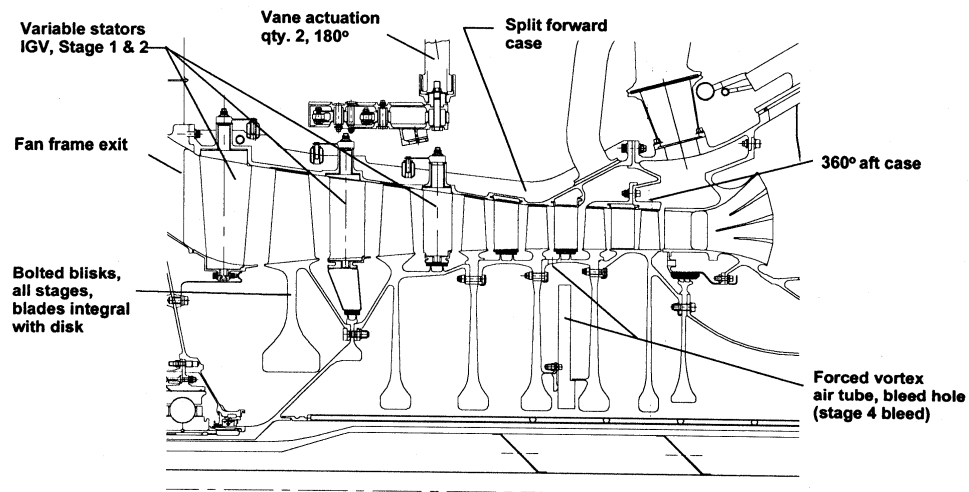
Figure 163.   Compressor Mechanical Configuration
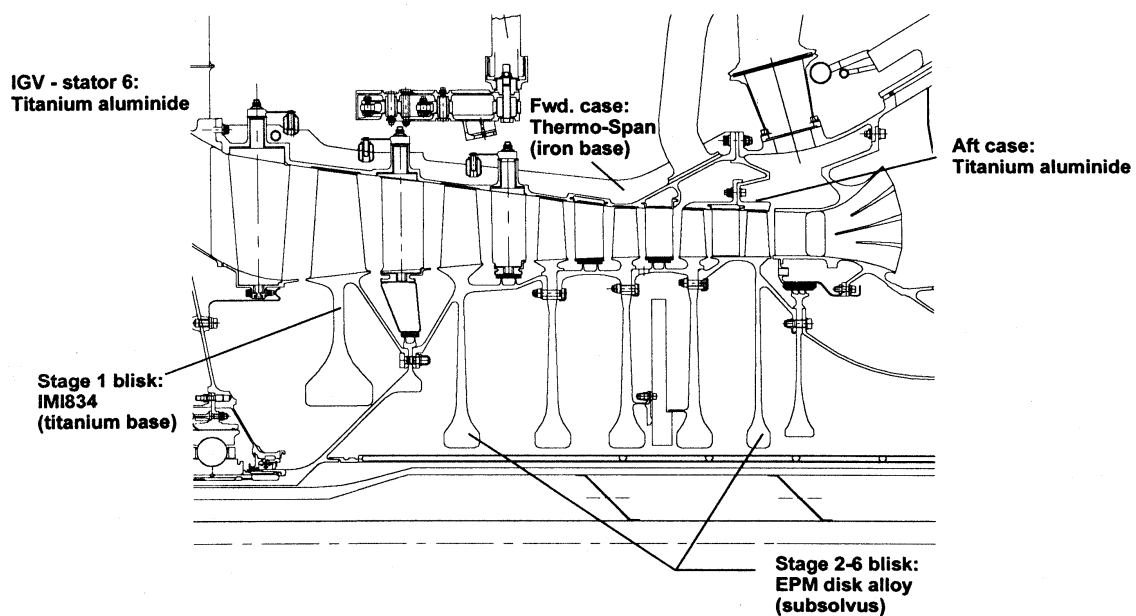
Figure 164.   Compressor Material Configuration

3.3.2.4 Turbine Aerodynamic, Cooling, and Mechanical Design

The GEAE turbine design effort to develop component configurations began in 1996. Prior to this, turbine definition had been captured in the FLOWPATH model used by the GEAE Preliminary Design organization to model engine/nozzle propulsion systems for use in the HSCT airplane system trade studies. This component definition was needed to develop an engine cross section to study system requirements for secondary flow, thrust balance, engine dynamics, weight, etc. Figure 165 shows the preliminary turbine module in the 3770 engine cross section.
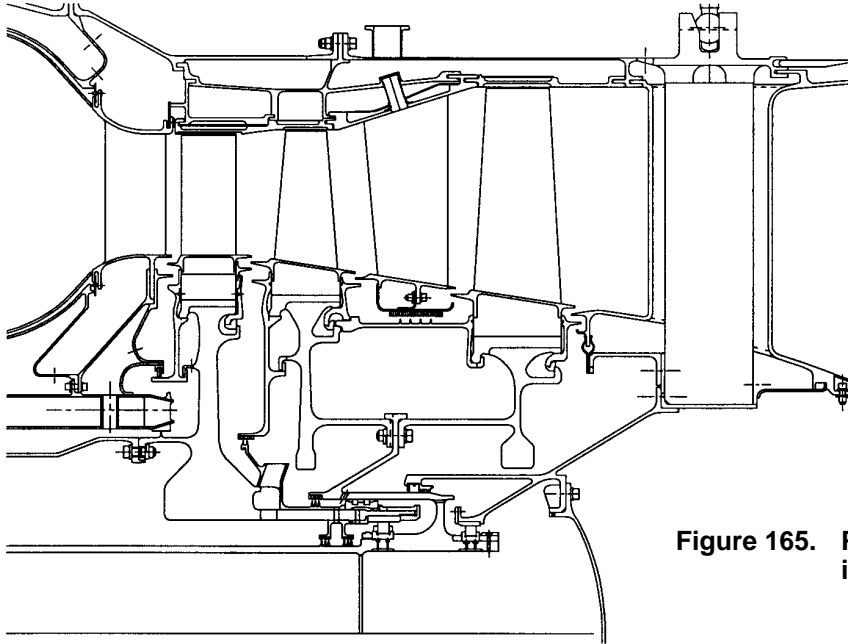
Figure 165.   Preliminary Turbine Module in 3770 Engine

The turbine aerodynamic design was based on the mission point requirements in the Usage Mission 2 definition as recorded in Coordination Memo GE96–057–S, dated April 19, 1996 and titled "HSCT Preliminary Usage Data for the 3770.54 Common Design Engine." Table 70 lists cycle requirements for takeoff, subsonic cruise, and supersonic cruise mission points for the high-pressure and low-pressure turbines.

Rotor thrust loads in general are greatest at takeoff, although HPT loading remains relatively constant over most significant operating conditions. The low-pressure turbine experiences the highest aerodynamic loading at subsonic cruise. Thus, subsonic cruise is considered to be the aerodynamic design point for the LPT. Since, however, a significant portion of each mission is spent at supersonic cruise, that leg must also be considered in the aerodynamic design. Supersonic cruise is also where the engine encounters the highest operating temperatures, so that leg is considered to be the heat transfer design point.

Turbine cooling analysis was performed based on the turbine cooling flow trends specified in Coordination Memo PW95–114–T, dated October 19, 1995, titled "Turbine Cooling & Efficiency Trends for 1996 Systems Studies." That Coordination Memo references the Enabling Propulsion Materials (EPM) Properties Document used for the blade materials and defines the current turbine cooling methods used in both the P&W and GEAE design configurations.

Table 70. Cycle Requirements for Takeoff and Cruise

Parameter		Mach 0.36 Sea Level, +18°F Day	Mach 0.9 34,000 ft, Std Day	Mach 2.4 55,560 ft, Std Day
HPT	T_{41}, °F	2570.0	1721.8	2772.0
	T_3, °F	942.3	623.3	1200.0
	W41GR	87.29	88.32	87.42
	$\Delta H/T$	0.0533	0.0530	0.0529
	$N/\sqrt{T}$	149.36	148.34	149.95
	η	90.98	90.94	91.09
	P_4/P_{49}	2.57	2.60	2.54
LPT	T_{49}, °F	1974.8	1265.3	2158.6
	W49GR	223.38	226.99	222.34
	$\Delta H/T$	0.0436	0.0507	0.0417
	$N/\sqrt{T}$	104.84	109.26	102.67
	η	91.73	91.57	91.60
	P_5/P_{49}	2.18	2.52	2.09

Figure 166 shows the HPT vane inlet radial temperature profile used in this study. This type of temperature profile is desirable for turbine blade/vane life but may not be achievable with the combustor designs needed to meet the emissions goals set for the HSCT.

Aerodynamic analyses of the turbine airfoils were conducted using the data described in the cooling memo above. Figure 167 shows the airfoil counts, aerodynamic flowpath, and radial and axial geometry that resulted from this analysis.

Key Turbine Characteristics

Table 71 details the key aerodynamic characteristics of the high-pressure and low-pressure turbine modules at the three key mission points: takeoff, subsonic cruise, and supersonic cruise. Most of the HPT characteristics change very little in the flight conditions listed. One exception is rotor speed; RPM varies together with related tip speed. Another exception is the parameter $AN^2 \times 10^9$. That parameter (annulus area times speed squared) was limited to 45×10^9 at supersonic cruise. Values for the LPT stage loading, exit Vz/U, exit swirl, and exit Mach number all have their highest values at subsonic cruise. Exit swirl varies from 9.5° to 20.6° between supersonic cruise and subsonic cruise. All these variations must be considered when designing the turbine frame.

Figures 168 and 169 show the turbine airfoil profiles that resulted from the 1996 3770.54 MFTF aerodynamic study. These airfoils are preliminary and were used to determine cooling flows, metal temperatures, and stresses in heat transfer and mechanical studies. The cooling flows listed in Table 72 were the status flows selected for the 1996 studies as specified in Coordination Memo PW95–114–T. These status flows were used in the aerodynamic analyses that included the turbine pitchline performance prediction program (TP3 or TP^3) and the circumferentially averaged flow determination (CAFD) program.
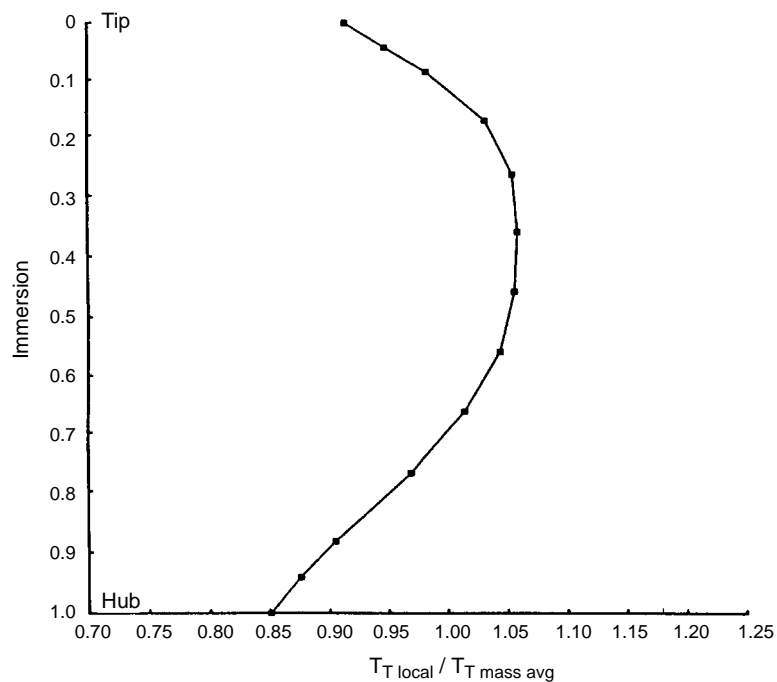
Figure 166.   HPT Vane Inlet Temperature Radial Profile
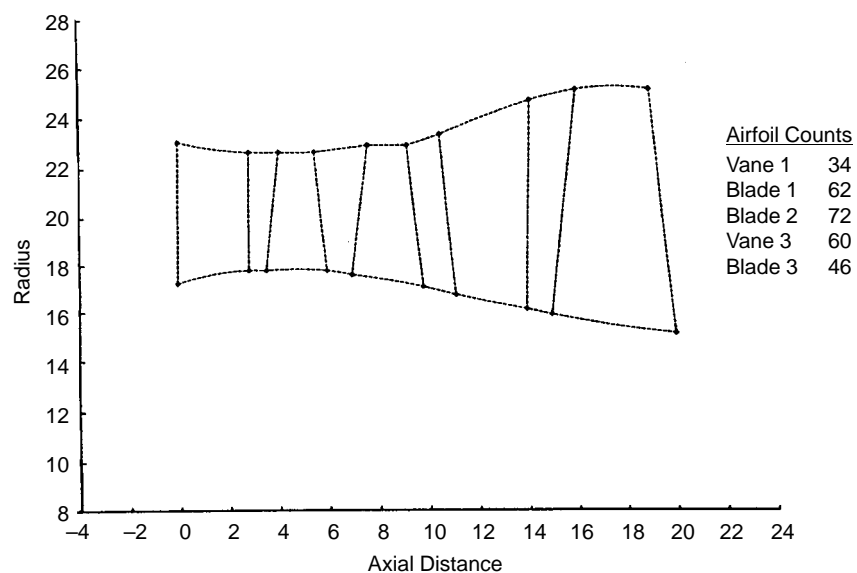
Figure 167.   Flowpath Defined by the Turbine Aerodynamic Analyses

Table 71. Turbine Aerodynamic Characteristics

	Parameter	Mach 0.36 Sea Level, +18°F Day	Mach 0.9 34,000 ft, Std Day	Mach 2.4 55,560 ft, Std Day
HPT	RPM	8221	6928	8524
	$AN^2(x10^{-9})$	41.8	29.7	45.0
	Tip Speed, ft/s	1626	1370	1686
	Flow Function	87.70	88.32	87.5
	Pressure Ratio	2.53	2.59	2.51
	Stage Loading	0.94	0.97	0.93
	Vz / U, exit	0.77	0.79	0.76
	Efficiency, %	90.8	90.9	91.1
	Pressure Reaction	0.57	0.58	0.57
	Exit Swirl, Degrees	38.6	39.1	38.4
	Exit Mach No.	0.63	0.65	0.63
	Mrel, exit	1.15	1.16	1.14
LPT	RPM	5173	4538	5254
	Pressure Ratio	2.01	2.46	1.93
	Avg Stage Loading	0.70	0.81	0.69
	Vz / U, exit	1.0	1.23	0.98
	Efficiency, %	92.3	92.0	92.2
	Swirl, exit	10.9	20.6	9.5
	Exit Mach No.	0.44	0.61	0.42

HSCT 3770.54
Turbine Aero Analysis
HPT Vane

HSCT 3770.54
Turbine Aero Analysis
HPT Blade

Figure 168. Aerodynamic Analysis of HPT Vane and Blade

HSCT 3770.54
Turbine Aero Analysis
LPT Stage 1 Blade

HSCT 3770.54
Turbine Aero Analysis
LPT Vane

HSCT 3770.54
Turbine Aero Analysis
LPT Stage 2 Blade

Figure 169. Aerodynamic Analysis of LPT Vanes
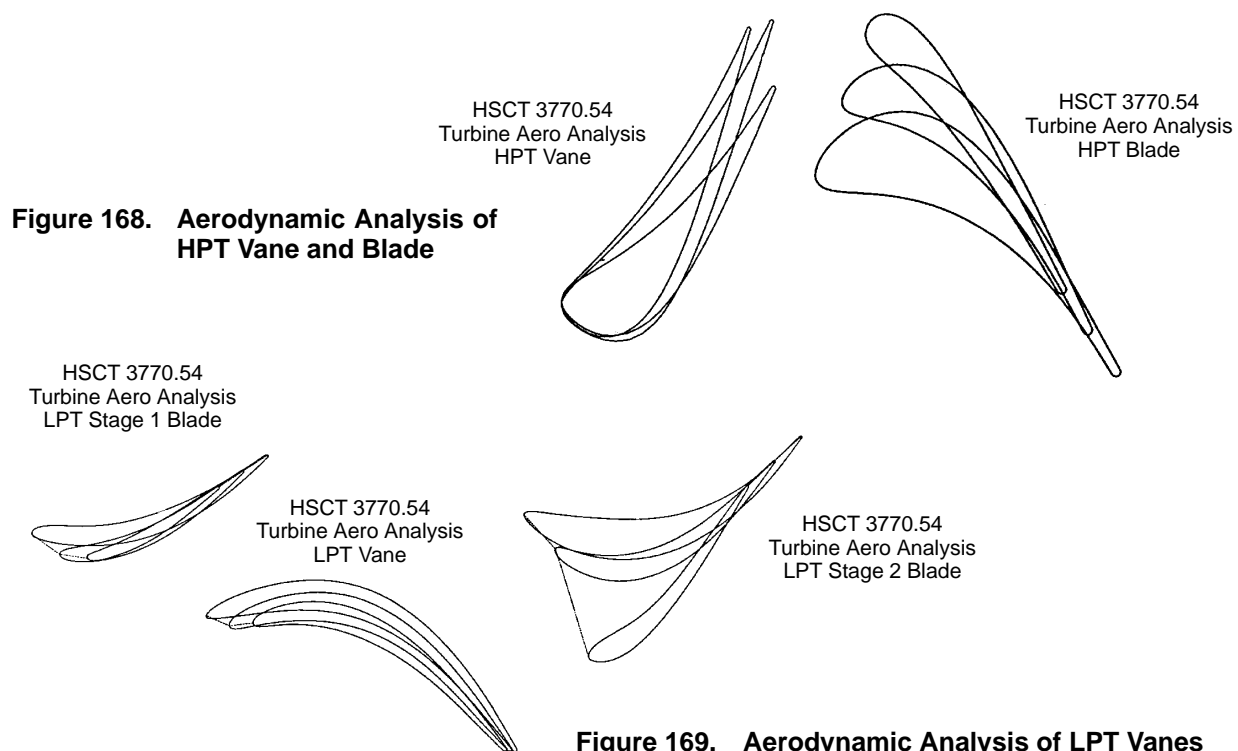
Table 72. Cooling Flows in Turbine Aerodynamic Analysis

Flow	%W$_{25}$
Vanes	9.322
Bands	1.45
Total HPT Nonchargeable	10.772
Vane Aft of Throat	1.138
Bands Aft of Throat	0.48
Blades	5.48
Shroud	0.64
Purge and Leakage	0.98
Total HPT Chargeable	8.718
Stage 1 Blades	2.81
Stage 2 Vanes	1.051
Stage 2 Blades	0.75
Shrouds	0.66
Purge and Leakage	2.009
Total LPT Chargeable	7.28

Analyses indicate that the predicted efficiencies from turbine prediction programs are in reasonable agreement with those used in the cycle deck.

Turbine Mechanical Design

Completion of the aerodynamic design activated the mechanical design approach with airfoil design conditions as shown in Figure 170. In 1996 design recommendations were made concerning the type of system material and the cooling-circuit technology necessary to meet the HSCT strength and life goals. For the HPT and LPT vanes, the EPM program recommended an advanced, single-crystal nickel-base alloy.

It was also proposed that the vanes should have a 0.010-inch EPM thermal-barrier coating. The HPT vanes were expected to require state-of-the-art vane cooling using film-cooled flowpath surfaces. The LPT vanes were expected to require both conventional vane cooling and film cooling.

The HPT blade and the LPT stages 1 and 2 blades were also expected to require the use of EPM advanced single-crystal nickel alloy. It was expected that the EPM TBC system would be necessary for the airfoil and platform surfaces of the HPT blade and for the airfoil surfaces of the LPT blades.

Later analysis determined that this HPT blade design with advanced cooling-circuit features would be able to meet design requirements for stress rupture, etc. with the specified cycle cooling flows. It was thought that the LPT blades with state-of-the-art cooling-circuit features would be challenged to meet the design requirements with the specified cycle cooling flows.

This conceptual design assessment identified additional thermal and mechanical design and analyses tasks needed to produce airfoil designs that could satisfy the strength and life requirements. It
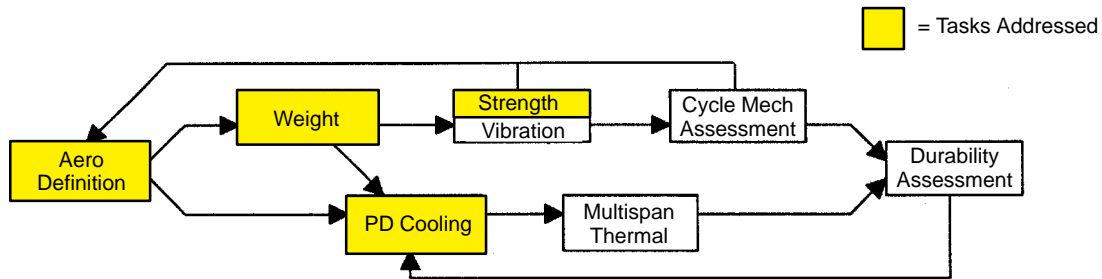
Parameter	Design Conditions				
	HPTV	**HPTB**	**LPTB1**	**LPTV**	**LPTB2**
Design Time (hr)	9000	9000	9000	9000	9000
% Wc	7%	3.8%	0.57%	13%	0.62%
TiTC (°F)	3546/1240	2794/1242	2279/1003	2162/1048	1936/1048
T_{bulk} capable (°F)	1700	1682	1827	1820	1734
Φ_{bulk}	0.80	0 .72	0.35	0.31	0.23
RPM	–	8524	5254	–	5254
No. of Airfoils	34	62	72	60	46

Figure 170. Mechanical Design Approach and Conditions

appears that additional design work is required for blade attachment (to disk) sizing and blade vibration criteria — primarily for the high-aspect-ratio, low-camber, LPT blades.

The objectives of the 1997 turbine aerodynamic, cooling, and mechanical design studies were to establish a preliminary design that would meet the strength and life requirements of the HSCT mission and to support the program weight reduction initiatives. The weight reduction initiatives were developing as the mission and cycle definition became more defined and the propulsion system components evolved due to better defined application requirements. The following approach was required to ensure that airfoil designs will meet the performance and cooling (life) design objectives:

- Turbine Pitch-Line Performance Program
  - Provides general turbine characteristics
  - Loss model, cooling flow prediction

- Circumferentially Averaged Through-Flow Analysis
  - Radial variations of angle, temperature, pressure loss, flow blockage, lean

- Airfoil Generator
  - Designed on streamlines established by through-flow analysis
  - Coupled with quasi-3D blade-to-blade solver

- 3D Viscous Analysis
  - Includes addition of cooling flow

- Airfoil Cavity Generator
  - Establishes number and size of internal cavities

- Internal Cooling Flow Model
  - Determines cooling flow and external metal temperatures
- 3D ANSYS
  - Temperature and stress

The mechanical design portion of the 1997 effort is described in a later subsection.

Cycle Requirements

The 1997 turbine cycle requirements and the key turbine design parameters used were the same as was shown in Tables 70 and 71. Execution of the detailed aerodynamic and cooling design approach presented here resulted in the airfoil designs described in Figure 171. The efforts completed to support these results are also illustrated in the figure. Note that the second-stage LPT changed to a design with 88 tip-shrouded blades as compared to the 1996 conceptual design which had 46 nonshrouded blades. This change was the result of a significant engine weight reduction activity in 1997. Several component and system approaches were evaluated by using the Preliminary Design organization FLOWPATH model as the initial-assessment tool. This weight reduction activity is described in Subsection 3.3.2.7.

Turbine Cooling

Where possible, the design feasibility of the weight reduction concepts was developed with preliminary component design work. Figure 172 shows the flowpath changes for the 1997 shrouded, second-stage LPT rotor design together with the estimated system level engine weight reduction. Figure 173 details the cooling flow results compared to the cycle values assumed. The cycle assumptions were excellent, and the actual design can be accomplished with a slightly lower cooling flow than was assumed.

Airfoil flows were calculated; shroud and band flows were scaled from existing designs. Leakage flows were assumed. The cooling flow sources for the LPT at this point were the compressor second-stage stator (piped to LPT vane and second-stage blade) and the compressor fourth-stage rotor (bore flow to LPT first-stage blade). Figure 174 shows the maximum temperature contours developed during 3D analysis and includes the cooling flow addition at the inner flowpath surface of the HPT vane. These preliminary results validate the acceptability of the design and would be used in the detail design to define the placement of the vane inner-flowpath, surface-film-cooling holes. Similar analyses were conducted to determine the outer flowpath temperatures and the vane surface temperatures.

Figure 175 shows the inlet and exit temperatures of the HPT vane based on 3D analysis with the cooling flow included. The graph also shows the changes in the radial temperature profile through the vane. The relative temperature profile that was developed from this 3D analysis was used in the blade cooling design. Figure 176 shows maximum metal temperatures for the HPT blade as developed by the 3D analysis. These temperatures are acceptable for the design requirements established.

Blade Analysis

Figure 177 shows the relative Mach number contours of the HPT blade at the blade pitch. This display shows evidence of the high-reaction design with low inlet Mach numbers and supersonic exit values. The LPT blades were analyzed in a similar manner to that used for the HPT airfoils.

HPTV1 Design Status

- Configuration
  - Nb = 34
  - EPM Alloy + TBC Materials
  - 3D Aerodynamics
  - Cooling 7.0% Wc (CDP)
  - T_{bulk} at pitch 1623°F
  - T_{max} at pitch 1885°F
  - Life limiting mechanism
    - Oxidation
    - Thermal mechanical fatigue
- Effort Completed
  - Preliminary Aero Design
  - Preliminary Cooling Circuit Design
  - 3D Viscous Euler Analysis

HPTB1 Design Status

- Configuration
  - Nb = 62
  - EPM Alloy + TBC Materials
  - Cooling 4.0% Wc (CDP)
  - T_{bulk} at pitch 1661°F
  - T_{max} at pitch 1999°F
  - Life limiting mechanism
    - Oxidation – TBC Bond Interface
    - Creep Rupture
- Effort Completed
  - Preliminary Aero Design
  - Preliminary Cooling Circuit Design
  - 3D Viscous Euler Analysis
  - P/A Weight + T_{bulk} Required

LPTB1 Design Status

- Configuration
  - Nb = 72
  - EPM Alloy + TBC Materials
  - Cooling 1.2% Wc (Stage 4)
  - T_{bulk} at pitch 1773°F
  - T_{max} at pitch 1911°F
  - Life limiting mechanism
    - Oxidation – TBC Bond Interface
    - Creep Rupture
- Effort Completed
  - Preliminary Aero Design
  - Preliminary Cooling Circuit Design
  - Prerliminary 3D FEM Vibration
  - P/A Weight + T_{bulk} Required

LPTB2 Design Status

- Configuration
  - Nb = 85
  - EPM Alloy
  - Cooling 1.2% Wc (Stage 2)
  - T_{bulk} at pitch 1685°F
  - T_{max} at pitch 1836°F
  - Life limiting mechanism
    - Creep
    - Creep Rupture
- Effort Completed
  - Preliminary Aero Design
  - Preliminary Cooling Circuit Design
  - Prerliminary 3D FEM Vibration
  - P/A Weight + T_{bulk} Required

Figure 171. Turbine Airfoil Design Status

(Solid) HSCT 3770–54 Shrouded LPT Blade 2
(Dashed) HSCT 3770–54 Status

Shrouded Stage 2 LPT Rotor Yields
Engine Weight Reduction of 181 lb
– Improved Producibility for LPT R2 Blade

Radial Distance, in

Axial Distance, in
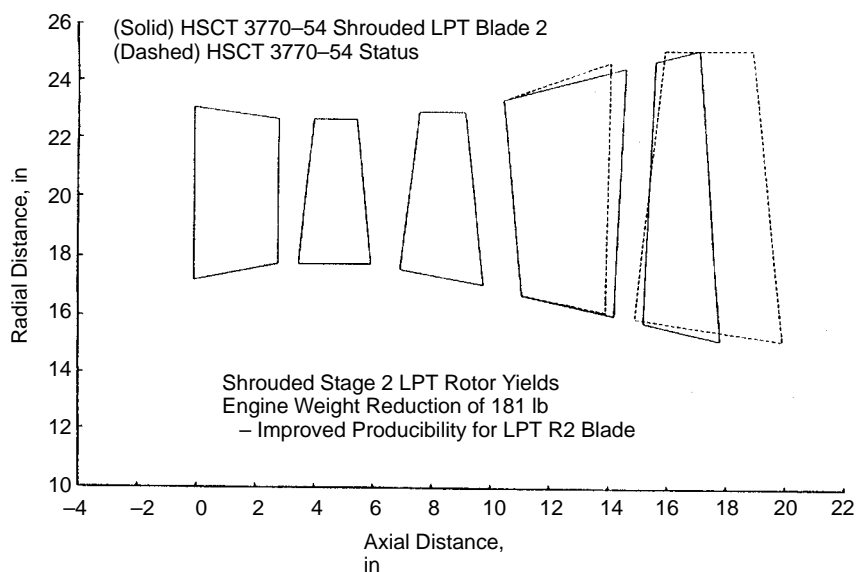
Figure 172. Turbine Weight Reduction Initiative

LPT Cooling and Leakage Flow Summary

All Flows are %W25

	CDP Chargeable	Stage 2 Chargeable	Stage 4 Chargeable
Blade 1			1.20
Shroud (includes lkg.)	0.52		
Leakage			0.37
Cavity Purge		0.50	0.50
Vane		1.15	
Ouier Band and lkg.		0.43	
B1ade 2		1.20	
Shroud (includes lkg.)		0.26	
Leakage		0.37	
Cavity Purge		1.00	
TotaL	0.52	4.91	2.07
			7.50
Cycle			7.35

HPT Cooling and Leakage Flow Summary

All Flows are %W25

	CDP Nonchargeable	CDP Chargeable
Vane	7.70	
Outer Band	1.51	
Inner Band	1.49	
OB Leakage	0.37	0.26
IB Leakage	0.37	0.26
Blade		4.30
Shroud (includes lkg.)		1.20
Leakage		0.37
Cavity Purge		0.50
Total	11.44	6.89
Cycle	12.39	7.10

CDP Nonchargeable	[11.44]	% W_{25}
CDP Chargeable HPT	[6.89]	% W_{25}
CDP Chargeable LPT	[0.52]	% W_{25}
Stage 2 Chargeable LPT	[4.91]	% W_{25}
Stage 4 (Bore) Chargeable LPT	[2.07]	% W_{25}
Total	[25.83]	% W_{25}

Total Calculated Cooling Flow Requirements 1% W_{25} Below Cycle

Figure 173.   Turbine Secondary Flows; Cooling and Leakage Summaries

The temperature scale on the right side of the figure shows (°F):
1300, 1400, 1500, 1600, 1700, 1800, 1900, 2000, 2100, 2200, 2300, 2400, 2500, 2600, 2700, 2800, 2900, 3000, 3100, 3200, 3300, 3400, 3500, 3600, 3700, 3800
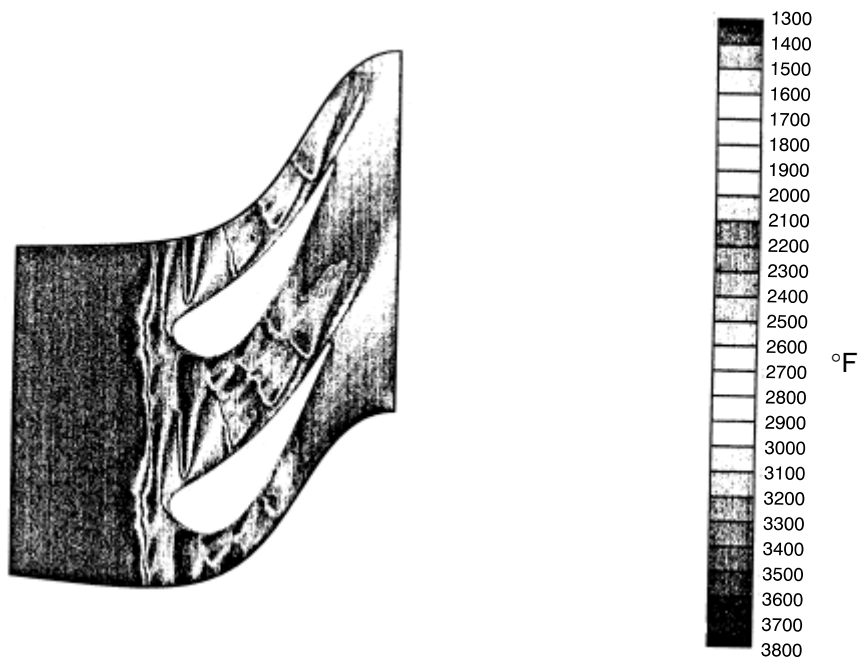
Figure 174.   HPV Viscous Euler Temperature (ABS) Solution

Figure 178 shows the preliminary analysis results of the LPT stage 1 blade. This blade was also characterized as acceptable. The LPT vane analysis was not completed then because the blade designs had higher priority. The LPT vane analyses were conducted subsequently as part of the LPT secondary flow circuit study executed as part of the 1998 effort.

The turbine mechanical design objectives and strength and life requirements established for the 1997 study effort were as follows.

Mechanical Design Objectives and Ground Rules

- Vibrations: No detrimental resonance in the engine operating range

- Containment: Blade failure shall be contained at maximum transient speed

- Cost, Weight, Maintainability: Design to meet target turbine module requirements

- Clearances: Target takeoff and supersonic cruise blade tip clearnace goals TBD

Mechanical Design Life Requirements

- Turbine Blade and Vane Minimum to Inspection

  - Inspection at 10,000 total hours = 4500 hot hours

  - Creep Rupture

  - Oxidation

  - TBC bond coat oxidation and spallation lives based on HSCT mission 2-hour dwell time

- Turbine Rotor Structures
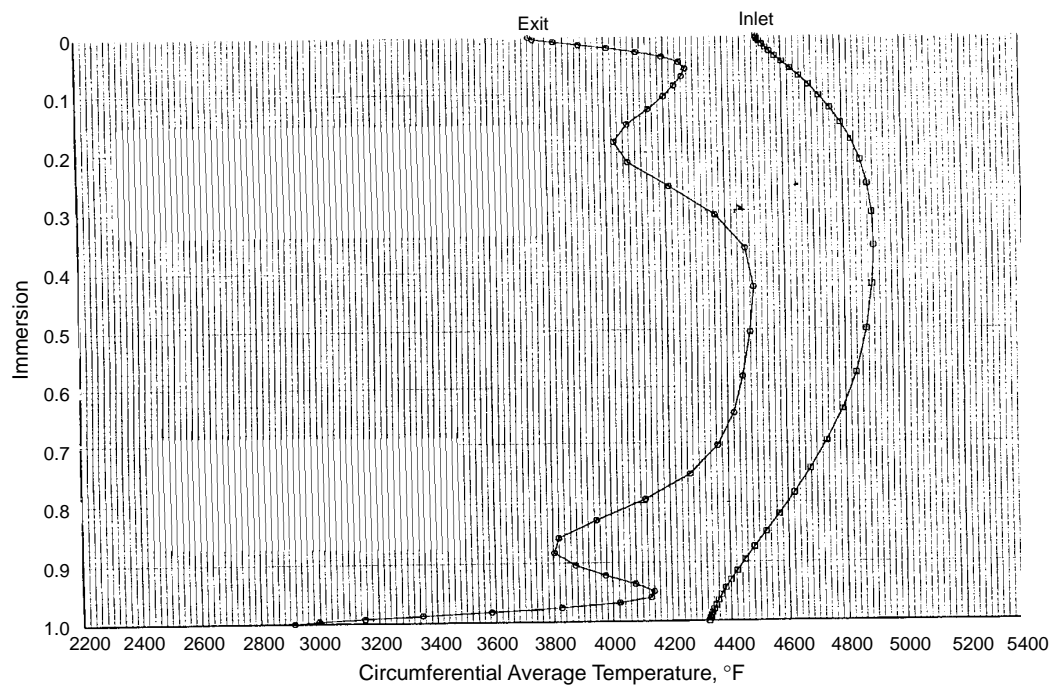
Figure 175.   HPV 3D Viscous Euler Inlet and Temperature (ABS) Solution Versus Immersion
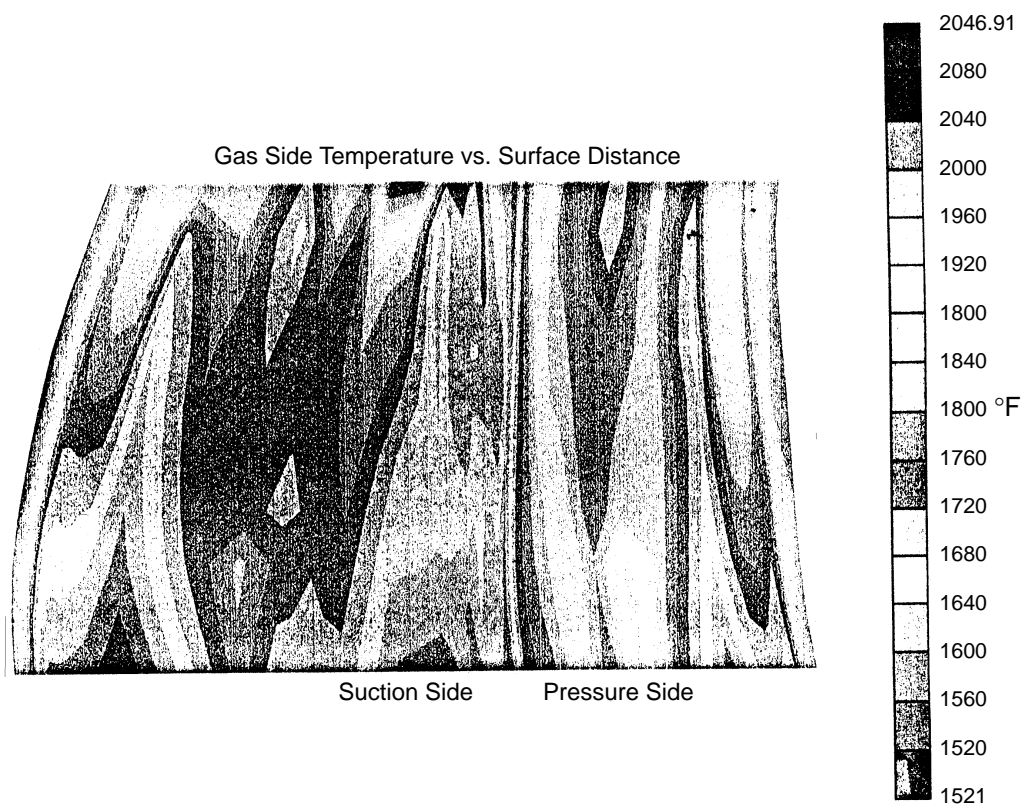
Figure 176.   HPB EPM Alloy/TBC Bond Interface Metal Temperature

0
0
0.57
0.114
0.171
0.228
0.285
0.342
0.399
0.456
0.513
0.57
0.627   °F
0.684
0.741
0.798
0.855
0.912
0.969
1.026
1.083
1.14
1.197
1.254
1.311
1.4231
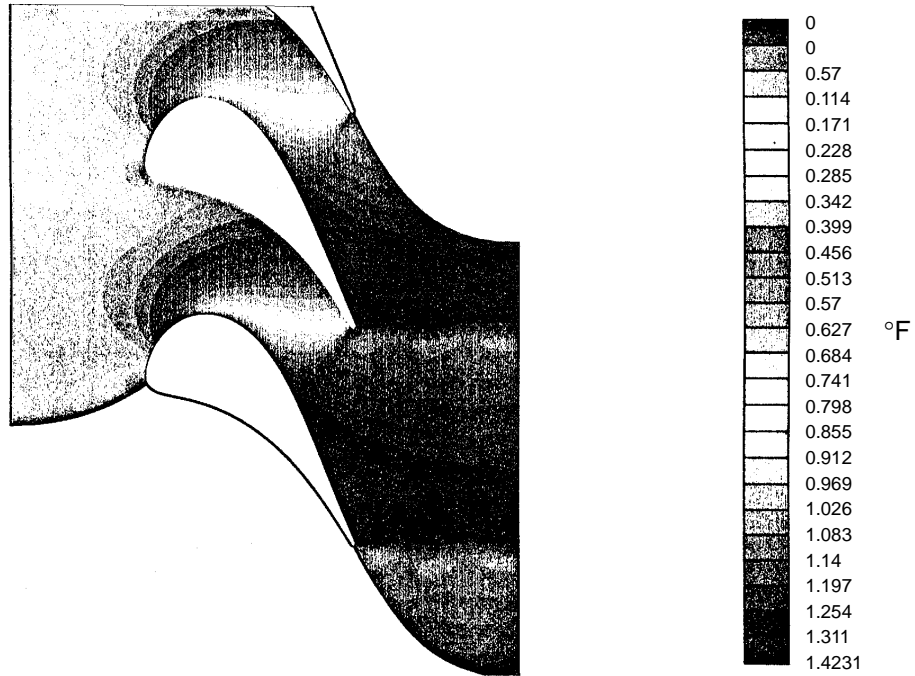
Figure 177.   Viscous Euler Mach Numbers (HPT Blade)

Gas Side Temperature vs. Surface Distance

1953.1
2000
1960
1920
1880
1840
1800
1760
1720   °F
1680
1640
1600
1560
1520
1480
1440
1472.5

Suction Side   Pressure Side

Figure 178.   LPTB1 EPM Alloy/TBC Bond Interface Metal Temperatures

- HPT: 5000 flight cycles; LP: 10,000 flight cycles

- Fracture mechanics life based on GEAE powder metal alloy probabilistic methodologies

- No creep to the extent that operation is impared during service life

- Burst margin 25% relative to redline for HPT and LPT rotors

During this study, the tip-shrouded, second-stage, LPT blade was a design challenge. Figures 179 and 180 show the design criteria considered during blade count selection, including the results of trade studies that dealt with critical shroud bending and dovetail space design issues.

Preliminary design work was also conducted to investigate the key design parameters involved in coupled turbine blade interaction in counterrotating and vaneless low pressure turbine systems. The approach used to assess the HSCT LPT first-stage blade design was as follows.

- GE experience with counterrotating and vaneless LPT systems provides a basis for addressing first-stage blade aeromechanical design balance

- Parameters of interest for coupled turbine blade interaction include:
  – LPT blade frequency placement
  – HPT blade count
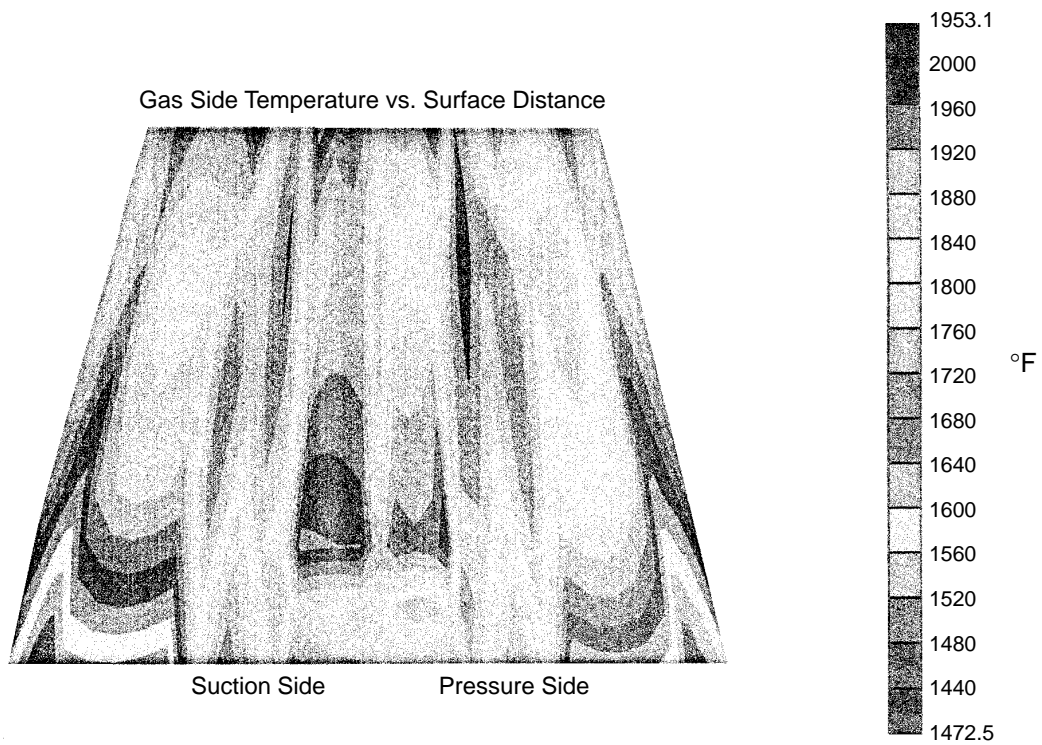 – LPT blade stiffness
  – Operating gaps and shock unsteady loading
  – Airfoil mode shape dependency
  – Mode-dependent damping effectiveness

- GEAE ongoing technology programs addressed analytically predicting and avoiding coupled turbine blade interactions

Figure 181 presents the results of a study performed to assess this design. This aeromechanical assessment established that the interaction would require more detailed design balance work, but the on-going work plus GEAE experience would be able to address the aeromechanical design required.

Secondary Cooling

A preliminary effort was also made to define the secondary flow system cooling flow design used in the HPT stage 1 blade. This effort evaluated the cooling flow and delivery system configuration to determine if it would meet blade life requirements. Before setting the secondary flow system hardware configuration, detailed trade studies must be conducted to balance the system level requirements for cooling flow levels, core rotor thrust balance, system weight, and blade and disk temperature levels. The 1997 turbine aerodynamic, cooling, and mechanical design accomplishments included the following.

- Aero and cooling design updated for 1.05 inlet profile

- Cooling flows analyzed/confirmed for all blades and vanes

- 3D Viscous Euler solutions prepared for HPT vanes and blades including cooling flows

- Cooling flow requirement 1% Wc less than assumed in cycle calculations

Blade Count Design Space
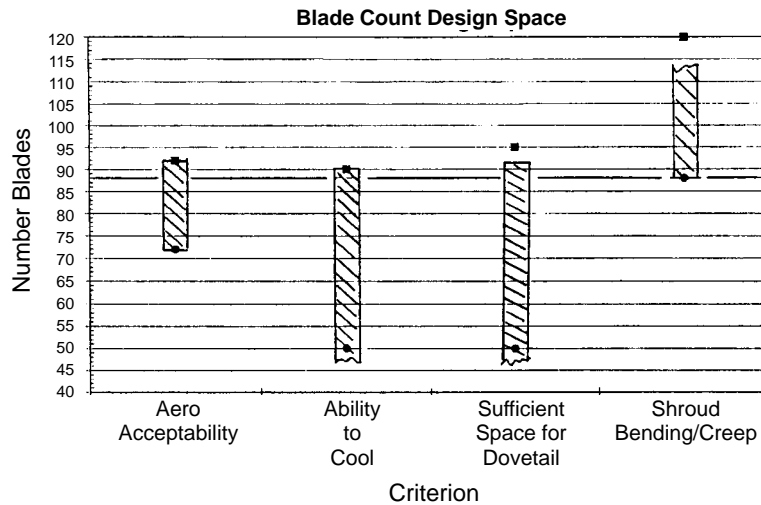
Figure 179.   LPT Second-Stage Blade Tip Shroud Design Trade Study

Shroud Bending / Creep

	Options		
Radius	25.14	25.14	25.14
# Blades	76	86	88
RPM	5400	5400	5400
L circum.	2.078	1.837	1.795
g load	20805	20805	20805
R(L*RPM)^2	3.17E+09	2.47E+09	2.36E+09

Shroud
Bending
Parameter

Baseline Experience:
Keep Parameter < 2.38 E9

Selection

Sufficient Space for Dovetail

HSCT LPT R2 Space for Blade Dovetail,
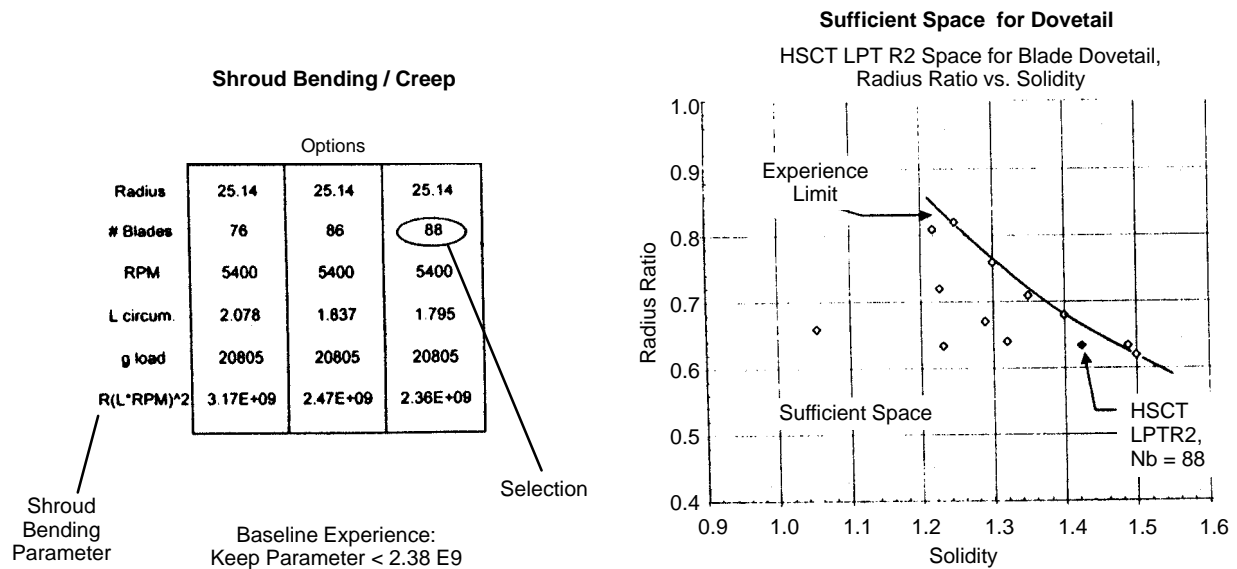Radius Ratio vs. Solidity

Figure 180.   LPT Second-Stage Rotor Tip Shroud Design Trade Study
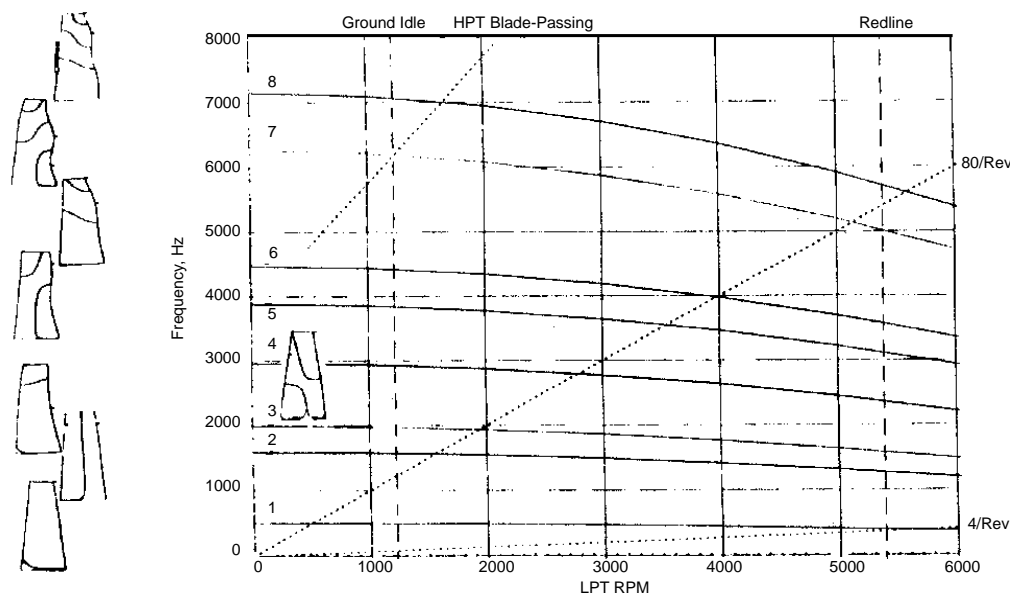
Figure 181.   LPT First-Stage Rotor Baseline Campbell Diagram

- Trade studies reduced turbine module weight
  - Turbine flowpath length reduced
  - Design assessment shows shrouded LPT second-stage rotor design feasible
- LPT first-stage blade aeromechanics evaluated; design parameters favorable for coupled turbine interaction
- Secondary flow system model generated
  - HPT blade coolant delivery system sized
  - Model adaptable to subsequent cycle system updates

Figure 182 shows the turbine module configuration that was developed from the 1997 design efforts.

Common Engine Configuration

In 1998, the GEAE/P&W Common Engine Configuration was established based on plans to execute a full-scale demonstrator engine design, build, and test program. The *Common Engine Configuration* shown in Figure 183 established the component design responsibilities. The figure also shows the design tasks that are to be addressed at the component and system level.

Two GEAE design tasks were selected. The first task was to design the turbine airfoils so that they would be compatible with the LPP staged combustor selected for the common engine configuration. The second task was to define the LPT architecture and secondary-flow circuit. The staged LPP combustor produced significant variations in radial temperature profile at different operating conditions. Figure 184 shows the leading-edge temperature variation of the turbine airfoils with supersonic cruise operation (flat profile: max = 1.05) compared to subsonic cruise operation (outboard peaked profile: max = 1.48).

Shrouds and Shroud Support
– Thermally matched to rotor for clearance control
– LPTR1 cooled with 4th stage air for improved performance
– René N5 shrouds (Qty = 17), René 77 hangers, Inco 718 support

HPT Blade (Qty = 62)
– EPM Alloy + TBC
– "ICE" cooling technology

LPT Stage 1 Blade (Qty = 72)
– EPM Alloy + TBC

LPT Vane (Qty = 54)
– EPM Alloy + TBC

HPT Vane (Qty = 34)
– EPM Alloy + TBC
– 3D aerodynamics

LPT Stage 2 Blade (Qty = 88)
– EPM Alloy
– Cooled/Shrouded

HPT Impeller
– Elimated flow holes
– ME2–9 (Subsolvus)

HPT Rotating Inducer
– ME2–9 (Subsolvus)

HPT Disk
– ME2–9 (Supersolvus)
– Single piece spool with weld
– ME2–9 (Subsolvus) aft shaft

Figure 182.   Coupled Turbine Design Features/Configuration

Design Lead
Pratt & Whitney
GE Aircraft Engines
HPT Aero (GEAE)
HPT Cooling (Joint)
HPT Structures (P&W)

Tasks

• Comoponent Flowpaths
• Component Performance
• Turbine Cooling Flows
• Secondary Flow System
• Structural Configuration
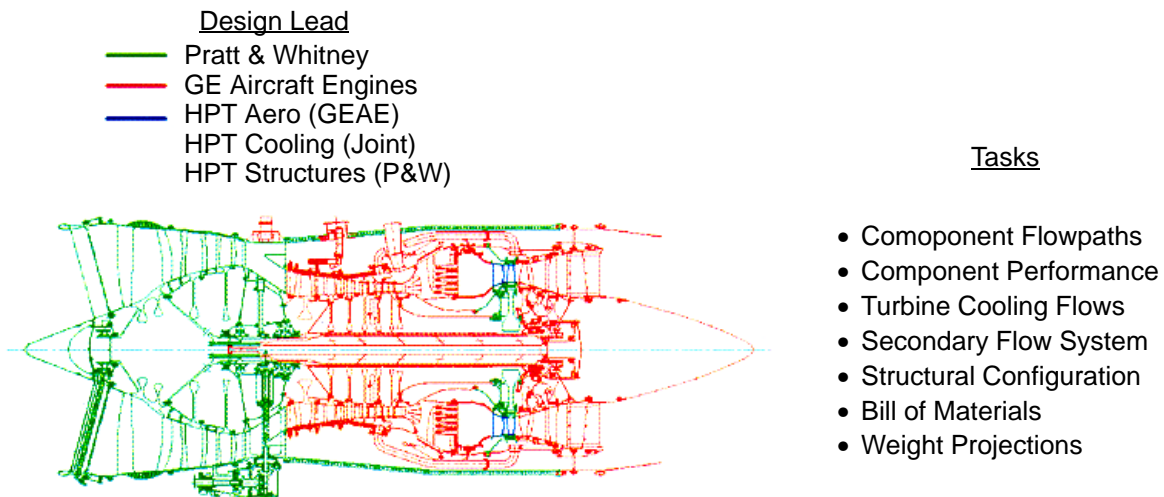• Bill of Materials
• Weight Projections

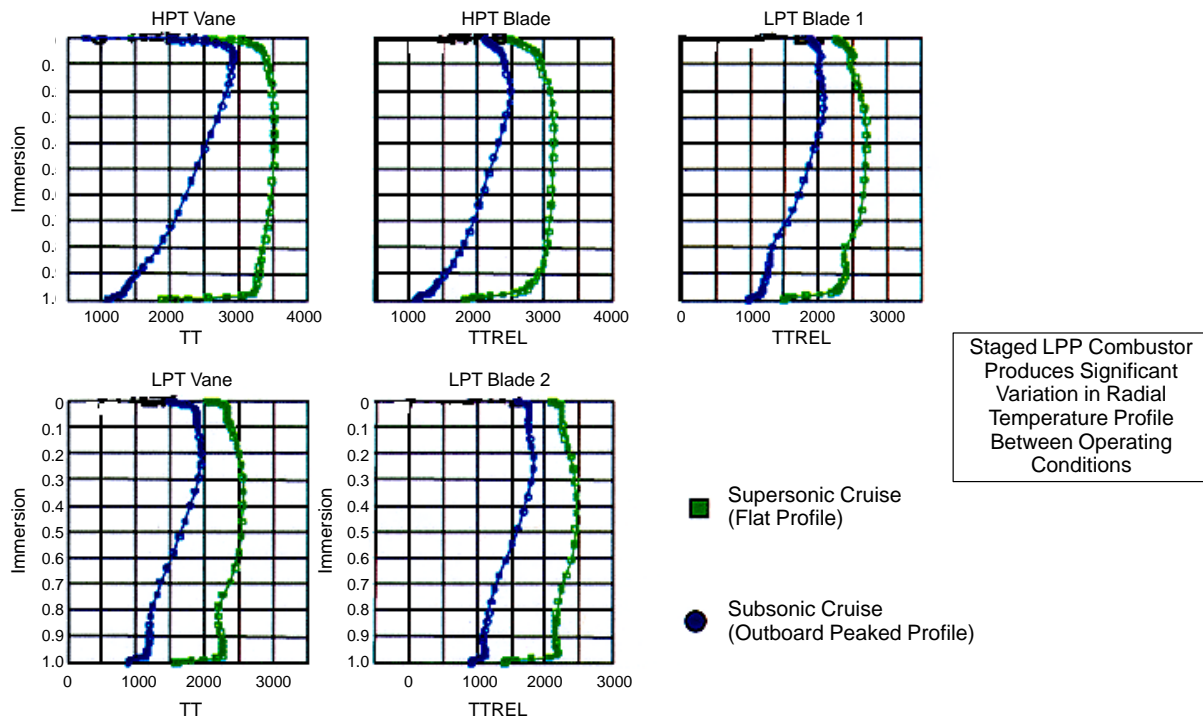**Figure 183.   P&W/GEAE Common Engine Configuration**

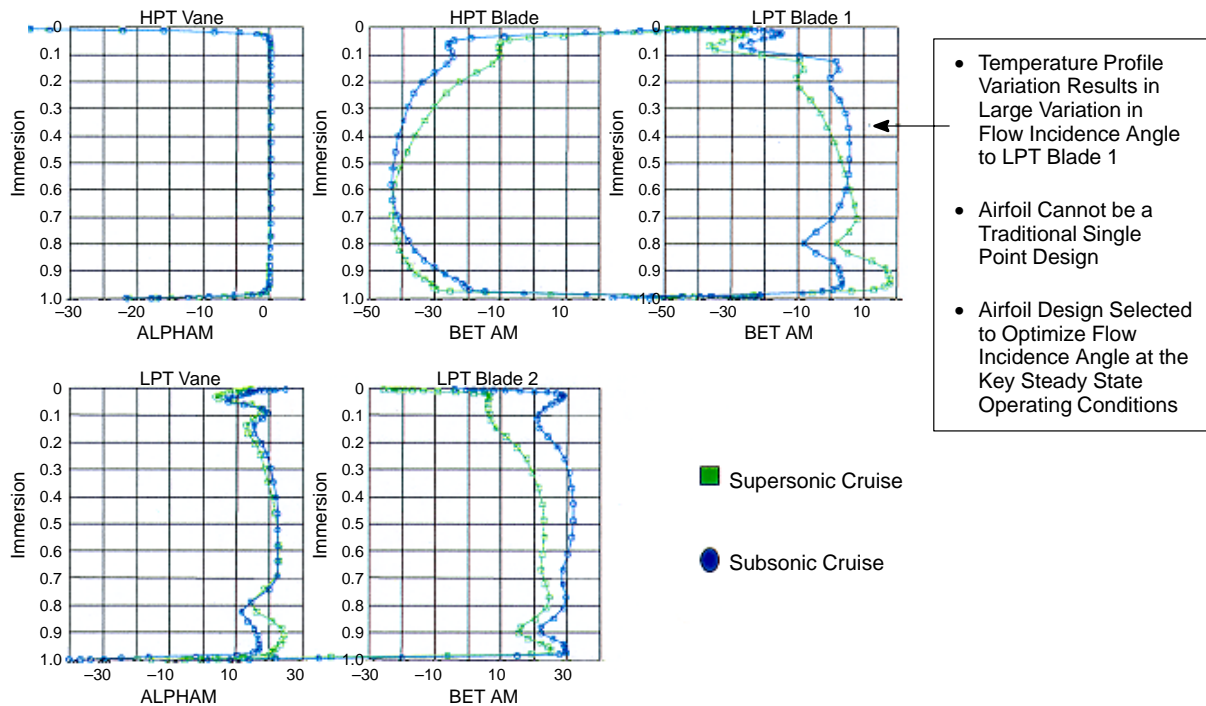**Figure 184.   Temperature at Leading Edge of Turbine Airfoils**

Figure 185.   Supersonic Cruise Versus Subsonic Cruise Incidence Angles

Figure 185 illustrates the challenge in the turbine airfoils aerodynamic design, especially the first-stage LPT blade. The turbine airfoils had to be aerodynamically designed to minimize the effects of flow incidence angle variation at key operating conditions and satisfy flow-stability guidelines.

Turbine airfoil temperatures were determined at subsonic cruise and supersonic cruise operating conditions to establish the effect of the combustor exit temperature profile. Figure 186 shows the results of the evaluation of the first-stage LPT blade. The evaluation determined that maximum blade temperatures at subsonic cruise (using the outboard-peaked temperature profile) were lower than blade temperatures at supersonic cruise (using the flat temperature profile). Therefore, at subsonic cruise operation, the outboard-peaked profile from the LPP combustor was not a design-limiting condition for turbine blade life.

- Maximum blade temperatures at subsonic cruise lower than supersonic
- Subsonic cruise temperature porfile does not contribute to blade life
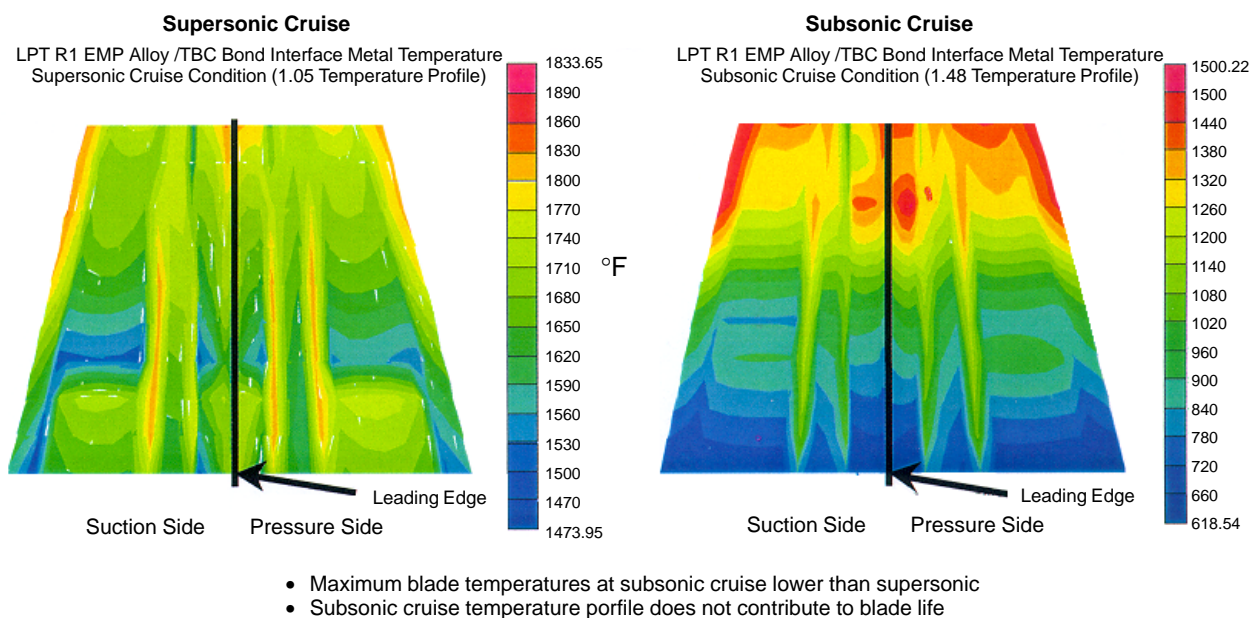
Figure 186.   Combustor Exit Temperature Profile Effect on LPT First-Stage Blade Temperature

Another task of the 1998 turbine design study was to determine theLPT secondary flow circuit and design configuration. The objectives and approach were as follows.

Objectives:

- Minimize engine system weight and turbine length

- Limit rotor bore temperature to 1000°F or less — residual life is reduced by hold-time effects above 1000°F

- Design robust secondary flow circuit design; minimize probability and impact of flow circuit failure (failed pipe, seals)

- Reduce disk temperature gradients — minimize bore stress and disk weight

Approach

- Investigate flow-circuit design options (four systems evaluated)

- Evaluate system based on key DOC+I variables: weight, performance, component life, etc.
- Consider impact on system safety

Figures 187 through 191 show the results of the effort. Configuration D satisfies all the design objectives.

1998 Design Summary

The GEAE turbine design effort for 1998 is summarized as follows:

Turbine Compatibility with LPP Combustor Exit Temperature Profiles

- Airfoil designs satisfy aero and cooling requirements
  - Minimize flow incidence angle variation at key operating conditions
  - Provide flow stability
  - Have no impact from subsonic cruise on airfoil durability

LP Secondary Flow Circuit

- Configuration D selected
  - Satisfactory HPT disk bore temp, no hold time effects on disk crack growth
  - Low disk weight for life requirement
  - Shorter LPT vane length, lower engine weight
  - Lower risk

This effort has proven that turbine airfoils can be designed to satisfy the aerodynamic and cooling requirements associated with the LPP combustor. Also, an extensive study of the LPT secondary flow circuit study was able to develop the design balance desired.

3.3.2.5 Core Engine Secondary Flow and Rotor Heat Transfer

Propulsion system mechanical design studies were initiated in 1995 to improve component and engine system design. These studies, which were conducted independently by GEAE and P&W, were to investigate component aerodynamic designs and engine system analyses including heat transfer, engine dynamics, and core rotor thrust balance. The results of these mechanical design studies were presented at the joint GEAE/P&W Mechanical Design Studies Review held in late September 1995 in Cincinnati, Ohio.

Previous to these studies, component and engine configurations had been based on preliminary design "FLOWPATH" models. The 1995 studies were conducted on the mixed-flow turbofan configuration designated 3770.42 MFTF, 800 lb/s. This engine featured a three-stage fan, five-stage compressor, single-stage HPT, and two-stage LPT.

Secondary Cooling Flow Circuits

Secondary cooling flow circuit design defines the coolant air sources, flow rates, pressures, and temperatures of an engine. The secondary cooling flow circuit of the 3770.42 engine had the following design objectives:

Figure 187.   Baseline 3770.54 Configuration A

LPT R1 supply external, Extract S4 tip exit (6 stage HPC), External pipes and duct through LP vane

LPT R2 supply external, Extract S4 tip exit (6 stage HPC), External pipes and duct through LP vane

To support the combined R1 and R2 cooling flow the LP vane would require an additional 1.3 in chord length and would result in increased engine weight

Figure 188.   Baseline 3770.54 Configuration B

LPT R1 supply external, Extract S4 tip exit (6 stage HPC), External pipes and duct through LP vane

LPT R2 supply external, Extract S4 tip exit (6 stage HPC), External pipes and duct through TRF

Cools HPT disk sufficiently but results in higher radial temperature gradient increasing disk max stress and requiring added weight to meet life

LPT R1 supply through bore, Extract R5 hub exit (6 Stage HPC)
LPT R2 supply external, Extract S4 tip exit (6 Stage HPC), External pipes and duct through LP vane

Stage 4 Stator
Bleed

Stage 5 Rotor
Bleed
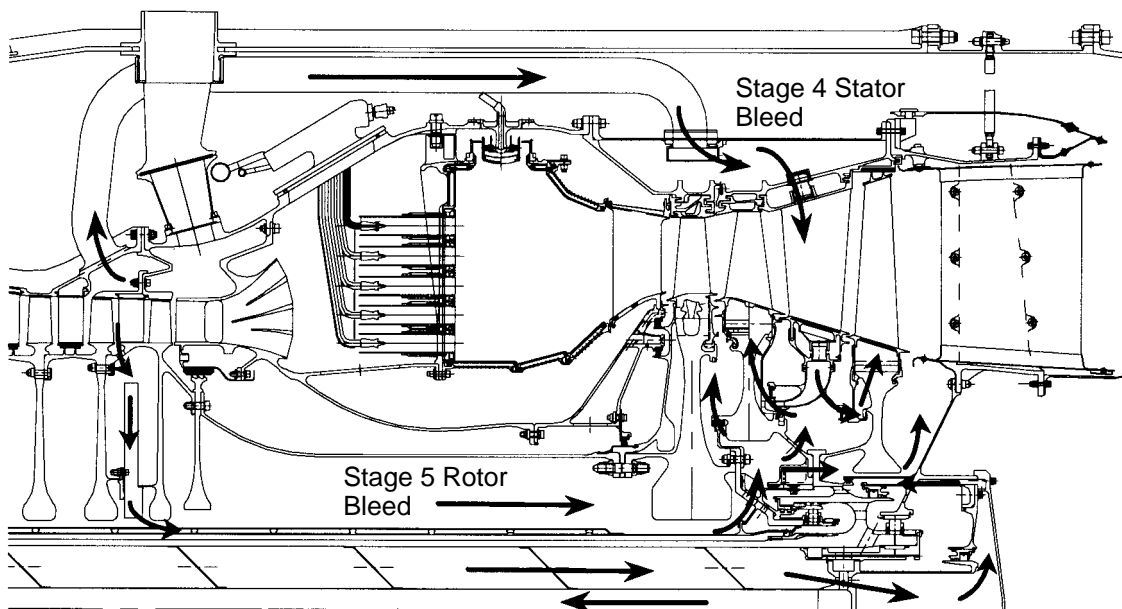
HPT Disk Bore Temperature > 1050°F (Reduced HPT Disk Life)

Figure 189.   Baseline 3770.54 Configuration C

LPT R1 supply external, Extract S4 tip exit (6 Stage HPC), External pipes and duct
through LP vane LPT R2 supply through bore, Extract R4 hub exit (6 Stage HPC)

Stage 4 Stator
Bleed

Stage 4 Rotor
Bleed
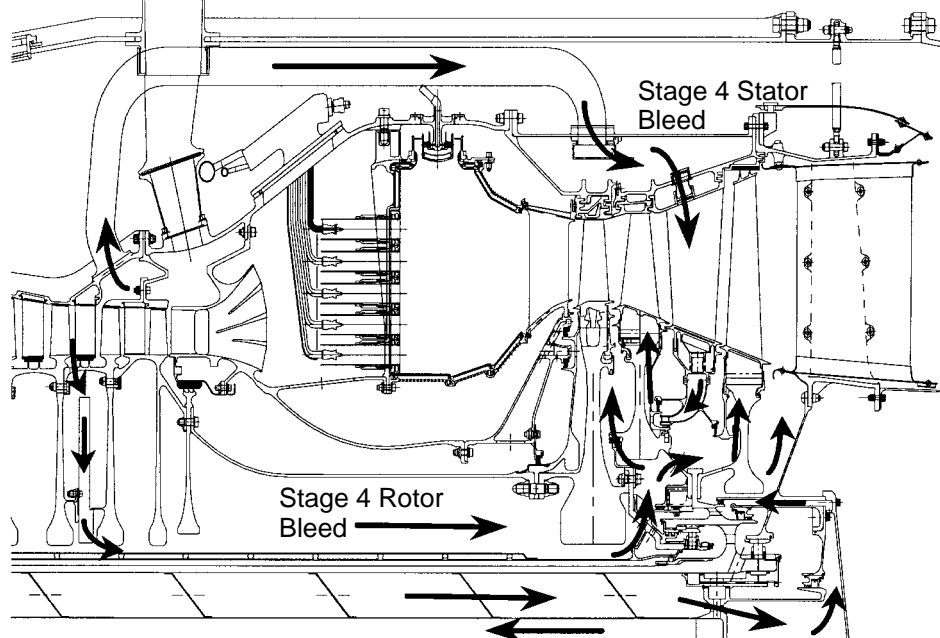
Balanced Design: HPT disk bore temperature = 1000°F with acceptable rim to bore temperature gradients

Figure 190.   Baseline 3770.54 Configuration D

Flows are %W**25**

Stage 4 Stator Bleed

3.85

1.55 3.27 0.57 1.35

0.77

0.40 0.53 0.41 0.36

0.23

0.04
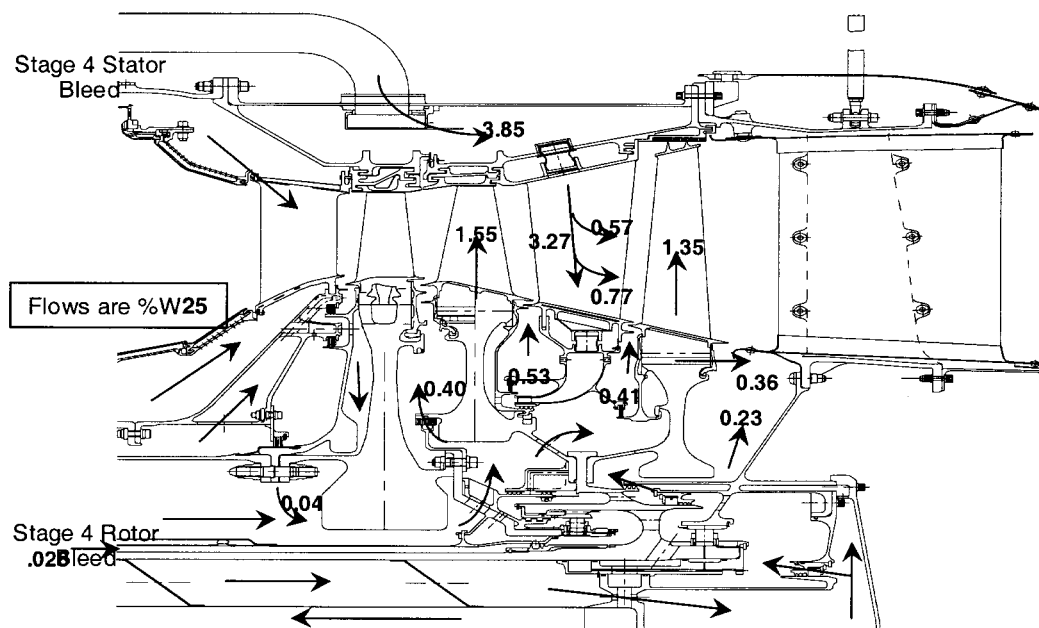
Stage 4 Rotor Bleed .02B

Figure 191.   Selected Configuration D LPT Cooling and Leakage Flows *LPT flow circuit satisfies turbine durability and blade cooling requirements failed seals considered.*

1. Control axial loads on the core rotor thrust bearing and ensure adequate bearing life
2. Provide adequate hot-parts cooling and acceptable disk radial temperature profiles
3. Ensure that internal cavities are purged to prevent hot gas ingestion

To achieve these ends, assumptions were made about the secondary cooling flow, and rotor thermal models were developed of the compressor rotor and turbine rotor and blades. These steps were necessary to be sure that the initial thermal values selected for were valid and that an acceptable thermal environment had been provided for the engine components.

Control of the thrust bearing axial loads was an important consideration in the design of the internal flow system to ensure desired bearing life. Interstage seals were used extensively to divide the internal passages and control the core rotor compartment pressures. The seal locations to control axial loads were evaluated and selected after careful consideration of the effects of all system factors including performance, weight, maintainability and reliability.

All cavities adjacent to the flowpath were pressurized above flowpath pressure to prevent ingestion of hot gases. The internal flow system was also designed to provide cooling and pressurization air to each bearing compartment for use in temperature and leakage control. The air provides a buffer to the bearing compartments, preventing unwanted hot gas from entering.

An accurate determination of the rotor thermal conditions was needed, both to size the components to meet life requirements and to establish the component weights. This mandated detailed secondary flow and heat transfer analyses.

Rotor Thermal Analysis

Analysis of the heat transfer of the GEAE high pressure rotor started in February 1995 and was completed in July 1995. For this analysis, detailed finite-element models were constructed of the

high-pressure compressor rotor and the turbine rotor (Figure 192). Cooling system trade studies were conducted on this model at the Mach 2.4 cruise condition.

Analysis of the trade study showed that design changes were required. As a result, the compressor rotor second-stage disk material was changed from Ti 6–2–4–2 to Inconel 718, and the compressor rotor stage 4/5 labyrinth seal was replaced with a smooth rotor (Figure 192). These changes reduced fifth-stage rim temperature approximately 25°F. The analysis also determined that application of a thermal-barrier coating at the compressor rotor stage 4/5 smooth rotor reduced the temperature by less than 10°F. The temperature of the HPT rotor disk post is approximately $T_3 + 20$°F.
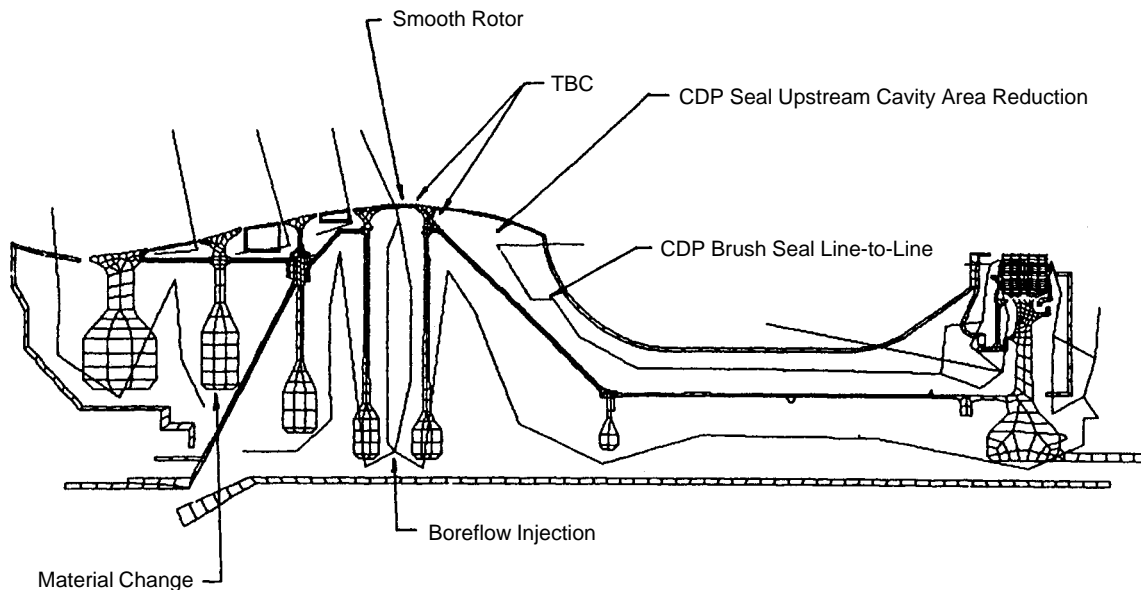

Figure 192.   Rotor Thermal Analysis Finite-Element Model

HSCT Mission Analysis

As a result of the configuration trade studies developed for steady-state, Mach 2.4, supersonic-cruise operating conditions, the heat transfer analysis was expanded to evaluate the HSCT mission. The mission was approximately four hours in duration, including a one-and-a-half-hour supersonic cruise segment that began at 61,000 feet and ended at 65,000 feet altitude.

Mission analysis verified the maximum metal temperatures at the end of supersonic cruise and established the rotor bore-to-rim thermal gradients to be used as part of the 1996 Mechanical Design Studies in follow-on rotor stress and life analyses. The core rotor heat transfer analysis also defined the best temperatures expected, see Figure 193. This enabled the HSCT EPM program to reevaluate the material capability requirements needed by the Compressor/Turbine Disk development program (EPM Task K), and others, for use in the HSCT 3770.42 MFTF configuration.

The high-pressure rotor heat transfer analysis was continued in 1996 in preparation for a detailed stress and life analysis using the rotor finite-element model. Although the 3770.54 MFTF engine cycle had been selected for the 1996 Mechanical Design Studies, the 1995 3770.42 heat transfer model continued to be used for the 1996 study. This was necessary because the 3770.54 configuration was not yet well enough defined to convert the heat transfer model and because both engine
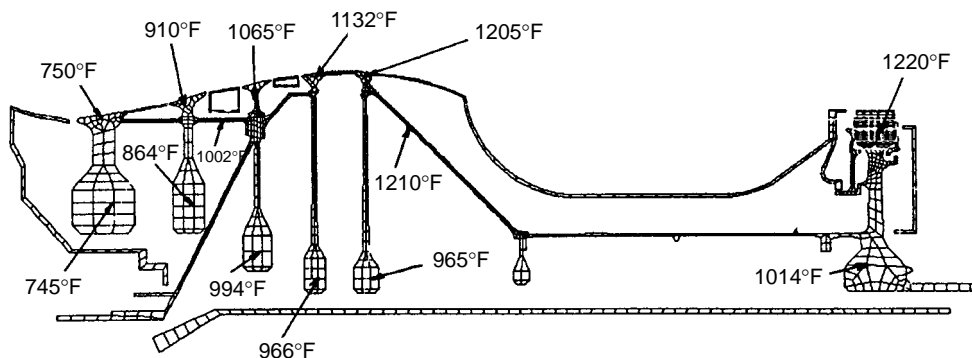
Figure 193.   Steady-State Mach 2.4 Cruise Metal Temperatures

cycles employed the same maximum T_3 and T_{41} conditions. It was felt that this variation would have only minor impact on the objectives of the study.

Potential Mission Configurations

Since the HSCT mission selection was not yet established in 1996, three potential mission configurations were studied:

- **Design Mission:**   1995 TCA; 5000 nmi, 5 hours total with 2.5-hour supersonic cruise leg and an ending 1+ hour (750-nmi) subsonic cruise leg.

- **Usage Mission 1**:   Based on old 3500-nmi economic mission; 4-hr total with a beginning 1-hr+ (700-nmi) subsonic cruise and a 1.75-hr supersonic cruise leg.

- **Usage Mission 2:**   Based on old 3500-nmi economic mission; 4 hours total with < 1 hour beginning and ending 350-nmi subsonic cruise legs and a 2-hour supersonic cruise leg between.

Figures 194 and 195 show the 1996 finite-element models for the high-pressure compressor and HPT rotors.

Bore-to-Rim Gradients

The mission analyses indicated that the maximum rotor bore-to-rim thermal gradients were nearly equal for the three missions studied. The fifth-stage compressor rotor maximum thermal gradient (approximately 450°F) occurs during acceleration to takeoff power, and the maximum thermal gradient for the compressor rotor (approximately 550°F) occurs at the third stage during the throttle chop from supersonic cruise. The HPT maximum bore-to-rim thermal gradient is approximately 420°F, as shown in Figure 196.

Stress and Life Analyses

The heat transfer results projected for the high-pressure rotor during the mission analyses were provided to the life management design group and incorporated into the stress and life analysis studies. Stress analysis of the high-pressure rotor was conducted in concert with the EPM Task K – Long Life Compressor/Turbine Disk Materials program. This analysis was used to update the
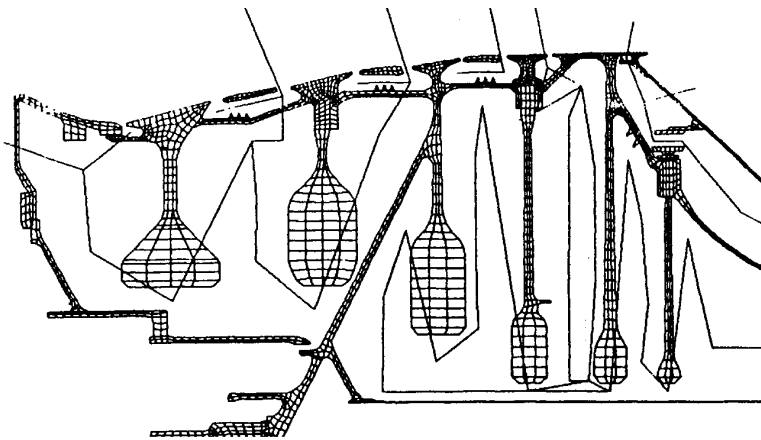
Figure 194. High-Pressure Compressor Rotor Analysis Model
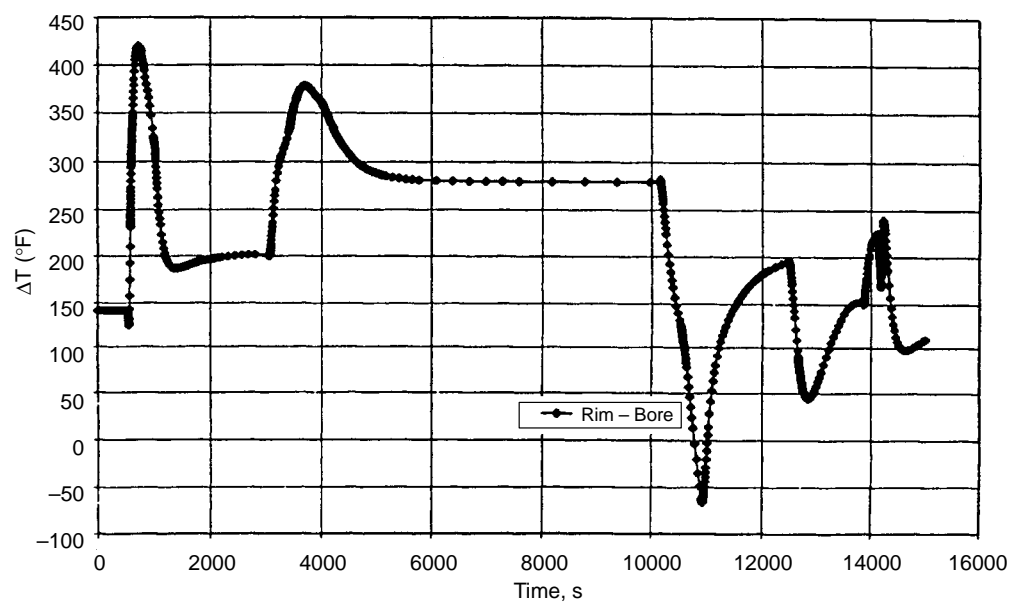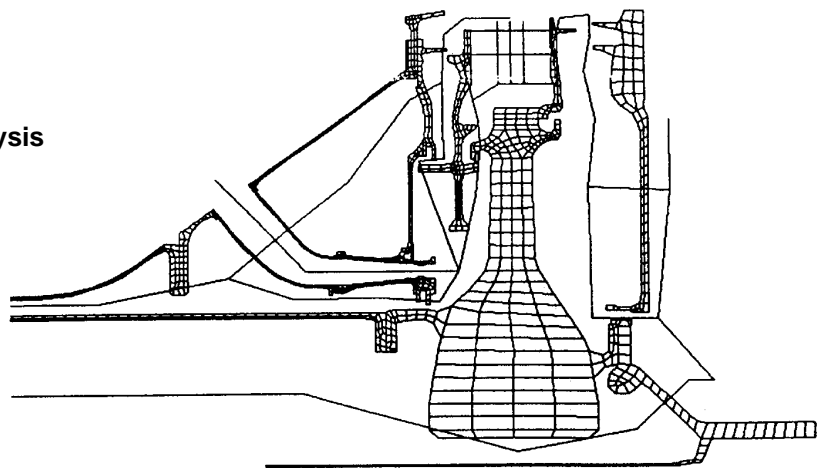
Figure 195. HPT Rotor Analysis Model

Figure 196. HPT Rotor Rim-to-Bore Temperature Gradient (Usage Mission 2)

results of a 1994 study conducted by the EPM Task K Team that estimated disk design configurations and design stress levels. The updated stress analysis values were used to establish the specifications for new disk alloys needed to meet the HSCT mission requirements.

The rotor thermal model must be able to correctly evaluate EPM materials, component life, and weight. This 1996 study allowed the mechanical design of the compressor and turbine disk configurations to be used for evaluation of the compatibility of various material candidates. The life-management design team developed a thermal analysis that incorporated 890+ time points for the mission and allowed mapping of temperature results onto stress-analysis models. The results of this thermal analysis provided insight into the impact of thermal transients on rotor.

Figures 197 and 198 show the critical locations selected for the stress and life analyses of the compressor and HPT rotors. These locations were used by the life management group to assess the rotor configurations versus candidate materials capabilities in creep, low-cycle fatigue, and fracture mechanics. Material selections and other guidance developed from these life studies were used by the component designers for sizing and assigning weights to the various rotor components.

3.3.2.6 Engine/Nozzle Dynamics and Mount Configurations

Preliminary Design

In 1995, a study of the 3770.42 MFTF and nozzle configuration was initiated using two-dimensional models to evaluate rotor criticals, bearing loads due to unbalance, turbomachinery clearance closures with maneuvers, and fan blade-out (missing blade) loads at engine mounts and other key structural locations. Figure 199 summarizes the study and lists continuing studies proposed because of the potential for component changes. This study indicated mounting the large, noise-suppressing, exhaust nozzle directly onto the engine structure did not introduce any rotor dynamics design issues.

As the engine and airplane concept configurations became better defined, the engine dynamics and mount configuration design work went from the concept study phase of 1995 to a preliminary design-evaluation phase to support engine component design and engine and airplane weight studies. An engine and nozzle analytical model was updated and used to refine critical speed calculations, the nominal unbalance response, the maneuver response, and the blade-out response.

A 3D NASTRAN model of the engine, nozzle, and airplane strut was completed by the third quarter of 1997. This 3D model, which incorporated nonaxisymmetric structures, was needed to determine the effects of engine case ovalization on the turbomachinery clearance closures and to calculate the absolute deflections at critical airframe interfaces. The model was also used to determine engine/airframe mount loads for maximum (limit) maneuver load conditions and for ultimate-load conditions including blade-out. Figure 200 shows both a 2D model and the NASTRAN 3D model.

By the time that the CPC Mechanical Design Studies Review was held at NASA–Lewis on October 8, 1997, the 3D engine, nozzle, and strut model was complete. Forward and aft mount concepts had been identified for study, and a matrix of load conditions had been created for the study.

Figures 201 and 202 present additional details of both models for the 1998 3770.54 engine.

Engine Dynamics

The following is a summary of the general engine dynamics behavior from the 1998 2D analysis study. Analysis results indicated that the engine design was acceptable.

Forward Rim Fillet

Rim

Forward Rabbet Fillet

Rim Bolt Hole
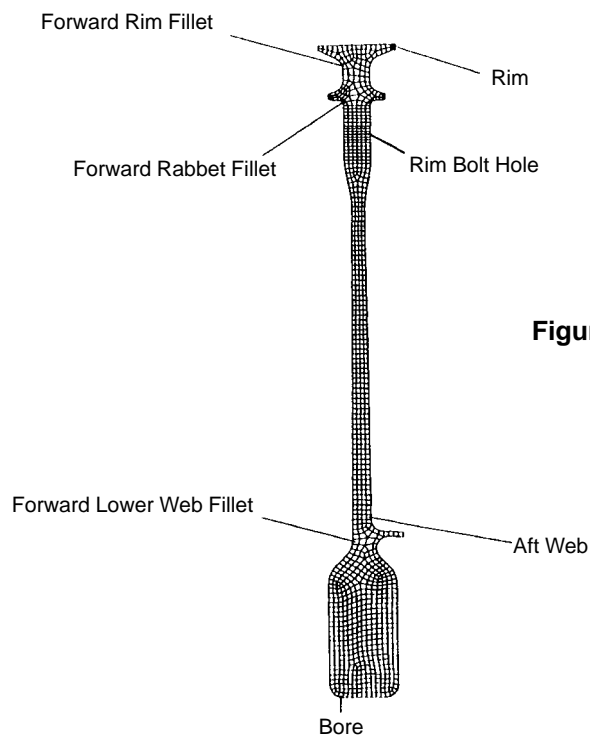
Figure 197. Stress and Life Analysis Critical Location for the HP Compressor Stage 4

Forward Lower Web Fillet

Aft Web

Bore

Upper Tang

Critical Locations for HPT Disk

Forward Rim Upper Fillet

Lower Tang

Slot Bottom

Forward Upper Arm Fillet

Aft Rim Upper Fillet

Figure 198. Stress and Life Analysis Critical Location for the HPT

Aft Web Upper Radius

Forward Web

Web Lower Radius

Forward LW Arm Up Fillet

Forward LW Arm LO Fillet

LW Arm Fillet

Forward Bolt Hole

Aft Bolt Hole

Aft Bore Face

Bore Corner

Bore
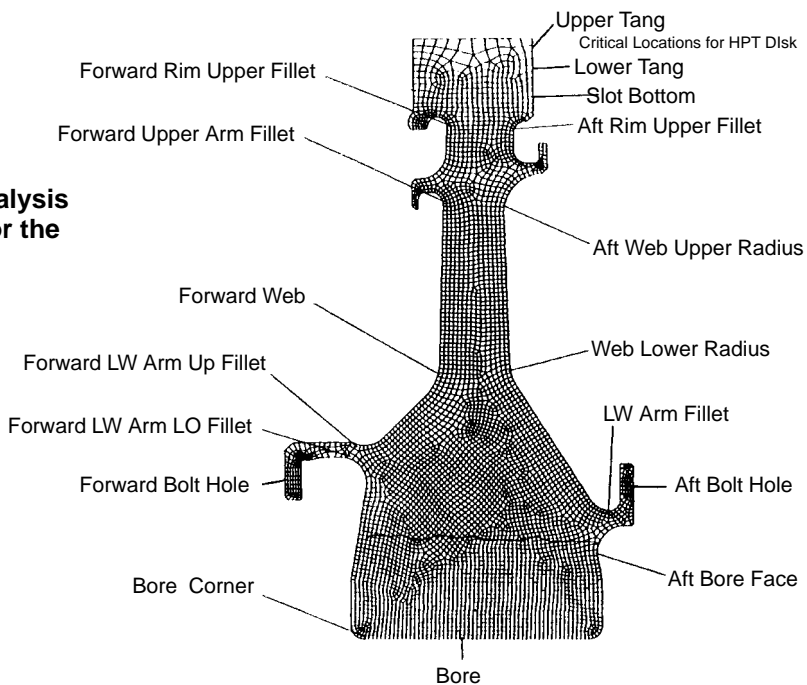
- Hard mounting exhaust nozzle does not significantly affect rotor dynamics
- Rotor criticals are above operating range
- Blade out loads are not excessive for cases and bearings
- May benefit from damper at No. 3 bearing

HSCT
LP Ref

RPM = 5738.6

4%K   4%K   4%K
4%P
6%K
10%K
10%P
33%P
7%K
10%K   13%P   7%K
5%P
9%P
8%P   8%K

Stick Model

Response Curve

Max

Fan Blade-Out Load, lbf (1000's)

5.0
4.5
4.0
3.5
3.0
2.5
2.0
1.5
1.0
0.5
0

0   1   2   3   4   5   6   7

Shaft Speed, RPM (1000's)
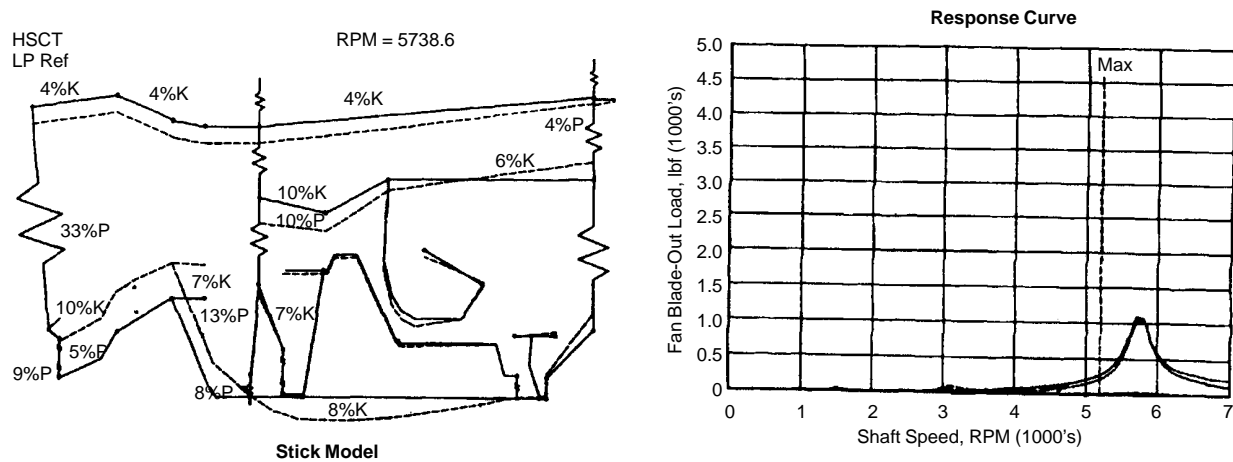
Figure 199.   Summary of 1995 Rotor Dynamics Study
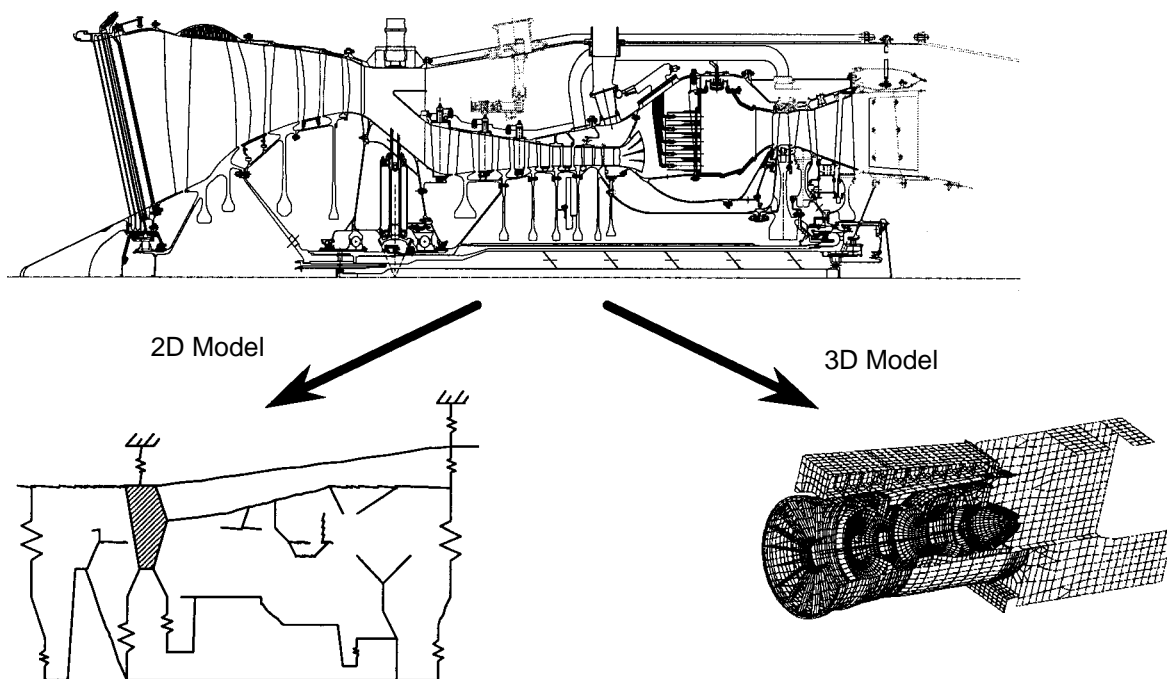
2D Model

3D Model

Figure 200.   Dynamic Model Cross Section With 2D And 3D Models
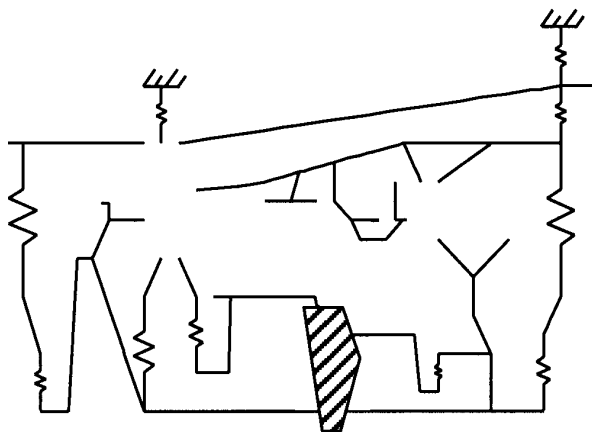
- 800 lbm/s MFTF3770.54 June 98 configuration
  - Common Design Engine components
    - P&W fan
    - GEAE 6-Stage HPC
    - LPP Combustor
    - GEAE/P&W turbine module
    - Bearing compartments, shaft (lengths), etc.
- Fan frame stiffness extracted from 3D model
- Weights from Preliminary Design FLOWPATH model and component designers

Figure 201.   HSCT 2D Analysis Model

3D NASTRAN Shell Model (CIRCA 3rd Quarter 1997)

- Complete System Model
  - Developed in conjuction with Boeing
  - Included mounting strut
  - Simulated Airplane Construction
  Simulated all clearances and loads
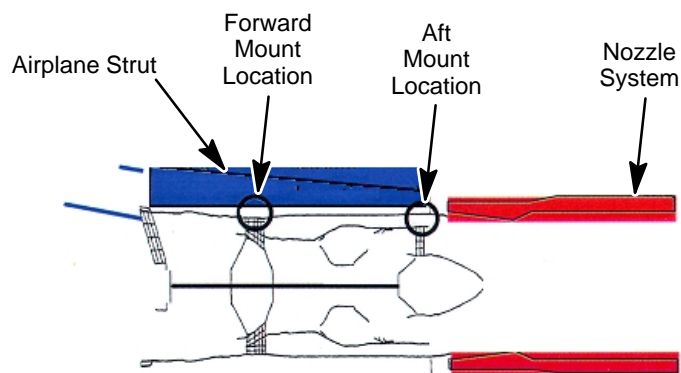
- Mount Configurations
  - Evaluated 6 forward and 2 aft mount concepts
  - Developed 11 concept combinations:
    9 statically redundant, 2 determinant

Figure 202.   HSCT 3D Analysis Model

- Sufficient critical speed margin achieved with proposed changes
- Maximum undetected unbalance
  - Clearance closures acceptable
  - Bearing loads acceptable, with proposed changes
- No bowed-rotor start problems
  - Clearance closures acceptable
  - Bearing loads acceptable
- No spring mount bearings or squeeze-film dampers required for bearing life
- No modal stability problems

Engine Mounting

Mounting concepts developed for thE common GEAE/P&W engine configuration are illustrated in Figure 203. These mounting concepts were formed into 11 combinations that were evaluated and compared to determine which was best. The engine mounting on the airframe is shown in Figure 204. Figure 205 shows a typical mounting and includes the strut and yoke required to attach the engine at the 3:00 and 9:00 o'clock mount locations.

Airframe Interface Loads

Analyses of the engine mounting concepts are documented in the following Coordination Memos:

1. GE97–150–S Rev1, "Preliminary Analysis of HSCT Turbomachinery Clearance Closures During Once/Flight Maneuver Conditions, May 7, 1998

2. GE98–038–S Rev1, "Preliminary Analysis of HSCT Loads During Limit Maneuver Conditions," May 6, 1998.

3. GE98–086–S, "Preliminary Analysis of HSCT Ultimate Loads From Bladeout Event," August 12, 1998.

Clearance Closures

In the 3D analyses, turbomachinery clearance closures, limit maneuver loads, fan blade-out loads, and mount configuration assessment were all considered. The analyses examined 11 candidate mount configuration combinations and 118 normal once/flight maneuver conditions. The turbomachinery clearance closures provided by the 3D model analysis included casing-ovalization effects and rotor/stator relative deflections.

In the 3D model, the criteria established for clearance-closures analyses was that there should be no rotor/stator rubbing during normal operation. Figure 206 shows that mount concepts Fwd–2 and Fwd–5 appear to be the best (most margin). Either aft mount configuration is acceptable with these two mount concepts.

Limit Maneuver Loads Analysis

The limit maneuver loads analyses examined 11 candidate mount concept combinations under 18 limit maneuver conditions. These analyses primarily looked at conditions that produced the maxi-

Forward Mount Concepts
(Aft looking forward)

Fwd–1 (On fan frame)
Fwd–4 (On front frame)

45°

Fwd–2 (On fan frame)

45°

Fwd–3 On fan frame)
(removes axial load from hinge)

Fwd–5 (On fan frame)

Fwd–6 (On fan frame)
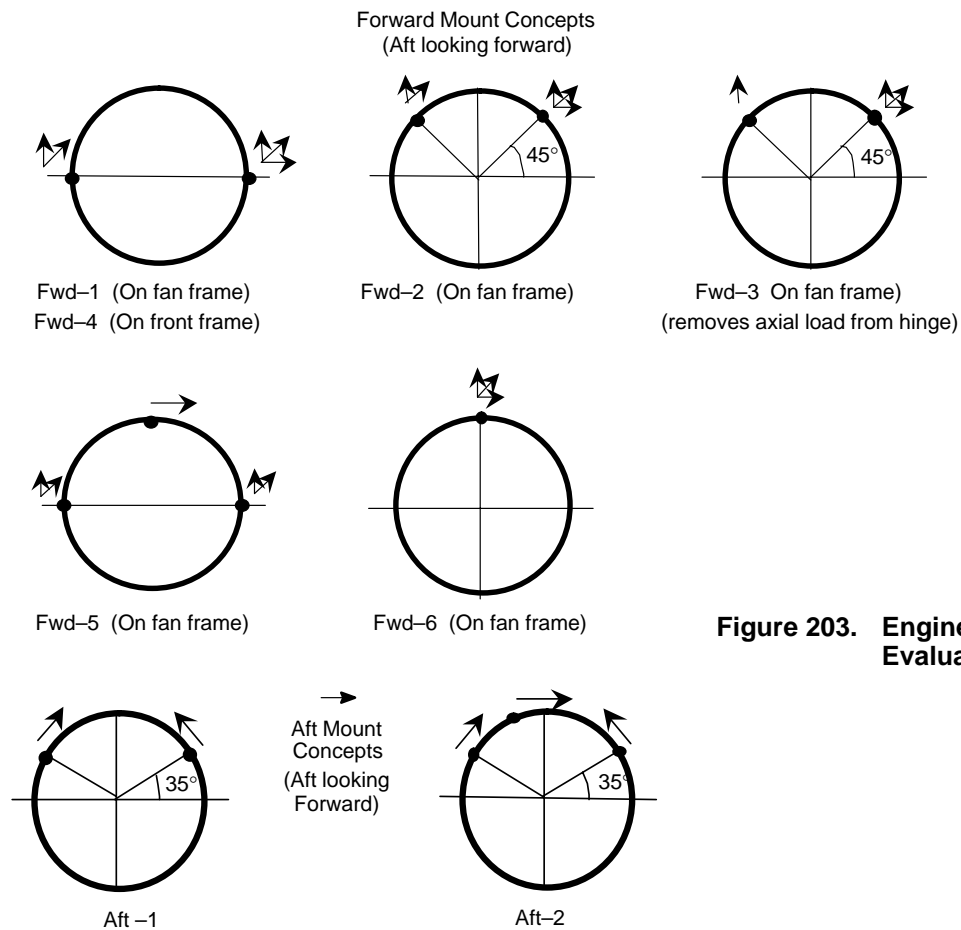
Figure 203.   Engine Mounting Concepts Evaluated

35°

Aft –1

Aft Mount
Concepts
(Aft looking
Forward)

35°

Aft–2
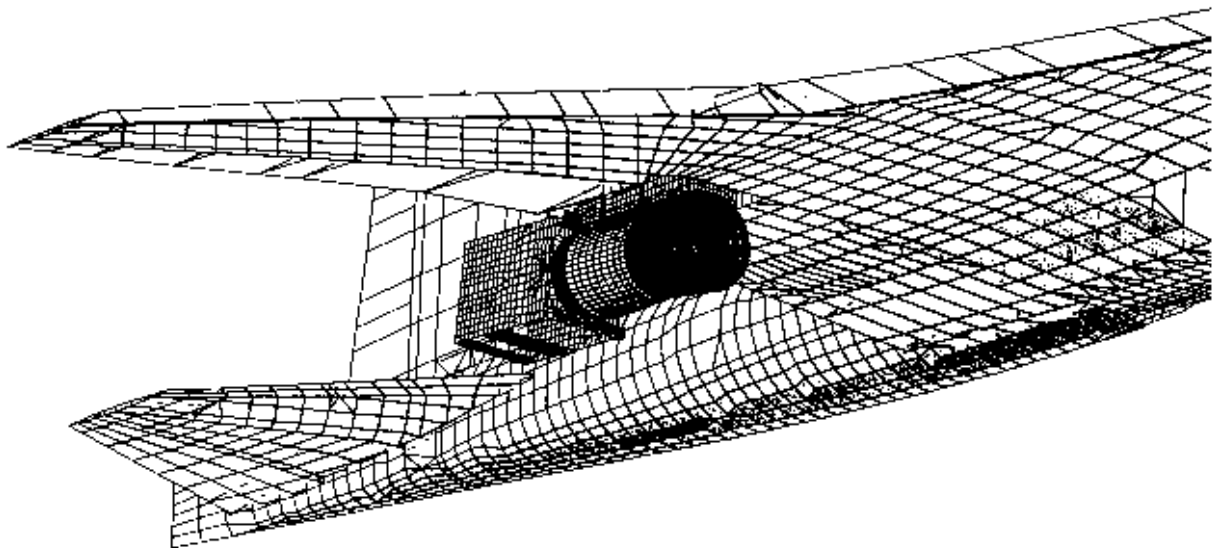
Figure 204.   NASTRAN Model of Airframe with Engine

Figure 205. Engine Mounting

Aircraft Strut for Engine Mounting

Aircraft Yoke to Engine Mounts

Engine Mounts at 3:00 and 9:00 (Fwd–5)
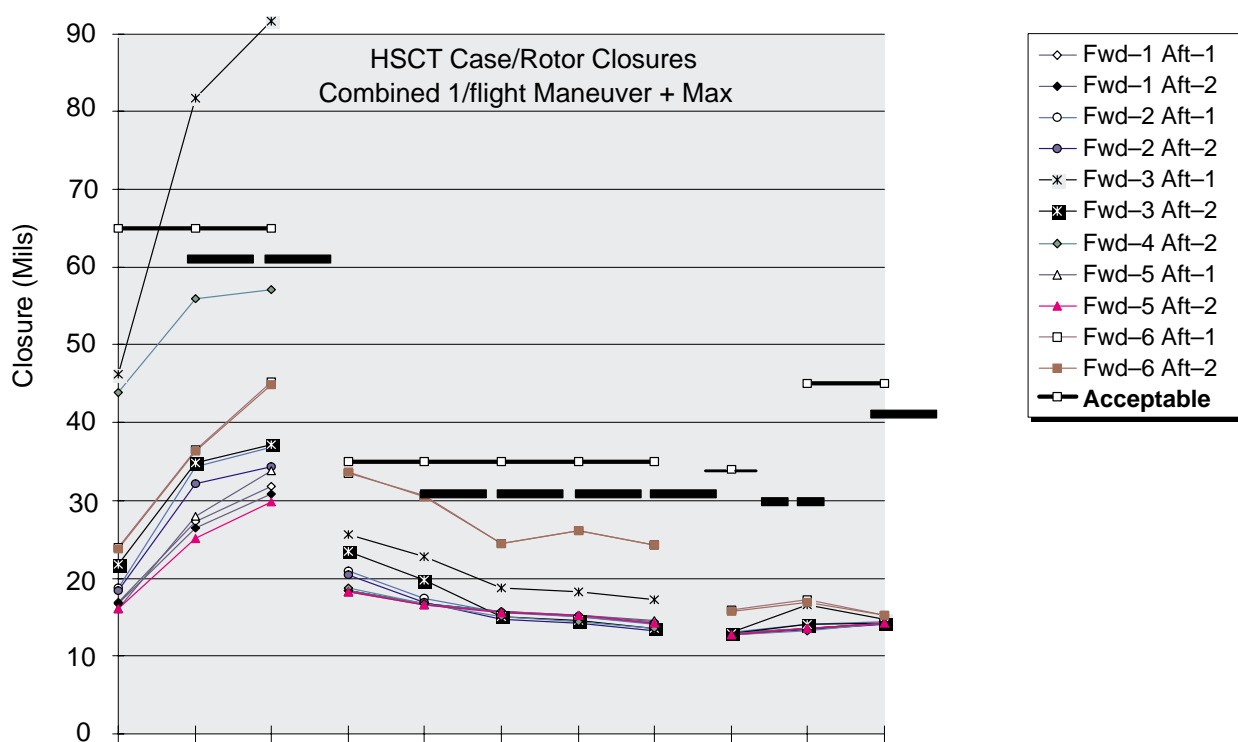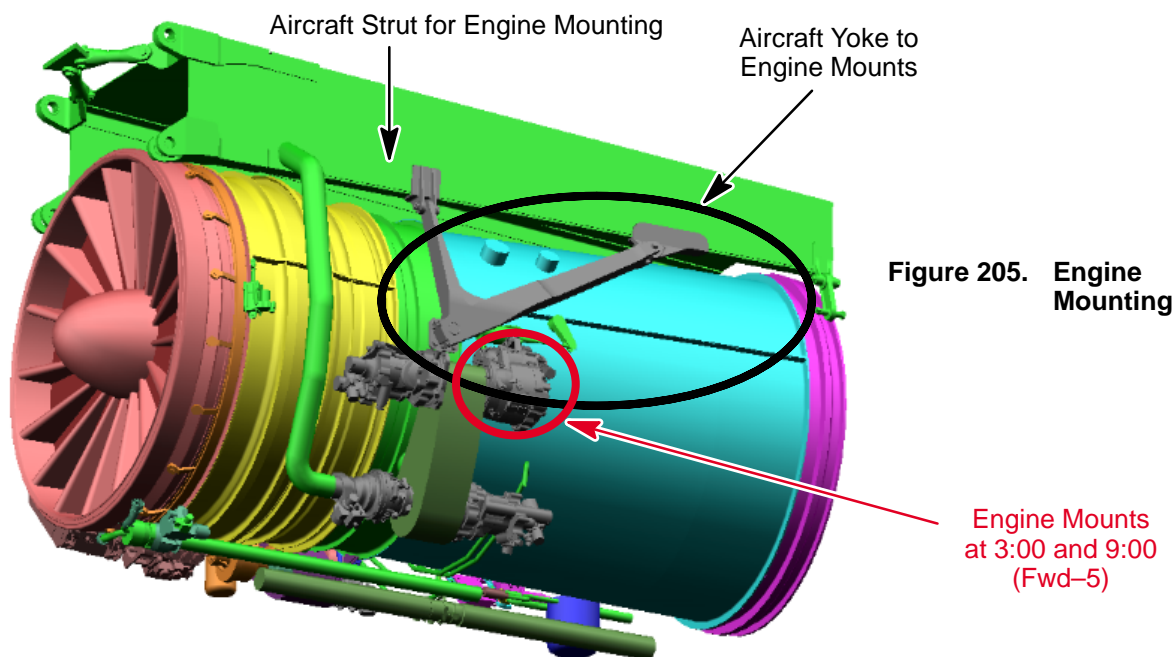

Figure 206. Comparison of Mount Combinations

mum loads expected in service. These analyses results were used to screen HSCT mount concepts and also to generate projected values for mounting loads, bearing loads, engine flange loads, and deflection at the engine forward interface location. Evaluation of the analyses revealed that the addition of an aft midlink to mounting concept Aft–2 significantly reduced the engine carcass loads and engine roll deflection due to lateral maneuvers. Either of the mount concepts, Fwd–2 or Fwd–5, in combination with mount concept Aft–2, resulted in the lowest mount loads and engine structure loads under limit maneuver conditions.

Fan Blade-Out Analysis

Fan blade-out (missing blade) is the ultimate-load analysis used as sizing criteria for engine mounts and engine structures. The analysis generated projected values for mount loads, bearing loads, internal engine flange loads, and aircraft strut-to-wing attachment loads. The mount concepts Fwd–2 and Fwd–5 combined with mount concept Aft–2 were selected for blade-out analysis based on the maneuver-load analyses.

Blade-out analysis results are shown in Table 73. The analysis determined that the combination of mount concepts Fwd–5 and Aft–2 offered a slight advantage. This would be critical only if loads were at the level used to size the specific component of interest. Based on the analyses above, Figure 207 shows the two recommended mounting concept combinations.

Table 73. Blade-Out Analysis *Influence of using Fwd–5 + Aft–2 mount configuration.*

Location	Effect on Load Relative to Fwd–2 + Aft–2
Forward Mount System	Decrease: 10% to 25%
Aft Mount System	Increase: 10% in lateral load
Bearings	No. 1 bearing the same; 5% decrease in No. 2 bearing, about 10% increase in Nos. 3, 4, and 5 bearings
Forward Bypass Duct	Shear load same; torque and moment load about 5% to 25% increase
Aft Bypass Duct	About the same
Compressor Forward Flange	Decrease: 11%
Front Frame Flange	About the same
Turbine Rear Frame Forward Mount Moment	Decrease: 15%
TRF Link Total Shear Load	Decrease: 10%
Nozzle Flange Moment	About the same
Wing Loads	Slight decrease in moment loads; 10% to 30% decrease in shear loads

The final results of the Engine Dynamics and Mount Configuration Studies for the HSCT are summarized as follows.

- The Aft–2 mount mid-link is strongly recommended

- Fwd–2 and Fwd–5 forward mounts emerged as best candidates from closure and limit loads analyses

Figure 207. Recommended Mount Systems
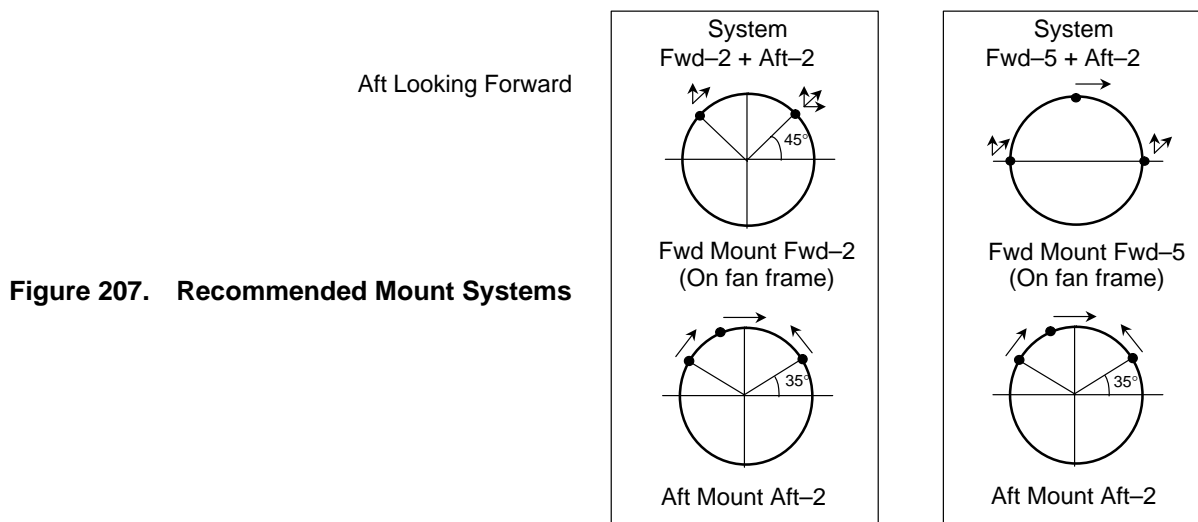
- The blade-out analysis slightly favors the Fwd–5 configuration; however, the Fwd–2 configuration may result in less overall weight despite favorable loads and clearance closures

3.3.2.7 Controls Architecture and Nacelle Integration

In 1997 a study was initiated to define the engine controls and accessories design and configuration required for the HSCT application. This effort would identify the turbomachinery and nozzle control systems, evaluate the lube and hydraulic fluid cooling provisions, and configure the installation of the controls and accessories components.

Figure 208 shows the turbomachinery control system envisioned for the HSCT requirements. Features of this system include dual-redundant electronics, a variable-displacement main fuel pump, a fuel return to aircraft, fuel-actuated variable-vane stages, and a combustor staging control.

The exhaust nozzle control system is shown in Figure 209, and nozzle components are shown in Figure 210. Variable nozzle components are the inner and outer doors at both the upper and lower surfaces, the convergent and divergent flaps, and the variable-area bypass air injectors. A 5000-psi hydraulic system was selected.

In-flight operation of the nozzle was accomplished with 50 to 100 gal/min hydraulics. Transition to thrust reverse (occurs at low engine power) requires 250 gal/min. The control system approach was to provide one 100-gal/min piston pump for the in-flight operation and add a 250-gal/min turbocentrifugal pump driven by compressor discharge bleed air for the thrust reverse transition.

For the exhaust nozzle temperature environment, the hydraulic fluid recommended is <u>nonflammable</u> and has a specific gravity of 1.8. Considering the amount required, approximately 19 gallons, this becomes a significant weight penalty, especially when compared to <u>fire resistant</u> fluids that have a specific gravity of 0.8.

A comprehensive thermal-management model was developed to evaluate fuel-cooling capability relative to the HSCT mission requirements. The system inputs were set up so that fuel temperature at the combustor manifold would be less than 300°F. Fuel at higher temperature would be returned
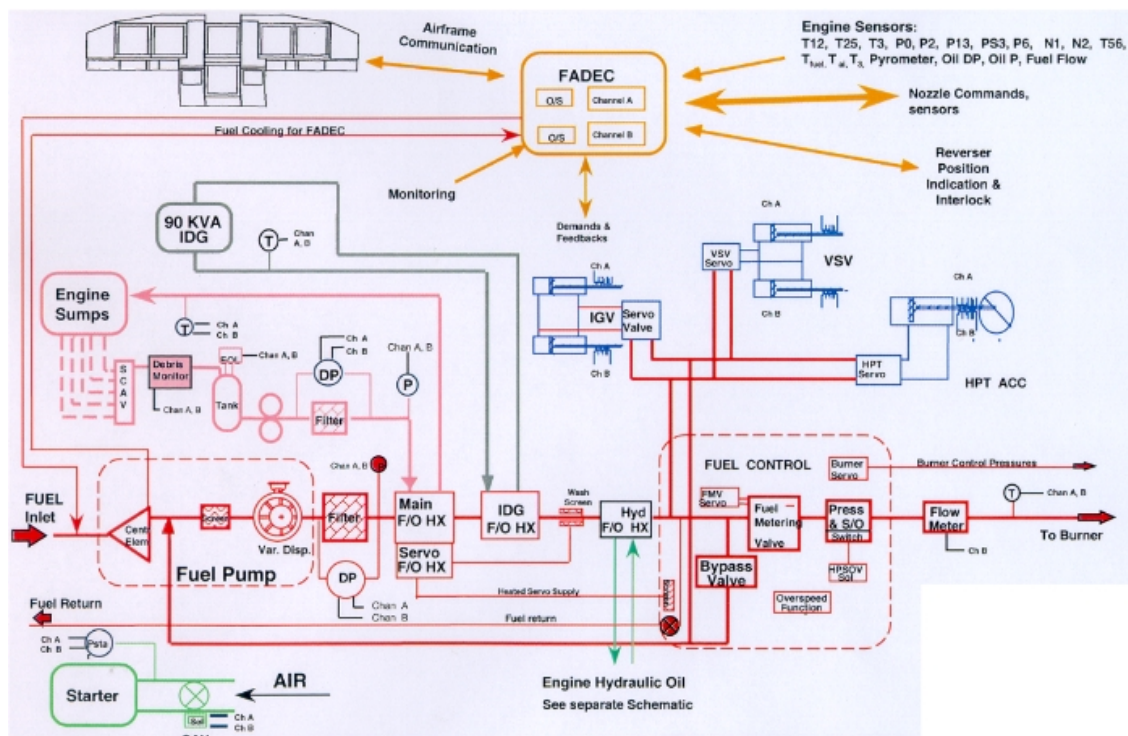
Figure 208.   Turbomachinery Control System

Notes:

1. 5000-psi pump operates in–flight Hydraulic pressure = f(P3) and 5000 psi max

2. Centrifugal hydraulic pump is air–turbine driven; off except during reverse cycles 1200 psi assumes reverser transition occurs at lower power

3. Actuators have 600°F ambient air

4. Boost pumps are integral with hydraulic pumps

5. Fluid is Perflouropolyalkyethers (PFPAE), nonflammable. Oil capability is 675°F. Predicted system max oil temperature is 400°F

6. Indicated peak loads are per actuator

7. Some servos will be paralled with a 4-way solenoid valve to reduce gains during flight, and operate on/off during reverse

8. The servo valves may be mounted on a single housing, "Nozzle Control"
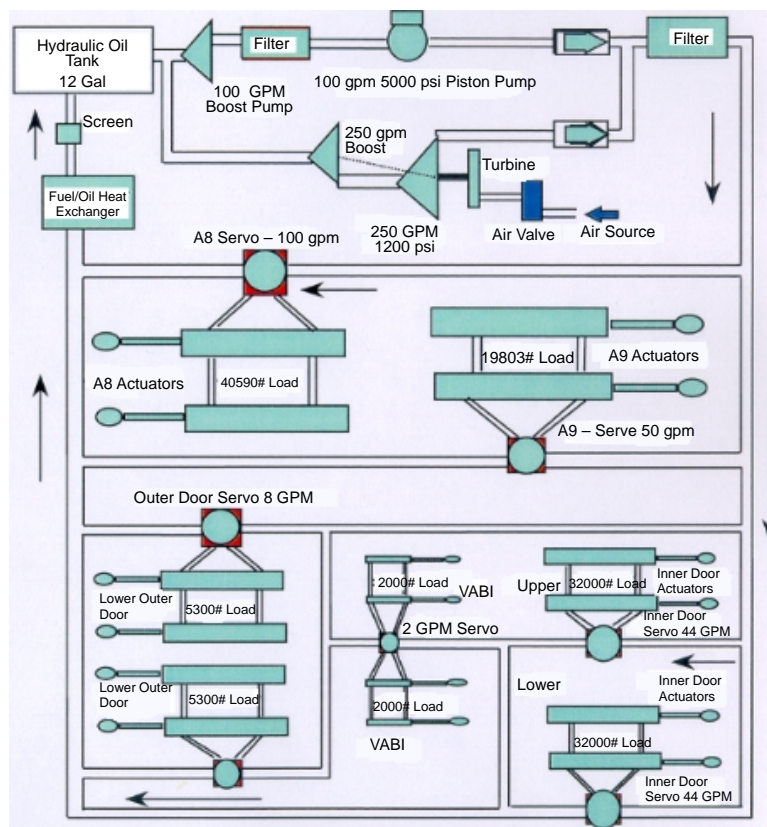
Figure 209.   Exhaust Nozzle Control System
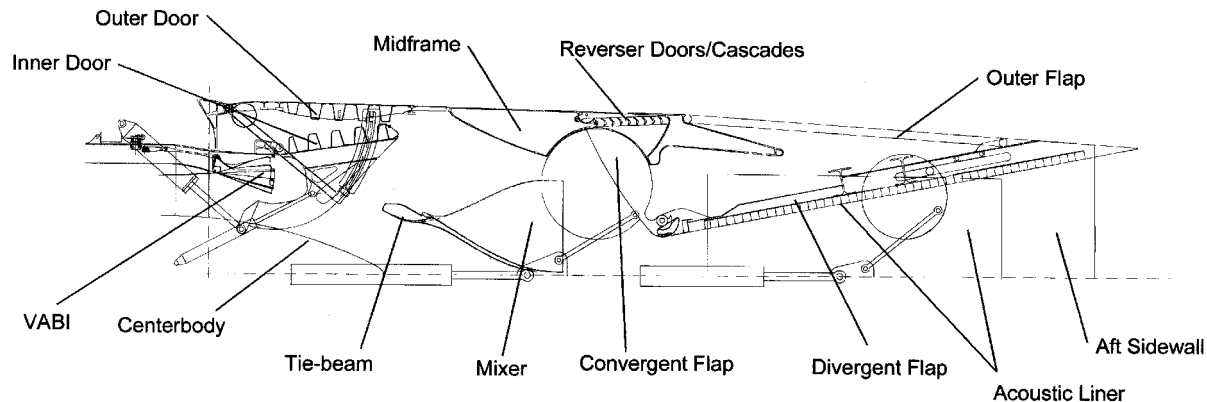
Figure 210. Exhaust Nozzle Components

to the tank. At maximum, the temperature of fuel fed to the engines (from the aircraft) would be 140°F.

The temperature of fuel fed to the engine affects the ability to cool control system electronics and engine oil, and this affects the selection of control system component materials. The engine heat model analysis determined that the cooling of control system fluids and components was adequate for most of the mission segments — including supersonic cruise. The analysis also found that engine heat removal was marginal when low engine fuel flow was experienced during descent and at ground idle.

All components required for the turbomachinery and nozzle control system were identified and sized based on similarities to existing product applications and on vendor estimates. A detailed parts list was prepared to establish the total weight of the system in the HSCT. This detailed list reflected the total installed weight of the system including the weight of components, fluids, and mounting hardware. Based on the initial 1997 configuration, the total weight estimated for HSCT controls and accessories is shown in Table 74. Total estimated weight of the HSCT control system is two to three times the weight required for current subsonic applications.

Table 74. Controls and Accessories Weight for 1997 HSCT Turbomachinery and Exhaust Nozzle

Item		Weight, lbm			
		Parts	**Fluid**	**Mounting**	**Installed Total**
Turbomachinery	Piping, Brackets	163.5	23.2	27.9	214.6
	Transducers	41.9	0	5.7	47.6
	Components	551.5	80.2	45.3	677.0
Nozzle – Suppressor, Reverser, Piping		931.4	303.9	87.8	1323.1
HSCT C&A Total		1688.3	407.3	166.7	2262.3

A nacelle integration effort was also conducted as part of the controls and accessories conceptual design effort. The purpose was to establish the physical locations for the engine controls and accessories and for the airframe accessories. The nacelle outline requirements were provided by the

airframer. Figures 211 through 215 show the locations selected for the controls and accessories on the HSCT configuration and also illustrate a concept that places engine controls and accessories on one side and airframe accessories on the other side. Figures 214 and 215 also show that, with minor exceptions, it was possible to configure the components within the conceptual design and within the requirements of the nacelle outline.

Following completion of the initial controls and accessories design and configuration definition in 1997, the exhaust nozzle team initiated weight-reduction activities that continued into 1999. These activities resulted in overall configuration changes which, in turn, caused changes to the (exhaust nozzle) control system design and to the controls and accessories components. The weights of the controls and accessories were included in the exhaust nozzle weight summaries.

Figure 216 shows the exhaust nozzle changes that were introduced for the reduced weight 6/99 configuration, which features a single door and linear actuation. Figure 217 shows the revised exhaust nozzle control system for the 6/99 configuration.

The weight of the controls and accessories for the 8/97 disk actuation nozzle configuration was estimated to be 1428 lbm, an increase from the initial 1997 estimate (1323 lbm). The 6/99 single-door linear actuation nozzle configuration were estimated to be reduced to 1355 lbm. Details of these configurations are summarized in Subsection 3.4.4.

3.3.2.8 Aft Sump and Lube System Design

In the 1998 preliminary design effort for the common engine configuration, GEAE was assigned responsibility for the overall turbine module. As part of this effort, GEAE initiated a system-design study for the aft sump and engine lubrication. The objectives of this study were:

- To establish the aft sump design including sump system pressurization and venting.
  - Assess compatibility with chosen engine cycle and secondary flow design. (See Subsection 3.3.2.4, LPT Secondary Flow Circuit Configuration D.)
  - Determine if sump vent temperatures are compatible with oil temperature limits.
- To conduct an engine heat-rejection analysis for the aircraft model. (See Subsection 3.3.2.6 Controls and Accessories Architecture.)
  - Determine engine oil temperatures.
  - Determine the requirement for fuel recirculation to the tank.
- To prepare an engine lubrication schematic.
  - Determine engine oil flow requirements.
  - Determine preliminary sizes for system components.

Figure 218 shows the aft sump design configuration, and Figure 219 details the sump pressurization and secondary flow circuit. Fan exit (hub) total pressure is used for seal pressurization. Internal venting is through a center (engine) vent tube to the (engine) midsump and then overboard. Table 75 lists the preliminary sizing criteria used for the aft sump bearings and seals. The 4R (roller) bearing and seal selections are challenging designs due to intershaft speeds. The remaining bearing and seal configurations are well within GEAE design experience.
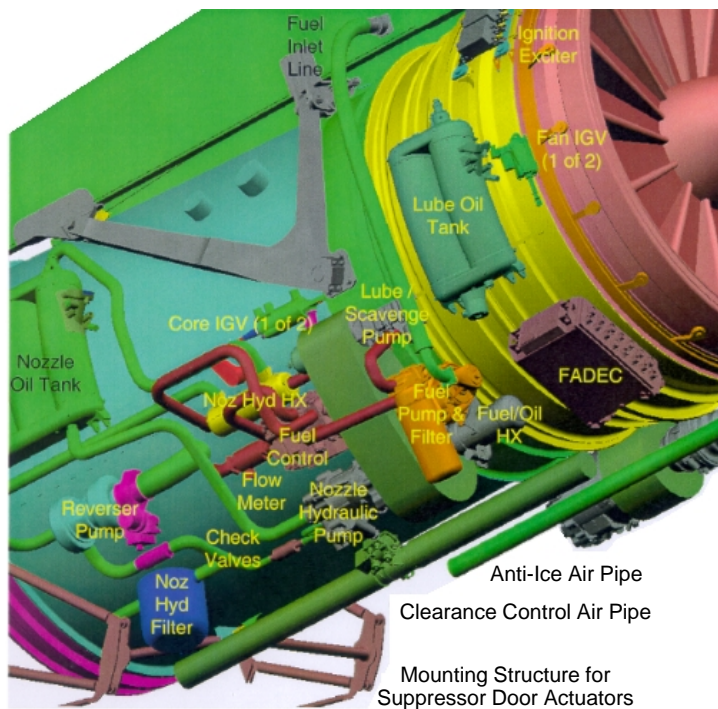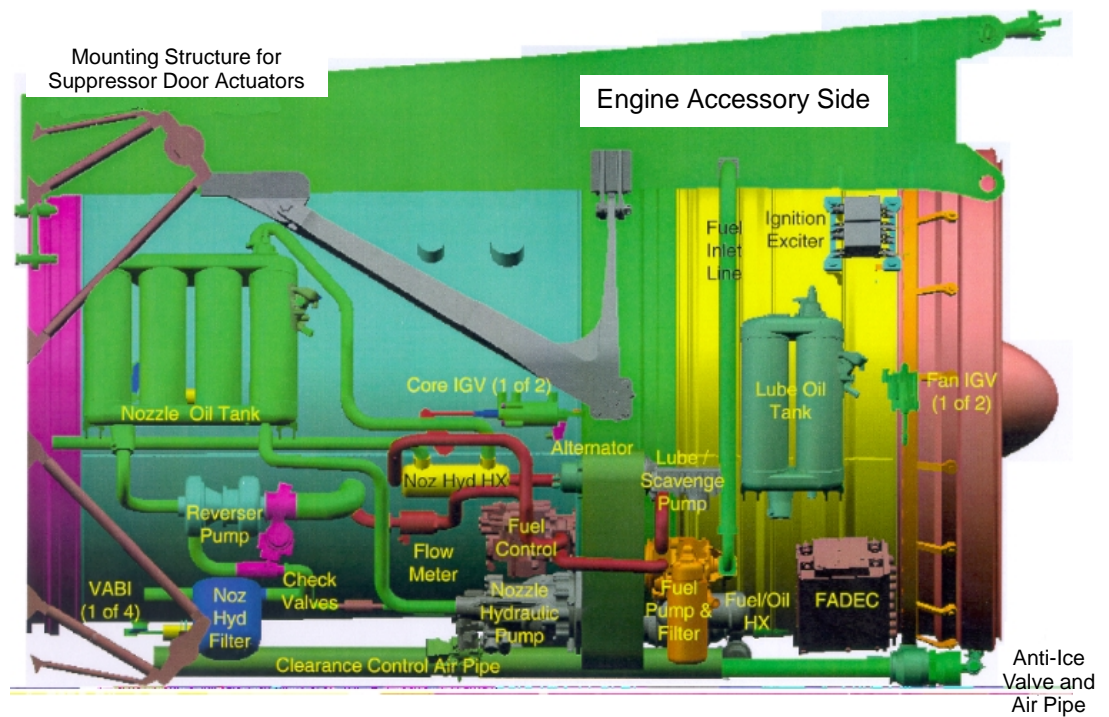
Engine Accessory Side, from Below

Figure 211.   Two Views, Engine Accessory Side
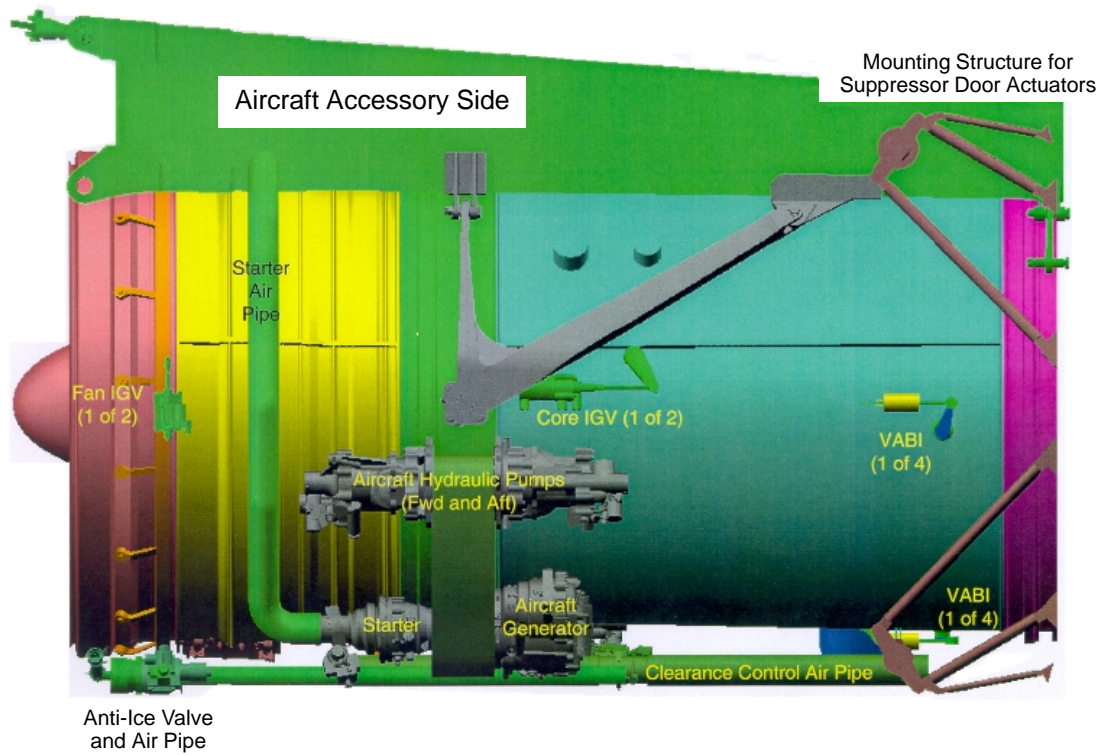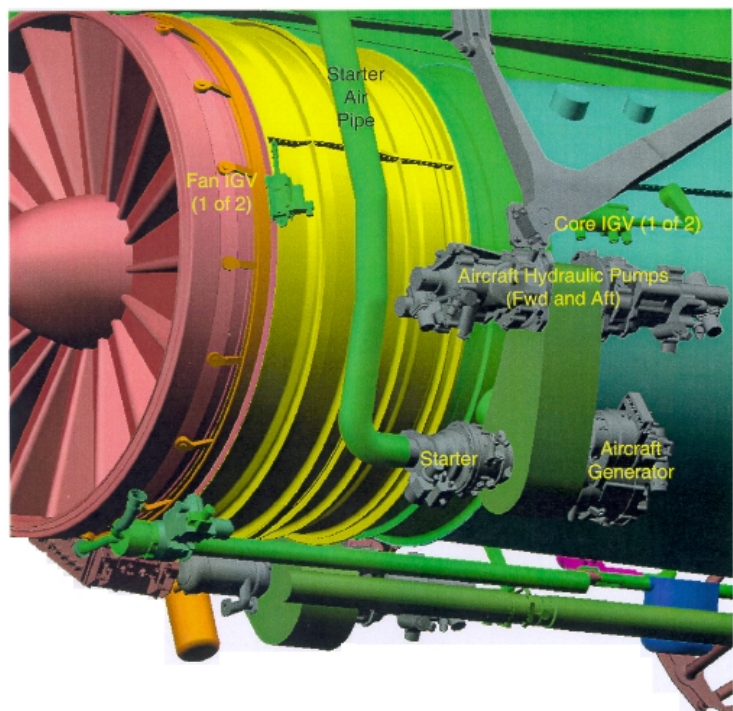
Figure 212.   Two Views, Aircraft Accessory Side

Outer Door Actuators (1 of 4)

Divergent Flap Actuators (1 of 2)

Engine and Nozzle, Accessory Side

Inner Door Actuators (1 of 4)

Convergent Flap Actuators (1 of 2)

Outer Door Actuators (1 of 4)

Divergent Flap Actuators (1 of 2)

Airframe Accessory Gearbox

Engine and Nozzle, Aircraft Side

Inner Door Actuators (1 of 4)

Convergent Flap Actuators (1 of 2)
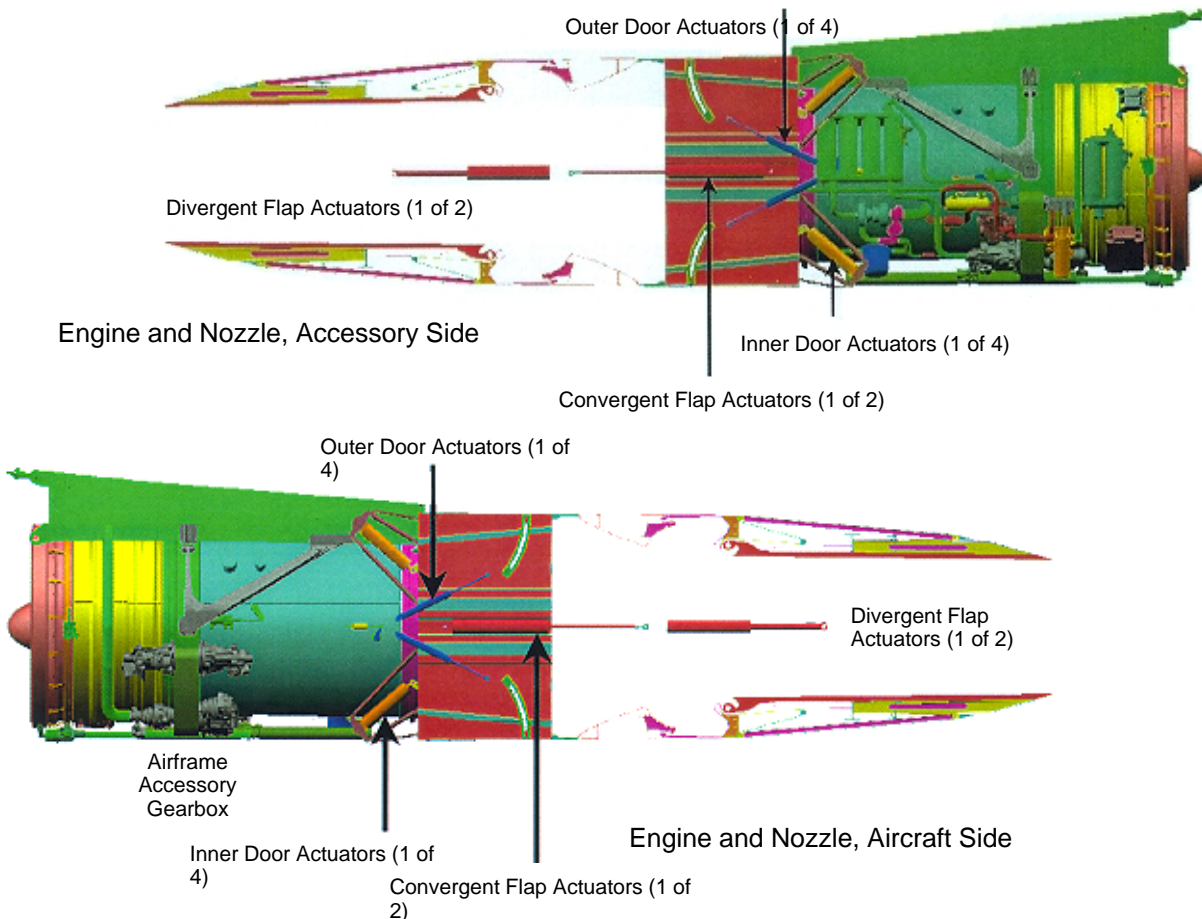
Figure 213.   Engine and Nozzle, Both Sides

Ignition Exciter

Fuel Inlet Line

Fan IGV (1 of 2)

Lube Oil Tank

Lube/Scavenge Pump (Forward)
Alternator (Aft)

Fuel Pump and Filter (Forward)
Nozzle Hydraulic Pump (Aft)

Fuel/Oil HX

FADEC

Engine Accessory
Gearbox

Anti-Ice Valve
and Air Pipe

Airframe Accessory Gearbox

Nacelle Outline

Fan IGV (1 of 2)

Airframe Hydraulic Pump(s)
(Forward and Aft)

Starter Air Pipe

Starter (Foward)
Generator (Aft)

Figure 214.   Component Locations in Relation to Nacelle, Forward Looking Aft
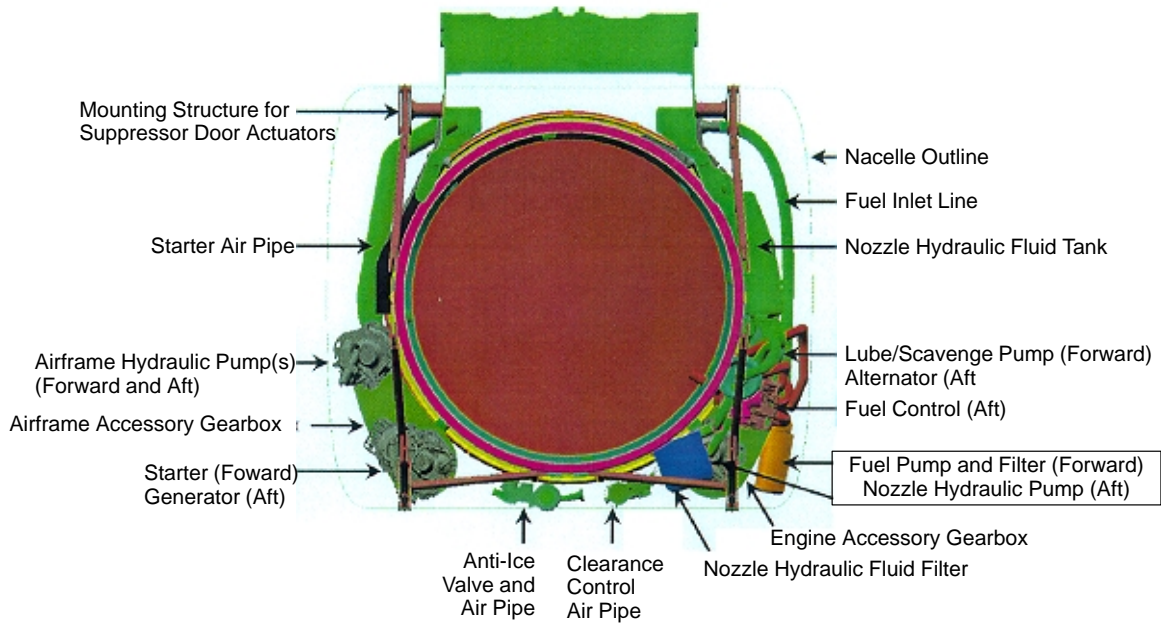
Figure 215. Component Locations in Relation to Nacelle, Aft Looking Forward at Turbine Rear Frame

A detailed model of the engine-sump heat-load analysis was developed including all bearings, seals, and gears. Engine oil temperatures were calculated for the mission flight conditions (51-point flight profile). The results of this calculation were compared against the design compatibility limits for standard commercial oils. The results were also used in aircraft thermal-management studies conducted by the Controls Design organization. Figure 220, an engine lubrication schematic, shows the fuel/oil-cooler interface to the aircraft thermal-management model. The oil temperatures calculated for mission flight conditions were within the design limits set for standard commercial oils. Figure 221 shows estimates of the sump-pressurization-system air temperature at the maximum cycle-temperature condition: Mach 2.4 supersonic cruise at 56,000-ft altitude. As shown in the figure, these temperatures are acceptable relative to design limits.

The aft sump and the engine lubrication system were designed to meet the requirements of the HSCT mission. The remaining challenges are:

- Lube system performance in a supersonic mission
  - Long times at maximum operating temperatures
  - Compatibility of standard commercial oils
  - Sump fire safety
  - Carbon seal life
- Challenging designs for 4R bearing and seal

3.3.3 Technical Requirements of Full-Scale Demonstrator Engine

The *Preliminary Technical Requirements* document was to provide a summary of the technical requirements for the anticipated full-scale demonstrator engine program. This document was in-

8/97 – Previous Baseline (Disk Actuation Nozzle)
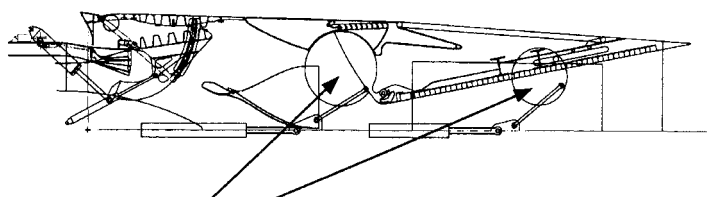
Convergent and Divergent Flap Actuation
Via Disks and Linear Actuators

Nozzle Features:
- Double Inlet Doors (4 total)
- R108 Uncooled Mixer (long)
- TiAl Div. Flaps
- TiAl Aft Sidewalls (cantilevered)
- $A_{trr}/A_{mix} > 6.0$
- 2 sec. Rev. Trans. Time
- 135.5 in. Mixing Length
- Latest Control Sys. Wt. Rollup
  (Adv. Mat'l)

6/99 – Current Baseline (Linear Actuation Nozzle)
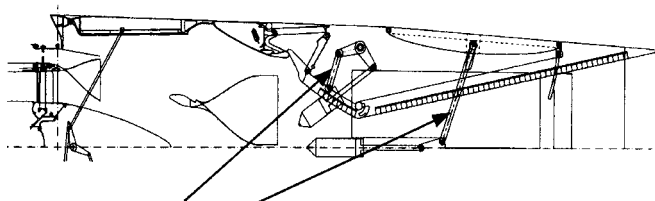
Convergent and Divergent Flap Actuation Via
Links, Bellcrank and Linear Actuators

Linear System Nozzle:
- Alternate Kinematics (linear actuation system)
- Single Inlet Door (total 2 per noz.)
- R108 Uncooled Mixer (Gen3.6-product scale)
- TiAl Div. Flaps
- TiAl Aft Sidewalls (non-cantilevered)
- Lower Density Bulk
- 2 sec. Rev. Trans. Time
- Fixed Fan/Core Mixer
- Adv. Mat'l Control System

Figure 216.   Current and Previous Baselines

Notes:

1. 5000-psi pump operates in–flight. Hydraulic pressure = f(P3) and 5000 psi max

2. Centrifugal hydraulic pump is air turbine driven; off except during reverse cycles 1500 psi assumes reverser transit occurs at low power

3. Actuators have 600°F abient

4. Boost pumps are integral with hydraulic pumps

5. Fluid is Perflouropolyalkyethers (PFPAE), nonflammable. Oil capability is 675°F. Predicted system max oil temperature is 350°F

6. Some servos will be paralled with a 4–way solenoid valve to reduce gains during flight, and operate on/off during reverse

Suppressor Door Actuation
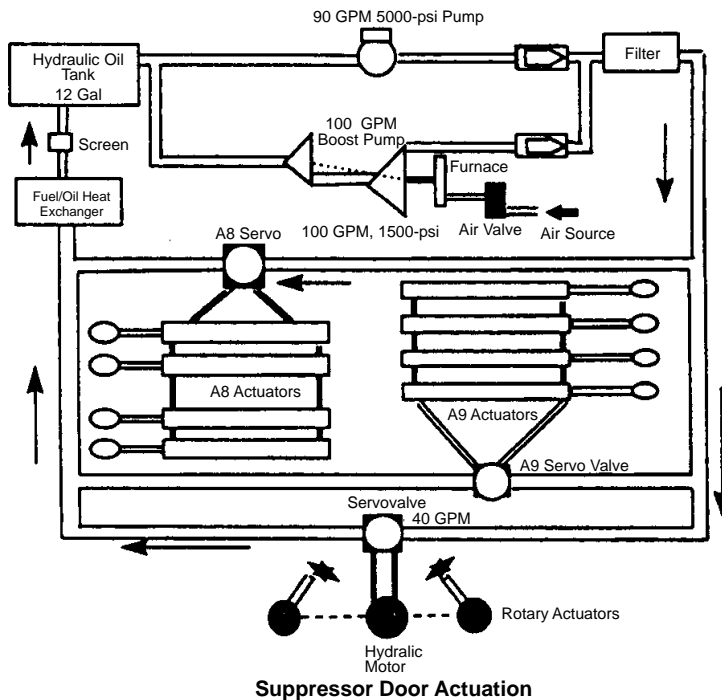
Figure 217.   Exhaust Nozzle Control System, 6/99 Configuration

Key Features

- Intershaft bearing and intershaft carbon seal
- Carbon seals for low leakage and low oil consumption
- Fan exit air used to pressurize seals
- Center vent to midsump via LP shaft
- Inverted No. 4 bearing
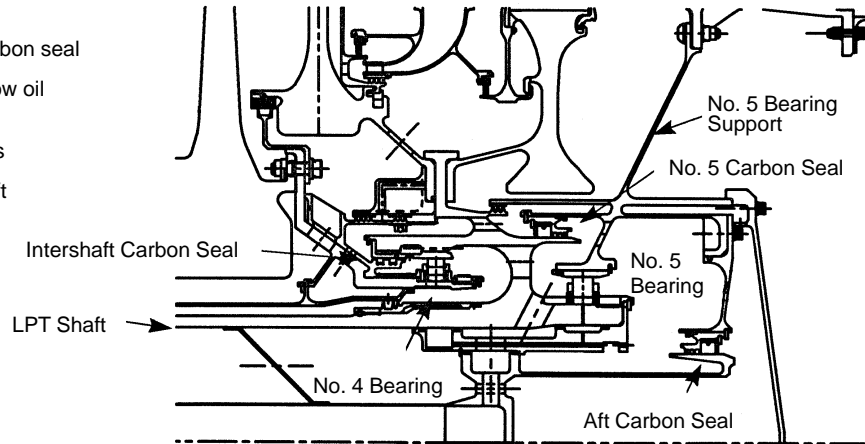
Figure 218. HSCT Aft Sump Compartment *Aft sump design is compatible with lube system requirements and turbine cooling-circuit temperatures.*

						Fan Shaft		Intershaft		Aft Seal		Vent	
Case	Description	Altitude (ft)	Mach Number	Power Code	ΔT_{amb} (°F)	Flow* (%W_{25})	Temp (°F)	Flow (%W_{25})	Temp (°F)	Press (%W_{25})	Temp (°F)	Flow (%W_{25})	Temp (°F)
4	Lift Off	0	0.36	100	18	0.012	384	0.016	622	0.0013	394	0.0304	536
18	Subsonic Cruise	34,000	0.9	38	0	0.009	233	0.025	453	0.0013	198	0.021	561
27	Supersonic Cruise	55,560	2.4	50	0	0.057	570	0.028	650	0.0014	629	0.0278	548
						* Used 50% recovery on source total pressure.							

Figure 219. Sump Pressurization, Secondary Flow Schematic

Table 75. HSCT Bearings and Seals *The 4R bearing and carbon seal are challenging designs. The inverted bearing configuration selected for clearance control increases critical design parameters. The other bearing and seal designs are within current design experience.*

Bearings	1R	2B	3B	4R	5R
Rolling Element	28x28 mm	$1^7/_{16}$ in	$1^9/_{16}$ in	13x13 mm	16 x 16 mm
Pitch Diameter, in	8.59	9.65	9.65	10.94	9.72
$DN \times 10^6$	0.975	1.03	1.73	**3.80**	1.2
Dynamic Capacity, lbf	86,000	47,500	49,400	32,500	45,100
Static Capacity, lbf	73,700	60,500	63,500	36,000	47,000
L_{10} Life Load, lbf	8,370	5,190	4,550	2,360	4,400
Carbon Seals	1R	2B	3B	4R I/S	5R
Rubbing Velocity, ft/s	11,041	11,514	19,139	**28,365**	18,400
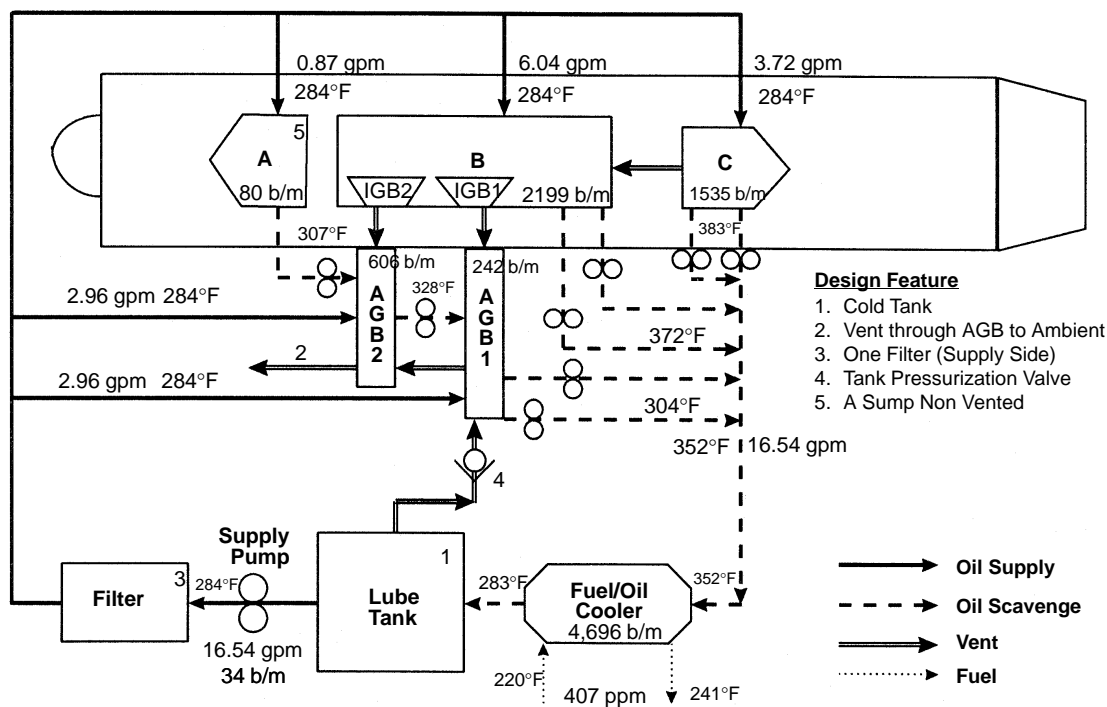
Figure 220.   HSCT Engine Lube Schematic   *Takeoff Case 5: 220° F fuel (coolant) temperature.*

Max Cycle Temperature Design Condition

Cycle Case 27, M=2.4, Alt=55,560' ft W25=304.46lbm/s
N2 = 5381 rpm, N25 = 9129 rpm

Rotor 4 Hub Exit Conditions
P = 101.71 psia
P_s = 79.18 psia
T_t = 942.3°F
T_s = 852.1°F

	W	T	P			W	T	P
	pps	F	psia			pps	F	psia
A. Vent	0.085	548	2.1		A. Vent	0.085	350	2.2
B. Fan Shaft	0.174	609	30.3		B. Fan Shaft	0.174	570	30.2
C. Inter Shaft	0.085	498	34.6		C. Inter Shaft	0.086	671	30.1
E. Aft Seal Press	0.004	671	34.8		D. LPT Cooling		743	

Figure 221.   Sump and Vent System Air Temperatures   *Temperatures are
below design limits for sump oil, vent coking, and carbon seals.*

tended to establish a specific set of requirements needed to support the design, build, and test objectives of that program. The Preliminary Technical Requirements document was developed in accord with the (Boeing) *Design Requirements and Objectives* (DR&O) document dated 1/17/97.

In 1998, the full-scale demonstrator program was dropped; consequently, the Preliminary Technical Requirement document was not completed. However, a prioritized list was drafted (Table 76).

Table 76. HSCT Preliminary Technical Requirements

1. Engine/Nozzle Bay Environment	13. Emergency Descent	25. Flight Envelope
2. Duty Cycle	14. Anti-Ice	26. Restart Envelope
3. Bleed and Power Extraction	15. Performance	27. Transient Requirements
4. Electrical Requirements	16. Fire Protection	27a. Transitions: Nozzle Mode Changes
5. Emissions	17. Mounting/Installation	28. Nozzle Failure Modes
6. Noise	18. Fuel Types	29. Inlet/Engine Control Interface
7. Thrust Requirement	19. Structural Integrity	30. Reliability
8. Time to Climb	20. Operability	31. Maintainability
9. Thrust Reverse	21. Certification	32. Autothrottle
10. Windmilling	22. Inlet Unstart/Recovery	33. Fuel Thermal Management
11. Starting	23. Maneuver Loads	34. Unique Environmental Issues
12. Engine-Out Mission Impact	24. Life Requirements	

3.3.4 FLOWPATH Engine Design and Weight-Reduction Studies

The HSCT TOGW proved to be very sensitive to engine weight. During every phase of the study, engine weight reduction became a key element. Engine weight estimates can be grouped into four time periods:

- The CPC Systems Study Engines
- 1996 Common Mechanical Design Engine
- 1997 Common Mechanical Design Engine – Status
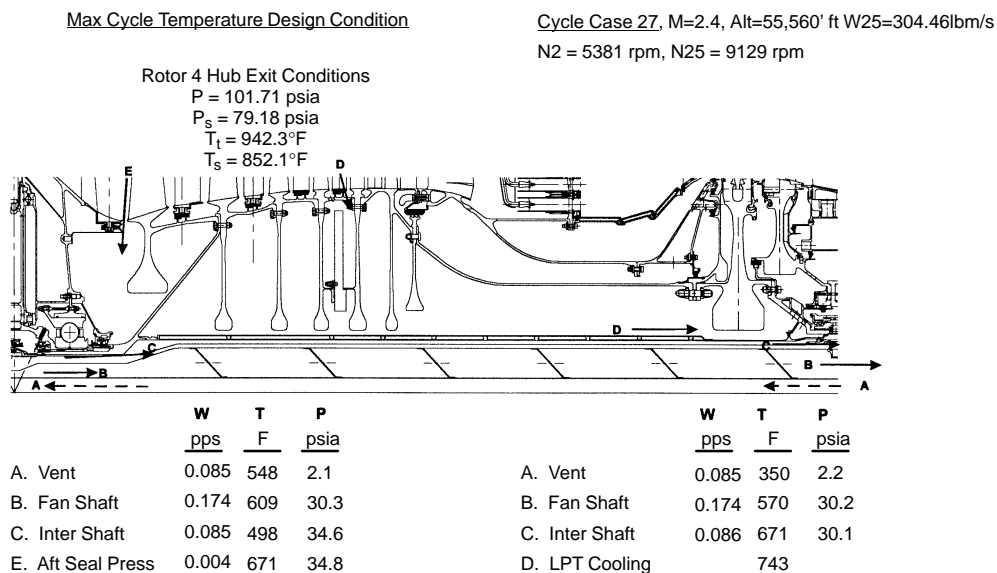- 1998 and 1999 "Ultimate MFTF" Configuration Studies

The first three are summarized in the following subsection; 1998 and 1999 "Ultimate MFTF" configuration studies are discussed in some detail in the next subsection.

3.3.4.1 Early Weight-Reduction Design Studies

The CPC systems study engine design work started in 1994. Engines developed in this study were designed to power the TCA wing planform. These engines incorporated Phase I design assumptions and the material suites developed through a two-year design activity.

The common mechanical design engine was developed as the baseline for the 1996 study. This engine was based on both the enabling propulsion materials (EPM) program and the component design activities that focused on the performance and life goals of the HSR program.

Further design development took place in 1997 and again in 1998. Engine design was continuously updated, and the first HSR component design efforts were included, both for the combustor and for the controls and accessories.

Significant weight problems were identified during 1997 and 1998, and specific weight-reduction activities focused on the problems. An effort was made to define the steps to establish an engine weight goal and to determine the technologies needed to achieve this goal.

The first major weight problem was addressed in 1997. Common engine design activity during 1996 identified significant component design changes needed to meet the severe life requirements of an HSR mission, and extensive component-geometry changes were then recommended for the HSCT3770.54:

<table>
<tr><td align="center">Assumptions:</td><td align="center">Material and Construction Changes:</td></tr>
<tr><td valign="top">

- F110 Style Front Frame
- P&W Fan Definition
- Updated GEAE Compressor
- Generic Combustor Match of LPP (Weight from Design Group)
- GEAE Turbines and Rear Frame

</td><td valign="top">

- Stages 2 and 3 Fan Disks to Ti 6242
- Fan Stators Shrouded
- Fan Frame to Ti 64 (Weight is for Additional Case)
- EPM Advanced Nickel Subsolvus Compressor Stage 4 and 5 Disks
- HPC Stator 5, Cantilevered
- TiAl Combustor Diffuser, Inco 930 Case
- EPM Advanced Nickel Subsolvus Turbine Disk Material
- LP Shaft Diameter and Thickness
- Inco 718 Rear Duct Links

</td></tr>
</table>

The engine configuration defined from these new components is shown in Figure 222. The new components are shown on the right-hand side of the figure. The engine schematic shows the 1997 3770.54 engine on top and the 1996 common engine underneath. The 3770.54 design was the first time that the LPP combustor characteristics were modeled in the full engine. The added length of the burner that resulted adversely impacted the core-stream components.

The 2274-lbm weight increase shown in Figure 222 caused a flurry of activity as steps were taken to identify what was needed to meet engine weight goals for the system. To start this process, the engine design was compared with a current product.

The FLOWPATH program was used to scale the GEAE F110–129 to the inlet flow size of the 1997 base engine. It should be noted that the two engines do not have similar missions or duty cycles. The F110 is used in fighter aircraft applications where missions are short duration and high thrust generation is the primary objective. The weight of the two turbofans, however, is nearly identical, as shown in Figure 223.

The technologies needed to reduce the weight of the HSR engine by increasing the cycle temperature exist and are used in the design of advanced military engines for the future. There are, however, two reasons why these technologies cannot be used for the HSR propulsion system, and these two reasons mandate engine technologies unique to the HSR system. First, system emission requirements restrict the compressor-exit and turbine-inlet temperatures to levels lower than those in
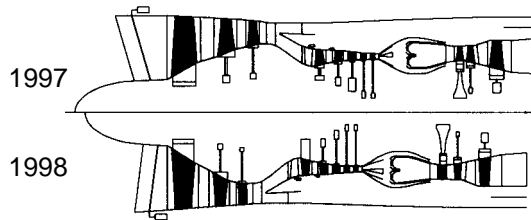
Engine Weight, lbm

Component	1996	1997 I	Diff
Front Frame	196	232	36
Fan Rotor	1087	1462	375
Stator	713	998	285
Main Frame	427	435	8
Compressor Rotor	871	1222	351
Stator	336	369	33
Combustor	661	1315	654
HP Turbine Rotor	731	703	−28
Stator	224	237	13
LPT Rotor	1059	1379	320
Stator	314	330	16
Rear Frame	562	530	−32
Outer Duct	348	347	−1
C&A	619	757	138
Core Engine	**8555**	**10830**	**2274**
HP Spool	3980	5196	1217
LP Spool	4576	5633	1057
Fan Containment	135	162	27
Core Engine with Cont	8691	10992	2302

- This is the initial 1997 Engine
- New P&W Fan
- New GEAE HPC
- LPP Combustor Length and Weight
- GEAE Turbine Aeromechanical Design
- Combustor Length Impacts Core:
  – HPC Rotor
  – HPT Rotor
  – LPT Rotor
  – LP Shaft Diameter

Figure 222.   Engine Comparison: 1997 versus 1996
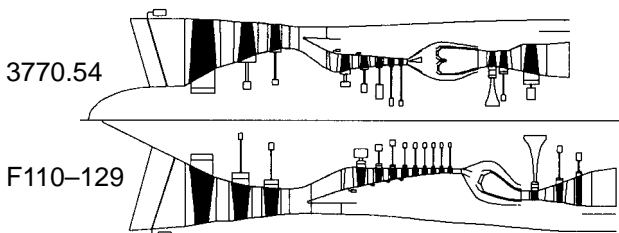
For Reference:

at 800 lbm/s
  » F110–129 –> 10,986 lbm
  » HSCT3770.54–> 10,992 lbm

Items That Make HSCT Heavier	Lighter
Life and Durability	Length
Low Emission Combustor	No Vane HPT–LPT
Cooled LP Turbine	Fan and Compressor Blisks
Low Aspect Ratio LP Turbine	5 vs. 9 Stage HPC

Figure 223.   Scaled F110–129 Vs HSCT 3770.54 Engine

current military engines. Second, noise-suppression requirements place a limit on engine exhaust jet velocity that restricts engine fan pressure ratio as well as the specific thrust of the system.

A program summit was held at NASA-Langley in June 1997 to address the system weight problems. In support of this activity, a second version of the 1997 3770.54 engine was defined. To create this new configuration, the components, including the fan, were returned to the previous architecture. Additional stretch goals were placed on the design of the other items that led to the heavy estimates.

New improvements that were tried included changes to the front two frames and to the tailored turbine geometries. Some modest length improvements were achieved with this design, and the weight problem was thought to have been cut roughly in half.

A comparison of these first two 1997 engines is shown in Figure 224. While the results were encouraging, the new engine was still heavier than the 1996 engine, and the economics of the system were threatened by this weight problem.
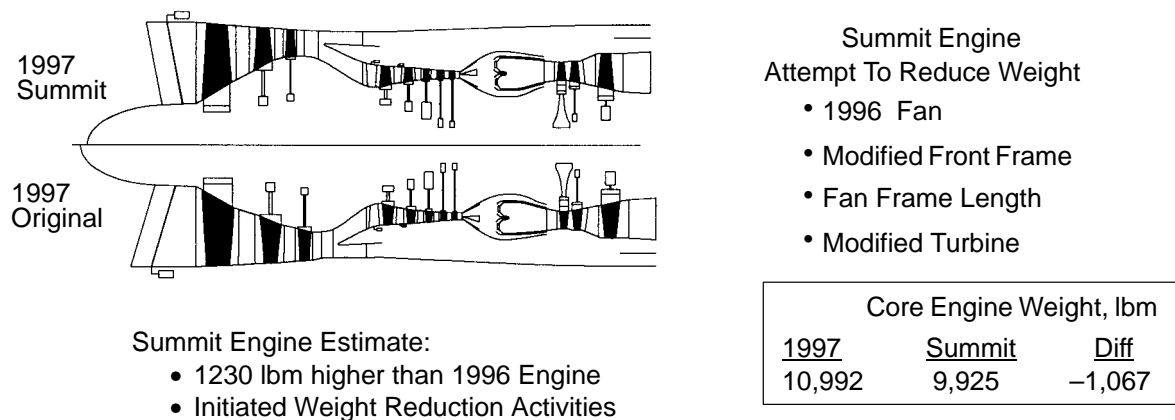
Figure 224. Summit 3770.54 Engine Vs 1997 Engine

It was agreed that a weight goal for the HSR propulsion system design would be identified by September 1997. To support this activity, the engine design team held a brainstorming session at GEAE in May 1997 where they identified 20 component items as potential weight drivers. Of these items, 12 were not found to have any beneficial impact on the HSR engine. The items that appeared to offer weight reduction were as follows:

- Shrouded Stage 2 LPT blade, increased aspect ratio
- Increased LPT tip slope
- Increased HPT blade root stress (AN^2)
- Reduced fan radius ratio
- Increased fan exit Mach number
- Increased HPC exit Mach number
- Six-stage versus five-stage HPC

The LPT rotor appeared to represent a significant portion of the increased engine weight. This problem was compounded by the low-aspect-ratio airfoil that was required on the turbine second

stage to provide sufficient vibration tolerance (aspect ratio equals height over chord). Therefore, an airfoil chord increase was required to achieve the desired vibration tolerance. This chord increase made the airfoil weights heavier and mandated a wider disk to hold the airfoil. Both factors increased disk weight.

It had been established that application of a tip shroud to a turbine stage would permit the use of airfoils with a shorter chord. Relatively high-aspect-ratio airfoils gain significant vibration tolerance when used with a shroud. In light of this feature, the goal became to design an airfoil that reduced rotor weight sufficiently to compensate for the added weight of a shroud. The task was complicated by the fact that cooling was required for the airfoils.

Initial FLOWPATH studies of this feature indicated that a significant weight reduction would be achieved by adding a shroud. Figure 225 summarizes the weight results of this design prediction and also shows an engine schematic comparison. The shrouded turbine engine is on top, and the 1997 summit engine is on the bottom.

LP Turbine Stage Two Blade and Disk
- Large Source of Weight – 456 lb
- Disk is large and Sensitive to Sump Size
- Blade Taper is large for Aeromechanics
  – Large root chord
  – Large dead mass on disk

Stage Two Shroud Impacts:
  – LP Turbine Design
  – LP Shaft Diameter
- Stage 2 Rotor Weight down 250 lb
  – Assumes F110 Parameters
    • Aspect ratio
    • Zwiefel Coefficient
    • Taper Ratio
- Very Significant Impact

Core Engine Weight	July Eng.	LPT Shd	Diff
HP Turbine Rotor	703	709	6
Stator	237	235	−2
LPT Rotor	943	726	−217
Stator	266	250	−16
Rear Frame	528	519	−9
Outer Duct	345	336	−9
	8988	8742	−246

Figure 225.   Shrouded Stage Two LPT Rotor

A second engine improvement thought to have promise was to increase the exit Mach number of the compression components, both the fan and compressor. The fan appeared to offer the most potential for improvement.

The geometry of the fan has been designed to produce the pressure rise and desired flow at the most practical level of efficiency. The design takes into account fan stall considerations. Design tip speed for the fan is selected to ensure that there will be sufficient tolerance to fan stalling during operation in a product environment. For the HSR fan, tip speed was limited by inlet noise during landing approach, since this noise has a direct relationship to fan tip speed.

The limit established by this noise requirement removed one of the design strategies that might have been used to establish sufficient stall tolerance in the component. Other variables that could have been used to influence the design are the length of the airfoil chord and the amount of static pressure

rise. The airfoil chord impacts the coefficient of airfoil lift. A longer chord reduces the coefficient of lift and thus increases the tolerance to the onset of stall.

A design total pressure rise has been specified (3.7). The design static pressure rise is dependent on this requirement, and the relationship is governed by the selection of the inlet and exit Mach numbers for the component. The exit Mach number that had been used in these designs was based on product experience.

To define the baseline, parameters were adjusted until a balanced fan was developed that could satisfy performance requirements and provide 25% stall margin. This margin was assumed to be adequate based on similar design experience.

The lift coefficient of the airfoils is also dependent on the static pressure rise of the fan. To achieve a lower exit static pressure, it was necessary to increase the fan exit mach number. This would allow shorter chords to be used to achieve stall tolerance. The shorter chords were used to negate the performance loss of the high Mach number, and it was hoped they would result in a component weight reduction.

As shown in Figure 226, a significant engine weight reduction was achieved by increasing the design exit Mach number from 0.45 to 0.50. Figure 226 also shows the issues and the impact of this Mach number change on the design. For the analysis shown here, only the fan was allowed to change, so weight reduction is limited to the fan module.

M 0.50

M 0.45

Fan Exit Mach Number
• Efficiency Best at Low Mach Number
• Increased Static Pressure Rise
• Increased Blade Chord => Weight

Initially Agreed to 0.45 – Current Products

Impact
• Limited to Fan and Frame
• Reduced Height in Fan
• Longer Length

Weight Improvement
• Lighter Airfoils
• Smaller Disks

Core Engine Weight			
	July Eng.	0.5 Me	Diff
Fan Rotor	1207	1031	−176.3
Stator	739	671	−68.6
	8989	8731	−258.1

Figure 226.   Fan Exit Mach Number Comparison
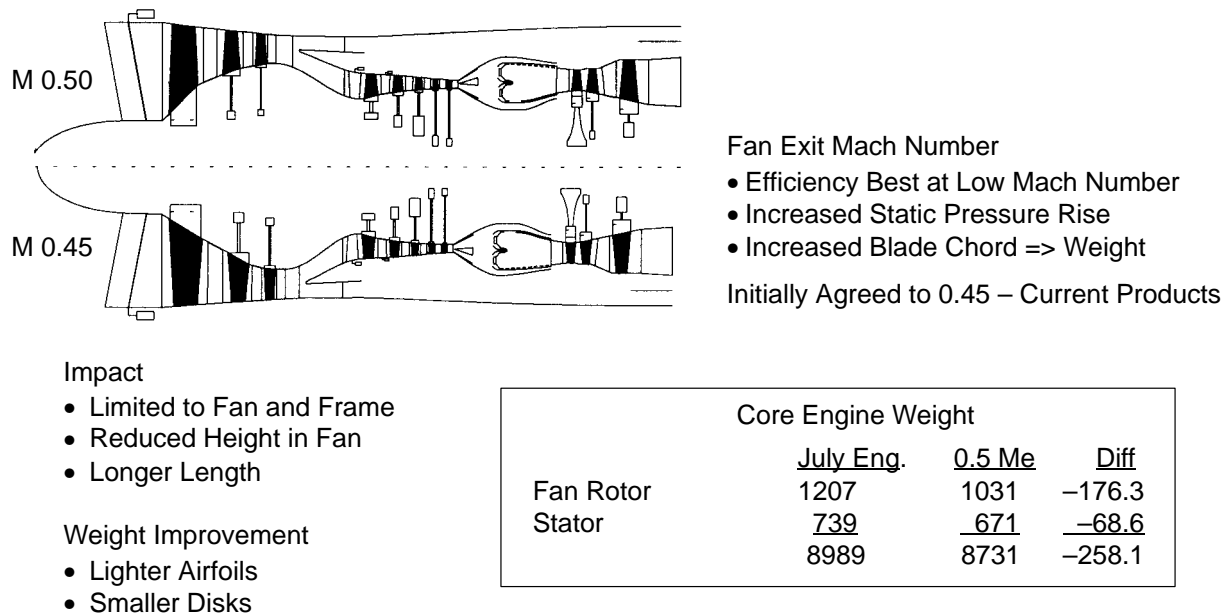
The items listed in Figure 226 were examined with the FLOWPATH model. Several showed significant improvements and were passed on for more detailed design consideration. Detail designers refined the fan design with a higher exit Mach number and a shrouded LPT. These configurations were incorporated into the FLOWPATH analysis, and the new weights were predicted as shown in Table 77.

The shrouded Stage 2 LPT rotor and increased fan exit Mach number offered the most potential weight reduction (about 250 lbm each). Changes in LPT slope (30 lbm) and fan inlet radius ratio (34 lbm) gave positive results but had to be designed with an eye on the actual weight impact on the feature.

Table 77. Engine Weight Estimates *Initial results stimulated design activity.*

Refinement	Component	Weight, lbm		
		July Engine	Refined	Δ
Higher Exit Mach Number Fan (M_e = 0.5)	Fan Rotor	1207	1130	−77.2
	Stator	739	717	−22.4
	Main Frame	448	434	−14.5
	Total	8989	8865	−124.0
LPT Stage 2 Shrouded Rotor	LPT Rotor	943	746	−197.0
	Stator	266	279	+12.8
	Rear Frame	528	546	+18.6
	Outer Duct	345	338	−6.7
	Total	8989	8808	−181.0

This engine configuration did not respond favorably to an increase in turbine blade root stress, AN^2. This was probably due to the engine rotor weight sensitivity as will be discussed later.

Proposed items were examined by limiting impact to the particular feature. Usually this approach overstates the cumulative impact of applying several features. Often benefits are gained from same part weight reductions. When combined, only part of the weight reduction is achieved; thus, a realization factor was applied to the FLOWPATH predictions to allow detailed design realities.

Compressor design variations were: exit Mach number was increased from 0.30 to as high as 0.40, and the stage count was changed from five to six stages. The exit Mach number benefits the compressor design strategy just as it did the fan discussed above. Adding a stage reduces the loading or lift coefficient per stage and allows the benefit of diameter reductions in the component.

The weight results of three variations relative to the summit engine are shown in Figure 227. Interestingly, all three variations were lighter than the summit engine, which had a five-stage compressor at a low exit Mach number. A 62-lbm reduction was achieved by integrating the aerodynamic choices with the summit engine mechanical requirements. As shown in Figure 227, the six-stage compressor was the lightest, and this configuration was chosen for the September 1997 weight estimate.

As is usually the case, the weight reduction features above were combined with additional system realities that had not been included in the calculations for the summit engine. These included incorporation of the fan rotor weight to handle distortion from the 2D inlet that had been used as the baseline during this activity. Additional weight was added for the controls and accessory gearboxes that were required for the engine and for the additional structure in the turbine rear frame.

The September 1997 (interim) engine design that resulted is shown in Figure 228. In the schematic, the interim engine is shown on top, and the summit engine is shown on the bottom. Features and weight projections are also shown. Because of the design activity described above, the engine core
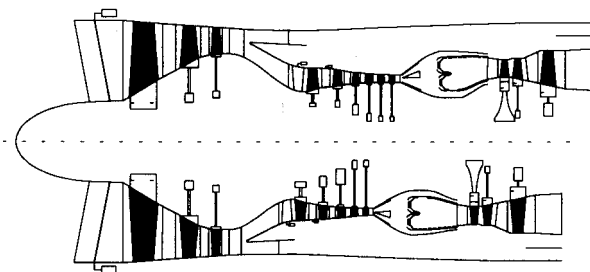
Compressor Refinement:
Exit Mach Number and Stage Count

- All Lighter than Base
- 0.4 Me Heaviest Choice
  - High Combustor Losses
  - Increased Turbine Flow Size
- Six-Stage Compressor Yields lightest Engine

Core Engine Weight						
	July Eng.	M0.35 5 Stg	Diff	M0.35 6 Stg	Diff	M0.40 5 Stg	Diff
HPC Rotor	970	915	−54.9	767	−203.3	881	−89.8
Stator	369	366	−3.3	391	21.9	370	1.0
Combustor	829	829	0.0	802	−27.0	802	−27.0
HPT Rotor	703	703	0.0	737	33.6	740	36.6
LPT Rotor	943	943	0.0	969	25.8	969	26.0
Rear Frame	528	528	0.0	528	0.0	539	11.5
Outer Duct	345	345	0.0	369	24.2	353	8.4
	8989	8927	−62.1	8856	−133.2	8958	−30.7

Figure 227.   Three Engine Comparison

Interim Engine

September 1997 HSCT3770.54 Estimate
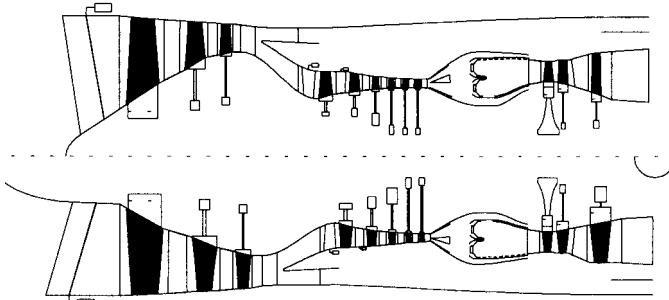
Summit Engine

Interim Engine

Combines Weight Reduction Elements

- Higher Exit Mach Number Fan
- Six Stage HPC
- Shrouded Stage Two LPT Rotor
- Low NOx Combustor
- HSCT Control Requirements
- High Suppression Nozzle

Engine Weight			
		Interim	
	Summit	Projection	Diff
Frame	208	221	13
Fan Rotor	1213	1285 **	72
Stator	739	654	−86
Main Frame	492	447	−45
HPC Rotor	838	765	−73
Stator	369	391	22
HPT Rotor	703	717	14
Stator	237	237	0
LPT Rotor	1249	746	−503
Stator	311	282	−29
Rear Frame	528	640	112
Outer Duct	345	363	18
Combustor	1381	1461	80
C&A	807	798	−9
Gear Boxes	0	290	290
Total Core	**9925**	**9767**	**−158**
Nozzle	**9900**	**8705**	**−1195**
Total Engine	**19825**	**18472**	**−1353**

** 160 lb added for Stg 1 Frequency

Figure 228.   September 1997 HSCT3770.54 Estimate

weight was reduced by 158 lbm. This, together with the nozzle weight reduction, drove the engine to a very significant reduction of 1353 lbm.

The management of the two engine companies (GEAE and P&W) decided that experience justified a weight challenge to the projected product weight of this engine system. The challenge was for a 10% cut across the board relative to the interim estimate above. This cut defined the product weight estimate for a 3.7 FPR engine with 800 lbm/s inlet flow to be 16675 lbm. There were a few caveats applied to this estimate, and these are listed in Figure 229. The engine schematic is identical to the top portion of the schematic in the previous figure. The weights listed were calculated with the weight challenge applied. The differences listed are related to the summit engine discussed earlier.
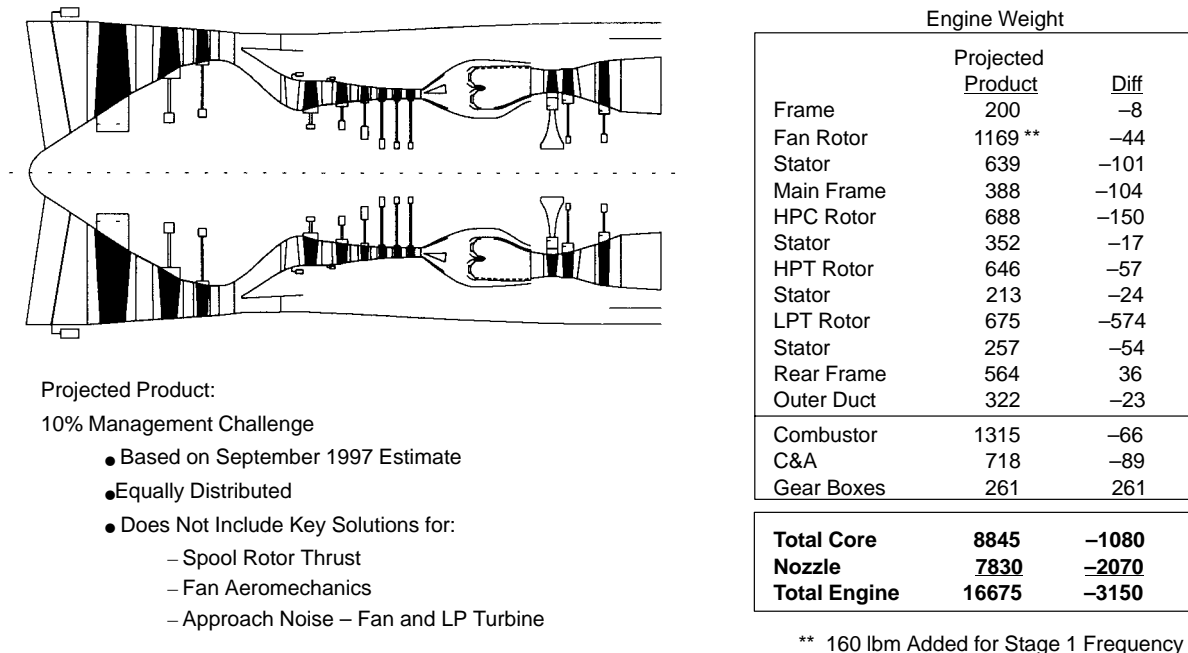

Projected Product:

10% Management Challenge

- Based on September 1997 Estimate
- Equally Distributed
- Does Not Include Key Solutions for:
  - Spool Rotor Thrust
  - Fan Aeromechanics
  - Approach Noise – Fan and LP Turbine

Engine Weight		
	Projected Product	Diff
Frame	200	−8
Fan Rotor	1169 **	−44
Stator	639	−101
Main Frame	388	−104
HPC Rotor	688	−150
Stator	352	−17
HPT Rotor	646	−57
Stator	213	−24
LPT Rotor	675	−574
Stator	257	−54
Rear Frame	564	36
Outer Duct	322	−23
Combustor	1315	−66
C&A	718	−89
Gear Boxes	261	261
Total Core	**8845**	**−1080**
Nozzle	**7830**	**−2070**
Total Engine	**16675**	**−3150**

** 160 lbm Added for Stage 1 Frequency

Figure 229.   September 1997 3770.54 Projected Product

The weight reduction effort is summarized as follows:

- September 1997 Interim Estimate Based on Preliminary Component Design Effort

- Product Projection Considered a Reasonable Challenge (10% Lighter than Interim Engine)
  - Requires additional work and new ideas
  - Does not include key turbomachinery solutions

3.3.4.2 1998 and 1999 "Ultimate MFTF" Configuration Studies

As discussed in the TC design sections, the 1998 engine design matrix used sophisticated design modeling and optimization processes to define the best propulsion system solution. Figure 230 describes the propulsion system configuration developed for the Technology Configuration aircraft (FY 98 milestone). The inlet, turbofan engine, and exhaust nozzle are shown and described in the figure, and features are listed that provide the balanced economics, risk, and environmental impact necessary for the TC.
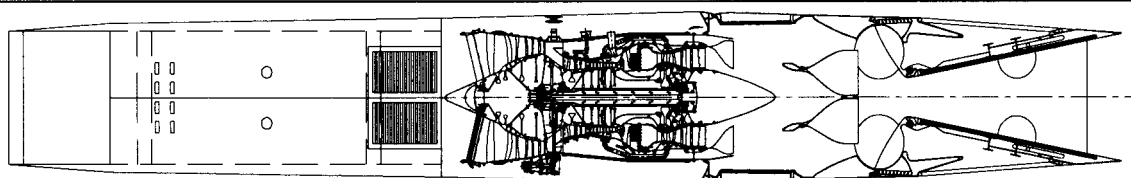
2D Bifurcated Mixed-Compression Inlet

- Lowest overall risk
- Low mechanical complexity
- Lightest when required acoustic treatment area is considered

3770.54 Mixed-Flow Turbofan

- Moderate-risk conventional turbomachinery
- Flexibility to match aircraft thrust and noise-suppression requirements

2D Mixer/Ejector Exhaust Nozzle

- Moderate-risk noise-suppression concept
- Avoids oversizing of inlet and engine

Figure 230.   TC Propulsion System 1998 Configuration
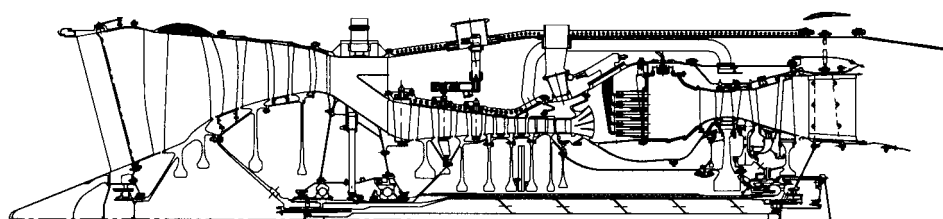
Component	Weight, lbm		
	June Brick Engine	August Engine	Difference
Turbomachinery	7,689	7,587	−101
Combustor	1,356	1,356	0
C&A	972	972	0
Total Core	13,351	10,250	−101
Exhaust Nozzle	8,465	7,833	−632
Total Engine	18,816	18,083	−733

October 1997 Projected Product	16,675
Status Weight Progression	
October 1997	18,467
March 1998	18,953
April 1998 Brick	20,833
June 1998 Brick	18,816
August 1998 (3770.54)	18,083

Figure 231.   Design Activities (1998) Focussed to Recover Weight Introduced with Increased Cycle Fidelity

The weight progression during 1998 is shown in Figure 231. Component updates throughout the engine and a reassessment of the controls and accessory hardware contributed to the March 1998 establishment of a new baseline that increased the weight by 486 lbm. In this model, the LP spool and the combustor actually went down in weight, but engine cycle redefinition to support the TC selection resulted in significant engine and nozzle weight increases for the 3770.54 MFTF engine. This was noted in the April 1998 "Brick" status.

Subsequent changes introduced in the cycle performance losses and part-power operation definition for the June cycle resulted in recovery from the April 1998 weight increase as well as some of the weight that was introduced by the March 1998 configuration definition. These weight-reduction activities used the FLOWPATH engine design process to leverage DOE techniques and achieve the best performance/weight configurations. Based on the June 1998 cycle, additional component design solutions in the fan, compressor, turbines, and nozzle were evaluated, and this resulted in the

August 1998 (3770.54) engine. The nozzle weight reflected incorporation of SAVE event weight-reduction features together with the June 1998 cycle update.

The August 1998 engine weight was significantly heavier than the projected goal weight of 16675 lbm. As a result, additional weight reduction activities were initiated in July 1998 to determine the lightest possible configuration. As part of this activity, the technical requirements imposed on the engine designs were relaxed. The work was specified without risk level, technology readiness date, or cost limitations to establish a perspective for the proposed "projected" product weight. The (higher risk) configuration that resulted was designated the "Ultimate MFTF" engine.

As shown in Figure 232, the initial list of 106 weight-reduction ideas (advanced technologies and advanced designs) was condensed to about 40 items. Rough order of magnitude (ROM) engine weight reductions were estimated in August. The component configurations that incorporated these weight reduction ideas were used in the "Flowpath" Engine Design Process to determine which combination provided the best performance/weight configuration (net configuration). This net configuration was the basis for performing the continuing 1999 "Ultimate MFTF" work.

Table 78 lists items evaluated by the FLOWPATH program, ranked by impact on overall TOGW as defined using the transfer function shown in Figure 232. Items shaded in green were deemed significant to the system. Items shaded in grey were judged to be a detriment to the system and were not carried into the 1999 work. The Table defines the total impact as well as the impact of the weight alone. The third column is the projected weight savings for each item in pounds (for weight change alone, not total impact). The second and eighth items are the same feature applied first to minimize the TOGW and then to minimize the item weight. This table points out that the lightest system does not yield the best TOGW answer. Here the turbine blade root stress (AN^2) can have twice the impact on the system by designing an engine that only saves half the weight of the lighest possible solution.

The results of this analysis were used to define the preliminary weight reductions based on the July 1998 assumptions that were identified by Nov 1998 for the "Ultimate MFTF." These projections are shown in Figure 233. The total weight reduction is a combination of items that were evaluated later in the FLOWPATH model (net configuration) plus assessed by engine and nozzle component designers. The results show that at the preliminary design level the weight reduction potential appears to be sufficient to achieve the "projected" product weight with the attendant risk, technology development, and acquisition cost factors that would be required.

This weight reduction activity defined the objective and approach used for the 1999 "Ultimate" MFTF work:

Objective: To establish the suite of materials and component technologies that define a "best case" solution for the MFTF propulsion system.

Approach:

- 2015 Technology Readiness Assumption – New program launch with mature technologies or well-defined risk-abatement plans in place.

- Extension of the 1998 Component Design and Weight-Reduction Work
  – Evaluate higher risk technologies for engine and exhaust nozzle
  – Improve fidelity of the 1998 weight-reduction estimates
    ▪ Layout or sketch
    ▪ Supporting analysis and/or substantiation

- Weight calculations
- Technology development plan, estimated schedule and costs
- Issues and risks
- Acquisition-cost estimate

Table 78.   Item Weights and Impact on TOGW

Item	ΔTOGW (%)		ΔTOGW (lbm)
	Total	Weight	
HPT and Stage 1 LPT Blisk	−1.13	−1.13	−440.0
Increase AN^2 to 48 – Min TOGW	−0.88	−0.22	−84.9
Forward-Swept Fan	−0.68	−0.20	−77.8
Composite Fan Stator	−0.62	−0.62	−243.3
Shrouded LPT Rotor 1	−0.58	−0.40	−155.6
Fan Suction-Side Bleed	−0.58	−0.24	−94.9
Reduced Radius Ratio and 43.3 W/A Fan	−0.47	−0.34	−131.1
Increase AN^2 to 48 – Min Weight	−0.43	−0.46	−177.8
Composite Fan Case	−0.42	−0.42	−162.3
Fan Stage 2/3 Tip Shroud	−0.38	−0.39	−152.7
All CMC Turbine Nozzle Airfoils	−0.37	−0.37	−143.2
Hollow-Bladed Fan Blisks	−0.29	−0.29	−113.4
Change LP Shaft Diameter	−0.28	−0.28	−110.0
CMC Fan Frame with Load Decoupler	−0.20	−0.20	−76.2
Eliminate Front Frame and Sump; Keep IGV's	−0.17	−0.17	−67.1
Eliminate HPC Stage 1 Variable Stator Vane	−0.17	−0.17	−66.0
Fan Stage 1 Midspan Shroud	−0.09	−0.30	−117.1
NiAl HPT Nozzle	−0.07	−0.07	−26.6
CMC Inlet Guide Vanes	−0.04	−0.04	−16.4
Cross 2/Rev on Fan Rotor 1	−0.04	0.01	5.6
42.3 W/A Fan	−0.01	−0.18	−70.9
Dual-Alloy Turbine Disks	0.01	0.01	3.1
Integrate Fan IGV's with Fan Frame	0.01	0.01	5.2
CMC HPC Vanes	0.02	0.02	6.0
Reduced Radius Ratio FAn	0.11	0.19	74.7
CMC Stage 2 LPT Uncooled Blade	0.25	0.25	98.7
Two-Stage Hollow Fan	0.75	−0.03	−10.6
Two-Stage Fan	1.17	0.39	151.5
Single-Stage LPT – Two-Stage Fan	2.31	1.33	520.1
Single-Stage LPT – Three-Stage Fan	2.76	2.33	907.1
Single-Stage LPT – Two-Stage Fan with Low RR	4.30	2.90	1132.0

"Ultimate MFTF" Proposed:

      July 1998:   Initial brainstorm generated 106 ideas; over 40 new ideas were evaluated.

      August 1998:   ROM weight-reductions were estimated.

FLOWPATH Engine Design Process Used

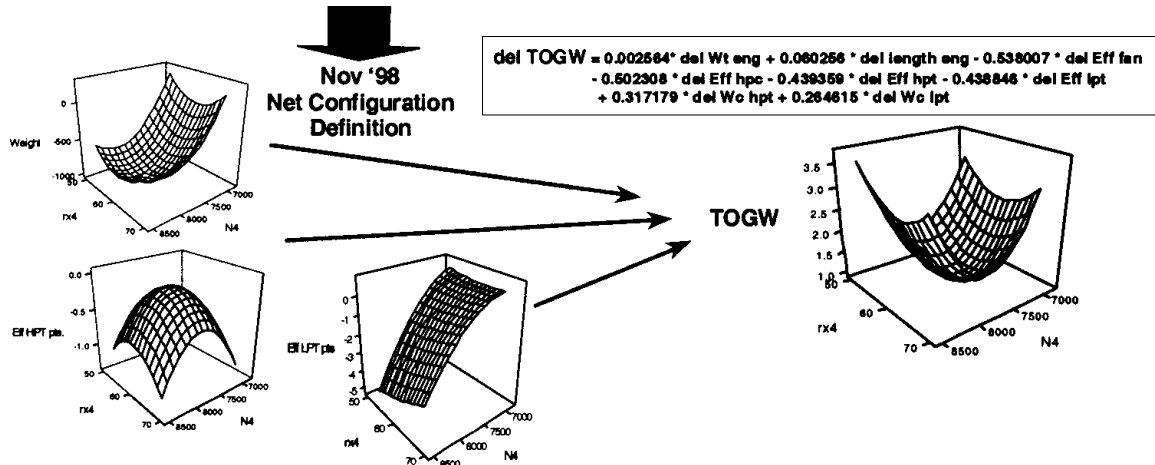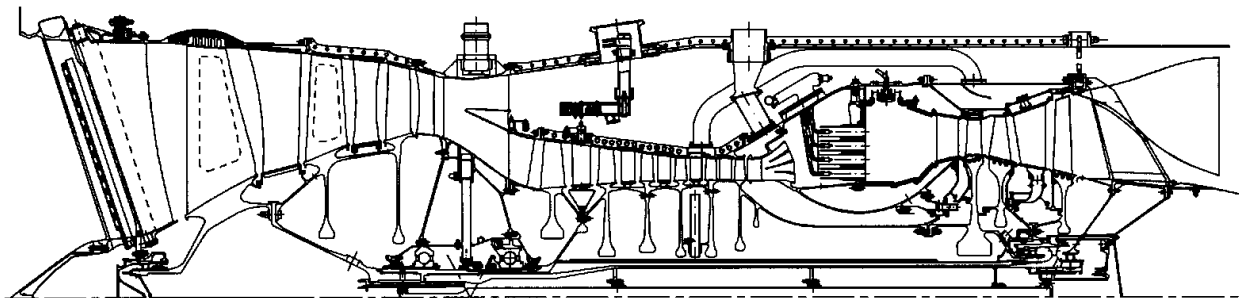   <u>Net Configuration</u> (Best Combinations) Approach

del TOGW = 0.002564* del Wt eng + 0.060256 * del length eng - 0.538007 * del Eff fan
- 0.502308 * del Eff hpc - 0.439359 * del Eff hpt - 0.436846 * del Eff lpt
+ 0.317179 * del Wc hpt + 0.264615 * del Wc lpt

Figure 232.   Process Used to Define the Ultimate MFTF Concept   *System performance is best served by a balanced design.*

FLOWPATH Net Configuration		Engine		Nozzle	
Fan	– 557	Eliminate CDP Seal	– 63	SAVE Reductions	– 632 Tier II (7833 lb)
Compressor	– 62	Single Wall HPC Case	– 50	SAVE Reductions	– 355 Teir III
Combustor	– 35	Combustor	– 337	CMC's, etc.	– 192
Turbines	– 425	Turb Vanes, Shrouds	– 150		
Structures	– 178	Bearings, Seals, Drives	– 47		
Brgs, Seals, Drives	– 5	Integrated TRF/Mixer	– 350		
		C&A – lighter hyd fluid	– 111		
	– 1262		–1108		–1179

Figure 233.   November 1998, Ultimate MFTF Net Configuration Weight Reductions

Figure 234 defines by module the weight-reduction technologies that provide weight reduction in the 1999 "Ultimate" MFTF configuration. Additional technologies were considered and evaluated but these were not included if no benefit was identified.
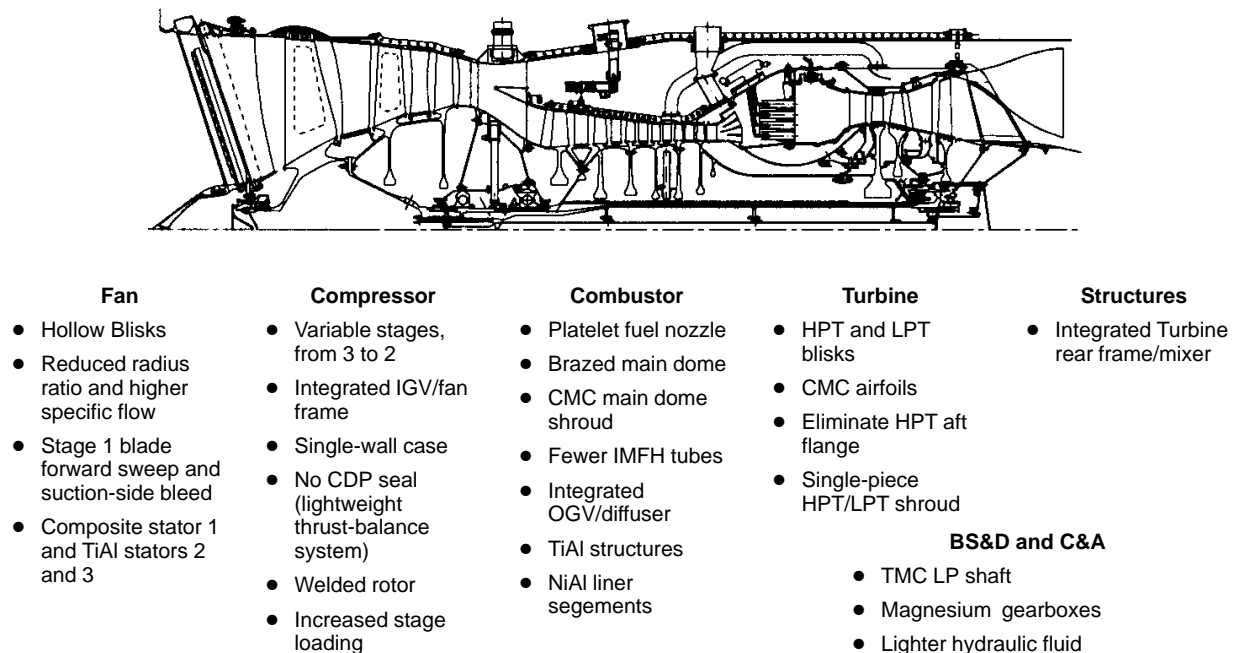

Fan
- Hollow Blisks
- Reduced radius ratio and higher specific flow
- Stage 1 blade forward sweep and suction-side bleed
- Composite stator 1 and TiAl stators 2 and 3

Compressor
- Variable stages, from 3 to 2
- Integrated IGV/fan frame
- Single-wall case
- No CDP seal (lightweight thrust-balance system)
- Welded rotor
- Increased stage loading

Combustor
- Platelet fuel nozzle
- Brazed main dome
- CMC main dome shroud
- Fewer IMFH tubes
- Integrated OGV/diffuser
- TiAl structures
- NiAl liner segements

Turbine
- HPT and LPT blisks
- CMC airfoils
- Eliminate HPT aft flange
- Single-piece HPT/LPT shroud

Structures
- Integrated Turbine rear frame/mixer

BS&D and C&A
- TMC LP shaft
- Magnesium gearboxes
- Lighter hydraulic fluid

Figure 234.   The 1999 Ultimate MFTF Weight Reduction Technologies *Additional technologies were evaluated but dropped from consideration if no benefit was identified.*

3.4 New Requirements

3.4.1 Requirements Definition

As the HSCT program progressed into the TCA development stage, it became apparent that noise tolerance was changing throughout the world. Noise levels produced by the subsonic fleet had been reduced and were scheduled to go to lower levels in the future (see Figures 235 and 236). Quieter subsonic aircraft would necessitate a quieter HSCT as a viable commercial aircraft. For this reason, Boeing initiated a study to reevaluate existing noise restrictions. The purpose of this study was to determine what the new noise requirements should be in light of the trend in subsonic aircraft noise.

During this process of reevaluation, it was assumed that the HSCT baseline aircraft would need to have a TOGW of approximately 650,000 lbm, both to meet mission economic goals and for noise robustness. This target weight imposed substantial technological challenges on the program, but after investigation and evaluation it was felt that the difficulties could be dealt with. Subsequently, the set of new system requirements shown in Table 79 was developed.
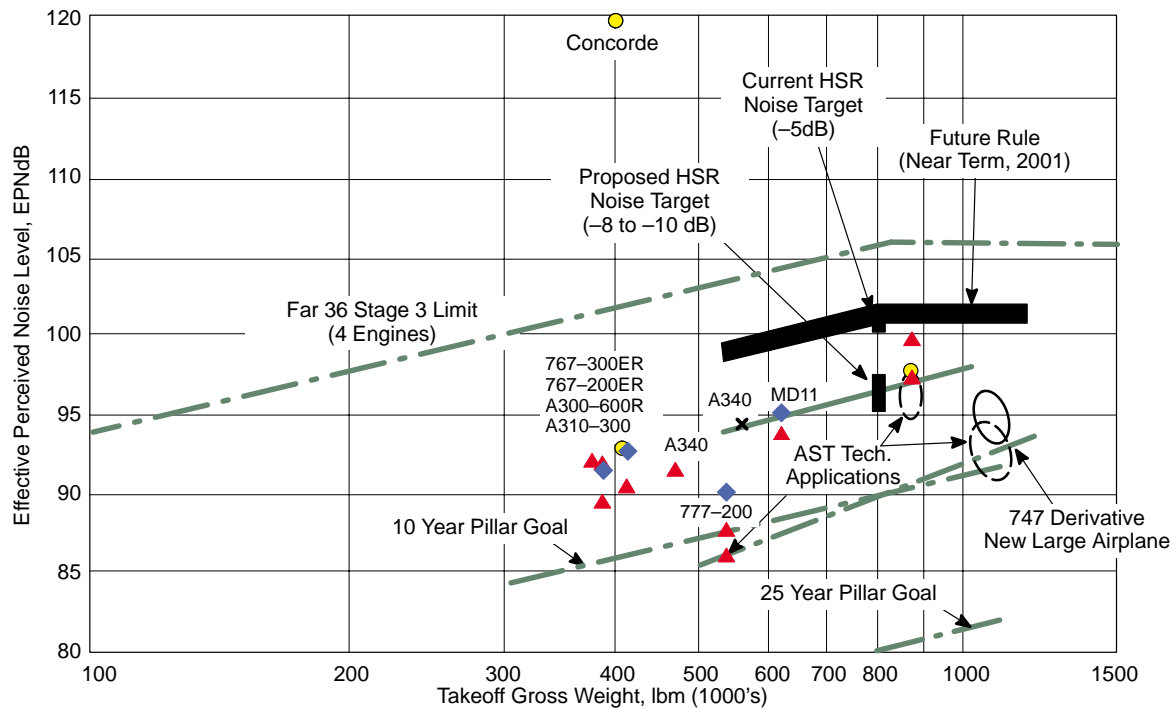
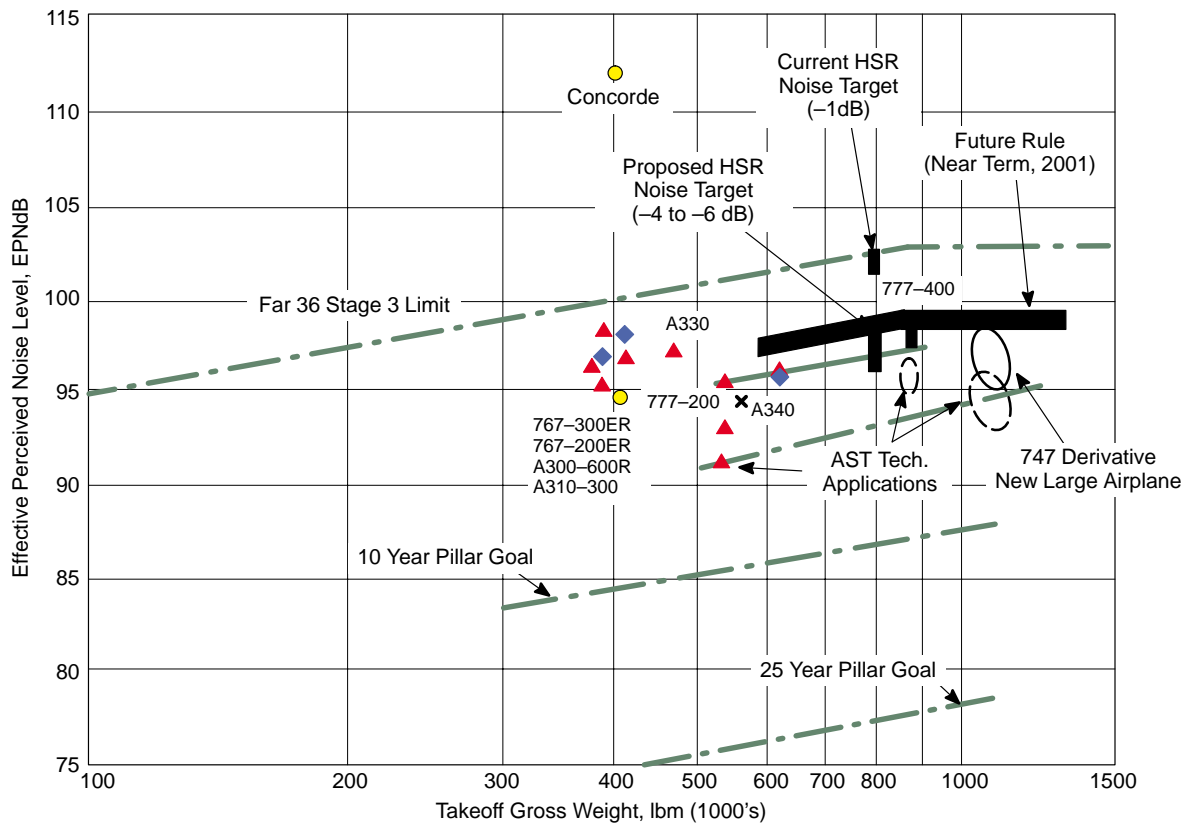**Figure 235.   FAR 36 Noise Levels, Takeoff with Cutback**

Figure 236.   FAR36 Noise Levels, Sideline

Table 79.   Revised Noise Requirements

Requirement		TC Requirement	New Program Requirement
Technology Readiness Date		2007	2015
Noise Level Relative to FAR36 Stage III	Sideline	−1	−4 to −6
	Cutback	−5	−8 to −10
	Approach	−1	−5 to −6
Comfort Level		737/757	767
Economic Viability		Surcharge < 20%, (About 750,000 lbm TOGW)	Surcharge < 10%, (About 650,000 lbm TOGW)

3.4.2 Advanced Concepts Screening

3.4.2.1 Background

In early 1998, evaluation of PTC development (version 1080–1504) for the Level I milestone indicated potential problems in the structural weight, drag, SFC, and engine thrust-to-weight ratio. It was the consensus opinion that these problems could, if unchecked, increase the weight of the HSCT 100,000 lbm beyond the 750,000-lbm weight limit mandated by economics. This realization sparked concern that the engine/airframe combination selected by the HSCT program might not be able to meet initial mission requirements and probably would not be sufficiently robust to meet future requirements.

At about the same time, changes in the resources available and industry market factors caused the production program schedule to slide out 5 to 10 years. This delay provided time for reevaluation of the entire HSR program. Subsequently, the HSR IIA program was divided into a series of phases to facilitate reassessment of the HSCT technologies selected.

During this interval, the airframe and propulsion management teams (AMT and PMT) working together with inputs from the environmental impact (EI) team developed a new set of requirements thought to be more appropriate for the design of a 2015 HSCT. These requirements included more stringent noise constraints than had been previously proposed, a lower takeoff weight to improve economic feasibility, containerized cargo-handling capability, and increased cabin comfort.

As a result of this scheduling slide and the proposal of new technology requirements, it became evident that the original date goals set for the HSCT technology readiness level (TRL) objectives should be adjusted. Table 80 shows the schedule proposed for these new requirements.

Preliminary sensitivity studies at NASA–Langley indicated that no single solution would enable the HSCT to meet the new requirements. The studies estimated that an improvement of 10% or more would be needed in all sizing inputs to achieve the goals proposed.

In an effort to develop new approaches to these problems, the TI team distributed survey forms to all the HSR industry participants and all the NASA aeronautics centers. The forms solicited new ideas that might lead to advanced technologies or alternative configuration concepts that could produce significant improvements in the HSCT. Basically, the survey asked three questions:

1. What new technologies or configuration concepts might produce significant improvements in the HSR TC baseline?

Table 80. Updated HSCT Viability Requirements

Requirement	Prior to 1998	End FY1998
Readiness Date	**2007**	**2015**

	2002:
	   Technologies at TRL 6
	
	2007:
	   Technologies at TRL 9
		2002:
		   Selected Technologies TRL 6
		
		2007:
		   Enhanced Technologies TRL 3 to 4
		
		2015:
		   All Technologies at TRL 9

Noise (Relative to FAR 36, Stage III)	**−1 EPNdB Sideline −5 EPNdB Cutback −1 EPNdB Approach**	**−4 to −6 EPNdB Sideline −8 to −10 EPNdB Cutback −5 to −6 EPNdB Approach**
Cabin Comfort Level	**737 / 757**	**767**
Economic Viability	**Surcharge < 20%, ≃ 750,000 lb**	**Surcharge < 10% ≃ 650,000 lb**

2. Can *any* HSCT achieve the year 2015 goals proposed without violating the laws of physics, and if so, what is it?

3. Would margins added for hot-day cruise or minimum engine performance cause unacceptable TOGW penalties, and would this margin change the cycle selection criteria for the HSCT engine?

Approximately 200 ideas were collected during the initial solicitation, and another 40 ideas were developed during the reply review process. All these ideas were catalogued, reviewed, and evaluated by appropriate IT teams. These evaluations were then reviewed by the Concept Selection Committee, and the ideas were ranked against each other. The committee then made recommendations as to which concepts should be given priority for further consideration. Figure 237 is a flow chart of this entire operation.

3.4.2.2 Concept Screening

The TI TMT commissioned a "panel of experts" to collect, interpret, and screen the concepts they had solicited. This panel consisted of 10 members and 6 alternates chosen to represent all of the technical disciplines involved and provide a crossdiscipline perspective of the concepts. The names of the members and alternate members of the screening panel are listed in Table 81 together with their affiliations and fields of expertise. Each panel member was assigned to review a certain number of concepts and then was required to shepherd the concepts through the entire process, including first-order analysis and evaluation of additional related ITD inputs. The main criteria used in this evaluation process are listed in Table 82. The screening effort was coordinated by NASA–Lewis.

3.4.2.3 Concepts Selected

The concepts that survived evaluation fell into three basic categories:

1. Concepts that could provide significant benefits

2. Concepts that probably wouldn't show large benefits individually but could produce benefits when combined with others.
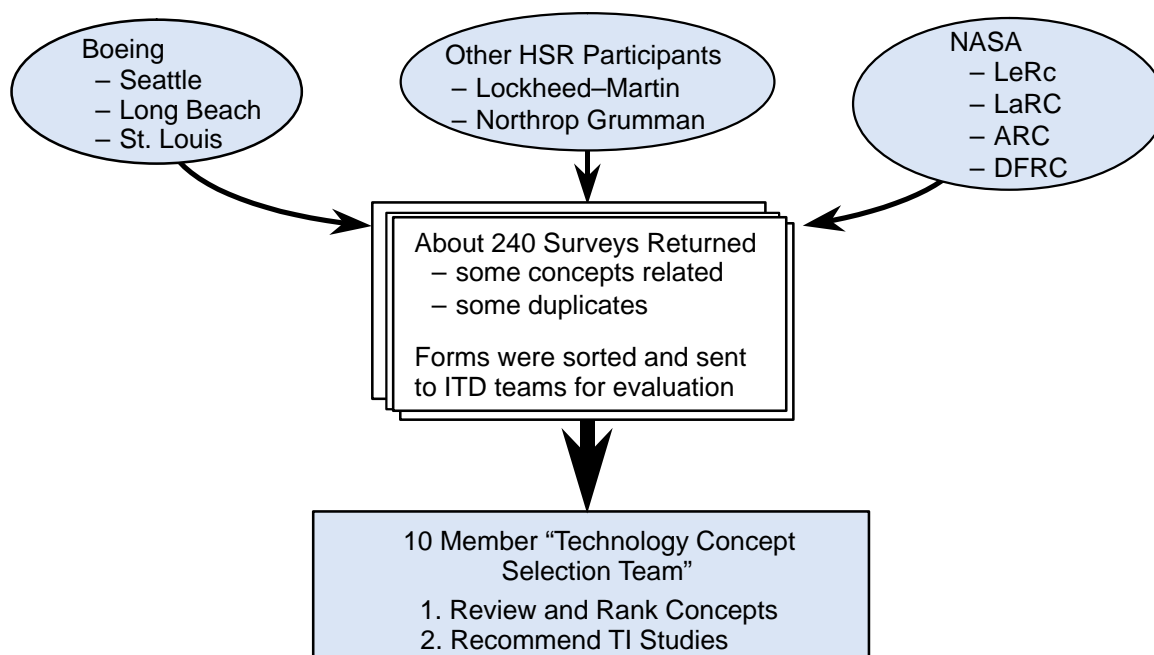
Figure 237. New Concept Solicitation and Screening, September 1998 to February 1999

Table 81. NASA/Industry Technology Concept Selection Team

Name		Home Discipline	Organization
Shreekant	Agrawal	Aerodynamics	Boeing Phantom Works
Kumar	Bhatia	Structures	Boeing Commercial
Ed	Coleman	Flt. Deck/Flt. Controls	Boeing Commercial
Steve	Jones	Prop. Components	Pratt & Whitney
Mahendra	Joshi	Environmental / Acoustics	Boeing Commercial
Martin	Manning	Prop. Syst. Integration	GE Aero Engines
Gary	Seng	Prop. Components	NASA Lewis Research Center
Ajay	Misra	Prop. Materials	NASA Lewis Research Center
Peter	Coen	Tech./Config. Integration	NASA Langlely Research Center
Chet	Nelson	Aero Integration	Boeing Commercial
"Deputies" for the above committee members:			
Bob	Patton	Aerodynamics	Boeing Commercial
Mark	Nazari	Structures	Boeing Commercial
		Flt. Deck/Flt. Controls	
George	Allen	Prop. Components	Pratt & Whitney
Gene	Nihart	Noise/Environmental	Boeing Commercial
		Prop. Syst. Integration	
Bob	Plencner	Prop. Components	NASA Lewis Research Center
		Prop. Materials	
Lori	Ozoroski	Tech./Config. Integration	NASA Langley Research Center
Peter	Coen	Tech./Config. Integration	NASA Langley Research Center

Table 82.   Concept Screening Criteria

1. Performance
    – SFC (subsonic, transonic, supersonic)
    – OEW (airframe OEW, engine–nozzle T/W)
    – L/D (subsonic, transonic, supersonic)
    – Noise (sideline, cutback, approach)
    – Emissions (NOx, fuel used)

2. Technical Feasibility/Readiness
    – TRL today
    – TRL under HSR2A
    – Confidence in TRL 6 by 2015
    – Certification/safety
    – Manufacturability
    – Design "Robustness"

3. Cost/Marketabililty Issues
    – Infrastructure/airport compatibility
    – Recurring/nonrecurring design and manufacturing costs
    – Reliability, maintainability
    – Payload / range / Mach tradeoffs

4. "Tie Breakers"
    – Broad applicability (across HSCT's, to subsonics, military etc.)

3. Concepts that probably wouldn't show large benefits individually but enabled the use of other beneficial configuration concepts that combined several ideas synergistically.

Many of the concepts selected were not new ideas. Several had been considered during the initial HSR effort but were shelved either for lack of program resources or because of excess complexity. A few of the concepts had been rejected earlier because they caused large penalties when used with the HSCT Stage III noise limits. These concepts were now reconsidered because it was felt that they might provide net benefits under the more restrictive noise constraints of the 2015 configuration. Table 83 lists the top 25 concepts that were developed from this screening process.

3.4.2.4 Additional Concepts Considered

The screening committee also developed a list of discarded past concepts (Table 84) they felt should be reevaluated against the new HSCT requirements. The concepts listed in Tables 83 and 84 provide a broad range of promising ideas, but the limited time and resources available to the TI team severely limited the amount of investigation that was possible.

3.4.2.5 Highly Integrated Concepts

The highest ranking concepts considered were for full configurations that incorporated a number of improvements into one vehicle to maximize the benefit. Two approaches in particular used highly integrated airplane technology. One such approach was the Concept 154 airplane, also known as the HISCAT (for *highly integrated supersonic cruise airplane technology*) shown in Figure 238. The other approach mentioned was the SCID (for *supersonic cruise integrated design*) airplane shown

Table 83.   Screening Process Selections January/February 1999

- **Concepts Ranked in the Top 25 Almost Regardless of Sorting Method**
    - Fully integrated configurations with integration synergism between features
    - Hybrid propulsion systems
    - "JBE" Jet Blade Ejector nozzle
    - Multipodded engines (XB–70)
    - Very high AR nozzles (banked miniengines, trailing-edge-slot fan exhaust)
    - Dual-podded nacelles, including long 2D inlet (Tu–144), diverterless horizontal ramp
    - Lighter simpler inlet ("Waverider" inlet design concept)
    - Enhanced mixing nozzles (fluidic mixers, lobe-on-lobe, etc.)
    - Water injection in nozzle for sideline noise reduction/frequency shift
    - Airframe shielding of exhaust and/or fan noise, S-duct ahead of fan
    - Combination of lighter materials, improved tabs, chevrons, fan ("Ultimate MFTF–ME")
    - Advanced flight systems (flutter/gust/load alleviation, envelope limiting, photonics)
    - Tailoring composite structure and outboard wing arrangement to reduce flutter
    - OEW savings due to smart trim panels, quiet composites for interior noise
- **Specific "Enablers" and Ideas with Large Potential Synergism**
    - Drag reduction through SLFC, riblets, base blowing, jet flaps
    - Application of multipoint nonlinear aero optimization in integrated design process (nacelle integration, wing/body integration)
    - High order analysis /design tools for loads, flutter, S&C, noise, engine/inlet /nozzle development, etc.
    - "Buried" boost engines (enables high-flow cycles, lower FPR's with minimal drag impact)
    - HHLEX/Superstrake integrated wing planforms
    - Folding high-aspect-ratio canards (Tu–144)
    - Interior noise-reduction schemes (smart trim panels, low noise composites)
- **Plasma Technology Concepts**
    - May be high payoff, but <u>extremely</u> low TRL
    - Little quantitative data available, scale-up is a big unknown
    - Best potential application to HSCT may be plasma-shielded nozzle
    - Much being done outside of the HSCT arena

Table 84.   Past Concepts Reconsidered

- Swing-wing (directly attacks conflicting high- versus low-speed drag)

- "High flow" engine cycles
    – VCE (Variable-Cycle Engine)
    – VCF (Variable-Capacity Fan)
    – MTF / Flade (Mid–Tandem Fan / Fan-on-Blade)

- Lower cruise Mach number?

    – Updated Mach 2 planform and engine better suited to new noise goals?
    – Updated material / tooling cost trade data and economics ?
    – Lower Mach, lower cruise altitude would improve emissions impact
    – Oblique "scissors wing" attractive if Mach 1.6 or smaller airplane economics OK

"Concept 154"*:   A highly integrated general arrangement synergistically combining several concepts to address key concerns...

Improve Cabin Comfort and Ride Quality
– Wide-body, twin-aisle cabin
– Improved turnaround time
– Large, stiff body cross section
– Canard for SMC (if required)

Maximize "Airframe Shielding" of Noise Sources
– S-duct inlet
– TE "reflection plane"
– Vertical tails
– Dual pod jet–jet shielding

Maintain / Improve Aerodynamics
– Increased wing span, AR ≃ 2.8–3.2
– "Diverterless" nacelles
– Extend strake, ovalize body
– "Sharknose" body apex
– Minimize midlength cross section
– Planform to minimize aircraft shift

Reduce Loads and Flutter Problems
– Wider, deeper inboard box
– Dual-podded nacelles
– No aft body or tail
– Better support of long nozzles
– Increase outboard taper 35%
– Less kink in rear spar
– Active loads/flutter alleviation

* Highly Integrated Supersonic
   Cruise Airplane Technology
   (HISCAT) Initial Concept Shown
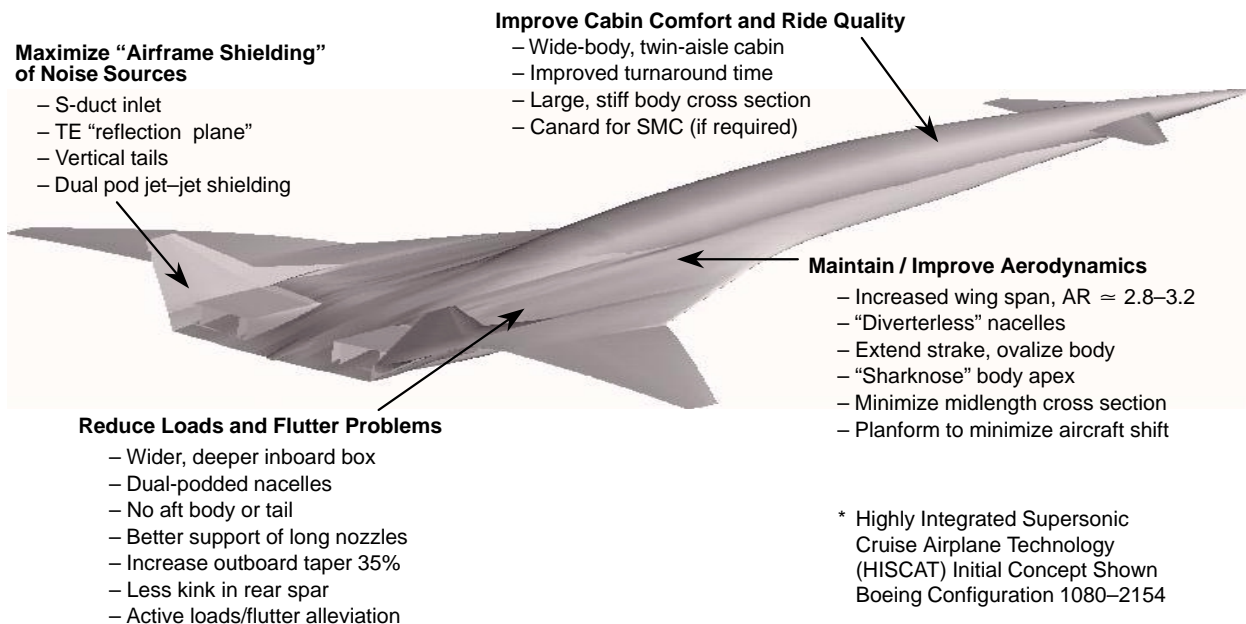   Boeing Configuration 1080–2154

Figure 238.   Concept 154 Airplane

in Figure 239. Salient features of each of these aircraft are listed in Table 85. Other approaches investigated included a swing-wing concept examined in both a blended wing/body and a conventional wing planform. Figure 240 summarizes the noise to TOGW relationships of the vehicles examined.

3.4.2.6 Summary

After completion of this advanced concept gathering and screening process, the TI TMT offered the following recommendations. Future development should:

1. Focus on applying reasonable-risk concepts on a TC-like airplane
   - Use the TC with 767-type comfort
   - Use the "Ultimate" MFTF engine with the waverider inlet
   - Use the 2015 airframe projections including dual-podded nacelles
2. Assess the potential of highly integrated general configurations.
3. Determine whether any previously discarded options might help meet the year 2015 goals:
   - Swing wing
   - Laminar flow control
   - Lower Mach number cruise
4. Assess the potential of selected advanced propulsion concepts, such as:
   - Hybrid propulsion system (with booster fan)
   - Jet blade ejector
   - Nozzle water ejector
   - Variable-cycle/high-flow engines (complete IR&D MTF study)
5. Prioritize to ensure optimum use of time.

3.4.3 Ultimate MFTF

The Ultimate MFTF effort continued into 1999 with the objectives of determining (1) which suite of materials and which component technologies would provide the optimum solution for the HSCT propulsion system and (2) which aerodynamic/thermodynamic relationships would be involved.

The approach was to continue the weight-reduction work initiated in July 1998 and identified as the ultimate MFTF design effort. The possibility had been proposed that the projected product weight goal could most easily be achieved if the constraints of technology readiness and risk/cost limitations were eliminated.

Figure 241 illustrates the propulsion system weight evolution and the projected product weight established in late 1997. The figure shows that even though weight-reduction efforts were ongoing in 1997 and 1998, the August 1998 engine and nozzle weight was still significantly higher (18,715 versus 16,675 lbm) than the projected product goal. This condition persisted even though system-

First Class at 61-in Pitch = 30
Business Class at 39-in Pitch = 88
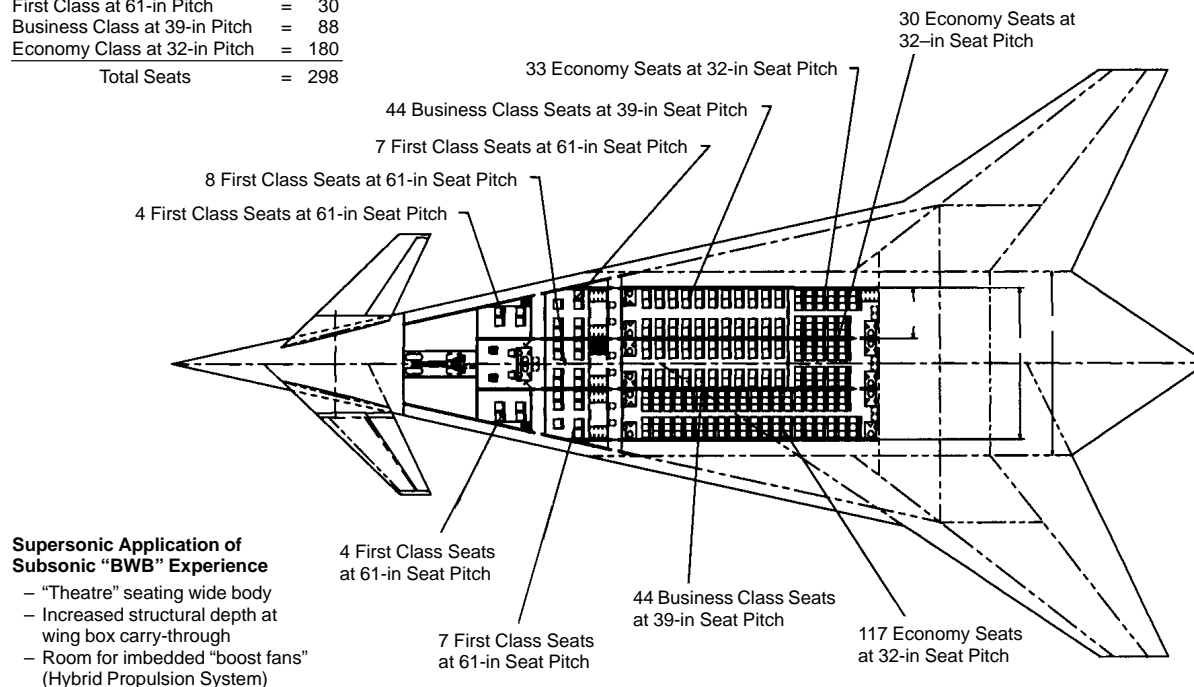Economy Class at 32-in Pitch = 180
Total Seats = 298

30 Economy Seats at 32–in Seat Pitch

33 Economy Seats at 32-in Seat Pitch

44 Business Class Seats at 39-in Seat Pitch

7 First Class Seats at 61-in Seat Pitch

8 First Class Seats at 61-in Seat Pitch

4 First Class Seats at 61-in Seat Pitch

Supersonic Application of Subsonic "BWB" Experience
– "Theatre" seating wide body
– Increased structural depth at wing box carry-through
– Room for imbedded "boost fans" (Hybrid Propulsion System)

4 First Class Seats at 61-in Seat Pitch

7 First Class Seats at 61-in Seat Pitch

44 Business Class Seats at 39-in Seat Pitch

117 Economy Seats at 32-in Seat Pitch

Figure 239.   SCID Blended Wing/Body Airplane

Table 85.   Fully Integrated Configurations Considered

- "SCID" Supersonic Cruise Integrated Design
    - Distinguishing feature is integrated delta wing-body with "theater seating" and no horizontal tail
    - "Q–SCID" (Quiet SCID) variant accommodates two to four boost engines (or boost fans) providing largest potential EI benefits
    - Swing-wing variant for improved L/D potential

- "Concept 154"
    - Configuration maximizes "airframe shielding" of jet and fan noise
    - A distinguishing feature is twin vertical tails integrated with extended nozzles behind the wing, joined by integral trailing edge / noise "reflection plate"
    - S–duct inlets below wing, mixer/ejector nozzle exits above wing (SERN–type ?)
    - Blended wing/body center section, eight-abreast twin-aisle cabin
    - Potential for structural weight/flutter and drag benefits relative to "TC"
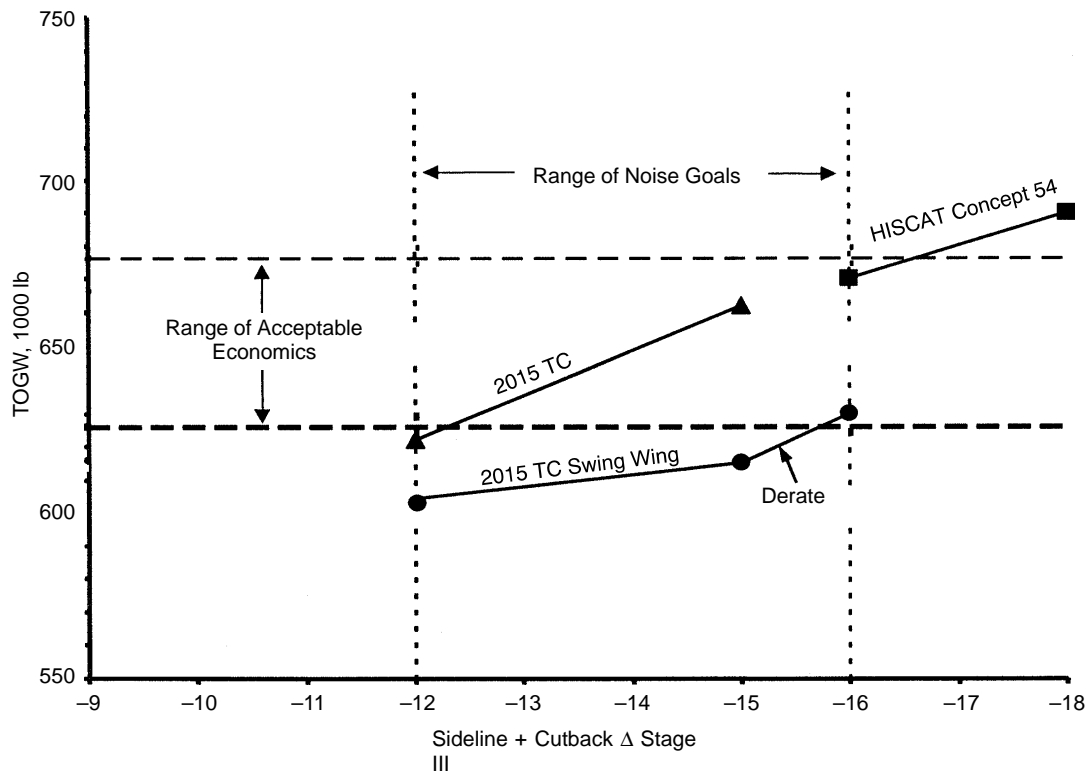
Figure 240.   System Evaluation of Wing Planforms Tested
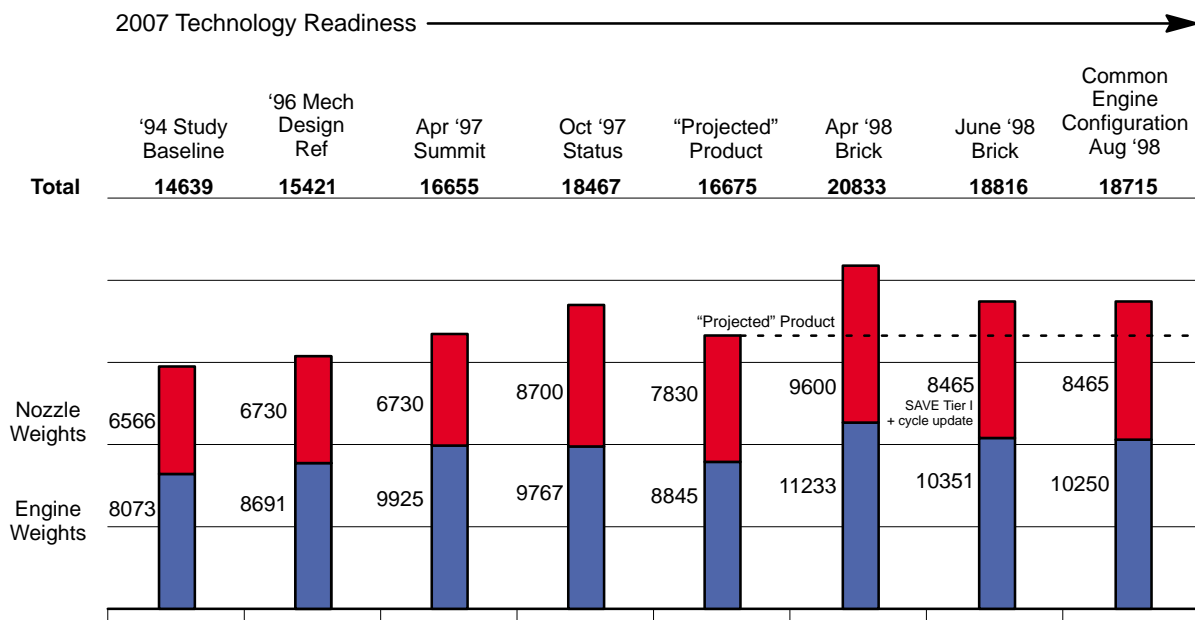
Figure 241.   Propulsion System Weight Evolution

level optimizations were incorporated from analyses of the preliminary design FLOWPATH model and component design fidelity improvements were developed for the common engine configuration.

In November, 1998, rough-order-of-magnitude estimates were made of the engine and nozzle weight-reduction ideas that had been developed. These estimates indicated that the ultimate MFTF weight goal should be achievable. Figure 233 (page 257) summarizes the November 1998 preliminary weight-reduction estimates, which indicated that the potential was present to achieve the approximately 2000-lbm reduction necessary to reach the projected product weight goal.

In 1999, the approach used in the ultimate MFTF study was to improve the fidelity of the 1998 weight-reduction studies. It was decided that continuing studies would use the 3770.54, 800-lbm/s, MFTF cycle. Higher risk materials and technologies would be evaluated for the engine and nozzle components with the assumption that they would have a 2015 Technology Readiness date. This implied that the technologies would achieve maturity in time for use in a new product launch (no more technology development required). It was also decided that, if the technologies had not reached full maturity, they could still be acceptable with risk-abatement plans in place.

The same design process as used in 1998 for general weight-reduction studies of the preliminary design FLOWPATH engine was used. It was expected that this process would best evaluate overall propulsion system changes such as component geometry, flowpath adjustments, component loading levels, and rotor speeds. The engine design process used DOE statistical analyses to establish the propulsion system solutions (response surfaces). This method has been found especially effective when several variables may change simultaneously.

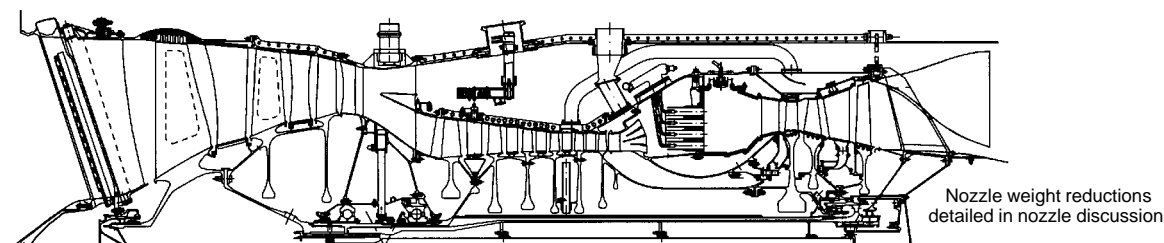The items determined by the 1999 ultimate MFTF study were:

- Changes in engine and nozzle weights
- Δ MTOW for the aircraft
- Δ engine price (nozzle price changes were not estimated)
- Development programs needed for the new materials and technologies

Figure 242 shows which of the materials and technologies studied resulted in weight reductions for the engine. Additional technologies were considered and evaluated but are not listed if no benefit was identified.

The *Systematic Approach to Value Engineering* (SAVE) event conducted by the nozzle team in December 1997 resulted in a set of low-to-medium risk weight-reduction ideas for the nozzle. These ideas, designated as the SAVE event Tier I ideas, projected a nozzle weight of 7764 lbm. The single-door concept and incorporation of alternate kinematics were two ideas that appeared to offer significant weight reduction. Figure 243 summarizes the major ideas from SAVE event, Tier I.

At the end of 1998, results from the aircraft system studies focused the requirements of the ultimate propulsion system on the 3770.54 cycle engine with a 2.7 SAR exhaust nozzle. The weight of the ultimate nozzle for this engine was estimated as 7296 lbm based on the (baseline) nozzle weight status, projections of applicable weight-reduction ideas, and the weight of available nozzles.

By June of 1999, the SAVE Tier I ideas had been evaluated by the nozzle team in detail, and a new baseline nozzle weight had been established. In addition to the Tier I ideas, high-risk items (designated Tier II) were available to be considered for use with the 2015 ultimate nozzle. Figure 244 shows the June 1999 baseline and the projection of that baseline to a 2015 ultimate nozzle weight

Nozzle weight reductions
detailed in nozzle discussion

Fan

- Hollow blisks
- Reduced r/r and higher specific flow
- Stage 1 blade fwd sweep and suction side bleed
- Composite stator 1 and TiAl stator 2&3
- Shortened fan frame

Compressor

- Eliminate Stage 2 VSV
- Integrate IGV into fan frame
- Single wall split case
- Lightweight thrust balance system
- Welded blisk spool
- Increased stage loading

Combustor

- Platelet fuel nozzle
- Brazed main dome construction
- CMC main dome shroud
- Fewer IMFH tubes
- Integrate OGV's and diffuser
- TiAl structures

Turbine

- HPT and LPT blisks
- CMC Nozzles
- Welded HPT aft shaft
- Single piece HPT/LPT shroud
- CMC shroud
- Increased AN squared

Structures

- Integrate dTRF/mixer

BS&D and C&A

- Hybrid LP shast
- Lightweigh fire resistant hydraulic fluid
- Lightweight gearboxes
- C&A component improvements

Figure 242.   Ultimate MFTF Weight Reduction Materials and Technologies *Additional technologies were evaluated but are not listed here if no benefit was identified.*

- August 1997 – Nozzle Weight = 9986 lb
  - A 50% increase from previous weight status
  - Nozzle >2000 lb over the goal weight of 7830 lb

- December 1997 – Value Engineering Event (SAVE) held with the objective of generating weight reduction ideas
  - 16 items were identified as Tier 1 weight reduction items with low to medium risk for a total of 2222 lb/nozzle (based on 3770.60 Cycle, 2.9 SAR)

Item	Weight Reduction
Single Inlet Door	364
Incorp H/C – Outer Skins T-Duct, Midframe, Sidewalls	123
Sidewall Cross Beam	170
Incorp. Titanium T-Duct, Aft-Flap, Sidewalls	223
Composite Outer Fairing	64
Fan/Core Mixer	60
Increased Structural Envelope	330
Incorporate Alt. Kinematics	457
Composite Outer Flaps	51
Composite Cascades	26
Optimize Door Kinematics (inlet)	85
CMC – Chute Vanes	51
Increased Suppresssed/Unsuppressed Transition Time	43
Low-Density Bulk Absorber	88
Minimize Liner Attachments	34
Reduced Liner Facesheet Thickness	55

Single Inlet Door

Alternate Kinematics

- Nozzle weight prediction = 9986 – 2222 = 7764 lb

- Single Door and Alternate Kinematics were the two largest weight reduction items evaluated
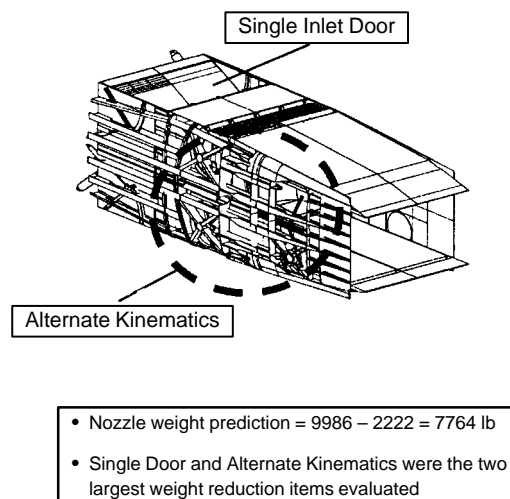
Figure 243.   SAVE Event, Tier I Weight Reduction Items, December 1997

of 7262 lbm. This projection increased confidence that the initial late-1998 estimate of 7296 lbm for the ultimate nozzle weight was achievable.

The total engine and nozzle weight reductions resulted in a weight status that was less than the projected product weight goal of 16675 lbm. Tables 86 through 88 summarize these ultimate MFTF study results.

Table 86. Summary of Weight Changes *"Ultimate" MFTF weighs 15,270-lbm vs projected product goal of 16,675 lbm.*

Configuration	Weight, lbm		
	Engine	**Nozzle**	**Total**
1998 (3770.54 MFTF) Common Engine	10,250	8,465	18,715
1999 (3770.54 MFTF) "Ultimate" MFTF	8,249	7,021*	15,270
Δ	*−2,001*	*−1,444*	*−3,445*
* The 2015 "Ultimate" exhaust nozzle with fan/core mixer removed (integrated into turbine rear frame) and with lighter hydraulic fluid.			

Table 87. Summary of Performance Changes *Component efficiency (points) and cooling flow changes for the 1999 (3770.54 MFTF) "Ultimate" MFTF.*

Component	Δ Efficiency	Δ Cooling Flow
Fan	+0.21	
Compressor	−1.31	
High-Pressure Turbine	+0.24	−0.09
Low-Pressure Turbine	−0.23	−0.17

June 1999 Baseline
3770.60 Cycle, 2.9 SAR
8015 lbm

Late 1998 Weight Projection (Goal)
3770.54 Cycle, 2.7 SAR
7296 lbm

1999 Ultimate Nozzle Weight Estimate (lbm)

June 1999 Baseline	+8015
3770.60 to 3770.54 Cycle Change*	+690
Open Tier I SAVE Event items**	−400
2.9 SAR to 2.7 SAR Change***	−500
Tier II SAVE Event Items	−243
Incorp. CC/CMC by 2015	−300
	7262

*Based on "06/98 Briquette" system studies
**Items with highest confidence at 100% realization
***Part of Tier II SAVE Event

Figure 244. Nozzle Weight Projection: June 1999 Baseline to 2015 Ultimate Nozzle *High confidence in achieving previously published ultimate nozzle weight.*

Table 88.   MTOW for Ultimate MFTF Configuration

Item	MTOW Δ lbm	MTOW Δ %
Engine weight (–2001 lbm)	–40,020	– 5.08
Nozzle weight (–1444 lbm)	–30,324	– 3.85
Engine length (–15 in)	– 7,050	– 0.90
Performance changes	+ 3,643	+0.46
Totals	73,751	– 9.37

As outlined earlier, the impact of all the changes executed during the ultimate MFTF study were included in an assessment of impact on the aircraft MTOW (Table 88). The system performance changes are listed in Table 87. The engine length change that resulted from engine component changes was approximately 15 inches. In this discussion, engine length is defined as the average of the estimated nacelle and pylon length reductions that resulted from engine component length reductions. The ΔMTOW values listed in Table 88 were developed using the available DOC+I propulsion sensitivities (defined in Coordination Memo GE98–027–S) for a base MTOW of 788,500 lbm. The ultimate MFTF configuration provided a substantial weight reduction in aircraft MTOW.

The weight-reduction technologies identified in Figure 242 would require development programs to support the Technology Readiness 2015 date assumed for the study. These programs are estimated to have durations and costs as listed in Table 89.

Table 89.   Development Programs Summary

Program	Duration (Years)	1999 Dollars ($M)
Hollow-Bladed Fan Blisks	7	20.5
Composite Fan Stator	6	9.8
Welded HPC Rotor and HPT Aft Shaft	7	10.2
Hybrid LP Shaft	9	11.7
Turbine Blisks	7	17.7
CMC Turbine Nozzles	6	10.4
CMC Turbine Shroud	6	10.4
Total		90.7
Note: Production facilities and associated costs have not been evaluated.		

The higher engine price due to more advanced technologies would also affect the economics of the HSCT ultimate MFTF application. As part of the 1999 studies, an estimate of the increased engine price of the ultimate MFTF configuration was compared to a reference engine price developed in 1995. In this case, the engine changes were evaluated but nozzle changes were not included. Current state-of-the-art COMPEAT™ cost models were developed and compared using the ultimate MFTF components instead of the corresponding components in the 1995 reference engine. The study found that the ultimate MFTF configuration changes reduced many components in size and length — which reduced material quantity, manufacturing time, etc. The configuration changes also reduced

the complexity and number of piece parts in the components. These reductions, combined with the addition of new materials and technologies, resulted in only a small (less than 1%) increase in engine price.

In summary (Table 90), the ultimate MFTF study was able to achieve the objectives proposed. Weight-reduction materials and technologies were identified and evaluated with analysis methods used for preliminary design fidelity of results. Associated technology development needs were estimated for cost and scheduling at rough-order-of-magnitude (ROM) levels. The impact of engine price changes was also evaluated. The study results show that the ultimate MFTF would be able to achieve a lower total weight than the projected product goal weight with a corresponding significant reduction in the aircraft MTOW. It was estimated that this engine could be produced with relatively minor impact on the engine price, but the engine would require a significant development effort in materials and technology.

Table 90. Ultimate MFTF Study Results

Item	Approximate Change
Δ Engine and Nozzle Weight 15,270 vs 16,675 lb Projected Product Goal	− 3,445 lb (from 18,715 base)
Δ MTOW Impact of Ultimate MFTF	− 73,750 lb or > − 9%
Δ Engine Price (vs Reference)	Net Change < +1 %
Development Plans ROM Cost Estimates	$91M over 7–9 years

3.4.4 Ultimate Mixer/Ejector Nozzle

3.4.4.1 General

The previous baseline fixed-chute nozzle (circa 8/97) was the disk-actuated configuration, developed for the 3770.60 cycle at a 2.9 suppression area ratio and a 1.5 aspect ratio. The total projected system weight of this configuration was verified at 9986 lbm through the use of finite-element analyses and hand calculations; see Figure 245. Subsequent aircraft system studies showed that HSCT program requirements mandated a nozzle weight of 7830 lbm or less.

For this reason, the nozzle team conducted a SAVE event for the purpose of generating weight-reduction ideas to be incorporated into the nozzle design at known levels of risk. This event resulted in a set of low-to-medium-risk ideas representing an estimated weight savings of 2222 lbm per nozzle (projected 7764-lbm nozzle weight). These were designated as the SAVE event, Tier I weight-reduction ideas.

The 6/99 baseline fixed-chute nozzle was a linear-actuation-system configuration developed from the alternate-kinematics downselect effort for the 3770.60 cycle at a 2.9 SAR and a 1.5 aspect ratio. After incorporation of SAVE event Tier I ideas that offered the greatest weight reduction, total system weight was verified at 8015 lbm through the use of finite-element analyses and hand calculations.

The ultimate fixed-chute mixer/ejector nozzle (circa 2015) is projected to have a total system weight of 7296 lbm. This nozzle configuration reflected the linear-actuation-system concept, based on the 3770.54 cycle at a 2.7 SAR and a 1.5 aspect ratio. The configuration incorporated weight-reduction ideas that had been developed during Tier II (higher risk) of the SAVE event.

(Based on Noise Goals of FAR 36, Stage III –1, –5, –1)

7830 (Goal: 2005 – 2007)
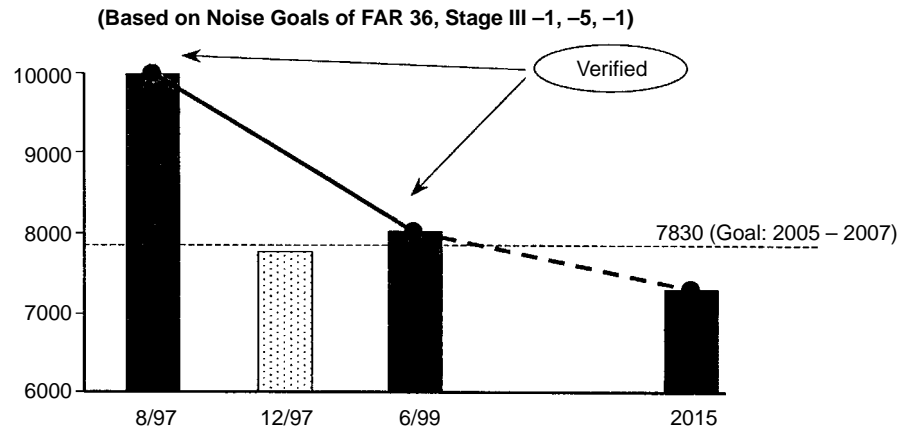
3770.60 Cycle, 2.9 SAR

8/97 – Previous Baseline FCN (Disk-Actuated Configuration)

12/97 – SAVE Event Tier I Weight-Reduction Ideas (Low to Moderate Risk)

6/99 – Final Baseline FCN (Linear Actuation System Configuration)

3770.54 Cycle, 2.7 SAR

2015 – Ultimate Fixed-Chute Mixer/Ejector Exhaust Nozzle

Figure 245.   Exhaust Nozzle Weight Reduction Summary

3.4.4.2 Nozzle Baseline 8/1997

The circa 8/97 baseline FCN was a disk-actuated configuration. The convergent and divergent flaps were positioned by the use of linear actuators and disks mounted within the midframe and aft sidewall structures, respectively. These disks were basically bellcranks made in the shape of disks so they would block the passage of flowpath gases from the external nozzle bay region. Figure 246 shows a typical layout of this configuration. Incorporation of the disks caused large voids within the midframe and aft wall structures. This is an inefficient structural configuration.
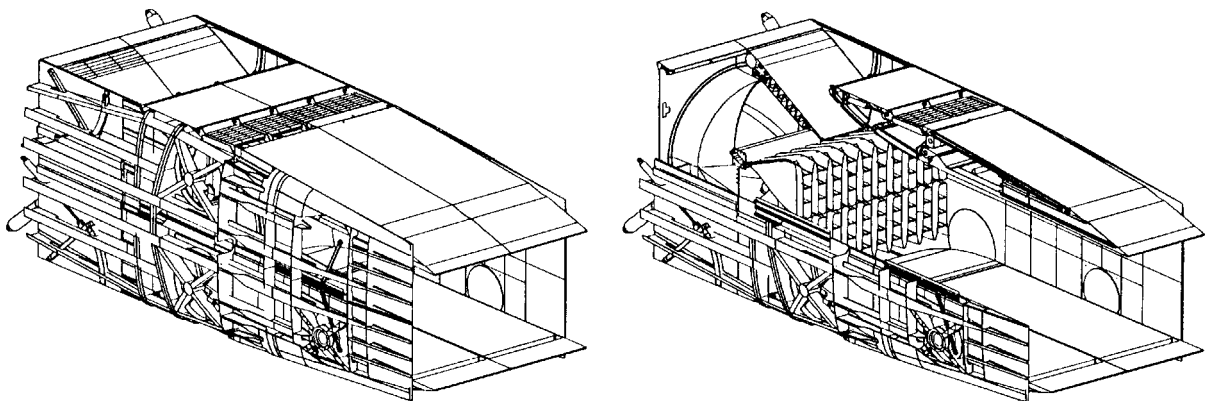
Figure 246.   Disk Actuation Configuration (Baseline 8/97)

3.4.4.3 Nozzle Components

The weight of the previous (8/97) baseline fixed-chute nozzle system was verified at 9986 lbm, The component weights are shown in Figure 247. The component complement of the nozzle was as follows:

Double Inlet Doors – The nozzle had two doors per inlet, a total of four doors per nozzle. There are two inner doors at the transition duct opening and two outer doors at the ejector inlet openings.

René 108 Uncooled Mixer – The ejector/mixer uses a René 108 superalloy casting with no active cooling. The geometry of the mixer was consistent with the aerodynamic requirements existing during 8/97. This geometry represented a long version of the mixer as compared to the final Gen 3.6 mixer design.

TiAl Divergent Flaps – The divergent flap configurations were based on the use of TiAl (TI 48–2–2).

TiAl Aft Sidewalls – The aft sidewall configurations were based on the use of TiAl (Ti 48–2–2). These aft sidewall structures were cantilevered from the aft end of the midframe and did not have any aft support structure.

$A_{trt}/A_{mix} > 6.0$ – The ratio of acoustic treatment area (A_{trt}) over mixing area (A_{mix}) was greater than 6.0 when both 2-in and 1-in thick acoustic bulk material was used. This ratio was based on a

8/97 – Preivous Baseline: Nozzle Weight Rollup (3770.60 Cycle, 2.9 SAR)

Component	Weight, lbm
Centerbody	68
Fan/Core Mixer (VABI)	271
Inlet and T–Duct Doors	830
Ejector Mixer	867
Transition Duct	1063
Midframe	1275
Aft Sidewalls	934
Convergent Flaps	634
Divergent Flaps	920
Outer Flaps	310
Rev. Doors and Cascades	190
Acoustic Liner Heat Shields	788
Subtotal	**8150**
Controls and Actuation	1428
Miscellaneous Mounts	408
Nozzle Total	**9986**
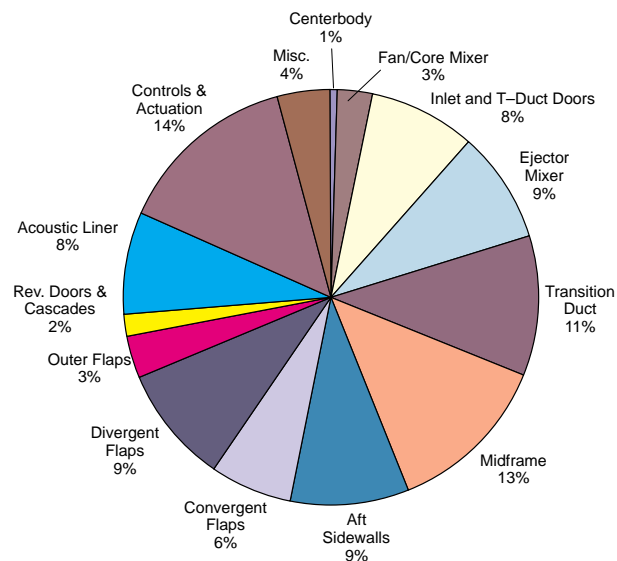
Nozzle Features:
– Double Inlet Doors (4 total)
– R108 Uncooled Mixer (long)
– TiAl Divergent Flaps
– TiAl Aft Sidewalls (cantilevered)
– $A_{trt}/A_{mix} > 6.0$
– 2 sec Rev. Trans. Time
– 135.5 in. Mixing Length
– Control System Weight Rollup (Advanced Material)

Figure 247.   Previous Baseline (8/97) Weights of Nozzle Components

requirement for the acoustic treatment to start at 10 mixer hot lobe widths aft of the exit plane of the ejector mixer.

Two Second Reverse Transition Time – The control system was sized to provide a two-second transition time between the suppressed takeoff mode and the full reverse thrust mode.

135.5-Inch Mixing Length – The mixing length was 135.5 inches for the nozzle in the suppressed takeoff condition. This dimension represents the distance from the exit plane of the ejector/mixer to the approximate midpoint between the trailing edge of the aft sidewalls and the divergent flaps.

Control System Advanced Materials – The control system weight is estimated on the assumption that advanced materials will be used for all appropriate control system components.

3.4.4.4 SAVE Event Initiation

The weight of the 8/97 baseline nozzle was estimated at 9986 lbm by a much more rigorous method than had been used for all previous nozzle weight estimates. For this reason, the estimated weight of the 8/97 nozzle showed a substantial increase (50%) over previous estimates. Subsequent aircraft system studies indicated that a nozzle weight of 7830 lbm or less was needed to meet HSCT program requirements. Therefore, the estimated weight of 9986 lbm had to be reduced by more than 2000 lbm, and nozzle weight reduction efforts were initiated immediately.

Accordingly, the nozzle team conducted a SAVE event to develop a set of weight-reduction ideas that could be incorporated into the nozzle design at known levels of risk. The SAVE event generated a set of low-to-medium-risk weight-reduction ideas that projected a possible weight reduction of 2222 lbm per nozzle (see Figure 243, page 270). These ideas were designated the SAVE event, Tier I weight reduction. When these ideas were incorporated, the nozzle estimated weight dropped to 7764 lbm, well within the limit stated above. The two most important changes are discussed next.

3.4.4.5 Single Door Weight Reduction

The single-door weight-reduction idea involved reducing the number of doors from two per ejector inlet to one per inlet, thus resulting in two doors per mixer ejector nozzle (see Figure 248). Benefits to the system from this change are expected to be the following:

- Reduced Weight – SAVE event weight savings were predicted to be 364 lbm per nozzle.

- Reduced Complexity – Complexity is reduced because elimination of the inner door reduces the number of structural components and allows incorporation of a more efficient actuation system. This more efficient system replaces eight linear actuators with only three rotary actuator components.

- Simplified Control System Logic – The control logic is simplified because the single-door configuration eliminates fail-safe concerns that existed for the double-door configuration. The fail-safe concerns involved synchronization of the inner and outer doors to avoid interference during transitions to different nozzle-operating modes.

3.4.4.6 Actuation System Selection

The alternate-kinematics effort was conducted to (1) develop a fixed-chute nozzle configuration that would eliminate the use of flap-actuation disks and (2) verify the weight reduction resulting from
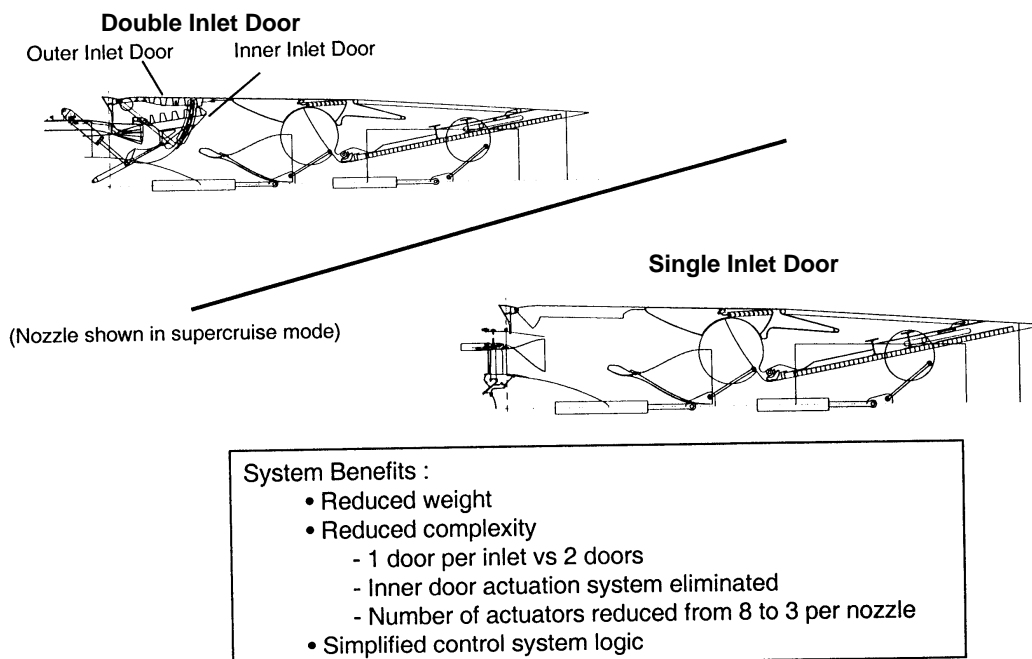
Double Inlet Door

Outer Inlet Door   Inner Inlet Door

Single Inlet Door

(Nozzle shown in supercruise mode)

System Benefits :
- Reduced weight
- Reduced complexity
  - 1 door per inlet vs 2 doors
  - Inner door actuation system eliminated
  - Number of actuators reduced from 8 to 3 per nozzle
- Simplified control system logic

Figure 248.   SAVE Event 12/97, Tier I Weight Reduction Items

the change. Two concepts were developed: the linear actuation system and the rotary actuation system. Both systems were developed to the level necessary to allow a valid downselection comparison. The result of this downselection was that the linear actuation system was designated the current baseline system (see Figure 249).

The flap actuation disks of the previous baseline (8/97) configuration were replaced by a kinematic system of links and bellcranks in the final baseline (6/99) configuration. This final baseline is a much more structurally efficient configuration for the midframe and aft sidewalls. Figure 250 shows the changes between the previous and final baselines.

3.4.4.7 Final Baseline (6/1999)

The final baseline fixed-chute nozzle system, developed in 6/1999, has a verified weight of 8015 lbm. Component weights are shown in Figure 251; component features are as follows:

Alternate Kinematics – The flap-actuation system was based on the kinematic approach for the linear actuation system. Weight was reduced substantially as a result of the more structurally efficient midframe and aft sidewall configurations.

Single Inlet Door – The nozzle had a single door per ejector inlet, a total of two doors per nozzle. The set of upper and lower doors was actuated and synchronized by a rotary actuation system.

René Uncooled Mixer – The ejector/mixer uses an René 108 superalloy casting with no active cooling. The mixer/ejector geometry is consistent with the Gen 3.6 mixer at product scale and therefore represented a short version of the mixer.

TiAl Divergent Flaps – The divergent flap configurations were based on the use of TiAl (Ti 48–2–2).
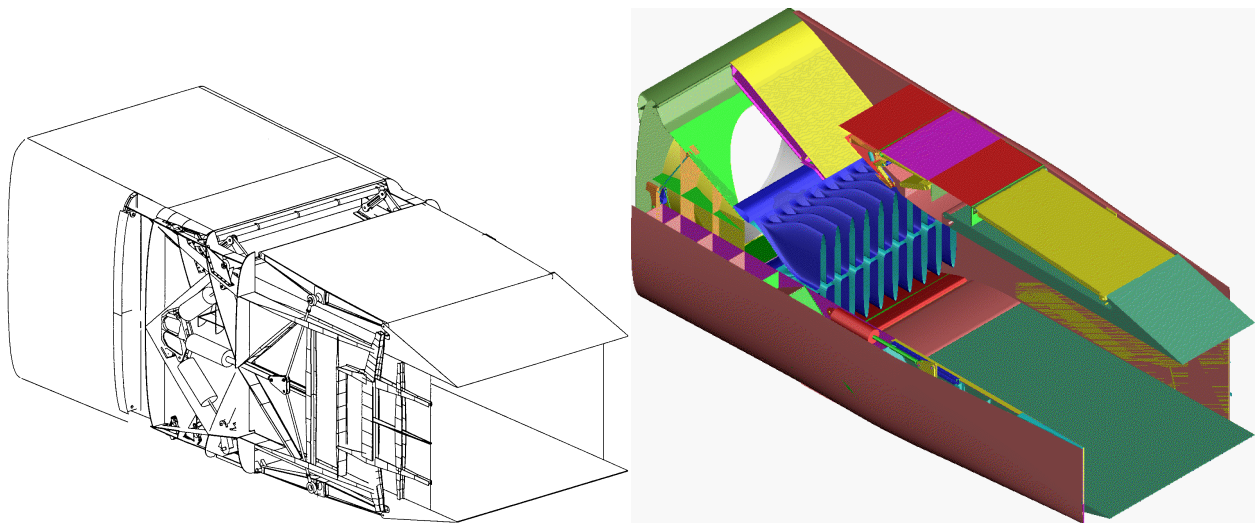
Figure 249.   Final (6/99) Baseline Linear Actuation System Configuration   *Linear actuation system was downselected as part of the alternate kinematics nozzle development effort.*

Previous Baseline (Disk Actuation Nozzle)
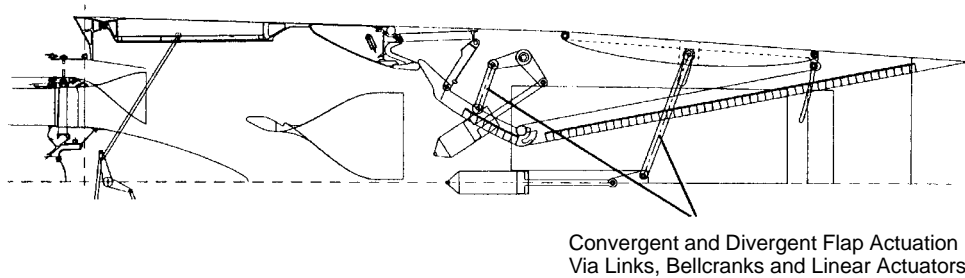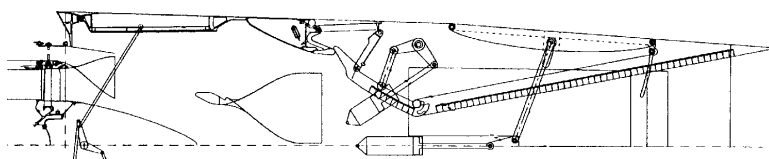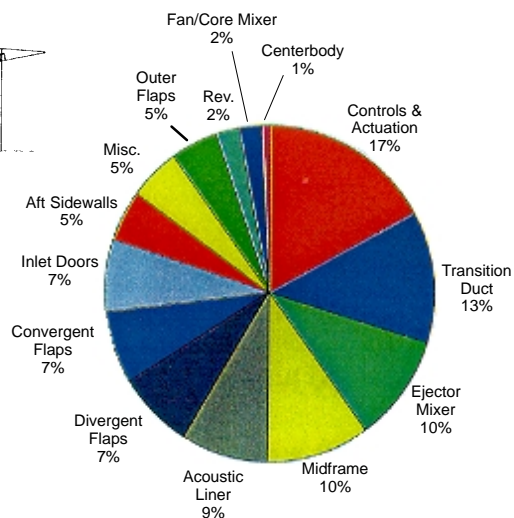

Convergent and Divergent Flap Actuation
Via Disks and Linear Actuators

Current Baseline (Linear Actuation Nozzle)

Convergent and Divergent Flap Actuation
Via Links, Bellcranks and Linear Actuators
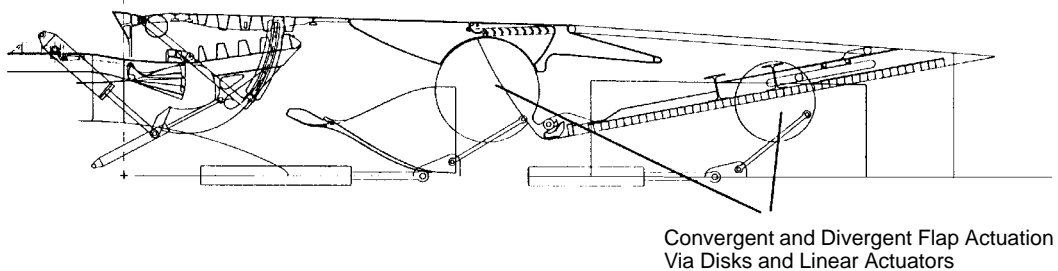
Figure 250.   Changes, Previous Baseline (8/97) to Final Baseline (6/99)

6/99 – Final Baseline: Nozzle Weight Rollup (3770.60 Cycle, 2.9 SAR)

Component	Status Weight, lbm
Centerbody	68
Fan/Core Mixer	175
Inlet Doors	550
Ejector Mixer	813
Transition Duct	1030
Midframe	801
Aft Sidewalls	403
Convergent Flaps	561
Divergent Flaps	599
Outer Flaps	361
Rev. Doors and Cascades	190
Acoustic Liner	700
Subtotal	6251
Controls and Actuation	1355
Misc.	408
Nozzle Total	8015

Linear System Nozzle:
– Alternate kinematics (linear actuation system)
– Single Inlet Door (total 2 per nozzle)
– R108 Uncooled Mixer (Gen 3.6 – product scale)
– TiAl Divergent Flaps
– TiAl Aft Sidewalls (noncantilevered)
– Lower density bulk acoustic liner
– 2 sec Rev. Trans. Time
– Fixed Fan/Core mixer
– Advanced Material Control System

Figure 251.   Final Baseline (6/99), Weights of Nozzle Components

TiAl Aft Sidewalls – The aft sidewall configurations were based on the use of TiAl (Ti 48–2–2). These aft sidewall structures were supported at the aft end through the incorporation of tierods. The tierods provided structural support by allowing the pressure loads to be counteracting. Substantial weight reduction was obtained as a result of changing from a cantilevered system to a noncantilevered system.

Lower Density Bulk Material – Additional weight reduction was realized through the incorporation of lower density bulk material for the acoustic treatment.

Two-Second Reverse Transition Time – The control system was sized to provide for a two-second transition time between the suppressed takeoff mode and the full reverse thrust mode.

Control System – The control system weight value reflects the use of advanced materials for the appropriate control system components.

3.4.4.8 Results of Weight Reduction Changes

Incorporation of the single door, the alternate kinematics, and a few other weight-reduction items exceeded the weight savings predicted by the SAVE event by a substantial amount. In fact, these items accounted for 89%, or 1971 lbm, of the Tier I total reduction goal of 2222 lbm per nozzle. The weight savings due to the alternate kinematics effort alone was a considerable 1454 lbm per nozzle

due to the significant weight reductions that occurred within the midframe, aft sidewalls, divergent flap, and control system. The SAVE event items that remain open represent potential or additional weight savings yet to be realized (see Table 91).

In addition to the Tier I weight reduction ideas discussed above, the SAVE event produced a set of Tier II weight reduction ideas categorized as high-risk items. This set of Tier II items offered potential additional weight savings of 243 lbm (see Table 92).

3.4.4.9 Ultimate Nozzle Weight

At the end of 1998, results from the aircraft system studies focussed the requirements for the ultimate propulsion system on the 3770.54 cycle at a 2.7 SAR. During this same time period, the ultimate nozzle weight was originally estimated to be 7296 lbm. More detailed analyses in 1999 projected the ultimate nozzle weight to be 7262 lbm. These detailed analyses included:

- Changes to the engine cycle and SAR
- Open SAVE events Tier I items
- Tier II items
- Advanced materials, such as carbon–carbon and ceramic-matrix composites, expected to be incorporated by 2015

As shown in Figure 244 (page 271), there is high confidence that 7296 lbm per nozzle can be achieved for the the 2015 ultimate nozzle configuration.

3.4.4.10 Summary

The current (6/99) baseline nozzle has the following features:

- Fixed-Chute Mixer/Ejector Configuration
- 3770.60 Cycle, 2.9 SAR
- 8015-lbm Weight (Verified)

The ultimate (2015) exhaust nozzle is projected to have the following features:

- Fixed-Chute Mixer/Ejector Configuration
- 3770.60 Cycle, 2.7 SAR
- High Confidence in 7296-lbm Weight

3.4.5 Final Technology Configuration (FTC) Evaluation

The early Technology Configuration (TC) aircraft design was designated the (year) 2007 TC. Shortly after this design was established, technical requirements for the HSCT were revised (Subsection 3.4.1). Subsequently, the Advanced Concept Screening Committee surveyed all propulsion possibilities and developed recommendations (Subsection 3.4.2) for a final TC (FTC) design. All these factors led to the FTC (or 2015 TC). Figure 252 shows this development. The FTC design proposed by Boeing and endorsed by both P&W and GEAE is shown in Figure253.

The airframe selected for the FTC is very similar to the airframe that had been used for the 2007 TC design except that it is lighter in structure, offers reduced flutter, and lends itself to improved propulsion integration.

Table 91.   Comparison of Weight Reduction to SAVE, Tier I Goals   *Positve numbers represent weight reductions.*

Weight Reduction Item	SAVE Goals Tier I Weight Reduction	Linear Actuation 05/99 Status Weight Reduction	Comment
Single Door	364	246*	Less than SAVE goal
Incorporate Honeycomb	123	– –	Open
Sidewall Cross Beam	170	– –	Part of Alternate Kinematics
Incorporate Ti	223	– –	Open
Composite Fairings	64	– –	Open
Fixed Fan/Core Mixer	60	96	Meets SAVE goal
Increased Structural Envelope	330	– –	Open
Incorporate Alternate Kinematics	457	1454**	Exceeds SAVE goal
Composite Outer Flap	51	– –	Open
Composite Cascade	26	– –	Open
Optimize Door Kinematics	85	– –	Open
CMC Vanes – Ejector Mixer	51	– –	Open
Increased Mode Transition Time	43	– –	Part of Alternate Kinematics
Lower Bulk Density Acoustic Material	88	88	Meets SAVE goal
Minimize Attachments – Acoustic Liner	34	– –	Open
Reduced Facesheet Thickness – Acoustic Liner	55	– –	Open
Reduced Ejector Mixer Length	N/A	54	
T–Duct Further Design Development	N/A	33	
Total	**2222**	**1971**	

 *Inlet Door = 280; C&A = –34(weight adders)

**Midframe = 474; Aft Sidewall = 31; Flap C&A = –23 (weight adders); Pump C&A = 130; Dflap = 321; Outer Flap = 51 (weight adder)

Table 92.   Save Event, Tier II (12/99) Weight Reduction Items
Tier II weight reduction items were incorporated into the ultimate nozzle weight projection.

Item	Weight Reduction
Outer Fairing as Structural Skin	50
Reduce Mixer Penetration – Side to Side	32
Reduce Mixer Wall Area – Chevron	21
Allow Stalled Actuators/Inerlocks on Door	30
Redesign TPS	30
Optimize Facesheet Thickness – Acoustic Liner	10
Ti Convergent Flap w/Cooling	60
Total	**243**
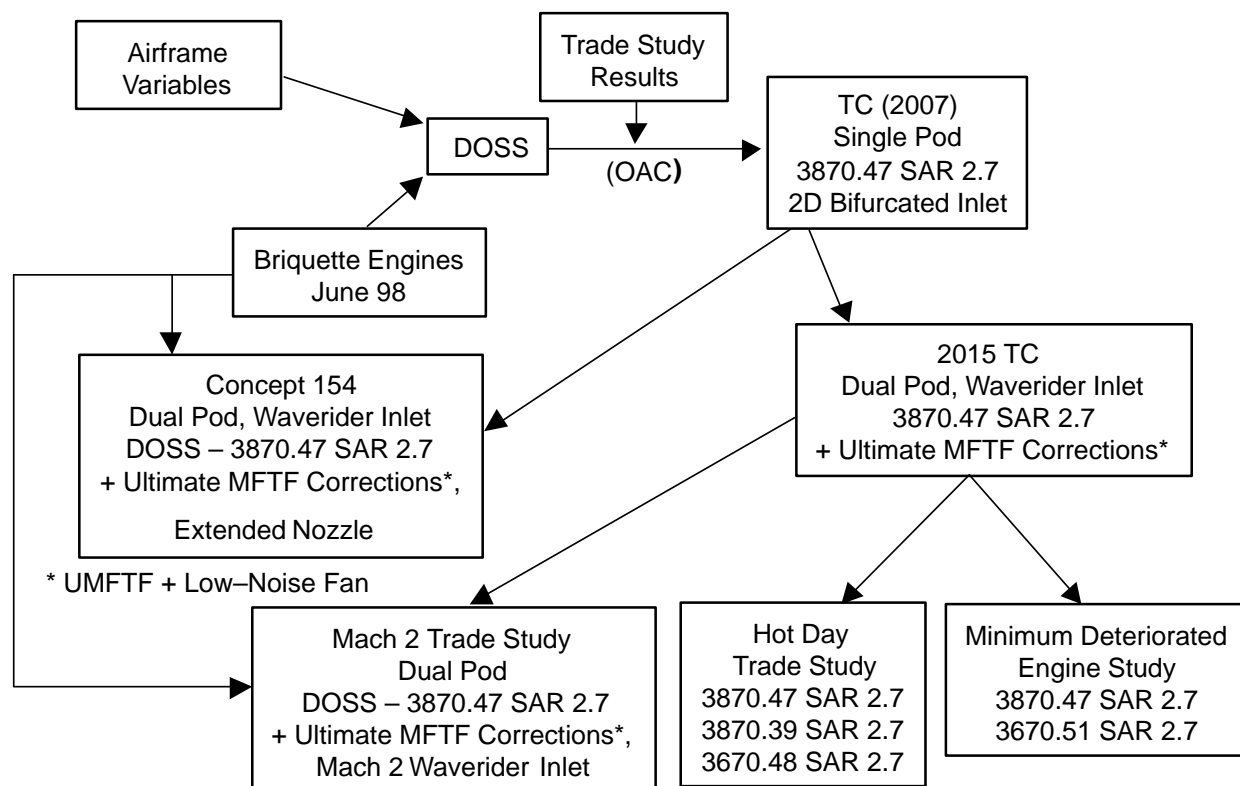
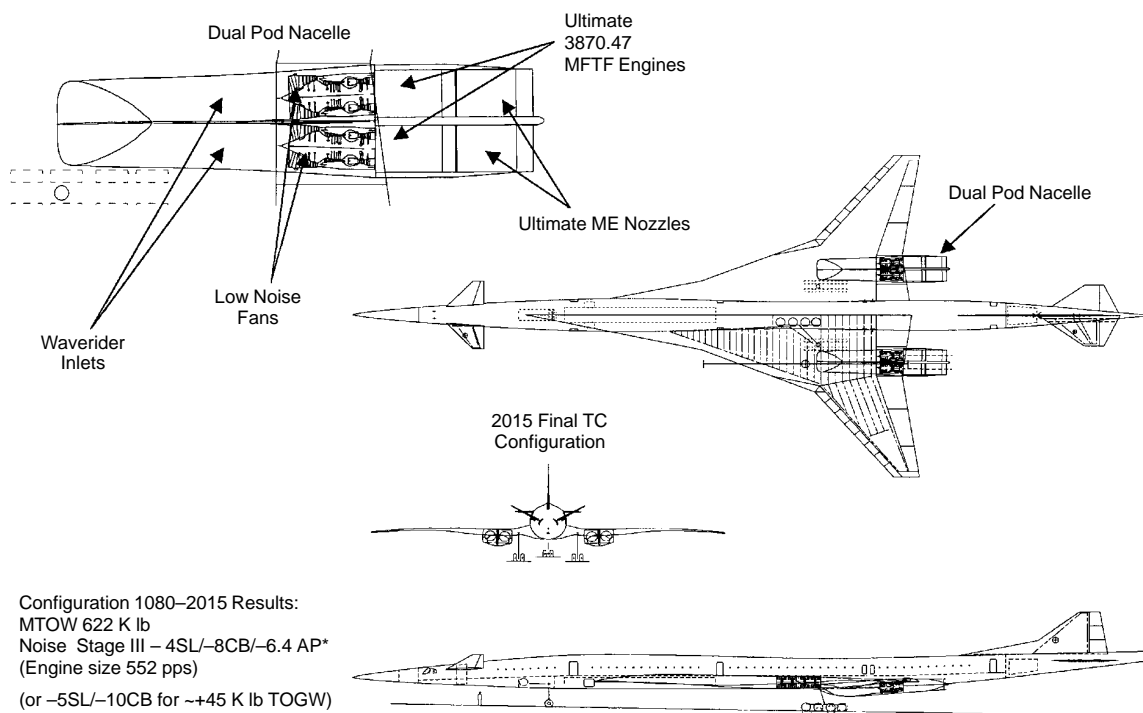**Figure 252.   Propulsion System Development**

Figure 253.   Final Technology Configuration – 2015 TC

The selected propulsion system is also similar to the 2007 TC design. The 2007 TC propulsion system used a 3870.47 SAR 2.7 MFTF–ME engine/nozzle combination with a 2D bifurcated inlet and a single-pod nacelle mounting. The propulsion system selected for FTC also used a 3870.47 SAR 2.7 MFTF–ME nozzle combination, but the FTC incorporated improvements that had been proposed for the Ultimate MFTF engine. Key features of the FTC propulsion system are as follows.

Waverider Inlet – A 3D external compression "waverider" inlet was incorporated into the FTC engine. This inlet is relatively "unstart free," relatively light, and offers reduced complexity compared to the 2D bifurcated inlet. In addition, the waverider inlet reduced engine weight by about 300 lbm since the fan and fan-containment system do not need to be designed to take the strong two-per-rev excitation from the inlet ramps. On the negative side, the waverider has a small cowl drag penalty, but this should be offset by the advantages of the inlet.

Low-Noise Fan – A low-noise fan was incorporated into the MFTF engine to enable the FTC to meet the new noise requirements. It should be noted that the low-noise fan increases engine weight by 300 lbm. This weight increase is cancelled out by the 300-lbm weight reduction that was enabled by the waverider inlet. The effective result is that the propulsion system weight is not changed by the addition of the fan and waverider inlet.

Ultimate Nozzle – The "Ultimate" nozzle was designed for use in the FTC. This nozzle had been completely optimized in flowpath, chevrons, tabs, and mixer length. The result of the optimization was to decrease projected noise levels. The TC engine/nozzle combination is projected to reduce noise by 3 dB at the sideline measuring point and 4 dB at the cutback measuring point. These noise reductions are achieved with only a 1% loss in thrust.

Dual-Pod Nacelle – The FTC engines and nozzles are designed to be mounted in a canted, common-sidewall configuration in dual-pod nacelles. The dual-pdo arrangement was chosen as the only apparent solution to wing flutter problems. The canted, common-sidewall configuration was selected because it is projected to have the least amount of boattail drag.

FTC Propulsion System – Analysis of engine/nozzle performance indicated that the propulsion system selected for the FTC produced the best economic result. The FTC propulsion system is projected to produce a net weight decrease of 1175 lbm and a net improvement in specific fuel consumption at cruise of 0.53% relative to the 2007 TC.

3.4.6 Alternate Aircraft System Evaluations

3.4.6.1 Concept 154 – HISCAT (Dual-Pod Configuration)

The Concept 154 or *high speed supersonic cruise airplane technology* concept used a blended wing/body with twin vertical tails, powered by two integrated, dual-pod, propulsion units each consisting of two mixed-flow turbofans and matching fixed-chute nozzles. This integrated approach was taken because it appeared to offer significant weight reductions beyond those achievable with the more traditional designs.

In the original drawings, the HISCAT was conceptualized with a single quad–podded engine nacelle. This design was discarded due to potential certification issues related to the risk of cascading engine failures. To mitigate these concerns, the HISCAT propulsion system is installed in two dual-pod nacelles, one beside each twin vertical tail (see Figure 238, page 265). Due to time constraints, the study of this HISCAT design was performed only with the ultimate MFTF (cycle 3870.47) engine.

Airflow variations were examined, but there was no consideration of other engine cycles, so study results cannot be considered optimized.

The HISCAT design used in the study included an S-duct inlet below the wing for each MFTF engine and four mixer/ejector nozzles extended behind the wing and connected by an integral trailing edge that is in effect a noise-deflection plate. The design placed the nozzle exits above the wing, as this configuration appeared to maximize the airframe shielding of jet and fan noise.

Both linear and rotary actuation linkages were considered for the HISCAT design, but ultimately the rotary actuated linked flap nozzles were selected as shown in Figure 254. The mounting of the nozzles adjacent to the vertical tails enabled the structural elements of the nozzles to be combined with the structural elements of the tails, thereby reducing overall weight.
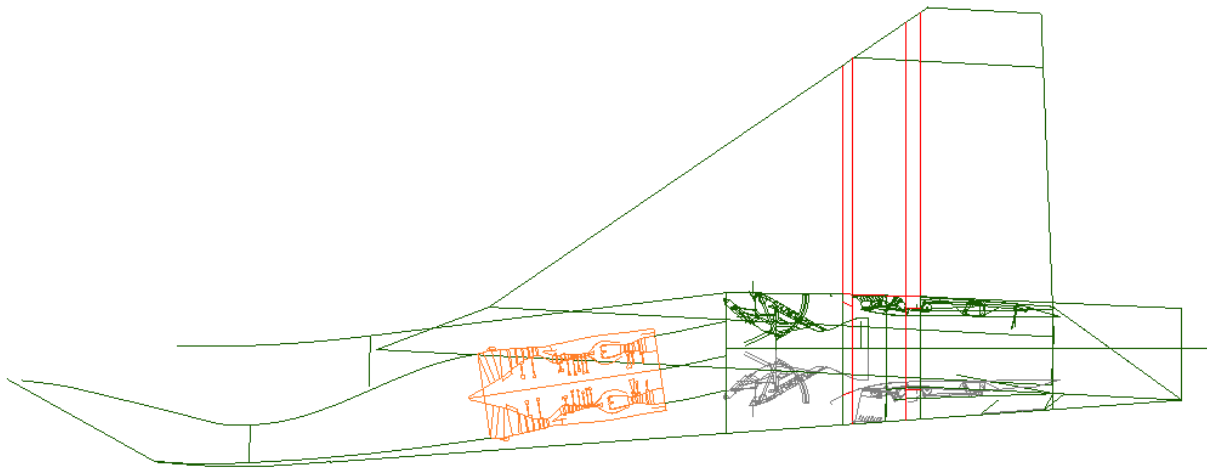
Figure 254.   Nozzle Installation, Side View

A number of designs for combining the nozzles and tail structures were examined, but many were found unsuitable. Figures 255 and 256 show an acceptable nozzle structure and support fully integrated into the airframe structure. Note that the design makes maximum use of all structural elements present and minimizes the use of single-function structures. Although in the illustration the structural supports are shown as midframe bulkhead elements, similar supports could have been located in other regions along the nozzle, such as in front of the mixer inlet doors or between the engine and nozzle inlet duct. Regardless of support location, nozzle installation would have to be performed by installing the nozzle components individually into the airframe. Nozzle servicing would be accomplished in a similar fashion.

Another nozzle system mounting approach considered involved installing the system at the recommended centerline of the tail as shown in figure Figure 257. In the figure, note the location and orientation of the inlet doors that feed the mixers. The top doors are unchanged from the earlier design, but the bottom door has been moved downward to the lower wing surface. This location lengthens the mixing passage, but it is not known whether the resulting configuration would cause the mixer to attenuate the noise sufficiently. It is apparent, however, that the angled duct feeding the nozzle from the engine would enable the upper door to be moved from the top of the nozzle to a more
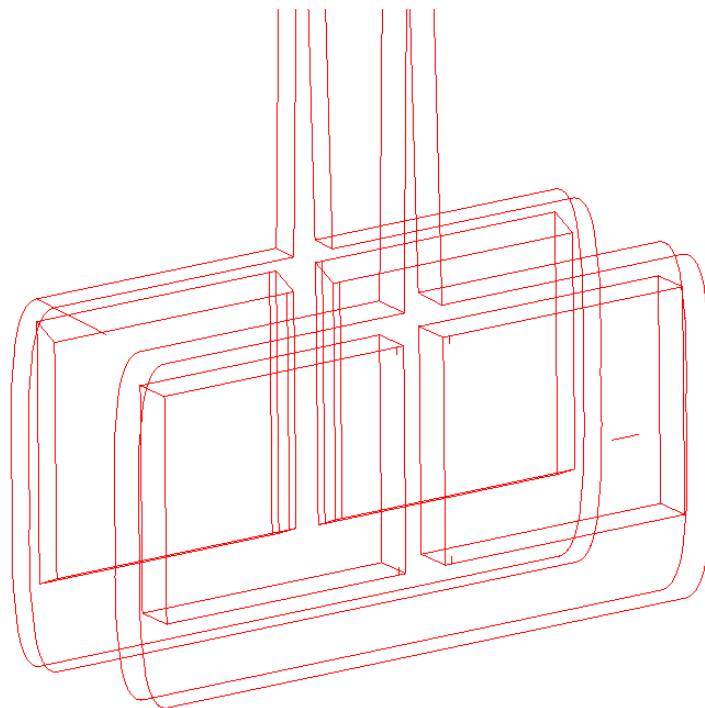
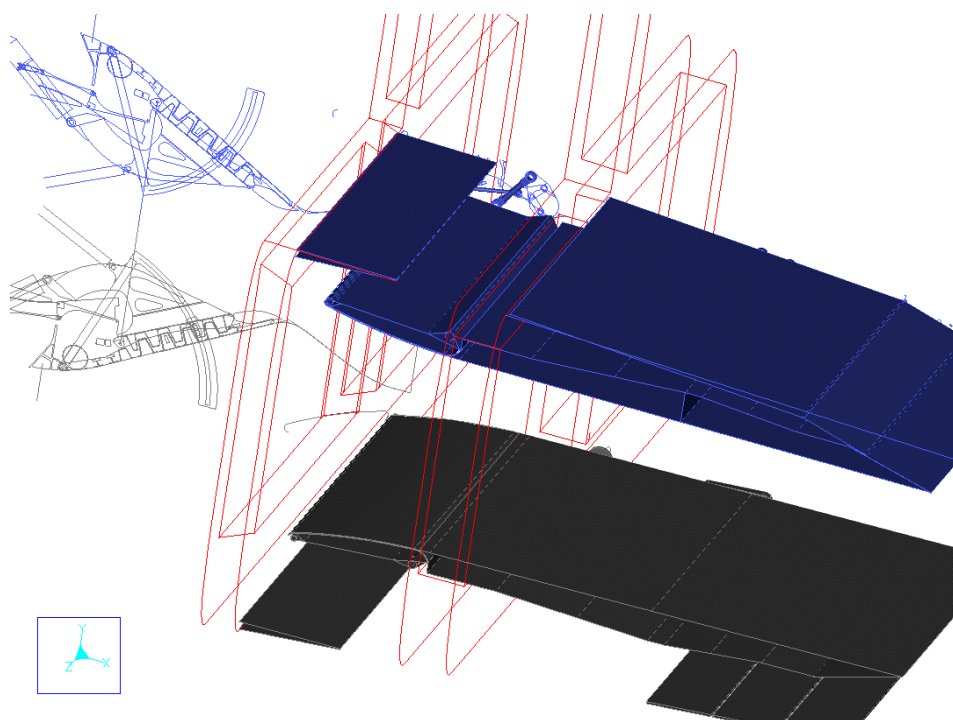**Figure 255.   Combined Nozzle Bulkhead and Tail Structure, Idealized View**

Figure 256.   Combined Structure with Flaps and Mixer Components
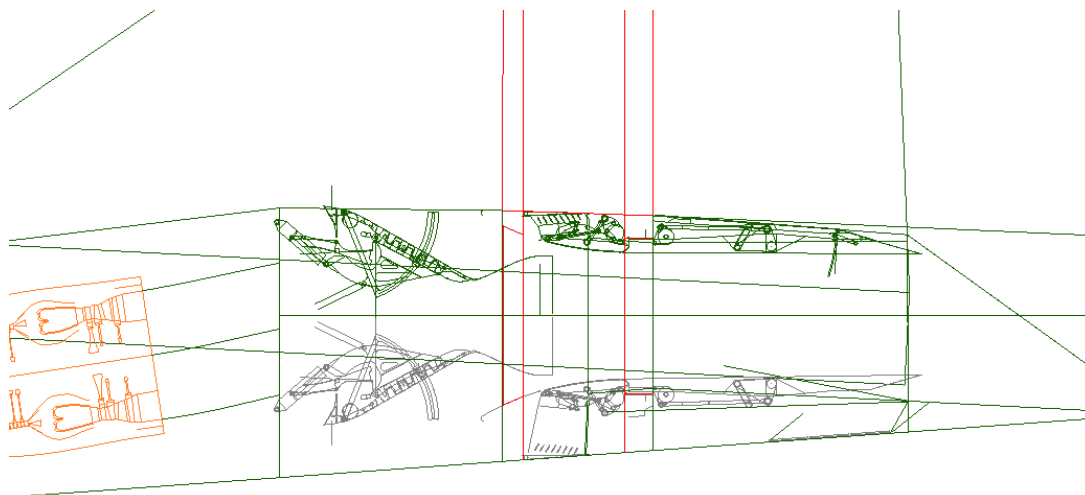
Figure 257. Nozzle/Mixer Installed on Recommended Centeline, Takeoff Position

forward location on the angled face of the duct. This repositioning would probably enable the inlet to provide higher feed pressure with a more direct (reduced loss) route to the mixer.

Additional benefits might be derived from moving the mixer and/or nozzle forward. This would improve the aircraft center of gravity and significantly increase the nozzle mixing length. It also appears likely that moving the mixer/transition into the curved feed duct would somewhat offset the added weight and cost of the curved duct. The new location may also permit rotation of the mixer into or out of the gas path as needed. If true, this configuration would enhance both cruise performance and mixer durability, in which case it is suggested that the lower mixer system be eliminated and efforts be made to reduce the lower sector noise emissions.

The rotary actuator systems used in the study of the HISCAT are of the same type as recommended in the actuator downselect study. However, after reevaluation, it appears that additional benefit might be derived by moving the hydraulic motors from the inboard and outboard ends of the system to a central location in the tail structure between the nozzles. In the central locations, the individual motors would need to be larger and heavier, but the number of motors could be reduced from 16 to 4. This would improve overall weight and simplify the hydraulic service, since there would need to be routing to only 4 locations instead of 12.

A thermal study was conducted to find out if the structural efficiency of the HISCAT might be improved by combining the hot and cold structural elements that make up the nacelle/tail assembly. Figure 258 shows the shell model used for thermal/structural analysis. This model included an 800°F inner sleeve to simulate a nozzle and an outer surface of 300°F to simulate the cooler airframe and resultant shear webs used to join these structures. The thermal study found that the bulk of the material was below 50 ksi (maximum Von Mises). This suggested that, although some handling would be necessary in heavily loaded areas, the basic approach of attaching the hot inner nozzle panels to the cold outer airframe surfaces through shear webs is achievable.

Structural analysis of the HISCAT configuration was conducted to determine what advantages might be expected by combining the nozzle and tail structures. Figure 259 shows the structural model of the combined nozzle and tail that was analyzed. The study found that the nested nozzle/tail
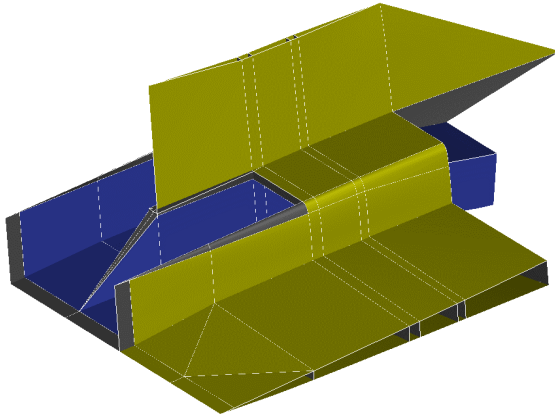
Figure 258.   Shell Model Used for Thermal Structural Analysis

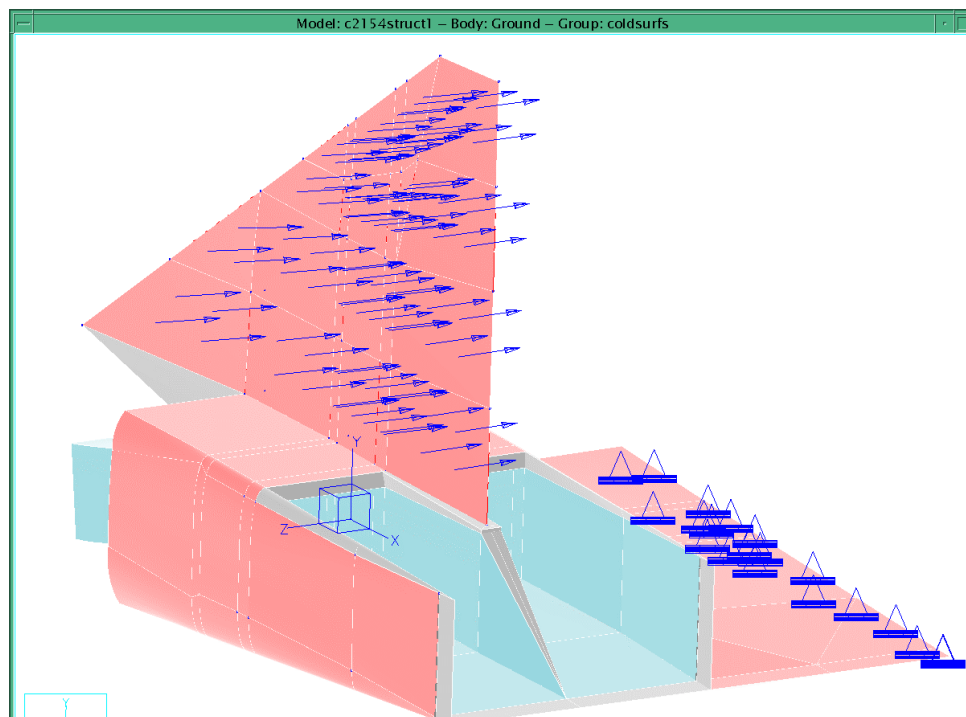Model: c2154struct1 – Body: Ground – Group: coldsurfs

Figure 259.   Combined Nozzle and Tail Structural Model

confguration might reasonably be expected to lower the system weight, not only because the tail is supported by the nozzle but also because the a sidewall in each nozzle is replaced with a structure that is both sidewall and tail structure.

Table 93 lists the component weights for the nozzle used in the studies cited above.

Table 93.   Nozzle Component Weights

Nozzle Component	No. Per Nozzle	Weight Each	Weight Per Nozzle	Comments
Convergent flap	2	137.2	274.4	note 1
Divergent flap	2	306.3	612.6	note 1
External flap	1	130	130	note 2
Midframe	1	259	259	note 3
Aft sidewalls, outboard	1	100	100	note 4
Aft sidewalls, inboard	1	40	40	note 5
Controls and actuation	1	1478	1478	note 1
Actuation linkage	1	194	194	notes 1, 6
Centerbody	1	68	68	
Fan/core mixer	1	175	175	
Inlet doors	2	225	450	
Ejector mixer	2	406	812	
Transition duct	1	1030	1030	
Reverser doors and cascades	2	95	190	
Accoustic tiles	1	700	700	
Total			6513	

Note 1: Unchanged from "downselect" configuration

Note 2: External flap exists on upper flap train only

Note 3   Midframe weight reduced by 40%. Inboard boundary provided by adjacent tail structure, lower boundary provided by adjacent wing structure

Note 4: Aft sidewalls, inboard are supported along 2 edges (1 edge support in "downselect" configuration), forward edge at midframe interface and lower edge at wing interface. Weight reduced by 40%.

Note 5: No additional structure required as pressure loads are absorbed by adjacent tail structure. Thermal barrier function estimated to add 40 lbs.

Note 6: Lower actuation systems of both convergent and divergent flaps are unchanged from "downselect" configuration.

3.4.6.2 2015 TC (Dual-Pod Configuration)

The 2015 TC "ultimate" aircraft design used two propulsion systems mounted in dual pods on each wing. Each propulsion system was to consist of a 3870.47 cycle MFTF and matching fixed-chute nozzle. The 3870.47 engine has a fan pressure ratio of 3.8, a flow lapse ratio of 70%, and a bypass ratio of 0.47. The mixer/ejector fixed chute nozzle has a suppression area ratio of 2.7, which represents the ratio between the (suppression) mixing area and the engine throat area (A_8) at suppressed takeoff conditions. Each nozzle also has an aspect ratio of 1.5, which is the ratio of gas flowpath width to height at the nozzle exit plane during suppressed takeoff conditions.

The GEAE nozzle design team was given the responsibility of evaluating these ultimate pod-mounted propulsion system nozzles and recording the nozzle geometery and weight data for use in further system studies. The mixer/ejector nozzle configuration developed uses the alternate kinematics/linear actuation system concept and incorporates Tier I and Tier II standards for weight reduction items from the SAVE event.

Design Approach

In developing the mounting to be used for the ultimate TC propulsion system, it was determined that the conventional method of podding two propulsion systems side by side resulted in an unacceptable base-drag region between the common sidewalls of the exhaust nozzles (Figure 260). To eliminate this problem, the team limited evaluations to those configuration candidates known to reduce or eliminate base drag. The intent of the study was to develop a design that minimized the base-drag region and effects to a level consistent with that of the baseline nozzle configuration.

Large Base-Drag
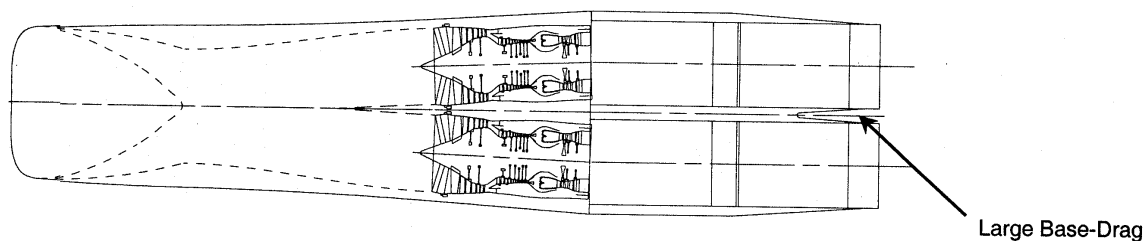
Figure 260.   Dual-Pod Nacelle Configuration (Generic)

Three candidate nozzle configurations were developed and evaluated; each appeared to reduce this base-drag concern. The candidate configurations were:

1. Canted common sidewalls

2. Canted nozzles

3. Kinked nozzles

Canted Common Sidewall Configuration

The canted common-sidewall nozzle configuration features a spacing of 12 inches between the flowpaths of the common sidewalls. This spacing produces a nacelle maximum area (A_{max}) of 13,900 in^2 and would be consistent with the initial spacing proposal.

In this design, the common sidewalls of the two propulsion units are mounted at a 4.42° angle from the nozzle centerline and canted towards each other (Figure 261). This mounting results in a trailing-edge base-drag effect consistent with that of the other sidewalls. The 12-inch spacing makes it necessary for the divergent actuators to be offset from the nozzle centerline to preclude interference between the actuators. One actuator would be positioned above the nozzle centerline; the other would be positioned below the centerline. It had been assumed that each nozzle would need two separate actuation systems to provide fail-safe protection, so use of a large common divergent actuator was not considered.

- 12 in. spacing between nozzle common sidewall flowpaths (at nozzle fore flange)
- Common sidewalls canted toward each other
- Common sidewall divergent actuators located offset from nozzle centerline
- Increased boattail angle due to closing-down of the divergent flaps
- About 0.55% C_{FG} loss at Mach 2.4 cruise
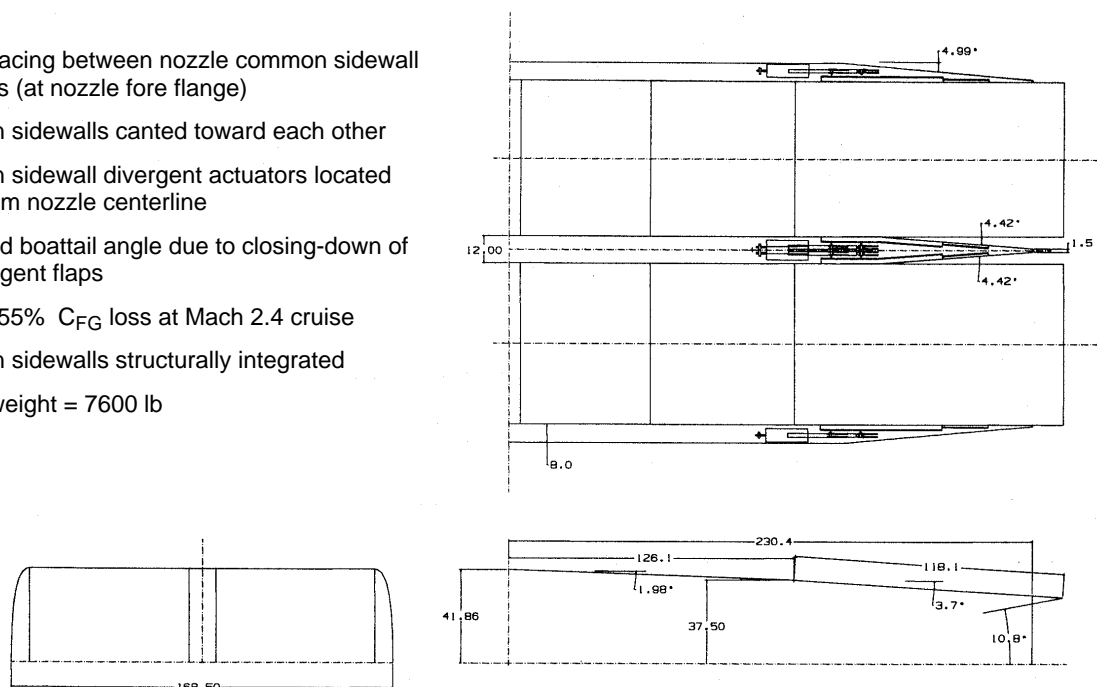- Common sidewalls structurally integrated
- Nozzle weight = 7600 lb

Figure 261.   Canted Common-Sidewall Configuration

The canting of the common sidewalls formed an additional leakage area between the divergent flaps and the respective sidewalls. For this reason, the divergent flaps had to be closed down to compensate for the increased leakage. This flap closure increased the boattail angle.

A performance evaluation determined that the canted common-sidewall configuration would have about a 0.55% loss in the coefficient of gross thrust (C_{FG}) at Mach 2.4 cruise. Approximately 0.4% of this can be assumed to be Prandtl–Meyer expansion loss at the sidewall. The remainder (about 0.15%) can be attributed to leakage loss at the triangular gap between the divergent flap and the sidewall.

The nozzle weight for the canted common-sidewall configuration was estimated at 7600 lbm. The initial nozzle weight had been reduced by 110 lbm by the structural integration of the common sidewalls and the reduction in area of the 2-in acoustic tile — caused by canting the common sidewalls. The initial weight had been increased, however, by an estimated 90 lb due to the reduced structural envelope between the nozzles and the increased loading from the divergent actuator. The end result was that the nozzle used in the canted common-sidewall configuration was 20 lbm lighter than the weight estimated for the ultimate 3870.47 baseline nozzle.

The main differences between the three configurations being evaluated involved changes needed in the divergent actuation at the common sidewalls. In the canted common-sidewall configuration, offsetting the divergent actuation seems to require the least amount of change in the adjacent nozzle structure and its components.

Canted Nozzle Configuration

In the canted nozzle configuration, the two nozzles were mounted at a 3.4° angle in relation to the engine centerline and canted towards each other (Figure 262). This resulted in a common-sidewall, trailing-edge, base-drag effect consistent with the other sidewalls. A 28.9-in space between the nozzle flowpaths at the nozzle forward flange affected the spacing of the interfacing engine turbo-machinery components. This spacing resulted in a nacelle A_{max} of 15,290 in^2.

The divergent actuation system designed for the common sidewalls was positioned forward relative to the baseline location to limit the canted angle and the spacing between flowpaths that results. Therefore, changes were needed in both the actuation linkages and the structural configurations of the aft sidewalls and midframes. As in the canted-sidewall configuration, it was assumed that each nozzle needed separate actuation systems for fail–safe purposes, so the use of a single large common divergent actuator was not considered.

Due to the cosine effect of the canted nozzles, an internal performance evaluation predicted a gross thrust loss of approximately 0.18% when measured at all forward thrust points.

The nozzle weight for the canted nozzle configuration was estimated at 7595 lbm. The initial weight had been reduced 100 lbm by the structural integration of the common sidewalls, the increased structural envelope between the nozzles at the forward end, and the reduction in area of the 2-in acoustic tile caused by the canting of the nozzles. The initial weight had been increased, however, an estimated 75 lbm due to the reduced structural envelope between the nozzles at the aft end and the increased loading and structural changes caused by moving the divergent actuation further
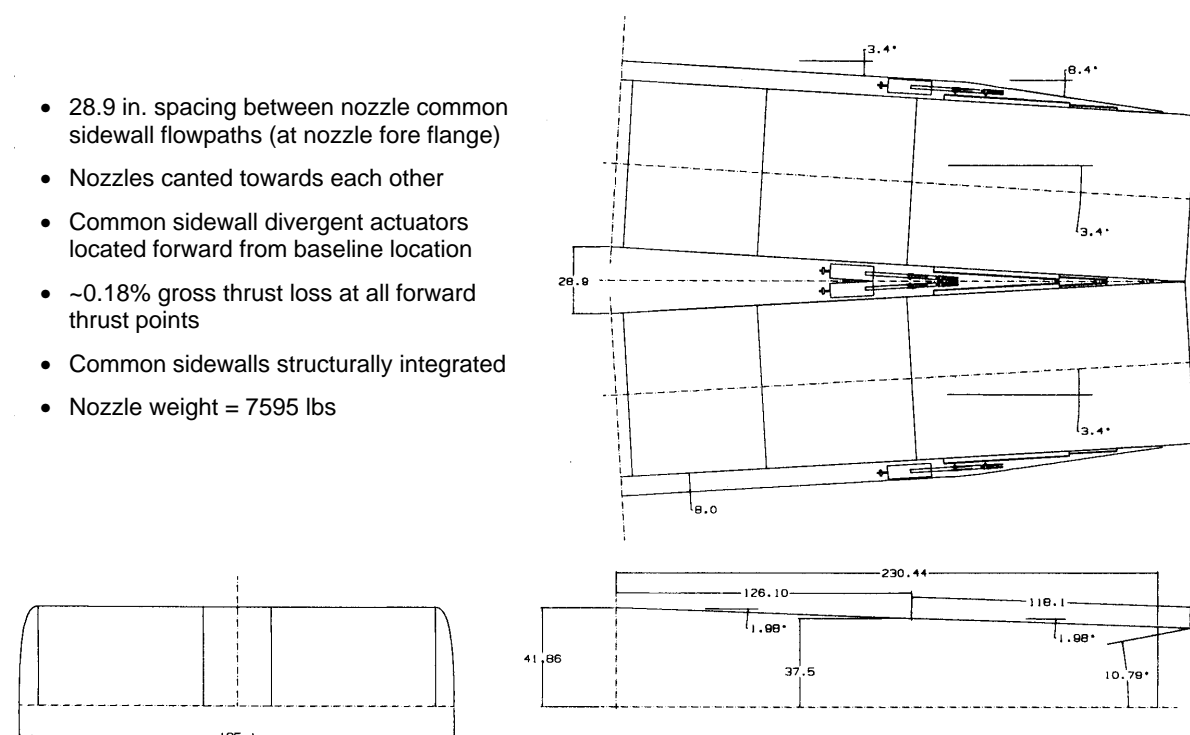
- 28.9 in. spacing between nozzle common sidewall flowpaths (at nozzle fore flange)
- Nozzles canted towards each other
- Common sidewall divergent actuators located forward from baseline location
- ~0.18% gross thrust loss at all forward thrust points
- Common sidewalls structurally integrated
- Nozzle weight = 7595 lbs

Figure 262.   Canted Nozzle Configuration

forward. The end result was that the canted nozzle configuration was 25 lbm lighter than the weight estimated for the ultimate 3870.47 baseline nozzle.

As stated before, the main differences between the configurations being evaluated involved the changes needed in the divergent actuation at the common sidewalls. Positioning the divergent actuation further forward as required for the canted nozzle configuration required more change to the associated nozzle structure and actuation linkages than was needed for the canted common-sidewall configuration.

Kinked Nozzles

For the kinked nozzle configuration, the forward halves of the two nozzles were mounted parallel to each other, but the aft halves were bent or kinked towards each other at a 3.4° angle relative to the nozzle centerline (Figure 263). This configuration resulted in a common-sidewall, trailing-edge, base-drag effect consistent with that of the other sidewalls. The configuration resulted in a spacing of 17.74 inches between the nozzle flowpaths at the nozzle fore flange, which affected the spacing of the interfacing engine turbomachinery components. This component spacing resulted in a nacelle A_{max} of 14,380 in^2.

- 17.74 inch spacing between nozzle common sidewall flowpaths (at nozzle fore flange)

- Nozzles kinked towards each other at midframe

- Common sidewall divergent actuators located forward from baseline location

- ~0.18% gross thrust loss at all forward thrust points

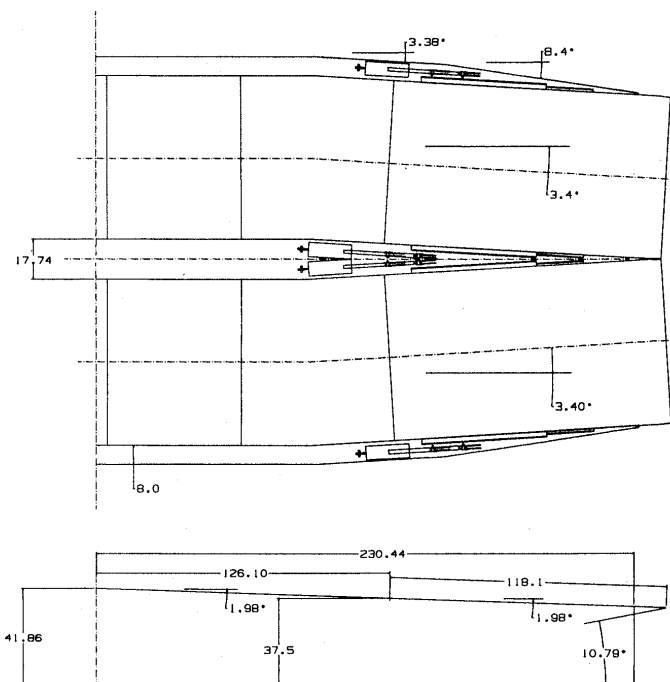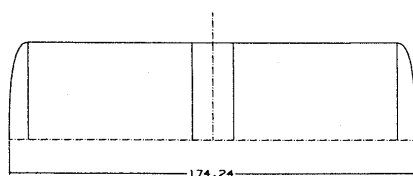- Common sidewalls structurally integrated

- Nozzle weight = 7635 lbs

Figure 263.   Kinked Nozzle Configuration

The divergent actuation designed for the common sidewalls was moved forward relative to the baseline location to limit the canted angle and the resulting spacing between the flowpaths. This meant that changes would be required, both in the actuation linkages and in the structure of the aft sidewalls and midframes. Once again, it was assumed that each nozzle needed separate actuation systems for fail-safe purposes, and so the use of a single large common divergent actuator was not considered.

As was the case in the canted nozzle configuration, an internal performance evaluation predicted a gross thrust loss of approximately 0.18%, when measured at all forward thrust points, due to the cosine effect of the canted nozzles

The nozzle weight for the kinked nozzle configuration was estimated at 7635 lbm. The initial weight had been reduced 100 lbm by the structural integration of the common sidewalls, the increased structural envelope between the nozzles at the forward end, and the reduction in the area of the 2-in acoustic tiles that resulted from canting the nozzles. The initial weight had been increased by an estimated 116 lbm due to the reduced structural envelope between the nozzles at the aft end, the structural changes to the midframe as the result of the kink, and the increased loading and structural changes that resulted from the divergent actuation being located further forward. The end result was that the kinked nozzle configuration was 15 lbm lighter than the weight estimated for the ultimate 3870.47 baseline nozzle.

In this case also, the main differences between the configurations involved changes required in the divergent actuation at the common sidewalls. The positioning of the divergent actuation further forward involved more changes to the associated nozzle structure and actuation linkage than were needed for the canted common sidewall configuration.

Summary

The objective of the exhaust nozzle evaluation was to supply geometry and weight data to be used for further aircraft studies of the 2015 TC. Table 94 summarizes the data submitted for further aircraft system studies as part of the nozzle data pack.

Table 94.   Summary of Nozzle Data Submitted for Further Aircraft System Studies

2.7 SAR, 1.5 Aspect Ratio, 142-in Mixing Length							
Nozzle Description	Nozzle Weight (lbs/noz)	Nozzle c.g. (in)	Nacelle* Amax (in²)	Supercruise Boattail Angle (°F)	Performance Losses	Atrt/ Amix	Flowpath Spacing** (in)
Baseline – Ultimate Mixer Ejector Nozzle	7620	87.9	7017	1.98	Reference	6.3	N/A
2015 TC – Canted Sidewalls***	7600	87.9	13900	3.7	0.55% Cfg (Cruise)	6.0	12.0
2015 TC – Canted Nozzles	7595	87.9	15290	1.98	0.18% gross fwd thrust	6.0	28.9
2015 TC – Kinked Nozzles	7635	87.9	14380	1.98	0.18% gross fwd thrust	6.0	17.7
* Single engine per nacelle for baseline; two engines per nacelle for others.							
** At nozzle for flange.							
*** Involves the least amount of changes to baseline nozzle design.							

The main differences between the three 2015 TC configurations involved the changes required in the divergent actuation needed for the common sidewalls. Offsetting the divergent actuation as required for the canted common sidewall configuration involves the least amount of change to the adjacent nozzle structure and components.

3.4.6.3 Mach 2.0 Studies (1998–1999)

In late 1998, a study was initiated of Mach 2.0 HSCT engines complying with Boeing-defined thrust requirements. Two engines, the 37685.38 and the 37689.40, were developed by P&W to match these requirements. Both of these engines were 3.76 FPR MFTF/ME types. GEAE generated flowpaths

for both of these engines. The 37685.38 engine was projected to weigh 9309 lbm, and the projected weight of the 37689.40 engine was 9178 lbm. A 2.7 SAR mixer/ejector nozzle was designed for each of these engines. The nozzle for the 37685.38 had a projected weight of 7833 lbm and the nozzle for the 37689.40 engine was projected to weigh 7591 lbm. The Mach 2.0 aircraft was not sized with these two engines.

At the suggestion of the Technology Integration team, a new evaluation of Mach 2.0 cruise was initiated. For this study, it was decided to apply factors to the Mach 2.4 "Briquette" engines so that it would not be necessary to generate new datapacks.

The two Mach 2.0 designed engines weights and lengths are compared to the 1998/1999 Mach 2.4 "Briquette engines in Table 95. The two Mach 2.0 engines are shown in the far right columns of Table 95. A nozzle with a SAR of 2.9 was not evaluated for the Mach 2.0 engines. Engie center of gravity for the 3270.8 and 3470.69 "Briquette" engines was not evaluated because the engines were defined near the end of the study and time ran out.

The 37689.40 engine has an 89% Mach 2.0 flow lapse, which is comparable to the Mach 2.0 flow lapse in the Briquette engines. A decision was made to maintain the thrust lapse relationship (Mach 2.0 cruise divided by hot day takeoff) in the Briquette. There are two Mach 2.4 engines in the Briquette that match the Mach 2.0 thrust lapse requirements specified by Boeing: the 3770.43 and the 3870.39. As can be seen in the table, weights for these two engines are almost identical to the weight of the 37689.40. However, these weights are all generated by the FLOWPATH program and do not take into account the fact that lower temperature materials introduced into the fan module would reduce weight a predicted 250 lbm (about 3% of engine weight). The nozzle is expected to be about 500 lbm lighter because of the lower Mach 2.0 cruise exhaust temperature and nozzle pressure ratio. It is recommended that, for Mach 2.0, the Briquette engine weight should be reduced by 250 lbm (about 3%), and the nozzle weight should be reduced by 500 lbm (about 6%).

Three more factors must be considered when dealing with Mach 2.0 operation: noise, SFC and thrust. The consensus opinion is that that suppressed operation at low speed is not significantly impacted by the design cruise Mach number; therefore, it should be assumed that noise and low-speed performance will not be impacted.

Figure 264 shows the Mach 2.0 thrust lapse plotted against the Mach 2.0 cruise SFC. This chart is based on several sets of Mach 2.0 design data and original Briquette data run at P&W. The Mach 2.0 designed engines are shown on the left of the chart, and the Mach 2.4 designed engines (Briquette) are shown on the right. The figure shows that the Mach 2.0 designed engines all have better SFC at Mach 2.0 than the engines designed for Mach 2.4. Because of the maximum T_3 limit at cruise, the engines actually designed for Mach 2.0 also have a better overall pressure ratio than engines designed for Mach 2.4. Hence, the Mach 2.0 engines have better fuel efficiency. The (old) Mach 2.4 3770.60 PTC engine, which is also shown on the chart, exhibits quite good SFC, but this is because the engine was designed to the original, more optimistic design assumptions. These assumptions were updated in June 1998.

Four variables on the plot affect SFC: thrust lapse (bypass ratio), flow lapse, fan pressure ratio, and overall pressure ratio (design Mach). The dotted line on the far left of the chart (Mach 2.0 engine) and the dashed lines on the far right (Mach 2.4 engines) represent 89% flow lapse engines. The solid lines in the middle of the chart (Mach 2.0 engine) represent 85% flow lapse engines. The SFC shift along the solid lines or dashed lines shows the impact of the FPR on SFC. This trend variation already

Weights in lbm, geometry in inches.

Table 95. Weights, CG's, and Geometry

| Engine Configuration	3270.8	3470.69	3670.60	3670.48	3770.54	3770.43	3870.47	3870.39	37789.40	37685.38
Design Mach No.	2.4	2.4	2.4	2.4	2.4	2.4	2.4	2.4	2.0	2.0
Thrust Lapse ID	0	0	0	10	0	10	0	10	10	10
SAR	2.5	2.5	2.7	2.7	2.7	2.7	2.7	2.7	2.7	2.7
Engine Weight	8804.77	8917.89	8755	9315	8845	9169	8848	9170	9178	9309
Nozzle Weight	7068	7139	7137	7900	7362	8037	7657	8185	7591	7833
Total Goal Proj. Prod. Weight	15872.8	16056.9	15892	17215	16207	17206	16505	17355	16769	17142
CG, Turbomachinery	67.3663	66.7747	65.29	66.91	65.60	65.60	63.68	68.73	64.76	69.88
CG, Nozzle (rel to RF aft Flange)	88.7	88.1	88.30	87.80	88.10	87.50	87.90	87.60	92.10	91.80
CG location, Engine			130.72	134.08	131.00	133.61	131.03	138.98	64.76	69.88
Turbine Rear Frame Aft Flange	119.669	117.125	122.69	125.47	121.48	123.70	120.96	130.07	117.92	126.09
Nozzle Length at Takeoff	224.4	221.4	227.84	230.40	229.25	231.37	230.44	232.20	227.60	226.80
	2.7	2.7	2.9	2.9	2.9	2.9	2.9	2.9	2.9	2.9
Engine Weight	8804.77	8917.89	8755	9315	8845	9169	8848	9170	9178	9309
Nozzle Weight	7579	7601	7629	8476	7830	8601	8145	8743		
Total Goal Proj. Prod. Weight	16383.8	16518.9	16384	17791	16675	17770	16993	17913		
CG, Turbomachinery	67.3663	66.7747	65.29	66.91	65.60	65.60	63.68	68.73	64.76	69.88
CG, Nozzle (rel to RF aft Flange)	89	87.8	90.20	89.50	88.70	88.10	87.80	87.60		
CG location, Engine			134.02	137.45	133.49	136.37	133.22	141.43		
Turbine Rear Frame Aft Flange	119.669	117.125	122.69	125.47	121.48	123.70	120.96	130.07	117.92	126.09
Nozzle Length at Takeoff	224.5	221.4	230.60	233.30	229.50	232.40	230.20	232.60		
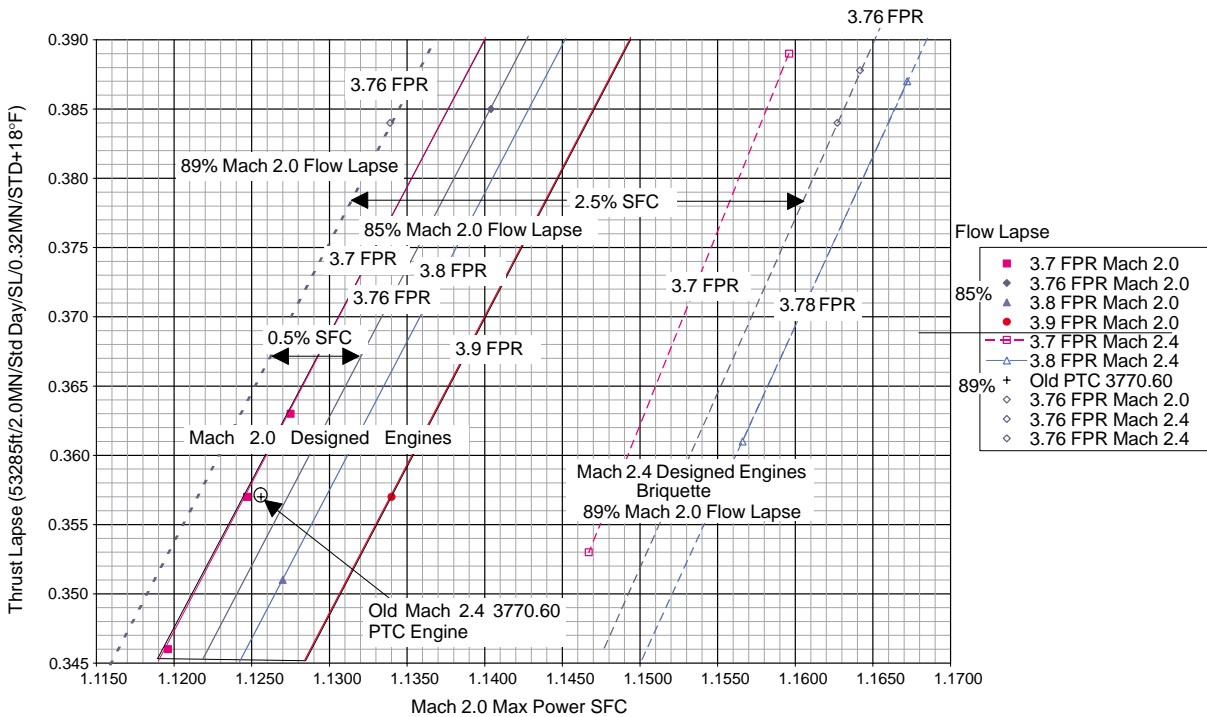
Figure 264. Mach 2.0 Cycle Performance
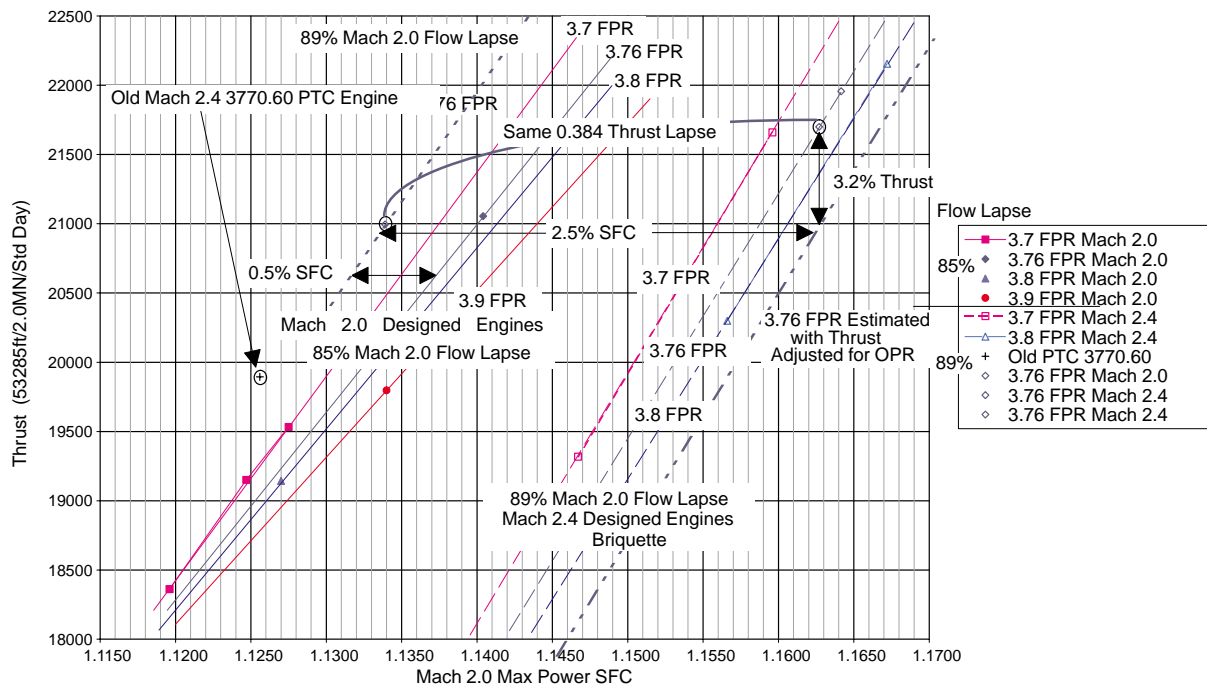
Figure 265. Mach 2.0 Cycle Performance

exists in the Briquette. The shift between the far-left dashed line and solid lines to the immediate right reveals the effect that flow lapse has on SFC. If the FPR is held constant, the transition from 89% flow lapse to 85% flow lapse costs about 0.5% in SFC. Finally, when a comparison is made between the far-left Mach 2.0 dashed line and an estimated 3.76 FPR Mach 2.4 dashed line, it is evident that at 89% flow lapse the OPR shift for a design Mach number of 2.0 reduces SFC about 2.5%.

Figure 265 establishes the thrust factor to be used in determining the impact of the OPR change on the Briquette engine. An increased OPR does improve the SFC, but it also reduces the thrust. The 0.384 thrust lapse points shown in Figure 264 are also shown in Figure 265 to illustrate the thrust change caused by the OPR shift. The chart shows that the 3.76 FPR line for the Mach 2.4 engine had to be shifted down 3% to match the thrust of the Mach 2.0 engine at the same thrust lapse, flow lapse, and FPR. When the 3% correction is made to the Briquette data, an SFC difference of 2.5% is apparent, as was seen in Figure 264.

An analysis similar to the above was performed on the subsonic data, and the result was an SFC shift of 3% with no reduction in thrust. Subsonic cruise thrust can be matched by adjusting the throttle. There is no significant change in SFC for a small (+3%) thrust adjustment because the SFC is still on the flat part of the curve. Therefore, the recommendation for estimating Mach 2.0 engines with the Briquette is:

- Reduce engine weight by 2.5%
- Reduce nozzle weight by 6%
- Use same NPD* tables for noise with 3% adjustment for thrust
- Decrease supersonic SFC by 2.5%
- Decrease subsonic SFC by 3.0%
- Decrease overall thrust by 3.0%
- For 85% flow lapse, increase SFC by about 0.5%

* NPD stands for *noise power distance* — the noise level at a given power at a given distance from the microphone. The NPD tables are output from Boeing's system studies.

REPORT DOCUMENTATION PAGE

1. AGENCY USE ONLY (Leave blank)	2. REPORT DATE	3. REPORT TYPE AND DATES COVERED
	May 2005	Final Contractor Report

4. TITLE AND SUBTITLE

Critical Propulsion Components

Volume 1: Summary, Introduction, and Propulsion Systems Studies

6. AUTHOR(S)

Pratt & Whitney and General Electric Aircraft Engines

5. FUNDING NUMBERS

WBS–22–714–09–447
NAS3–27235

7. PERFORMING ORGANIZATION NAME(S) AND ADDRESS(ES)

Pratt & Whitney
Advanced Engineering Operations
P.O. Box 109600
West Palm Beach, Florida 33410

8. PERFORMING ORGANIZATION REPORT NUMBER

E–15051–1

9. SPONSORING/MONITORING AGENCY NAME(S) AND ADDRESS(ES)

National Aeronautics and Space Administration
Washington, DC 20546–0001

10. SPONSORING/MONITORING AGENCY REPORT NUMBER

NASA CR—2005-213584-VOL1

12a. DISTRIBUTION/AVAILABILITY STATEMENT

Unclassified - Unlimited
Subject Categories: 01, 05, and 07

Available electronically at http://gltrs.grc.nasa.gov

This publication is available from the NASA Center for AeroSpace Information, 301–621–0390.

12b. DISTRIBUTION CODE

13. ABSTRACT (Maximum 200 words)

Several studies have concluded that a supersonic aircraft, if environmentally acceptable and economically viable, could successfully compete in the 21st century marketplace. However, before industry can commit to what is estimated as a 15 to 20 billion dollar investment, several barrier issues must be resolved. In an effort to address these barrier issues, NASA and Industry teamed to form the High-Speed Research (HSR) program. As part of this program, the Critical Propulsion Components (CPC) element was created and assigned the task of developing those propulsion component technologies necessary to: (1) reduce cruise emissions by a factor of 10 and (2) meet the ever-increasing airport noise restrictions with an economically viable propulsion system. The CPC-identified critical components were ultra-low emission combustors, low-noise/high-performance exhaust nozzles, low-noise fans, and stable/high-performance inlets. Propulsion cycle studies (coordinated with NASA Langley Research Center sponsored airplane studies) were conducted throughout this CPC program to help evaluate candidate components and select the best concepts for the more complex and larger scale research efforts. The propulsion cycle and components ultimately selected were a mixed-flow turbofan (MFTF) engine employing a lean, premixed, prevaporized (LPP) combustor coupled to a two-dimensional mixed compression inlet and a two-dimensional mixer/ejector nozzle. Due to the large amount of material presented in this report, it was prepared in four volumes; Volume 1: Summary, Introduction, and Propulsion System Studies, Volume 2: Combustor, Volume 3: Exhaust Nozzle, and Volume 4: Inlet and Fan/Inlet Acoustic Team.

14. SUBJECT TERMS

High speed civil transport; High speed research; Mixed-flow turbofan; Mixer/ejector; Nozzles

15. NUMBER OF PAGES

327

16. PRICE CODE

17. SECURITY CLASSIFICATION OF REPORT	18. SECURITY CLASSIFICATION OF THIS PAGE	19. SECURITY CLASSIFICATION OF ABSTRACT	20. LIMITATION OF ABSTRACT
Unclassified	Unclassified	Unclassified	